

Organometallic Chemistry

Research Perspectives

Contributors

Uwe Böhme

Vladimir I. Bregadze

Isabella Chiarotto

Dipak Kumar Dutta

Jun Hou

Alexander Jakob

Heinrich Lang

Kazuyoshi Ohta

Xiaojun Peng

Tahereh Sedaghat

Igor B. Sivaev

Yoshiyuki Sugahara

Seiichi Tahara

Yosuke Takeda

Abbas Tarassoli

Yuko Uchimaru

Wai-Yeung Wong

Satoru Yoshioka

Richard P. Irwin
Editor

NOVA

ORGANOMETALLIC CHEMISTRY RESEARCH PERSPECTIVES

ORGANOMETALLIC CHEMISTRY

RESEARCH PERSPECTIVES

RICHARD P. IRWIN
EDITOR

Nova Science Publishers, Inc.
New York

Copyright © 2007 by Nova Science Publishers, Inc.

All rights reserved. No part of this book may be reproduced, stored in a retrieval system or transmitted in any form or by any means: electronic, electrostatic, magnetic, tape, mechanical photocopying, recording or otherwise without the written permission of the Publisher.

For permission to use material from this book please contact us:

Telephone 631-231-7269; Fax 631-231-8175

Web Site: <http://www.novapublishers.com>

NOTICE TO THE READER

The Publisher has taken reasonable care in the preparation of this book, but makes no expressed or implied warranty of any kind and assumes no responsibility for any errors or omissions. No liability is assumed for incidental or consequential damages in connection with or arising out of information contained in this book. The Publisher shall not be liable for any special, consequential, or exemplary damages resulting, in whole or in part, from the readers' use of, or reliance upon, this material.

Independent verification should be sought for any data, advice or recommendations contained in this book. In addition, no responsibility is assumed by the publisher for any injury and/or damage to persons or property arising from any methods, products, instructions, ideas or otherwise contained in this publication.

This publication is designed to provide accurate and authoritative information with regard to the subject matter covered herein. It is sold with the clear understanding that the Publisher is not engaged in rendering legal or any other professional services. If legal or any other expert assistance is required, the services of a competent person should be sought. FROM A DECLARATION OF PARTICIPANTS JOINTLY ADOPTED BY A COMMITTEE OF THE AMERICAN BAR ASSOCIATION AND A COMMITTEE OF PUBLISHERS.

LIBRARY OF CONGRESS CATALOGING-IN-PUBLICATION DATA

Organometallic chemistry research perspectives / Richard P. Irwin, editor.

p. cm.

Includes index.

ISBN-13: 978-1-60692-874-5

1. Organometallic chemistry--Research. I. Irwin, Richard P.

QD411.O665 2006

547'.05--dc22

2007019178

Published by Nova Science Publishers, Inc. • New York

CONTENTS

Preface	vii
Chapter 1 Polyhedral Boron Hydrides in Use: Current Status and Perspectives <i>Igor B. Sivaev and Vladimir I. Bregadze</i>	1
Chapter 2 Hydrosilylation of CH ₂ =CH- Groups Immobilized on the Interlayer Surface of an Ion-Exchangeable Layered Perovskite with Hydorochlorosilanes and Oligosiloxanes <i>Seiichi Tahara, Kazuyoshi Ohta, Satoru Yoshioka, Yosuke Takeda, Yuko Uchimaru and Yoshiyuki Sugahara</i>	61
Chapter 3 Use of Electrochemistry and Palladium Catalysts for an Efficient Synthesis of Carbonyl Compounds <i>Isabella Chiarotto</i>	83
Chapter 4 Mixed Transition Metal Acetylides with Different Metals Connected by Carbon-Rich Bridging Units: On the Way to Heteromultimetallic Organometallics <i>Heinrich Lang and Alexander Jakob</i>	99
Chapter 5 Recent Advances in Organometallic Materials Derived from Ferrocenylacetylide <i>Wai-Yeung Wong</i>	165
Chapter 6 The Bio-Organometallic Chemistry of [2Fe2S] Models Related to Iron Hydrogenase Active Site <i>Xiaojun Peng and Jun Hou</i>	197
Chapter 7 Recent Advances in Organotin(IV) Complexes Containing Sn-S Bonds <i>Abbas Tarassoli and Tahereh Sedaghat</i>	221

Chapter 8	Organometallic Complexes of Rhodium(I), Iridium(I) and Ruthenium(II) Containing Hemilabile Functionalized Phosphine-Chalcogen Donor Ligands : Synthesis, Reactivities and Applications <i>Dipak Kumar Dutta</i>	249
Chapter 9	Electronic Properties of Transition Metal Carbene and Silylene Complexes - A Quantum Chemical Study at Selected Model Complexes <i>Uwe Böhme</i>	289
Index		299

PREFACE

Organometallic chemistry is based on the reactions and use of a class of compounds ($R-M$) that contain a covalent bond between carbon and metal. They are prepared either by direct reaction of the metal with an organic compound or by replacement of a metal from another organometallic substance. Research in organometallic chemistry is also conducted in the areas of cluster synthesis, main-group derivatives in unusual oxidation states, organometallic polymers, unstable organometallic compounds and intermediates in matrices, structure determination of organometallic compounds in the solid state [X-ray diffraction] and gaseous states [electron diffraction], and mechanisms of reactions of transient silylenes and related species. In addition to the traditional metals and semimetals, elements such as selenium, lithium and magnesium are considered to form organometallic compounds, e.g. organomagnesium compounds $MeMgI$, iodo(methyl)magnesium and diethylmagnesium which are Grignard reagents an organo-lithium compound $BuLi$ butyllithium; Organometallic compounds often find practical uses as catalysts, in the processing of petroleum products and in the production of organic polymers. This book presents leading-edge new research in the field.

Chapter 1 - This review is designed to highlight the current status and perspectives of application of polyhedral boron compounds and their metal complexes. The main attention is paid to application of polyhedral boron hydrides in medicine including boron neutron capture therapy for cancer, radionuclide diagnostics and therapy, as well as antitumor activity of some metal derivatives of carboranes. Boron neutron capture therapy - a binary cancer treatment based upon the interaction of two relatively harmless species, a ^{10}B nucleus and a thermal neutron, which results in the formation of the highly energetic 4He and 7Li as products. These fission products have an effective range of $\sim 10 \mu m$ in tissue, thus, effectively limiting the extent of cellular damage to approximately one cell diameter. Therefore, the selective concentration of boron compounds within the tumor cells, followed by their capturing of thermal neutrons, should result in localized destruction of the malignant cells in the presence of the normal cells. Another possible medical application of polyhedral boron hydrides is radionuclide diagnostics and therapy of cancer, where these compounds can be used for attachment of radionuclide labels to various cancer-targeting biomolecules. Other fields of potential application of polyhedral boron hydrides and their metal complexes are synthesis of new materials (liquid crystals, NLO materials, magnets, semiconductors, etc.), radionuclide extraction from nuclear wastes, ion-selective electrodes, production of thermally stable

polymers and high burning composite propellants, development of new catalysts for organic synthesis.

Chapter 2 - Novel preparation of inorganic-organic hybrids using ion-exchangeable layered perovskites *via* hydrosilylation has been explored. $\text{CH}_2=\text{CH}-$ groups were immobilized on the interlayer surface through an alcohol-exchange-type reaction between an *n*-propoxy derivative of $\text{HLaNb}_2\text{O}_7\cdot x\text{H}_2\text{O}$ (HLaNb) with 4-penten-1-ol or 9-decen-1-ol to form a $\text{CH}_2=\text{CH}(\text{CH}_2)_n\text{O}$ -derivative of HLaNb (*n* = 3 or 8), and hydrosilylation of the $\text{CH}_2=\text{CH}-$ groups of the $\text{CH}_2=\text{CH}(\text{CH}_2)_n\text{O}$ - groups with SiH groups in hydrochlorosilanes, hydride-terminated polydimethylsiloxane (H-PDMS) or octahydridosilsesquioxane (OHSQ) was conducted subsequently. When the $\text{CH}_2=\text{CH}(\text{CH}_2)_3\text{O}$ -derivative of HLaNb was reacted with dichloromethylsilane, trichlorosilane or H-PDMS, X-ray diffraction (XRD) patterns, infrared (IR) adsorption, and ^{13}C and ^{29}Si CP/MAS nuclear magnetic resonance (NMR) spectra showed the occurrence of hydrosilylation in the interlayer space. Although the XRD pattern of the product of the reaction between the $\text{CH}_2=\text{CH}(\text{CH}_2)_8\text{O}$ -derivative of HLaNb and OHSQ showed no notable increase in interlayer distance, the IR and ^{13}C and ^{29}Si CP/MAS NMR spectra suggested the occurrence of hydrosilylation. The occurrence of hydrosilylation between the $\text{CH}_2=\text{CH}-$ groups and OHSQ in the interlayer space was also indicated by a comparison of the pyrolysis behavior of the product of the reaction between the $\text{CH}_2=\text{CH}(\text{CH}_2)_8\text{O}$ -derivative of HLaNb and OHSQ with those of pyrolyzed HLaNb and the pyrolyzed $\text{CH}_2=\text{CH}(\text{CH}_2)_8\text{O}$ -derivative of HLaNb . These results clearly demonstrate that hydrosilylation in the interlayer space is a potential new method for preparing various organic derivatives of ion-exchangeable layered perovskites.

Chapter 3 - The great utility of carbonylic compounds as starting materials is well known; the importance of the carbonyl group derives from its reactivity, being susceptible to nucleophilic attack at carbon and electrophilic attack at oxygen. Transition metals can be used as reagents and catalysts to bring carbon monoxide into many organic compounds. Among transition metals, used in organic synthesis, palladium complexes offer versatile and very useful synthetic methods for carbonylation reaction and, generally, for carbon-carbon bond formation.

A lot of investigations aimed at the use of electrochemistry as a selective and environment friendly tool in organic synthesis, have allowed to develop a new methodology for palladium(II) catalyst recycling by means of its anodic oxidation at a graphite electrode in the absence of any other co-catalyst or stoichiometric oxidant. This methodology was applied to the synthesis of carbonyl compounds such as methyl acetylenecarboxylates, starting from alkynes, oxazolidin-2-ones, in very good yields, starting from 2-amino-1-alkanols, and N,N'-disubstituted ureas starting from amines, in an very efficient synthesis.

The advantage of the anodic recycling at a graphite electrode of Pd(II) is that it proceeds efficiently under atmospheric pressure of carbon monoxide, avoids the use of copper or halide ions and high pressure of O_2 gas which also implies the formation of water and causes undesired side reactions.

Chapter 4 - The chemistry of mono- and bis(alkynyl) transition metal complexes, modified ferrocenes, functionalized alkynyls, diaminoaryl NCN pincer molecules ($\text{NCN} = [\text{C}_6\text{H}_2(\text{CH}_2\text{NMe}_2-2,6)_2]^+$), and 1,4- and 1,3,5-substituted benzene derivatives towards diverse metal fragments will be discussed and serves to understand the manifold and sometimes unexpected reaction behavior of such species. Interesting novel (hetero)bi- to undecametallic compounds with often uncommon structural motifs are formed in which the respective

transition metal building blocks are connected by carbon-rich π -conjugated organic and/or inorganic bridging units. The reactions based on the modular molecular “Tinkertoys” approach depend upon the steric and electronic properties of the metal centers and ligands involved, which also will be discussed. The electrochemical behavior of such 1-dimensional molecular wire molecules, coordination polymers, star-like structured and dendritic oriented transition metal systems, respectively, is presented as well.

Chapter 5 - There is a flurry of interest in the research community in the development of carbon-rich bi- or multi-metallic assemblies containing π -conjugated chains. It has been demonstrated that molecular wires comprising mixed-valence bimetallic fragments or remote redox-active organometallic building blocks linked by all-carbon chains could be used in molecular electronics, optoelectronic devices and chemical sensing appliances. In recent years, the author has been engaged in the chemistry and material properties of oligoacetylenic ferrocenyl complexes and their organometallic derivatives by virtue of their potential in various areas of materials science. The synthesis, characterization, crystal structures, optical spectroscopy and electrochemistry of a series of homometallic and heterometallic alkynyl complexes end-capped with ferrocenyl entities which contain conjugated organic bridges will be presented. The electronic and redox properties will be examined as a function of the chain length and nature of the spacer group and the data are compared with the results obtained from theoretical computational studies.

Chapter 6 - Hydrogenases are enzymes that catalyze the reversible uptake/evolution hydrogen. The X-ray single crystal structure determinations have shown that the active site of iron hydrogenase features the organometallic community of [2Fe2S] compounds. Small molecular synthetic models, which structurally mimic the [2Fe2S] centre, serve as important probes of structure and chemistry at the active site of Fe-only hydrogenase. The azadithiolate-bridged diiron compounds that have been developed as structural model systems for Fe-only hydrogenase are reviewed in this article. The functionalized diiron complexes which show some ability to generate hydrogen are surveyed, with emphasis on the synthesis and the electrocatalytic properties. The electrocatalytic properties of all complexes investigated by cyclic voltammetry in the presence and absence of acid are described. In addition, the application of electrochemical and IR spectroelectrochemical (SEC) techniques to the elucidation of the details of the electrocatalytic proton reduction is described. The functional mechanistic proposals are discussed from these work.

Chapter 7 - In view of widespread industrial and biomedical applications of organotin(IV) compounds containing Sn-S bond, the synthesis, spectroscopic characterization and X-ray strucrural studies of some novel organotin complexes with 2-amino-1-cyclopentene-1-carbodithioic acid (ACDA) and its N-alkyl derivatives (RACDA) are investigated and reviewed. The presence of competing reactive center in these aminodithiocarboxylato ligands and the remarkable diversity in structure of organotin dithiolates lead to the interest in the study of such sulfur-nitrogen containing ligands. X-ray crystallographic studies of these organotin complexes show the bonding take place through the dithioate moiety and reveal a variety of coordination geometry around the Sn atom. These studies also show that an intramolecular hydrogen bond is formed between NH proton of amine group and one of sulfur atoms from dithiolate moiety. In ACDA complexes the neighboring molecules are oriented in such a way that an intermolecular hydrogen bond is also formed between another NH proton and one sulfur atom of the neighboring molecule, so that this sulfur atom is involved in one intra- and one inter-molecular hydrogen bonding. In

this chapter the reaction of ACDA and RACDA ($R = Et, Bu$ and Bz) with di- and tri-organotin chlorides will be discussed and the characterization of complexes will be investigated in solution and in solid state by spectroscopic methods and X-ray crystallography.

Chapter 8 - Organometallic complexes of rhodium, iridium and ruthenium have gained much importance because of their novelty, reactivity and applications in diverse fields. Some important examples of applications of such metal complexes as commercial homogeneous catalysts are : *L-DOPA* synthesis(Rhodium(I)-chiral catalyst); Monsanto / B. P. Chemicals process for carbonylation of methanol to acetic acid (Rhodium(I) catalyst) and the process called ‘*Cativa*’ (Iridium(I) catalyst with Ru-complex activator). Neutral and cationic rhodium(I), iridium(I) and ruthenium(II) complexes of functionalized phosphine-chalcogen donors $P-X$ ($X = O, S, Se$) ligands are of much interest in recent time because of expected novel structures and stereo-chemical control in catalytic applications in various important organic synthesis. Different types of $P-X$ ligands like $R_2P-(CH_2)_n-COOX'$, $X' = H / alkyl$, $n = 1-3$; $R_2P-(CH_2)_n-XR$, $R = alkyl/aryl$; $Ph_2PC_6H_4COOMe$; mono-, di- and tri-chalcogen functionalized poly-phosphines such as $Ph_2P(CH_2)_nP(X)Ph_2$, ($n = 1-4$), $MeC(CH_2PPh_2)_2(CH_2P(X)Ph_2)$ and other ligands CO , COD (1,5-cyclooctadiene) etc. form interesting metal complexes. Rhodium(I) carbonyl complexes containing bidentate chelating ligand such as diphenylphosphinomethane oxide / sulphide / selenide have shown interesting structural features. The chelated complex of the type $[Rh(CO)Cl(2-Ph_2PC_6H_4COOMe)]$ has been synthesized and the X-ray structure indicates a long range intramolecular ‘Secondary’ $Rh...O$ interactions ($Rh - O$ distance 3.18 \AA). The effect of chain length of the bifunctional i.e. ‘Soft and Hard’ donors chelating ligands of tertiary phosphines with functional carboxylic acid or ester, or unequal softness of the chelating donors i.e. tertiary phosphines functionalised with sulfur or selenium donors having aliphatic and aromatic backbones on the ‘*Hemilability*’ of the metal - $O / S / Se$ bonds are discussed. In chelate metal complexes containing hemilabile ligands like $P-X$, the labile $M-X$ bonds cleave and provide a vacant potential coordination site for reversible binding of substrates to metal centre by dynamic chelating ability i.e. by ‘*Opening and Closing*’ mechanism. The steric effect, electronic effect and kinetics of oxidative addition (OA) reactions of the complexes with different electrophiles like CH_3I , C_2H_5I , $C_6H_5CH_2Cl$ etc. are discussed. The activation of small molecules like CO , CH_3I , I_2 , etc. by the metal complexes and evaluation as catalysts precursors for carbonylation of alcohol are also discussed. The catalytic activities of suitable metal complexes are reported for carbonylation, hydrogenation and hydroformylation of important substrates for potential industrial organic compounds. The metal complexes of types $[Rh(CO)_2Cl(P\sim O)]$ and $[Rh(CO)Cl(P\sim O)_2]$; show high catalytic carbonylation reactions of methanol to acetic acid / ester with high Turn Over Number(TON) of about 1500. The metal complexes and the products were characterized mainly by Infrared, UV-Visible spectroscopy, NMR studies, X-ray crystallography and GCMS technique.

Chapter 9 - Common features and principal differences between carbene and silylene complexes of early and late transition metals are analyzed from a quantum chemical point of view. $Cp_2Ti=EH_2$ and $(OC)_4Fe=EH_2$ with $E = C, Si$ were chosen as representative examples for that purpose. The nature of the transition metal carbon and silicon bond was analyzed with CDA, NBO and the EHT-method. The distinctive properties of transition metal silylene complexes are caused by two main reasons: the silylene substituent acts mainly as σ -donor, and there is very weak π -bonding in silylene complexes.

Chapter 1

POLYHEDRAL BORON HYDRIDES IN USE: CURRENT STATUS AND PERSPECTIVES

Igor B. Sivaev and Vladimir I. Bregadze

A.N.Nesmeyanov Institute of Organoelement Compounds,
Russian Academy of Sciences, Moscow, Russia

ABSTRACT

This review is designed to highlight the current status and perspectives of application of polyhedral boron compounds and their metal complexes. The main attention is paid to application of polyhedral boron hydrides in medicine including boron neutron capture therapy for cancer, radionuclide diagnostics and therapy, as well as antitumor activity of some metal derivatives of carboranes. Boron neutron capture therapy - a binary cancer treatment based upon the interaction of two relatively harmless species, a ^{10}B nucleus and a thermal neutron, which results in the formation of the highly energetic ^4He and ^7Li as products. These fission products have an effective range of $\sim 10 \mu\text{m}$ in tissue, thus, effectively limiting the extent of cellular damage to approximately one cell diameter. Therefore, the selective concentration of boron compounds within the tumor cells, followed by their capturing of thermal neutrons, should result in localized destruction of the malignant cells in the presence of the normal cells. Another possible medical application of polyhedral boron hydrides is radionuclide diagnostics and therapy of cancer, where these compounds can be used for attachment of radionuclide labels to various cancer-targeting biomolecules. Other fields of potential application of polyhedral boron hydrides and their metal complexes are synthesis of new materials (liquid crystals, NLO materials, magnets, semiconductors, etc.), radionuclide extraction from nuclear wastes, ion-selective electrodes, production of thermally stable polymers and high burning composite propellants, development of new catalysts for organic synthesis.

1. INTRODUCTION

After the discovery of the first boranes by Alfred Stock in 1912 [1], these compounds were considered for a long time as academic curiosities. The boom in borane chemistry

started at the end of 1940's when some of them (B_5H_9 and $B_{10}H_{14}$) were believed to be most powerful rocket fuels superior to the available hydrocarbon fuels.

The US Army launched Project HERMES in the late 1940's, in 1952 the US Navy Bureau of Aeronautics started Project ZIP, and in 1956 the US Air Force sponsored Project HEF (High Energy Fuels). Many gifted scientists and engineers were mobilized for these projects, all working under a veil of secrecy. At least five boron fuel production plants were built in the USA and one plant was built in the USSR. In 1955 the US government launched a major project to build a boron-fuel-powered long-range strategic bomber called the Valkyrie XB-70A ("Boron Bomber"). Two of these magnificent jet aircraft were eventually built. One XB-70A was destroyed in a mid-air collision with a fighter jet over California's Mojave Desert, but the remaining bomber is on display at the Wright Patterson Air Force Base in Ohio, USA. Although they never flew solely on boron fuel, their construction led to technological advancements in the design of high speed aircraft. In fact, the XB-70A served as a model for the design of the Concorde supersonic jet.

Ultimately, the era of boron fuels came to a close. By the end of the 1950s, new generations of jet engines and new fuels involving liquid hydrogen and hydrazine made boron fuels obsolete. Technical problems with boron fuels - including byproducts that decreased engine function and high fuel consumption rates - had proved too hard to overcome. In 1959, the US military cancelled the boron fuels program, having invested the equivalent in modern currency rates of more than one billion dollars. Documents concerning the boron fuel projects were declassified some later and the public could finally see the monumental scale of these efforts [2].

2. MAIN TYPES OF POLYHERAL BORON HYDRIDES. SYNTHESIS AND PROPERTIES

One of the most important and exciting events in the chemistry of the XX century was the discovery of polyhedral boron hydrides at the end of 1950-s. Polyhedral boron hydrides are characterized by electron-deficient bonding, meaning that there are too few valence electrons for bonding to be described exclusively in terms of two-centered two-electron bonds. One characteristic of electron-deficient structures is the aggregation of atoms to form unusual three-centered two-electron bonds, which typically results in formation of trigonal boron faces and hypercoordination [3]. In contrast to the known boron hydrides, the polyhedral boron hydrides were shown to be exceptionally stable. Investigation of the properties of these compounds led to the conclusion that these compounds have aromatic properties [4]. It was the first example of non-planar three-dimensional aromatic compounds and resulted to development of concept of three-dimensional aromaticity that is generally accepted at the present time [5].

The *closo*-decaborate anion $[B_{10}H_{10}]^{2-}$ (Figure 1) is the first known representative of family of the *closo*-polyhedral boron hydrides. Its synthesis was first reported by Hawthorne and Pitichelli in 1959 [6]. The classical method of synthesis of the *closo*-decaborate anion is based on the reaction of decaborane(14) $B_{10}H_{14}$ and triethylamine in boiling toluene resulting in the desired product in 92% yield [7]. The other method is based on the solid state pyrolysis of tetraethylammonium tetrahydroborate (Et_4N) BH_4 and gives the target product in the yield

up to 80 % [8,9]. Synthesis of numerous derivatives of the *closo*-decaborate anion has been developed [4,10-19].

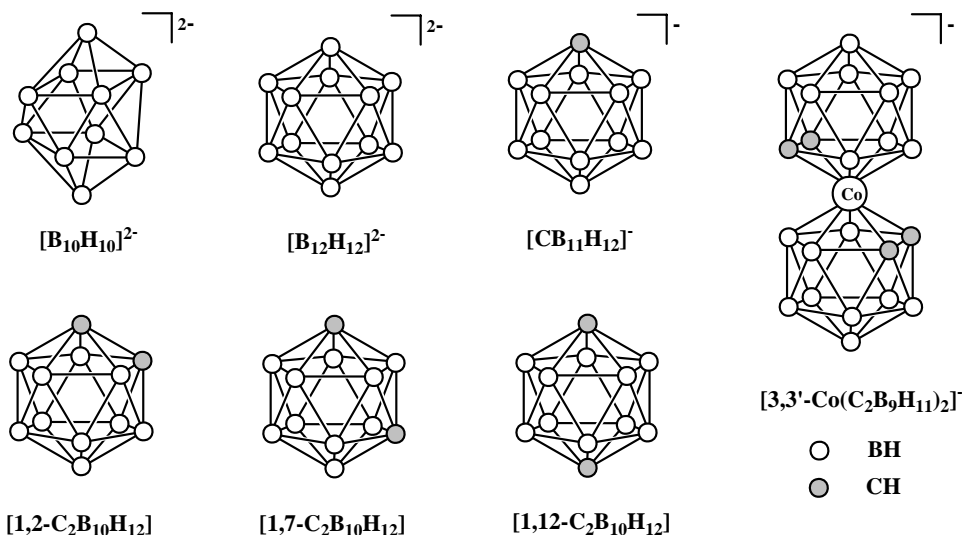


Figure 1. Main types of stable polyhedral boron hydrides.

The *closo*-dodecaborate anion $[B_{12}H_{12}]^{2-}$ (Figure 1) was first prepared by Hawthorne and Pitochelli in 1960 as a side-product of the reaction of 2-iododecaborane and triethylamine [20]. This synthesis was the brilliant verification of the results of quantum-chemical calculations performed by Longuet-Higgins and Roberts, who predicted in 1955 that the icosahedral boron hydride system would be stable only as the $[B_{12}H_{12}]^{2-}$ dianion [21]. A few years later several high-yield methods of its synthesis were proposed by different research groups [22-26]. At present there are several preparative methods for synthesis of the $[B_{12}H_{12}]^{2-}$ anion. Some of them are based on decaborane. Thus, pyrolysis of decaborane with triethylamine-borane $Et_3N \cdot BH_3$ at 190 °C in ultrasene gives the desired product in 92 % yield [23,24,27]. Another widely used in laboratory practice method is reaction of decaborane with $NaBH_4$ in refluxing diglyme giving the target product in 91% yield [25,28]. Other methods are based on commercial bulk chemicals and avoid highly toxic and expensive decaborane. Thus, pyrolysis of $Na[B_3H_8]$ generated *in situ* by oxidation $NaBH_4$ with iodine in diglyme gives the desired product in the yield up to 90 % [29]. The solid-state synthesis from potassium tetrafluoroborate KBF_4 and calcium hydride CaH_2 results in the target product in more than 90% yield [30]. Another method includes use widely available boron materials, such as boric acid and sodium borates in combination with various reducing agents [31]. Further development of this approach can give the $[B_{12}H_{12}]^{2-}$ anion in large amounts at a reasonable price.

The B-H bonds in the *closo*-dodecaborate anion have a hydridic character and amenable to attack by electrophilic reagents resulting in substitution of hydrogen atoms. There are two distinct mechanisms for substitution in polyhedral boron hydrides, ordinary aromatic electrophilic substitution and electrophile-induced nucleophilic substitution (EINS). The last one includes abstraction of a hydride anion from a BH vertex under electrophilic attack (or by Lewis acid) followed by attack of the “boronium ylide” formed with nucleophile [32].

Synthesis and chemical properties of the *closo*-dodecaborate anion and its derivatives have been reviewed recently [33,34], some more recent reports are included [35-41].

The carba-*closo*-dodecaborate anion $[CB_{11}H_{12}]^-$ (Figure 1) was first prepared by Knowth in 1967 in the multi-step synthesis starting from decaborane and sodium cyanide [42,43]. A safer and more convenient modification of the synthesis was proposed later by Hermanek's group [44]. In an important recent advance, the two-step synthesis of the $[CB_{11}H_{12}]^-$ anion from decaborane by Brelochs reaction with formaldehyde followed by insertion of two BH vertices gives the desired product in yield up to 65 % [45]. Using substituted benzaldehydes instead of formaldehyde at the first stage, the corresponding C-phenyl derivatives can be prepared [46,47]. An alternative approach of the $[CB_{11}H_{12}]^-$ anion synthesis is the carbon vertex insertion into the 11-vertex *nido*-precursor $Na[B_{11}H_{14}]$ that is accessible in 50 % yield in one-step reaction from $NaBH_4$ and $BF_3 \cdot OEt_2$. The reaction of $[B_{11}H_{14}]^-$ with chloroform under basic conditions results in the desired product in 20-25 % yield [48]. In the similar way, the substituted C-phenyl derivatives can be prepared by the reaction of the $[B_{11}H_{14}]^-$ anion with substituted benzyl chlorides [49].

The C-H bond in the $[CB_{11}H_{12}]^-$ anion is weakly acidic and can be deprotonated by strong bases, whereas the B-H bonds have hydridic character and are amenable to attack by electrophilic reagents. Synthesis and chemical properties of the carba-*closo*-dodecaborate anion and its derivatives have been reviewed very recently [50].

The synthesis of *ortho*-carborane (1,2-dicarba-*closo*-dodecaborane 1,2- $C_2B_{10}H_{12}$, figure 1) and some its C-substituted derivatives were first reported in 1963 independently by chemists from the USSR and USA [51-54]. *ortho*-Carboranes are prepared by the reaction of acetylenes (including both mono and disubstituted alkynes) with $B_{10}H_{12}L_2$ generated *in situ* from decaborane $B_{10}H_{14}$ and a weak Lewis base ($L = MeCN, R_2S, R_3N$). The reaction can be performed in the presence of a wide range of functional groups except the ones containing acidic hydrogen atoms (acids, alcohols, amines, etc.). These functionalities must be protected prior to conversion of an alkyne to a carborane. The *meta*- and *para*-carboranes (1,7- and 1,12- $C_2B_{10}H_{12}$, Figure 1) are prepared by thermal isomerization of *ortho*-carborane. At 400-500 °C *ortho*-carborane converts to the *meta*-isomer, which in turn rearranges to the *para*-isomer between 600-700 °C [55].

The CH groups in the carboranes are weakly acidic and can be readily deprotonated by strong bases (n -BuLi, $NaNH_2$, etc.) generating carboranyl anions (or organometallic derivatives CM) that are sufficiently nucleophilic to react with a wide range of electrophiles including alkyl halides, carbon dioxide, aldehydes, acid chlorides [55-57]. In contrast, the boron vertices can be derivatized using reactive electrophilic reagents [56-58].

One of the boron atoms adjacent to the both carbon atoms of *ortho*-carborane 1,2- $C_2B_{10}H_{12}$ and its derivatives can be removed using alkoxide bases [55], amines [59], or fluoride ion [60] to generate 7,8-dicarba-*nido*-undecaborate anion $[7,8-C_2B_9H_{12}]^-$ or its derivatives. The $[7,8-C_2B_9H_{12}]^-$ anion contains a bridging hydrogen atom which can be readily removed with base to yield the dicarbollide dianion $[7,8-C_2B_9H_{11}]^{2-}$. The dicarbollide dianion is formally isolobal to cyclopentadienide and has therefore been used to prepare a wide range of organometallic complexes, including a carborane analogue of ferrocene, first reported by Hawthorne and coworkers [61]. The cobalt bis(1,2-dicarbollide) anion $[3,3'-Co(1,2-C_2B_9H_{11})_2]^-$ (Figure 1), one of the very first metallacarboranes synthesized [62], is, probably, the most studied and the most used at present time metallacarborane [63-72].

All the polyhedral boron hydrides described above are available from commercial sources. It should be noted, however, that the polyhedron boron hydrides, especially those produced from decaborane, are very expensive and find practical applications only in some exclusive areas where no alternative exists. On the other hand, a revival in industrial production of boron cluster compounds and their price reducing can be expected only after the development of some important applications for these species.

Since the first review on potential applications of polyhedral boron hydrides published by Plešek fifteen years ago [73] apparent progress in this fields has been demonstrated and in this article we will make emphasis on the directions that have received the most development since that time.

3. APPLICATION OF POLYHEDRAL BORON HYDRIDES

The era of boron chemistry aimed at advanced jet and rocket propulsion systems ended in the early 1960s, however, the interest in the polyhedral boron hydrides as high energy density materials still persists and some salts of the *closo*-decaborate and the *closo*-dodecaborate anions were proposed as components of components of high burning composite propellants [74]. However, the main interest in application of the polyhedral boron hydrides is connected with medicine [57,75] and traditionally centered on their use in boron neutron capture therapy for cancer [76,77].

3.1. Boron Neutron Capture Therapy

3.1.1. General Principles

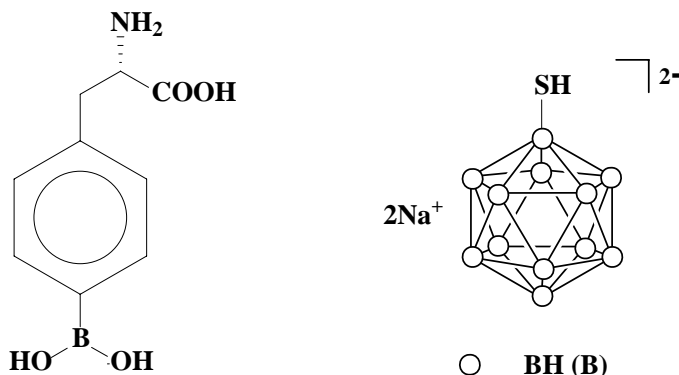
Boron neutron capture therapy (BNCT) for cancer is a binary method for the treatment of cancer, which is based on the nuclear reaction of two essentially nontoxic species, nonradioactive ^{10}B and low-energy thermal neutrons. The neutron capture reaction by ^{10}B produces an α -particle $^{4}\text{He}^{2+}$ and $^{7}\text{Li}^{3+}$ ion together with 2.4 MeV of kinetic energy and a 480 keV photon. These high-linear-energy transfer ions dissipate their kinetic energy before traveling one cell diameter (5-9 μm) in biological tissues, ensuring their potential for precise cell-killing. Therefore, high accumulation and selective delivery of boron into the tumor tissue are the most important requirements to achieve efficient neutron capture therapy of cancer. There are three most important requirements for development of boron compounds: (1) achieving minimal tumor concentrations in the range of 20-35 μg of ^{10}B per gram of tumor tissue; (2) selective delivery of boronated compounds to tumor cells, while at the same time, the boron concentration in the cells of surrounding normal tissue should be kept low to minimize the damage to normal tissue; (3) sufficiently low toxicity [78,79]. Ideally, only tumor cells will be destroyed without damage to healthy tissues in the irradiated bulk. The absence of an adverse effect on the surrounding healthy tissues is attributed to the fact that the thermal neutron capture cross-sections of elements involved in tissues are 4-7 orders of magnitude smaller than that of the ^{10}B isotope (table 1).

Table 1. Thermal neutron capture cross-sections of isotopes characterized by the largest capture cross-sections and cross-sections of isotopes of some physiologically important elements

Isotope	Capture cross-section (barn)	Isotope	Capture cross-section (barn)	Average content in tissues
^{10}B	3.8×10^3	^1H	0.33	(10.0 %)
^{113}Cd	2.0×10^4	^{12}C	3.4×10^{-3}	(18.0 %)
^{149}Sm	4.2×10^4	^{14}N	1.8	(3.0 %)
^{151}Eu	5.8×10^3	^{16}O	1.8×10^{-4}	(65.0 %)
^{155}Gd	6.1×10^4	^{31}P	0.18	(1.16 %)
^{157}Gd	2.6×10^5	^{32}S	0.53	(0.20 %)

Despite the fact that the thermal neutron capture cross-section of the ^{10}B isotope is smaller (see table 1) than those of some other elements (^{113}Cd , ^{149}Sm , ^{151}Eu , ^{155}Gd , or ^{157}Gd), at present the ^{10}B isotope is virtually an alternativeless element for neutron capture therapy for cancer because it readily forms stable covalent compounds. Moreover, the use of boron clusters containing ten or more boron atoms per molecule “increases” the neutron capture cross-section by an order of magnitude considering a boron cluster as a structure element alternative to a single metal atom. At the same time, the synthesis of stable *in vivo* complexes of cadmium and *f*-elements capable of undergoing modifications is quite an intractable problem presently. Only ^{157}Gd complexes currently have potential use in nuclear capture therapy [80].

The only two BNCT agents currently used for clinical trials are L-*p*-dihydroxy-borylphenylalanine (BPA), a boronated aminoacid analogue, and disodium mercaptoundecahydro-*closso*-dodecaborate $\text{Na}_2\text{B}_{12}\text{H}_{11}\text{SH}$ (BSH), both are the so-called ‘second generation’ BNCT drugs (Figure 2).



L-*p*-boronophenylalanine (BPA)

sodium mercapto-*closso*-dodecaborate (BSH)

Figure 2. Clinically used BNCT agents.

Both these drugs are very far from ideal. Therefore, many different types of boron containing compounds have been designed and synthesized for testing as BNCT drugs over the past 30 years. In order to fulfill the requirements for the BNCT agents, these new compounds should consist of a boron-containing part connected *via* a hydrolytically stable linkage to a tumor-targeting part responsible for delivering of a boron fragment to the tumor cell and its retention there (Figure 3).

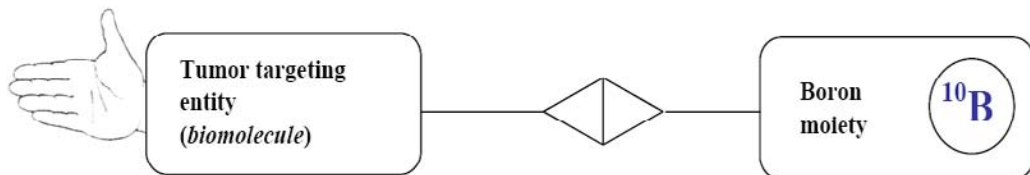


Figure 3. Principal scheme of BNCT agent.

The BNCT agents currently under investigation are the ‘third generation’ boron carriers and can be classified either according to their chemical structure and compound category, their high molecular weight or their biological target recognition properties.

3.1.2. Low Molecular Weight Boron Compounds

Synthesis of low molecular weight boron compounds is in a focus of attention of many groups of chemists. The most widespread chemical effort has been related to the design and synthesis of boron-containing cellular building blocks. The rationale for their synthesis is that, in contrast with normal cells, tumor cells have an elevated requirement for certain constituents necessary for cell replication (nucleic acid precursors, amino acids, carbohydrates, etc.).

Nucleotides and Nucleosides

Boron-containing nucleosides are good candidates for BNCT. The rationale for their synthesis was suggested to be hypothetical incorporation of boron-containing nucleoside triphosphates into DNA reducing effectively minimal therapeutic concentration to 20-35 µg $^{10}\text{B}/\text{g}$ [79,81-84]. More recently, it was recognized that active triphosphates, due to their cytotoxicity, are responsible for the most of the severe toxic side-effects in antimetabolite chemotherapy. Triphosphates of boron-containing nucleoside prodrugs could exert a similar toxicity profile without neutron radiation when administered systemically at high doses, and it is uncertain if this toxicity can be tolerated [85].

At present, however, boron-containing nucleosides are still considered as promising candidates for BNCT because of their potential to be retained in rapidly dividing tumor cells after 5'-monophosphorylation by phosphorylating enzymes, thymidine kinase 1 and deoxycytidine kinase. Thymidine kinase 1 is pyrimidine specific, phosphorylating thymidine and 2'-deoxyuridine, whereas deoxycytidine kinase has a broad substrate specificity, phosphorylating 2'-deoxycytidine, 2'-deoxyadenosine, and 2'-deoxyguanosine. Cellular efflux of such 5'-monophosphates would be retarded due to the negatively charged phosphate moiety. Design strategy for BNCT nucleoside prodrugs should focus on structures which enter tumor cells either by passive diffusion or via nucleoside membrane transporter and are

selectively trapped intracellularly as anabolically and catabolically stable non-toxic 5'-monophosphates and/or 5'-diphosphates [85].

Syntheses and results of biological studies of carborane-containing nucleosides have been reviewed several times during the last 10 years [81-85]. Based on the results of phosphoryl transfer assays of a few series of carborane-containing nucleosides, three-dimensional quantitative structure-activity relationship has been developed [86]. Structures of some carborane-containing nucleosides synthesized are presented in Figure 4.

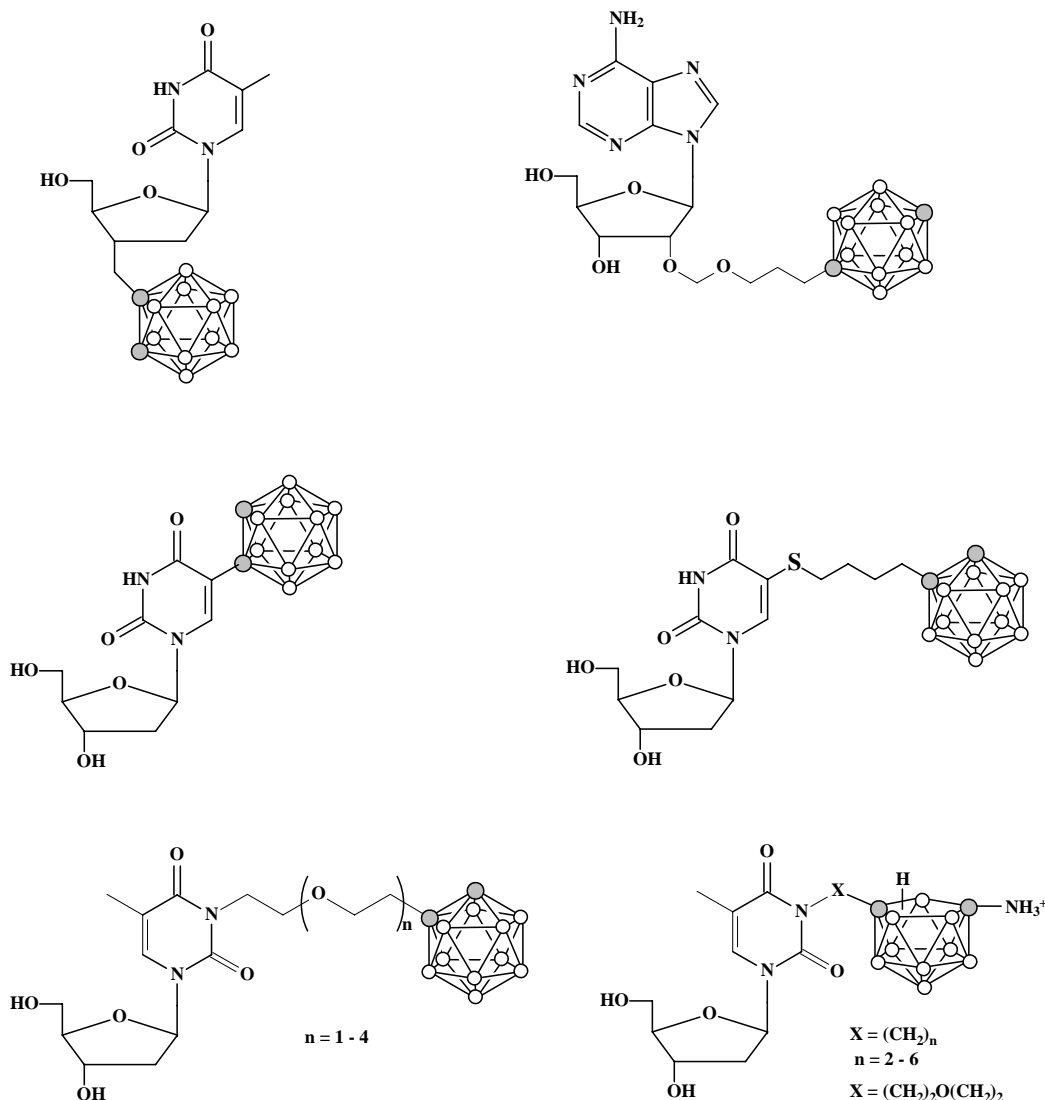


Figure 4. Structures of some carborane-containing nucleosides.

Synthesis and biological evaluation of the first cobalt bis(dicarbollide) analogues of thymidine have been reported recently by Lesnikowski et al. [70,87,88] (Figure 5).

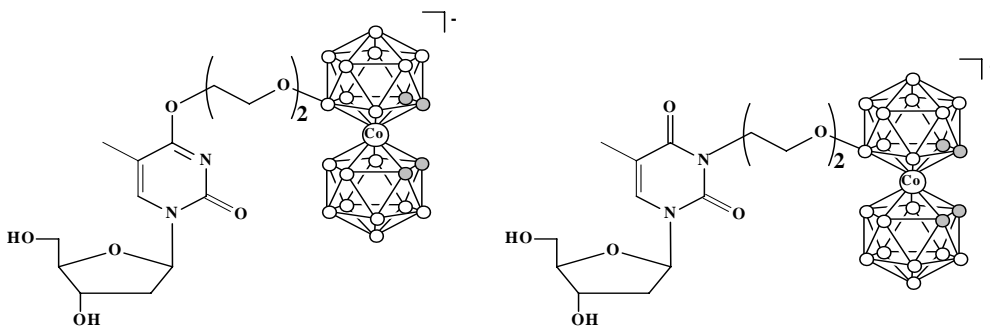


Figure 5. Structures of cobalt bis(dicarbollide) based nucleosides.

Aminoacids

The interest in the development of carborane-containing amino acids arose soon after the first carboranes were synthesized and *o*-carboranylalanine was one of the earliest described carborane-based analogues of biomolecules. It was first synthesized as the racemic mixture independently by Brattsev [89] and Zakharkin [90]. Subsequently, other methods of its synthesis in high yield [91-93] as well as the stereoselective synthesis of the *L*-isomer [94] have been proposed. More recently several more useful stereoselective syntheses of the *L*- and *D*-isomers have been developed [95-97]. At present time, a number of various carborane-containing amino acids are synthesized including the *p*-carborane analog of tyrosine [98], carborane derivatives of 1-amino-cyclobutanecarboxylic acid [99-102], and β -carboranyl- α -trifluoromethyl- α -aminoacid [103,104] (Figure 6). Synthesis and use of carborane-containing aminoacids have been reviewed very recently [105].

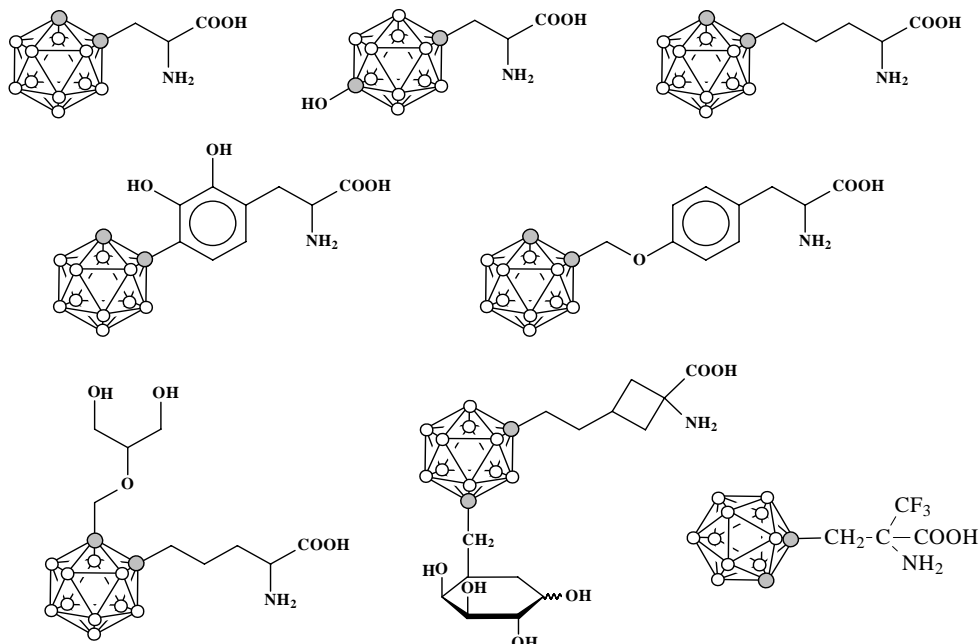


Figure 6. Structures of some carborane-containing aminoacids.

Due to the hydrophobicity of carborane, most carborane-containing amino acids are not soluble in water. In order to increase solubility, some hydrophilic substituents were introduced or the carborane was transformed to the *nido*-form. Several amino acids based on anionic boron hydrides [78,106] and metallacarboranes [67] have been prepared (Figure 7).

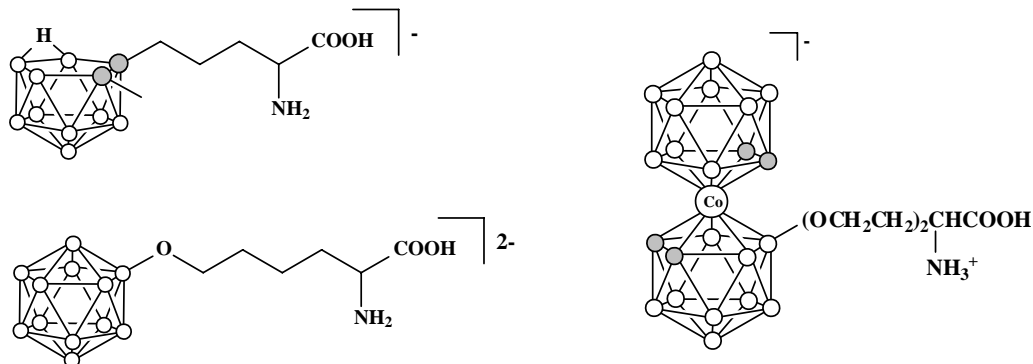


Figure 7. Structures of anionic boron-containing aminoacids.

Besides numerous polyhedral boron hydride based α -aminoacids, a few compounds with carborane cage incorporated between amino and carboxylic groups were reported [107,108].

Carbohydrates

Synthesis of the first carborane-containing carbohydrates was described more than 25 years ago as a way to compensate for the hydrophobicity of the carborane cage and to enhance the water solubility of carborane biomolecules [109-112]. The concept still persists [102,113-115], however nowadays much more attention is paid to using carbohydrates as tumor-targeting agents. This form of biomolecular recognition involves binding of a carbohydrate to a lectin receptor. Endogenous lectins are found on surfaces of many normal and malignant cells and involved in various biological functions, acting as specific receptors and/or mediating endocytosis of specific glycoconjugates. Because lectins recognize and bind to the terminal (non-reducing) sugar residues of oligosaccharides, endocytosis is relatively uninfluenced by the size or composition of the aglycon. This feature has stimulated interest in carbohydrate-mediated delivery (glycotargeting) of various compounds (including drugs and polynucleotides) to cells expressing the corresponding lectins [116]. Transformation of a normal cell to a tumor cell often results in the change of lectin composition of the cell surface and is usually accompanied by over-expression of the certain lectins. Attachment of boron moiety to an oligosaccharide ligand of the lectin will lead to the preparation of boron-containing neoglycoconjugates, which can be used for targeted delivery of boron to the tumor tissues. Recently, syntheses of various boron-containing conjugates have been reported by several research groups [40, 117-129]. Some examples of lactose conjugates with various polyhedral boron hydrides are presented in Figure 8.

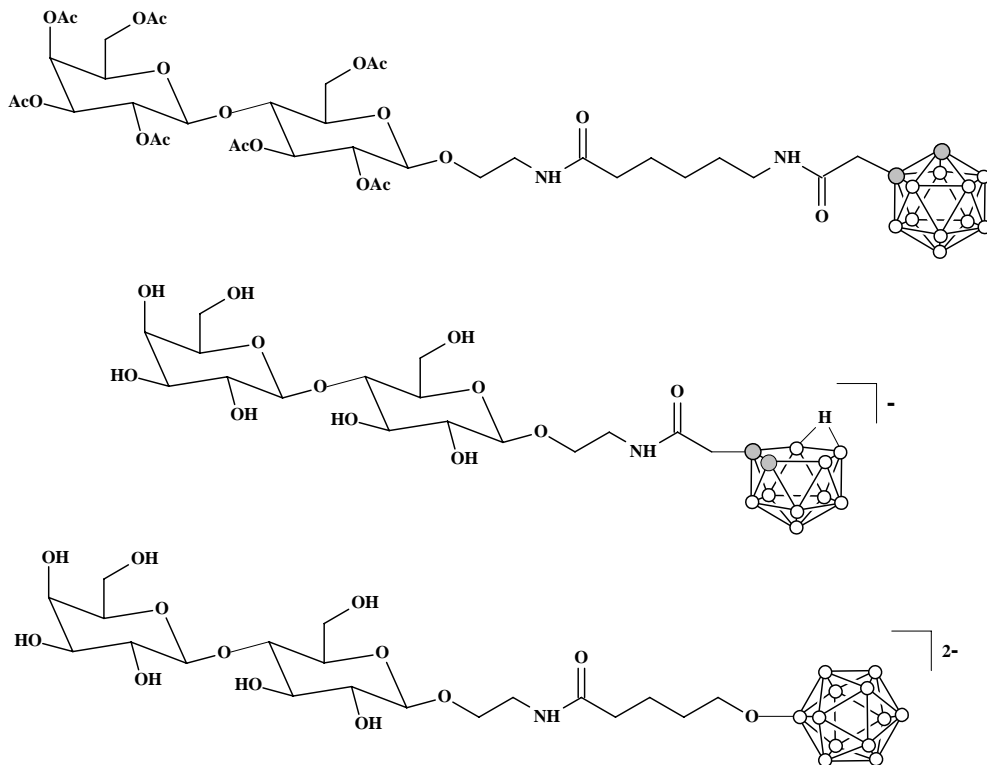


Figure 8. Structures of some boron-containing lactoses.

Porphyrins and Phthalocyanines

Porphyrins and phthalocyanines have been observed by nearly a century to accumulate selectively in a variety of tumors [130]. Photodynamic therapy (PDT) has become a clinically established bimodal cancer therapy whereby superficial tumors loaded with a photosensitizing porphyrin or related macrocycle are irradiated with red laser light to form an excited triplet state which reacts with molecular oxygen and other substrates to generate highly cytotoxic species (e.g. single oxygen, superoxide anion, hydroxyl radicals) that cause irreversible destruction of tumor cells [131]. Although only two porphyrins Photofrin® and Visudyne™ have been approved by the U.S. Food and Drug Administration many others are currently being evaluated in animal models for the treatment of certain cancers and other diseases.

In the past two decades boron-containing porphyrins have been investigated as possible BNCT agents and BNCT/PDT dual sensitizers in preclinical studies. Two approaches have been used for the synthesis of these compounds - condensation of boron-containing building blocks, on the one hand, and attachment of boron cages to natural or synthetic porphyrins and phthalocyanines, on the other hand. The first carborane-containing porphyrins were reported by Haushalter and Rudolph in 1978 [132,133] and this field is under extensive development [131, 134-136]. The most of the prepared carborane-containing porphyrins are based on the *meso*-tetraphenylporphyrin skeleton and contain from one to eight *closo*- or *nido*-carborane cages (Figure 9). Beside carborane-based porphyrins, syntheses of *meso*-tetraarylporphyrins containing cobalt bis(dicarbollide) [71,72,137], *closo*-dodecaborate [138] and carba-*closo*-dodecaborate [139] moieties were reported (figure 9).

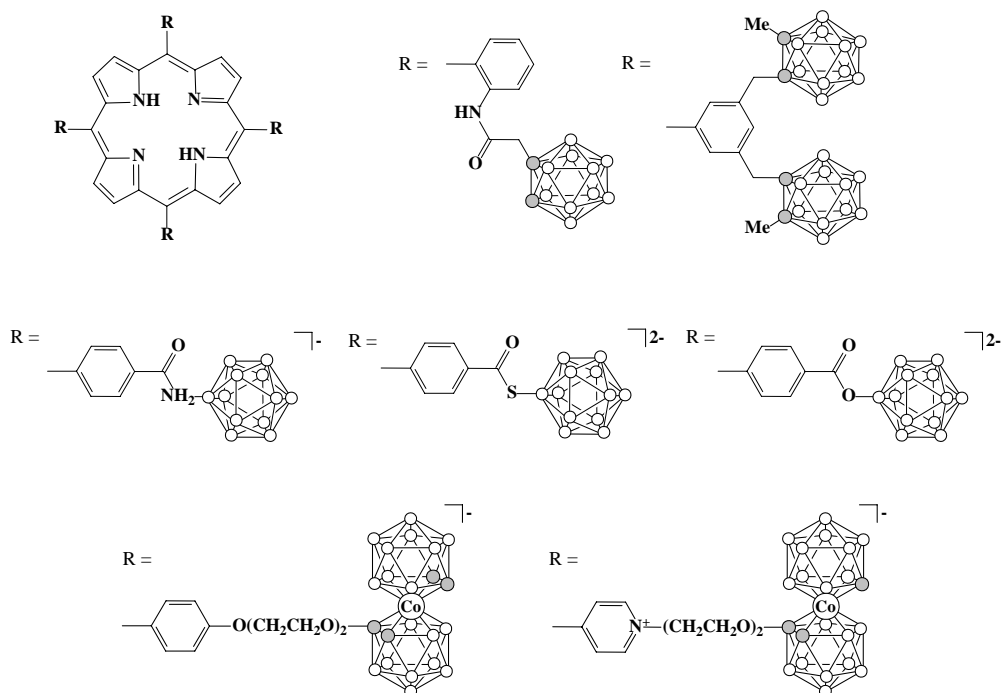


Figure 9. Structures of some boron-containing porphyrins.

A number of carboranyl porphyrins have been obtained on the basis of the natural porphyrin derivatives such as deuteroporphyrin IX and hematoporphyrin IX and two of them, VCDP and BOPP (Figure 10), have been extensively studied in animals. BOPP was reported to have a tumor-normal brain ratio from 13:1 to 400:1 for different glioma models [140,141]. High boron levels in tumor ($> 60 \mu\text{g}^{10}\text{B/g tumor}$) were achieved in these animal studies. However, data obtained from a human Phase I clinical trial showed that BOPP does not deliver therapeutic concentrations of boron to the tumors of glioblastoma patients, and dose escalation is prevented by the toxicity of this compound. Nevertheless, BOPP has shown promise as an effective PDT photosensitizer [142-145].

More recently, syntheses of *cis*-dodecaborate derivatives of naturally occurring porphyrin systems pyropheophorbide *a* [146] and bacteriochlorin *p* [147] have been reported.

Syntheses and results of biological studies of boron-containing porphyrins have been reviewed several times during the last 5 years [131,134-136] and some more recent publications include [137-139,147-150].

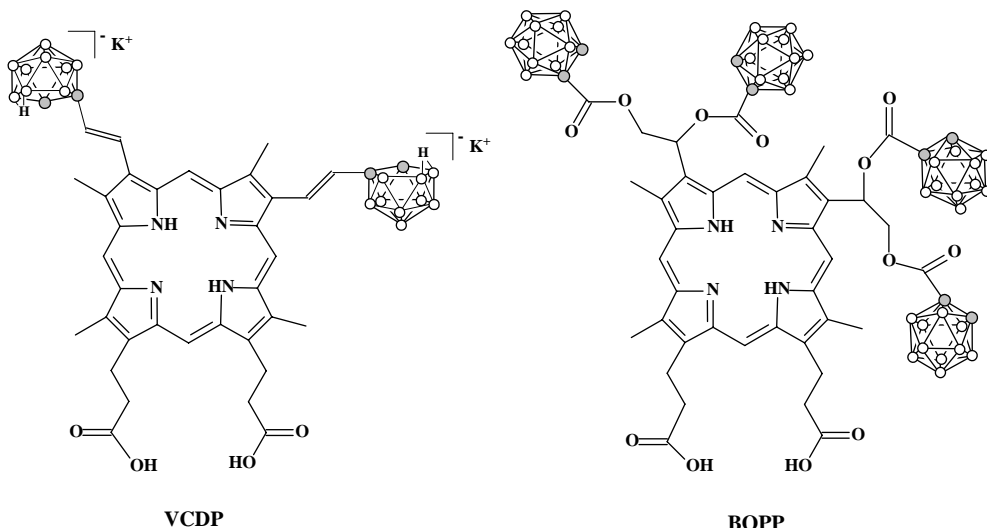


Figure 10. Structures of some carborane-containing porphyrins.

Synthesis of boron hydride based phthalocyanines has received much less development. After the first paper reviewed this field [134], only four reports have been published during the last 5 years [151-154] (Figure 11).

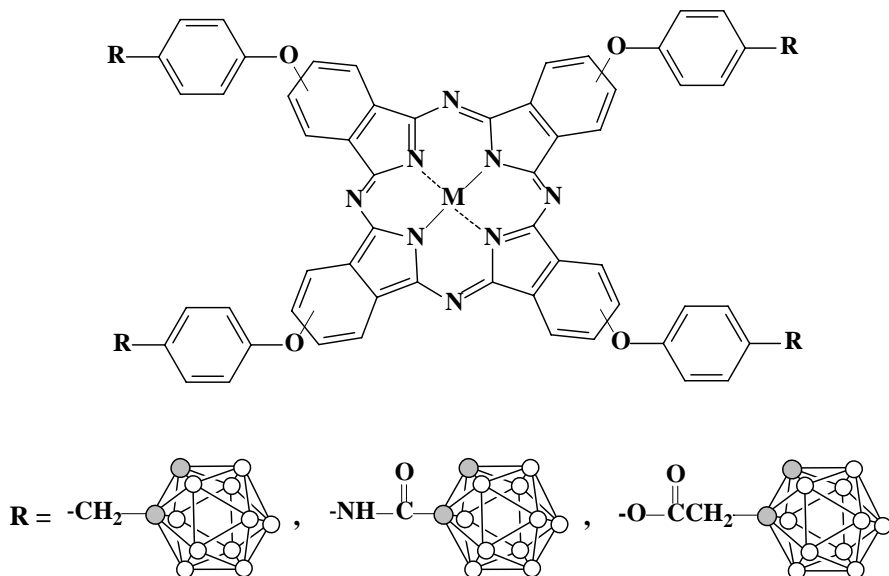


Figure 11. Structures of some boron-containing phthalocyanines.

DNA Binders

Another group of low molecular weight boron compounds received great attention for the last years is DNA binders. BNCT agents that target DNA are attractive because, as mentioned previously, the amount of boron required for successful therapy is reduced if the ^{10}B is deposited in proximity to the DNA. Acridine dyes have been shown to stain the nuclei of

many different cell types and therefore have the potential of being boron delivery agents to tumor cells. A series of carborane containing analogues of DNA intercalating compounds, acridine and phenanthridine, were prepared by Sjöberg *et al.* [155-158] (Figure 12) and analyzed in cultured human malignant glioma spheroids. These compounds, however, were found to be not specific to cancer cells, thus to gain tumor specificity, the proposed strategy is to prepare conjugates with tumor targeting agents (*vide infra*).

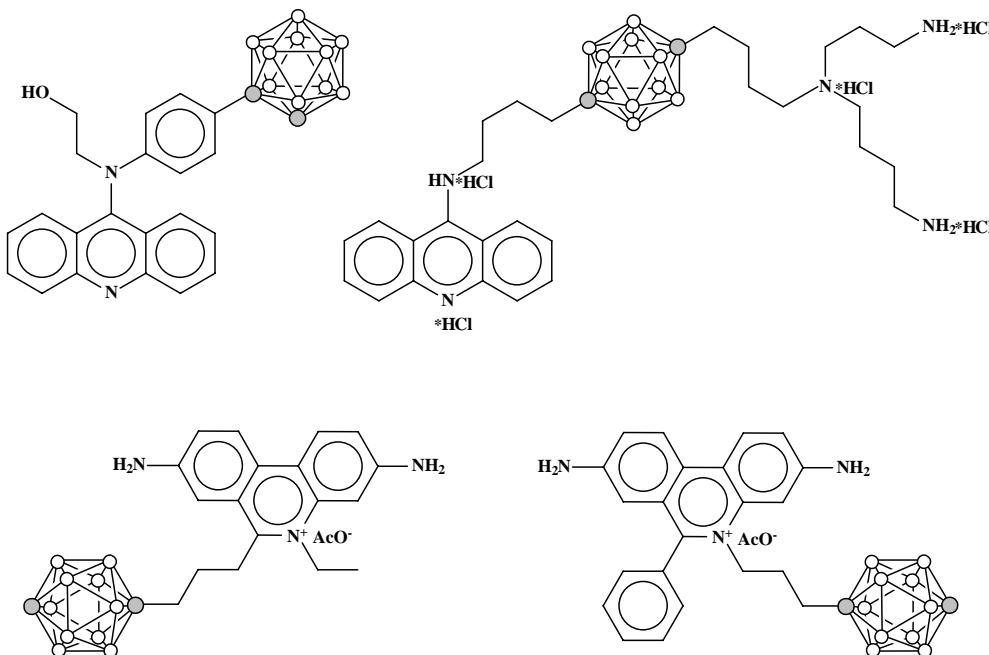


Figure 12. Structures of some carborane-containing acridines and phenanthridines.

Recently a series of Pt-based DNA metallointercalators with carborane-containing ligands have been synthesized and found to have significant anti-cancer activity (see below).

Related to the intercalators are DNA groove binders. The initial focus was to use bibenzimidazole compounds related to Hoechst 33258, a compound that has been shown to target the minor groove of DNA with a great deal of specificity. A series of carborane analogues of Hoechst 33258 was synthesized and their DNA binding capacity was evaluated [159,160] (Figure 13).

Polyamines, such as putrescine, spermidine, and spermine, are important biochemical constituents that are essential for cell growth and differentiation. Elevated concentrations of these substances were found in rapidly proliferating tumor cells whose polyamine transport system is upregulated. These structures, under physiological conditions, exist as cationic moieties and bind very tightly to DNA via electrostatic interactions. A series of carboranyl derivatives of spermidine and spermine were synthesized [155,161-164] (figure 14). These compounds demonstrate rather high cellular uptake *in vitro* but, at the same time, high cellular and *in vivo* toxicity [163,164].

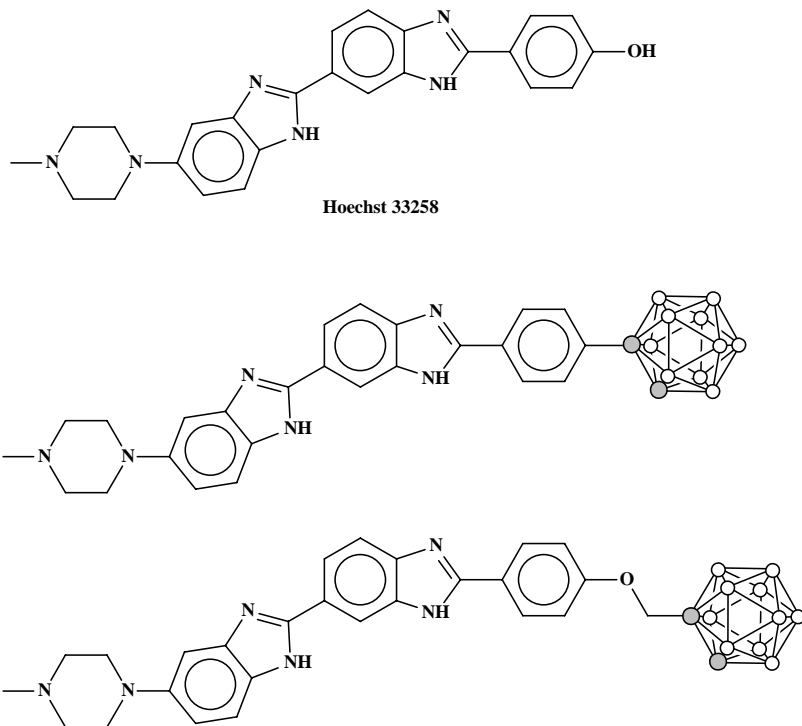


Figure 13. Structures of some carborane-containing analogues of Hoechst 33258.

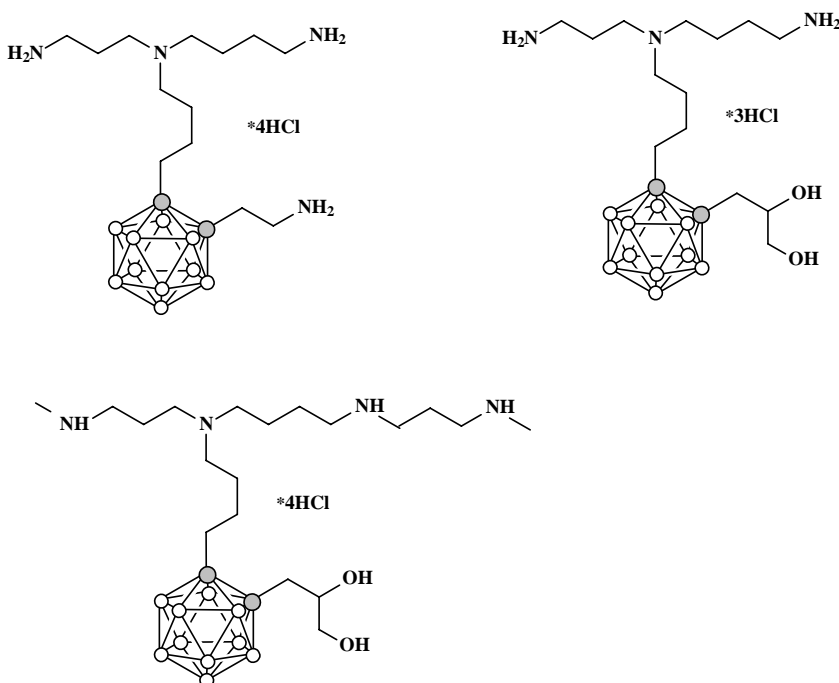


Figure 14. Structures of some carborane-containing polyamines.

There are many synthesized and partially evaluated boron-containing low molecular weight compounds which do not fall into any of the above classifications [57,79]. However, there is at least one factor that unifies practically all low molecular weight boron compounds: they have not reached the stage of being evaluated clinically. Many have been screened in cell culture: some using purified enzymes to determine their metabolism; other have been evaluated in rodents with a variety of subcutaneously transplanted animal and human tumors; and fewer have been screened against these same tumors that were implanted intracranially; and many and many compounds have been synthesized but have not been evaluated at all. Based on the data available, how does one decide to eliminate or further evaluate a compound, since additional studies are both costly and time-consuming? The key question in BNCT agent development is assessing the usefulness of enzymatic, cell culture, and animal studies in determination of clinical potential of the compounds. Another question is, how do these newer agents compare with those two compounds that are now being used clinically? Probably, we are very close to synthesis of a compound that could work in BNCT much better than BSH and BPA or, perhaps, someone already has synthesized such compound and put it on a laboratory shelf. It should be noted here that some boron compounds demonstrating high cellular uptake but being not specific to cancer cells or/and high *in vivo* toxicity could be used in BNCT as conjugates with tumor targeting agents, e.g. targeted liposomes [79,165].

3.1.3. High Molecular Weight Boron Delivery Agents

High molecular weigh delivery agents usually contain a boron cluster linked through a hydrolytically stable bond to a tumor-targeting moiety, such as monoclonal antibodies (mAbs) or low molecular weight receptor targeting ligands. Examples of these include epidermal growth factor (EGF) or the mAb cetuximab (IMC-C225) to target the EGF receptor or its mutant isoform EGFRvIII, which are over-expressed in a variety of malignant tumors [165].

The use of antibodies to deliver boron to tumor cells was suggested in the 1960s. The initial investigation of boron-conjugation chemistry with model protein substrates such as bovine serum albumin and human γ -globulin was initiated nearly simultaneously in several laboratories in the 1970s. The studies focused on the type of boron compounds that were to be used, the linkages that would be required, and the effect of such covalent attachment and its boron moiety on the physiochemical properties of the conjugate formed. The results of these early studies were surveyed in Hawthorne's review [78]. However, some fundamental strategic problems arose soon after the first boron-containing conjugates were obtained. It was estimated that the boronated antibody molecule must contain 10^3 ^{10}B atoms (approx. 100 boron cages) to provide the necessary therapeutic boron concentration in tumor [166]. The question is: could that number of boron cages introduced to the antibody molecule with retention of its conformational and targeting specificity? It was demonstrated that the introduction of approx. 1300 ^{10}B atoms per molecule of 17-1A Mab monoclonal antibody using N-succinimidyl 3-(2-undecahydro-*clos*o-dodecaboranyldithio) propionate $[\text{B}_{12}\text{H}_{11}\text{SS}(\text{CH}_2)_2\text{COO}(\text{N}(\text{CO})_2(\text{CH}_2)_2)]^{2-}$ resulted in 90 % loss of its immunoreactivity [167]. This result indicates that attaching 100 functional groups on the antibody molecule apparently results in the loss of its targeting specificity. It means that the minimum modification of the antibody molecule is needed for retention of its immunoreactivity. Thus, there emerged two requirements in order to prepare boron-containing antibodies for BNCT: 1) synthesis of a

boronated macromolecules containing up to 100 boron cages, and 2) development linkage technology to attach such structures to antibodies.

The initial approach included the use of a preformed macromolecule containing a large number of functional groups to which the boron polyhedron could be covalently attached. The first macromolecule that has been used as a platform for delivery of boron compounds was polylysine, a polymer having multiple reactive amino groups. The protein-binding polyhedral boron derivative, isocyanato-*closو*-dodecaborate $[B_{12}H_{11}NCO]^{2-}$, was linked to polylysine and subsequently to the anti-B16 melanoma mAb IB16-6 [168]. The bioconjugate had an average of 2700 boron atoms per molecule and retained 58 % of the native antibody immunoreactivity. Other bioconjugates prepared by this method had more 1000 boron atoms per molecule of antibody and retained 40-90 % of the immunoreactivity. Using site-specific linkage of boronated polylysine to the carbohydrate moieties of anti-TSH antibody resulted in a bioconjugate that had approx. 6000 boron atoms with retention of its immunoreactivity [169]. One of the limitations of this approach is that the polymer itself is not a discrete and homogeneous entity and that heterogeneity is markedly increased following boronation since the number of boron groups attached to each polymeric molecule could vary.

Dendrimers are one of the most attractive polymers that have been used as boron carriers due to their well-defined structure and large number of reactive terminal groups. Initially, second- and fourth-generation polyamidoamino (PAMAM) dendrimers, which have 12 and 48 reactive terminal amino groups, respectively, were reacted with the isocyanato derivative of *closو*-decaborate anion $[Me_3NB_{10}H_8NCO]^-$. The boronated dendrimer then was linked to mAb IB16-6 directed against the murine B16 melanoma [170,171]. More recently, the fifth-generation PAMAM dendrimers was boronated with the same polyhedral borane anion and linked to the anti-EGFR mAb cutuximab or the EGFRvIII specific mAb L8A4. The resulting bioconjugate contained ~ 1100 boron atoms per molecule and was found to retain the native antibody immunoreactivity [172,173].

Besides monoclonal antibodies, boronated PAMAM dendrimers can be targeted to tumor using epidermal growth factors [174,175], vascular endothelial growth factor [176], and folic acid, vitamin that is transported into cells *via* folate receptor mediated endocytosis [177].

Synthesis of a few other boronated dendrimers that potentially could be used as boron delivery agents for BNCT were described recently [178,179].

Another type of polymers that could be used as boron carriers are dextrans, glucose polymers that consist mainly of a linear α -1,6-glucosidic linkage with some degree of branching *via* a 1,3-linkage. Several examples of $[B_{12}H_{11}SH]^{2-}$ coupling to modified dextran derivatives were described [180-184].

Two different approaches to tumor targeting of boronated polymers using streptavidin-biotin strategy [185] and bispecific antibodies [171,186] were considered in earlier review [79].

One of the observed differences between tumor cells and their normal counterparts is the rate of metabolism of low-density lipoproteins (LDLs). The LDL vesicle comprises a phospholipids/cholesterol shell with a diameter of approximately 15-20 nm, filled with cholestryl and glyceryl esters of long-chain alkyl carboxylic acids. This difference is based on the increased need that tumor cells possess for cholesterol in order to facilitate new membrane formation. The overexpression of the LDL receptors on the tumor cell membrane is responsible for its LDL accretion. This provides a basis for cellular differentiation and the

targeting of tumor cells with boron if cholestryl esters of the LDL core are replaced with a boron species that would simulate cholesterol in its physiochemical properties.

This concept was proposed by Kahl at the beginning of 1990s. The initial compounds synthesized were esters of carborane carboxylic acid with various fatty acid alcohols [187]. Later some other derivatives of cholesterol were synthesized [188-193]. More recently LDLs were proposed as tumor delivery agents for carborane-containing porphyrins [194].

While LDLs are natural lipoproteins with a proclivity for those tumor cells in which the receptors for these vesicles are overexpressed, liposomes can be considered as related synthetic vesicles. The liposomes consist of a phospholipids bilayer that forms a spherical shell surrounding an aqueous core. Modification of the liposomal surface by PEGylation or attachment of antibodies or receptor ligands will increase their circulation time and improve their selective targeting. Design strategies for boron-containing liposomes for BNCT centered on both non-targeted and tumor-targeted formulations [165]. The latter includes liposomes conjugated to transferrin [195-197], EGF [198-201], antibodies [202], vascular endothelial growth factor [203], $\alpha(v)$ -integrin specific arginine-glycine-aspartate peptides [204], and folic acid [205-208].

Most liposomes designed for BNCT contained hydrophilic low molecular weight boron agents, which presumably localized in the aqueous core of the liposomes during preparation. These boron agents include BSH [196,209-211] and BPA [212,213], anionic polyhedral boron hydrides with or without simple substitution patterns [206-208,214-218], carborane-containing amines [219], polyamines [206], acridines [198-202], porphyrins [220], carbohydrates [221], and nucleosides [222].

Phospholipids are common lipid bilayer components of liposomes and they have been proven to be effective anchors for boron compounds in the form of single- [205,223] or dual-chain *nido*-carborane [197,224,225] or *closso*-dodecaborate [41] phospholipid mimetics. Cholesterol is another major component of the mammalian cell membrane and most liposomal formulations. Therefore, the development of carborane-containing derivatives of cholesterol [188-193] is potentially an effective approach for delivery of boron to cancer cells via both liposomes and LDL. More recently, a novel strategy for the design and synthesis of carboranyl cholesterol mimics has been proposed. In this mimics, both the B and the C rings of cholesterol were replaced with a carborane cluster (Figure 15). The novel carboranyl cholesterol mimics are excellent lipid bilayer components for construction of nontargeted and receptor-targeted boronated liposomes for BNCT of cancer [203].

3.1.3. Second Component: Neutron Sources

Neutron sources for BNCT are currently limited to nuclear reactors and several reactors with very good neutron beam quality have been developed and currently are being used clinically [226]. The advantage of a reactor is that the neutrons from reactors are relatively cheap, if capital costs are discounted. The disadvantages of reactors are that the capital costs are very high and reactors are too complicated for an ordinary clinic to operate, so these clinics cannot afford to build and maintain a small nuclear reactor to use as a neutron source.

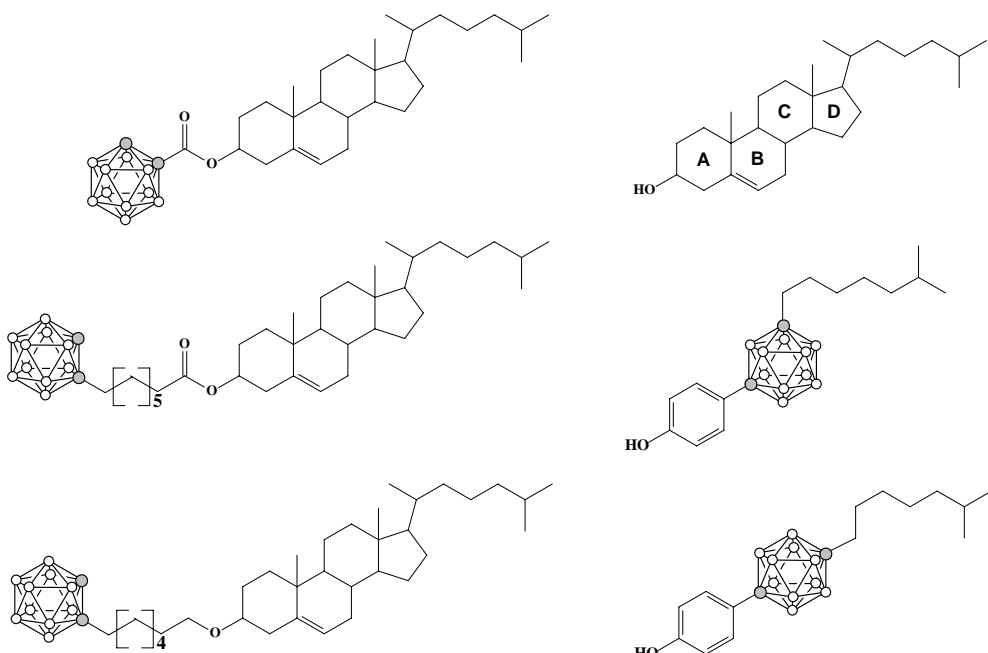


Figure 15. Structures of some carborane-containing analogues of cholesterol.

Another approach is to use accelerators and accelerator-based neutron sources are being developed in several countries [227-229]. Accelerators offer a number of potential advantages over reactor-based neutron sources for clinical applications. First, accelerators can be easily turned off when the neutron field is no longer required. This, and the fact that neutrons are not produced via a critical assembly of fissile material, means that licensing and regulations associated with maintaining the neutron source are substantially simplified. Second, the variety of neutron-producing reactions that are accessible to accelerators, allows for a number of neutron energy source spectra to be produced. Consequently, for some accelerator types, a number of clinically useful epithermal neutron fields can be produced by the same accelerator, and the neutron flux energy spectrum of the field can be tailored to the spatial characteristics of a particular patient's tumor. Third, the capital expenses of an accelerator-based BNCT system will be substantially lower than those associated with installation of a reactor system in or near a hospital. And finally, accelerators have been prominent features of radiotherapy departments in hospitals for years; clinicians have a longstanding and comfortable experience with such devices for patient irradiation. It is likely that accelerator hardware for BNCT irradiations could be sited within an existing radiotherapy room with the addition of extra shielding [227].

3.1.4. Clinical Status of BNCT

Although the clinical potential of BNCT was recognized in the 1930s, the clinical trials were carried out up to recently only in two countries, in USA (1954-1961, 1994-present) and Japan (1968-present). The BNCT geography has expanded sharply for the last 10 years when the clinical trials started in European Union (at Petten, 1997), Finland (1999), Sweden (2001-2004), Czech Republic (2001), and Argentina (2003). Significant growth and wider development of the clinical trials could be expected with further development of accelerator-

based neutron sources that can be incorporated into medical surroundings and with development of a new generation of BNCT agents.

High-grade gliomas, and specifically glioblastoma multiforme, that are still extremely resistant to all current forms of therapy, including surgery, chemotherapy, radiotherapy, immunotherapy, and gene therapy, are the main subject of BNCT. Melanomas, which cannot be treated by either surgical excision or stereotactic radiosurgery, are other candidates for the BNCT treatment. The use of BNCT for treatment of the head and neck recurrent tumors (squamous cell carcinomas, sarcomas, parotid tumor) and adenocarcinoma of the colon that had metastasized to the liver have been reported recently [77].

3.2. Boron Neutron Capture Synovectomy

Rheumatoid arthritis is an autoimmune disease characterized by recurrent swollen, inflamed and painful joints. It afflicts 1–2 % of the US population. Since the cause of rheumatoid arthritis is unknown, patients are treated symptomatically. Anti-inflammatory drugs are effective in approximately 90% of all patients. In the remaining 10% patients, the inflammation in one or more joints will not respond to drugs and a more severe approach is taken. In the USA, the only option is surgical synovectomy, a costly and painful procedure followed by extensive physical therapy and rehabilitation. Symptomatic relief lasts roughly 2–5 years since the cause of rheumatoid arthritis has not been addressed. Radionuclide synovectomy using beta-particle emitters injected directly into the joint is routinely used in Europe and elsewhere and gives about the same symptomatic relief, for the same fraction of patients, for the same length of time, as surgery. Radionuclide synovectomy is less costly, less painful and requires no rehabilitation time relative to surgery. It is, however, not approved for routine clinical use in the USA due to concerns regarding healthy tissue irradiation caused by leakage of the β -emitter away from the joint.

Boron Neutron Capture Synovectomy (BNCS) was proposed as a way to carry out radiation synovectomy without the concern regarding leakage of a radioactive substance. A ^{10}B -labeled compound injected into the joint space would be followed by local irradiation with a beam of low-energy neutrons. The experimental parameters required for the successful implementation of BNCS as a treatment modality for rheumatoid arthritis [230,231]. The boron neutron capture reaction could be used to selectively ablate arthritic tissue, without causing damage to other tissue and organs so long as highly selective and efficient boron delivery vehicles could be developed [232,233].

3.3. Polyhedral Boron Hydrides in Radionuclide Diagnostics and Therapy [75]

Initially, labeling polyhedral boranes with radionuclides was performed with the aim to study biodistribution and pharmacokinetics of boron compounds for BNCT [234]. For *in vivo* imaging of boron compounds, radiolabeled derivatives are of particular interest since their biodistribution can be easily monitored by using single-photon emission computed tomography (SPECT) and positron emission tomography (PET), depending on the radionuclide employed. In many cases, radiolabeling gives detailed information about boron

pharmacokinetics that can be used to generate improved patient treatment protocols, for example by providing information about the required dosage of tumor-seeking boron conjugates, and optimal treatment time.

Another important field is use of boron clusters as pendant groups for attachment of radionuclides to tumor-seeking biomolecules for targeted radionuclide therapy. The principle of this mode of treatment is based on selective delivery of radionuclide to cancer cells. Due to very high cytotoxicity of radionuclides, the use of highly tumor-specific transport system is required. The targeting vectors used in radionuclide diagnostics and therapy are of protein nature. These may be monoclonal antibodies directed toward tumor-specific antigens or regulatory peptides binding to receptors overexpressed on or by malignant cells. The important advantage of targeted radionuclide therapy over boron neutron capture therapy is that the therapeutic concentration of radionuclides in tumor are, as a rule, a few order of magnitude less than the therapeutic concentration required for BNCT. As a consequence, the less modification of the tumor-seeking molecule is required, which prevents loss of tumor specificity. The same tumor-seeking compounds may also be used for detection and characterization of tumors.

3.3.1. Polyhedral Boron Hydrides as Carriers of Radiohalogen Label

The most common procedures employed for radiolabeling proteins are radiohalogenations and labeling with radioactive metal ions. Halogen radioisotopes are especially attractive since they share many chemical properties and possess a variety of half-lives and decay modes (table 2), which enables optimization of half-life and emitted radiation, depending on the biomedical problem to be solved. Radiohalogens used in nuclear medicine today fall into two main categories, those useful in imaging applications and those useful in therapy applications [235].

Table 2. Radiohalogens used in imaging and therapy

Nuclide	Half-life	Mode of decay	Possible application
¹⁸ F	1.8 h	β^+	PET Imaging
⁷⁵ Br	1.6 h	β^+	PET Imaging
⁷⁶ Br	16 h	β^+	PET Imaging
⁷⁷ Br	2.4 days	electron capture	SPECT Imaging
^{80m} Br	4.4 h	Auger e ⁻	Therapy
⁸² Br	35.3 h	β^-	Therapy
¹²³ I	13.2 h	electron capture	SPECT Imaging
¹²⁴ I	4.2 days	β^+	PET Imaging
¹²⁵ I	59.4 days	electron capture	Therapy
¹³¹ I	8.0 days	β^-	Therapy
²¹¹ At	7.2 h	A	Therapy

Today, nuclear medicine imaging is carried out with highly sophisticated SPECT instruments available in most hospitals worldwide. Another imaging modality, PET, is being used clinically, but is not as widely available. The radioactive decay property that allows the use of radionuclides for imaging in emission of photons with sufficient energy to detect in a device external to the body. Radionuclides that are useful for SPECT imaging emit photons in high abundance and have sufficient energy (>100 keV) to escape the body and be detected. In

PET imaging, positrons emitted by the radionuclide interact with electrons in an annihilation process to produce two coincident 511 keV photons, which are detected simultaneously in a detector ring. An important characteristic is the energy of the emitted positron. The higher its energy, the further a positron will travel before the annihilation occurs. A longer distance of positron travel in tissue results in an overall loss of spatial resolution. Another important characteristic is the abundance of the positron emissions since a low abundance requires more radioactivity to be administrated.

^{123}I is a commercially available SPECT isotope that has very favorable SPECT imaging properties (159 keV) and a reasonable half-life (13.2 h). This isotope is widely used in nuclear medicine and can be shipped around the world. ^{77}Br is a single photon and positron emitter with a 57 h half-life. However, its limited availability and two higher energy gamma rays, as well as low percent positron emission (1%), make it less desirable as a SPECT or PET isotope.

From a purely physical point of view, ^{18}F has the most favorable nuclear properties for imaging with PET. The half-life (110 min), high percentage of β^+ emission (97%), and relatively low positron energy (0.635 MeV) make it the ideal PET halogen for high-resolution images. However, radiofluorination reactions of polyhedral boron hydrides have not yet been reported. ^{75}Br is a potential PET imaging isotope with a reasonable half-life (97 min). However, compared to ^{18}F , it suffers from a higher positron energy (1.74 MeV), a 71% positron emission and second high energy gamma, all of which contribute to its overall poorer resolution for imaging. ^{76}Br is a possible radionuclide for PET studies. This nuclide has a half-life of 16.2 h and emits 54% positrons per decay, properties that are well suited for labeling. ^{124}I is a positron-emitting radionuclide that has gained considerable interest recently. The interest comes from the fact that it has a relatively long half-life (4.2 d) and both imaging (PET) and therapeutic properties. However, the emission properties of this radionuclide are far from ideal.

Radiohalogens used for therapy applications have particle emissions such that they provide more or higher quality interaction (ionization) in biological tissues than the radionuclides used in imaging. In principle, any radiohalogen that emits an electron (β , β^+ , or Auger electron) or α -particle (^4He nucleus) might be used for therapy.

The most commonly used radiohalogen for therapy is ^{131}I . The factors that have made this radionuclide widely used are its availability and reasonably long half-life (8.0 d). This has made it relatively inexpensive and readily transported to clinical sites. The β -particle emissions of ^{131}I travel a few mm in tissue. This distance is important in tumors as the β -particle travels well beyond the cell it is attached to or internalized in, providing a radiation field effect. It is useful for solid tumors where penetration of the carrier molecule is difficult, or targeted receptors are not available on all cells. Unfortunately, ^{131}I does not have optimal properties as its decay produces high energy photons. These photons are problematic as they make it difficult to conduct labeling at the required high levels and can cause the patient to be isolated to minimize the radiation exposure to health care professionals and family members. On the other hand, the photons do allow imaging of the distribution of radioiodine within a patient by SPECT. It is important to be able to evaluate the distribution of radionuclide in a patient and to estimate the radiation dose to the target and non-target tissues. This provides information regarding the biological effect on normal tissues and the potential for an effective therapy of the tumor.

Another radiohalogen nuclide of interest for therapy is ^{125}I . The particle emitted in radioactive decay of ^{125}I , that makes it of particular interest, is an Auger electron. The Auger electrons deposit there energy in a very short distance (e.g. a few Å), which makes it high linear energy transfer (LET). While this short distance requires the Auger electron emitting radiohalogen to be internalized and localized in a specific location (i.e. associated with double strand DNA) to provide an effective therapy, it causes little damage to non-target tissues. Although ^{125}I is readily available, it is not an ideal radionuclide for therapy as it has a relatively long half-life (59.4 d), so other Auger electron-emitting radiohalogens are of interest. The SPECT imaging radionuclide ^{123}I has Auger electron emissions and a much shorter half-life; few studies have been performed with this radionuclide to determine its effectiveness in therapy.

^{211}At is another radiohalogen of interest for therapy. Although the half-life of ^{211}At is relatively short (7.2 h), it is the only α -emitting radiohalogen nuclide that is considered acceptable for use in humans. In contrast to β -particle emission, the α -particles emitted by ^{211}At decay have a range of 50-70 mm due to their much higher interaction with tissue. This high LET makes ^{211}At particularly attractive for therapy of metastatic cancer or in applications where single cells are targeted. While it is estimated to take several hundred (e.g. > 400) β -particle emitting radionuclides on a single cell to kill that cell due to the fact that most of the particles' energy is deposited outside of the cell, it is estimated that only a few (e.g. 1-14) associated α -particle emitting radionuclides can kill a cell. The closer the ^{211}At atom decays to the nucleus, the fewer atoms are required to kill the cell, making internalizing targeting agents particularly attractive.

Thus, specific targeting of halogen radionuclides is a promising approach to improved diagnosis and treatment of tumors. A problem in using radiohalogens for labeling of tumor-targeting proteins and peptides is that the commonly used radiohalogenation methods provide labels, which, after internalization and lysosomal digestion, rapidly "leak" from malignant cells as radiohalogenated degradation products. The main reason for such leakage is free diffusion of the radiometabolites through lysosomal and cellular membranes [236]. Dehalogenases and peptidases have been considered as enzyme systems responsible for the dehalogenation of radiohalogenated proteins *in vivo*. This results in increased accumulation of the radioiodide in the thyroid, whereas the radiobromide anion is not excreted but remains distributed in the extracellular space, decreasing the contrast of the image. If the radiometabolite cannot penetrate the cellular membrane, it will be trapped intracellularly until its excretion by exocytosis. Since exocytosis is relatively slow in comparison with diffusion, the cellular retention and, consequently, the tumor accumulation of radionuclide are improved. This resulted in a new concept in which the cellular retention can be improved by placing radiohalogen label on a structure that cannot penetrate the cellular membrane and remain trapped inside the cell.

The polyhedral borane anions were found to be reasonable linkers for attachment of radiohalogens to tumor-targeting proteins and peptides. For such applications, the following features of these compounds are important: 1) the high strength of the boron-halogen bonds (higher than in their carbon-halogen counterparts); 2) the absence of enzymatic systems for cleavage of the boron-halogen bond due to the very exogenous nature of such compounds and 3) the negative charges of polyhedral borane anions which may improve intracellular retention of bound radiohalogens without elevated uptake in kidneys.

Radionuclide targeting using polyhedral borane anions as pendant groups can in many cases utilize compounds which have been developed for use as boron carriers in BNCT. Functional groups which enable boron hydride coupling with tumor-seeking molecules are amino acids ($-\text{CH}(\text{NH}_2)\text{COOH}$), amines ($-\text{NH}_2$), acids ($-\text{COOH}$), isocyanates ($-\text{NCO}$), and isothiocyanates ($-\text{NCS}$). A number of derivatives containing these functionalities were prepared and described above.

One example is a *p*-isothiocyanatophenyl derivative of *nido*-carborane [$7\text{-}(4\text{-SCNC}_6\text{H}_4)\text{-7,8-C}_2\text{B}_9\text{H}_{11}]^-$] synthesized earlier for coupling with anticarcinoembryonic antigen IgG for BNCT [237]. This compound was labeled with the positron-emitting nuclide ^{76}Br and coupled to anti-HER2 antibody trastuzumab used for therapy of breast cancer. The label was found to be stable *in vitro* under physiological and denaturing conditions, and retention of immunoreactivity of trastuzumab after labeling was demonstrated in a cell binding test (Figure 16) [238].

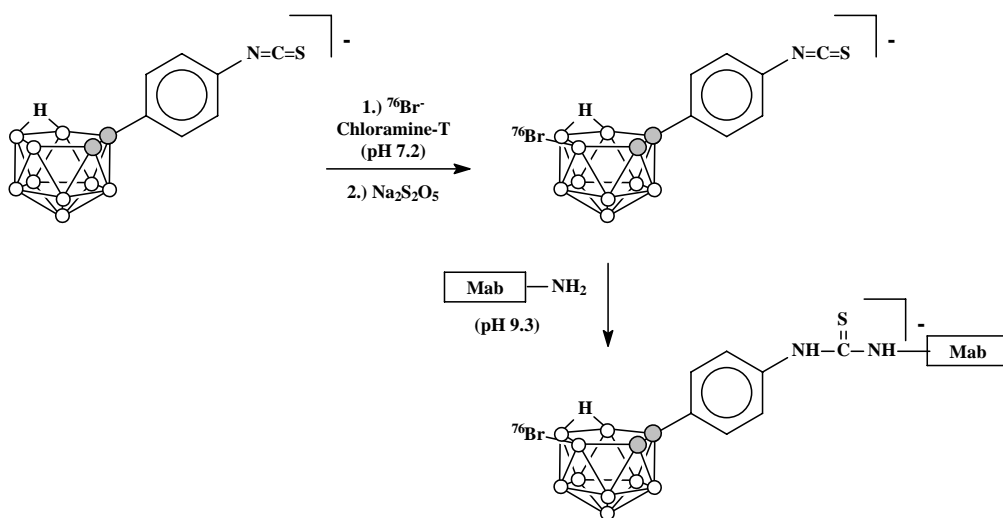


Figure 16. Labelling of antibodies with ^{76}Br -brominated $[7\text{-}(4\text{-SCNC}_6\text{H}_4)\text{-7,8-C}_2\text{B}_9\text{H}_{11}]^-$.

Similarly, the isothiocyanate derivative of the *closo*-dodecaborate anion $[\text{B}_{12}\text{H}_{11}\text{NH}_2\text{CH}_2\text{C}_6\text{H}_4\text{-4-NCS}]^-$ prepared previously for a BNCT project [239] was used for radiolabeling of proteins. This compound was labeled with the Auger electron-emitting nuclide ^{125}I and coupled to anti-HER2/neu humanized antibody trastuzumab [240] (Figure 17). The study of the biodistribution of a radioconjugate prepared in mice revealed decreased radioactivity uptake in thyroid in comparison with the directly radiolabeled antibody. Effective targeting of a head and neck squamous cell carcinoma xenograft model using chimeric monoclonal antibody cMAb U36 radioiodinated with *closo*-dodecaborate linker was demonstrated [241,242]. The labeling of the isothiocyanate derivative with ^{76}Br followed by coupling to anti-HER2/neu humanized antibody trastuzumab was also described (Figure 17) [243]. At the same time, the use of the isocyanate derivative for labeling low-molecular weight Affibody ZHER2:342 was found to be non-effective [244].

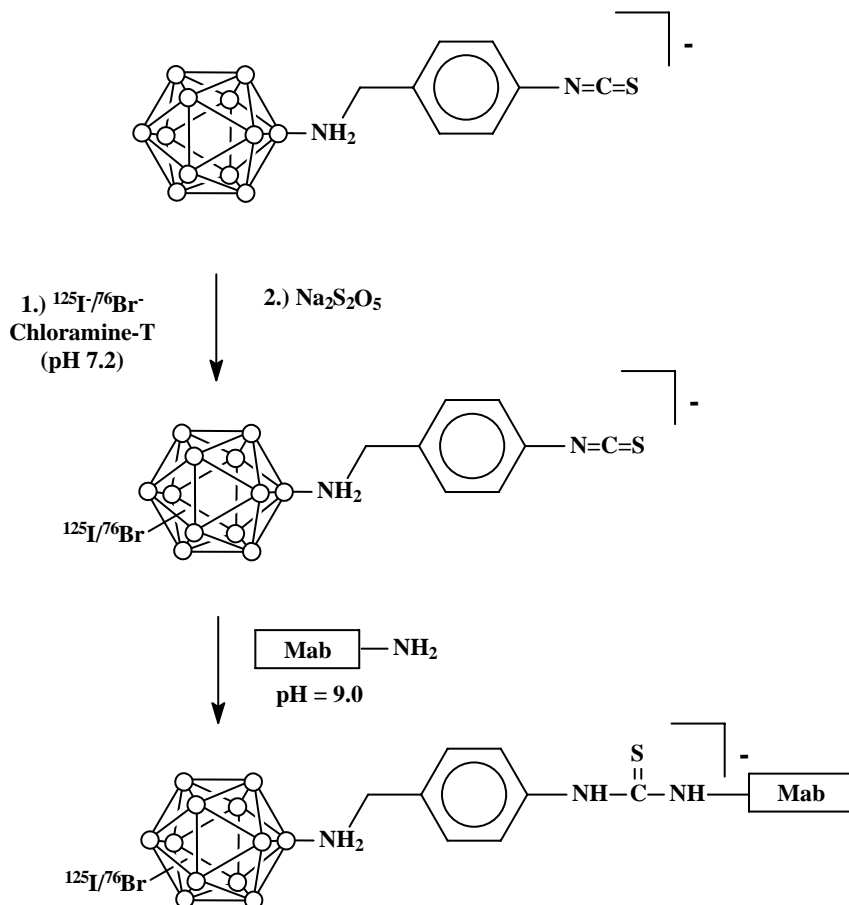


Figure 17. Labelling of antibodies with ^{125}I -iodinated and ^{76}Br -brominated $[\text{B}_{12}\text{H}_{11}\text{NH}_2\text{CH}_2\text{C}_6\text{H}_4\text{-4-NCS}]^-$.

^{131}I -labeling of protein conjugates with isothiocyanate derivatives of the 7,8-dicarba-*nido*-undecaborate and *closso*-decaborate anions have reported (Figure 18) [245].

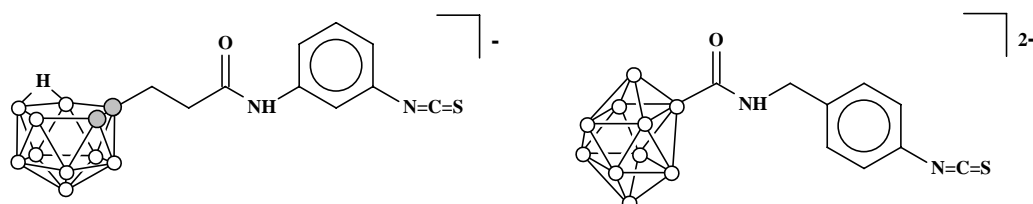


Figure 18. Anionic boron hydride isothiocyanates.

nido-Carborane derivatives were also suggested as pendant groups for direct iodination of proteins that either lack tyrosine residues or in which the tyrosine residues are buried inside the protein structure [246].

Polysaccharides are known to be not degradable by proteolytic enzymes in lysosomes and do not diffuse through cellular membranes. Thus, attached to an internalizing targeting protein, such polysaccharide linkers will remain intracellularly after protein degradation. The stability of the *nido*-carborane-dextran conjugate labeled with ^{125}I was evaluated in rat liver homogenates to be higher than one of labeled albumin (Figure 19) [247].

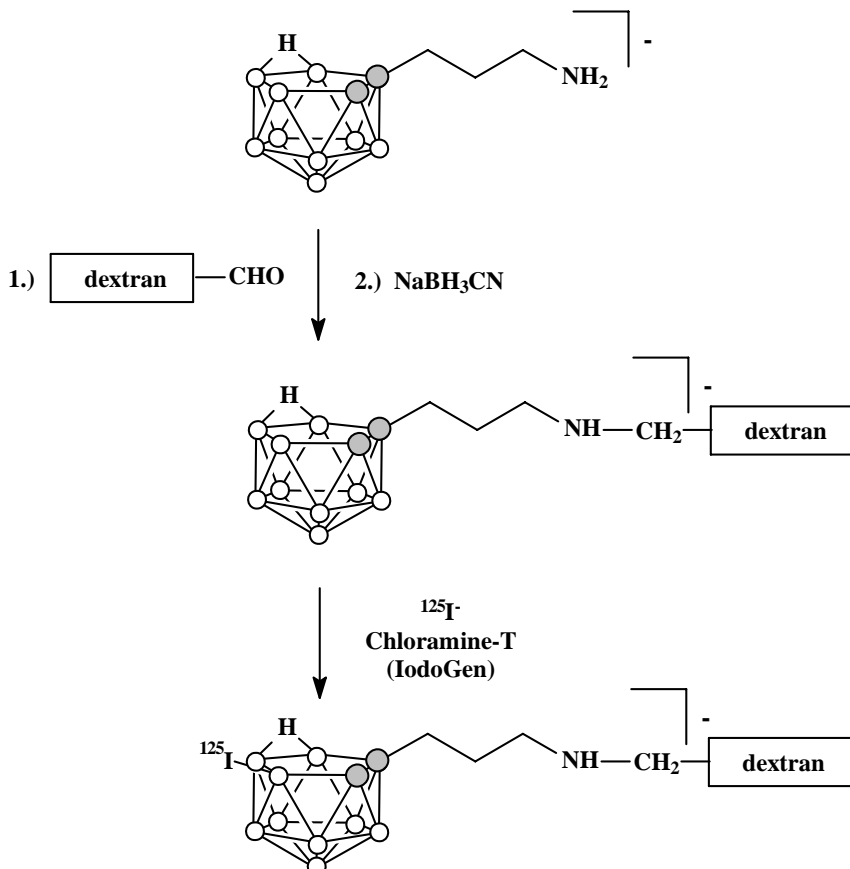


Figure 19. Labelling of dextran with ^{125}I -iodinated $[7-(3-\text{NH}_2\text{CH}_2\text{CH}_2\text{CH}_2)-7,8-\text{C}_2\text{B}_9\text{H}_{11}]$.

A radiolabeled borane-dextrane conjugate was prepared by coupling mercapto-*closo*-dodecaborate $[\text{B}_{12}\text{H}_{11}\text{SH}]^{2-}$ with allyl-functionalized dextran followed by radioiodination [248] (Figure 20).

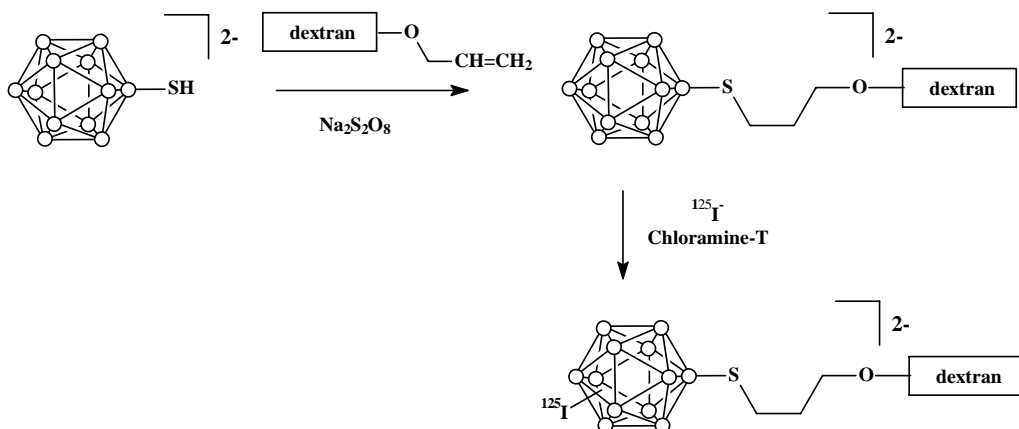


Figure 20. Labelling of dextrane with ^{125}I -iodinated $[\text{B}_{12}\text{H}_{11}\text{SH}]^{2-}$.

Another approach termed “pretargeting”, employs biotin (vitamin H) derivatives to deliver therapeutic radionuclides to cancer cells *in vivo*. In the pretargeting approach, a monoclonal antibody-streptavidin conjugate (mAb-SAv) is injected and allowed to bind antigens on cancer cells. After a period of time sufficient for adequate tumor targeting (e.g. 24 h), a clearing agent is used to remove excess mAb-ASv conjugate from blood. After an appropriate time (e.g. 1-3 h), the radiolabeled biotin derivative is administered such that it can bind with the pretargeted mAb-SAv on cancer cells due to the extraordinarily high biotin-streptavidin affinity. At present, a number of boron-containing derivatives of biotin were synthesized and radioiodinated and their biodistribution studied [249-251] (Figure 21).

The use of polyhedral borane anions as pendant groups for attachment of the α -emitting radionuclide ^{211}At to tumor-seeking biomolecules is of special interest. The problem is that direct oxidative astatin labeling of proteins gives a very weak astatin-protein bond, which prohibits its application in targeted radionuclide therapy. This problem may be circumvented by astatin labeling of N-succinimidyl 3-(tributylstannyl) benzoate or N-succinimidyl 5-(tributylstannyl)pyridine-3-carboxylate, followed by conjugation to the targeting protein. However, all *in vivo* distribution studies performed so far indicate a release of astatin from the targeting conjugate. Study of the *nido*-carborane conjugates with tumorbinding protein human epidermal growth factor hEGF revealed higher labeling yield (70%) than that obtained by indirect labeling using N-succinimidyl astatobenzoate whereas *in vitro* stability is close to stability hEGF labeled with astatobenzoate (Figure 22) [252,253].

Wilbur and coworkers concentrating on the use of *nido*-carborane derivatives for astatination of biotin found that *nido*-carborane can be directly labeled in 70-80% yield and the biotin derivatives containing astatinated *nido*-carborane moieties are more stable to *in vivo* deastatination than aryl astatin derivatives; however, the astatinated *nido*-carborane derivatives undergo some deastatination [249,250,254].

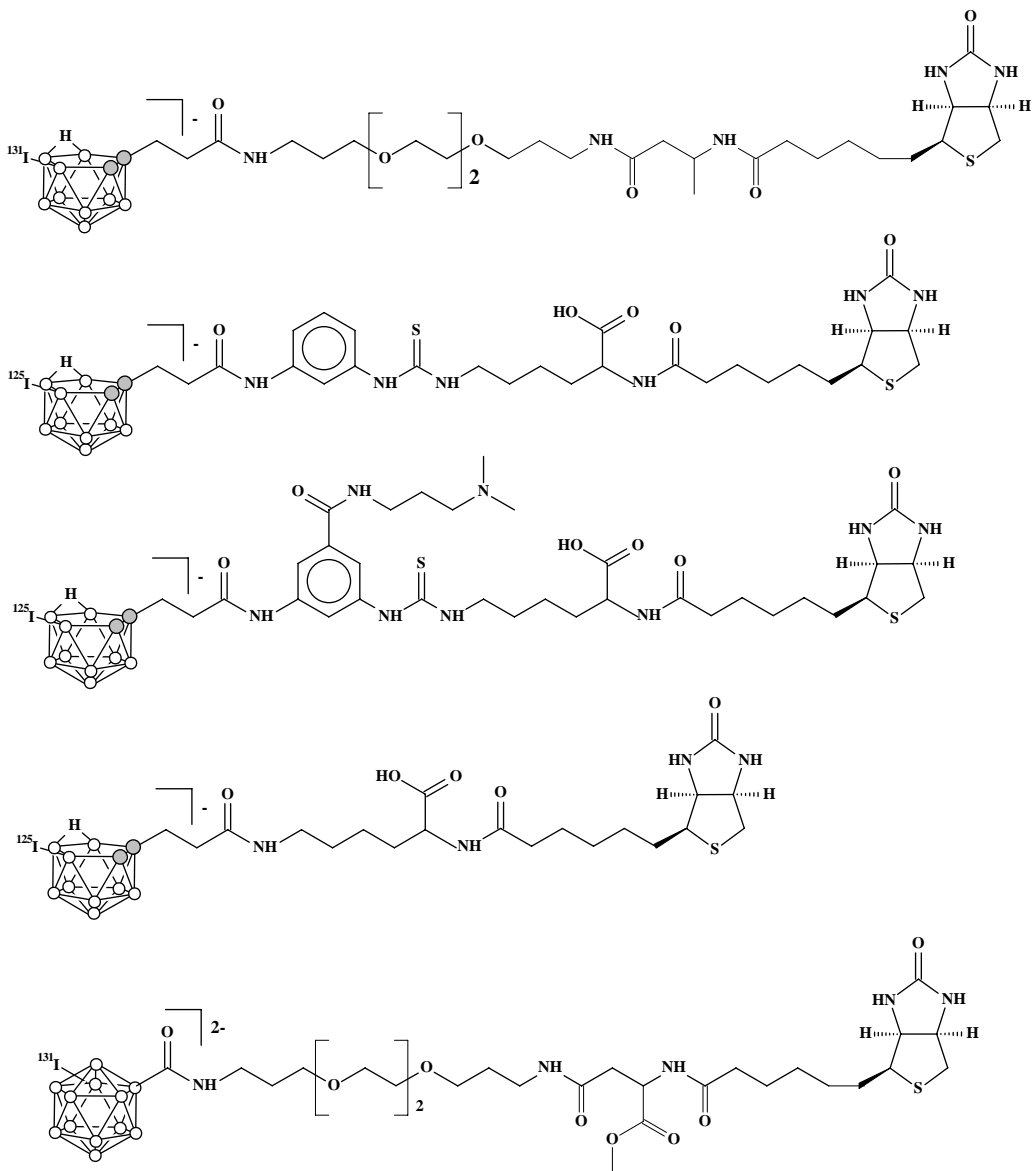


Figure 21. Radioiodinated boron-containing derivatives of biotin.

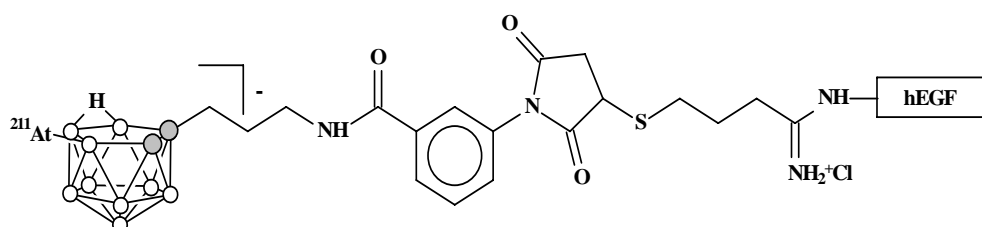


Figure 22. Labelling of hEGF with astatinated nido-carborane.

3.3.2. Polyhedral Boron Hydrides as Chelators for Radiometals

An alternative approach involves the radiolabeling of proteins that have been covalently modified with metalchelating groups. The ligand systems used for metal complexation include derivatives of EDTA, DTPA, DOTA, TETA, NOTA, etc. It is essential for effective imaging that the radioactive metal ions remain complexed by the protein-chelator conjugate. A particular concern in this regard is the competition for metal binding from serum transferrin, which is known to remove metal ions from chelates *in vivo*. Of utmost importance is the magnitude of the radionuclide-chelator dissociation rate, which must be minimal. Most desired would be an especially robust chelation system that is promptly excreted along with tightly-held radiometal even if the antibody or the chelate-antibody linker molecule suffered catabolic degradation. One possible solution to this problem was proposed using an extraordinarily stable metallacarborane clusters readily prepared in aqueous solution and bearing organic substituents for conjugation purposes. A pendant arm, such as a carboxylate functional group, can be used to form an amide linkage with biomolecules *via* established peptide coupling methodology [234].

^{99m}Tc is one of the most widely used radionuclides for nuclear medicine imaging. This is due to the favorable properties of this isotope: the emission of a 140 keV γ -ray with an abundance of 89% and a half-life of 6.0 h [255-257]. The *nido*-carborane cage has been proposed as pendant group for labeling proteins with ^{99m}Tc . The high-yield preparative methods of synthesis of $[3,3,3-(\text{CO})_3-3,1,2-\text{MC}_2\text{B}_9\text{H}_{11}]^-$ and $[1-\text{HOOCCH}_2\text{CH}_2-3,3,3-(\text{CO})_3-3,1,2-\text{MC}_2\text{B}_9\text{H}_{10}]^-$ ($\text{M} = \text{Re, } ^{99}\text{Tc}$) were developed [258] (Figure 23). More recently, the radiolabeling of the *nido*-carborane derivatives with ^{99m}Tc in water under weakly basic conditions was described (Figure) [259-261].

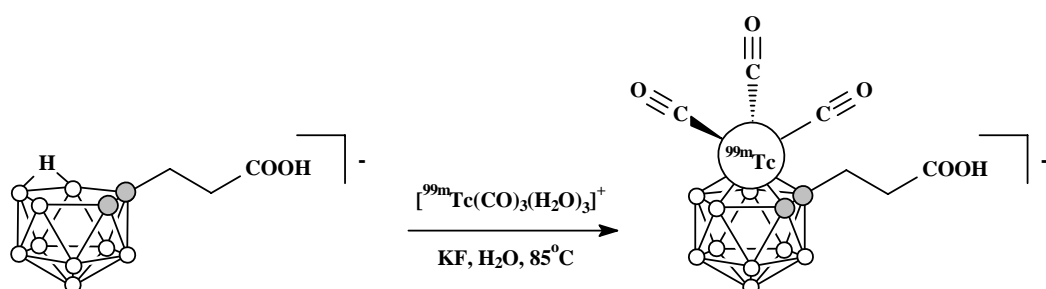


Figure 23. Synthesis of ^{99m}Tc -labeled metallacarborane.

High stability of the radiometallacarborane obtained was demonstrated by its incubation with a 1000-fold excess of cysteine or histidine in phosphate buffered saline (pH 7.2) at 37°C for 24 h [259].

3.4. Boron Clusters as X-Ray Contrast Agents

Another possibility of medical application of the polyhedral boron hydrides is X-ray contrasting imaging. Highly iodinated molecules have application in medicine as X-ray contrast agents due to the opacity of the iodine atoms to low energy X-rays [262]. Even with the recent phenomenal growth of MRI and ultrasound procedures, X-ray imaging studies

remain the workhorse of modern radiology (currently 75-80% of all diagnostic imaging procedures are X-ray related). Today, iodinated X-ray contrast agents are used in about 20 million procedures annually in the United States, mainly in computed tomography and angiographic applications. The U.S. market for X-ray contrast media has grown from \$ 103 million in 1985 to more than \$ 550 million in 1997, and approximately \$ 1 billion today with a worldwide market worth \$3.2 billion.

Current X-ray contrast agents are principally composed of substituted iodinated benzene compounds and their dimers. Most of the iodinated benzene derivatives have three iodine atoms substituted in an alternating fashion with other substituents that are designed to increase water solubility and decrease *in vivo* toxicity. Although the current radiographic contrast media have been optimized over many years of development, improvements are still being sought. One of the methods of improving contrast agents is to increase the iodine content in the molecules. An increase in the percentage of molecular weight due to iodine in a contrast agent from 28.7 to 37.5 % is known to double the contrast of the radiographic image at selected X-ray energies. This fact suggests that chemical moieties other than benzene rings, which can be more highly iodinated, might present new alternatives for contrast agents. The anionic polyhedral boron hydrides could be easily halogenated and have the potential for incorporation of a large number of iodine atoms per molecule (molecules containing 65-85 wt. % of iodine can be obtained) [263-265].

3.5. Carboranes as Pharmacophores

The exceptional hydrophobic character and the spherical geometry of the carboranes [266,267] might allow them to work effectively as hydrophobic pharmacophores. This approach was first applied when phenylalanine and tyrosine residues in various bioactive peptides and polypeptides were replaced with the *o*-carborane cluster [91,94,268,269]. Later synthesis of carborane analogue of the anti-estrogen tamoxifen containing the carborane fragment in place of the A ring phenyl group was reported [270].

Endo *et al.* proposed to use carboranes as the cores from which to construct a series of potent estrogen receptor agonists [271-275] and antagonists [275-277]. The rationale behind the design of the agonists was that hydrophobic carborane cluster could be used in place of the C and D rings of 17 β -estradiol, which play an important role in the binding of the steroid to the estrogen receptors through hydrophobic interactions. Good binding to the receptors and estrogenic activity requires the appropriate hydrophobic group be located adjacent to a phenolic ring, in addition to the having an appropriately positioned H-bonding substituent. As a result, a series of carborane derivatives containing phenolic substituents were prepared. The position of the phenolic OH group, the nature of the substituents off the remaining carborane CH group, and the choice of carborane isomer were all varied to obtain structure-activity relationships. One of the carborane compounds prepared was found to be ten times more active than 17 β -estradiol in a luciferase reporter gene assay (Figure 24).

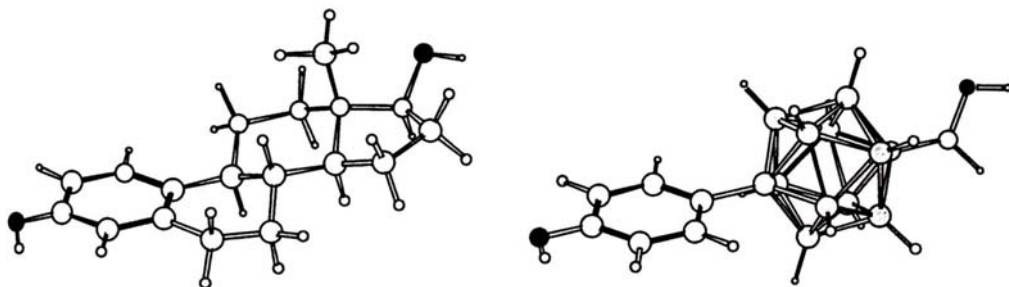


Figure 24. Molecular structures of 17β -estradiol and its p-carborane analogue.⁷

Consequently, Endo *et al.* prepared and screened a series of carborane-based retinoic acid receptor agonists [278-280] and antagonists [281,282] having both amide and amine cores, containing carborane substituents at the 3 and 4 positions of the central aryl group. More recently, syntheses of novel carboranyl testosterone (Figure 25) [283-285] and cholesterol (Figure 15) [203] mimics were reported.

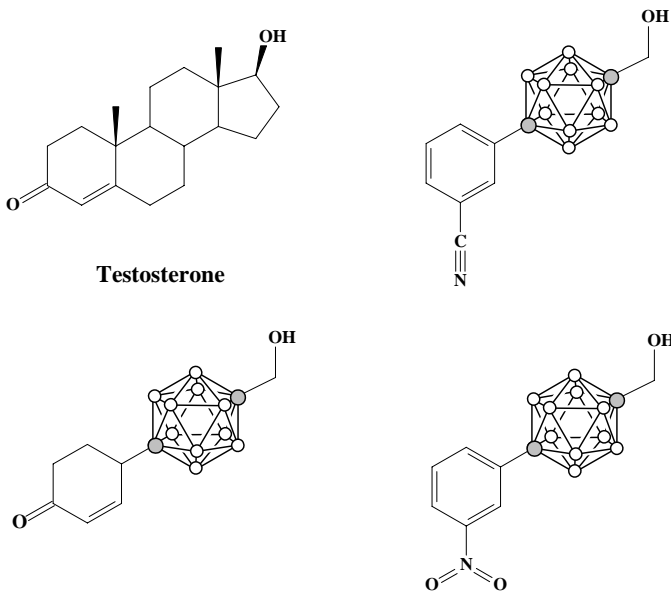


Figure 25. Structures of some carborane-based analogues of testosterone.

3.6. Carborane-Based Antitumour Agents

3.6.1. Platinum(II) Complexes with Carborane-Containing Ligands

The clinical utility of platinum anticancer agents is well proved. One leading anticancer agent, cisplatin, is useful in treating some human cancers but is limited by both its side-affects and the ability of some cancer cells to acquire a resistance to the drug [286]. Therefore, it is desirable to develop a new platinum-based anticancer drug with broader spectrum of activity, improved clinical efficacy and reduced toxicity, better than cisplatin.

As it was mentioned above, a series of platinum(II) complexes containing carborane-based ligands were prepared as DNA metallointercalators for BNCT [287-292] by Rendina *et al.* (Figure 26). Some of them were found to have rather high anti-cancer *in vitro* activity against L1210 murine leukaemia cell line and its cisplatin-resistant variant (L1210/DDP) as well as against 2008 human ovarian cancer cell line and its cisplatin-resistant variant (2008/C13) (table 3).

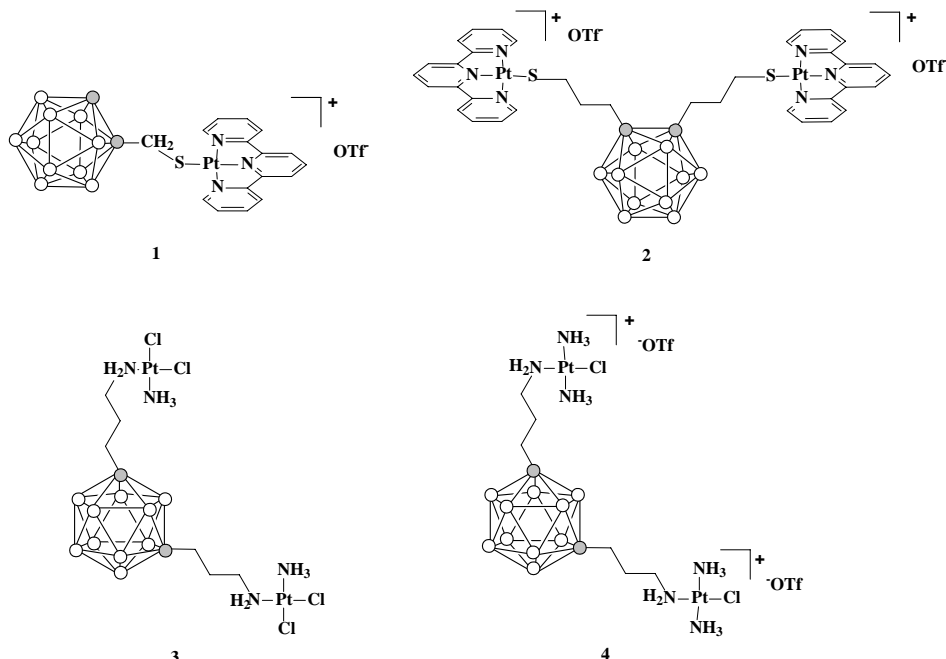


Figure 26. Structures of some platinum(II) complexes with carborane-containing Ligands.

Table 3. IC₅₀ (μM) values for some platinum(II) carborane complexes against selected tumor cell lines

Compound	L1210	L1210/DDP	2008	2008/C13
1	1.6	0.9	1.7	2.1
2	0.9	0.8	-	-
3	2.0	2.5	13	13
4	1.1	1.4	5.5	5.6
Cisplatin	0.5	6.9	0.6	10

The relative cytotoxicities of the Pt(II) carborane complexes are similar in both the cisplatin-sensitive and cisplatin-resistant cell lines. This clearly indicates that the mechanism of cytotoxicity of the Pt(II) carborane complexes is not affected by the cisplatin resistance mechanism(s). Preliminary *in vitro* DNA-binding experiments indicate that the complexes are capable of targeting plasmid DNA.

Several other potentially DNA-intercalating carborane-based platinum(II) complexes were prepared [293-295], however no data on their biological activity were reported.

3.6.2. Organotin Derivatives of Carboranes

Antitumor *in vitro* activity of many organotin derivatives have been well documented [296-298]. A number of organotin derivatives of carboranes were synthesized and antitumor activity of some of them was determined (Figure 27) [299-303].

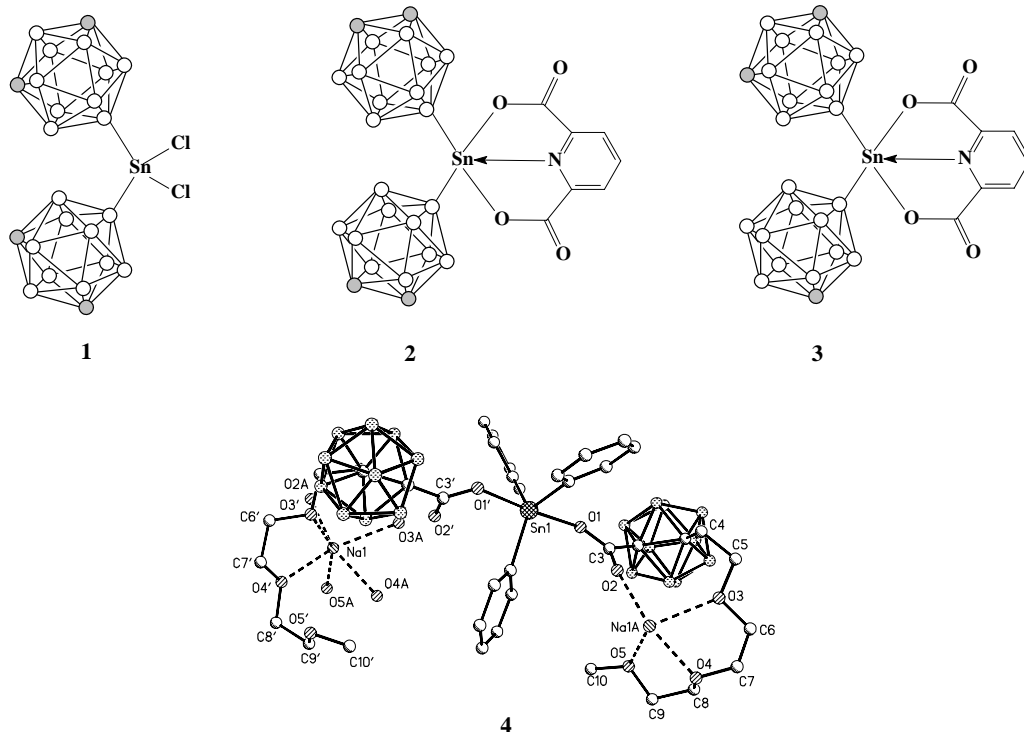


Figure 27. Structures of someorganotin derivatives of carboranes.

Table 4. IC₅₀ (ng/ml) values for some organotin carboranes against selected tumor cell lines

Compound	1	2	3	4	cisplatin	Doxorubicin
MCF-7	5	10	11	44	800	1200
WiDr	31	102	45	37	8	20

The compounds studied were shown to be somewhat less active than doxorubicin and more active than cisplatin, suggesting that the carborane derivatives have intermediate anti-cancer activity.

3.7. Weakly Coordinating Anions

There is considerable interest to weakly coordinating anions for numerous applications. Probably, the most appreciated is the need for inert counterions in the preparation of extremely reactive cations, especially strong Brønsted acids, and cationic catalysts.

Weakly coordinating anions are bulky anions with a low overall charge, preferably -1, highly delocalized over the entire anion [304,305]. The carba-*closo*-dodecaborate anion $[CB_{11}H_{12}]^-$ is weakly coordinating, but its hydridic hydrogens in positions 7-12 coordinate quite readily. Their hydridic nature poses an even more serious limitation due to increased reactivity towards cationic electrophiles. A solution is to replace the hydrogens in $[CB_{11}H_{12}]^-$, particularly those in positions 7-12, with halogens giving $[CB_{11}H_6X_6]^-$ or $[HCB_{11}X_{11}]^-$, where X = F, Cl, Br, I. Probably, the fluoro derivative $[HCB_{11}F_{11}]^-$ is the best choice, but it has not seen much use so far because they are best prepared only with elemental fluorine in liquid hydrogen fluoride, that few laboratories are equipped for [50].

Acids derived from halogen derivatives of the carba-*closo*-dodecaborate anion were found to be the strongest isolable acids presently known [306-308]. Due to this fact together with very low (the least) nucleophilicity and very high chemical inertness of halogenated carborane anions, these acids have received name of “strong yet gentle” acids [309]. Carborane acids are moisture-sensitive, white solids with extremely high thermal stability. They sublime under vacuum at temperatures in the range 150-200 °C. Crystals of the free acid H $[CB_{11}Cl_{11}]$ were found to contain linear polymeric chains with proton bridges between chlorines located in the lower belt [308].

A demonstration of the strength of carborane acids is their ready protonation of benzene. Protonated arenas are important as the intermediates of electrophilic aromatic substitution – so-called Wheland intermediates. Triflic acid does not protonate benzene, the strongest known neat liquid acid, HFSO₃, does so only to a very small extent, the HF/SbF₅ mixture has enough high acidity to protonate benzene, however stability of the resulting benzenium ion is limited by temperatures below ambient. On the other hand, when carborane acid is used, the resulting benzenium ion salt, $[C_6H_7]^+[HCB_{11}Me_5Br_6]^-$, is stable to 150 °C. X-ray crystal structure analysis of the protonated toluene $[CH_3C_6H_6]^+[CB_{11}H_6Br_6]^-$ revealed that protonated arenium ion has structure of a σ complex (Figure 28) [310].

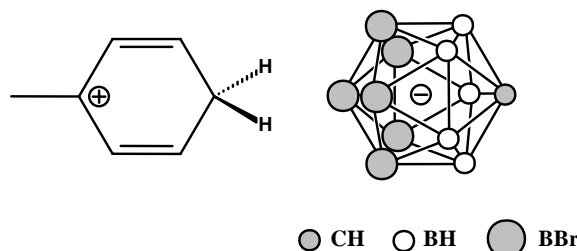


Figure 28. Structure of the protonated toluene salt.

A more powerful illustration of the strong-yet-gentle characteristics of the carborane acids is their protonation of fullerenes. A decade of attempts to observe protonation of C₆₀ with traditional strong and superacids failed due to oxidative/nucleophilic decomposition of the fullerene by the conjugate bases of the acid used. On the other hand, H $[CB_{11}H_6Cl_6]$ was found to cleanly and reversibly protonate C₆₀ in dry halocarbon solvents [311]. The formed $[HC_{60}]^+[CB_{11}H_6Cl_6]^-$ salt was characterized by ¹³C CPMAS NMR spectroscopy to have a 1,2-carbocation static structure [312,313]. In solution the proton in the $[HC_{60}]^+$ cation is a true “globetrotter”, rapidly migrating between all 60 carbon atoms.

The carborane acids pick up water from solvents and glassware forming hydronium ion salts. Using a large non-nucleophilic counterion makes possible the isolation and characterization of stable crystalline hydronium salts with precisely defined hydration. The first example of the hydronium ion carborane salt was $[(\text{H}_3\text{O})(\text{H}_2\text{O})_3][\text{CB}_{11}\text{H}_6\text{Br}_6]$, containing discrete $[(\text{H}_3\text{O})(\text{H}_2\text{O})_3]^+$ ions [314]. Other examples are structures of $[\text{H}(\text{H}_2\text{O})_2][\text{HCB}_{11}\text{Cl}_{11}] \cdot \text{C}_6\text{H}_6$, containing $[\text{H}(\text{H}_2\text{O})_2]^+$ ions, and $[(\text{H}_3\text{O})(\text{C}_6\text{H}_6)_3][\text{CB}_{11}\text{H}_6\text{Br}_6] \cdot \text{C}_6\text{H}_6$, displaying coordination of the hydronium cation to three molecules of benzene [315]. Several additional O-solvated H^+ species have been characterized, including $[\text{H}(\text{H}_2\text{O})(\text{Et}_2\text{O})]^+$ and $[\text{H}(\text{Et}_2\text{O})_2]^+$ [316].

The extremely weak nucleophilicity of halogenated carborane anions has been used to develop a new class of alkylating reagents $[\text{R}]^+[\text{HCB}_{11}\text{Me}_5\text{X}_6]^-$, where R = Me, Et, *i*-Pt and X = Cl, Br. These reagents are stronger electrophiles than methyl triflate and more thermally stable than fluoroantimonate alkylating reagents [317]. $[\text{Me}][\text{HCB}_{11}\text{Me}_5\text{Br}_6]$ was found to be sufficiently electrophilic to abstract hydride from alkanes at or below room temperature [318]. For example, the reaction with butane results in elimination of methane and formation of the *t*-butyl cation salt $[\text{t-Bu}]^+[\text{HCB}_{11}\text{Me}_5\text{Br}_6]^-$ that is stable indefinitely at room temperature in absence of moisture and nucleophiles and was characterized by X-ray diffraction [318]. The first X-ray structure of a vinyl cation, the two-coordinate unsaturated analogue of a carbenium ion, was recently obtained using a carborane as counterion [319].

The existence and mechanistic importance of the carbenium ion (R_3C^+) in organic chemistry has inspired the long search for its silicon analogue, the silylium ion (R_3Si^+). Presently, the closest structurally-characterized approach to trialkylsilylium ion is $[\text{i-Pr}_3\text{Si}]^+[\text{CB}_{11}\text{H}_6\text{Cl}_6]^-$ [320,321]. The bonding between the R_3Si^+ cation and the carborane anion is weak and probably largely ionic. A truly three-coordinate sp^2 silylium ion was isolated using bulky mesityl substituents on silicon, $[\text{Mes}_3\text{Si}]^+[\text{CB}_{11}\text{H}_6\text{Cl}_6]^- \cdot \text{C}_6\text{H}_6$ [322].

There has been considerable interest in using weakly coordinating anions in catalytic active complexes. They could have the ability to move to the side, allowing the substrate to coordinate to the metal but still remaining available for stabilization of the active intermediate. Carba-*closو*-dodecaborate based silver catalysts with phosphine and N-carbene ligands were shown to have high activity as catalysts for hetero-Diels-Alder reactions [323,324]. Zirconium-based catalysts were used for polymerization of olefins [325] and for conversion of alkynes and alkenes to ketones [326]. Rhodium catalyst found application in the conversion of arylboronic acids to aldehydes [327] and in hydrogenation of olefins [328]. An iridium complex with $[\text{CB}_{11}\text{H}_6\text{Br}_6]^-$ anion was used in the room temperature and pressure hydrogenation of internal alkenes, including sterically hindered ones [329]. Lithium salt $\text{Li}[\text{MeCB}_{11}\text{Me}_{11}]$ was found to catalyze pericyclic reactions [330], as well as radical polymerization of alkenes, alkadienes, and alkynes at ambient pressure [331]. Lithium salt of another weakly coordinating anion, $\text{Li}[3,3'\text{-Co}(1,2\text{-C}_2\text{B}_9\text{H}_{11})_2]$, is a mild and effective catalyst for the conjugate addition of silyl ketene acetals to α,β -unsaturated carbonyl compounds and for the substitution of allylic acetates with various nucleophiles [332,333].

3.8. Metallacarboranes as Catalysts

Besides transition metal complexes with weakly coordinating *closو*-borate anions, metallacarboranes in which metal atom incorporated into carborane cage are of great interest

as catalyst or catalyst precursors. The use of rhodacarboranes as catalysts for the hydrogenation and isomerisation of alkenes under mild conditions was first reported by Hawthorne *et al.* It was found that the Rh(III) *closو* complex [*closо*-3,3-(PPh₃)₂-3H-3,2,1-RhC₂B₉H₁₁] is in equilibrium with the *exo-nido* Rh(I) isomer [*exo-nido*-5,10-{(PPh₃)₂Rh}-4,9-(μ-H)₂-7,8-C₂B₉H₁₀] (Figure 29) and the last species is catalytically active [334].

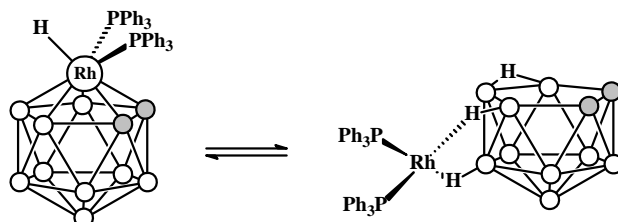


Figure 29. *Closо – exo-nido* equilibrium of rhodium carborane complexes.

As an example of possible practical use, rhodacarboranes were found to be exceptionally effective for stereoselective hydrogenation of methacycline to doxocycline [335,336]. Catalytic activity of Rh- and Ru-based metallacarboranes in reactions of some other types of reactions was demonstrated [337-341]. According to the results obtained by Hawthorne *et al.*, the *exo-nido* metal disposition with B-H coordination to the carborane cage is one of the main factors governing catalytic activity of metallacarboranes. With the aim to avoid the *exo-nido* to *closо* tautomerism and to force B-H-M interactions a series of rhoda- and ruthenacarboranes based on RS- and R₂P-substituted dicarbollide ligands were prepared. In this case the *exo-nido* coordination of metal is forced by coordination with mercapto or phosphine ligand. Some of the metallacarboranes synthesized were found to demonstrate high catalytic activity in reactions of hydrogenation and cyclopropanation of olefins [342]. More recently, the use of rhodacarborane catalyst in (R)-Binap mediated asymmetric hydrogenation reactions was reported [343].

Metallacarboranes of the Group 4 metals (Ti, Zr, Hf) are of interest as analogues of Ziegler-Natta catalysts for polymerization of olefins. A series of such metallacarboranes were prepared, however they were found to exhibit only moderate catalytic activity [344-348].

A few examples of synthesis and catalytic activity of polymer- [349] and single-wall carbon nanotube- [350] supported metallacarboranes were reported. It should be noted that despite of that reports on catalytic activity of metallacarboranes continue to appear, only catalytic activity of rhoda- and ruthenacarboranes was studied more or less systematically.

3.9. Polyhedral Boron Hydrides in Molecular Engineering

Due to their axially directed terminal bonds and rigid cage structures, polyhedral boron hydrides offer a unique opportunity in the area of molecular engineering for their potential application as a molecular anchor between two or more active reaction centers [351-354]. In this context, homo- and hetero- substituted derivatives with substituents attached to the antipodal positions of the 10- and 12-vertex borane clusters are of a great interest. Syntheses of antipodally substituted boranes and carboranes have been reviewed recently [355]. Another attracting attention feature is electronic properties of polyhedral boron hydrides. Through-

cage electron transmission effects and electronic interactions between the 10- and 12-vertex borane clusters and π substituents are of particular interest.

3.9.1. NLO Materials

The main reason of this interest is potential use of polyhedral boron hydrides as components of nonlinear optic (NLO) materials. NLO materials have increasingly attracted attention owing to their direct application in the development of efficient optical telecommunication networks lacking electrical-to-optical, and *vice versa*, signal conversion. Such application requires thermally robust materials with highly NLO response (first hyperpolarizability β). Typical organic NLO compounds include donor and acceptor moieties bridged by a π -conjugated linker. Until now, most efforts to obtain better hyperpolarizability (β) have been directed to finding both the right combination of donor and acceptor species and the right length of the conjugated bridge between donor and acceptor.

It is well accepted that *C*-carboranyl groups act as electron-withdrawing groups [56]. It is true, however, for the compounds in the ground state and NLO activity concerns the properties of the excited states. Previously a series of carboranes containing various donor groups were synthesized [356,357], but their hyperpolarizable properties were not satisfactory and comparable with the one for the standard *p*-nitroaniline benchmark often used for evaluating new NLO compounds. More recently synthesis of the 12-vertex carborane–ferrocene dyads bridged by the ethenyl-*p*-phenyl or iminyl-*p*-phenyl π systems as well as their NLO properties were reported. It was shown that carboranes act as an acceptor in the hyperpolarizable activity and the order of electron withdrawing ability is $\text{NO}_2 > \text{carboranes} > \text{H}$. Among isomeric carborane derivatives, the *p*-carborane-based ones exhibit the highest β values [358]. Surprisingly high β values were found in a series of the 12-vertex carborane–fullerene hybrids bridged by the ethynyl-*p*-phenyl π system, where fullerene is electron-withdrawing group (acceptor-acceptor system). As in the case of the carborane–ferrocene series, the highest β value ($\beta = 1189 \times 10^{-30}$ esu) was found for the *p*-carborane-based compound [359].

UV spectroscopy provides a convenient tool for studying intramolecular electronic effects. The spectroscopic studies demonstrated a rather moderate effect of the 12-vertex carboranes on π substituents of different types [360,361]. In contrast to carboranes, the strong donor effect of the B_{12} cage was found in a series of Schiff bases derived from the *closododecaborate* anion [36,37]. Another example is tropilium derivative of the *closododecaborate* anion [$\text{B}_{12}\text{H}_{11}\text{C}_7\text{H}_6^-$] demonstrating strong charge-transfer band due to charge transfer from the negatively charged boron cage to the positively charged aromatic ring [362–364]. The recent molecular study revealed that the tropilium derivative has additional low lying π orbital in which pair of the cage electrons is completely delocalized throughout the cage and the ring that results in its extraordinary stability [365]. The similar strong charge transfer band and rather high first hyperpolarizability β were found in the *B*-substituted tropilium derivative of the carba-*closododecaborate* anion [$12\text{-C}_7\text{H}_6\text{-1-CB}_{11}\text{H}_{11}$] [366].

The studies concerning the 10-vertex boron hydrides demonstrated significantly stronger electronic interactions between the cluster and π substituents than those observed in the 12-vertex analogues. This is evident from intense and relatively low energy absorption bands observed for derivatives of 10-vertex boranes with various π substituents at apical position of a cage [361,367–371].

Another important question concerning design of NLO materials is the electron transfer properties of 10-and 12-vertex boron clusters. As it was shown above, the electronic interactions between 12-vertex carboranes and π substituents are rather small being the strongest for *p*-carborane. The study of the transmission of the electronic effect through *p*-carborane substituted with aryl electron-donor and -withdrawing groups revealed that 12-vertex *p*-carborane cage is completely ineffective as a π -conjugated linker for NLO materials [360]. Electrochemical experiments on a series of π -CpFe(CO)₂-substituted *p*-carborane derivatives [372,373] and *p*-carborane functionalized by dicobalt-dicarbon cobalt clusters [374] suggested that the metal centers are weakly coupled. The absence of extensive electron delocalization through the 1,4-C₆H₄-*p*-CB₁₀H₁₀C-1,4-C₆H₄ bridge was found in binuclear Ru complex involving the *p*-carborane framework in the bridging ligand [375]. On the other hand, quantum mechanical calculations that are effectively employed in evaluation of the NLO properties of new materials showed that when substituted with a powerful donor and acceptor, 12-vertex carborane could act as an electron conduit [376]. More recently the matrix elements relevant to electron tunneling through 10- and 12-vertex *p*-carborane cages have been calculated [377].

In general, the 10-vertex borane clusters with its high symmetry and rather strong electronic interactions appear to be well suited for the design of NLO chromophores both as acceptor/donor elements and as π -conjugated linkers, whereas the 12-vertex borane clusters having weaker electron-transfer properties could be used as acceptor/donor elements for construction of new NLO materials.

3.9.2. Molecular Magnets and Conductors

The NLO properties of a series of salts of the iron bis(dicarbollide) anion [3,3'-Fe(1,2-C₂B₉H₁₁)₂]⁻ with dipolar and polarizable cations were studied but the results obtained were disappointed [378]. On the other hand, the metallocarborane anions [3,3'-M(1,2-C₂B₉H₁₁)₂]⁻ (M = Co, Fe, Ni, Cu) and their derivatives would be of interest as structural elements for design of new molecular ferri- and ferromagnets, synthetic metals and semiconductors [379-386]. Nickel(IV) bis(dicarbollide) [3,3'-Ni(1,2-C₂B₉H₁₁)₂] was proposed as candidate for a molecular rotary motor with electrical or photocontrol of the intramolecular rotation of the carborane ligands around a nickel axis [387,388].

3.9.3. Carborane Based Liquid Crystals

The highly symmetric 10- and 12-vertex boron hydrides are also of particular interest for designing photochemically and thermally stable calamitic (rod-like) liquid crystals. Liquid crystals are organic or organometallic compounds that exhibit a birefringent fluid phase between the crystal solid and ordinary (isotropic) liquid. The synthesis of stable, room temperature liquid crystal compounds suitable for use in electro-optic devices produced revolution in display industry. Calamatic molecules are typically composed of a rigid core comprising several rings (phenyl, cyclohexyl, bicyclo[2.2.2]octyl) joined directly or through linking group (ester, azo, alkene, azomethene). It is the mesogenic core that provides the anisotropic interactions necessary for the formation of the liquid crystal phase and has the dominating effect on bulk properties. To reduce the crystal melting point and, as sequence, to reveal the liquid crystal behavior flexible substituents (alkyl chains) should be attached to the mesogenic core (Figure 30) [389].

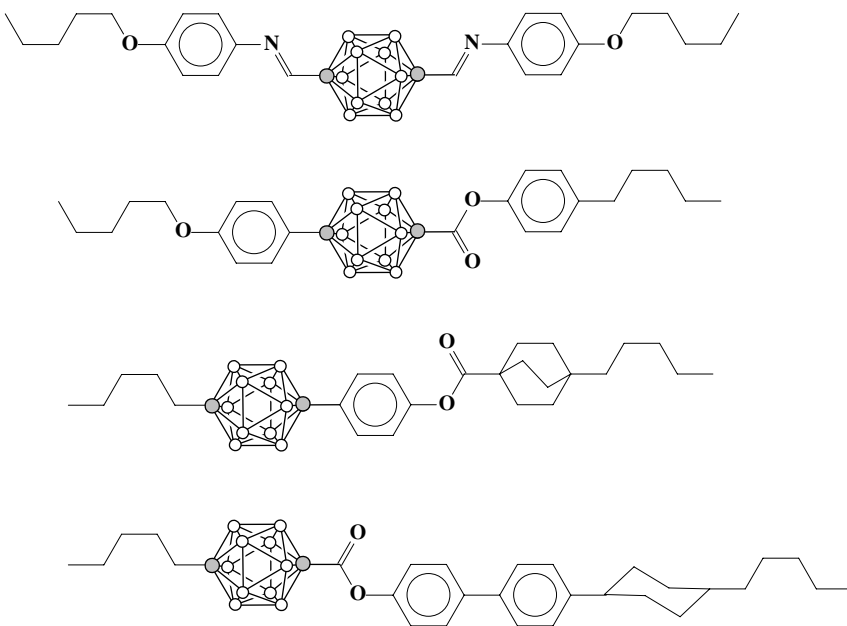


Figure 30. Structures of some p-carborane based liquid crystals.

The 10- and 12-vertex boron hydrides satisfy well to the geometric requirements for structural elements for liquid crystal rigid cores. The electronic structure of the polyhedral boron hydrides is also very attractive for use in synthesis of liquid crystals. They have only a marginal electronic absorption above 200 nm [390] and demonstrate significant electronic polarizability [391,392]. As it was mentioned above, electronic interactions of the 12-vertex borane clusters with π substituents are rather marginal and they typically have only modest influence on the electronic spectra. That means that the 12-vertex borane clusters are of particular interest for designing liquid crystals, however the potential of the 10-vertex clusters cannot be discarded [389]. At present a large variety of liquid crystals based on the *closo*-decaborate [355,393], 1,10-dicarba-*closo*-decaborane [394-399], carba-*closo*-dodecaborate [355,400], and 1,12-dicarba-*closo*-dodecaborane [393,395-399,401-408] cages were synthesized and their properties were investigated. Other examples include liquid crystals with the 1,1'-bis(1,10-dicarba-*closo*-decaborane) [409] and 1,1'-bis(1,12-dicarba-*closo*-dodecaborane) [409] moieties as a mesogenic core, as well as liquid crystalline carborane-containing polymers [410,411].

3.10. Carborane-Based Polymers

The extreme thermal stability of icosahedral carboranes attracted the interest of polymer chemists immediately after these compounds were discovered in the early 1960s. In the mid 1960s several groups of polymer chemists studied the effect of incorporation of carborane cages into chains and networks of almost any known type of polymers [412]. The best results were achieved with the family of poly(*m*-carborane-siloxane)s [413,414] that have even been manufactured on an industrial scale under the trade name DEXSIL (Figure 31). Some of these

polymers with appropriate fillers retain their properties even around 500 °C. Tubings, insulation jackets, gaskets, membranes, coatings, etc. have all been made of such polymers. Synthesis and chemistry of the poly(carborane-siloxane) polymers were reviewed [415].

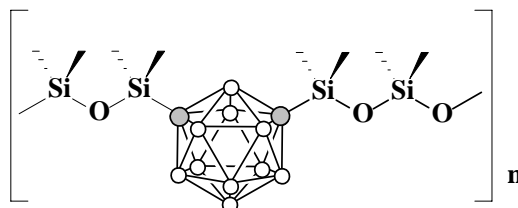


Figure 31. Structure of poly(m-carborane-siloxane) polymer.

A systematic research program on all aspects of carborane-modified polymers has been operated for decades in the Soviet Union/Russia. The results obtained were reviewed in a few domestic reports [416,417]. Some recent reviews are related to arylene carborane polymers [418-420].

3.11. Solvent Extraction of Radiometals

High solubility of inorganic salts in organic solvents is characteristic property of polyhedral borane monoanions, especially of cobalt bis(dicarbollide) $[3,3'-\text{Co}(1,2-\text{C}_2\text{B}_9\text{H}_{11})_2]^-$ [73]. This property, together with its high thermal and chemical stability (including resistance to acids, bases, and radiation) attracted attention for use in the extraction of radionuclides from nuclear waste. The solubility and other properties of cobalt bis(dicarbollide) can be improved and refined by introduction of various substituents. Thus, the hexachloro derivative $[8,8',9,9',12,12'-\text{Cl}_6-3,3'-\text{Co}(1,2-\text{C}_2\text{B}_9\text{H}_8)_2]^-$ was found to be much more resistant than the parent anion to 3 M HNO₃, that is a requirement for the large-scale selective recovery of ¹³⁷Cs and ⁹⁰Sr. The first application of cobalt bis(dicarbollide) for solvent extraction of radionuclides was first reported in mid 1970s [421]. An industrial separation facility based on cobalt bis(dicarbollide) started operation at the Mayak plant near Chelyabinsk in Russia in 1996 and the industrial extraction experiment showed excellent results with real high-level waste. More recently, the Cobalt Dicarbollide Universal Extraction (UNEX) Process has been jointly developed at the Khlopin Radium Institute (St. Petersburg, Russia) and the Idaho National Engineering and Environmental Laboratory (USA). This process removes cesium, strontium, and actinides from acidic waste in a single step. The original process removed only cesium and strontium using cobalt dicarbollide and polyethylene glycol in a nitrobenzene diluent. Since nitrobenzene is considered to be hazardous in the U.S., alternate diluents were developed. This process provides a simplified and cost-effective method for waste treatment as compared to the currently used method that utilizes two or three separate processes [422-425]. A series of novel cobalt bis(dicarbollide) derivatives containing substituents of various types (alkyl, aryl, ether, oligoethylene glycol, calixarene, etc.) have been synthesized for the last years and their extraction properties have been investigated [68,69,426-432].

3.12. Miscellaneous

Ionic liquids are salts that are liquid at or near room temperature. Carba-*closo*-dodecaborate anion and its derivatives can serve as counterions in the development of new types of ionic liquids [433]. Use of ionic liquids based on $[CB_{11}H_{12}]^-$ anion in synthetic organic chemistry has been reported [434,435].

High solubility in non-aqueous solvents and high chemical stability of the polyhedral borane anions make some of them candidates for use as electrolytes in lithium-ion batteries [436-438] and components of ion-exchange membranes and ion-selective electrodes [439-445].

o-Carborane is widely used for boronization of inner surfaces of tokamaks and stellarators to improve plasma parameters [446-453].

Some derivatives of polyhedral boron hydrides were found to form stable host-guest complexes with anions of various types. Thus, carborane-based macrocyclic Lewis acid [9]mercuracarborand-3 (Figure 32) acts as anticrown towards some monoanions [454]. Its use in electrochemical [455,456] and photochemical sensors [457] for chloride ion has been proposed. The greatly enhanced Lewis acidity of mercury centers attached to electron-withdrawing carborane cages in mercuracarborand structures allowed these hosts to complex also uncharged electron-rich molecules. A novel neutral host-guest complex of hexamethyl[9]mercuracarborand-3 complexing two water and one benzene molecules has been reported [458]. Each of the water oxygens in this structure is η^3 -coordinated to all three mercury centers of one of the cycles, and both sides of the benzene ring encapsulated in the center of the sandwich structure are π -H hydrogen bonded with one of the two complexed water molecules. This is the first solid-state structure of a benzene-water hydrogen-bonded complex. *Closo*-dodecaborate based bis(guanidinium) ionophore (Figure 32) gives stable host-guest complexes with various oxoanions [459-461] and can be used in ion-selective electrodes for detection of monohydrogen phosphate and sulfate anions [462].

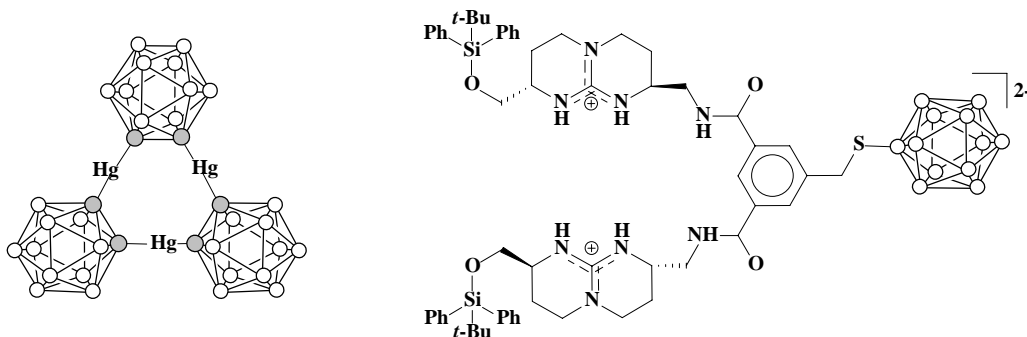


Figure 32. Structures of anion-selective borane-based host molecules.

4. CONCLUSION

It is practically impossible to cover all areas of potential application of polyhedral boron hydrides. In the present review we tried to highlight directions that are of the most common interest or that are very interesting in our opinion. We don't know where breakthrough will be done, but we put trust in it. Time will tell.

5. ACKNOWLEDGMENTS

This work was financially supported by the Russian Foundation for Basic Research (grants 05-03-32429 and 07-03-00712). IBS thanks Dr. V.V.Semioshin and all staff of the 4th Moscow anti-tuberculosis clinic, where the most part of this review was written, for their care and patience.

6. REFERENCES

- [1] Stock, A. *Hydrides of Boron and Silicon*, Cornell University Press, Ithaca, NY, 1933.
- [2] Schubert, D. (2001) From Missiles to Medicine: The development of boron hydrides. <http://www.borax.com/pioneer54.html>
- [3] Lipscomb, W. N. *Boron Hydrides*, W.A. Benjamin, Inc., New York, NY, 1963.
- [4] Hawthorne, M. F. In: *The Chemistry of Boron and Its Compounds*; Muettterties, E. L.; Ed., John Wiley and Sons, Inc., New York, NY, 1967, pp. 223-323.
- [5] King, R. B. *Chem. Rev.* 2001, *101*, 1119-1152.
- [6] Hawthorne, M. F.; Pitochelli, A. R. *J. Am. Chem. Soc.* 1959, *81*, 5519.
- [7] Hawthorne, M. F.; Pilling, R. L. *Inorg. Synth.*, 1967, *9*, 16-19.
- [8] Manhlouf, J. M.; Hough, W. V.; Hefferan, G. T. *Inorg. Chem.*, 1967, *6*, 1196-1198.
- [9] Guillevic, G.; Dazord, J.; Mongeot, H.; Cueilleron J. *J. Chem. Res.*, 1978, 402-403.
- [10] Leyden, N.; Hawthorne, M. F. *Inorg. Chem.* 1975, *14*, 2444-2446.
- [11] Shelly, K.; Knobler, C. B.; Hawthorne, M. F. *Inorg. Chem.* 1992, *31*, 2889-2892.
- [12] Naoufal, D.; Grüner, B.; Bonnetot, B.; Mongeot, H. *Polyhedron*. 1999, *18*, 931-939.
- [13] Zhizhin, K. Yu.; Vovk, O. O.; Malinina, E. A.; Mustyatsa, V. N.; Goeva, L. V.; Polyakova, I. N.; Kuznetsov, N. T. *Russ. J. Coord. Chem.* 2001, *27*, 613-619.
- [14] Sivaev, I. B.; Votinova, N. A.; Bragin, V. I.; Starikova, Z. A.; Goeva, L. V.; Bregadze, V. I.; Sjöberg, S. *J. Organomet. Chem.* 2002, *657*, 163-170.
- [15] Bernard, R.; Cornu, D.; Perrin, M.; Schaff, J.-P.; Miele, P. *J. Organomet. Chem.*, 2004, *689*, 2581-2585.
- [16] Zhizhin, K. Yu.; Mustyatsa, V. N.; Malinina, E. A.; Votinova, N. A.; Matveev, E. Yu.; Goeva, L. V.; Polyakova, I. N.; Kuznetsova, N. T. *Zh. Neorgan. Khim.* 2004, *49*, 221-230.
- [17] Sivaev, I. B.; Bragin, V. I.; Bregadze, V. I.; Votinova, N. A., Sjöberg S. *Russ. Chem. Bull., Int. Ed.* 2004, *53*, 2092-2095.

- [18] Zhizhin, K. Yu.; Mustyatsa, V. N.; Malinina, E. A.; Votinova, N. A.; Matveev, E. Yu.; Goeva, L. V.; Polyakova, I. N.; Kuznetsov, N. T. *Zh. Neorgan. Khim.* 2005, 50, 243-249.
- [19] Bragin, V. I.; Sivaev, I. B.; Bregadze, V. I.; Votinova, N. A. *J. Organomet. Chem.* 2005, 690, 2847-2849.
- [20] Hawthorne, M. F.; Pitochelli, A. R. *J. Am. Chem. Soc.* 1960, 82, 3228-3229.
- [21] Longuet-Higgins, H. C.; Roberts M. de V. *Proc. R. Soc. London, Ser. A* 1955, 230, 110-119.
- [22] Miller, H. C.; Miller N. E.; Muetterties E. L. *Inorg. Chem.* 1964, 3, 1456-1463.
- [23] Miller, H. C.; Miller N. E.; Muetterties E. L. *J. Am. Chem. Soc.* 1963, 85, 3885.
- [24] Greenwood, N. N.; Morris, J. H. *Proc. Chem. Soc.* 1963, 338.
- [25] Adams, R. M.; Siedle, A. R.; Grant, J. *Inorg. Chem.* 1964, 3, 461.
- [26] Ellis, I. A.; Gaines, D. F.; Schaeffer R. *J. Am. Chem. Soc.* 1963, 85, 3885-3886.
- [27] Miller, H. C.; Muetterties E. L. *Inorg. Synth.* 1967, 10, 88-92.
- [28] Kuznetsov, N. T.; Klimchuk, G. S. *Russ. J. Inorg. Chem.* 1971, 16, 645-648.
- [29] Wang, F.; Wang, Y.; Wang, X. *Yingyong Huaxue.* 1988, 15(5), 111.
- [30] Solntsev K. A.; Saldin, V. I.; Kuznetsov, N. T. Pat. USSR 1,695,619.
- [31] Harzdorf, C.; Niederprüm, H.; Oclenbach H. Z. *Naturforsch.* 1970, 25B, 6-10.
- [32] Bregadze, V. I.; Timofeev, S. V.; Sivaev, I. B.; Lobanova, I. A. *Russ. Chem. Rev.* 2004, 73, 433-453.
- [33] Sivaev, I. B.; Bregadze, V. I.; Sjöberg, S. *Collect. Czech. Chem. Commun.* 2002, 67, 679-727.
- [34] Sivaev, I. B.; Bregadze, V. I.; Kuznetsov, N. T. *Russ. Chem. Bull., Int. Ed.* 2002, 51, 1362-1374.
- [35] Bernard, R.; Cornu, D.; Luneau, D.; Naoufal, D.; Scharff, J.-P.; Miele, P. *J. Organomet. Chem.* 2005, 690, 2745-2749.
- [36] Bernard, R.; Cornu, D.; Baldeck, P. L.; Časlavsky, J.; Letoffe, J.-M.; Scharff, J.-P.; Miele, P. *Dalton Trans.* 2005, 3065-3071.
- [37] Bernard, R.; Cornu, D.; Scharff, J.-P.; Chiriac, R.; Miele, P.; Baldeck, P. L.; Časlavsky, J. *Inorg. Chem.* 2006, 45, 8743-8748.
- [38] Orlova, A. W.; Kondakov, N. N.; Kimel, B. G.; Kononov, L. O.; Kononova, E. G.; Sivaev, I. B.; Bregadze, V. I. *Appl. Organomet. Chem.* 2007, 21, 98-100.
- [39] Hoffmann, S.; Justus, E.; Ratajski, M.; Lork, E.; Gabel, D. *J. Organomet. Chem.* 2005, 690, 2757-2760.
- [40] Leichtenberg, B.; Gabel, D. *J. Organomet. Chem.* 2005, 690, 2780-2782.
- [41] Lee, J.-D.; Ueno, M.; Miyajima, Y.; Nakamura, H. *Org. Lett.* 2007, 9, 323-326.
- [42] Knoth, W. H. *J. Am. Chem. Soc.* 1967, 89, 1274.
- [43] Knoth, W. H. *Inorg. Chem.* 1971, 10, 598-605.
- [44] Plešek, J.; Jelinek, T.; Drdakova, E.; Heřmanek, S. *Collect. Czech. Chem. Commun.* 1984, 49, 1559-1562.
- [45] Franken, A.; Bullen, N. J.; Jelinek, T.; Thornton-Pett, M.; Teat, S. J.; Clegg, W.; Kennedy, J. D.; Hardie, M. J. *New J. Chem.* 2004, 28, 1499-1505.
- [46] Franken, A.; Kilner, C. A.; Thornton-Pett, M.; Kennedy, J. D. *Collect. Czech. Chem. Commun.* 2002, 67, 869-912.
- [47] Franken, A.; Jelinek, T.; Taylor, R. G.; Ormsby, D. L.; Kilner, C. A.; Clegg, W.; Kennedy, J. D. *Dalton Trans.* 2006, 5753-5769.

- [48] Franken, A.; King, B. T.; Rudolph, J.; Rao, P.; Noll, B. C.; Michl, J. *Collect. Czech. Chem. Commun.* 2001, **66**, 1238-1249.
- [49] Körbe, S.; Sowers, D. B.; Franken, A.; Michl, J. *Inorg. Chem.* 2004, **43**, 8158-8161.
- [50] Körbe, S.; Schreiber, P. J.; Michl, J. *Chem. Rev.* 2006, **106**, 5208-5249.
- [51] Heying, T. L.; Ager, J. W.; Clark, S. L.; Mangold, D. J.; Goldstein, H. L.; Hillman, M.; Polak, R. J.; Szymanski, J. W. *Inorg. Chem.* 1963, **2**, 1089-1092.
- [52] Fein, M. M.; Bobinski, J.; Mayes, N.; Schwartz, N.; Cohen, M. S. *Inorg. Chem.* 1963, **2**, 1111-1115.
- [53] Zakharkin, L. I.; Stanko, V. I.; Brattsev, V. A.; Chapovsky, Yu. A.; Struchkov, Yu. T. *Russ. Chem. Bull.* 1963, **12**, 1911.
- [54] Zakharkin, L. I.; Stanko, V. I.; Brattsev, V. A.; Chapovsky, Yu. A.; Okhlobystin, O. Yu. *Russ. Chem. Bull.* 1963, **12**, 2074.
- [55] Grimes, R. N. *Carboranes*, Academic Press: New York, NY, 1970.
- [56] Bregadze, V. I. *Chem. Rev.* 1992, **92**, 209-223.
- [57] Valliant, J. F.; Guenther, K. J.; King, A. S.; Morel, P.; Schaffer, P.; Sogbein, O. O.; Stephenson, K. A. *Coord. Chem. Rev.* 2002, **232**, 173-230.
- [58] Grushin, V. V.; Bregadze, V. I.; Kalinin, V. N. *J. Organomet. Chem. Libr.* 1988, **20**, 1-68.
- [59] Zakharkin, L. I.; Kirillova, V. S. *Russ. Chem. Bull.* 1975, **12**, 2484-2486.
- [60] Tomita, H.; Luu, H.; Onak, T. *Inorg. Chem.* 1991, **30**, 812-815.
- [61] Hawthorne, M. F.; Young, D. C.; Wegner, P. A. *J. Am. Chem. Soc.* 1965, **87**, 1818-1819.
- [62] Hawthorne, M. F.; Young, D. C.; Andrews, T. D.; Hove, D. V.; Pilling, R. L.; Pitts, A. D.; Reinjes, M.; Warren, L. F.; Wegner, P. A. *J. Am. Chem. Soc.* 1968, **90**, 879-896.
- [63] Sivaev, I. B.; Bregadze, V. I. *Collect. Czech. Chem. Commun.* 1999, **64**, 783-805.
- [64] Gashti, A. N.; Huffman, J. C.; Edwards, A.; Szekely, G.; Siedle, A. R.; Karty, J. A.; Reilly, J. P.; Todd, L. J. *J. Organomet. Chem.* 2000, **614-615**, 120-124.
- [65] Santos, E. C.; Pinkerton, A. B.; Kinkead, S. A.; Hurlburt, P. K.; Jasper, S. A.; Sellers, C. W.; Huffman, J. C.; Todd, L. J. *Polyhedron* 2000, **19**, 1777-1781.
- [66] Plešek, J.; Grüner, B.; Bača, J.; Fusek, J.; Cisařova, I. *J. Organomet. Chem.* 2002, **649**, 181-190.
- [67] Sivaev, I. B.; Starikova, Z. A.; Sjöberg, S.; Bregadze, V. I. *J. Organomet. Chem.* 2002, **649**, 1-8.
- [68] Plešek, J.; Grüner, B.; Hermanek, S.; Baca, J.; Marecek, V.; Janchenova, J.; Lhotsky, A.; Holub, K.; Selucky, P.; Rais, J.; Cisařova, I.; Caslavsky, J. *Polyhedron*. 2002, **21**, 975-986.
- [69] Teixidor, F.; Pedrajas, J.; Rojo, I.; Viñas, C.; Kivekäs, R.; Sillanpää, R.; Sivaev, I.; Bregadze, V.; Sjöberg, S. *Organometallics*. 2003, **22**, 3414-3423.
- [70] Olejniczak, A. B.; Plešek, J.; Kriz, O.; Lesnikowski, Z. *J. Angew. Chem. Int. Ed.* 2003, **42**, 5740-5743.
- [71] Hao, E.; Vivente, M. G. H. *Chem. Commun.* 2005, 1306-1308.
- [72] Hao, E.; Jensen, T. J.; Courtney, B. H.; Vicente, M. G. H. *Bioconjugate Chem.* 2005, **16**, 1495-1502.
- [73] Plešek, J. *Chem. Rev.* 1992, **92**, 269-278.
- [74] Schroeder, M. A. *J. Propul. Power.* 1998, **14**, 981-990.

- [75] Bregadze, V. I.; Sivaev, I. B.; Glazun S. A. *Anti-Cancer Agents Med. Chem.* 2006, *6*, 75-109.
- [76] Barth, R. F.; Soloway A. H.; Fairchild, R. G. *Cancer Res.* 1990, *50*, 1061-1070.
- [77] Barth, R. F.; Coderre, J. A.; Vicente, M. G. H.; Blue, T. E. *Clin. Cancer Res.* 2005, *11*, 3987-4002.
- [78] Hawthorne, M. F. *Angew. Chem., Int. Ed. Engl.* 1993, *32*, 950-984.
- [79] Soloway, A. H.; Tjarks, W.; Barnum, B. A.; Rong, F.-G.; Barth, R. F.; Codogni, I. M.; Wilson, J. G. *Chem. Rev.* 1998, *98*, 1515-1562.
- [80] Salt, C.; Lennox, A. J.; Takagaki, M.; Maguire, J. A.; Hosmane, N. S. *Russ. Chem. Bull. Int. Ed.*, 2004, *53*, 1871-1888.
- [81] Schinazi, R. F.; Lesnikowski, Z. J. *Nucleosides Nucleotides.* 1998, *17*, 635-647.
- [82] Soloway, A. H.; Zhuo, J.-C.; Rong, F. G.; Lunato, A. J.; Ives, D. H.; Barth, R. F.; Anisuzzaman, A. K. M.; Barth, C. D.; Barnum, B. A. *J. Organomet. Chem.* 1999, *581*, 150-155.
- [83] Lesnikowski, Z. J.; Shi, J.; Schinazi, R. F. *J. Organomet. Chem.* 1999, *581*, 156-169.
- [84] Tjarks, W. *J. Organomet. Chem.* 2000, *614-615*, 37-47.
- [85] Byun, Y.; Narayanasamy, S.; Johnsamuel, J.; Bandyopadhyaya, A. K.; Tiwari, R.; Al-Madhoun, A. S.; Barth, R. F.; Eriksson, S.; Tjarks, W. *Anti-Cancer Agents Med. Chem.* 2006, *6*, 127-144.
- [86] Bandyopadhyaya, A. K.; Tiwari, R.; Tjarks, W. *Bioorg. Med. Chem.* 2006, *14*, 6924-6932.
- [87] Lesnikowski, Z. J.; Paradowska, E.; Olejniczak, A. B.; Studzinska, M.; Seekamp, P.; Schüßler, U.; Gabel, D.; Schinazi, R. F.; Plešek, J. *Bioorg. Med. Chem.* 2005, *13*, 4168-4175.
- [88] Olejniczak, A. B.; Plešek, J.; Lesnikowski, Z. J. *J. Exp. Psychology-Apppl.* 2007, *13*, 311-318.
- [89] Brattsev, V. A.; Stanko, V. I. *Zh. Obshch. Khim.* 1969, *39*, 1175-1178.
- [90] Zakharkin, L. I.; Grebennikov, A. V.; L'vov, A. I. *Russ. Chem. Bull.* 1970, *19*, 97-102.
- [91] Leukart, O.; Caviezel, M.; Eberle, A.; Escher, E.; Tun-Kyi, A.; Schwyzer, R. *Helv. Chim. Acta.* 1976, *59*, 2184-2187.
- [92] Wyzlic, I. M.; Soloway A. H. *Tetrahedron Lett.* 1992, *33*, 7489-7490.
- [93] Wyzlic, I. M.; Tjarks, W.; Soloway, A. H.; Perkins, D. J.; Burgos, M.; O'Reilly, K. P. *Inorg. Chem.* 1996, *35*, 4541-4547.
- [94] Fauchere, J. L.; Leukart, O.; Eberle, A.; Schwyzer, R. *Helv. Chim. Acta.* 1979, *62*, 1385-1395.
- [95] Karnbrock, W.; Musiol, H.-J.; Moroder, L. *Tetrahedron.* 1995, *51*, 1187-1196.
- [96] Radel, P. A.; Kahl, S. B. *J. Org. Chem.* 1996, *61*, 4582-4588.
- [97] Lindström, P.; Naeslund, C.; Sjöberg S. *Tetrahedron Lett.* 2000, *41*, 751-754.
- [98] Ujvary, I.; Nachman, R. *J. Peptides.* 2001, *22*, 287-290.
- [99] Srivastava, R. R.; Singhaus, R. R.; Kabalka, G. W. *J. Org. Chem.* 1997, *62*, 4476-4478.
- [100] Srivastava, R. R.; Kabalka, G. W. *J. Org. Chem.* 1997, *62*, 8730-8734.
- [101] Das, B. C.; Kabalka, G. W.; Srivastava, R. R.; Bao, W.; Das, S.; Li, G. *J. Organomet. Chem.* 2000, *614-615*, 255-261.
- [102] Kabalka, G. M.; Das, B. C.; Das, S.; Li, G.; Srivastava, R.; Natarajan, N.; Khan, M. K. *Collect. Czech. Chem. Commun.* 2002, *67*, 836-842.

- [103] Beletskaya, I. P.; Bregadze, V. I.; Osipov, S. N.; Petrovskii, P. V.; Starikova, Z. A.; Timofeev S. V. *Synlett.* 2004, 1247-1248.
- [104] Timofeev, S. V.; Bregadze, V. I.; Osipov, S. N.; Titanyuk, I. D.; Petrovskii, P. V.; Starikova, Z. A.; Glukhov, I. V.; Beletskaya, I. P. *Russ. Chem. Bull.* 2007, 56, 761-767.
- [105] Kabalka, G. W.; Yao, M.-L. *Anti-Cancer Agents Med. Chem.* 2006, 6, 111-125.
- [106] Sivaev, I. B.; Semioshkin, A. A.; Brelochs, B.; Sjöberg, S.; Bregadze, V. I. *Polyhedron.* 2000, 19, 627-632.
- [107] Kasar, R. A.; Knudsen, G. M.; Kahl, S. B. *Inorg. Chem.* 1999, 38, 2936-2940.
- [108] Ol'shevskaya, V. A.; Ayuob, R.; Brechko, Zh. G.; Petrovskii, P.V.; Kononova, E. G.; Levit, G. L.; Krasnov, V. P.; Charushin, V. N.; Chupakhin, O. N., Kalinin, V. N. *J. Organomet. Chem.* 2005, 690, 2761-2765.
- [109] Maurer, J. L.; Serino, A. J.; Hawthorne, M. F. *Organometallics* 1988, 7, 2519-2524.
- [110] Maurer, J. L.; Berchier, F.; Serino, A. J.; Knobler, C. B.; Hawthorne, M. F. *J. Org. Chem.* 1990, 57, 838-843.
- [111] Tjarks, W.; Anisuzzaman, A. K. M.; Liu, L.; Soloway, A. H.; Barth, R. F.; Perkins, D. J.; Adam, D. M. *J. Med. Chem.* 1992, 35, 1628-1633.
- [112] Dahlhoff, W. V.; Bruckmann, J.; Angermund, K.; Krüger, C. *Liebigs Ann. Chem.* 1993, 831-835.
- [113] Das, B. C.; Das, S.; Li, G.; Bao, W.; Kabalka, G. W. *Synlett.* 2001, 1419-1420.
- [114] Raddatz, S.; Marcello, M.; Kliem, H.-C.; Tröster, H.; Trendelenburg, M. F.; Oeser, T.; Granzow, C.; Wiessler, M. *Chem. Bio. Chem.* 2004, 474-482.
- [115] Ronchi, S.; Prosperi, D.; Compostella, F.; Panza, L. *Synlett.* 2004, 1007-1010.
- [116] Yamazaki, N.; Kojima, S.; Bovin, N. V.; Andre, S.; Gabius, S.; Gabius, H.-J. *Adv. Drug Deliv. Rev.* 2000, 43, 225-244.
- [117] Giovenzana, G. B.; Lay, L.; Monty, D.; Palmisano, G.; Panza, L. *Tetrahedron.* 1999, 55, 14123-14136.
- [118] Tietze, L. F.; Bothe, U. *Chem. Eur. J.* 1998, 4, 1179-1183.
- [119] Tietze, L. F.; Bothe, U.; Schuberth, I. *Chem. Eur. J.* 2000, 6, 836-842.
- [120] Tietze, L. F.; Bothe, U.; Griesbach, U.; Nakaichi, M.; Hasegawa, T.; Nakamura, H.; Yamamoto, Y. *Bioorg. Med. Chem.* 2001, 9, 1747-1752.
- [121] Tietze, L. F.; Bothe, U.; Griesbach, U.; Nakaichi, M.; Hasegawa, T.; Nakamura, H.; Yamamoto, Y. *ChemBioChem.* 2001, 2, 326-334.
- [122] Tietze, L. F.; Griebach, U.; Schuberth, I.; Bothe, U.; Marra, A.; Dondoni, A. *Chem. Eur. J.* 2003, 9, 1296-1302.
- [123] Basak, P.; Lowary, T. L. *Can. J. Chem.* 2002, 80, 943-948.
- [124] Orlova, A. V.; Zinin, A. I.; Malysheva, N. N.; Kononov, L. O.; Sivaev, I. B.; Bregadze, V. I. *Russ. Chem. Bull. , Int. Ed.* 2003, 52, 2766-2768.
- [125] Kononov, L. O.; Orlova, A. V.; Zinin, A. I.; Kimel, B. G.; Sivaev, I. B.; Bregadze, V. I. *J. Organomet. Chem.* 2005, 690, 2769-2774.
- [126] Orlova, A. V.; Kononov, L. O.; Kimel, B. G.; Sivaev, I. B.; Bregadze, V. I. *Appl. Organomet. Chem.* 2006, 20, 416-420.
- [127] Orlova, A. V.; Kondakov, N. N.; Zinin, A. I.; Kimel, B. G.; Kononov, L. O.; Sivaev, I. B.; Bregadze, V. I. *Russ. Chem. Bull. , Int. Ed.*, 2005, 54, 1352-1353.
- [128] Orlova, A. V.; Kondakov, N. N.; Zinin, A. I.; Kimel, B. G.; Kononov, L. O.; Sivaev, I. B.; Bregadze, V. I. *Russ. J. Bioorg. Chem.* 2006, 32, 568-577.

- [129] Ronchi, S.; Prosperi, D.; Thimon, C.; Morin, C.; Panza, L. *Tetrahedron Asym.*, 2005, **16**, 39-44.
- [130] Hausman, W. *Biochem. Z.* 1909, **14**, 275-278.
- [131] Vicente, M. G. H. *Curr. Med. Chem. - Anti-Cancer Agents*. 2001, **1**, 175-194.
- [132] Haushalter, R. C.; Rudolph, R. W. *J. Am. Chem. Soc.* 1978, **100**, 4628-4629.
- [133] Haushalter, R. C.; Butler, W. M.; Rudolph, R. W. *J. Am. Chem. Soc.* 1981, **103**, 2620-2627.
- [134] Bregadze, V. I.; Sivaev, I. B.; Gabel, D.; Wöhrle, D. *J. Porphyrins Phthalocyanines*. 2001, **5**, 767-781.
- [135] Evstigneeva, R. P.; Zaitsev, A. V.; Luzgina, V. N.; Ol'shevskaya, V. A.; Shtil, A. A. *Curr. Med. Chem. - Anti-Cancer Agents*. 2003, **3**, 383-392.
- [136] Renner, M. W.; Miura, M.; Easson, M. W.; Vicente, M. G. H. *Anti-Cancer Agents Med. Chem.* 2006, **6**, 145-157.
- [137] Sibrian-Vazquez, M.; Hao, E.; Jensen, T. J.; Vicente, M. G. H. *Bioconjugate Chem.* 2006, **17**, 928-934.
- [138] Koo, M.-S.; Ozawa, T.; Santos, R. A.; Lamborn, K. R.; Bollen, A. W.; Deen, D. F.; Kahl, S. B. *J. Med. Chem.* 2007, **50**, 820-827.
- [139] Ol'shevskaya, V. A.; Zaitsev, A. V.; Luzgina, V. N.; Kondratieva, T. T.; Ivanov, O. G.; Kononova, E. G.; Petrovskii, P. V.; Mironov, A. F.; Kalinin, V. N.; Hofmann, J.; Shtil, A. A. *Bioorg. Med. Chem.* 2006, **14**, 109-120.
- [140] Hill, J. S.; Kahl, S. B.; Kaye, A. H.; Stylli, S. S.; Koo, M. S.; Gonzales, M. F.; Verdaxis, N. J.; Johnson, C. I. *Proc. Natl. Acad. Sci. USA*. 1992, **89**, 1785-1789.
- [141] Ceberg, C. P.; Brun, A.; Kahl, S. B.; Koo, M. S.; Persson, B. R. R.; Salford, L. G. *J. Neurosurg.* 1995, **83**, 86-92.
- [142] Hill, J. S.; Kahl, S. B.; Stylli, S. S.; Nakamura, Y.; Koo, M.-S.; Kaye, A. H. *Proc. Natl. Acad. Sci. USA*. 1995, **92**, 12126-12130.
- [143] Tibbitts, J.; Fike, J. R.; Lamborn, K. R.; Bollen, A. W.; Kahl, S. B. *Photochem. Photobiol.* 1999, **69**, 587-594.
- [144] Tibbitts, J.; Sambol, N. C.; Fike, J. R.; Bauer, W. F.; Kahl, S. B. *J. Pharm. Sci.* 2000, **89**, 469-477.
- [145] Ozawa, T.; Afzal, J.; Lamborn, K. R.; Bollen, A. W.; Bauer, W. F.; Koo, M. S.; Kahl, S. B.; Deen, D. F. *Int. J. Rad. Oncol. Biol. Phys.* 2005, **63**, 247-252.
- [146] Ratajski, M.; Osterloh, J.; Gabel, D. *Anti-Cancer Agents Med. Chem.* 2006, **6**, 159-166.
- [147] Grin, M.A.; Semioshkin, A. A.; Titeev, R. A.; Nizhnik, E. A.; Grebenyuk, J. N.; Mironov, A. F.; Bregadze, V. I. *Mendeleev Commun.* 2007, **17**, 14-15.
- [148] Luguya, R.; Jensen, T. J.; Smith, K. M.; Vicente, M. G. H. *Bioorg. Med. Chem.* 2006, **14**, 5890-5897.
- [149] Gottumukkala, V.; Ongayi, O.; Baker, D. G.; Lomax, L. G.; Vicente, M. G. H. *Bioorg. Med. Chem.* 2006, **14**, 1871-1879.
- [150] Wu, H.; Micca, P. L.; Makar, M. S.; Miura, M. *Bioorg. Med. Chem.* 2006, **14**, 5083-5092.
- [151] Fabris, C.; Jori, G.; Giuntini, F.; Rincucci, G. *J. Photochem. Photobiol. B* 2001, **64**, 1-7.
- [152] Giuntini, F.; Raoul, Y.; Dei, D.; Municchi, M.; Chiti, G.; Fabris, C.; Colautti, P.; Jori, G.; Roncucci, G. *Tetrahedron Lett.* 2005, **46**, 2979-2982.
- [153] Tsaryova, O.; Semioshkin, A., Wöhrle, D.; Bregadze, V. I. *J. Porphyrins Phthalocyanines*. 2005, **9**, 268-274.

- [154] Semioshkin, A.; Tsaryova, O.; Zhidkova, O.; Bregadze, V.; Wöhrle, D. *J. Porphyrins Phthalocyanines*. 2007, *10*, 1293-1300.
- [155] Ghaneolhosseini, H.; Tjarks, W.; Sjöberg, S. *Tetrahedron*. 1998, *54*, 3877-3884.
- [156] Tjarks, W.; Ghaneolhosseini, H.; Hensen, C. L. A.; Malmquist, J.; Sjöberg S. *Tetrahedron Lett.* 1996, *37*, 6905-6908.
- [157] Ghaneolhosseini, H.; Tjarks, W.; Sjöberg, S. *Tetrahedron*. 1997, *55*, 17519-17526.
- [158] Gedda, L.; Ghaneolhosseini, H.; Nilsson, P.; Nyholm, K.; Pettersson, J.; Sjöberg, S.; Carlsson, J. *Anti-Cancer Drug Design*. 2000, *15*, 277-286.
- [159] Kelly, D. P.; Bateman, S. A.; Martin, R. E.; Reum, M. E.; Rose, M.; Whittaker, A. D. *Aust. J. Chem.* 1994, *47*, 247-262.
- [160] Bateman, S. A.; Kelly, D. P.; Martin, R. F.; White, J. M. *Aust. J. Chem.* 1999, *52*, 291-301.
- [161] Hariharan, J. R.; Wyzlic, I. M.; Soloway, A. H. *Polyhedron*. 1995, *14*, 823-825.
- [162] Cai, J.; Soloway, A. H. *Tetrahedron Lett.* 1996, *37*, 9283-9286.
- [163] Cai, J.; Soloway, A. H.; Barth, R. F.; Adams, D. M.; Hariharan, J. R.; Wyzlic, I. M.; Radcliffe, K. *J. Med. Chem.* 1997, *40*, 3887-3896.
- [164] Zhuo, J.-C.; Cai, J.; Soloway, A. H.; Barth, R. F.; Adams, D. M.; Ji, W.; Tjarks, W. *J. Med. Chem.* 1999, *42*, 1282-1292.
- [165] Wu, G.; Barth, R. F.; Yang, W.; Lee, R. J.; Tjarks, W.; Backer, M. V.; Backer, J. M. *Anti-Cancer Agents Med. Chem.* 2006, *6*, 167-184.
- [166] Alam, F.; Soloway, A. H.; Barth, R. F. *Antibody Immunoconjugates Radiopharm.* 1989, *2*, 145-163.
- [167] Alam, F.; Soloway, A. H.; McGuire, J. E.; Barth, R. F.; Carey, W. E.; Adams, D. M. *J. Med. Chem.* 1985, *28*, 522-525.
- [168] Alam, F.; Soloway, A. H.; Barth, R. F.; Mafune, N.; Adams, D. M.; Knoth, W. H. *J. Med. Chem.* 1989, *32*, 2326-2330.
- [169] Novick, S.; Quastel, M. R.; Marcus, S.; Chipman, D.; Shani, G.; Barth, R. F.; Soloway, A. H. *Nucl. Med. Biol.* 2002, *29*, 159-167.
- [170] Barth, R. F.; Adams, D. M.; Soloway, A. H.; Alam, F.; Darby, M. V. *Bioconjugate Chem.* 1994, *5*, 58-66.
- [171] Liu, L.; Barth, R. F.; Adams, D. M.; Soloway, A. H.; Reisfeld, R. A. *Anticancer Res.* 1996, *16*, 2581-2588.
- [172] Wu, G.; Barth, R. F.; Yang, W.; Chatterjee, M.; Tjarks, W.; Ciesielski, M. J.; Fenstermaker, R. A. *Bioconjugate Chem.* 2004, *15*, 185-194.
- [173] Barth, R. F.; Wu, G.; Yang, W.; Binns, P. J.; Riley, K. J.; Patel, H.; Coderre, J. A.; Tjarks, W.; Bandyopadhyaya, A. K.; Thirumamagal, B. T.; Ciesielski, M. J.; Fenstermaker, R. A. *Appl. Radiat. Isot.* 2004, *61*, 899-903.
- [174] Capala, J.; Barth, R. F.; Bendayan, M.; Lauzon, M.; Adams, D. M.; Soloway, A. H.; Fenstermaker, R. A.; Carlsson, J. *Bioconjugate Chem.* 1996, *7*, 7-15.
- [175] Yang, W.; Barth, R. F.; Wu, G.; Bandyopadhyaya, A. K.; Thirumamagal, B. T.; Tjarks, W.; Binns, P. J.; Riley, K.; Patel, H.; Coderre, J. A.; Ciesielski, M. J.; Fenstermaker, R. A. *Appl. Radiat. Isot.* 2004, *61*, 981-985.
- [176] Backer, M. V.; Gaynutdinov, T. I.; Patel, V.; Bandyopadhyaya, A. K.; Thirumamagal, B. T.; Tjarks, W.; Barth, R. F.; Claffey, K.; Backer, J. M. *Mol. Cancer Ther.* 2005, *4*, 1423-1429.

- [177] Shukla, S.; Wu, G.; Chatterjee, M.; Yang, W.; Sekido, M.; Diop, L. A.; Muller, R.; Sudimack, J. J.; Lee, R. J.; Barth, R. F.; Tjarks, W. *Bioconjugate Chem.* 2003, **14**, 158-167.
- [178] Parrott, M. C.; Marchington, E. B.; Valliant, J. F.; Adronov, A. *J. Am. Chem. Soc.* 2005, **127**, 12081-12089.
- [179] Thomas, J.; Hawthorne, M. F. *Chem. Commun.* 2001, 1884-1885.
- [180] Holmberg, A.; Meurling, L. *Bioconjugate Chem.* 1993, **4**, 570-573.
- [181] Carlsson, J.; Gedda, L.; Gronvik, C.; Hartman, T.; Lindström, A.; Lindström, P.; Lundqvist, H.; Lovqvist, A.; Malmqvist, J.; Olsson, P.; Essand, M.; Ponten, J.; Sjöberg, S.; Westermark, B. *Int. J. Radiat. Oncol. Biol. Phys.* 1994, **30**, 105-115.
- [182] Gedda, L.; Ollson, P.; Ponten, J.; Carlsson, J. *Bioconjugate Chem.* 1996, **7**, 574-591.
- [183] Mehta, S. C.; Lu, D. R. *Pharm. Res.* 1996, **13**, 344-51.
- [184] Olsson, P.; Gedda, L.; Goike, H.; Liu, L.; Collins, V. P.; Ponten, J.; Carlsson, J. *Anticancer Drug Des.* 1998, **13**, 279-289.
- [185] Sano, T. *Bioconjugate Chem.* 1999, **10**, 905-911.
- [186] Primus, F. J.; Pak, R. H.; Rickard-Dickson, K. J.; Szalai, G.; Bolen, J. L.; Kane, R. R.; Hawthorne, M. F. *Bioconjugate Chem.* 1996, **7**, 532-535.
- [187] Kahl, S. B. *Tetrahedron Lett.* 1990, **31**, 1517-1520.
- [188] Feakes, D. A.; Spinler, J. K.; Harris, F. R. *Tetrahedron*. 1999, **55**, 11177-11186.
- [189] Ji, B.; Peacock, G.; Lu, D. R. *Bioorg. Med. Chem. Lett.* 2002, **12**, 2455-2458.
- [190] Alanazi, F.; Li, H.; Halpern, D. S.; Øie, S.; Lu, D. R. *Int. J. Pharm.* 2003, **255**, 189-197.
- [191] Peacock, G. F.; Ji, B.; Wang, C. K.; Lu, D. R. *Drug. Deliv.* 2003, **10**, 29-34.
- [192] Peacock, G.; Sidwell, R.; Pan, G.; Øie, S.; Lu, D. R. *J. Pharm. Sci.* 2004, **93**, 13-19.
- [193] Pan, G.; Øie, S.; Lu, D. R. *Pharm. Res.* 2005, **21**, 1257-1262.
- [194] Dozzo, P.; Koo, M.-S.; Berger, S.; Forte, T. M.; Kahl, S. B. *J. Med. Chem.* 2005, **48**, 357-359.
- [195] Maruyama, K. *Drug Delivery Syst.* 2005, **20**, 35-41.
- [196] Maruyama, K.; Ishida, O.; Kasaoka, S.; Takizawa, T.; Utoguchi, N.; Shinohara, A.; Chiba, M.; Kobayashi, H.; Eriguchi, M.; Yanagie, H. *J. Control Rel.* 2004, **98**, 195-207.
- [197] Miyajima, Y.; Nakamura, H.; Kuwata, Y.; Lee, J.-D.; Masunaga, S.; Ono, K.; Maruyama, K. *Bioconjugate Chem.* 2006, **17**, 1314-1320.
- [198] Bohl Kullberg, E.; Bergstrand, N.; Carlsson, J.; Edwards, K.; Johnsson, M.; Sjöberg, S.; Gedda, L. *Bioconjugate Chem.* 2002, **13**, 737-743.
- [199] Bohl Kullberg, E.; Nestor, M.; Gedda, L. *Pharm. Res.* 2003, **20**, 229-236.
- [200] Bohl Kullberg, E.; Carlsson, J.; Edwards, K.; Capala, J.; Sjöberg, S.; Gedda, L. *Int. J. Oncol.* 2003, **23**, 461-467.
- [201] Bohl Kullberg, E.; Wei, Q.; Capala, J.; Giusti, V.; Malmström, P.-U.; Gedda, L. *Int. J. Radiat. Biol.* 2005, **81**, 621-629.
- [202] Wei, Q.; Bohl Kullberg, E.; Gedda, L. *Int. J. Oncol.* 2003, **23**, 1159-1165.
- [203] Thirumamagal, B. T. S.; Zhao, X. B.; Bandyopadhyaya, A. K.; Narayanasamy, S.; Johns Samuel, J.; Tiwari, R.; Golightly, D. W.; Patel, V.; Jehning, B. T.; Backer, M. V.; Barth, R. F.; Lee, R. J.; Backer, J. M.; Tjarks, W. *Bioconjugate Chem.* 2006, **17**, 1141-1150.
- [204] Krijger, G. C.; Fretz, M. M.; Woroniecka, U. D.; Steinebach, O. M.; Jiskoot, W.; Storm, G.; Koning, G. A. *Radiochim. Acta*. 2005, **93**, 589-593.

- [205] Sudimack, J. J.; Adams, D.; Rotaru, J.; Shukla, S.; Yan, J.; Sekido, M.; Barth, R. F.; Tjarks, W.; Lee, R. *J. Pharm. Res.* 2002, **19**, 1502-1508.
- [206] Pan, X. Q.; Wang, H.; Shukla, S.; Sekido, M.; Adams, D. M.; Tjarks, W.; Barth, R. F.; Lee, R. *J. Bioconjugate Chem.* 2002, **13**, 435-442.
- [207] Pan, X. Q.; Wang, H.; Lee, R. *J. Anticancer Res.* 2002, **22**, 1629-1633.
- [208] Stephenson, S. M.; Yang, W.; Stevens, P. J.; Tjarks, W.; Barth, R. F.; Lee, R. *J. Anticancer Res.* 2003, **23**, 3341-3345.
- [209] Mehta, S. C.; Lai, J. C. K.; Lu, D. R. *J. Microencapsul.* 1996, **13**, 269-279.
- [210] Ji, B.; Chen, W.; Lu, D. R.; Halpern, D. S. *Drug Deliv.* 2001, **8**, 13-17.
- [211] Awad, D.; Tabod, I.; Lutz, S.; Wessolowski, H.; Gabel, D. *J. Organomet. Chem.* 2005, **690**, 2732-2735.
- [212] Pavanetto, F.; Perugini, P.; Genta, I.; Minoia, C.; Ronchi, A.; Prati, U.; Roveda, L.; Nano, R. *Drug. Deliv.* 2000, **7**, 97-103.
- [213] Martini, S.; Ristori, S.; Pucci, A.; Bonechi, C.; Becciolini, A.; Martini, G.; Rossi, C. *Biophys. Chem.* 2004, **111**, 27-34.
- [214] Shelly, K.; Feakes, D. A.; Hawthorne, M. F.; Schmidt, P. G.; Krisch, T. A.; Bauer, W. F. *Proc. Natl. Acad. Sci. USA.* 1992, **89**, 9039-9043.
- [215] Feakes, D. A.; Shelly, K.; Knobler, C. B.; Hawthorne, M. F. *Proc. Natl. Acad. Sci. USA.* 1994, **91**, 3029-3033.
- [216] Hawthorne, M. F.; Shelly, K.; Li, F. *Chem. Commun.* 2002, 547-554.
- [217] Feakes, D. A., Waller, R. C.; Hathaway, D. K.; Morton, V. S. *Proc. Natl. Acad. Sci. USA.* 1999, **96**, 6406-6410.
- [218] Watson-Clark, R. A.; Banquerigo, M. L.; Shelly, K.; Hawthorne, M. F.; Brahn, E. *Proc. Natl. Acad. Sci. USA.* 1998, **95**, 2531-2534.
- [219] Moraes, A. M.; Santana, M. H. A.; Carbonell, R. G. *J. Microencapsul.* 1999, **16**, 647-664.
- [220] Zhou, R.; Balasubramanian, S. V.; Kahl, S. B.; Straubinger, R. M. *J. Pharm. Sci.* 1999, **88**, 912-917.
- [221] Ristori, S.; Oberdisse, J.; Grillo, I.; Donati, A.; Spalla, O. *Biophys. J.* 2005, **88**, 535-547.
- [222] Rossi, S.; Schinazi, R. F.; Martini, G. *Biochim. Biophys. Acta* 2005, **1712**, 81-91.
- [223] Feakes, D. A.; Shelly, K.; Hawthorne, M. F. *Proc. Natl. Acad. Sci. USA* 1995, **92**, 1367-1370.
- [224] Nakamura, H.; Miyajima, Y.; Takei, T.; Kasaoka, S.; Maruyama, K. *Chem. Commun.* 2004, 1910-1911.
- [225] Li, T.; Hamdi, J.; Hawthorne, M. F. *Bioconjugate Chem.* 2006, **17**, 15-20.
- [226] Harling, O. K.; Riley, K. *J. J. Neurooncol.* 2003, **62**, 7-17.
- [227] Blue, T. E.; Yanch, J. C. *J. Neurooncol.* 2003, **62**, 19-31.
- [228] Culbertson, C. N.; Green, S.; Mason, A. J.; Picton, D.; Baugh, G.; Hugtenburg, R. P.; Yin, Z.; Scott, M. C.; Nelson, J. M. *Appl. Radiat. Isot.* 2004, **61**, 733-738.
- [229] Pisent, A.; Colautti, P.; Esposito, J.; De Nardo, L.; Conte, V.; Agosteo, D.; Jori, G.; Posocco, P. A.; Tecchio, L. B.; Tinti, R.; Rosi, G. *J. Phys.: Conf. Ser.* 2006, **41**, 391-399.
- [230] Yanch, J. C.; Shortkroff, S.; Shefer, R. E.; Johnson, S.; Binello, E.; Gierga, D.; Jones, A. G.; Young, G.; Vivieros, C.; Davison, A.; Sledge, C. *Med. Phys.* 1999, **26**, 364-375.
- [231] Gierga, D. P.; Yanch, J. C.; Shefer, R. E. *Med. Phys.* 2000, **27**, 203-214.

- [232] Watson-Clark, R. A.; Banquerigo, M. L.; Shelly, K.; Hawthorne, M. F.; Brahn, E. *Proc. Natl. Acad. Sci. USA.* 1998, **95**, 2531-2534.
- [233] Valliant, J. F.; Schaffer, P.; Britten, J. F.; Davison, A.; Jones, A. G.; Yanch, J. C. *Tetrahedron Lett.* 2000, **41**, 1355-1358.
- [234] Hawthorne, M. F.; Maderna, A. *Chem. Rev.* 1999, **99**, 3421-3434.
- [235] Adam, M. J.; Wilbur, D. S. *Chem. Soc. Rev.* 2005, **34**, 153-163.
- [236] Tolmachev, V.; Sjöberg, S. *Collect. Czech. Chem. Commun.* 2002, **67**, 913-935.
- [237] Mizusawa, E. A.; Thompson, M. R.; Hawthorne, M. F. *Inorg. Chem.* 1985, **24**, 1911-1916.
- [238] Winberg, K. J.; Persson, M.; Mamström, P.-U.; Sjöberg, S.; Tolmachev, V. *Nucl. Med. Biol.* 2004, **31**, 425-433.
- [239] Sivaev, I. B.; Bruskin, A. B.; Nesterov, V. V.; Antipin, M. Yu.; Bregadze, V. I.; Sjöberg, S. *Inorg. Chem.* 1999, **38**, 5887-5893.
- [240] Orlova, A.; Bruskin, A.; Sivaev, I.; Sjöberg, S.; Lundqvist, H.; Tolmachev, V. *Anticancer Res.* 2006, **26**, 1217-1223.
- [241] Nestor, M.; Persson, M.; Cheng, J.; Tolmachev, V.; van Dongen, G.; Anniko, M.; Kairemo, K. *Bioconjugate Chem.* 2003, **14**, 805-810.
- [242] Cheng, J.; Persson, M.; Tolmachev, V.; Sivaev, I.; Orlova, A.; Kairemo, K.; Anniko, M. *Acta Otolaryngol.* 2004, **124**, 1078-1085.
- [243] Bruskin, A.; Sivaev, I.; Persson, M.; Lundqvist, H.; Carlsson, J.; Sjöberg, S.; Tolmachev, V. *Nucl. Med. Biol.* 2004, **31**, 205-211.
- [244] Tran, T.; Orlova, A.; Sivaev, I.; Sandström, M.; Tolmachev, V. *Int. J. Mol. Med.* 2007, **19**, 485-493.
- [245] Hanlin, D. K.; Chyan, M.-K.; Wilbur, D. S. *Abstr. 5th Int. Symp. Radiohalogens*, Whistler, Canada, 2004, CS18.
- [246] Wilbur, D. S.; Hamlin, D. K.; Pathare, P. M.; Kegley, B. B. *J. Label. Compd. Radiopharm.* 1999, **42**, S288-S290.
- [247] Tolmachev, V.; Bruskin, A.; Carlsson, J.; Lundqvist, H.; Sjöberg, S. *J. Radioanal. Nucl. Chem.* 2004, **261**, 107-112.
- [248] Tolmachev, V.; Koziorowski, J.; Sivaev, I.; Lundquist, H.; Carlsson, J.; Orlova, A.; Gedda, L.; Olsson, P.; Sjöberg, S.; Sundin, A. *Bioconjugate Chem.* 1999, **10**, 338-345.
- [249] Wilbur, D. S.; Hamlin, D. K.; Foulon, C. F.; Zalutsky, M. R.; Pathare, P. M. *J. Label. Compd. Radiopharm.* 1997, **40**, 76-78.
- [250] Wilbur, D. S.; Hamlin, D. K.; Chyan, M.-K.; Kegley, B. B.; Quinn, J.; Vessella, R. L. *Bioconjugate Chem.* 2004, **15**, 601-616.
- [251] Chyan, M.-K.; Hamlin, D. K.; Wilbur, D. S. *Abstr. 5th Int. Symp. Radiohalogens*, Whistler, Canada, 2004, CS23.
- [252] Sjöström, A.; Tolmachev, V.; Koziorowski, J.; Lebeda, O.; Einarsson, L.; Sjöberg, S.; Carlsson, J.; Lundqvist, H. *Nucl. Med. Commun.* 2000, **21**, 594.
- [253] Sjöström, A.; Tolmachev, V.; Lebeda, O.; Koziorowski, J.; Carlsson, J.; Lundqvist, H. *J. Radioanal. Nucl. Chem.* 2003, **256**, 191-197.
- [254] Wilbur, D. S.; Chyan, M.-K.; Hamlin, D. K.; Kegley, B. B.; Risler, R.; Pathare, P. M.; Quinn, J.; Vessella, R. L.; Foulon, C.; Zalutsky, M.; Wedge, T. J.; Hawthorne, M. F. *Bioconjugate Chem.* 2004, **15**, 203-223.
- [255] Dilworth, J. R.; Parrott, S. J. *Chem. Soc. Rev.* 1998, **27**, 43-55.
- [256] Jurisson, S. S.; Lydon, J. D. *Chem. Rev.* 1999, **99**, 2205-2218.

- [257] Liu, S.; Edwards, D. S. *Chem. Rev.* 1999, **99**, 2235-2268.
- [258] Valliant, J. F.; Morel, P.; Schaffer, P.; Kaldis, J. H. *Inorg. Chem.* 2002, **41**, 628-630.
- [259] Sogbein, O. O.; Merdy, P.; Mordel, P.; Valliant, J. F. *Inorg. Chem.* 2004, **43**, 3032-3034.
- [260] Sogbein, O. O.; Green, A. E. C.; Valliant, J. F. *Inorg. Chem.* 2005, **44**, 9585-9591.
- [261] Green, A. E. C.; Causey, P. W.; Louie, A. S.; Armstrong, A. F.; Harrington, L. E.; Valliant J. F. *Inorg. Chem.* 2006, **45**, 5727-5729.
- [262] Grainger, R. G. *Br. J. Radiol.* 1982, **55**(649), 1-18.
- [263] Wilbur, D. S. *PCT Int. Appl.* WO 95 05,202.
- [264] Meyer, D.; Spielvogel, B. F. *PCT Int. Appl.* WO 93 08,122.
- [265] Martin-Jimenez, J. L.; Carretero-Colon, J. M.; Martinez-Sanz, A.; Krause, W. *PCT Int. Appl.* WO 95 26,353.
- [266] Leukart, O.; Caviezel, M.; Eberle, A.; Escher, E.; Tun-Kyi, A.; Schwyzer, R. *Helv. Chim. Acta* 1976, **59**, 2184-2187.
- [267] Fauchere, J. L.; Do, K. Q.; Jow, P. Y. C.; Hansch, C. *Experientia*. 1980, **36**, 1203-1204.
- [268] Fischli, W.; Leukart, O.; Schwyzer, R. *Helv. Chim. Acta*. 1977, **60**, 959-963.
- [269] Nachman, R. J.; Teal, P. E. A.; Radel, P. A.; Holman, G. M.; Abernathy, R. L. *Peptides*. 1996, **17**, 747-752.
- [270] Valliant, J. F.; Schaffer, P.; Stephenson, K. A.; Britten, J. F. *J. Org. Chem.* 2002, **67**, 383-387.
- [271] Endo, Y.; Iijima, T.; Yamakoshi, Y.; Yamaguchi, M.; Fukusawa, H.; Shudo, K. *J. Med. Chem.* 1999, **42**, 1501-1504.
- [272] Endo, Y.; Iijima, T.; Yamakoshi, Y.; Kubo, A.; Itai, A. *Bioorg. Med. Chem.* 1999, **9**, 3313-3318.
- [273] Endo, Y.; Iijima, T.; Yamakoshi, Y.; Fukasawa, H.; Miyaura, C.; Kubo, A.; Itai, A. *Chem. Biol.* 2001, **8**, 341-355.
- [274] Ogawa, T.; Ohta, K.; Yoshimi, T.; Yamazaki, H.; Suzuki, T.; Ohta, S.; Endo, Y. *Bioorg. Med. Chem. Lett.* 2006, **16**, 3943-3946.
- [275] Endo, Y.; Yoshimi, T.; Ohta, K.; Suzuki, T.; Ohta, S. *J. Med. Chem.* 2005, **48**, 3941-3944.
- [276] Endo, Y.; Yoshimi, T.; Iijima, T.; Yamakoshi, Y. *Bioorg. Med. Chem. Lett.* 1999, **9**, 3387-3392.
- [277] Endo, Y.; Yoshimi, T.; Yamakoshi, Y. *Chem. Pharm. Bull.* 2000, **48**, 312-314.
- [278] Iijima, T.; Endo, Y.; Tsuji, M.; Kawachi, E.; Kagechika, H.; Shudo, K. *Chem. Pharm. Bull.* 1999, **47**, 398-404.
- [279] Endo, Y.; Iijima, T.; Ohta, K.; Kagechika, H.; Kawachi, E.; Shudo, K. *Chem. Pharm. Bull.* 1999, **47**, 585-587.
- [280] Endo, Y.; Iijima, T.; Yaguchi, K.; Kawachi, E.; Kagechika, H. *Bioorg. Med. Chem. Lett.* 2001, **11**, 1307-1311.
- [281] Endo, Y.; Yaguchi, K.; Kawachi, E.; Kagechika, H. *Bioorg. Med. Chem. Lett.* 2000, **10**, 1733-1736.
- [282] Ohta, K.; Iijima, T.; Kawachi, E.; Kagechika, H.; Endo, Y. *Bioorg. Med. Chem. Lett.* 2004, **14**, 5913-5918.
- [283] Fujii, S.; Hashimoto, Y.; Suzuki, T.; Ohta, S.; Endo, Y. *Bioorg. Med. Chem. Lett.* 2005, **15**, 227-230.

- [284] Fujii, S.; Goto, T.; Ohta, K.; Hashimoto, Y.; Suzuki, T.; Ohta, S.; Endo, Y. *J. Med. Chem.* 2005, **48**, 4654-4662.
- [285] Goto, T.; Ohta, K.; Suzuki, T.; Ohta, S.; Endo, Y. *Bioorg. Med. Chem.* 2005, **13**, 6414-6424.
- [286] Wong, E.; Giandomenico, C. M. *Chem. Rev.* 1999, **99**, 2451-2466.
- [287] Todd, J. A.; Rendina, L. M. *Inorg. Chem.* 2002, **41**, 3331-3333.
- [288] Todd, J. A.; Turner, P.; Ziolkowski, E. J.; Rendina, L. M. *Inorg. Chem.* 2005, **44**, 6401-6408.
- [289] Crossley, E. L.; Caiazza, D.; Rendina, L. M. *Dalton Trans.* 2005, 2825-2826.
- [290] Woodhouse, S. L.; Ziolkowski, E. J.; Rendina, L. M. *Dalton Trans.* 2005, 2827-2829.
- [291] Woodhouse, S. L.; Rendina, L. M. *Chem. Commun.* 2001, 2464-2465.
- [292] Woodhouse, S. L.; Rendina, L. M. *Dalton Trans.* 2004, 3669-3677.
- [293] Base, K.; Grinstaff, M. W. *Inorg. Chem.* 1998, **37**, 1432-1433.
- [294] Base, K.; Tierney, M. T.; Fort, A.; Muller, J.; Grinstaff, M. W. *Inorg. Chem.* 1999, **38**, 287-289.
- [295] Yoo, J.; Do, Y. *Bull. Korean Chem. Soc.* 2005, **26**, 231-232.
- [296] Gielen, M. *Coord. Chem. Rev.* 1996, **151**, 41-51.
- [297] Gielen, M. *Appl. Organomet. Chem.* 2002, **16**, 481-494.
- [298] Gielen, M.; Biesemans, M.; Willem, R. *Appl. Organomet. Chem.* 2005, **19**, 440-450.
- [299] Gielen, M.; Kayser, F.; Zhidkova, O. B.; Kampel, V. Ts.; Bregadze, V. I.; de Vos, D.; Biesemans, M.; Mahieu, B.; Willem, R. *Metal Based Drugs.* 1995, **2**, 37-42.
- [300] Tiekink, E. R. T.; Gielen, M.; Bouhdid, A.; Willem, R.; Bregadze, V. I.; Ermanson, L. V.; Glazun, S. A. *Metal-Based Drugs.* 1997, **4**, 75-80.
- [301] Gielen, M.; Bouhdid, A.; Willem, R.; Bregadze, V. I.; Ermanson, L. V.; Tiekink, E. R. T. *J. Organomet. Chem.* 1995, **501**, 277-281.
- [302] Bregadze, V. I.; Glazun, S. A.; Petrovskii, P. V.; Starikova, Z. A.; Rochev, V. Ya.; Dalil, H.; Biesemans, M.; Willem, R.; Gielen, M.; de Vos, D. *Appl. Organomet. Chem.* 2003, **17**, 453-457.
- [303] Bregadze, V. I.; Glazun, S. A.; Petrovskii, P. V.; Starikova, Z. A.; Buyanovskaya, A. G.; Takazova, R. U.; Gielen, M.; de Vos, D.; Kemmer, M.; Biesemans, M.; Willem, R. *Appl. Organomet. Chem.* 2004, **18**, 191-194.
- [304] Strauss, S. H. *Chem. Rev.* 1993, **93**, 927-942.
- [305] Reed, C. A. *Acc. Chem. Res.* 1998, **31**, 133-139.
- [306] Juhasz, M.; Hoffmann, E.; Stoyanov, E.; Kim, K.; Reed, C. A. *Angew. Chem. Int. Ed.* 2004, **43**, 5352-5355.
- [307] Stoyanov, E. S.; Kim, K.; Reed, C. A. *J. Am. Chem. Soc.* 2006, **128**, 1948-1958.
- [308] Stoyanov, E. S.; Hoffmann, S.; Juhasz, M.; Reed, C. A. *J. Am. Chem. Soc.* 2006, **128**, 3160-3161.
- [309] Reed, C. A. *Chem. Commun.* 2005, 1669-1677.
- [310] Reed, C. A.; Kim, K.-C.; Stoyanov, E. S.; Stasko, D.; Tham, F. S.; Mueller, L. J.; Boyd, P. D. *W. J. Am. Chem. Soc.* 2003, **125**, 1796-1804.
- [311] Reed, C. A.; Kim, K.-C.; Bolksar, R. D.; Mueller, L. *Science*, 2000, **289**, 101-104.
- [312] Mueller, L. J.; Elliott, D. W.; Kim, K.-C.; Reed, C. A.; Boyd, P. D. *W. J. Am. Chem. Soc.* 2002, **124**, 9360-9361.
- [313] Mueller, L. J.; Elliott, D. W.; Leskowitz, G. M.; Struppe, J.; Olsen, R. A.; Kim, K.-C.; Reed, C. A. *J. Magn. Reson.* 2004, **168**, 327-335.

- [314] Xie, Z.; Bau, R.; Reed, C. A. *Inorg. Chem.* 1995, **34**, 5403-5404.
- [315] Stoyanov, E. S.; Hoffmann, S. P.; Kim, K.-C.; Tham, F. S.; Reed, C. A. *J. Am. Chem. Soc.* 2005, **127**, 7664-7665.
- [316] Stasko, D.; Hoffmann, S. P.; Kim, K.-C.; Fackler, N. L. P.; Larsen, T.; Drovetskaya, T.; Tham, F. S.; Reed, C. A.; Rickard, C. E. F.; Boyd, P. D. W.; Stoyanov, E. S. *J. Am. Chem. Soc.* 2002, **124**, 13869-13876.
- [317] Kato, K.; Stoyanov, E. S.; Geier, J.; Grutzmacher, H.; Red, C. A. *J. Am. Chem. Soc.* 2004, **126**, 12451-12457.
- [318] Kato, K.; Reed, C. A. *Angew. Chem. Int. Ed.* 2004, **43**, 2907-2911.
- [319] Müller, T.; Juhasz, M.; Reed, C. A. *Angew. Chem. Int. Ed.* 2004, **43**, 1543-1546.
- [320] Reed, C. A.; Xie, Z.; Bau, R.; Benesi, A. *Science* 1993, **263**, 402-404.
- [321] Reed, C. A. *Acc. Chem. Res.* 1998, **31**, 325-332.
- [322] Kim, K.-C.; Reed, C. A.; Elliott, D. W.; Mueller, L. J.; Tham, F.; Lin, L. J.; Lambert, J. B. *Science*. 2002, **297**, 825-827.
- [323] Patmore, N. J.; Hague, C.; Cotgreave, J. H.; Mahon, M. F.; Frost, C. G.; Weller, A. S. *Chem. Eur. J.* 2002, **8**, 2088-2098.
- [324] Fox, M. A.; Mahon, M. F.; Patmore, N. J.; Weller, A. S. *Inorg. Chem.* 2002, **41**, 4567-4573.
- [325] Crowther, D. J.; Borkowsky, S. L.; Swenson, D.; Meyer, T. Y.; Jordan, R. F. *Organometallics*. 1993, **12**, 2897-2903.
- [326] Guram, A. S.; Jordan, R. F. *J. Org. Chem.* 1993, **58**, 5595-5597.
- [327] Moreau, C.; Hauge, C.; Weller, A. S.; Frost, C. G. *Tetrahedron Lett.* 2001, **42**, 6957-6960.
- [328] Rifat, A.; Patmore, N. J.; Mahon, M. F.; Weller, A. S. *Organometallics*. 2002, **21**, 2856-2865.
- [329] Rifat, A.; Kociok-Köhn, G.; Steed, J. W.; Weller, A. S. *Organometallics*. 2004, **23**, 428-432.
- [330] Moss, S.; King, B.; de Meijere, A.; Kozhushkov, S.; Eaton, P.; Michl, J. *Org. Lett.* 2001, **3**, 2375-2377.
- [331] Vyakaranam, K.; Barbour, J. B.; Michl, J. *J. Am. Chem. Soc.* 2006, **128**, 5610-5611.
- [332] DuBay, W. J.; Grieco, P. A.; Todd, L. J. *J. Org. Chem.* 1994, **59**, 6898-6899.
- [333] DuBay, W. J.; Grieco, P. A.; Todd, L. J. *Tetrahedron Lett.* 1996, **48**, 8707-6710.
- [334] Hawthorne, M. F. In *Advances on Boron and the Boranes*; Liebman, J. F; Greenberg, A.; Williams, R. E.; Eds.; VCH Publishers, New York, NY, 1988, pp 225-246.
- [335] Pirotte, B.; Felekidis, A.; Fontaine, M.; Demonceau, A.; Noels, A. F.; Delarge, J.; Chizhevsky, I. T.; Zinevich, T. V.; Pisareva, I. V.; Bregadze, V. I. *Tetrahedron Lett.* 1993, **34**, 1471-1474.
- [336] Felekidis, A.; Goblet-Stachow, M.; Liegeois, J. F.; Pirotte, B.; Delarge, J.; Demonceau, A.; Fontaine, M.; Noels, A. F.; Chizhevsky, I. T.; Zinevich, T. V.; Bregadze, V. I.; Dolgushin, F. M.; Yanovsky, A. I.; Struchkov, Yu. T. *J. Organomet. Chem.* 1997, **536**, 405-412.
- [337] Belmont, J. A.; Soto, J.; King, R. E.; Donaldson, A. J.; Hewes, J. D.; Hawthorne, M. F. *J. Am. Chem. Soc.* 1989, **111**, 7475-7486.
- [338] Kang, H. C.; Hawthorne, M. F. *Organometallics*. 1990, **9**, 2327-2332.
- [339] Lebedev, V. N.; Balagurova, E. V.; Dolgushin, F. M.; Yanovskii, A. I.; Zakharkin, L. I. *Russ. Chem. Bull.* 1997, **46**, 550-558.

- [340] Demonceau, A.; Saive, E.; de Froidmont, Y.; Noels, A. F.; Hubert, A. J.; Chizhevsky, I. T.; Lobanova, I. A., Bregadze, V. I. *Tetrahedron Lett.* 1992, **33**, 2009-2012.
- [341] Demonceau, A.; Fontaine, M. A.; Messere, R.; Noels, A. F.; Chizhevsky, I. T.; Zinevich, T. V.; Bregadze, V. I. *Rhodium Express.* 1995, **12**, 32-39.
- [342] Teixidor, F.; Nuñez, R.; Flores, M. A.; Demonceau, A.; Viñas, C. *J. Organomet. Chem.* 2000, **614-615**, 48-56.
- [343] Zhu, Y. H.; Carpenter, K.; Bun, C. C.; Bahnmueler, S.; Ke, C. P.; Srid, V. S.; Kee, L. W.; Hawthorne, M. F. *Angew. Chem. Int. Ed.* 2003, **42**, 3792-3795.
- [344] Hlatky, G. G.; Turner, H. W.; Eckman, R. R. *J. Am. Chem. Soc.* 1989, **111**, 2728-2729.
- [345] Yoshida, M.; Crowther, D. J.; Jordan, R. F. *Organometallics.* 1997, **16**, 1349-1351.
- [346] Yoshida, M.; Crowther, D. J.; Jordan, R. F. *Organometallics.* 1997, **16**, 4508-4510.
- [347] Kim, D.-H.; Won, J. H.; Kim, S.-J.; Ko, J.; Kim, S. H.; Cho, S.; Kang, S. O. *Organometallics.* 2001, **20**, 4298-4300.
- [348] Yinghuai, Z.; Yulin, Z.; Carpenter, K.; Maguire, J. A.; Hosmane, N. S. *J. Organomet. Chem.* 2005, **690**, 2802-2808.
- [349] Kats, G. A.; Komarova, L. G.; Rusanov, A. L. *Russ. Chem. Bull.* 1991, **40**, 855-857.
- [350] Yinghuai, Z.; Sia, S. L. P.; Carpenter, K.; Kooli, F.; Kemp, R. A. *J. Phys. Chem. Solids* 2006, **67**, 1218-1222.
- [351] Schwab, P. F. H.; Levin, M. D.; Michl, J. *Chem. Rev.* 1999, **99**, 1863-1933.
- [352] Yang, X. G.; Jiang, W.; Knobler, C. B.; Hawthorne, M. F. *J. Am. Chem. Soc.* 1992, **114**, 9719-9721.
- [353] Muller, J.; Baše, K.; Magnera, T.; Michl, J. *J. Am. Chem. Soc.* 1992, **114**, 9721-9722.
- [354] Schöberl U.; Magnera, T. F.; Harrison, R. M.; Fleischer, F.; Pflug, J. L.; Schwab, P. F.; Meng, X.; Lipiak, D.; Noll, B. C.; Allured, V. S.; Rudalevige, T.; Lee, S.; Michl, J. *J. Am. Chem. Soc.* 1997, **119**, 3907-3917.
- [355] Kaszynski, P. *Collect. Czech. Chem. Commun.* 1999, **64**, 895-926.
- [356] Murphy, D. M.; Mingos, D. M. P.; Forward, J. M. *J. Mater. Chem.* 1993, **3**, 67-76.
- [357] Murphy, D. M.; Mingos, D. M. P.; Haggit, J. L.; Powell, H. R.; Westcott, S. A.; Marder, T. B.; Taylor, N. J.; Kanis, D. R. *J. Mater. Chem.* 1993, **3**, 139-148.
- [358] Tsuboya, N.; Lamrani, M.; Hamasaki, R.; Ito, M.; Mitsuishi, M.; Miyashita, T.; Yamamoto, Y. *J. Mater. Chem.* 2002, **12**, 2701-2704.
- [359] Lamrani, M.; Hamasaki, R.; Mitsuishi, M.; Miyashita, T.; Yamamoto, Y. *Chem. Commun.* 2000, 1595-1596.
- [360] Fox, M. A.; MavBride, J. A. H.; Peace, R. J.; Wade, K. *J. Chem. Soc., Dalton Trans.* 1998, 401-411.
- [361] Kaszynski, P.; Pakhomov, S.; Young, V. G. *Collect. Czech. Chem. Commun.* 2002, **67**, 1061-1083.
- [362] Harmon, A. B.; Harmon, K. M. *J. Am. Chem. Soc.* 1966, **88**, 4093-4094.
- [363] Harmon, K. M.; Harmon, A. B.; MacDonald, A. A. *J. Am. Chem. Soc.* 1969, **91**, 323-329.
- [364] Harmon, K. M.; Nelson, T. E.; Stachoeski, B. M. *J. Mol. Struct.* 1995, **359**, 135-145.
- [365] Harmon, K. M.; Gill, S. H. *J. Mol. Struct.* 2002, **607**, 181-188.
- [366] Grüner, B.; Janoušek Z.; King, B. T.; Woodford, J. N.; Wang, C. H.; Všetečka, V.; Michl, J. *J. Am. Chem. Soc.* 1999, **121**, 3122-3126.
- [367] Hawthorne, M. F.; Olsen, F. P. *J. Am. Chem. Soc.* 1965, **87**, 2366-2372.

- [368] Zakharkin, L. I.; Pisareva, I. V.; Sulaimankulova, D. D.; Antonovich, V. A. *J. Gen. Chem. USSR* 1990, **60**, 2453-2455.
- [369] Knoth, W. H. *J. Am. Chem. Soc.* 1966, **88**, 935-939.
- [370] Hertler, W. R.; Knoth, W. H.; Muetterties, E. L. *Inorg. Chem.* 1964, **4**, 288-293.
- [371] Pakhomov, S.; Kaszynski, P.; Young, V. G. *Inorg. Chem.* 2000, **39**, 2243-2245.
- [372] Bitner, T. W.; Wedge, T. J.; Hawthorne, M. F.; Zink, J. I. *Inorg. Chem.* 2001, **40**, 5428-5433.
- [373] Wedge, T. J.; Herzog, A.; Huertas, R.; Lee, M. W.; Knobler, C. B.; Hawthorne, M. F. *Organometallics* 2004, **23**, 482-489.
- [374] Fox, M. A.; Paterson, M. A. J.; Nervi, C.; Galeotti, F.; Puschmann, H.; Howard, J. A. K.; Low, P. *J. Chem. Commun.* 2001, 1610-1611.
- [375] Ghirotti, M.; Schwab, P. F. H.; Indelli, M. T.; Chiorboli, C.; Scandola, F. *Inorg. Chem.* 2006, **45**, 4331-4333.
- [376] Allis, D. G.; Spencer, J. T. *J. Organomet. Chem.* 2000, **614-615**, 309-313.
- [377] Pati, R.; Pineda, A. C.; Pandey, R.; Karna, S. P. *Chem. Phys. Lett.* 2005, **406**, 483-488.
- [378] McKinney, J. D.; McQuillan, F. S.; Chen, H.; Hamor, T. A.; Jones, C. J.; Slaski, M.; Cross, G. H.; Harding, C. J. *J. Organomet. Chem.* 1997, **547**, 253-262.
- [379] Forward, J. M.; Mingos, D. M. P.; Powell, A. V. *J. Organomet. Chem.* 1994, **465**, 251-258.
- [380] Forward, J. M.; Mingos, D. M. P.; Muller, T. E.; Williams, D. J.; Yan, Y. K. *J. Organomet. Chem.* 1994, **467**, 207-216.
- [381] Yan, Y. K.; Mingos, D. M. P.; Kurmoo, M.; Li, W. S.; Scowen, I. J.; McPartlin, M.; Coomber, A. T.; Friend, R. H. *J. Chem. Soc., Chem. Commun.* 1995, 997-998.
- [382] Yan, Y. K.; Mingos, D. M. P.; Kurmoo, M.; Li, W. S.; Scowen, I. J.; McPartlin, M.; Coomber, A. T.; Friend, R. H. *J. Chem. Soc., Dalton Trans.* 1995, 2851-2860.
- [383] Yan, Y. K.; Mingos, D. M. P.; Williams, D. J.; Kurmoo, M. *J. Chem. Soc., Dalton Trans.* 1995, 3221-3230.
- [384] Kazheva, O. N.; Chekhlov, A. N.; Alexandrov, G. G.; Buravov, L. I.; Kravchenko, A. V.; Starodub, V. A.; Sivaev, I. B.; Bregadze, V. I.; Dyachenko, O. A. *J. Organomet. Chem.* 2006, **691**, 4225-4233.
- [385] Yan, Y. K.; Mingos, D. M. P.; Muller, T. E.; Williams, D. J.; Kurmoo, M. *J. Chem. Soc. Dalton Trans.* 1994, 1735-1741.
- [386] Yan, Y. K.; Mingos, D. M. P.; Williams, D. J. *J. Organomet. Chem.* 1995, **498**, 267-274.
- [387] Hawthorne, M. F.; Zink, J. I.; Skelton, J. M.; Bayer, M. J.; Liu, C.; Livshits, E.; Baer, R.; Neuhauser, D. *Science*. 2004, **303**, 1849-1851.
- [388] Hawthorne, M. F.; Ramachandran, B. M.; Kennedy, R. D.; Knobler, C. B. *Pure Appl. Chem.* 2006, **78**, 1299-1304.
- [389] Kaszynski, P.; Douglass, A. G. *J. Organomet. Chem.* 1999, **581**, 28-38.
- [390] Thibault, R. M.; Hepburn, D. R.; Klingen, T. J. *J. Phys. Chem.* 1974, **78**, 788-792.
- [391] Kaczmarszyk, A.; Kolski, G. B. *J. Phys. Chem.* 1964, **68**, 1227-1229.
- [392] Kaczmarszyk, A.; Kolski, G. B. *Inorg. Chem.* 1965, **4**, 665-671.
- [393] Kaszynski, P.; Huang, J.; Jenkins, G. S.; Bairamov, K. A.; Lipiak, D. *Mol. Cryst. Liq. Cryst.* 1995, **260**, 315-332.
- [394] Douglass, A. G.; Czuprynski, K.; Mierzwa, M.; Kaszynski, P. *Chem. Mater.* 1998, **10**, 2399-2402.

- [395] Douglass, A. G.; Both, B.; Kaszynski, P. *J. Mater. Chem.* 1999, **9**, 683-686.
- [396] Czuprynski, K.; Kaszynski, P. *Liq. Cryst.* 1999, **26**, 775-778.
- [397] Piecek, W.; Kaufman, J. M.; Kaszynski, P. *Liq. Cryst.* 2003, **30**, 39-48.
- [398] Januszko, A.; Kaszynski, P.; Wand, M. D.; More, K. M.; Pakhomov, S.; O'Neil, M. *J. Mater. Chem.* 2004, **14**, 1544-1553.
- [399] Januszko, A.; Glab, K. L.; Kaszynski, P.; Patel, K.; Lewis, R. A.; Mehl, G. H.; Wand, M. D. *J. Mater. Chem.* 2006, **16**, 3183-3192.
- [400] Douglass, A. W.; Janousek, Z.; Kaszynski, P.; Young, V. G. *Inorg. Chem.* 1998, **37**, 6361-6365.
- [401] Douglass, A. W.; Czuprynski, K.; Mierzwa, M.; Kaszynski, P. *J. Mater. Chem.* 1998, **8**, 2391-2398.
- [402] Czuprynski, K. *Liq. Cryst.* 1999, **26**, 261-269.
- [403] Douglass, A. G.; Pkhomov, S.; Reeves, B.; Janoušek, Z.; Kaszynski, P. *J. Org. Chem.* 2000, **65**, 1434-1441.
- [404] Ohta, K.; Januszko, A.; Kaszynski, P.; Nagamine, T.; Sasnouski, G.; Endo, Y. *Liq. Cryst.* 2004, **31**, 671-682.
- [405] Nagamine, T.; Januszko, A.; Ohta, K.; Kaszynski, P.; Endo, Y. *Liq. Cryst.* 2005, **32**, 985-995.
- [406] Ringstrand, B.; Vroman, J.; Jensen, D.; Januszko, A.; Kaszynski, P.; Dziaduszek, J.; Drzewinski, W. *Liq. Cryst.* 2005, **32**, 1061-1070.
- [407] Januszko, A.; Kaszynski, P.; Drzewinski, W. *J. Mater. Chem.* 2006, **16**, 452-461.
- [408] Nagamine, T.; Januszko, A.; Kaszynski, P.; Ohta, K.; Endo, Y. *J. Mater. Chem.* 2006, **16**, 3836-3843.
- [409] Kaszynskii, P.; Pakhomov, S.; Tesh, K. F.; Young, V. G. *Inorg. Chem.* 2001, **40**, 6622-6631.
- [410] Voitekunas, V. Y.; Vasnev, V. A.; Markova, G. D.; Dubovik, I. I.; Vinogradova, S. V.; Papkov, V. S.; Abdullin, B. M. *Polymer Sci., Ser. A* 1997, **39**, 604-611.
- [411] Vinogradova, S. V.; Vasnev, V. A. In *Polycondensation Processes and Polymers*; Nauka, MAIK "Nauka/Interperiodika": Moscow, 2000, pp 175-188.
- [412] Williams, R. E. *J. Pure Appl. Chem.* 1972, **29**, 569-583.
- [413] Mayes, N.; Greene, J.; Cohen, M. S. *J. Polym. Sci. Part A-1* 1967, **5**, 365-379.
- [414] Papetti, S.; Schaeffer, B. B.; Grey, A.; Heying, T. L. *J. Polym. Sci. Part A-1* 1966, **4**, 1623-1636.
- [415] Peters, E. N. *J. Macromol. Sci., Rev. Macromol. Chem. C*. 1979, **17**, 173-208.
- [416] Bekasova, N. I.; Komarova, L. G. In *Advances in the Field of Synthesis of Organoelement Polymers*; Korshak, V. V.; Ed.; Nauka: Moscow, 1988, pp 56-87.
- [417] Vinogradova, S. V.; Vasnev, V. A. In *Polycondensation Processes and Polymers*; Nauka, MAIK "Nauka/Interperiodika": Moscow, 2000, pp 251-287.
- [418] Vinogradova, S. V.; Vasnev, V. A.; Valetskii, P. M. *Russ. Chem. Rev.* 1994, **63**, 833-851.
- [419] Vinogradova, S. V.; Valetskii, P. M.; Kabachii, Yu. A. *Russ. Chem. Rev.* 1995, **64**, 365-388.
- [420] Colquhoun, H. M.; Lewis, D. F.; Herbertson, P. L.; Wade, K.; Baxter, I. Williams, D. J. In *Contemporary Boron Chemistry*; Davidson, M.; Hughes, A. K.; Marder, T. B.; Wade, K.; Eds.; Royal Society of Chemistry: Cambridge, 2000, pp 59-66.
- [421] Rais, J.; Selucky, P.; Kyrš M. *J. Inorg. Nucl. Chem.* 1976, **38**, 1376-1378.

- [422] Romanovskiy, V. N.; Smirnov, I. V.; Babain, V. A.; Todd, T. A.; Law, J. D.; Herbst, R. S.; Brewer, K. N. *Solv. Extr. Ion Exch.* 2001, 19, 1-21.
- [423] Law, J. D.; Herbst, R. S.; Todd, T. A.; Romanovskiy, V. N.; Babain, V. A.; Esimantovskiy, V. M.; Smirnov, I. V.; Zaitsev, B. N. *Solv. Extr. Ion Exch.* 2001, 19, 23-36.
- [424] Romanovskiy, V. N.; Smirnov, I. V.; Babain, V. A.; Todd, T. A.; Brewer, K. N. US Patent 6258333 (2001).
- [425] Zaitsev, B. N.; Esimantovskiy, V. M.; Lazarev, L. N.; Dzekun, E. G.; Romanovskiy, V. N.; Todd, T. A.; Brewer, K. N.; Herbst, R. S.; Law, J. D. US Patent 6270737 (2001).
- [426] Viñas, C.; Gomez, S.; Bertran, J.; Barron, J.; Teixidor, F.; Dozol, J. F.; Rouquette, H.; Kivekäs, R.; Sillanpää, R. *J. Organomet. Chem.* 1999, 581, 188-193.
- [427] Viñas, C.; Bertran, J.; Gomez, S.; Teixidor, F.; Dozol, J. F.; Rouquette, H.; Kivekäs, R.; Sillanpää, R. *J. Chem. Soc., Dalton Trans.* 1998, 2849-2854.
- [428] Viñas, C.; Gomez, S.; Bertran, J.; Teixidor, F.; Dozol, J. F.; Rouquette, H. *Inorg. Chem.* 1998, 37, 3640-3643.
- [429] Viñas, C.; Gomez, S.; Bertran, J.; Teixidor, F.; Dozol, J. F.; Rouquette, H. *Chem. Commun.* 1998, 191-192.
- [430] Grüner, B.; Plešek, J.; Baca, J.; Dozol, J. F.; Lamare, V.; Cisarova, I.; Belohradsky, M.; Caslavsky, J. *New J. Chem.* 2002, 26, 867-875.
- [431] Plešek, J.; Grüner, B.; Cisarova, I.; Baca, I.; Selucky, P.; Rais, J. *J. Organomet. Chem.* 2002, 657, 59-70.
- [432] Grüner, Mikulasek, L.; Cisarova, I.; Bohmer, V.; Danila, C.; Reinoso-Garcia, M. M.; Verboom, W.; Reinhoudt, D. N.; Casnati, A.; Ungaro, R. *Eur. J. Org. Chem.* 2005, 2022-2039.
- [433] Larsen, A. S.; Holbrey, J. D.; Tham, F. S.; Reed, C. A. *J. Am. Chem. Soc.* 2000, 122, 7264-7272.
- [434] Zhu, Y.; Ching, C.; Carpenter, K.; Xu, R.; Selvaratnam, S.; Hosmane, N. S.; Maguire, J. A. *Appl. Organomet. Chem.* 2003, 17, 346-356.
- [435] Yinghuai, Z.; Bahnmueller, S.; Hosmane, N. S.; Maguire, J. A. *Chem. Lett.* 2003, 32, 730-731.
- [436] Johnson, J. W.; Brody, J. F. *J. Electrochem. Soc.* 1982, 129, 2213-2219.
- [437] Rupich, M. W.; Foss, J. S.; Brummer, S. B. *J. Electrochem. Soc.* 1985, 132, 119-122.
- [438] Lee, H. S.; Ma, F. F.; Yang, X.-Q.; Sun, X.; McBreen J. *J. Electrochem. Soc.* 2005, 151, A1429-A1435.
- [439] Bobacka, J.; Väänänen, V.; Lewenstam, A.; Ivaska, A. *Talanta*, 2004, 63, 135-138.
- [440] Peper, S.; Telting-Diaz, M.; Almond, P.; Albrecht-Schmitt, T.; Bakker, E. *Anal. Chem.* 2002, 74, 1327-1332.
- [441] Peper, S.; Qin, Y.; Almond, P.; McKee, M.; Telting-Diaz, M.; Albrecht-Schmitt, T.; Bakker, E. *Anal. Chem.* 2003, 75, 2131-2139.
- [442] Qin, Y.; Bakker, E. *Anal. Chem.* 2003, 75, 6002-6010.
- [443] Krondak, M.; Volf, R.; Kral, V. *Collect. Czech. Chem. Commun.* 2001, 66, 1659-1664.
- [444] Tutsch, J.; Krondak, M.; Volf, R.; Grüner, B.; Kral, V. *Chem. Listy.* 2005, 99, 186-189.
- [445] Masalles, C.; Teixidor, F.; Borros, S.; Viñas, C. *J. Organomet. Chem.* 2002, 657, 239-246.
- [446] Sharapov, V. M.; Kanaev, A. I.; Zakharov, A. P.; Gorodetsky, A. E. *J. Nucl. Mater.* 1992, 191-194, 508-511.

- [447] Buzhinsky, O. I.; Azizov, E. A.; Belov, A. M.; Grashin, S. A.; Krasilnikov, A. V.; Kovan, I. A.; Mirnov, C. V.; Petrov, A. A.; Petrov, V. G.; Portnov, D. V.; Pulinets, T. S.; Romannikov, A. N.; Skvortsova, A. A.; Sotnikov, S. M.; Tugarinov, S. N.; Fedorenko, S. I.; Chernobaj, A. P.; Kanaev, A. I.; Sharapov, V. M.; Rybakov, S. Y.; Gorodetsky, A. E.; Zakharov, A. P.; Vasilyev, A. A.; Luzganov, S. N.; Fokin, V. P.; Chulkov, A. N. *J. Nucl. Mater.* 1992, 191-194, 1413-1416.
- [448] Alimov, V. Kh.; Bogomolov, D. B.; Churaeva, M. N.; Gorodetsky, A. E.; Kanashenko, S. L.; Kanaev, A. I.; Rybakov, S. Yu.; Sharapov, V. M.; Zakharov, A. P.; Zalavutdinov, R. Kh.; Buzhinsky, O. I.; Chernobay, A. P.; Grashin, S. A.; Mirnov, S. V.; Bregadze, V. I.; Usyatinsky, A. Yu. *J. Nucl. Mater.* 1992, 196-198, 670-675.
- [449] Sharapov, V. M.; Mirnov, S. V.; Grashin, S. A.; Lebedev, S. V.; Kovan, I. A.; Krasilnikov, A. V.; Krupin, V. A.; Levin, L. S.; Romannikov, A. N.; Zakharov, A. P. *J. Nucl. Mater.* 1995, 220-222, 730-735.
- [450] Peng, L.; Wang, E.; Zhang, N.; Yan, D.; Wang, M.; Wang, Z.; Deng, B.; Li, K.; Luo, J.; Liu, L. *Nucl. Fusion*. 1998, 38, 1137-1147.
- [451] Wan, B.N.; Zhao, Y. P.; Li, J.G.; Song, M.; Wu, Z. W.; Luo, J. R.; Li, C. F.; Wang, X. M. *Plasma Sci. Techol.* 2002, 4, 1375-1382.
- [452] Tafalla, D.; Tabares, F. L. *Vacuum*. 2002, 67, 393-397.
- [453] Buzhinskij, O. I.; Otroshchenko, V. G.; Whyte, D. G.; Baldwin, M.; Conn, R. W.; Doerner, R. P.; Seraydarian, R.; Luckhardt, S.; Kugel, H.; West, W. P. *J. Nucl. Mater.* 2003, 313-316, 214-218.
- [454] Wedge, T. J.; Hawthorne, M. F. *Coord. Chem. Rev.* 2003, 240, 111-128.
- [455] Badr, I. H. A.; Diaz, M.; Hawthorne, M. F.; Bachas, L. G. *Anal. Chem.* 1999, 71, 1371-1377.
- [456] Johnson, R. D.; Badr, I. H. A.; Diaz, M.; Wedge, T. J.; Hawthorne, M. F.; Bachas, L. G. *Electroanalysis*. 2003, 15, 1244-1250.
- [457] Badr, I. H. A.; Johnson, R. D.; Diaz, M.; Hawthorne, M. F.; Bachas, L. G. *Anal. Chem.* 2000, 72, 4249-4254.
- [458] Lee, H.; Knobler, C. B.; Hawthorne, M. F. *Angew. Chem. Int. Ed.* 2001, 40, 3058-3060.
- [459] Berger, M.; Schmidtchen, F. P. *J. Am. Chem. Soc.* 1996, 118, 8947-8948.
- [460] Berger, M.; Schmidtchen, F. P. *Angew. Chem. Int. Ed.* 1998, 37, 2694-2696.
- [461] Berger, M.; Schmidtchen, F. P. *J. Am. Chem. Soc.* 1999, 121, 9986-9993.
- [462] Fibbioli, M.; Berger, M.; Schmidtchen, F. P.; Pretsch, E. *Anal. Chem.* 2000, 72, 156-160.

Chapter 2

HYDROSILYLATION OF CH₂=CH- GROUPS IMMOBILIZED ON THE INTERLAYER SURFACE OF AN ION-EXCHANGEABLE LAYERED PEROVSKITE WITH HYDROCHLOROSILANES AND OLIGOSILOXANES

*Seiichi Tahara¹, Kazuyoshi Ohta¹, Satoru Yoshioka¹,
Yosuke Takeda¹, Yuko Uchimaru² and Yoshiyuki Sugahara¹*

¹ Department of Applied Chemistry, School of Science and Engineering,
Waseda University, Ohkubo-3, Shinjuku-ku, Tokyo 169-8555, Japan

² National Institute of Advanced Industrial Science and Technology,
AIST Tsukuba Central 5-2, Tsukuba, Ibaraki 305-8565, Japan

ABSTRACT

Novel preparation of inorganic-organic hybrids using ion-exchangeable layered perovskites *via* hydrosilylation has been explored. CH₂=CH- groups were immobilized on the interlayer surface through an alcohol-exchange-type reaction between an *n*-propoxy derivative of HLaNb₂O_{7-x}H₂O (HLaNb) with 4-penten-1-ol or 9-decen-1-ol to form a CH₂=CH(CH₂)_nO-derivative of HLaNb (*n* = 3 or 8), and hydrosilylation of the CH₂=CH- groups of the CH₂=CH(CH₂)_nO- groups with SiH groups in hydrochlorosilanes, hydride-terminated polydimethylsiloxane (H-PDMS) or octahydridosilsesquioxane (OHSQ) was conducted subsequently. When the CH₂=CH(CH₂)₃O-derivative of HLaNb was reacted with dichloromethylsilane, trichlorosilane or H-PDMS, X-ray diffraction (XRD) patterns, infrared (IR) adsorption, and ¹³C and ²⁹Si CP/MAS nuclear magnetic resonance (NMR) spectra showed the occurrence of hydrosilylation in the interlayer space. Although the XRD pattern of the product of the reaction between the CH₂=CH(CH₂)₈O-derivative of HLaNb and OHSQ showed no notable increase in interlayer distance, the IR and ¹³C and ²⁹Si CP/MAS NMR spectra suggested the occurrence of hydrosilylation. The occurrence of hydrosilylation between the CH₂=CH- groups and OHSQ in the interlayer space was also indicated by a comparison of the pyrolysis behavior of the product of the reaction between the CH₂=CH(CH₂)₈O-derivative of HLaNb and OHSQ with those of pyrolyzed HLaNb and the pyrolyzed CH₂=CH(CH₂)₈O-derivative of HLaNb. These results clearly demonstrate

that hydrosilylation in the interlayer space is a potential new method for preparing various organic derivatives of ion-exchangeable layered perovskites.

INTRODUCTION

Extensive research has been conducted on the preparation of inorganic-organic hybrids with a focus on the achievement of novel structures, compositions and tunable properties.[1-8] The preparation of inorganic-organic hybrids has been widely studied employing various techniques, including intercalation [1,7-10] and the sol-gel process.[3,5,6] "Intercalation" is utilized to accommodate organic ions and/or molecules in the interlayer space of layered compounds to form intercalation compounds, which consist of alternatively stacked inorganic nano-sheets and layers of organic ions/molecules. Since the intercalation compounds exhibit not only photofunctional properties[7,8] and anisotropic electro/ion conductivities[1,11,12] based on the properties of guest ions/molecules but also enhanced properties based on the inorganic nanosheets[13] and adsorptive properties[7,8], various functional organic ions/molecules have been intercalated in the interlayer space. The interfaces between interlayer surfaces and organic ions and/or molecules generally consist of weak interactions such as ionic bonds and hydrogen bonds. The organic ions/molecules are therefore easily removed under appropriate conditions. Some layered compounds can bind organic and organometallic groups on the interlayer surface with covalent bonds, on the other hand, by employing "grafting" reactions to form stable interfaces. Layered polysilicate can react with chlorosilanes or alkoxy silanes to form Si-O-Si bonds,[14,15] for example, and kaolinite can react with alcohols to form Al-O-C bonds.[16,17] In addition, immobilization of organic or organometallic groups is reported for FeOCl[18] and zirconium phosphate.[19]

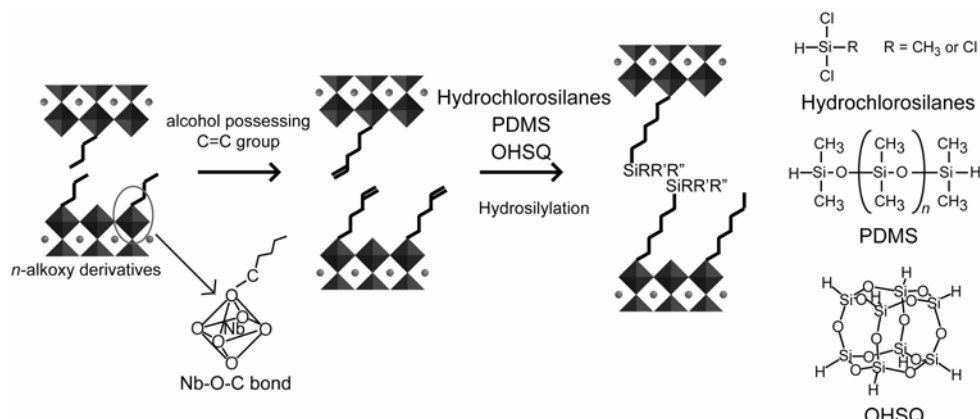
Perovskites and perovskite-related compounds are interesting materials, since these compounds can exhibit excellent magnetic,[20] dielectric[21,22] and optical properties,[23] which originate in their perovskite-related structures and the compositions. Ion-exchangeable layered perovskites consist of interlayer cations, M, and perovskite-like slabs, $[A_{m-1}B_mO_{3m+1}]$ (such as $[LaNb_2O_7]$ where A = La, B = Nb and m = 2).[24] Perovskite-like slabs, $[A_{m-1}B_mO_{3m+1}]$, possess a (100) sliced perovskite structure with an A-site cation coordinated by 12 oxygen atoms and a B-site cation positioned at the center of the BO_6 octahedra. The thickness of a perovskite-like slab is expressed by m. Ion-exchangeable layered perovskites can be classified into two phases based on the number of exchangeable cations, M, per $[A_{m-1}B_mO_{3m+1}]$: Dion-Jacobson phases, $M[A_{m-1}B_mO_{3m+1}]$, and Ruddlesden-Popper phases, $M_2[A_{m-1}B_mO_{3m+1}]$.[24] Acid treatment of these phases easily leads to formation of the protonated forms of ion-exchangeable layered perovskites, $H[A_{m-1}B_mO_{3m+1}]$ and $H_2[A_{m-1}B_mO_{3m+1}]$. The protonated forms of ion-exchangeable layered perovskites have been reported to exhibit photocatalytic activities[25,26] and proton conductivities.[27]

Intercalation of organic bases into the protonated forms of ion-exchangeable layered perovskites via acid-base reactions has been attracting attention, since the intercalation compounds could exhibit enhanced properties based on their perovskite-related structures.[24] Intercalation of n-alkylamine into $HSr_2Nb_3O_{10}$ leads, for example, to excellent fatigue behavior of the dielectric properties.[28] Dion-Jacobson type niobates, $HLaNb_2O_7 \cdot xH_2O$ ($HLaNb$) and $HCa_2Nb_3O_{10} \cdot xH_2O$ ($HCaNb$), on the other hand, can react with n-alcohols to form n-alkoxy derivatives of $HLaNb$ and $HCaNb$ possessing Nb-O-C

covalent bonds.[29-31] These *n*-alkoxy derivatives of HLaNb and HCaNb are stable compared to the intercalation compounds, since covalent bonds are more stable than ionic and hydrogen bonds. The reactions of *n*-alkoxy derivatives of HLaNb with other alcohols, such as *sec*-alcohol and alkanediol, lead to the formation of organic derivatives of HLaNb through alcohol-exchange-type reactions.[32] Although the alcohol-exchange-type reactions enable us to prepare additional organic derivatives, bulky alcohols, such as *tert*-alcohol, are grafted onto the interlayer surface only partially. These facts suggest the need for an additional method of binding organic molecules in the interlayer space of layered perovskites is required.

Hydrosilylation has been well known for decades in silicon chemistry and industry.[33-35] For hydrosilylation, transition metal complex catalysts, such as chloroplatinic acid and Pt₂(dvs)₃ (dvs = 1,3-divinyl-1,1,3,3-tetramethyl-1,3-disiloxane), are used to obtain hydrosilylated products with high yields. Hydrosilylation of CH₂=CHR groups with ≡SiH groups generally yields a large amount of ≡SiCH₂CH₂R via β -addition, but the structure of the hydrosilane compounds, the R group in the CH₂=CHR groups and the selection of catalysts could affect the distribution of adducts formed via α - and β -addition.[33,36] Since hydrosilylation usually forms no by-products, it is applied extensively to surface modification of solids possessing ≡SiH and CH₂=CH- groups on their surfaces to form inorganic-organic hybrids.[37-39] In addition, hydrosilylation between alkenyl groups bound on the interlayer surface and pentametyldisiloxane using a layered mineral, appophlite, has also been reported.[40,41] Application of hydrosilylation to appropriate organic groups (such as CH₂=CH-, CH≡C- or SiH groups) immobilized on the interlayer surface of ion-exchangeable layered perovskites can therefore be expected to form new organic derivatives of ion-exchangeable layered perovskites.

Here, we report the immobilization of CH₂=CH- groups in the interlayer space through a reaction between an *n*-propoxy derivative of HLaNb and 4-penten-1-ol or 9-decen-1-ol and subsequent hydrosilylation between CH₂=CH- groups immobilized on the interlayer surface of HLaNb and hydrochlorosilanes, (CH₃)_{3-x}(H)SiCl_x (*x* = 2, 3),[42] hydride-terminated polydimethylsiloxane (H-PDMS), HSi(CH₃)₂O-[Si(CH₃)₂O]_{*n*}-(CH₃)₂SiH, and octahydridosilsesquioxane (OHSQ), H₈Si₈O₁₂. (scheme 1) Successful formation of these hydrosilylated products indicates that hydrosilylation can be a versatile method for the preparation of novel inorganic-organic hybrids.



Scheme 1. Overview of the reaction of hydrochlorosilanes and oligosiloxanes via the hydrosilylation.

EXPERIMENTAL SECTION

Instrumentation

The X-ray diffraction (XRD) patterns of the products were recorded on a Mac Science M03XHF²² diffractometer with Mn-filtered FeK α radiation. The solid-state ¹³C and ²⁹Si nuclear magnetic resonance (NMR) spectra were obtained using a JEOL CMX-400 spectrometer operated at 100.54 MHz (¹³C) and 79.427 (²⁹Si) MHz with cross-polarization (CP) and magic angle spinning (MAS) techniques. The contact times were 1.5 ms (¹³C) and 5 ms (²⁹Si). The sample spinning rate was about 5 kHz and the pulse delay was 5 s. In the solid-state ²⁹Si MAS NMR measurement without cross-polarization techniques, the pulse delay was set for 250 s. The infrared (IR) adsorption spectra of the products were recorded with a Perkin-Elmer Spectrum One instrument or a JASCO FT/IR-460 Plus instrument using KBr disc techniques. The amounts of carbon were determined by an internal service at the Waseda University Materials Characterization Center. The Si/Nb ratios of the products were determined by X-ray fluorescence (XRF) (Rigaku RIX-2100) analysis employing the fundamental parameter method.

Starting Materials

RbLaNb₂O₇ and HLaNb₂O₇·xH₂O were prepared based on the previous reports.[32,43] A mixture of Rb₂CO₃, La₂O₃ and Nb₂O₅ (with a 30-mol% excess amount of Rb₂CO₃) was calcined at 1200°C for 48 h with intermittent grinding after 24 h. After calcination, the product was washed with distilled water to remove the residual Rb and dried at 120°C. The XRD pattern of the product was indexed for a tetragonal cell with $a = 0.3888(4)$ nm and $c = 1.0991(6)$ nm, parameters consistent with the previous report ($a = 0.3885(2)$ nm and $c = 1.0989(3)$ nm).[43] Inductively coupled plasma emission spectrometry (ICP) showed that the cation ratio of the product was consistent with RbLaNb₂O₇. To prepare HLaNb₂O₇·xH₂O (HLaNb), RbLaNb₂O₇ was treated with 6 mol/L HNO₃ at 60°C for 3 d. After acid treatment, the product was centrifuged, washed with distilled water and dried at ambient temperature. The XRD pattern of the product after drying at 120°C was indexed for a tetragonal cell with $a = 0.3896(5)$ nm and $c = 1.045(1)$ nm, parameters consistent with the reported values for anhydrous HLaNb₂O₇ ($a = 0.3894(3)$ nm and $c = 1.0479(7)$ nm).[43] ICP showed that all the Rb ions were essentially removed by acid treatment and that the La/Nb ratio was consistent with HLaNb₂O₇. The amount of protons estimated by thermogravimetry (TG) was 1.0 per [LaNb₂O₇].

For the preparation of an *n*-propoxy derivative of HLaNb, 3 g of HLaNb were typically refluxed with a mixture of *n*-propanol and distilled water (10mass% of water) for 3 d.[32] After centrifugation, the product was washed with acetone and dried at room temperature. The XRD pattern of the product was assigned to the *n*-propoxy derivative of HLaNb with lattice parameters, $a = 0.389(1)$ nm and $c = 1.540(3)$ nm. The solid-state ¹³C CP/MAS NMR spectrum of the product exhibited a signal at 80 ppm, which was indicative of the formation of Nb-O-C bonds.[32] All the analytical results indicated that an *n*-propoxy derivative of HLaNb was obtained.[32]

Trichlorosilane was supplied by Tokyo Kasei Kogyo Co., and dichloromethylsilane and H-PDMS, HSi(CH₃)₂O-[Si(CH₃)₂O]_n-(CH₃)₂Si-H (number average molecular weight, M_w , = 580 and $n \approx 6$) and Pt₂[(CH₂=CH(CH₃)₂Si)₂O]₃ (0.1 mol/L in xylene) were purchased from Aldrich. Trichlorosilane and dichloromethylsilane were distilled under reduced pressure. Toluene, *n*-hexane and tetrahydrofuran were supplied by Kanto Kagaku Co. Methanol, FeCl₃, CaCl₂, *p*-xylene and H₂PtCl₆·6H₂O were purchased from Wako Pure Chemical Industries. Distillation of toluene, *p*-xylene and tetrahydrofuran was performed with sodium and benzophenone.

Octahydridosilsesquioxane (OHSQ) was prepared under a protective nitrogen atmosphere by a method based on the previous report.[44] Typically, 50 g of anhydrous FeCl₃, 20 mL of 12 mol/L HCl, 40 mL of methanol, 350 mL of *n*-hexane and 50 mL of toluene were mixed in a round-bottomed flask. This suspension was stirred vigorously with a mechanical stirrer. A mixture of trichlorosilane (25 mL) and *n*-hexane (150 mL) was added dropwise to the suspension over a period of 9 h. After an additional 30-min stirring, the suspension was filtered to remove FeCl₃. Fourteen g of K₂CO₃ and 10 g of CaCl₂ were then added to the filtrate and stirred overnight. The solution was filtrated, and the solvent was removed under reduced pressure to obtain a crude product. The crude product was recrystallized from a mixture of 20 mL of tetrahydrofuran and 30 mL of *n*-hexane and washed with *n*-hexane. The ¹H NMR spectrum (C₆D₆) of the product showed the presence of a signal at 4.2 ppm. The ²⁹Si NMR (C₆D₆) spectrum (DEPT) showed a signal at -84 ppm assignable to an HSi(OSi)₃ environment. These NMR results indicated the formation of OHSQ.[45] In addition, the IR spectrum of the product showed the presence of a weak band at 3416 cm⁻¹ due to the $\nu_{(OH)}$ mode, indicating the formation of impurities containing the ≡SiOH group.

Immobilization of 4-Penten-1-Ol and 9-Decen-1-Ol on the Interlayer Surface of HLaNb₂O₇·*x*H₂O (HLaNb)

For the reaction between the *n*-propoxy derivative of HLaNb and 4-penten-1-ol, 1.3 g of the *n*-propoxy derivative of HLaNb and 40 mL of 4-penten-1-ol were sealed in a glass ampoule and heated at 80°C for 7 d. After centrifugation, the product was washed with acetone and dried at ambient temperature (CH₂=CH(CH₂)₃O-HLaNb). For the reaction between the *n*-propoxy derivative of HLaNb and 9-decen-1-ol, 2 g of the *n*-propoxy derivative of HLaNb were reacted with 25 mL of 9-decen-1-ol in a glass ampoule at 80°C for 7 d. The product was centrifuged and washed with acetone. The product was dried at ambient temperature (CH₂=CH(CH₂)₈O-HLaNb).

Reaction of Immobilized CH₂=CH- Groups on the Interlayer Surface with Hydrochlorosilanes, H-PDMS or OHSQ

The reaction procedures with hydrochlorosilanes and OHSQ were performed using the standard Schlenk techniques under a protective nitrogen atmosphere[46] or in a globe box filled with nitrogen.

For the reactions with hydrochlorosilanes, about 0.3 g of $\text{CH}_2=\text{CH}(\text{CH}_2)_3\text{O}-\text{HLaNb}$ and 20 mL of $\text{Cl}_x(\text{H})\text{Si}(\text{CH}_3)_{3-x}$ ($x = 2, 3$) were refluxed for 3 d. As a catalyst, $\text{H}_2\text{PtCl}_6 \cdot 6\text{H}_2\text{O}$ (as an acetonitrile solution) was added with a Pt/Si ratio of 5×10^{-4} . The resultant product was washed with *n*-hexane and dried under reduced pressure.

For the reaction with H-PDMS, about 0.3 g of $\text{CH}_2=\text{CH}(\text{CH}_2)_8\text{O}-\text{HLaNb}$ and 17 mL of H-PDMS (with an approximate $\text{HSi}\equiv/\text{CH}_2=\text{CH}(\text{CH}_2)_8\text{O}$ -molar ratio of 100) were stirred at 80°C for 10 d under a nitrogen atmosphere. $\text{CH}_2=\text{CH}(\text{CH}_2)_8\text{O}-\text{HLaNb}$ was used after drying under reduced pressure for 1 h, and the water was removed from H-PDMS using molecular sieves 3A before use. As a catalyst, $\text{Pt}_2[(\text{CH}_2=\text{CH}(\text{CH}_3)_2\text{Si})_2\text{O}]_3$ (as a *p*-xylene solution) was added with a Pt/ $\text{CH}_2=\text{CH}$ - ratio of 5×10^{-2} . After centrifugation, the resultant product was washed with *p*-xylene and tetrahydrofuran and dried under reduced pressure.

For the reaction with OHSQ, about 0.3 g of $\text{CH}_2=\text{CH}(\text{CH}_2)_8\text{O}-\text{HLaNb}$ and 0.4 g of OHSQ (with an approximate $\text{H}_8\text{Si}_8\text{O}_{12}/\text{CH}_2=\text{CH}(\text{CH}_2)_8\text{O}$ - molar ratio of 2) were refluxed in toluene at 110°C for 10 d. $\text{CH}_2=\text{CH}(\text{CH}_2)_8\text{O}-\text{HLaNb}$ and OHSQ were used after drying under reduced pressure for 1 h. As a catalyst, $\text{H}_2\text{PtCl}_6 \cdot 6\text{H}_2\text{O}$ was added with a Pt/ $\text{CH}_2=\text{CH}$ - ratio of about 5×10^{-2} . The resultant product was washed with *p*-xylene and tetrahydrofuran and dried under reduced pressure.

The pyrolysis of HLaNb, $\text{CH}_2=\text{CH}(\text{CH}_2)_8\text{O}-\text{HLaNb}$ and the product of the reaction between $\text{CH}_2=\text{CH}(\text{CH}_2)_8\text{O}-\text{HLaNb}$ and OHSQ using a tube furnace was performed at 350°C and 400°C for 10 min in air with a heating rate of 5°C/min.

RESULTS AND DISCUSSIONS

Immobilization of 4-Penten-1-Ol and 9-Decen-1-Ol on the Interlayer Surface of $\text{HLaNb}_2\text{O}_{7+x}\text{H}_2\text{O}$ (HLaNb)

The XRD patterns of the *n*-propoxy derivative of HLaNb and the products of the *n*-propoxy derivative of HLaNb with 4-penten-1-ol and 9-decen-1-ol are shown in Figure 1 ($\text{CH}_2=\text{CH}(\text{CH}_2)_3\text{O}-\text{HLaNb}$) and Figure 2 ($\text{CH}_2=\text{CH}(\text{CH}_2)_8\text{O}-\text{HLaNb}$). The *d* values for the low-angle reflections correspond to the interlayer distances. The interlayer distance increases from 1.53 nm to 1.85 (4-penten-1-ol) or 2.67 nm (9-decen-1-ol). The (100) reflections at $2\theta = 28.8^\circ$, due to the crystal structure of the perovskite-like slabs, do not shift after the reactions, thus indicating the preservation of the perovskite-like slab structure.

The IR spectra of the products, $\text{CH}_2=\text{CH}(\text{CH}_2)_3\text{O}-\text{HLaNb}$ and $\text{CH}_2=\text{CH}(\text{CH}_2)_8\text{O}-\text{HLaNb}$, are shown in Figure 3 and Figure 4, respectively. The IR spectrum of $\text{CH}_2=\text{CH}(\text{CH}_2)_3\text{O}-\text{HLaNb}$ shows new bands at 3074 and 1641 cm^{-1} . These bands are assignable to the $\nu_{(\text{CH})}$ mode (3074 cm^{-1}) and the $\nu_{(\text{C}=\text{C})}$ (1640 cm^{-1}) mode of the $\text{CH}_2=\text{CH}$ - groups. In the IR spectrum of $\text{CH}_2=\text{CH}(\text{CH}_2)_8\text{O}-\text{HLaNb}$, the $\nu_{(\text{CH})}$ band (3075 cm^{-1}) and $\nu_{(\text{C}=\text{C})}$ band (1640 cm^{-1}) of the $\text{CH}_2=\text{CH}$ - groups are observed in a similar fashion.

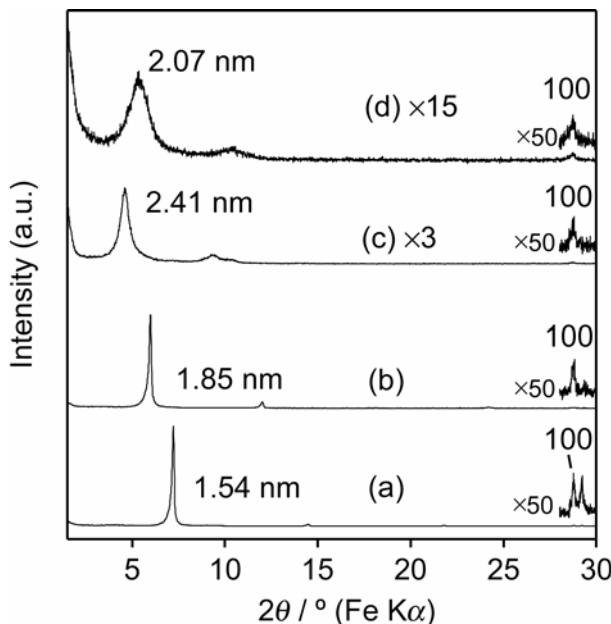


Figure 1. XRD patterns of (a) *n*-propoxy derivatives of HLaNb, (b) $\text{CH}_2=\text{CH}(\text{CH}_2)_3\text{O}-\text{HLaNb}$, (c) the product of the reaction between $\text{CH}_2=\text{CH}(\text{CH}_2)_3\text{O}-\text{HLaNb}$ and dichloromethylsilane and (d) the product of the reaction between $\text{CH}_2=\text{CH}(\text{CH}_2)_3\text{O}-\text{HLaNb}$ and trichlorolsilane.

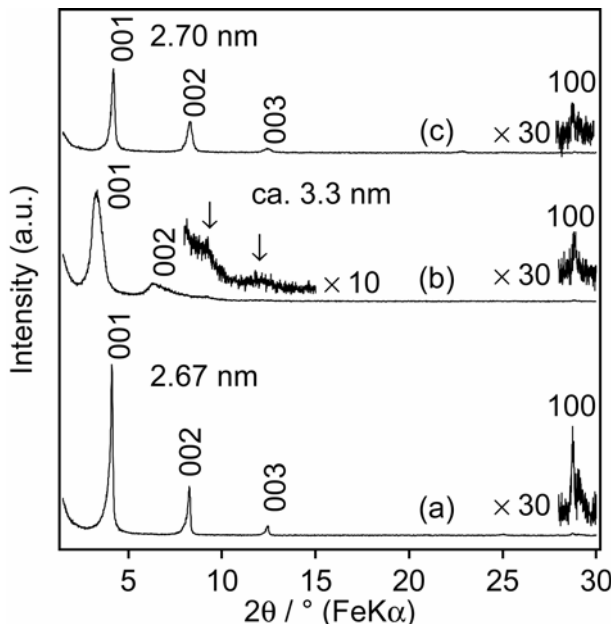


Figure 2. XRD patterns of (a) $\text{CH}_2=\text{CH}(\text{CH}_2)_8\text{O}-\text{HLaNb}$, (b) the product of the reaction between $\text{CH}_2=\text{CH}(\text{CH}_2)_8\text{O}-\text{HLaNb}$ with H-PDMS and (c) the product of the reaction between $\text{CH}_2=\text{CH}(\text{CH}_2)_3\text{O}-\text{HLaNb}$ with OHSQ.

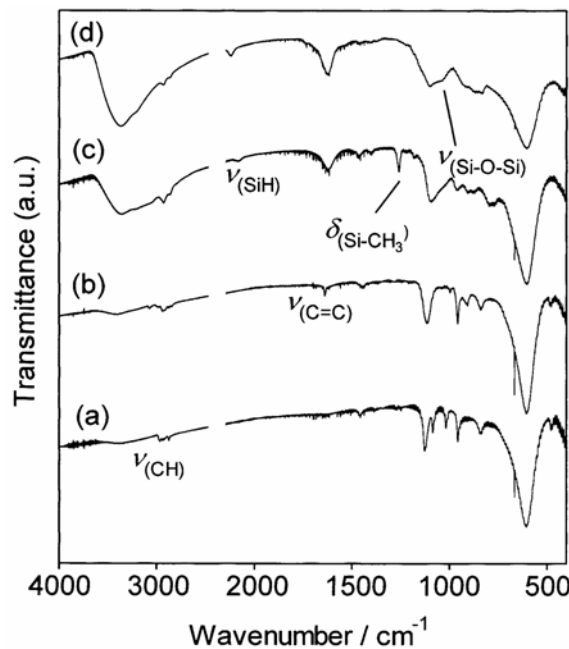


Figure 3. IR spectra of (a) *n*-propoxy derivatives of HLaNb, (b) the $\text{CH}_2=\text{CH}(\text{CH}_2)_3\text{O}-\text{HLaNb}$, (c) the product of the reaction between $\text{CH}_2=\text{CH}(\text{CH}_2)_3\text{O}-\text{HLaNb}$ with dichloromethylsilane and (d) the product of the reaction between $\text{CH}_2=\text{CH}(\text{CH}_2)_3\text{O}-\text{HLaNb}$ with trichlorolsilane.

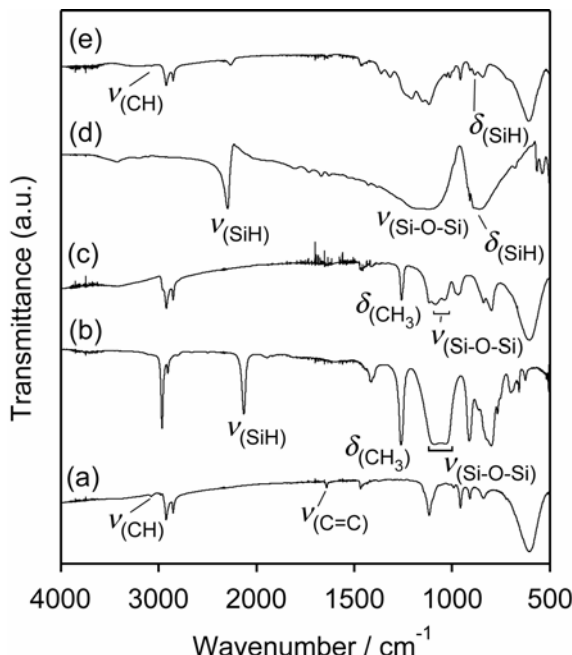


Figure 4. IR spectra of (a) $\text{CH}_2=\text{CH}(\text{CH}_2)_8\text{O}-\text{HLaNb}$, (b) H-PDMS, (c) the product of the reaction between $\text{CH}_2=\text{CH}(\text{CH}_2)_8\text{O}-\text{HLaNb}$ with H-PDMS, (d) OHSQ and (e) the product of the reaction between $\text{CH}_2=\text{CH}(\text{CH}_2)_3\text{O}-\text{HLaNb}$ with OHSQ.

The ¹³C CP/MAS NMR spectra of the *n*-propoxy derivative of HLaNb and its products of the reactions with 4-penten-1-ol and 9-decen-1-ol are shown in Figure 5 (CH₂=CH(CH₂)₃O-HLaNb) and Figure 6 (CH₂=CH(CH₂)₈O-HLaNb). The A, B and C signals in the spectrum of the *n*-propoxy derivative of HLaNb are assigned to *n*-propoxy groups (Figure 5-a). The spectra of both CH₂=CH(CH₂)₃O-HLaNb and CH₂=CH(CH₂)₈O-HLaNb show the disappearance of these signals due to the *n*-propoxy groups. New signals at 31 (signal F), 33 (signal G), 80 (signal H), 115 (signal D) and 140 (signal E) ppm appear in the spectrum of CH₂=CH(CH₂)₃O-HLaNb, on the other hand, and are assignable to the CH₂=CH(CH₂)₃O-groups, as shown in Figure 5(b). The spectrum of CH₂=CH(CH₂)₈O-HLaNb also shows new signals at 28 (signal O), 31 (signal M), 32 (signal N), 34 (signal P), 35 (signal L), 80 (signal Q), 115 (signal J) and 139 (signal K). These signals can be assigned to the CH₂=CH(CH₂)₈O-groups, as shown in Figure 6-a. The chemical shifts for the carbon atoms attached to oxygen atoms (-CH₂O-) are 80 ppm for the products of the reactions with both 4-penten-1-ol and 9-decen-1-ol. The typical chemical shifts in liquid-state ¹³C NMR spectra of 4-penten-1-ol and 9-decen-1-ol molecules, on the contrary, were 62 and 63 ppm, respectively, and downfield shifts for the -CH₂O- environments were reported to be indicative of the formation Nb-O-C bonds.[30] With increases in the interlayer distances and IR results taken into account, the ¹³C CP/MAS NMR results provide sufficient evidence for the successful immobilization of 4-penten-1-ol or 9-decen-1-ol on the interlayer surface.

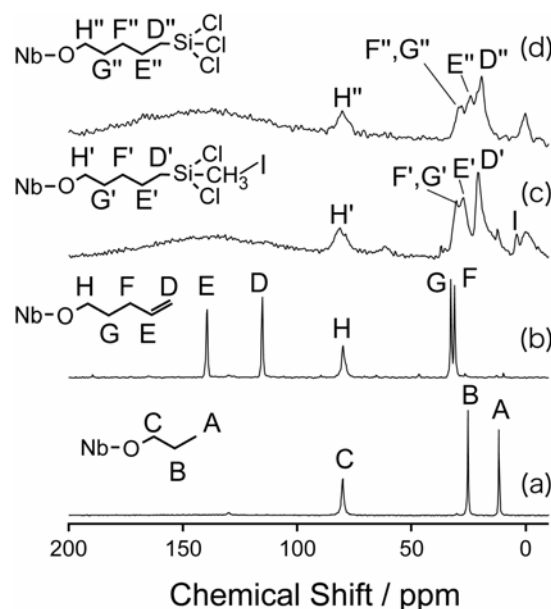


Figure 5. Solid-state ¹³C CP/MAS NMR spectra of (a) *n*-propoxy derivatives of HLaNb, (b) CH₂=CH(CH₂)₃O-HLaNb, (c) the product of the reaction between CH₂=CH(CH₂)₃O-HLaNb with dichloromethylsilane and (d) the product of the reaction between CH₂=CH(CH₂)₃O-HLaNb with trichloroilsilane.

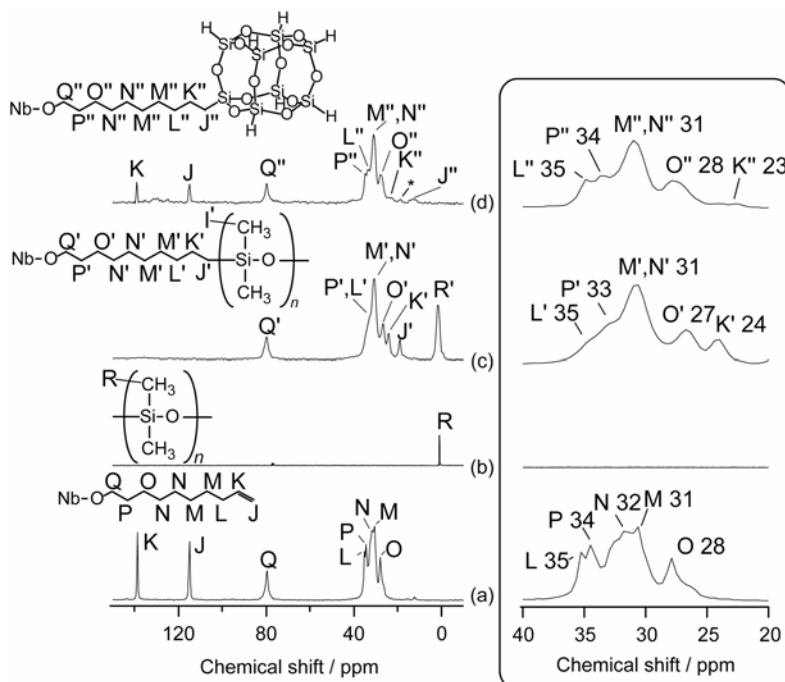


Figure 6. Solid-state ^{13}C CP/MAS NMR spectra of (a) $\text{CH}_2=\text{CH}(\text{CH}_2)_8\text{O}-\text{HLaNb}$, (b) PDMS, (c) the product of the reaction between $\text{CH}_2=\text{CH}(\text{CH}_2)_8\text{O}-\text{HLaNb}$ with H-PDMS and (d) the product of the reaction between $\text{CH}_2=\text{CH}(\text{CH}_2)_3\text{O}-\text{HLaNb}$ with OHSQ. The figure in the box (right) is the image expanded in the range 20–40 ppm.

The amounts of the $\text{CH}_2=\text{CH}(\text{CH}_2)_n\text{O}$ - groups are estimated from the carbon contents, 9.96 ($\text{CH}_2=\text{CH}(\text{CH}_2)_4\text{O}$ -) and 19.23 mass% ($\text{CH}_2=\text{CH}(\text{CH}_2)_4\text{O}$ -). Thus, the amount of the $\text{CH}_2=\text{CH}(\text{CH}_2)_4\text{O}$ - groups is 0.81 per $[\text{LaNb}_2\text{O}_7]$ and that of the $\text{CH}_2=\text{CH}(\text{CH}_2)_8\text{O}$ - groups is 0.90 per $[\text{LaNb}_2\text{O}_7]$.

Hydrosilylation of $\text{CH}_2=\text{CH}(\text{CH}_2)_3\text{O}-\text{HLaNb}$ with Hydrochlorosilanes

The XRD patterns of the products of the reactions between $\text{CH}_2=\text{CH}(\text{CH}_2)_3\text{O}-\text{HLaNb}$ and hydrochlorosilanes are shown in Figure 1. The XRD patterns of the products of the reactions with dichloromethylsilane, $[\text{CH}_3(\text{H})\text{SiCl}_2]$, and trichlorosilane, (HSiCl_3) , show the disappearance of the reflection due to $\text{CH}_2=\text{CH}(\text{CH}_2)_3\text{O}-\text{HLaNb}$, and new low-angle reflections are observed at $d = 2.41$ nm (trichlorosilane) and $d = 2.07$ nm (trichlorosilane). In addition, these XRD patterns of the products of the reactions with dichloromethylsilane and trichlorosilane show (100) reflections at 28.8° , indicating preservation of the perovskite-like slab structure after the reactions. We also attempted a reaction with dimethylchlorosilane $[(\text{CH}_3)_2(\text{H})\text{SiCl}]$, but the XRD pattern of the product (not shown) showed a low-angle reflection corresponding to the interlayer distance of $\text{CH}_2=\text{CH}(\text{CH}_2)_3\text{O}-\text{HLaNb}$ at $d = 1.85$ nm with a very weak shoulder at $d = 2.43$ nm, indicating much lower reactivity, which seems to be ascribable to an electronic effect of the chlorine substitute on the hydrosilanes.[35,47]

The solid-state ^{13}C CP/MAS NMR spectra of the products of the reactions with hydrochlorosilanes are shown in Figure 5. In the spectrum of the product of the reaction with

dichloromethylsilane, the signals due to the CH₂=CH- groups disappear and new signals appear at 4 (signal I), 21 (signal D'), 27 (signal E'), 30 (signal F' and G') and 82 (signal H') ppm. These signals are assignable to carbon atoms in the expected hydrosilylated product, [CH₃(Cl)₂Si(CH₂)₅-O-Nb], as shown in Figure 5-c. In similar fashion, the signals due to the CH₂=CH- groups disappear in the spectrum of the product of the reaction with trichlorosilane, and new signals appear at 22 (signal D''), 27 (signal E''), 31 (signal F'' and G'') and 83 (signal H'') ppm. These signals are assignable to carbon atoms in the expected hydrosilylated product, [Cl₃Si(CH₂)₅-O-Nb], as shown in Figure 5-d. No signals assignable to α -addition-type hydrosilylated products are detected, indicating the occurrence of β -addition only.

The IR spectra of the products of the reactions with hydrochlorosilanes are shown in Figure 3. In the spectrum of the products of the reactions with dichloromethylsilane, a new band is observed at 1259 cm⁻¹, which is assignable to the $\delta_{(Si-CH_3)}$ mode.[48] Both the spectra show the disappearance of the $\nu_{(CH)}$ mode of the CH₂=CH- groups, indicating the occurrence of hydrosilylation. In addition, both the spectra show the $\nu_{(SiH)}$ band at either 2160 cm⁻¹ (dichloromethylsilane) or at 2238 and 2248 cm⁻¹ (trichlorosilane).[48] In the spectrum of the product of the reaction with trichlorosilane, a weak shoulder assignable to the $\nu_{(Si-O-Si)}$ mode is detected at 1039 cm⁻¹. The presence of the $\nu_{(SiH)}$ and $\nu_{(Si-O-Si)}$ bands is discussed below.

Figure 7 shows the solid-state ²⁹Si CP/MAS NMR spectra of the products of the reactions with hydrochlorosilanes. Both the spectra show signals assignable to the expected hydrosilylation products, a Cl₂(CH₃)SiCH₂- environment at 33 ppm (dichloromethylsilane) and a Cl₃SiCH₂- environment at 14 ppm (trichlorosilane),[49] which are consistent with the solid-state ¹³C CP/MAS NMR results. Some additional signals are also observed, however, in upfield regions of both the spectra. In the solid-state ²⁹Si CP/MAS NMR spectrum of the product of the reaction with dichloromethylsilane, the signals at 6, -20 and -35 ppm are ascribable to the CH₃Si(O-)₂CH₂-, (CH₃)ClSi(O-)CH₂- and H(CH₃)Si(O-)₂ environments, respectively. The solid-state ²⁹Si CP/MAS NMR spectrum of the product of the reaction with trichlorosilane shows signals at -35, -62 and -86 ppm, which can be assigned to the HSiCl₂(O-), HSiCl(O-)₂ and HSi(O-)₃ environments, respectively. These environments, observed in both spectra, indicate the occurrence of hydrolysis and condensation reactions to form siloxane bonds, which is consistent with the presence of the $\nu_{(Si-O-Si)}$ band observed in the IR results. In addition, ≡Si-H groups are present in the silyl groups formed by the hydrolysis and condensation reactions without hydrosilylation. These results are consistent with the observation of the $\nu_{(SiH)}$ bands in the IR spectra of the products of the reactions with dichloromethylsilane and trichlorosilane. Hydrolysis and condensation reactions are expected to occur during the process of synthesis and/or washing with impurity water, since the ≡SiCl groups are highly moisture-sensitive.

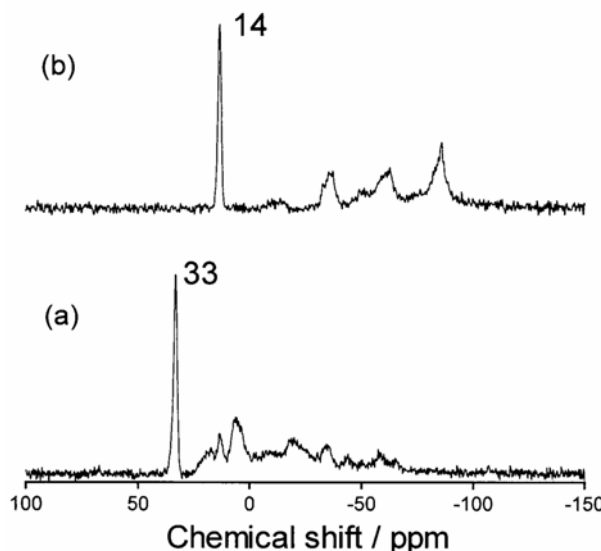


Figure 7. Solid-state ^{29}Si CP/MAS NMR spectra of (a) the product of the reaction between $\text{CH}_2=\text{CH}(\text{CH}_2)_3\text{O}-\text{HLaNb}$ with dichloromethylsilane and (b) the product of the reaction between $\text{CH}_2=\text{CH}(\text{CH}_2)_3\text{O}-\text{HLaNb}$ with trichloroisilane.

Hydrosilylation of $\text{CH}_2=\text{CH}(\text{CH}_2)_8\text{O}-\text{HLaNb}$ with H-PDMS

The XRD pattern of the product of the reaction between $\text{CH}_2=\text{CH}(\text{CH}_2)_8\text{O}-\text{HLaNb}$ and H-PDMS, $\text{HSi}(\text{CH}_3)_2\text{O}-[\text{Si}(\text{CH}_3)_2\text{O}]_n-(\text{CH}_3)_2\text{Si-H}$ ($n \approx 6$), is shown in Figure 2. The XRD pattern of the product of the reaction with H-PDMS shows the disappearance of the reflection of $\text{CH}_2=\text{CH}(\text{CH}_2)_8\text{O}-\text{HLaNb}$, and new broad reflections are observed at $d = 3.33$ nm and $d = 1.61$ nm. These reflections are indexed as (001) and (002), respectively, to give an approximate interlayer distance of ca. 3.3 nm. The interlayer distance can not be determined precisely, however, since weak reflections (marked by arrows) overlap at ca. 9.1° (ca. 1.2 nm) and ca. 12.1° (ca. 0.92 nm), indicating that the product of the reaction with H-PDMS is composed of compounds with different interlayer distances. Preliminary analysis of the BET specific surface area of $\text{CH}_2=\text{CH}(\text{CH}_2)_8\text{O}-\text{HLaNb}$ and the product of the reaction between $\text{CH}_2=\text{CH}(\text{CH}_2)_8\text{O}-\text{HLaNb}$ and H-PDMS also showed non-porous features for these products. The (100) reflection at 28.8° is observed at the same position, indicating preservation of the perovskite-like slab structure.

The IR spectrum of the product of reaction between $\text{CH}_2=\text{CH}(\text{CH}_2)_8\text{O}-\text{HLaNb}$ and H-PDMS is shown in Figure 4. Bands are observed at 1260 cm^{-1} and $1090\text{--}1020\text{ cm}^{-1}$ due to the $\delta_{(\text{Si-CH}_3)}$ and $\nu_{(\text{Si-O-Si})}$ modes of the PDMS chain,[50] while the band due to the $\nu_{(\text{SiH})}$ mode of H-PDMS at 2160 cm^{-1} disappears (Figures 4-b and -c). The band due to the $\nu_{(\text{CH})}$ mode of the $\text{CH}_2=\text{CH-}$ groups at 3074 cm^{-1} is also no longer observed. These observations suggest the occurrence of hydrosilylation.

The solid-state ^{13}C CP/MAS NMR spectrum of the product of the reaction between $\text{CH}_2=\text{CH}(\text{CH}_2)_8\text{O}-\text{HLaNb}$ and H-PDMS is shown in Figure 6. Signals at 115 and 139 ppm due to the $\text{CH}_2=\text{CH}(\text{CH}_2)-$ and $\text{CH}_2=\text{CH}(\text{CH}_2)\text{-}$ groups disappear, and new signals appear at

18 (signal J') and 24 (signal K') ppm. These new signals can be assigned to the -OSi(CH₃)₂CH₂CH₂- (18 ppm) and -OSi(CH₂)₂CH₂CH₂- (24 ppm) environments,[51] providing additional evidence for the occurrence of β -addition-type hydrosilylation.

The solid-state ²⁹Si CP/MAS NMR spectrum of the product of the reaction between CH₂=CH(CH₂)₈O-HLaNb and H-PDMS is shown in Figure 8. The new signal at -22 ppm is assignable to a (CH₃)₂Si(OSi)₂ environment of the PDMS chains.[49] Another new signal at 8 ppm can be assigned to a (CH₃)₂Si(OSi)CH₂- environment (signal B'),[49] which is consistent with the occurrence of hydrosilylation. No H(CH₃)₂Si(OSi)- environment (signal B) is not detected at -7 ppm, moreover, indicating that all the SiH groups in H-PDMS are involved in the hydrosilylation with immobilized CH₂=CH- groups. Assignment of the additional weak signals at 2 and 29 ppm (marked by asterisks) has not yet been possible.

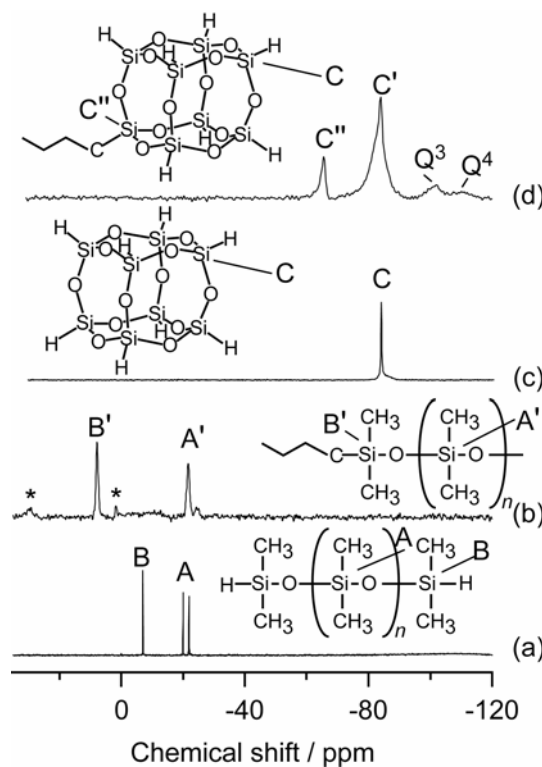
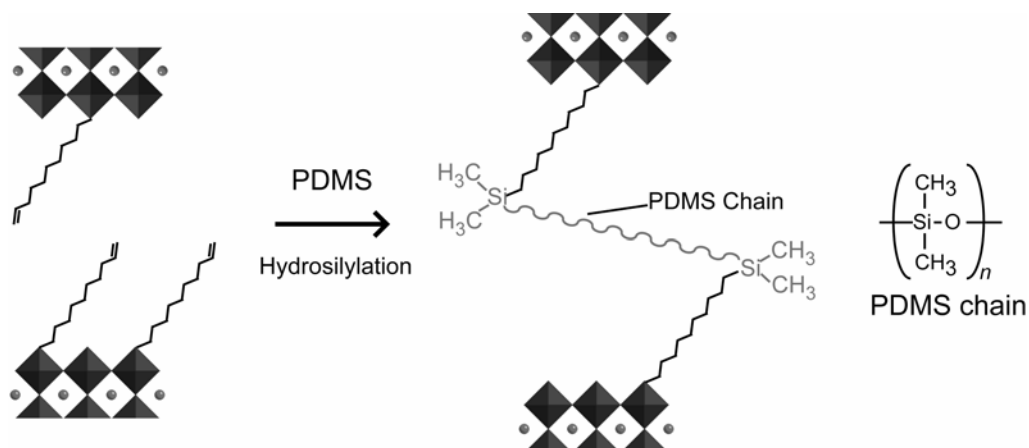
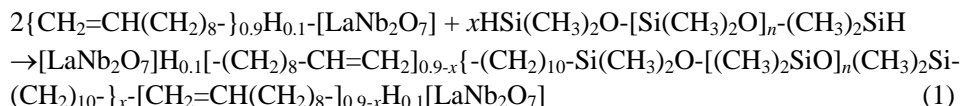


Figure 8. Solid-state ²⁹Si CP/MAS NMR spectra of (a) H-PDMS, (b) the product of the reaction between CH₂=CH(CH₂)₈O-HLaNb with H-PDMS, (c) OHSQ and (d) the product of the reaction between CH₂=CH(CH₂)₃O-HLaNb with OHSQ.

The expansion of the interlayer distance demonstrated by the XRD results and the presence of the $\delta_{\text{Si}-\text{CH}_3}$ and $\nu_{\text{Si}-\text{O}-\text{Si}}$ modes of the PDMS chains in the IR spectra indicate the presence of PDMS chains in the interlayer space of HLaNb. The disappearance of the ν_{SiH} band suggests, moreover, that all the SiH groups attached to the PDMS chains are involved in hydrosilylation. The proposed reactions are illustrated as scheme 2 and can also be expressed by the following equation:



Scheme 2. The proposed reaction between $\text{CH}_2=\text{CH}(\text{CH}_2)_8\text{-HLaNb}$ and H-PDMS.

Although intercalation compounds with polymers generally exhibit their own uniform interlayer distances,[1] XRD analysis demonstrates that the interlayer distance is not uniform. The absence of a uniform interlayer environment seems to be characteristic of the grafting reactions of polymer chains: since intercalated H-PDMS is involved in hydrosilylation, the formation of a variety of interlayer configurations of PDMS chains is likely.

The XRF results showed that the Si/Nb ratio was 0.60. The amount of the PDMS chain per $[\text{LaNb}_2\text{O}_7]$ cannot be determined precisely, however, since unidentified side reactions occurred, as evidenced by the solid-state ^{29}Si CP/MAS NMR. The amount of the PDMS chain is therefore estimated roughly assuming that the product consists of the hydrosilylated product only. From the XRF results, the x value of equation (1) is calculated as $0.60 \times 4/(n+2) = 0.30$. (Since four Nb atoms are present in two $[\text{LaNb}_2\text{O}_7]$ units, the 0.60×4 Si atoms are present. The average number of Si atoms in a PDMS chain is expressed by '($n+2$)'. The calculation is performed with $n = 6$). This result indicates that about 30% of the $\text{CH}_2=\text{CH}$ groups originally present in the $\text{CH}_2=\text{CH}(\text{CH}_2)_8\text{O-}$ derivative of HLaNb react with H-PDMS. The ^{13}C CP/MAS NMR shows the absence of unreacted $\text{CH}_2=\text{CH-}$ groups, however, which is inconsistent with the estimated amount of reacted $\text{CH}_2=\text{CH-}$ groups. We have tentatively interpreted these observations as resulting from hydrolysis of the unreacted $\text{CH}_2=\text{CH}(\text{CH}_2)_8\text{O-}$ groups during the experimental process.

Hydrosilylation of $\text{CH}_2=\text{CH}(\text{CH}_2)_8\text{O-HLaNb}$ with OHSQ

The XRD pattern of the product of the reaction between $\text{CH}_2=\text{CH}(\text{CH}_2)_8\text{O-HLaNb}$ and OHSQ is shown in Figure 2. The low-angle reflection corresponds to a d value of 2.70 nm, indicating that the interlayer distance of the product increases only slightly. The intensity of the low-angle reflection of $\text{CH}_2=\text{CH}(\text{CH}_2)_8\text{O-HLaNb}$ decreases drastically, however, after the

reaction with OHSQ. The (100) reflection at 28.8° is observed in the same position, indicating preservation of the perovskite-like slab structure.

The IR spectra of OHSQ and the product of reaction between CH₂=CH(CH₂)₈O-HLaNb and OHSQ are shown in Figures 4-d and 4-e, respectively. In the IR spectrum of OHSQ, the ν_(SiH) band at 2280 cm⁻¹, the δ_(SiH) band at 864 cm⁻¹, and the broad ν_(Si-O-Si) band centered at 1120 cm⁻¹ are observed.[52] The IR spectrum of the product of the reaction between CH₂=CH(CH₂)₈O-HLaNb and OHSQ shows the ν_(SiH) band at 2250 cm⁻¹, the δ_(SiH) band at 850 cm⁻¹, and the ν_(Si-O-Si) band at 1124 cm⁻¹, indicating the presence of OHSQ in the product. The relative intensity of the ν_(CH) bands of the CH₂=CH- groups at 3075 cm⁻¹ with respect to the ν_(Nb-O-Nb) band at 608 cm⁻¹[53] decreases, suggesting the occurrence of hydrosilylation.

The ¹³C CP/MAS NMR spectrum of the product of the reaction between CH₂=CH(CH₂)₈O-HLaNb and OHSQ is shown in Figure 6. Signals are detected at 13 (signal J") and 23 ppm (signal K"), which are assignable to (SiO)₃SiCH₂CH₂- (13 ppm) and (SiO)₃SiCH₂CH₂- (23 ppm) environments formed by β-addition-type hydrosilylation.[54,55] The signal at 18 ppm (marked by asterisk) may be assigned to (SiO)₃SiCH(CH₃)- groups, moreover, indicating the simultaneous occurrence of an α-addition reaction. Signals are also detected at 115 and 139 ppm, indicating the presence of unreacted CH₂=CH- groups.

The ²⁹Si CP/MAS NMR spectrum of OHSQ and the product of the reaction between CH₂=CH(CH₂)₈O-HLaNb and OHSQ are shown in Figure 8. In the ²⁹Si CP/MAS NMR spectrum of OHSQ, a signal due to an HSi(OSi)₃ environment is observed at -84 ppm (signal C). The ²⁹Si CP/MAS NMR spectrum of the product of the reaction between CH₂=CH(CH₂)₈O-HLaNb and OHSQ shows a new signal at -65 ppm (signal C"). This signal can be assigned to an -CH₂Si(OSi)₃ environment,[56] which is consistent with the occurrence of hydrosilylation. A signal due to the HSi(OSi)₃ environment is present at -84 ppm. Since the -CH₂Si(OSi)₃ : HSi(OSi)₃ ratio was estimated by ²⁹Si MAS NMR (not shown) to be ca. 1 : 4.9, 1.4 SiH groups in an OHSQ molecule are involved in hydrosilylation, on average. Signals at -100 and -110 ppm are assignable to Si(OSi)₃(O-) and Si(OSi)₄ environments, respectively.[49] These signals originate from impurities in the starting OHSQ, as described in the experimental section.

Although the occurrence of hydrosilylation is shown by ¹³C and ²⁹Si CP/MAS NMR, the interlayer distance does not clearly increase after the reaction, as shown by the XRD results (Figure 2). For the investigation of the presence of OHSQ in the interlayer space, HLaNb, CH₂=CH(CH₂)₈O-HLaNb and the product of the reaction between CH₂=CH(CH₂)₈O-HLaNb and OHSQ were pyrolyzed at 350°C and 400°C. The XRD patterns of the pyrolyzed products are shown in Figure 9. The XRD pattern of HLaNb does not change after pyrolysis (Figure 9-a), because the TG curves of HLaNb showed the onset temperature of dehydroxylation for HLaNb as ca. 400°C.[57,58] The XRD patterns of both the pyrolyzed residues from CH₂=CH(CH₂)₈O-HLaNb show decreases in the interlayer distance from 2.67 nm to 1.08 (350°C) and 1.06 nm (400°C), indicating the decomposition of CH₂=CH(CH₂)₈O-groups in the interlayer space. Broad reflections (1.84 nm in Figures 9-b and 9-c) are also observed (marked by arrows), indicating that the decomposition is not complete. On the other hand, the XRD pattern of the pyrolyzed product of the reaction between CH₂=CH(CH₂)₈O-HLaNb and OHSQ at 350° shows a new reflection at 1.60 nm (Figure 9-d). In the residue of the product of the reaction between CH₂=CH(CH₂)₈O-HLaNb and OHSQ pyrolyzed at 400°C, a reflection is observed at ca. 1.3 nm (Figure 9-e). In addition, (100) reflections due to

the crystal structures of perovskite-like slabs are observed in the XRD patterns of all the pyrolyzed products at 28.9°. These results clearly indicate that the pyrolysis behavior of the product of the reaction between $\text{CH}_2=\text{CH}(\text{CH}_2)_8\text{O}-\text{HLaNb}$ and OHSQ is different from that of HLaNb and $\text{CH}_2=\text{CH}(\text{CH}_2)_8\text{O}-\text{HLaNb}$, a finding ascribable to the presence of OHSQ in the interlayer space of HLaNb. Based on the ^{13}C and ^{29}Si CP/MAS NMR results, therefore, the presence of OHSQ in the interlayer space strongly suggests the occurrence of hydrosilylation in the interlayer space.

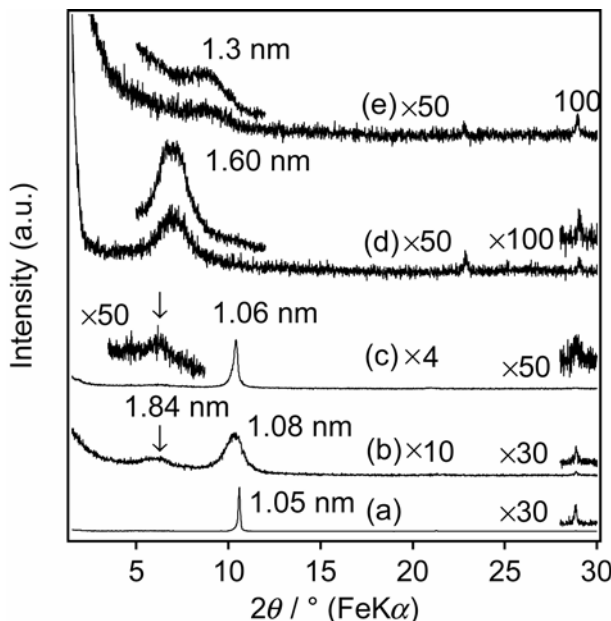


Figure 9. The XRD patterns of (a) the pyrolyzed HLaNb at 400°C, (b) the pyrolyzed $\text{CH}_2=\text{CH}(\text{CH}_2)_8\text{O}-\text{HLaNb}$ at 350°C, (c) the pyrolyzed $\text{CH}_2=\text{CH}(\text{CH}_2)_8\text{O}-\text{HLaNb}$ at 400°C, (d) the pyrolyzed product of the reaction with OHSQ at 350°C and (e) the pyrolyzed product of the reaction with OHSQ at 400°C. The inset patterns in (d) and (e) are recorded at a scan speed of 0.3°/min in the range of 5–12°.

The reason for the very small change in the interlayer distance is attributable to the alkyl chain conformation. The ^{13}C CP/MAS NMR spectrum (Figure 6) of $\text{CH}_2=\text{CH}(\text{CH}_2)_8\text{O}-\text{HLaNb}$ shows a signal of - CH_2- chains (signal N) at 32 ppm (we do not discuss the position of signal M, since the $\text{CH}_2=\text{CH}$ bond may affect the environment of carbon atoms, $\text{CH}_2=\text{CHCH}_2\text{CH}_2\text{CH}_2-\text{CH}_2-$), and signal of the - CH_2- chains of the product of the reaction between $\text{CH}_2=\text{CH}(\text{CH}_2)_8\text{O}-\text{HLaNb}$ and OHSQ are detected at 31 ppm (signals M'' and N''). The chemical shifts of the - CH_2- groups generally reflect the conformation of - CH_2- chains; signals for trans-conformation are detected at 32.6 ppm, while the presence of a larger amount of gauche-conformations leads to a greater upfield shift.[59,60] The conformation of the - CH_2- chains should change, therefore, after the occurrence of hydrosilylation between $\text{CH}_2=\text{CH}(\text{CH}_2)_8\text{O}-\text{HLaNb}$ and OHSQ to form a substantial amount of gauche-conformations. Gauche-conformation formation could consequently lead to a decrease in the length of the $\text{CH}_2=\text{CH}(\text{CH}_2)_8\text{O}-$ groups to cancel out the expected increase in the interlayer distance due to the presence of OHSQ in the interlayer space.

When OHSQ is assumed to be a cube (Figure 10), the length of one side is estimated by the Si-O bond length, Si-O-Si bond angle and ionic diameter of oxygen to be 0.635 nm.[61,62] The volume of OHSQ is therefore estimated to be $0.635^3 = 0.256 \text{ nm}^3$. Since the diagonal length of OHSQ is $0.635 \times \sqrt{3} = 1.10 \text{ nm}$, a maximum cross-section is estimated by assuming a circle with a diameter of 1.10 nm to be 0.951 nm^2 , an area corresponding to 6.28 [LaNb₂O₇] units. The volume of the space between two adjacent nano-sheets for 6.28 [LaNb₂O₇] units is calculated as follows:

$$\Delta d \times (\text{area of } 6.28 \text{ [LaNb}_2\text{O}_7\text{] units}) = (2.70 - 1.03) \times 0.389^2 \times 6.28 = 1.60 \text{ nm}^3$$

(The thickness of the perovskite-like slab is calculated to be $1.03 = 0.389 \times 2 + 0.25 \text{ nm}$ (ionic diameter of oxygen)[62])

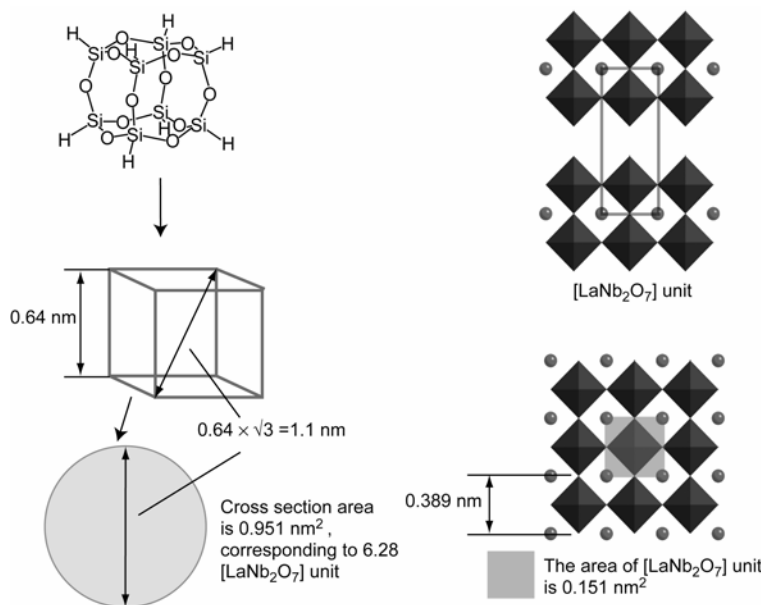


Figure 10. The length of a side assuming OHSQ to be a cube and the cross-section area of OHSQ are demonstrated. The area of the [LaNb₂O₇] unit is shown (right).

The volume of the CH₂=CH(CH₂)₈- group is roughly estimated to be $0.186 \times 0.127 \times 10 = 0.24 \text{ nm}^3$ (a cross-section area of the -CH₂- chains is 0.186 nm^2 [63] and the increase in the *all-trans* -CH₂- chain is 0.127 nm[64]). Since the 6.28×0.9 of CH₂=CH(CH₂)₈- groups are present in 6.28 [LaNb₂O₇] units (the average amount of CH₂=CH(CH₂)₈- group per [LaNb₂O₇] is '0.9'), the estimated free volume is $0.263 (= 1.60 - 0.24 \times 6.28 \times 0.9) \text{ nm}^3$, which is larger than the estimated volume of OHSQ (0.256 nm^3). An OHSQ molecule could therefore fit into 6.28 [LaNb₂O₇] units bearing the CH₂=CH(CH₂)₈- groups, corresponding to an Si/Nb ratio of 0.64 (0.16 OHSQ per [LaNb₂O₇].) The XRF results, on the contrary, showed the Si/Nb ratio to be 0.51, indicating that OHSQ can be spatially accommodated in the space between two adjacent nano-sheets. The amount of OHSQ is estimated from the Si/Nb ratio, to be 0.13 per [LaNb₂O₇], indicating that OHSQ occupies 80% ($0.51/0.64$) of the total free volume (0.263 nm^3). The actual amount of OHSQ per [LaNb₂O₇] seems to be lower; impurities are also present to a certain extent in OHSQ.

The amount of carbon, on the other hand, is determined by CHN analysis to be 18.1%. After the reaction between $\text{CH}_2=\text{CH}(\text{CH}_2)_8\text{-HLaNb}$ with OHSQ, the general formula is expressed by $\{(H_7\text{Si}_8\text{O}_{12}\text{-}(\text{CH}_2)_{10})_x\{\text{CH}_2=\text{CH}(\text{CH}_2)_8\text{-}\}^{0.9-x}\text{H}_{0.1}\text{LaNb}_2\text{O}_7$. The amount of OHSQ is therefore calculated by the following equation:

$$10 \times 0.9 \times (\text{atomic weight of C}) / [\text{Mw}_{\{(H_7\text{Si}_8\text{O}_{12}\text{-}(\text{CH}_2)_{10})_x\{\text{CH}_2=\text{CH}(\text{CH}_2)_8\text{-}\}^{0.9-x}\text{H}_{0.1}\text{LaNb}_2\text{O}_7}}] = 0.181$$

The amount of OHSQ, x value, is estimated to be 0.09 per $[\text{LaNb}_2\text{O}_7]$, which is smaller than the value estimated from the XRF results (0.13). This difference could be partially attributed to the presence of silicon containing impurities. Based on the two types of estimations, we assume that the space between two adjacent nano-sheets is occupied by the $\text{CH}_2=\text{CH}(\text{CH}_2)_8\text{-}$ groups (~85%) and hydrosilylated OHSQ (~9–14%).

CONCLUSION

We have investigated the hydrosilylation of the $\text{CH}_2=\text{CH-}$ groups immobilized on the interlayer surface of an ion-exchangeable layered perovskite, $\text{HLaNb}_2\text{O}_7\text{-}x\text{H}_2\text{O}$, with SiH groups in hydrochlorosilanes, hydride-terminated polydimethylsiloxane and octahydridosilsesquioxane. Immobilization of the $\text{CH}_2=\text{CH-}$ groups on the interlayer surface was conducted by reacting the *n*-propoxy derivative of $\text{HLaNb}_2\text{O}_7\text{-}x\text{H}_2\text{O}$ with 4-penten-1-ol or 9-decen-1-ol to form the $\text{CH}_2=\text{CH}(\text{CH}_2)_n\text{O}$ -derivative ($n = 3$ or 8) of $\text{HLaNb}_2\text{O}_7\text{-}x\text{H}_2\text{O}$. The $\text{CH}_2=\text{CH-}$ groups on the interlayer surface can be reacted with hydrochlorosilanes, hydride-terminated polydimethylsiloxane or octahydridosilsesquioxane to give a hydrosilylated product. The spectroscopic analyses and the increases in the interlayer distances clearly indicate that hydrosilylation with hydrochlorosilanes and hydride-terminated polydimethylsiloxane occurs in the interlayer space. Although the XRD pattern of the product of the reaction between the $\text{CH}_2=\text{CH}(\text{CH}_2)_n\text{O}$ -derivative of HLaNb and octahydridosilsesquioxane shows a slight increase in the interlayer distance, the ^{13}C and ^{29}Si CP/MAS NMR spectra indicate the occurrence of hydrosilylation. The hydrosilylation with octahydridosilsesquioxane in the interlayer space is demonstrated by its pyrolysis behavior, and the lack of an increase in the interlayer distance is explained by the change in the conformation of the - CH_2- chain. In addition, the XRD results for all the hydrosilylated products show the (100) reflection at 28.8° , indicating the preservation of the perovskite-like slab structure during hydrosilylation. This study clearly demonstrates, therefore, that grafting of the $\text{CH}_2=\text{CH}(\text{CH}_2)_n\text{O}$ groups and subsequent hydrosilylation is a versatile approach to grafting functional groups on the interlayer surface of ion-exchangeable layered perovskites. Various inorganic-organic hybrids can be expected to be prepared via hydrosilylation by applying other reactions involving various organic and organometallic molecules.

ACKNOWLEDGEMENTS

The authors express their gratitude to Prof. Kazuyuki Kuroda of Waseda University, Department of Applied Chemistry, for his valuable advice. We also wish to acknowledge the

technical support provide for the experiments by Dr. Ichiro Fujiwara and Dr. Yusuke Mori. This work was supported financially by the Grant-in-Aid for Scientific Research (No. 14350462) from the Ministry of Education, Science, Sports, and Culture, Japan, and by 21COE "Practical Nano-Chemistry" from MEXT, Japan.

REFERENCES

- [1] Alexandre, M.; Dubois, P. *Mater. Sci. Eng.* 2000, *R28*, 1-63.
- [2] Choy, J.-H. *J. Phys. Chem. Solid* 2004, *65*, 373-383.
- [3] Corriu, R. J. P.; Leclercq, D. *Angew. Chem. Int. Ed. Engl.* 1996, *35*, 1420-1436.
- [4] Judeinstein, P.; Sanchez, C. *J. Mater. Chem.* 1996, *6*, 511-525.
- [5] Sanchez, C.; Ribot, F. *New J. Chem.* 1994, *18*, 1007-1047.
- [6] Sanchez, C.; Soler-Illia, G. J. d. A. A.; Ribot, F.; Lalot, T.; Mayer, C. R.; Cabuil, V. *Chem. Mater.* 2001, *13*, 3061-3083.
- [7] Ogawa, M.; Kuroda, K. *Chem. Rev.* 1995, *95*, 399-438.
- [8] Ogawa, M.; Kuroda, K. *Bull. Chem. Soc. Jpn.* 1997, *70*, 2593-2618.
- [9] *Intercalation Chemistry.*, Whittingham, M. S.; Jacobson, A. J., Eds. Academic Press: New York, 1982.
- [10] O'Hare, D., *Inorganic Materials*, 2nd ed. John Wiley and Sons: Chichester, 1996; p 171.
- [11] Kanatzidis, M. G.; Wu, C.-G.; Marcy, H. O.; Kannewurf, C. R. *J. Am. Chem. Soc.* 1989, *111*, 4139-4141.
- [12] Mehrotra, V.; Giannelis, E. P. *Solid State Ionics*. 1992, *51*, 115-122.
- [13] Ebina, Y.; Tanaka, A.; Kondo, J. N.; Domen, K. *Chem. Mater.* 1996, *8*, 2534-2538.
- [14] Ruiz-Hitzky, E.; Rojo, J. M. *Nature*. 1980, *287*, 28-30.
- [15] Ogawa, M.; Okutomo, S.; Kuroda, K. *J. Am. Chem. Soc.* 1998, *120*, 7361-7362.
- [16] Tunney, J. J.; Detellier, C. *J. Mater. Chem.* 1996, *6*, 1679-1685.
- [17] Komori, Y.; Enoto, H.; Takenawa, R.; Hayashi, S.; Sugahara, Y.; Kuroda, K. *Langmuir*. 2000, *16*, 5506-5508.
- [18] Kikkawa, S.; Kanamaru, F.; Koizumi, M. *Inorg. Chem.* 1976, *15*, 2195-2197.
- [19] Alberti, G.; Casciola, M.; Constantino, U.; Vivani, R. *Adv. Mater.* 1996, *8*, 291-303.
- [20] Goodenough, J. B.; Longo, J. M., "Landolt-Börnstein" New Series, Group III, Vol. 4, Part a. Springer: Berlin, 1970.
- [21] Cross, L. E., *Ferroelectric Ceramics*. Brinkhauser Verlag: Basel, 1993.
- [22] Du, X. F.; Chen, I.-W. *Ferroelectrics*. 1998, *208*, 237-256.
- [23] Kurtz, S. K.; Perry, T. T. *J. Appl. Phys.* 1968, *39*, 3798-3813.
- [24] Schaak, R. E.; Mallouk, T. E. *Chem. Mater.* 2002, *14*, 1455-1471.
- [25] Yoshimura, J.; Ebina, Y.; Kondo, J. N.; Domen, K.; Tanaka, A. *J. Phys. Chem.* 1993, *97*, 1970-1973.
- [26] Kudo, M.; Tsuzuki, S.; Katshumata, K.; Yasumori, A.; Sugahara, Y. *Chem. Phys. Lett.* 2004, *393*, 12-16.
- [27] Sato, M.; Abo, J.; Jin, T.; Ohta, M. *J. Alloys Compd.* 1993, *192*, 81-83.
- [28] Zhong, Z.; Ding, W.; Hou, W.; Chen, Y.; Chen, X.; Zhu, Y.; Min, N. *Chem. Mater.* 2001, *13*, 538-542.

- [29] Tahara, S.; Sugahara, Y., *Recent Res. Dev. Inorg. Chem.*, 2004, **4**, 13-34.
- [30] Takahashi, S.; Nakato, T.; Hayashi, S.; Sugahara, Y.; Kuroda, K. *Inorg. Chem.* 1995, **34**, 5065-5069.
- [31] Tahara, S.; Sugahara, Y. *Langmuir*. 2003, **19**, 9473-9478.
- [32] Suzuki, H.; Notsu, K.; Takeda, Y.; Sugimoto, W.; Sugahara, Y. *Chem. Mater.* 2003, **15**, 636-641.
- [33] Speier, J. L., *Advances in Organometallic Chemistry*. Academic Press: New York, 1979; Vol. 17, p 407-447.
- [34] Ojima, I., The Chemistry of Organic Silicon compounds. (Chapter 25). Wiley: Chichester, 1989.
- [35] Marciniec, B.; Gulinski, J.; Urbaniak, W.; Kornetka, Z. W., *Comprehensive Handbook on Hydrosilylation*. Pergamon press: Oxford, 1992.
- [36] Musolf, M. C.; Speier, J. L. *J. Org. Chem.* 1964, **29**, 2519-2524.
- [37] Buriak, J. M. *Chem. Commun.* 1999, 1051-1060.
- [38] Boukherroub, R.; Morin, S.; Bensebaa, F.; Wayner, D. D. M. *Langmuir*. 1999, **15**, 3831-3835.
- [39] Fyfe, C. A.; Niu, J., *Macromolecules*. 1995, **28**, 3894-3897.
- [40] Katsoulis, D. E.; Chao, T. C.-S.; McQuiston, E. A.; Chen, C.; Kenney, M. E. *Mater. Res. Soc. Symp. proc.* 1998, **519**, 321-326.
- [41] Chao, T. C.; Katsoulis, D. E.; Kenney, M. E. *Chem. Mater.* 2001, **13**, 4269-4277.
- [42] Yoshioka, S.; Takeda, Y.; Uchimaru, Y.; Sugahara, Y. *J. Organomet. Chem.* 2003, **686**, 145-150.
- [43] Gopalakrishnan, J.; Bhat, V.; Raveau, B. *Mater. Res. Bull.* 1987, **22**, 413-417.
- [44] Agaskar, P. A. *Inorg. Chem.* 1991, **30**, 2707-2708.
- [45] Agaskar, P. A.; Klemperer W. G. *Inorg. Chim. Acta* 1995, **229**, 355-364.
- [46] Shriver, D. F.; Dreizdon, M. A., *The Manipulation of Air-Sensitive Compounds*, second ed. Wiley-Interscience: New York, 1986.
- [47] Eaborn, C.; Bott, B. W., *Organometallic Compounds of the Group IV Elements Part 2*. Marcel Dekker: New York, 1986; Vol. 1, p 1968.
- [48] Shurvell, H. F., Sample Characterization and Spectral Data Processing. In *Handbook of Vibrational Spectroscopy*, Chalmers, J. M.; Griffiths, P. R., Eds. Wiley: Chichester, 2002; Vol. 3, p 1783.
- [49] Marsmann, H., NMR 17, Basic Principals and Progress, Oxygen-17 and Silicon-29. In *NMR 17, Basic Principles and Progress, Oxygen-17 and Silicon-29*, Diehl, P.; Fluck, E.; Cosfeld, R., Eds. Springer-Verlag: Berlin, 1981.
- [50] Marchand, A.; Valade, J. *J. Organomet. Chem.* 1968, **12**, 305-322.
- [51] Henkensmeier, D.; Abele, B. C.; Candussio, A.; Thiem, J. *Macromol. Chem. Phys.* 2004, **205**, 1851-1857.
- [52] Frye, C. L.; Collins, W. T. *J. Am. Chem. Soc.* 1970, **92**, 5586-5588.
- [53] Vandeborre, M. T.; Husson, E.; Chubb, M. *Spectrochim. Acta*. 1984, **A40**, 361-365.
- [54] Tsuchida, A.; Bolln, C.; Sernetz, F. G.; Frey, H.; Mühaupt, R. *Macromolecules*. 1997, **30**, 2818-2824.
- [55] Sellinger, A.; Laine, R. M. *Chem. Mater.* 1996, **8**, 1592-1593.
- [56] Auner, N.; Bats, J. W.; Katsoulis, D. E.; Suto, M.; Tecklenburg, R. E.; Zank, G. A. *Chem. Mater.* 2000, **12**, 3402-3418.
- [57] Ollivier, P. J.; Mallouk, T. E. *Chem. Mater.* 1998, **10**, 2585-2587.

- [58] Jacobson, A. J.; Lewandouski, J. T.; Johnson, J. W. *J. Less-Common Met.* 1986, **116**, 137-146.
- [59] Pursch, M.; Strohschein, S.; Händel, H.; Albert, K. *Anal. Chem.* 1996, **68**, 386-393.
- [60] Pursch, M.; Brindle, R.; Ellwanger, A.; Sander, L. C.; Bell, C. M.; Händel, H.; Albert, K. *Solid State Nucl. Magn. Reson.* 1997, **9**, 191-201.
- [61] Rattay, M.; Fenske, D.; Jutzi, P. *Organometallics.* 1998, **17**, 2930-2932.
- [62] Shannon, R. D. *Acta Crystallogr.* 1976, **A32**, 751-767.
- [63] Goñi, A.; Ruis, J.; Insausti, M.; Lezama, L. M.; Pizarro, J. L.; Arriortua, M. I.; Rojo, T. *Chem. Mater.* 1996, **8**, 1052-1060.
- [64] Jacobson, A. J.; Johnson, J. W.; Lewandouski, J. T. *Mater. Res. Bull.* 1987, **22**, 45-51.

Chapter 3

USE OF ELECTROCHEMISTRY AND PALLADIUM CATALYSTS FOR AN EFFICIENT SYNTHESIS OF CARBONYL COMPOUNDS

Isabella Chiarotto

Università degli studi di Roma "La Sapienza".

Dipartimento di Ingegneria Chimica, dei Materiali delle Materie Prime e Metallurgia. 7, via Castro Laurenziano Roma I-00161, Italy

ABSTRACT

The great utility of carbonylic compounds as starting materials is well known; the importance of the carbonyl group derives from its reactivity, being susceptible to nucleophilic attack at carbon and electrophilic attack at oxygen. Transition metals can be used as reagents and catalysts to bring carbon monoxide into many organic compounds. Among transition metals, used in organic synthesis, palladium complexes offer versatile and very useful synthetic methods for carbonylation reaction and, generally, for carbon-carbon bond formation.

A lot of investigations aimed at the use of electrochemistry as a selective and environment friendly tool in organic synthesis, have allowed to develop a new methodology for palladium(II) catalyst recycling by means of its anodic oxidation at a graphite electrode in the absence of any other co-catalyst or stoichiometric oxidant. This methodology was applied to the synthesis of carbonyl compounds such as methyl acetylencarboxylates, starting from alkynes, oxazolidin-2-ones, in very good yields, starting from 2-amino-1-alkanols, and N,N'-disubstituted ureas starting from amines, in an very efficient synthesis.

The advantage of the anodic recycling at a graphite electrode of Pd(II) is that it proceeds efficiently under atmospheric pressure of carbon monoxide, avoids the use of copper or halide ions and high pressure of O₂ gas which also implies the formation of water and causes undesired side reactions.

INTRODUCTION

In the last year the scientific research has been engaged to discover novel and environmentally clear catalytic routes for the synthesis of the fine chemical. Electrochemistry can be considered in this contest, because represents a convenient synthetic method were the electrons are clean and energetically efficient reagents.

On the other side, palladium catalysis results to be a well established and very useful methodology in organic synthesis.[1] Electrochemical methodology was very useful to study Pd(0) and Pd(II) complex and their use in the synthesis and transformation of organic compounds.[2]

Although the majority of the organic synthesis involve catalytic amount of Pd catalyst, some reactions requiring stoichiometric quantities of transition metals. In these reactions the active form of Pd (II) is reduced to Pd(0); in order to render the reaction catalytic in palladium(II), reoxidative systems must be used.

The intend of this chapter is to prove how palladium catalysts and eletrochemical method can be used to bring carbon monoxide into reaction with a few organic compounds , under very mild conditions.

In fact, studing the reactivity of Pd(II) and Pd(0) complex in the presence of carbon monoxide, under electrochemycal conditions, using cyclic voltammetry and coulometric analysis, it was found out that, CO is capable of replacing the halides (when present), or the solvent molecules, or the base electrolyte, in the bimolecular interactions complexes of zerovalent palladium present in the solution.

The results, based upon electrochemical analysis, have shown that, when CO is bubbled into a solution of $\text{Pd}^{\text{II}}(\text{PPh}_3)_2\text{Cl}_2$, low coordinated species $\text{Pd}^{\circ}(\text{PPh}_3)_2\text{CO}$ is formed, by two-electron reduction of $\text{Pd}^{\text{II}}(\text{PPh}_3)_2\text{Cl}_2$. This species is obtained from the reduction of $\text{Pd}^{\text{II}}(\text{PPh}_3)_2\text{Cl}_2$ and the exchange of the Cl^- of species $\text{Pd}^{\circ}(\text{PPh}_3)_2\text{Cl}^-$ with CO. The electrochemical behaviour of the two species results different in fact, the $\text{Pd}^{\circ}(\text{PPh}_3)_2\text{CO}$ species, can be oxidized at 0.34V while $\text{Pd}^{\circ}(\text{PPh}_3)_2\text{Cl}^-$ is oxidized at 0.02V.[3]

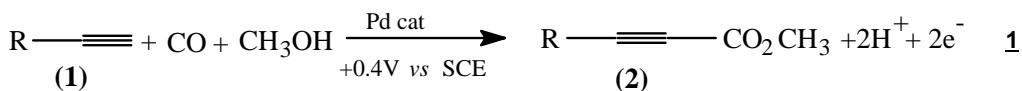
From these investigations, during the electrochemical studies, was been possible to value the applicability of the palladium electrochemical reoxidation to develop a system, that not use conventional chemistry to report palladium zero in oxidation form. A selective and environment friendly methodology, based on the use of electrochemistry and palladium catalysts, for fine chemical preparation is here reported.

ELECTROCHEMICAL SYNTHESIS OF METHYL ACETYLENECARBOXYLATES

One of the first applications of this electrochemical methods, palladium catalyzed, was been the carbonylation of terminal alkynes. Terminal acetylenes were carbonylated under very mild conditions to yield acetylenecarboxylates under atmospheric pressure of carbon monoxide at room temperature using palladium(II) catalyst in combination with its anodic recycling at graphite electrodes.[4]

Generally, these reactions are carried out using PdCl_2 as catalyst and stoichiometric amounts of CuCl_2 as reoxidant.[5] However, from a synthetic and environmental point of view, it is important to develop a halogen-free and copper-free reoxidant system. Sakurai *et al* reported a innovative oxidation system, $\text{Pd}(\text{OAc})_2$ /chlorohydroquinone/molybdovanadophosphate (NPMoV), to render the reaction catalytic in palladium(II); in this case, a high pressure of carbon monoxide and dioxygen are still required.[6] The electrochemical reoxidation of $\text{Pd}(0)$ in the carbonylation of acetylenic compounds has also been reported, but none of these methods occur without reducing the triple bonds and acetylenecarboxylates are not produced. [7]

A new procedure, for the electrochemical synthesis of methyl acetylenecarboxylates starting from alkynes, under mild conditions, is reported using a palladium complex as catalyst, carbon monoxide ($\text{p CO}=1 \text{ atm}$) and methanol at room temperature. The process is outlined in the following reaction.



The reaction proceeds under atmospheric pressure of carbon monoxide at 25°C in a $\text{CH}_3\text{CN}-\text{CH}_3\text{OH}$ solvent in the presence of bases (NaOAc or NEt_3) using a catalytic amount of a palladium(II) complex regenerated by oxidation of an intermediate $\text{Pd}(0)$ complex at the anode. The following general procedure was used: in a cell with three separated compartments, the electrolysis was carried out on solution of phenylacetylene in $\text{CH}_3\text{CN}-\text{CH}_3\text{OH}$ (70:30) as sovent, in the presence of $n\text{-Bu}_4\text{NBF}_4$, as supporting electrolyte, of Pd complexes as catalyst, and NaOAc , as base, under one atmosphere of CO at $+0.4 \text{ V vs SCE}$. A graphite electrode, was used as the working electrode. The counter-electrode was a Pt wire and the reference was a saturated calomel electrode (SCE). At the end of the electrolyses, yields were calculated by GC analysis of crude reaction mixtures by comparison with authentic samples of standards. The results for the electrolyses using various palladium complexes are reported in table 1. The use of a graphite anode is required to eliminate the necessity for a homogeneous electron transfer agent as "co-catalyst".[6] Accordingly, phenylacetylene 1a was recovered in 90% yield when it was reacted in $\text{CH}_3\text{OH}-\text{CH}_3\text{CN}$ (30:70) solution containing $n\text{-Bu}_4\text{NBF}_4$ (0.2M) in the presence of 10 mol% of $\text{Pd}(\text{OAc})_2(\text{PPh}_3)_2$, and 2 equivalents of base, under one atmosphere of carbon monoxide, without any electrochemical oxidation; methyl phenylacetylenecarboxylate 2a was obtained in only 8% yield.

The $\text{Pd}(\text{OAc})_2(\text{PPh}_3)_2$ /electrode system resulted an efficient catalyst, as good as the $\text{PdCl}_2(\text{PPh}_3)_2$ /electrode system. Interestingly, $\text{PdCl}_2(\text{PPh}_3)_2$ and $\text{Pd}(\text{OAc})_2(\text{PPh}_3)_2$ gave higher yields of methyl phenylacetylenecarboxylates than PdCl_2 (table 1). The effect of PPh_3 ligands was to stabilize the intermediate $\text{Pd}(0)$ complex. $\text{Pd}(\text{OAc})_2(\text{PPh}_3)_2$ may generate a $\text{Pd}(0)$ complex in a slow reaction; however, this latter will be oxidized at the anode back to $\text{Pd}(\text{OAc})_2(\text{PPh}_3)_2$. The electrochemical reoxidation of $\text{Pd}(0)$ under atmospheric pressure of

CO appears to be an interesting alternative to the $\text{PdCl}_2/\text{CuCl}_2$ or $\text{Pd(II)}/\text{HQ-Cl/NPMoV}$ procedures working under high pressure of carbon monoxide and dioxygen.

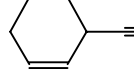
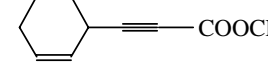
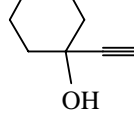
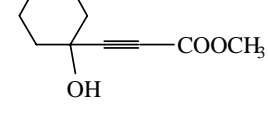
Table 1. Carbonylation of phenylacetylene (1a) to methyl acetylencarboxylate (2a) in the presence of palladium(II) complexes^a

Catalyst	Recovered 1a %	Yield 2a % ^b	Current efficiency % ^c
$\text{Pd}(\text{PPh}_3)_2(\text{OAc})_2$	23	56 (73)	93
$\text{Pd}(\text{PPh}_3)_2\text{Cl}_2$	20	57 (71)	95
PdCl_2	48	22 (42)	85
$\text{Pd}(\text{PPh}_3)_4$	22	45 (58)	77

^a The electrolysis was carried out using 1a (1 mmol) in 30 mL of $\text{CH}_3\text{CN}-\text{CH}_3\text{OH}$ (70:30) containing $n\text{-Bu}_4\text{NBF}_4$ 0.2 mol dm^{-3} , palladium complex (0.1 mmol), NaOAc (2 mmol) under CO (1 atm) at +0.4 V vs SCE at $25^\circ \pm 0.1^\circ\text{C}$.

^b Yields are relative to the initial 1a and determined by GC analyses. Yields in parentheses are relative to the disappearance of 1a.^c Current efficiency was calculated in comparison with theoretic coulomb (2F/mol).

Table 2. Carbonylation of various terminal alkynes 1 to methyl acetylencarboxylate 2^a

No	Alkyne 1	Time(h)	Product 2	Recovered alkyne 1(%) ^c	Yield(%) ^{c, d}
1	Ph— \equiv 1a	7	Ph— \equiv —COOCH ₃ 2a	23	56
2	 1b	8	 2b	20	56
3	 1c	6	 2c	35	53
4	 1d	10	 2d	18	56
5 ^b	1a	8	2a	10	70
6 ^b	1b	6	2b	5	87

^a The electrolyses of 1a phenylacetylene, 1b 1-ethynylcyclohexene, 1c 1-ethynyl-1-cyclohexanol, 1d 1-hexyne, (1 mmol), were carried out in $\text{CH}_3\text{CN}-\text{CH}_3\text{OH}$ (70:30) containing $n\text{-Bu}_4\text{NBF}_4$ 0.2 mol dm^{-3} , $\text{Pd}(\text{OAc})_2(\text{PPh}_3)_2$ (0.1 mmol) and NaOAc (2 mmol) under CO (1 atm) at +0.4 V vs SCE at 25°C .

^b Triethylamine (2 mmol) was used instead of NaOAc .

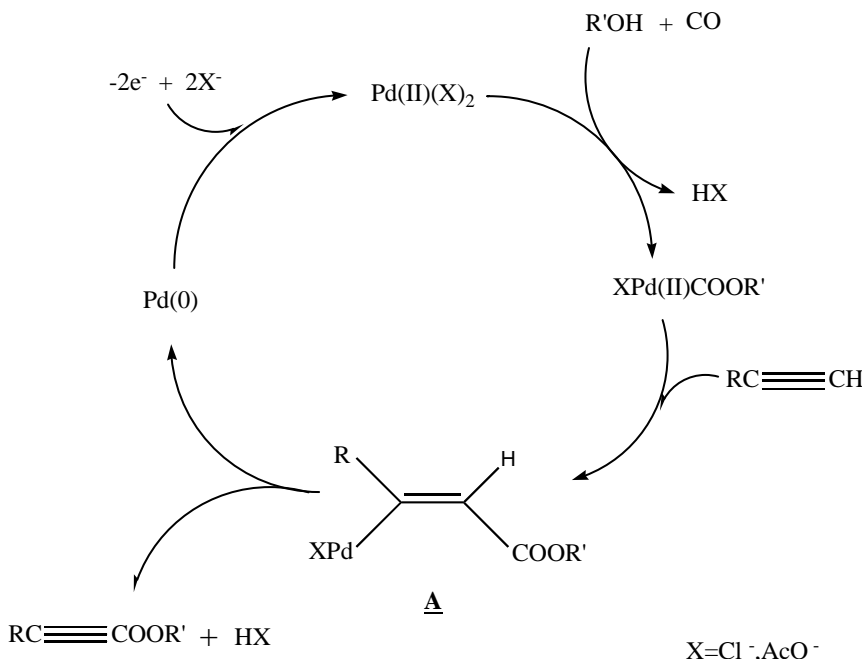
^c Yields of 1a-d and 2a-d were determined by GC analysis.

^d Yields relative to the initial 1a-d.

As proposed by Heck for the carbonylation of olefins and acetylenes, the electrocarbonylation of terminal alkynes is considered to proceed via a similar mechanism.[8]

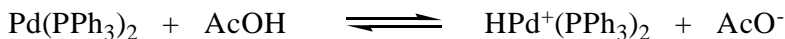
Because of the *syn* addition of $L_2(OAc)PdCOOR'$ on the alkyne, the formation of $HPd(OAc)(PPh_3)_2$ by a β -hydride *syn* elimination is impossible. The presence of the base is essential as a proton trapper by elimination of the H^+ from the β position.[9]

In table 2 are reported the results for the carbonylation of various terminal alkynes by using $Pd(OAc)_2(PPh_3)_2$ as catalyst and $NaOAc$ or NEt_3 as bases. It seems that the use of NEt_3 as a base is in favour of a more efficient catalytic cycle (compare entries 1,5 and 2,6, table 2).[10] When NEt_3 was used as base, the reaction occurs in shorter times suggesting that the $Pd(II)$ catalyst is more efficiently recycled in the presence of NEt_3 than with $NaOAc$.



Scheme 1.

The reaction is considered to proceed by the elimination of H^+ in the β position in complex [A], induced by the base (Scheme 1). NEt_3 is probably more efficient than AcO^- in this reaction. The $Pd(0)$ is then generated in higher concentrations from complex [A] in the presence of NEt_3 and can be reoxidized to $Pd(II)$ at the anode. Moreover, when acetate was used as base, acetic acid is formed from complex [A] concomitantly with the $Pd(0)$ complex. It was been reported that $Pd(0)$ undergoes oxidative addition with acetic acid to form a cationic palladium(II)hydride.[11]



Under such conditions the Pd(0) complex generated from [A] (Scheme 1) would be partially stored under the form of $\text{HPd}(\text{II})\text{L}_2^+$, a reaction which is in competition with its reoxidation at the anode.

ELECTROCHEMICAL SYNTHESIS OF N,N'-DISUBSTITUTED UREAS

An other application of the electrochemical method for the reoxidation of Pd(0), was been the efficient synthesis of N,N'-disubstituted ureas. In this case, aromatic and aliphatic primary amines undergo oxidative carbonylation under atmospheric pressure of carbon monoxide, using Pd(II) catalyst in combination with its anodic recycling at a graphite electrode.[12]

Substituted ureas have been of recent interest due to the appearance of this functionality in drug candidates such as HIV protease inhibitors;[13] in addition, ureas have found widespread use as agricultural chemicals, resin precursors, dyes and additives to petroleum compounds and polymers.[14]

For these reasons, many efforts have been made to find new efficient syntheses of ureas to replace the classical reactions of amines with phosgene [15] or related compounds (isocyanates, [16] carbonyldiimidazole [17] or disuccinimide carbonate [18]).

The synthesis of symmetrical ureas from amines can be accomplished by oxidative carbonylation of amines by means of carbon monoxide and a transition metal catalyst (W, [19] Ni, [20] Mn, [21] Co, [22] Rh, [23] Ru, [24] and Pd [25]). Among them, the most commonly used is Pd.

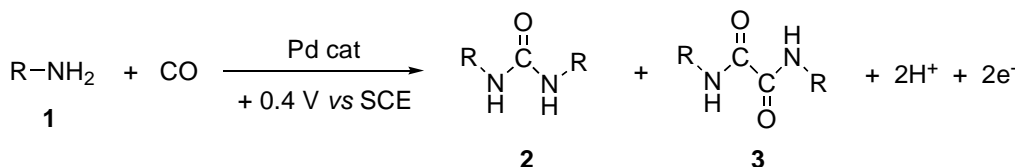
The reaction with a Pd catalyst implies the use of a reoxidant reagent in stoichiometric amount to transform Pd(0) (that results from the reaction) into Pd(II) (the reactive specie of the catalyst); usually high pressures of CO and O₂ are necessary sometimes, in combination with I₂;[26] alternatively, CO, O₂ and copper salts can be used.[27]

Electrochemistry has also been used as reoxidizing system: Deng and co-workers have applied electrochemistry to the synthesis of symmetrical dialkyl ureas using Pd(PPh₃)₂Cl₂ as catalyst and Cu(OAc)₂ as co-catalyst, instead of high pressure of CO/O₂. In this case, it was reported that Cu(OAc)₂ "acted as not only an electron transfer agent but also a catalyst".[28]

In all these syntheses of ureas, a side reaction of either double carbonylation to oxamides takes place, or the formation of isocyanates probably by amine-elimination reaction from urea. It was been, therefore, important to find a synthesis with high selectivity, to minimize the side reactions.

The electrochemical reoxidation of Pd(0) to Pd(II) was applied to the efficient synthesis of N,N'-disubstituted ureas, starting from amines and carbon monoxide. The advantage the anodic recycling at a graphite electrode of Pd(II) is that it proceeds efficiently under atmospheric pressure of carbon monoxide, avoids the use of copper or halide ions and high pressure of O₂ gas which also implies the formation of water and causes undesired side reactions; this way, the performances of the catalysts should be enhanced.

The reaction can be outlined as follow



In a cell with three separated compartments, the electrolysis was carried out on a solution of amine, in CH_3CN as solvent containing $n\text{-Bu}_4\text{NBF}_4$ (0.20M) as supporting electrolyte, in the presence of Pd(OAc)_2 (10%) and NaOAc as base, under 1 atm of CO at +0.4 V vs SCE. A graphite electrode, was used as working electrode, the counter-electrode was a Pt wire and the reference was a saturated calomel electrode (SCE).

Benzylamine was used as a model compound to study the influence of catalyst and ligands. The effect of different catalytic systems on the carbonylation of benzylamine is presented in table 1.

Table 3. Electrochemical synthesis of *N,N*-Dibenzylurea using different Pd(II) complexes as catalyst

catalyst	base	ligand	urea 2, yield (%) ^a	oxamide 3, yield (%) ^a	current yield (%)
Pd(OAc)_2	AcONa	-	62	12	81
Pd(OAc)_2	AcONa	TFP ^c	32	2	68
Pd(OAc)_2	AcONa	PPh_3	59	10	73
Pd(OAc)_2	AcONa	dppp ^d	57	16	85
$\text{Pd}_2(\text{dba})_3$ ^b	AcONa	-	67	5	90
$\text{Pd}(\text{PPh}_3)_4$	AcONa	-	83	10	86
$\text{PdCl}_2(\text{PPh}_3)_2$	AcONa	-	73	6	81
PdCl_2	AcONa	-	48	<1	99
PdCl_2	NEt_3	-	50	6	77

^a Yields determined by HPLC, yields relative to starting benzylamine.

^b Tris(dibenzylideneacetone)di-palladium(0).

^c TFP = Tri-2-furylphosphine. dppp = 1,3-Bis(diphenylphosphino)propane.

Among the examined catalytic systems, $\text{Pd}_2(\text{dba})_3$ exhibited good selectivity to afford the urea in 67% and oxamide in 5% yields, whereas the best yield in urea (83%) was obtained using $\text{Pd}(\text{PPh}_3)_4$ as catalyst. This suggests that the palladium(0) complexes, such as $\text{Pd}(\text{PPh}_3)_4$ and $\text{Pd}_2(\text{dba})_3$, are good catalytic systems in this transformation. From the electrochemical point of view, the most efficient catalytic system was PdCl_2 , as it appears from the current yield (99%) and from the selectivity of this reaction, but the reaction resulted very slow. The use of a base is necessary to avoid the formation of HPd(II)(L)_2^+ or of HPd(II)^+ , that do not react in this transformation.[11] In the presence of PdCl_2 as catalyst, the use of NEt_3 , instead of AcONa, seems to decrease the electrocatalytic system; in fact the current yield affords 77% in the presence of NEt_3 , respect to 99% in the presence of AcONa.

To test its applicability, this electrochemical synthesis, using two different catalytic systems, a complex of Pd(0), i.e. $\text{Pd}(\text{PPh}_3)_4$, and a complex of Pd(II) i.e. $\text{Pd}(\text{OAc})_2$, were applied to a variety of primary aliphatic and aromatic amines. The preparative results are reported in table 4.[29]

Table 4. Electrochemical synthesis of aliphatic and aromatic ureas using palladium catalyst^a

Entry	amine R	catalyst ^b	urea yield (%) ^c	oxamide yield (%) ^c
1	4-MeOPh	A	10	0
2	4-MeOPh	B	41	0
3	4-ClPh	A	20	0
4	4-ClPh	B	31	0
5	Ph	A	49	0
6	Ph	B	57	0
7	PhCH ₂	A	83	10
8	PhCH ₂	B	62	12
9	2-Py	A	30	0
10	2-Py	B	21	0
11	C ₆ H ₁₁	A	57	0
12	C ₆ H ₁₁	B	71	0
13	C ₅ H ₉	A	35	1
14	C ₅ H ₉	B	37	1
15	Bu	A	70	3
16	Bu	B	71	0

^a General procedure: the same described in the text.

^b A, $\text{Pd}(\text{PPh}_3)_4$; B, $\text{Pd}(\text{OAc})_2$

^c Yields determined by HPLC, yields relative to starting amine.

The yields in urea and the selectivity with respect to the formation of oxamide (side product) depend both on the structure of the starting amine and on the kind of catalyst system: the aromatic amines seem less reactive than the aliphatic ones, while the best catalyst seems to be a complex of Pd(II). In all cases (except benzylamine, entries 7 and 8), the selectivity was very high and oxamide was formed only in a very small amount or it was totally absent. It is to be underlined that in no case isocyanate was evidenced, so only two products were formed during the electrocatalytic carbonylation: diaryl or dialkylurea and oxamide. [30]

The choice of solvent also appeared to be significant; among the solvents used in the electrocarbonylation, CH_3CN gave the best yields of urea and easiness in the electrolysis work up. Changing the solvent to THF or DMF resulted in a change in the carbonylation products and selectivity (no urea could be evidenced) and further studies are in progress to understand the influence of those solvents on the selectivity of the product.

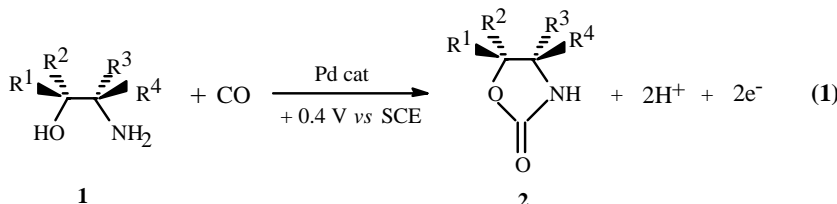
So that, the electrochemical methodology has permitted a mild, selective and environmental friendly reoxidation of Pd(0) into Pd(II) in oxidative carbonylation of amines to ureas. The reaction was very selective (in most cases, no side product was formed) and good yields in ureas were obtained from aliphatic amines.

ELECTROCHEMICAL SYNTHESIS OF OXAZOLIDIN-2-ONES AND BENZOXAZOLINONES

Oxazolidin-2-ones, a well-known class of organic compounds, have many chemical and biological uses; they are, in fact, utilized as chiral auxiliaries (Evans' chiral auxiliaries) [31] in asymmetric synthesis and some oxazolidin-2-ones have been found to have activity as immunosuppressant [32] and as antimicrobial. [33]

Oxazolidin-2-ones are usually obtained by reaction of 1,2-amino alcohols with phosgene or derivatives. [31] Also palladium catalyzed carbonylation of 2-amino alcohols has been described in literature: Tam [34] used 3 atm of CO and a quite high temperature (80°C) to afford oxazolidin-2-ones in 34-94% yields. This method has the disadvantage of not being suitable for primary amines, and CuCl_2 is used to reoxidize palladium (0) to palladium (II), which is the reactive species. Imada and coworkers [35] carried out this reaction with atmospheric pressure of a mixture of CO and O_2 , at 50°C and CuI as reoxidant, with fair to good yields in oxazolidin-2-ones; but also in this case the reaction does not work with primary amines. 80 atm of CO are necessary to carbonylate primary amines. More recently, Gabriele and coworkers [36] synthesized oxazolidin-2-ones by direct palladium catalyzed oxidative carbonylation of 2-amino-1-alkanols in good yields (with primary amines), but this method suffers from several drawbacks. A high pressure of gases (CO, O_2 and air, 60 atm) and the temperature of 100°C are requested.

The electrochemical synthesis of oxazolidinones from 2-amino-1-alkanols, under very mild conditions, using a palladium(II) complex as catalyst and carbon monoxide ($p\text{ CO}=1\text{ atm}$),[37] is outlined in the following reaction:



The electrolysis was carried out on a solution of 2-amino-2-phenylethanol in CH_3CN containing $n\text{-Bu}_4\text{NBF}_4$ (0.2 M) as supporting electrolyte, in the presence of $\text{Pd}(\text{OAc})_2$ (10%) and NaOAc as base, under atmospheric pressure of CO, at $+0.4$ V vs SCE. A graphite electrode was used as working electrode, the counter-electrode was a Pt wire and the reference was a saturated calomel electrode (SCE). The results for the electrolyses using various palladium complexes are presented in table 5.

Table 5. Electrochemical carbonylation of (*R*)-(−)-2-amino-2-phenylethanol to (*R*)-(−)-4-phenyloxazolidin-2-one using different Pd(II) complexes as catalyst

Catalyst	Base	F/mol ^a	2, yield (%) ^b	Current yield (%)
PdCl ₂	AcONa	1.04	62	100
Pd(PPh ₃) ₂ (OAc) ₂	AcONa	1.63	79	85
Pd(OAc) ₂	AcONa	1.27	75	100
PdCl ₂	NEt ₃	1.27	75	99

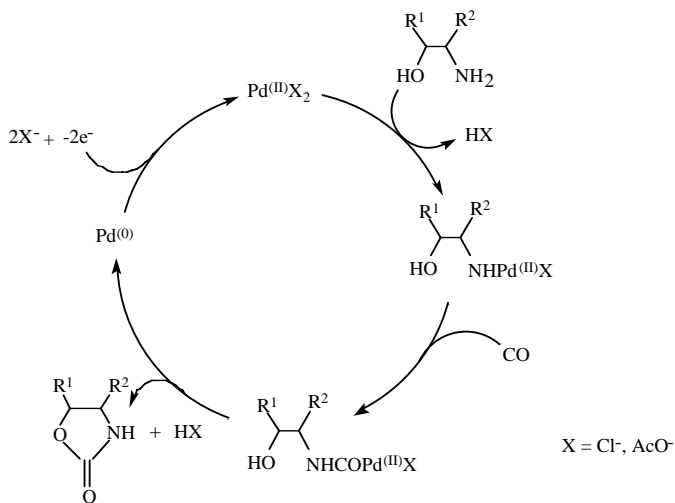
^a With respect to starting 1.

^b Isolated yields relative to starting 1

It was found that the reaction efficiently proceeded under atmospheric pressure of carbon monoxide with all the catalyst systems taken into account. The choice of the Pd(OAc)₂/NaOAc system derives from the necessity to use a chloride-free system and to avoid the presence of triphenylphosphines during the work-up, in order to improve the non-polluting aspects.[38] On the bases of these considerations, this catalyst system was used in the reaction with various 2-amino-1-alkanols (table 6).

Oxazolidin-2-ones were obtained in very good current yields, with all the 2-amino-1-alkanols bearing a primary amino group. In the case of *N*-benzyl-2-phenyl-2-amino-1-ethanol (table 2, entry 5) the reaction was very slow; it was probably due to the lower reactivity of this secondary amino group versus the palladium catalyst in this reaction conditions.

The possible reaction mechanism is outlined in Scheme 2. The use of a base is necessary to avoid the formation of HPd(II)(OAc)₂⁺, that does not work in this reaction. [11]



Scheme 2.

Table 6. Electrochemical carbonylation of 2-amino-1-alkanols 1, by $\text{Pd}(\text{OAc})_2$ catalyst, to oxazolidin-2-ones 2

Entry	1	2	Yield (%) ^a	Current yield (%)	F/mol ^b
1			75	100	1.27
2			96	96	1.80
3			58	57	1.70
4			79	95	1.45
5			29	57	0.64
6			86	84	1.80
7			69	97	1.22

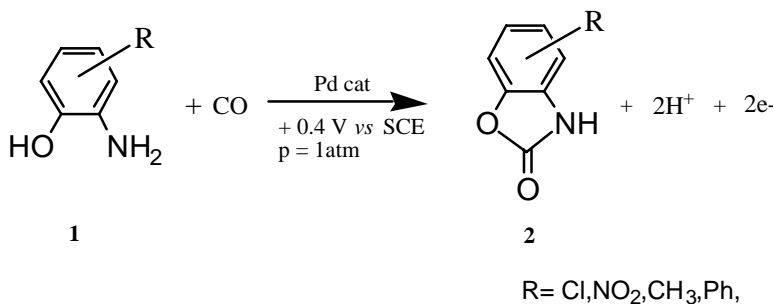
^a Isolated yields relative to starting 1.

^b With respect to starting 1.

The possibility to accomplish the reaction under mild conditions has also permitted the application of this electrochemical methodology to substrates particularly sensitive to oxidative conditions. The preparation of benzoxazolidin-2-ones required the use of 2-aminophenols of starting materials. Most of the aminophenols are very sensitive to oxidizing agents. However, benzoxazolidin-2-ones are a very interesting class of organic compounds.

Their importance is related with their medicinal properties. Several potentially useful drugs and pharmacological tools based on these pharmacophores have been developed in recent years.[39]

The reaction conditions, for the syntheses of benzoxazolidin-2-ones, are the same reported for the synthesis of oxazolidin-2-ones, and the reaction can be schematized as follows:



The controlled-potential electrolyses were carried out in a cell with three separated compartments. The cathode was a reticulated carbon rod and the anode was a platinum wire. As reference electrode was used a modified SCE. The catholyte was prepared by dissolving 2-aminophenol in CH₃CN, containing n-Bu₄NBF₄ (0.2M), as well as an excess of base and dichlorobis(triphenylphosphine) palladium(II) or palladium(II) acetate as catalyst. Carbon monoxide was bubbled through a glass capillary into the cathodic solution that subsequently was kept under a CO pressure of 1 atm. The electrolyses were interrupted when the current dropped to the value of the background current.

Table 7. Electrochemical carbonylation of 2-aminophenol to 2-benzoxazolinone using different Pd(II) complexes and bases

Catalyst	Base	Time (h)	2-aminophenol, yield (%) ^a
Pd(OAc) ₂	DABCO ^b	3	60
Pd(OAc) ₂	DBU ^c	2	60
Pd(OAc) ₂	Cs ₂ CO ₃	4	65
Pd(OAc) ₂	Et ₃ N	4	75
Pd(OAc) ₂	EtN(Pr ¹) ₂	2	85
Pd(OAc) ₂	KOH	4	45
Pd(OAc) ₂	AcONa	4	60
PdCl ₂ (PPh ₃) ₂	Cs ₂ CO ₃	4	60
PdCl ₂ (PPh ₃) ₂	AcONa	5	65

^a Yields determined by HPLC, yields relative to starting 2-aminophenol. Reaction conditions: 2-aminophenol (1mmol), CH₃CN containing n-Bu₄NBF₄ (0.2M), base (3mmol), T=50°C pCO=1atm.

^b 1,4-diazabicyclo-[2,2,2]-octane (DABCO) (c) 1,8-diazabicyclo-[5,4,0]-undec-7-ene (DBU).

The results obtained show that benzoxazolidin-2-ones can be obtained in moderate good yields with both catalysts used. Concerning the bases activity, the two bases triethylamine and diisopropylethylamine give the best results combined with Pd(OAc)₂ catalyst. On the other hand PdCl₂(PPh₃)₂ and AcONa as base gives a good result. This data confirm the results

obtained in the synthesis of oxazolidin-2-ones from β -amino alcohols were the best yield was obtained with $\text{Pd}(\text{OAc})_2/\text{AcONa}$ system.

CONCLUSION

Electrochemistry provides an easy way to generate a desired oxidation state of metal complex that becomes the active catalytic species for an organic reaction. In this particular case, of redox processes, the active catalytic species can be recycled continually by the electrode oxidation reaction. So that, this method results very versatile and his application to a varius chemical systems make its a valuable alternative to the use of hight pressure of carbon monoxide in addition to chemical reoxidant systhems. The applications of this methodologies confirm that electrochemistry in conjunction with organometallic catalysis provides mild and selective processes that can be exploiod to organic synthesis.

REFERENCES

- [1] H. M. Colquhoun, D. J. Thompson, M. V. Twigg, *Carbonilation, in Direct Syntheses of Carbonilic Compounds*, Penum Press, New York, 1991.
- [2] J. Tsuji, *Palladium Reagents and Catalysts*, Wiley, Chichester, 1995.
- [3] Chiarotto, I.; Carelli, I.; Carnicelli, V.; Marinelli, F.; Arcadi, A. *Electrochimica Acta* 1996, **41**, 2503-2509.
- [4] Chiarotto, I.; Carelli, I. *Synthetic Comm.* 2002, **32**, 881-886.
- [5] Tsuji, J.; Takahashi, M.; Takahashi, T. *Tetrahedron Lett.* 1980, **21**, 849-850.
- [6] Sakurai, Y.; Sakaguchi, S.; Ishii, Y. *Tetrahedron Lett.* 1999, **40**, 1701-1704.
- [7] (a) Alper, H.; Despeyroux, B.; Woell, J. B. *Tetrahedron Lett.* 1983, **24**, 5691-5694.(b) Hartstok, F. W.; McMahon, L. B.; Tell, I. P. *Tetrahedron Lett.* 1993, **34**, 8067-8070.(c) Hartstok, F. W.; Wayner, D. D. M. *Tetrahedron Lett.* 1994, **35**, 8137-8140.
- [8] Heck, R. F. *J. Am. Chem. Soc.* 1972, **94**, 2712-2719.
- [9] Negishi, E. *Acc. Chem. Res.* 1982, **15**, 340-348.
- [10] Amatore, C.; Jutand, A.; M'Barki, M. A. *Organometallics*. 1992, **11**, 3009-3013.
- [11] Amatore, C.; Jutand, A.; Meyer, G.; Carelli, I.; Chiarotto, I. *Eur. J. Inorg. Chem.* 2000, **8**, 1855-1859.
- [12] Chiarotto, I.; Feroci, M. *J. Org. Chem.* 2003, **68**, 7137-7139.
- [13] (a) Lam, P. Y. S.; Jadhav, P. K.; Eyermann, C. J.; Hodge, C. N.; Ru, Y.; Bacheler, L. T.; Meek, J. L.; Otto, M. J.; Rayner, M. M.; Wong, Y. N.; Chang, C. H.; Weber, P. C.; Jackson, D. A.; Sharpe, T. R.; Erickson-Viitanen, S. *Science* 1994, **263**, 380-384. (b) Lam, P. Y. S.; Ru, Y.; Jadhav, P. K.; Aldrich, P. E.; DeLucca, G. V.; Eyermann, C. J.; Chang, C. H.; Emmett, G.; Holler, E. R.; Daneker, W. F.; Li, L. Z.; Confalone, P. N.; McHugh, R. J.; Han, Q.; Li, R. H.; Markwalder, J. A.; Seitz, S. P.; Sharpe, T. R.; Bacheler, L. T.; Rayner, M. M.; Klabe, R. M.; Shum, L. Y.; Winslow, D. L.; Kornhauser, D. M.; Jackson, D. A.; Erickson-Viitanen, S.; Hodge, C. N. *J. Med. Chem.* 1996, **39**, 3514-3525.

- [14] Dragovich, P. S.; Barker, J. E.; French, J.; Imbacuan, M.; Kalish, V. J.; Kissinger, C. R.; Knighton, D. R.; Lewis, C. T.; Moomaw, E. W.; Parge, H. E.; Pelletier, L. A. K.; Prins, T. J.; Showalter, R. E.; Tatlock, J. H.; Tucker, K. D.; Villafranca, J. E. *J. Med. Chem.* 1996, 39, 1872-1884.
- [15] For use of phosgene and its derivatives see: (a) Hegarty, A. F.; Drennan, L. J. in *Comprehensive Organic Functional Group Transformations*, Katritzky, A. R., Meth-Cohn, O., Rees, C. W., Eds.; Pergamon: Oxford, 1995; Vol. 6, pp. 499-526. (b) Guichard, G.; Semetery, V.; Didierjean, C.; Aubry, A.; Briand, J. P.; Rodriguez, M. J. *Org. Chem.* 1999, 64, 8702-8705. (c) Majer, P.; Randal, R. S. *J. Org. Chem.* 1994, 59, 1937-1938. (d) Scialdone, M. A., Shuey, S.W.; Soper, P.; Hamuro, Y.; Burns, D. M. *J. Org. Chem.* 1998, 63, 4802-4807.
- [16] Satchell, R. S.; Satchell, D. P. N. *Chem. Soc. Rev.* 1975, 4, 231-250.
- [17] Zhang, X.; Rodrigues, J.; Evans, L.; Hinckle, B.; Ballantyne, L.; Pena, M.; *J. Org. Chem.* 1997, 62, 6420-6423.
- [18] Takeda, K.; Akagi, Y.; Saiki, A.; Tsukahara, T.; Ogura, H. *Tetrahedron Letters.* 1983, 24, 4569-4572.
- [19] (a) McCusker, J. E.; Grasso, C. A.; Main A. D.; McElwee-White, L. *Org. Lett.* 1999, 1, 961-964. (b) McCusker, J. E.; Qian, F.; McElwee-White, L. *J. Mol. Cat. A.: Chem.* 2000, 159, 11-17. (c) McCusker, J. E.; Main A. D.; Johnson, K. S.; Grasso, C. A.; McElwee-White, L. *J. Org. Chem.* 2000, 65, 5216-5222.
- [20] Giannoccaro, P.; Nobile, C. F.; Mastrorilli, C.; Ravasio, J. *J. Organomet. Chem.* 1991, 419, 251-258.
- [21] Srivastva, S. C.; Shrimal, A. K.; Srivastva, A. *J. Organomet. Chem.* 1991, 414, 65-69.
- [22] Bassoli, A.; Rindone, B.; Tollari, S.; Chioccara, F. *J. Mol. Cat.* 1990, 60, 41-48.
- [23] Mulla, S. A. R.; Gupte, S. P.; Chaudhari, R. V. *J. Mol. Cat.* 1991, 67, L7-L10.
- [24] Mulla, S. A. R.; Rode C. V.; Kelkar, A. A.; Gupte, S. P. *J. Mol. Cat. A.: Chem.* 1997, 122, 103-109.
- [25] (a) Valli, V. L. K.; Alper, H. *Organometallics* 1995, 14, 80-82. (b) Gupte, S. P.; Chaudhari, R. V. *J. Catal.* 1988, 114, 246-258.
- [26] (a) Pri-Bar, I.; Alper, H. *Can. J. Chem.* 1990, 68, 1544-1547. (b) Shi, F.; Deng, Y.; SiMa, T.; Yang, H. *Tetrahedron Letters.* 2001, 42, 2161-2163.
- [27] Giannoccaro, P. *J. Organomet. Chem.* 1987, 336, 271-278.
- [28] Yang, H.; Deng, Y.; Shi, F. *J. Mol. Cat. A.: Chem.* 2001, 176, 73-78.
- [29] Amines were purchased from commercial sources and were purified prior to use. Standard of disubstituted ureas and oxamides synthesized in that paper, are commercially available. The ureas and oxamides were characterized by comparison of infrared, nuclear magnetic resonance, and mass spectra with those for authentic materials and literature data.
- [30] The HPLC analysis of the electrolysis carried out in DMF solvent showed the presence of both isocyanate and carbammic acid, but no qualitative analysis was possible because carbammic acid can be also produced, by hydrolysis of isocyanate in the HPLC column.
- [31] (a) Evans, D. A. *Aldrichim. Acta* 1982, 15, 23-32. (b) Ager, D. J.; Prakash, I.; Schaad, D. R. *Chem. Rev.* 1996, 96, 835-875.
- [32] Seki, M.; Mori, K. *Eur. J. Org. Chem.* 1999, 2965-2967.

- [33] (a) Seneci, P.; Caspani, M.; Ripamonti, F.; Ciabatti, R. *J. Chem. Soc., Perkin Trans I* 1994, 2345-2351. (b) Barbachyn, M. R.; et al. *J. Med. Chem.* 1996, 39, 680-695. (c) Lohray, B. B.; Baskaran, S.; Srinivasa Rao, B.; Yadi Reddy, B.; Nageswara Rao, I. *Tetrahedron Lett.* 1999, 40, 4855-4856.
- [34] Tam, W. *J. Org. Chem.* 1986, 51, 2977-2981.
- [35] Imada, Y.; Mitsue, Y.; Ike, K.; Washizuka, K.-I.; Murahashi, S.-I. *Bull. Chem. Soc. Jpn.* 1996, 69, 2079-2090.
- [36] Garbriale, B.; Salerno, G.; Brindisi, D.; Costa, M.; Chiusoli, G. P. *Org. Lett.* 2000, 2 (5), 625-627.
- [37] Chiarotto, I.; Feroci, M. *Tetrahedron Letters.* 2001, 42, 3451-3453
- [38] After the end of the electrolysis, the anodic solution was concentrated, analyzed by TLC, and the reaction products purified by flash-chromatography (*n*-hexane/ethyl acetate 6:4). The isolated oxazolidin-2-ones were identified by comparison of their physical and spectral data ($^1\text{H-NMR}$, $^{13}\text{C-NMR}$, MS, aD) with those of authentic samples.
- [39] (a) Diouf, O.; Carato, P.; Depreux, P.; Bonte, J. P.; Caignard, D.H.; Guardiola-Lamaitre, B.; Rettori, M. C.; Belzung, C.; Lesieur, D. *Bioorg. Med. Lett.* 1997, 7, 2579-2584. (b) Diouf, O.; Carato, P.; Lesieur, I.; Rettori, M. C.; Caignard, D. H. *Eur. J. Med. Chem.* 1999, 34, 69-73. (c) Carato, P.; Bonte, J. P.; Lesieur, D.; Depreux, P.; Caignard, D. H.; Milan, M.; Newman-Tancredi, A.; Renard, P.; Rettori, M. C. *Eur. Patent Chem. Abstr.*, 1998, P4662x. (d) Carato, P.; Depreux, P.; Lesieur, D.; Milan, M.; Newman-Tancredi, A.; Rettori, M. C.; Caignard, D.H. *Drug Des. Disc.* 2000, 17, 173. (e) Lesieur, D.; Delmas, E.; Your, S.; Depreux, P.; Guillaumet, G.; Dacquet, C.; Levens, N.; Boutin, J.; Bennejean, C.; Renard, P. *French Patent* 00-01289, 2000. (f) Lesieur, D.; Blac-Delmas, E.; Bennejean, C.; Chavatte, P.; Guillaumet, G.; Dacquet, C.; Levens, N.; Boutin, J.; Renard, P. *French Patent* 01-12205, 2001.

Chapter 4

**MIXED TRANSITION METAL ACETYLIDES WITH
DIFFERENT METALS CONNECTED BY CARBON-RICH
BRIDGING UNITS: ON THE WAY TO HETERO-
MULTIMETALLIC ORGANOMETALLICS**

Heinrich Lang* and Alexander Jakob

Technische Universität Chemnitz, Fakultät für Naturwissenschaften,
Institut für Chemie, Lehrstuhl für Anorganische Chemie,
Straße der Nationen 62, 09111 Chemnitz, Germany

ABSTRACT

The chemistry of mono- and bis(alkynyl) transition metal complexes, modified ferrocenes, functionalized alkynyls, diaminoaryl NCN pincer molecules ($\text{NCN} = [\text{C}_6\text{H}_2(\text{CH}_2\text{NMe}_2-2,6)_2]$), and 1,4- and 1,3,5-substituted benzene derivatives towards diverse metal fragments will be discussed and serves to understand the manifold and sometimes unexpected reaction behavior of such species. Interesting novel (hetero)bi- to undecametallic compounds with often uncommon structural motifs are formed in which the respective transition metal building blocks are connected by carbon-rich π -conjugated organic and/or inorganic bridging units. The reactions based on the modular molecular “Tinkertoys” approach depend upon the steric and electronic properties of the metal centers and ligands involved, which also will be discussed. The electrochemical behavior of such 1-dimensional molecular wire molecules, coordination polymers, star-like structured and dendritic oriented transition metal systems, respectively, is presented as well.

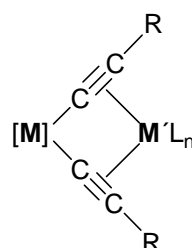
* Heinrich Lang: E-mail: heinrich.lang@chemie.tu-chemnitz.de

INTRODUCTION

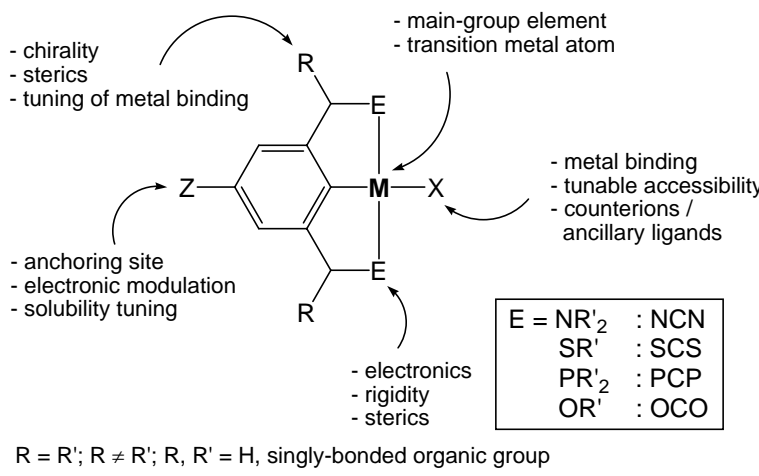
The coordinative and covalent linking of modular constructed transition metal building blocks to generate heteromultimetallic assemblies increasingly gained interest during the last years because such species may offer diverse applications in, for example, the field of electroluminescence, information storage materials and photochemical molecular devices [1]. Also, they are of interest since they may be used as representative model compounds in the fundamental study of electron-transfer and photoinduced energy-transfer processes [1]. One possibility to synthesize such complexes includes the principle of molecular manufacturing [2, 3]. This generally requires the prior preparation of multifunctional organic molecules which allow the stepwise synthesis of multitopic organometallic assemblies. In particular, as different binding sites of the bridging ligands reactive groups such as acetylides, phosphines, N,N,(N)-donor systems ($N,N,(N) =$ bi- or tri-dentate Lewis-base), ... can be used to control the synthesis of multimetallic complexes. In this respect, metal-containing alkynyls have been studied extensively due to their rigid structures, their stability and, for example, their rich spectroscopic, photophysical and electrochemical properties [1d, 4]. Examples of such connectivities are 1,4-diethynyl benzene [5, 6], 1,3,5-triethynyl benzene [7, 8], 1-ethynyl-4-diphenylphosphino benzene [9], 5-ethynyl-2,2'-bipyridine [10] and 2,5-bis(alkynyl) thiophenes [11, 12]. Based on these cores mainly homometallic assemblies have been synthesized, while only less is known about heteromultimetallic transition metal species.

In context with this background we focus in this chapter on the synthesis of heterodi- to heterohexametallic transition metal complexes, a hitherto barely explored class of compounds, supported by applying multitopic organometallic and organic building blocks. This article is a continued amendment of recently published reviews in this field of chemistry by one of the authors including recent developments made in organometallic π -tweezer chemistry [13].

Bis(alkynyl) transition metal complexes of type $RC\equiv C-[M]-C\equiv CR$ with $[M] = 12 - 16$ valence electron complex fragment, R = singly-bonded organic or organometallic group [13, 14], have recently been applied as organometallic bidentate chelating ligands (organometallic π -tweezers) for the stabilization of low-valent metal fragments $M'L_n$ (M' = element of groups 1, 2, 4, or 6 – 12 of the periodic table of the elements; L = neutral or ionic organic or inorganic 2-electron donor ligand; n = 1, 2, 3, 4) [14]. In the thus accessible heterobimetallic $\{[M](\mu-\sigma,\pi-C\equiv CR)_2\}M'L_n$ tweezer molecules the alkynyl groups $RC\equiv C$ act as σ -donors to M and as π -donors to M' , and hold the metals M (preferentially an early transition metal atom, such as Ti, Zr or Hf) and M' (vide supra) in close proximity to each other [14]. Synergistic and cooperative effects between M and M' are observed and apparently, these complexes show a versatile reaction chemistry and many applications [14].



A further extensively investigated chelating ligand in organometallic chemistry is the potentially η^3 -chelating, monoanionic diaminoaryl pincer molecule NCN ($\text{NCN} = [\text{C}_6\text{H}_3(\text{CH}_2\text{NMe}_2-2,6)_2]$) [13, 15]. Together with related diphosphino- and disulfido-aryl anions many pincer metal complexes are accessible, which possess a remarkable stability, and at the same time show excellent catalytic properties [15]. Recently, this approach could be successfully extended to synthesize pincer main-group element compounds [15].



Functionalized ferrocenes can act as bidentate chelating ligands towards many diverse transition metal and main-group element entities [16]. In addition, the ferrocene moiety is an exceptional building block in the preparation of, for example, multimetallic coordination complexes which provide interesting electronic, optical and/or magnetic properties [17]. Moreover, ferrocenes are very robust materials and show a versatile and interesting redox chemistry associated with, for example, polycarbon or related ligands derived from polyynes, since ferrocenes are excellent organometallic one-electron reservoirs [17]. Although, ferrocene celebrated its 50th anniversary six years ago [18], it still is a fountain of youth for the synthesis of new types of transition metal complexes with specific properties.

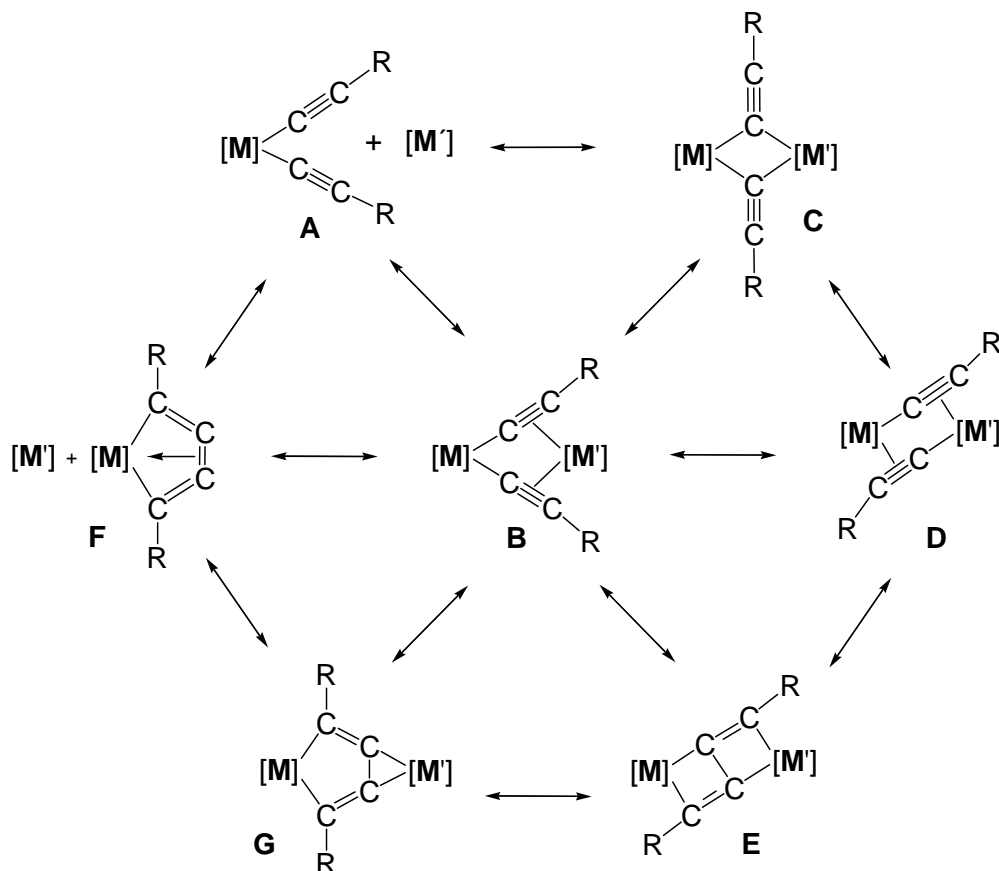
The concept of “molecular Lego®” was independently established by Michl [2a] and Stoddart [3a]. Individual functionalized inorganic, organic and/or organometallic molecules can be considered as modular “Tinkertoys” and can be assembled according to a specific building design to give new complexes with unique chemical head structures. This construction process should be reversible. The thus prepared parts can be maintained until the next “molecular Lego®” process starts anew.

Herein we focus in the following on the use of mainly mono and bis(alkynyl) transition metal complexes, ferrocenes, NCN pincer molecules, 1,4-/1,3,5-substituted benzenes, functionalized acetylenes etc. as molecular “Tinkertoys” in the modular synthesis of heteroatomic multinuclear assemblies with up to six different transition metal atoms. (For other organic and/or inorganic connecting units, such as carboxylates, halides and pseudo-halides see refs. [13, 15, 18]). In this respect, special attention will be paid to the most recent results from our group and others. We hope that we will be able to give new impetus to the path-breaking and rapidly developing field of multiheterometallic organometallic chemistry and applications of the systems. Therefore, this chapter is divided into two sections (i)

RECENT DEVELOPMENTS IN ORGANOMETALLIC π -TWEEZER CHEMISTRY, and in particular, (ii) MULTIHETEROMETALLIC TRANSITION METAL COMPLEXES. In all organometallic systems different transition metals are spanned by carbon-rich π -conjugated organic and/or inorganic units, allowing (more or less) electronic communication between the metals along the bridging entities. However, clusters, or (linear) transition metal complexes with direct metal-metal interactions will not be considered [19].

RECENT DEVELOPMENTS IN ORGANOMETALLIC π -TWEEZER CHEMISTRY

Complexes of type $\text{RC}\equiv\text{C}-[\text{M}]-\text{C}\equiv\text{CR}$ ($[\text{M}] = 12 - 16$ valence electron complex fragment, R = singly-bonded organic or organometallic group) (type A molecule) [14n] with their two alkynyl units act towards different metal fragments as organometallic bidentate chelating ligands, or like the motto “an old principle but a new name” as organometallic π -tweezers to afford heterobimetallic species of type B – G in which the respective metals M and M' are bridged by alkynyl ligands (Scheme 1) [14n].



Scheme 1. Interconversion of alkynyl coordination modes in type A – G molecules [14n].

The structures adopted by complexes B - G strongly depend on the relative affinity of the metals M and M' for electron density. If one metal atom (*e.g.*, M) is more electrophilic than the other (M'), then the alkynyl ligands $\text{RC}_\beta\equiv\text{C}_\alpha$ will preferentially bind to M through the C_α atoms. This results in the formation of type B species in which both alkynyl ligands are σ -bound to M and π -coordinated to the second metal M'. This is the preferred structure for many early-late heterobimetallic complexes [14n]. In most complexes of the latter type, *e. g.*, $\{[\text{Ti}](\mu-\sigma,\pi\text{-C}\equiv\text{CR})_2\}\text{M}'\text{X}$ ($[\text{Ti}] = (\eta^5\text{-C}_5\text{H}_5)_2\text{Ti}$, $(\eta^5\text{-C}_5\text{H}_4\text{Me})_2\text{Ti}$, $(\eta^5\text{-C}_5\text{H}_4\text{SiMe}_3)_2\text{Ti}$, ...; M' = Cu, Ag, Au, ...; X = neutral or ionic inorganic or organic 2-electron donor ligand; M' = Ni, Co; X = CO, PR₃, ...) the metals M' within the tweezer framework have coordination number 3 and possess a planar environment [14].

If the metals M and M' are competitive in their affinities towards the alkynyl ligands $\text{RC}\equiv\text{C}$, or if steric factors prevent the formation of type B tweezer complexes, then structural type C or D species are formed. In these molecules, the ligands $\text{RC}\equiv\text{C}$ are more evenly shared, either with both metals, μ -bridged by both alkynyl ligands (type C) or with each metal σ -bonded by one alkynyl unit and π -coordinated to the other (type D) [14].

In view of the fact that the two alkynyl ligands in type B molecules are held in close proximity by [M], coupling reactions between the two $\text{RC}\equiv\text{C}$ ligands are possible, forming molecules of type E and G [14f, r, aa]. Steric and electronic effects appear to play an essential role in determining the feasibility of the carbon-carbon bond forming reactions, as small changes in the alkynyl-bonded groups R or in the ancillary ligands of M and M' can induce or prevent these reactions.

The state-of-the-art in the field of organometallic π -tweezer chemistry until 2000 is depicted in Scheme 1. Many examples to date confirm this picture [14n]. While in the beginning of this chemistry we have been increasingly attracted by the use of type A molecules as organometallic chelating ligands [14n], we recently became interested in the application of such systems to study, for example, electron transfer [14i, h, s, v, x], to create self-assembled monolayers (SAMs) [20], and to prepare 1-dimensional molecular wire molecules, which can be used in molecular electronics to span metal surfaces/electrodes [20].

Regarding these topics, special attention was drawn to low-valent alkynyl-stabilized organo-copper(I) and -silver(I) compounds in which the respective metals possess a planar surrounding [14]. While the use of alkyne- and alkynyl-stabilized inorganic and organic group-11 metal fragments have lately been reviewed in detail [14], we focus here on recent results obtained in the field of electron transfer.

Since the path-breaking and pioneering work of Creutz and Taube in early 1969 [21], there has been a rapidly growing interest in the preparation as well as chemical and physical properties of homo- and heterobimetallic organometallic and metal organic assemblies in which the respective transition metals are connected by organic and/or inorganic (carbon-rich) π -conjugated bridging units [22, 23]. As this, many redox-active model compounds have been synthesized, such as $(\eta^5\text{-C}_5\text{H}_5)(\eta^5\text{-C}_5\text{H}_4)\text{Fe-C}\equiv\text{C-Pt(dppe)}(\text{R})$ (1) [22t] (dppe = diphenylphosphino ethane; R = aryl), $[(\eta^5\text{-C}_5\text{H}_5)\text{Fe}(\eta^5\text{-C}_5\text{H}_4\text{-C}\equiv\text{C}-\eta^5\text{-C}_5\text{H}_4)\text{Co}(\eta^5\text{-C}_5\text{H}_5)]^+$ (2) [24], *trans*-(PEt₃)₂(Ph)Pt-C≡C-C₆H₄-C≡C-ML_n (3a, ML_n = Ru(Cl)(Ph₂PCH₂PPh₂)₂; 3b, ML_n = Ru($\eta^5\text{-C}_5\text{H}_5$)(PPh₃)₂, ...) [6b], $(\eta^5\text{-C}_5\text{Me}_5)(\text{dppe})\text{Fe-C}\equiv\text{C-C}\equiv\text{C-Fe}(\eta^5\text{-C}_5\text{Me}_5)(\text{dppe})$ (4) [22w, y], and $[(\eta^5\text{-C}_5\text{Me}_5)(\text{NO})(\text{Ph}_3\text{P})\text{Re-C}\equiv\text{C-C}\equiv\text{C-C}\equiv\text{Mn}(\eta^5\text{-C}_5\text{H}_5)(\text{CO})_2]^+$ (5) [23p, 25] in which a molecular wire consisting of an all-carbon C₂-, C₄- or C₅-chain bridges the two

metals M and M' ($M/M' = Fe/Fe$, Re/Mn , Fe/Co , Fe/Pt), giving rise to an electronic coupling through three, five or even six bonds. Further examples of molecular wire molecules are, for example, $(R'_2PCH_2CH_2PR'_2)(RC\equiv C)Mn-C\equiv C-C\equiv C-Mn(C\equiv CR)(R'_2PCH_2CH_2PR'_2)$ [26] (6) ($R = SiEt_3$, Si^iPr_3 , Si^iBuMe_2 ; $R' = Me$, Et), $(\eta^5-C_5H_4Me)(Me_2PCH_2CH_2PMe_2)Mn=C=C=Mn-(Me_2PCH_2CH_2PMe_2)(\eta^5-C_5H_4Me)$ (7) [27], $(\eta^5-C_5H_5)(NO)(Ph_3P)Re-(C\equiv C)_n-Re(\eta^5-C_5H_4-Me)(NO)(PPh_3)$ (8) ($n = 1 - 10$) [28], [*trans*-($R-4-C_6H_4$)(Ph_3P)₂Pd $\leftarrow N^{\wedge}N \rightarrow$ Pd(PPh_3)₂(C_6H_4-4-R)]^{m+} (9) ($N^{\wedge}N = 4,4'$ -bipy, $C_6H_4-1,4-(C\equiv N)_2$, $(C_6H_4-4-C\equiv N)_2$, $C_5H_4N-CH=CH-C_6H_4-CH=CH-C_5H_4N$, ...; $R = Me(O)CS$, $m = 2$; $R = Ph_3P$, $m = 4$) and [$(R-4-C_6H_2(CH_2NMe_2-2,6)_2)Pt\leftarrow N^{\wedge}N \rightarrow Pt(C_6H_2(CH_2NMe_2-2,6)_2-4-R\right)^{2+}$ (10) [20]. In 10 the group-10 platinum redox termini can be adjusted in variable distances to each other by the connecting entities $N^{\wedge}N$ [20]. Besides these species, further binuclear assemblies with two different redox sites in close proximity were synthesized containing the cyano acetylide ligand as bridging unit. The isomeric heterobimetallic Fe-Ru complexes $(\eta^5-C_5H_5)(Ph_3P)_2Ru-C\equiv C-C\equiv N-Fe(\eta^5-C_5H_5)(dppe)$ (11) and $(\eta^5-C_5H_5)(dppe)Fe-C\equiv C-C\equiv N-Ru(\eta^5-C_5H_5)(PPh_3)_2$ (12) are readily available [29], and the electrochemical response of each complex is characterized by two oxidation waves found at 0.62 and 1.22 V (11) and at 0.66 and 1.37 V (12), respectively [29]. IR spectro-electrochemical investigations of the respective mono cationic species revealed a noteworthy decrease in the energy of the $\nu(C\equiv C, C\equiv N)$ vibrations, which is consistent with a contribution from the ligand to the redox active orbitals. [29] In addition, a intense NIR band is observed at $\nu = 9600\text{ cm}^{-1}$ ($\varepsilon = 5600\text{ M}^{-1}\text{ cm}^{-1}$) for $[(\eta^5-C_5H_5)(Ph_3P)_2Ru-C\equiv C-C\equiv N-Fe(\eta^5-C_5H_5)(dppe)]^+$, while for $[(\eta^5-C_5H_5)(dppe)Fe-C\equiv C-C\equiv N-Ru(\eta^5-C_5H_5)(PPh_3)_2]^+$ a band at $\nu = 9600\text{ cm}^{-1}$ ($\varepsilon = 5600\text{ M}^{-1}\text{ cm}^{-1}$) is typical [29]. From oxidation potentials of model alkynyl and cyano complexes featuring the $(\eta^5-C_5H_5)(dppe)Fe$ and $Ru(\eta^5-C_5H_5)(PPh_3)_2$ fragments, respectively, it looks like that initial oxidation of these two assemblies takes place at the iron ion [29]. Examples of another type of binuclear compounds are shown in Figure 1. It must be noted that since the first generation of the mixed-valence of diferrocenyl acetylene in 1974 [30], the interest in these sandwich complexes has significantly increased [31], because the ferrocenyl moiety is robust in its neutral and oxidized form. It also was shown that oligoyne and polyyne chains can be stabilized next to the direct linking of sp carbon atoms to the metals (vide supra) by joining the triple-bonded systems to the ligand periphery as typical for the molecules represented in Figure 1. The electrochemical response of these systems has been selectively reported with a focus on the variation of the connecting unit and the nature of the metal groups [32]. There it is found that the doubly bridged diiron species ($\Delta E = 0.25\text{ V}$) exhibit two sequential one electron oxidations with greater separation in the $E_{1/2}$ potentials than the singly bridged analogues [32]. From NIR studies it is assumed that the doubly bridged ferrocenes are more strongly coupled than the singly bridged ones [32]. The binuclear cobalt complex shown in Figure 1 possesses two potentials at 0.846 and 0.947 V in the cyclic voltammogram [33]. Apparently, in the radical cationic state the two cobalt atoms interact via the butadiyne chain. Although the complexes gave no ESR signals, the cyclic voltammetric results are in good agreement with a valence-trapped species.

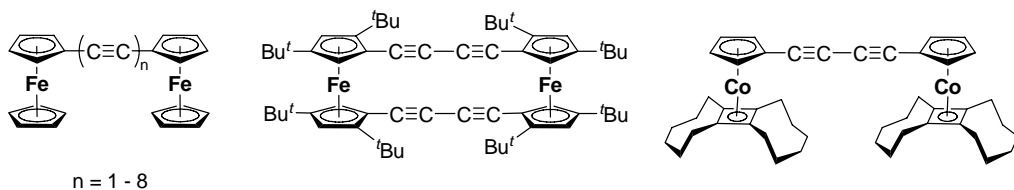


Figure 1. Selected oligometallic complexes featuring acetylide-based connecting ligands [32, 33].

Diethynyl di- and triferrocenyls have also been considered as potential connecting units. [34] Interactions between the remote ferrocenyl redox probes through the Fc_n core ($n = 1, 2, 3$) were investigated [34]. However, it was found that the interpolation of the Fc_2 moiety does not impede electronic communication between the two Fc units, although more attention is apparent with the Fc_3 entity. This means that the terminal groups and the oligo-frocene skeleton act almost independently. For an excellent review on this topic see ref. [29b].

Next to the high variety of late-late transition metal complexes (vide supra), also a number of early-late species, *e.g.* $(\eta^5-C_5H_5)(Me_3P)_2Ru-C\equiv C-Zr(\eta^5-C_5H_5)_2(Cl)$ (13) are known [23]. Further examples of this family are depicted in Figure 2. Complexes 14 - 16 are suited to transport electrons along the organic π -system between the redox-active metal termini.

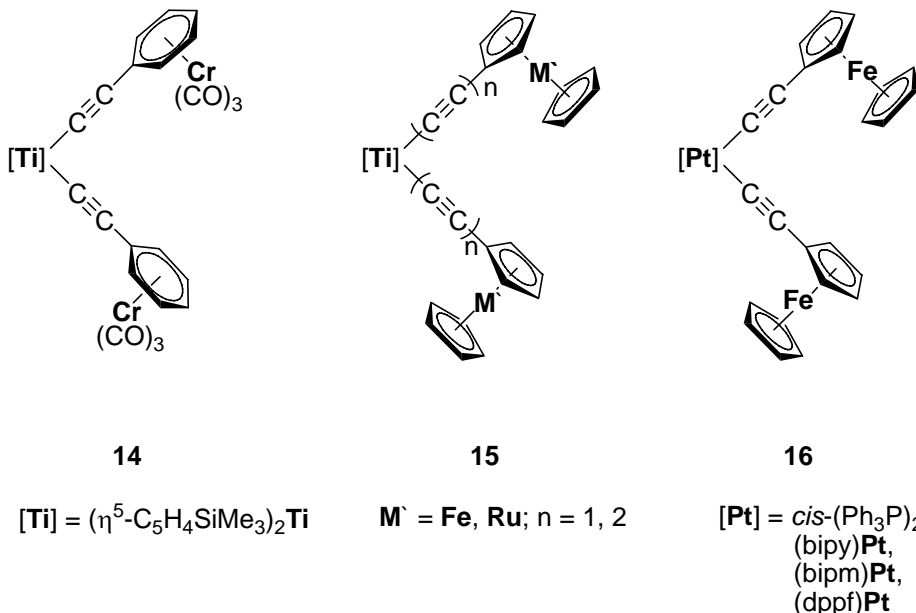


Figure 2. Organometallic π -tweezer molecules with (benzene tricarbonyl) chromium (14), ferrocenyl (15, 16) and ruthiocenyl (15) (redox-active) termini [14n, v, w, aa, 35 - 38].

Cyclic voltammetric studies of 14 show a reversible wave at $E_0 = -1.6$ V ($\Delta E = 100$ mV) which can be assigned to the $Ti(IV)/Ti(III)$ redox couple [35]. For the $(\eta^6-C_6H_5)Cr(CO)_3$ unit the appearance of irreversible oxidation waves is typical [39]. Replacement of this fragment in 14 by less electron withdrawing groups such as ferrocenyl or ruthiocenyl units affords the organometallic π -tweezers $[Ti][(C\equiv C)_mMc][(C\equiv C)_nM'c]$ (15a, $m = n = 1$, $Mc = M'c = Fc$; 15b, $m = n = 1$, $Mc = M'c = Rc$; 15c, $m = n = 2$, $Mc = M'c = Fc$; 15d, $[Ti] = (\eta^5-C_5H_5)_2Ti$, $m = n = 2$, $Mc = M'c = Fc$).

= n = 2, Mc = M'c = Fc; 15e, m = n = 2, Mc = Fc, M'c = Rc; 15f, m = 1, n = 2, Mc = M'c = Fc; 15g, m = 1, n = 2, Mc = Rc, M'c = Fc; Fc = (η^5 -C₅H₄)Fe(η^5 -C₅H₅), Rc = (η^5 -C₅H₄)Ru(η^5 -C₅H₅)) (Figure 2) [14v, x, aa]. Oxidation of 15 leads to an instantaneously coupling of the acetylidyne-ferrocenyl or –ruthiocenyl entities Mc(C≡C)_m and M'c(C≡C)_n to give the appropriate all-carbon complexes by an electron transfer from Ti-C_{C≡C} to Mc or M'c across the π -conjugated acetylides (C≡C)_m and (C≡C)_n, respectively. The oxidatively induced coupling of the Mc(C≡C)_m and M'c(C≡C)_n moieties is not even averted when the alkynyl ligands in 15 are η^2 -coordinated to an additional transition metal fragment as given in, *i.e.*, {[Ti](μ - σ , π -C≡CFc)₂}CuBr (17) and {[Ti](μ - σ , π -C≡CFc)₂}PdPPh₃ (18) [14s, ee].

To prevent the metal–carbon cleavage in 15 the titanocene moiety was exchanged by [Pt] since Pt–C bonds are significant more stable than Ti–C ones. In *cis*–[Pt](C≡CFc)₂ (16a, [Pt] = (bipy)Pt; 16b, [Pt] = (Ph₃P)₂Pt; 16c, [Pt] = (dppf)Pt; 16d, [Pt] = (bipm)Pt; bipy = 2,2'-bipyridine; dppf = 1,1'-bis(diphenylphosphino)ferrocene; bipm = 2,2'-bispyrimidine) a d⁸-electron configurated and hence, square-planar coordination of the Pt(II) ion is typical, which contrasts with the tetrahedral surrounding of the titanium(IV) ion in [Ti]. The electrochemical response of 16a and 16b shows two reversible one-electron oxidations centered on the Fc moieties at E_0 = -0.1 V (ΔE = 180 mV) and +0.05 V (ΔE = 115 mV) for 16a and E_0 = +0.1 V (ΔE = 200 mV) and +0.17 V (ΔE = 200 mV) for 16b. This indicates a moderate electronic interaction between the iron cores through the connecting organic chains and the platinum atom. Nevertheless, the electronic interaction found in 16a and 16b is stronger as in all-carbon Fc–C≡C–C≡C–Fc (ΔE = 100 mV) [37, 38]. Next to the two reversible oxidation processes, irreversible one-electron reductions are found at -1.55 and -2.19 V for 16b and at -1.46 V for 16a, which can be assigned to the reduction of Pt(II) to Pt(0). The second reduction wave for 16a (Pt(I)/Pt(0)) is covered by the reversible reduction of the 2,2'-bipyridine ligand (bipy/bipy⁻ = -1.78 V (ΔE = 140 mV), bipy⁻/bipy²⁻ = -2.47 V (ΔE = 180 mV)) [37]. In addition, the electrochemical properties of *cis*-(dppf)Pt(C≡CFc)₂, (16c) [{*cis*-(dppf)Pt-(C≡CFc)₂}CuBr] (19a), and [{*cis*-(dppf)Pt(C≡CFc)₂}AgClO₃] (19b) were investigated [40]. Oxidation of 16c gives by an oxidative coupling of the FcC≡C fragments the all-carbon butadiyne FcC≡C–C≡CFc along with [(dppf)Pt]²⁺ (Figure 3) [40].

The oxidatively induced coupling of the FcC≡C units is averted, when the alkynyl ferrocene ligands in 16c are π -bonded to a low-valent CuBr moiety, *i.e.*, [{*cis*-(dppf)-Pt(C≡CFc)₂}CuBr] (19a), which differs from the appropriate titanocene species (*vide supra*). [40] When instead of the CuBr moiety the higher homologue of copper is used then again the coupling of the FcC≡C ligands takes place. Next to the formation of FcC≡C–C≡CFc the mononuclear cationic platinum compound [(dppf)Pt(L)(OH)]X (L = thf, CH₃C≡N; X = Br, ClO₄) along with elemental silver was produced. A detailed mechanism for the formation of the latter species is presented in ref. [40]. The higher oxidation potentials for the silver complexes as compared with the copper counter parts suggest that there is less stabilization of the silver in the bis(alkynyl) platinum complexes than in the copper-platinum-iron assemblies [40]. A similar behavior was found for *cis*-(dppf)Pt(C≡CPh)₂ [41]. When the Fc units in 16 and 19 are replaced by Rc moieties (Rc = (η^5 -C₅H₄)(η^5 -C₅H₅)Ru), then more stable compounds are obtained, which most likely is attributed to the higher oxidation potential of the Rc fragments.

Extending the idea of connecting early-late and late-late transition metal building blocks from all-carbon to other carbon-rich μ - σ , π -conjugated organic bridging units enables the synthesis of a large variety of further organometallic compounds by applying the modular “Tinkertoy” approach.

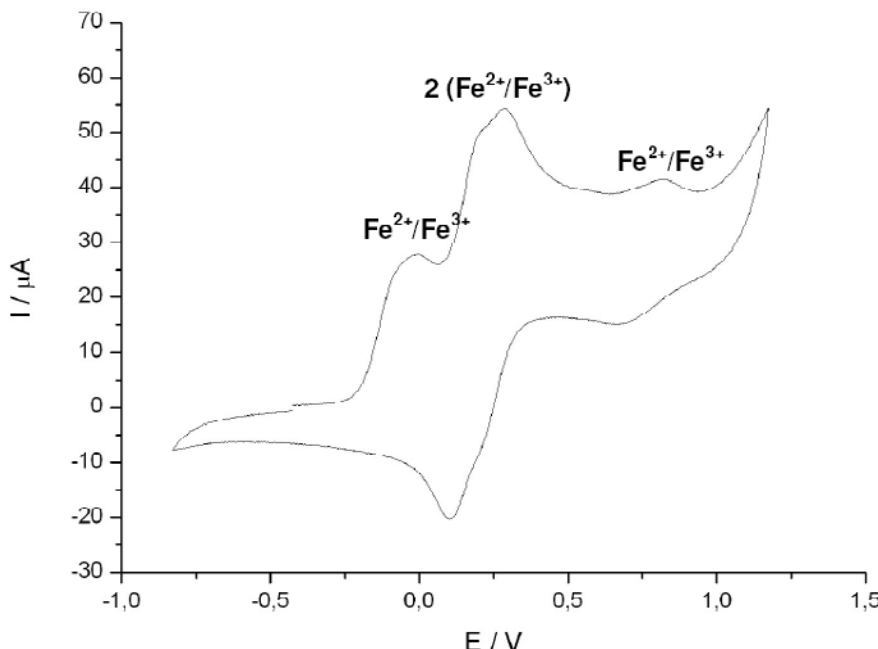


Figure 3. Cyclic voltammogram of 16c in dichloromethane at 25 °C, [$^n\text{Bu}_4\text{N}$]PF₆ supporting electrolyte (0.1 M), scan rate = 100 mV s⁻¹. All potentials are referenced to the FcH/FcH⁺ redox couple (FcH = ($\eta^5\text{-C}_5\text{H}_5$)₂Fe) with $E_0 = 0.00$ V ($\Delta E_p = 150$ mV) [40].

MULTIHETEROMETALLIC TRANSITION METAL COMPLEXES

Within this Section the modular preparation of multimetallic transition metal compounds featuring two, three, four, five, or even six different redox active early and/or late transition metals will be discussed. This idea can be extended even to complexes of higher nuclearity (undecametallic systems) possessing a variety of two, three or four distinct metal atoms. Concertedly for all heteromultimetallic species is that the individual metals are bridged by π -conjugated carbon-rich organic and/or inorganic building blocks. To limit the scope of this article we focus in the following on the synthesis, reaction chemistry, structure and bonding of mainly multimetallic complexes based on mono- and bis(alkynyl) transition metal complexes, functionalized diaminoaryl NCN (NCN = [C₆H₂(CH₂NMe₂-2,6)₂]⁺) and NN'N (NN'N = C₅H₃N(CH₂NMe₂-2,6)₂) pincer molecules, modified ferrocenes as well as 1,4- and 1,3,5-substituted benzenes.

(HETERO)BIMETALLIC TRANSITION METAL COMPLEXES

Besides early-late organometallic π -tweezer complexes of structural type **B** (Scheme 1), also titanocene and zirconocene mono-acetylides enable the synthesis of a series of heterobimetallic compounds featuring early-late transition metal atoms [42]. Two selected examples based on a titanocene ($\eta^5\text{-C}_5\text{H}_4\text{SiMe}_3\right)_2\text{Ti}$ core are depicted in Figure 4 [44].

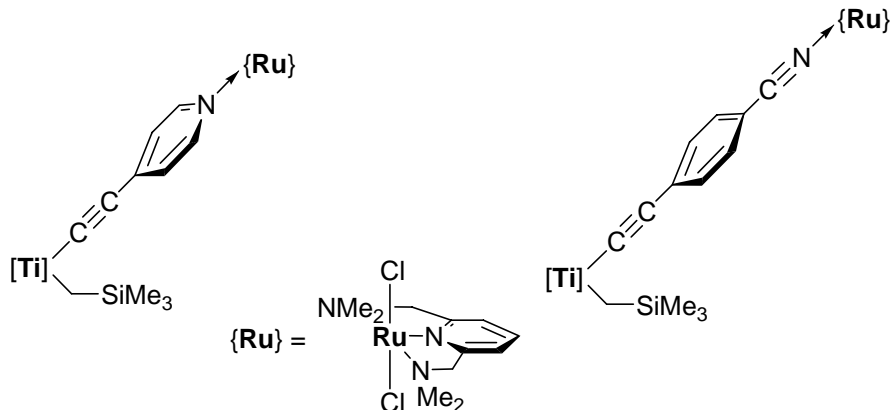
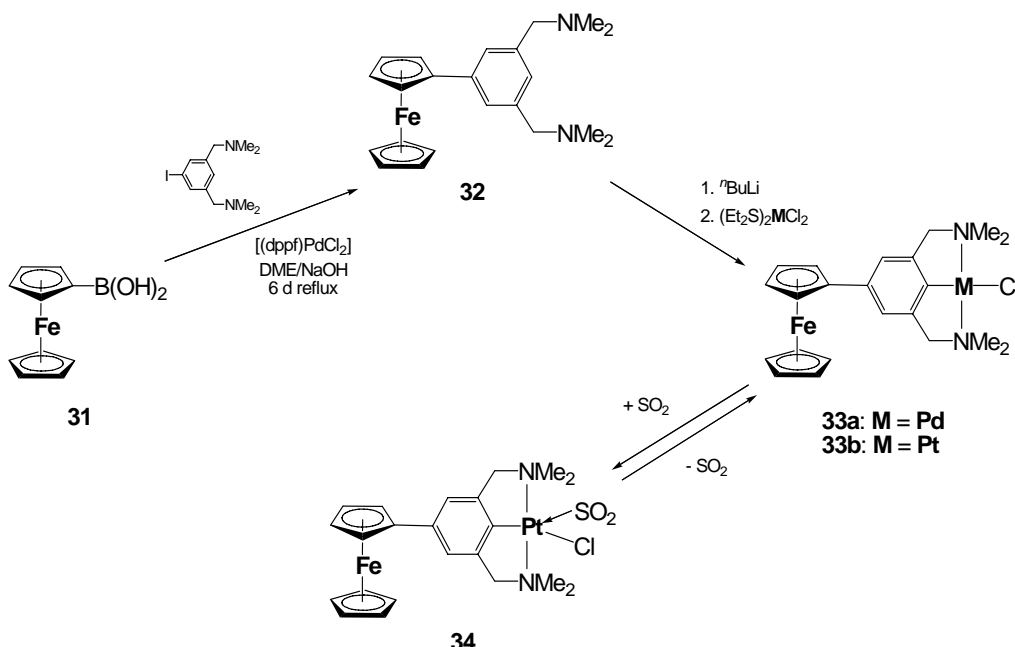


Figure 4. Complexes 20 (left) and 21 (right) [44].

Replacement of the $\text{C}_5\text{H}_4\text{N} \rightarrow \{\text{Ru}\}$ and $\text{C}_6\text{H}_4\text{-4-C}\equiv\text{N} \rightarrow \{\text{Ru}\}$ coordination complex fragments in 20 and 21 by an organometallic sandwich moiety Fc ($\text{Fc} = (\eta^5\text{-C}_5\text{H}_4)(\eta^5\text{-C}_5\text{H}_5)\text{Fe}$) leads to $[\text{Ti}](\text{CH}_2\text{SiMe}_3)(\text{C}\equiv\text{CFc})$ (22). Compound 22 represents a mixed early-late transition metal molecule with a reasonable electron transfer between the reducible $[\text{Ti}]$ and oxidizable Fc groups *via* a $\text{C}\equiv\text{C}$ connecting unit [44, 45]. A further example is $(\eta^5\text{-C}_5\text{H}_5)_2(\text{Me}_3\text{P})_2\text{Ru-C}\equiv\text{C-Zr}(\eta^5\text{-C}_5\text{H}_5)_2(\text{Cl})$ (13) in which the zirconium(IV) ion is directly linked with a ruthenium(II) fragment by an acetylide unit [46]. Likewise, $\{\text{Pt}\}(\text{C}\equiv\text{C-C}_6\text{H}_4\text{-4-C}\equiv\text{N})$ (23) ($\{\text{Pt}\} = (\text{C}_6\text{H}_3(\text{CH}_2\text{NMe}_2\text{-2,6})_2)\text{Pt}$) can act as starting source for the synthesis of linear heterobimetallic complexes of type $\{\text{Pt}\}\text{-C}\equiv\text{C-C}_6\text{H}_4\text{-4-C}\equiv\text{N} \rightarrow \text{M'L}$ (24a, $\text{M'L} = \{\text{Pt}\}\text{BF}_4$; 24b, $\text{M'L} = \{\text{Ru}\}$; 24c, $\text{M'L} = \text{AuCl}$) [47].

A series of supplementary heterobimetallic complexes based on Fc moieties is accessible by applying different synthesis methodologies. Sonogashira cross-coupling of ethynyl-ferrocene (26) with 4-bromobenzonitrile or 5-bromo-2,2'-bipyridine afforded $\text{Fc-C}\equiv\text{C-C}_6\text{H}_4\text{-4-C}\equiv\text{N}$ (27) and $\text{Fc-C}\equiv\text{C-bipy}$ (28), respectively. Treatment of 27 and 28 with $\{\text{Pt}\}\text{BF}_4$, $\{\text{Ru}\}\text{N}\equiv\text{N}\{\text{Ru}\}$, $(\text{nbd})\text{Mo}(\text{CO})_4$ (nbd = norbornadiene), $\text{Mn}(\text{CO})_5\text{Br}$, $\text{Ru}(\text{bipy})_2\text{Cl}_2$ or $(\text{Et}_2\text{S})_2\text{PtCl}_2$ gave the appropriate binuclear complexes $\text{Fc-C}\equiv\text{C-C}_6\text{H}_4\text{-4-C}\equiv\text{N} \rightarrow \text{M'L}$ (29a, $\text{M'L} = \{\text{Pt}\}\text{BF}_4$; 29b, $\text{M'L} = \{\text{Ru}\}$) and $\text{Fc-C}\equiv\text{C-bipy(M'L)}$ (30a, $\text{M'L} = \text{Mo}(\text{CO})_4$; 30b, $\text{M'L} = \text{Mn}(\text{CO})_3\text{Br}$; 30c, $\text{M'L} = \text{Ru}(\text{bipy})_2(\text{PF}_6)_2$; 30d, $\text{M'L} = \text{PtCl}_2$) in which a rigid-rod structured alkynyl benzonitrile entity spans the ferrocene and the M'L building blocks [13, 14a, 48].

Heterobimetallic iron-platinum and iron-palladium complexes based on the pincer functionalized ferrocene Fc-NCN ($\text{NCN} = [\text{4-C}_6\text{H}_2(\text{CH}_2\text{NMe}_2\text{-2,6})_2]$) are available by the synthesis protocol shown in Scheme 3 [49, 50].



Scheme 3. Synthesis of heterobimetallic 33a and 33b and their reaction behavior towards SO₂ (formation of 34) [49, 50].

Compound 33b possesses the ability to reversibly bind sulfur dioxide and hence, can successfully be used as a gas sensor for the detection of SO₂ (Scheme 3) [49, 50].

Related Fc-C≡C-NCNH (35) in which the NCNH and the Fc moieties are separated by an acetylidyne unit is accessible from FcC≡CH by applying the Sonogashira cross-coupling protocol. Lithiation of 35 and reaction of 35-Li with stoichiometric amounts of [(Et₂S)₂MCl₂] (M = Pd, Pt) produced Fc-C≡C-NCN-MCl (36a, M = Pd; 36b, M = Pt) [49, 50]. The introduction of a PdI unit into ferrocene NCN pincer molecules is realizable by the oxidative addition of the carbon-iodide bond in Fc-NCN-I or Fc-C≡C-NCN-I to palladium (*e. g.*, [Pd₂(dba)₃], dba = di(benzylidene) acetone). After appropriate work-up, complexes Fc-NCN-PdI (33c) and Fc-C≡C-NCN-PdI (35c) could be isolated in good yields.

The influence of the connecting alkynyl-aromatic moieties has been considered through electrochemical measurements of closely related complexes (*vide supra*) with a metal-ligand combination and a range of ethynyl-aromatic bridging entities.

(HETERO)TRIMETALLIC TRANSITION METAL COMPLEXES

Recent work of our group has been concerned with (hetero)trimetallic complexes derived from organometallic π -tweezers $\{[Ti](\mu-\sigma,\pi-C\equiv CR)_2\}M'X$ and $\{[Pt](\mu-\sigma,\pi-C\equiv CR)_2\}M'X$ (R = singly-bonded organic or organometallic fragment; M'X = 12 – 14 valence electron transition metal building block; [Pt] = (bipy)Pt, ...) (type B molecule) in which the M'X unit is complexed by both alkynyl ligands of the bis(alkynyl) transition metal fragments [Ti](C≡CR)₂ and [Pt](C≡CR)₂ [14n]. In complexes of type $\{[Ti](\mu-\sigma,\pi-C\equiv CR)_2\}M'X$ the

chelated metal atoms M' and the $[\text{Ti}](\text{C}\equiv\text{CR})_2$ fragments are coplanar, while in $\{[\text{Pt}](\mu-\sigma,\pi-\text{C}\equiv\text{CR})_2\}\text{M}'\text{X}$ the M' center is displaced from the plane defined by the Pt atom and the alkynyl ligands and hence, are *non-planar* [14n]. Within these studies a closely related series of diverse complexes with interesting properties could be prepared.

An approach to transition metal complexes with linear heterotrimetallic assemblies is given by starting from the alkyne-stabilized copper(I) methyl compound $\{[\text{Ti}](\mu-\sigma,\pi-\text{C}\equiv\text{CR})_2\}\text{CuCH}_3$ (37a, R = SiMe₃; 37b, R = 'Bu). Reaction of 37a and 37b with equimolar amounts of FcC≡CH produces upon loss of methane the appropriate copper(I) acetylide $\{[\text{Ti}](\mu-\sigma,\pi-\text{C}\equiv\text{CR})_2\}\text{CuC}\equiv\text{CFc}$ (38) in which a rigid-rod structured Ti-Cu-C≡C-Fc unit is present [14o]. Compounds similar to 38 can be obtained, when FcC≡CH is reacted with 4-ethynylbenzonitrile or 5-ethynyl-2,2'-bipyridine which contain further N-ligated sites. Thus formed $\{[\text{Ti}](\mu-\sigma,\pi-\text{C}\equiv\text{CR})_2\}\text{CuC}\equiv\text{CR}'$ (39a, R' = C₆H₄-4-C≡N; 39b, R' = bipy) reacts with, for example, {Ru}N≡N{Ru} ($\{\text{Ru}\}$ = RuCl₂(NN'N); NN'N = [C₅H₃N(CH₂NMe₂-2,6)₂]⁻) or (nbd)Mo(CO)₄ to afford heterotrimetallic 40 (Ti-Cu-Ru) and 41 (Ti-Cu-Mo), respectively, (Figure 5) [14j, 48].

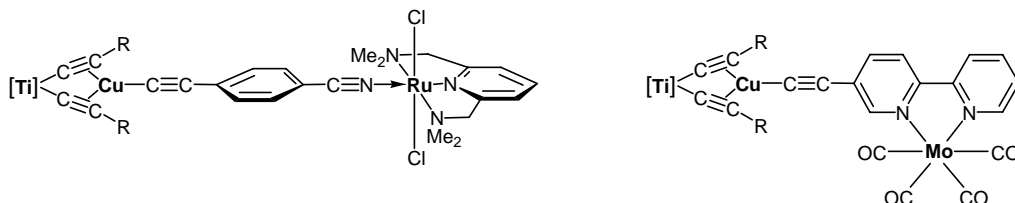


Figure 5. Trimetallic 40 (left) and 41 (right) (R = SiMe₃, 'Bu) [14j, 48].

In 40 and 41 three different transition metals (TiCuRu, TiCuMo) are connected *via* σ,π -bound acetylides and datively-bound benzonitrile (40) and 2,2'-bipyridine (41) ligands. In 40 a linear Ti-Cu-C≡C-C₆H₄-C≡N-Ru-NN'N building block is characteristic as evidenced by single X-ray structure analysis [LIT]. A further example of a similar compound is $\{[\text{Ti}](\mu-\sigma,\pi-\text{C}\equiv\text{CSiMe}_3)_2\}\text{Cu}-\text{C}\equiv\text{N}\rightarrow\text{Cr}(\text{CO})_5$ (42) which is accessible by treatment of the copper(I) cyanide $\{[\text{Ti}](\mu-\sigma,\pi-\text{C}\equiv\text{CSiMe}_3)_2\}\text{CuC}\equiv\text{N}$ (43) with the metal carbonyl Cr(CO)₅(thf) in a 1:1 molar ratio [52]. However, the latter molecule could only be characterized spectroscopically, due to its great instability in solution at room temperature.

A further effort to include metal atoms within organic connecting moieties is possible by treatment of the early-late titanium-copper and titanium-silver tweezers $\{[\text{Ti}](\mu-\sigma,\pi-\text{C}\equiv\text{CSiMe}_3)_2\}\text{M}'\text{X}$ (44a, M'X = Cu(N≡CMe)BF₄; 44b, M'X = AgFBF₃) with Ph₃PAuC≡N in a 1:1 molar ratio [52]. Complex 44a affords upon elimination of MeC≡N cationic 45 (Figure 6) in which the linear Cu-N≡C-Au-P arrangement is stabilized by the chelating effect of the organometallic π -tweezer $[\text{Ti}](\text{C}\equiv\text{CSiMe}_3)_2$. However, when 44b is reacted with the same gold(I) precursor then heterotrimetallic 46 is obtained (Figure 6) [52].

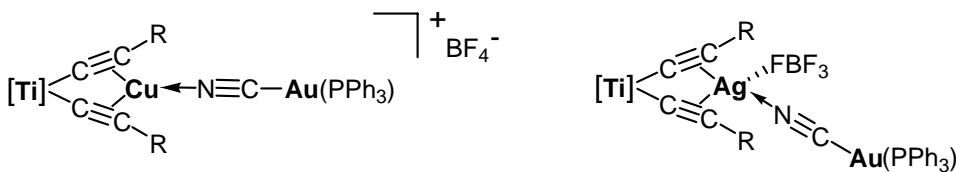
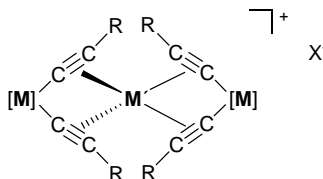


Figure 6. Complexes 45 (left) and 46 (right) ($R = SiMe_3$) [52].

In 45 the copper(I) ion is tri-coordinate and shows a planar surrounding set-up by the η^2 -coordinated $Ti(C\equiv CSiMe_3)_2$ unit and the datively-bonded $(Ph_3P)AuC\equiv N$ building block counting to 16-valence electrons at the copper center, while in 46 the coordination number of silver(I) expands to four and an 18-valence electron fragment is formed [52]. Complex 46 displays a *non-linear* $Ti-Ag-N\equiv C-Au$ array as required by the pseudo-tetrahedral geometry around silver(I). For the different coordination behavior of copper(I) and silver(I) towards Lewis-bases see refs. [14] and [53].

Although the reaction of $[M](C\equiv CR)_2$ π -tweezers ($[M] = [Ti], [Pt]$; $R =$ singly-bonded organic or organometallic ligand) with different metal sources in a 1:1 ratio results in the formation of heterobimetallic structural type B complexes (Scheme 1), an interesting class of oligometallic species is produced in a straightforward manner, when two equivalents of the organometallic π -tweezer $[M](C\equiv CR)_2$ are allowed to react with copper(I) or silver(I) salts $[M'X]$, forming molecules of type $\{[M](\mu-\sigma,\pi-C\equiv CR)_2\}_2M'X$ (47 – 50) (Table 1). In these complexes a single metal M' ($M' = Cu, Ag$) is tetrahedrally coordinated by two organometallic π -tweezer fragments [14]. However, it appeared that the counter-ion X must be a poor ligand, such as BF_4^- , ClO_4^- and PF_6^- to prevent the formation of structural type B molecules. Complexes 47 - 50 are summarized in Table 1.



47 - 50

The molecular solid state structures of selected species of multimetallic 47 - 50 were determined by single X-ray structure analysis. The cationic $\{[M](\mu-\sigma,\pi-C\equiv CR)_2\}_2M'\]^+$ part is set-up by two almost orthogonal positioned bis(alkynyl) transition metal fragments $[M](\mu-\sigma,\pi-C\equiv CR)_2$ which are connected by a $d^{10} M'^+$ metal ion. All four $RC\equiv C$ ligands are thereby η^2 -coordinated to M'^+ forming a linear $M-M'-M$ assembly. A characteristic feature of complexes 47 – 50 is the *non-equivalent* linkages of C_α and C_β to M' ($M-C_\alpha\equiv C_\beta$), which is even more pronounced as it is the case in type B molecules [14]. In 49c the copper ion lies only slightly out of the best $Pt(C\equiv CC_{Ph})_2$ plane to presumably minimize steric interactions between the phenylethynyl ligands and the dppe chelate, in 50b an asymmetric structure is typical, which means that the silver(I) ion is more closely situated to one $Pt(C\equiv CC_{Ph})_2$ fragment than to the other ($Pt(1)-Ag$ 3.384 Å, $Pt(2)-Ag$ 3.513 Å) [14, 54, 59].

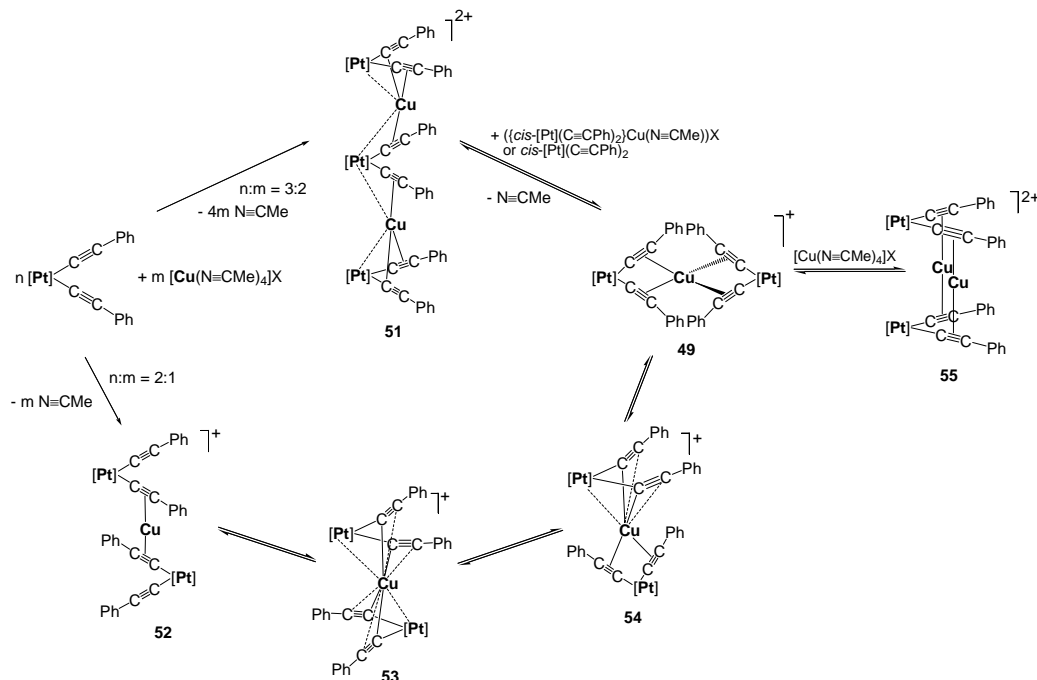
Table 1. Synthesis of Complexes 47 – 50

Compd.	[M]	R	M ⁺	X	Refs.
47a	(η^5 -C ₅ H ₄ SiMe ₃) ₂ Ti	Ph	Cu	BF ₄	14d, 87
47b	(η^5 -C ₅ H ₄ SiMe ₃) ₂ Ti	Ph	Cu	PF ₆	14d, 87
47c	(η^5 -C ₅ H ₄ SiMe ₃) ₂ Ti	Fc	Cu	BF ₄	14d
48a	(η^5 -C ₅ H ₄ SiMe ₃) ₂ Ti	Ph	Ag	BF ₄	14d, 87
48b	(η^5 -C ₅ H ₄ SiMe ₃) ₂ Ti	Ph	Ag	PF ₆	14d, 87
48c	(η^5 -C ₅ H ₄ SiMe ₃) ₂ Ti	Ph	Ag	ClO ₄	14d, 87
48d	(η^5 -C ₅ H ₄ SiMe ₃) ₂ Ti	Fc ^{a)}	Ag	PF ₆	14w
48e	(η^5 -C ₅ H ₄ SiMe ₃) ₂ Ti	Fc ^{a)}	Ag	ClO ₄	14d
48f	(η^5 -C ₅ H ₅) ₂ Ti	C≡CFC ^{a)}	Ag	PF ₆	14w
48g	(η^5 -C ₅ H ₄ SiMe ₃) ₂ Ti	C≡CFC ^{a)}	Ag	PF ₆	14w
48h	(η^5 -C ₅ H ₄ SiMe ₃) ₂ Ti	Rc ^{b)}	Ag	PF ₆	14w
49a	(bipy)Pt ^{c)}	Ph	Cu	BF ₄	55, 59
49b	(bipy')Pt ^{d)}	Ph	Cu	BF ₄	55, 59
49c	(dppe)Pt ^{e)}	Ph	Cu	BF ₄	55, 59
49d	(bppz)Pt ^{f)}	SiMe ₃	Cu	BF ₄	55, 59
49e	(bipy)Pt ^{c)}	Fc ^{a)}	Cu	Br	61
49f	(bipy)Pt ^{c)}	Fc ^{a)}	Cu	BF ₄	61
49g	(dppf)Pt ^{g)}	Ph	Cu	BF ₄	58
50a	(bipy)Pt ^{c)}	Ph	Ag	BF ₄	55, 59
50b	(bipy)Pt ^{c)}	Ph	Ag	PF ₆	55, 59
50c	(bipy)Pt ^{c)}	Ph	Ag	ClO ₄	55, 59
50d	(bipy')Pt ^{d)}	Ph	Ag	BF ₄	55, 59
50e	(bipy')Pt ^{d)}	Ph	Ag	PF ₆	55, 59
50f	(bipy')Pt ^{d)}	Ph	Ag	ClO ₄	55, 59
50g	(bipy)Pt ^{c)}	Fc ^{a)}	Ag	ClO ₄	61
50h	(bppz)Pt ^{f)}	SiMe ₃	Ag	ClO ₄	55, 59
50i	(PPh ₃) ₂ Pt	Ph	Ag	ClO ₄	54
50j	(PEt ₃) ₂ Pt	Ph	Ag	ClO ₄	54
50k	(dppe)Pt ^{e)}	Ph	Ag	ClO ₄	54
50l	(PPh ₃) ₂ Pt	¹ Bu	Ag	ClO ₄	54
50m	(dppe)Pt ^{e)}	¹ Bu	Ag	ClO ₄	54
50n	(dppf)Pt ^{g)}	Ph	Ag	BF ₄	58

a) Fc = (η^5 -C₅H₄)Fe(η^5 -C₅H₅). b) Rc = (η^5 -C₅H₄)Ru(η^5 -C₅H₅). c) bipy = 2,2'-bipyridine. d) bipy' = 4,4'-dimethyl-2,2'-bipyridine. e) dppe = 1,2-diphenylphosphinoethane. f) bppz = 2,5-bis(2-pyridyl)pyrazine. g) dppf = 1,1'-bis(diphenylphosphino) ferrocene.

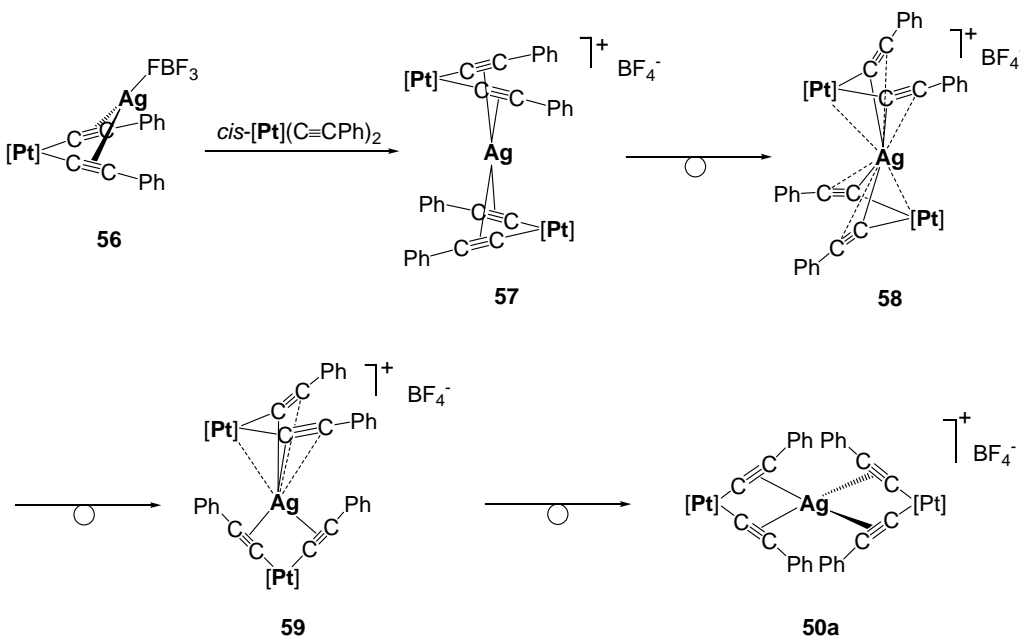
Further possibilities to prepare 49a – 49c are presented in Scheme 4. The reactions shown there are based on the stoichiometry of the reactants *cis*-[Pt](C≡CPh)₂ and [Cu(N≡CMe)₄]X (X = BF₄, PF₆, ClO₄) as well as on the temperature and the reaction time (Scheme 4) [14gg, 56, 57, 59]. It was found that, when *cis*-[Pt](C≡CPh)₂ is reacted with [Cu(N≡CMe)₄]X in the ratio of 3:2, pentametallic Pt₃Cu₂ (51) is formed in which three helically arranged *cis*-[Pt](C≡CPh)₂ building blocks are connected by two copper(I) ions. In 51 the two outer [Pt](C≡CPh)₂ entities are coordinated by only one copper atom. For this, we reacted 51 with a further type B molecule to obtain even higher oligomeric structures. To our surprise only trimetallic 49 could be isolated. However, treatment of *cis*-[Pt](C≡CPh)₂ with the copper source [Cu(N≡CMe)₄]X and using the molar ratio of 2:1 at low temperature gave 52, a compound in which the copper(I) ion is π -bound by one PhC≡C ligand of individual *cis*-[Pt]C≡CPh₂ units, thus resulting in a linear alkyne-copper-alkyne arrangement (alkyne =

midpoint of the C≡C triple bond). This complex can be considered as an intermediate in the formation of 49 (Scheme 4). Slowly warming a tetrahydrofuran solution containing this species to 45 °C, 52 smoothly rearranges *via* the formation of 53 and 54 to give 55 as evidenced by spectroscopic and single crystal X-ray diffraction studies [14gg, 45, 56 57, 58, 59]. When 49 is further reacted with one equivalent of $[\text{Cu}(\text{N}\equiv\text{CMe})_4]\text{X}$ the incoming Cu(I) adds to the alkynyl ligands of 49 resulting in the formation of 55 (Scheme 4). In 55 two bis(alkynyl) platinum entities are linked by copper(I) ions, whereby two PhC≡C units, one associated with each platinum atom, are π -bonded to the group-11 metal copper.



Scheme 4. Reaction chemistry of *cis*-[Pt](C≡CPh)₂ towards $[\text{Cu}(\text{N}\equiv\text{CMe})_4]\text{X}$; formation of 49 and 51 – 55 [55, 57, 59].

Another possibility to synthesize trimetallic 50a is given by treatment of the platinum-silver species $\{\text{cis}-[\text{Pt}](\mu-\sigma,\pi-\text{C}\equiv\text{CPh})_2\}\text{AgFBF}_3$ (56) with stoichiometric amounts of *cis*-[Pt](C≡CPh)₂ as depicted in Scheme 5 [55, 57, 59]. The first step in the preparation of 50a involves the elimination of BF_4^- from 56 upon addition of the organometallic chelate *cis*-[Pt](C≡CPh)₂. Initially formed $\{[\text{cis}-[\text{Pt}](\mu-\sigma,\pi-\text{C}\equiv\text{CPh})_2]_2\text{Ag}\}\text{BF}_4$ (57) contains two *cis*-[Pt](C≡CPh)₂ moieties which are η^2 -coordinated to a silver(I) cation by all of the PhC≡C ligands. The two *cis*-[Pt](C≡CPh)₂ units are oriented parallel to the platinum atoms on opposite sites. This complex isomerizes in solution to produce 58 and then 59, which afterward rearranges to give 50a. IR spectroscopic studies gave the first hint for the different bonding modes of the alkynyl groups in 56 - 59 and 50a. Additionally, the molecular solid state structures of these species were confirmed by single crystal X-ray structure determinations [14gg, 45, 56, 59].



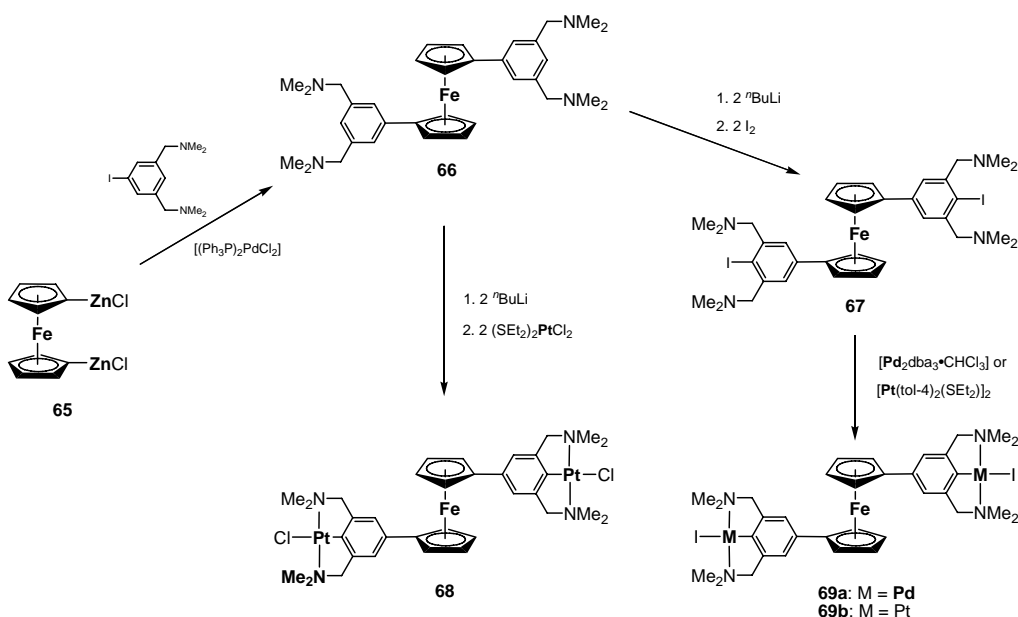
Scheme 5. Synthesis of 50a by reacting 56 with $cis\text{-[Pt]}(\text{C}\equiv\text{CPh})_2$ [55, 57, 59].

Trimetallic $\text{M}_2\text{M}'$ compounds of type ($\text{M} = \text{Fe}$, $\text{M}' = \text{Hg, Cd, Zn, Pd}$; $\text{M} = \text{Pd, Pt}$, $\text{M}' = \text{Fe}$; ...) can be synthesized in a straightforward manner by applying different synthesis methodologies [60, 61]. Treatment of two equivalents of $\text{FcC}\equiv\text{CH}$ with mercuric acetate (Hg(OAc)_2) in different solvents produced $(\text{FcC}\equiv\text{C})_2\text{Hg}$ (60) along with acetic acid [60, 61]. The reaction mechanism is discussed in the light of the mercurated and non-mercurated reaction intermediates (depending on the solvents used), involving $\text{FcC(OCH}_2\text{HgX}$, FcC(OMe)=CH_2 , FcC(O)Me , and FcC(OAc)=CH_2 , whereby X appeared to contain another mercury atom [60a]. For comparison the reaction behavior of ethynylbenzene with the same mercurating systems has also been investigated [60, 61].

Isostructural $(\text{FcC}\equiv\text{C})_2\text{M}$ complexes (61, $\text{M} = \text{Cd}$; 62, $\text{M} = \text{Zn}$) are accessible in a much more straightforward reaction when $\text{FcC}\equiv\text{CLi}$ is treated with MCl_2 ($\text{M} = \text{Cd, Zn}$) in a 2:1 molar ratio [61]. After appropriate work-up, these complexes were obtained in good yield. In the latter molecules group-11 and group-12 transition metal atoms are linking two ferrocene ethynyl building blocks. Electrochemical studies, however, showed that between the $\text{FcC}\equiv\text{C}$ units no coupling is observed [61].

A Fe_2Pd trinuclear complex of composition $[(\text{Fc-C}\equiv\text{C-1-C}_6\text{H}_4\text{-4-C}\equiv\text{N})_2\text{Pd}(\text{PPh}_3)_2](\text{OTf})_2$ (63) is available by the reaction of $\text{Fc-C}\equiv\text{C-1-C}_6\text{H}_4\text{-4-C}\equiv\text{N}$ (64) with $\text{Pd}(\text{PPh}_3)_2(\text{OTf})_2$ [62]. Electrochemical studies of 63 showed that only one reversible redox couple is found for the Fc units and hence, no electron transfer *via* the connecting metal palladium atom takes place.

As shown earlier Fc-NCNH pincer molecules can successfully be used in the synthesis of heterobimetallic complexes. The introduction of a further NCNH unit in Fc-NCNH opens the possibility to prepare the ferrocene-based trimetallic FeM_2 complexes 68 and 69 ($\text{M} = \text{Pd, Pt}$) by starting from ferrocene 65 (Scheme 6). The reactions shown in Scheme 6 include metallation-*transmetallation* and oxidative addition processes [49, 63].

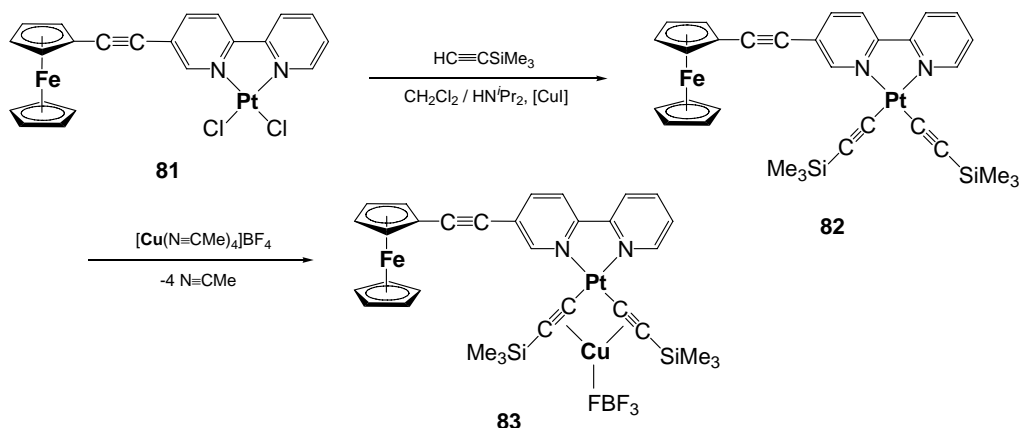


Scheme 6. Synthesis of FeM_2 complexes 68, 69a and 69b from 65 [49, 63].

Replacing the NCN pincer unit in $(\eta^5\text{-C}_5\text{H}_4\text{-NCN})_2\text{Fe}$ sandwich compounds by diphenyl phosphino coordinating groups allows the synthesis of a series of trimetallic assemblies of structural type $(\eta^5\text{-C}_5\text{H}_4\text{PPh}_2\text{ML}_n)_2\text{Fe}$ ($\text{ML}_n = \text{M}(\text{CO})_5$: 70a, $\text{M} = \text{Cr}$; 70b, $\text{M} = \text{Mo}$; 70c, $\text{M} = \text{W}$; 71, $\text{ML}_n = (\eta^6\text{-C}_6\text{H}_4\text{-1-}'\text{Pr-4-Me})\text{RuCl}_2$; 72a, $\text{ML}_n = \text{AuCl}$; 72b, $\text{ML}_n = \text{AuC}\equiv\text{Cbipy}$) [64, 65]. Molecules 72a and 72b can be used as starting materials for the preparation of complexes of higher nuclearity and of, e.g., coordination polymers [64].

Other trimetallic MM'_2 metal complexes are $\{[(\eta^5\text{-C}_5\text{H}_4\text{PPh}_2)_2\text{CuCl}]\text{Ti}(\mu-\sigma,\pi-\text{C}\equiv\text{C}'\text{Bu})_2\}\text{CuCl}$ (73) [65], $\text{Pt}[(\mu-\sigma,\pi-\text{C}\equiv\text{CPh})\text{CdCl}_2]_2$ (74) [66], $\text{Pt}[(\text{C}\equiv\text{C-C}_6\text{H}_4\text{-2-C}\equiv\text{C-C}_6\text{H}_4\text{-2-C}\equiv\text{C})\text{HgCl}_2]_2$ (75) [67], $(^n\text{Bu}_3\text{P})_2(\text{L})(\text{CO})\text{Ru}(\text{C}\equiv\text{CFc})_2$ (76a, $\text{L} = \text{CO}$; 76b, $\text{L} = \text{C}_5\text{H}_5\text{N}$; 76c, $\text{L} = \text{P}(\text{OMe})_3$) [68], $(\text{Ph}_2\text{P}(\text{CH}_2)_n\text{PPh}_2)_2\text{Ru}(\text{C}\equiv\text{CFc})_2$ (77a, $n = 1$; 77b, $n = 2$) [69], $(\text{R}_3\text{P})_2\text{Pt}(\text{C}\equiv\text{CFc})_2$ (78) [70], $(\text{R}_3\text{P})_2\text{Pt}(\text{C}\equiv\text{C-Y-C}\equiv\text{CFc})_2$ (79a, $\text{Y} = 1,4\text{-C}_6\text{H}_4$; 79b, $\text{Y} = 2,5\text{-thiophene}$, ...; $\text{R} = \text{alkyl, aryl}$) [12a, 71], and $[(\eta^5\text{-C}_5\text{H}_4\text{terpy})\text{Fe}(\eta^5\text{-C}_5\text{H}_4\text{PPh}_2)]_2\text{MCl}_2$ (80a, $\text{M} = \text{Pt}$; 80b, $\text{M} = \text{Pd}$; terpy = terpyridine) [61]. Trimetallic 80b can be used in the preparation of pentametallic complexes featuring three different transition metals, since it possesses with the terpy ligands further N-ligated coordination sites (see below). From 77 – 79 detailed spectro-electrochemical investigations were carried out. These complexes display a degree of electronic interaction between the metal-based redox groups located at the ligand termini. The electrochemical response of these systems has been selectively reviewed, with a focus on the variation in properties that accompany changes in the structure of the bridging ligand and the nature of the metal groups [69-71].

So far, trimetallic molecules with two different transition metals have been discussed. A straightforward synthesis method to prepare heterotrimetallic organometallic π -tweezer-based derivatives with three different metal atoms is depicted in Scheme 7 [14a, 48].



Scheme 7. Synthesis of heterotrimetallic 83 by subsequent treatment of 81 with $\text{HC}\equiv\text{CSiMe}_3$ followed by complexation of 82 with $[\text{Cu}(\text{N}\equiv\text{CMe})_4]\text{ClO}_4$ [14a, 48].

Compound 83 is accessible in a consecutive way by the alkynylation of $\text{FcC}\equiv\text{C}-\text{bipy}(\text{PtCl}_2)$ (81) with $\text{HC}\equiv\text{CSiMe}_3$ in presence of diisopropyl amine and catalytic amounts of $[\text{CuI}]$ to give $\text{FcC}\equiv\text{C}-\text{bipy}[\text{Pt}(\text{C}\equiv\text{CSiMe}_3)_2]$ (82) which yields with $[\text{Cu}(\text{N}\equiv\text{CMe})_4]\text{BF}_4$ the trimetallic Fe-Pt-Cu complex 83 (Scheme 7) [14a, 48]. The cyclic voltammograms of 82 and 83 are shown in Figure 7.

For heterobimetallic 82 two redox waves are observed for the bipy ligand at $E_{0,1} = -1.59 \text{ V}$ ($\Delta E_p = 120 \text{ mV}$) and $E_{0,2} = -2.24 \text{ V}$ ($\Delta E_p = 130 \text{ mV}$) in the cyclic voltammogram (Figure 7, top) which is typical for chelate-bonded bipy ligands in platinum transition metal chemistry [14a, 48]. The cyclic voltammogram of 82 also exhibits, as 81, a reversible oxidation for the ferrocene moiety at $E_0 = 0.17 \text{ V}$ ($\Delta E_p = 130 \text{ mV}$) showing that this unit is more difficult to oxidize than 81 and FcH , taken as standard [72]. Complexation of $[\text{CuFBF}_3]$ as given in 83 does not influence on the oxidation or reduction potentials of the $\text{FcC}\equiv\text{C}-\text{bipy}[\text{Pt}(\text{C}\equiv\text{CSiMe}_3)_2]$ moiety ($\text{Fe}^{2+}/\text{Fe}^{3+}$: $E_0 = 0.16 \text{ V}$ ($\Delta E_p = 120 \text{ mV}$); bipy: $E_{0,1} = -1.60 \text{ V}$ ($\Delta E_p = 130 \text{ mV}$) $E_{0,2} = -2.23 \text{ V}$ ($\Delta E_p = 120 \text{ mV}$)). The coordinated copper(I) ion shows a irreversible reduction wave at $E_{p,\text{red}} = -1.82 \text{ V}$ (Figure 7, bottom). This observation may imply that the copper(I) reduction occurs initially resulting in fragmentation of $\text{FcC}\equiv\text{C}-\text{bipy}\{[\text{Pt}((\mu-\sigma,\pi-\text{C}\equiv\text{CSiMe}_3)_2]\text{CuFBF}_3\}$. A similar phenomenon was found for other organometallic π -tweezers, *i.e.* $\{[\text{Ti}](\mu-\sigma,\pi-\text{C}\equiv\text{CR})_2\}\text{CuX}$ [14a, 48].

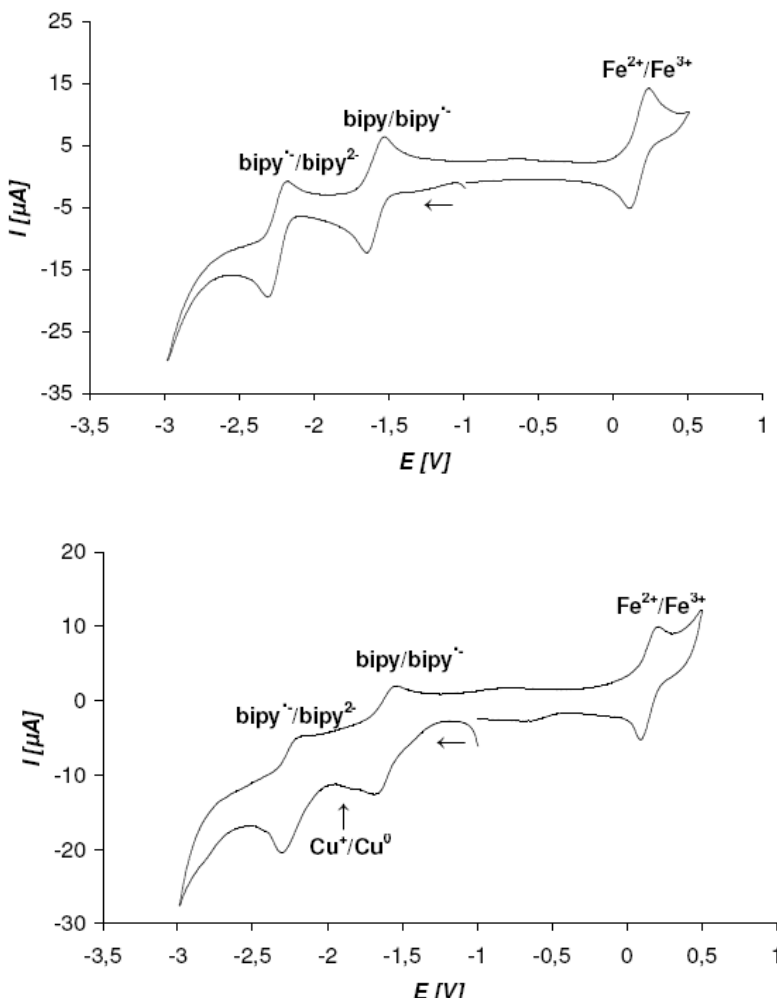
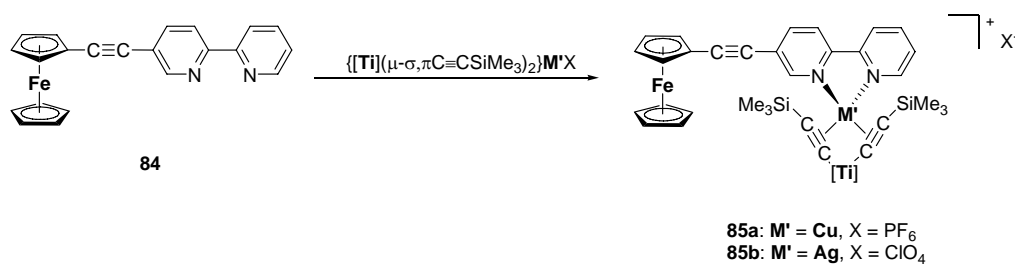


Figure 7. Cyclic voltammograms of 82 (top) and 83 (bottom) in tetrahydrofuran at 25 °C, [$^n\text{Bu}_4\text{N}$]PF₆ supporting electrolyte (0.1 M), scan rate = 100 mV s⁻¹. All potentials are referenced to the FcH/FcH⁺ redox couple (FcH = ($\eta^5\text{-C}_5\text{H}_5$)₂Fe) with $E_0 = 0.00$ V ($\Delta E_p = 150$ mV) [14a, 48].

In neutral 83 a Fc-C≡C-bipy unit is chelate-bonded to a Pt-Cu tweezer moiety. A similar structural motif is also found in $\{[[\text{Ti}](\mu-\sigma,\pi\text{-C}\equiv\text{CSiMe}_3)_2]\text{M}'\}\text{bipy-C}\equiv\text{CFc}]X$ (85a, M' = Cu, X = PF₆; 85b, M' = Ag, X = ClO₄), where the 2,2'-bipyridine entity is coordinated to a heterobimetallic $\{[\text{Ti}](\mu-\sigma,\pi\text{-C}\equiv\text{CSiMe}_3)_2\}\text{M}'^+$ tweezer fragment [14a, 48]. In this molecule the group-11 metal ions copper and silver are chelate-bound by the organometallic π -tweezer $[\text{Ti}](\text{C}\equiv\text{CSiMe}_3)_2$ and the 2,2'-bipyridine ligand resulting in tetra-coordination at M'. These complexes are accessible by combining the mononuclear ferrocene acetylide FcC≡C-bipy (84) with heterobimetallic early-late $\{[\text{Ti}](\mu-\sigma,\pi\text{-C}\equiv\text{CSiMe}_3)_2\}\text{M}'X$ (M'X = Cu(N≡CMe)PF₆; M'X = AgOCLO₄). While trimetallic 85a and 85b are stable in the solid state, they slowly start to decompose in solution on exposure to air, *i. e.*, 85b gives metallic silver along with $[\text{Ti}](\text{C}\equiv\text{CSiMe}_3)_2$ [14a, 48].



Exemplary, the solid state structure of 85a was determined by single X-ray structure analysis. The result thereof is shown in Figure 6 [14a, 48].

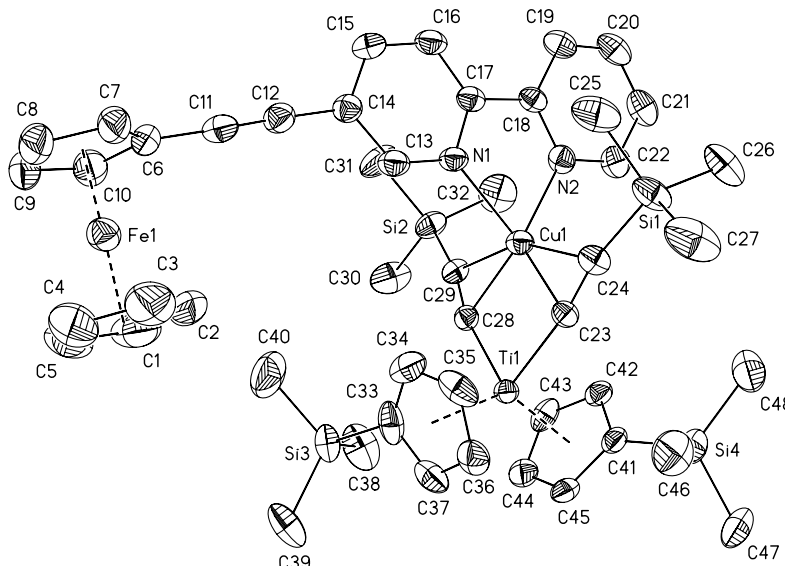


Figure 6. ORTEP plot (30 % probability level) of 85a with the atom numbering scheme (the hydrogen atoms, the PF₆⁻ counter ion, and the distortion of one Me₃Si group are omitted for clarity). For selected bond distances (Å) and angles (°) see ref. [14a, 48].

Heterotrimetallic 85a shows a pseudo-tetrahedral coordination geometry around Cu1 with two η^2 -coordinated Me₃SiC≡C groups (C23-C24, C28-C29) and the chelate-bonded bipy ligand (N1, N2). Noteworthy to mention is the difference between Cu1-N1 (2.225(4) Å) and Cu1-N2 (2.044(4) Å) which verifies an asymmetrical chelate binding of the bipyridine ligand to Cu1. The large dissimilarity between Cu1-N1 and Cu1-N2 in 85a most probably can be ascribed to electronic effects resulting from the electron rich FcC≡C unit.

For comparison, [FcC≡C-bipy{[Ti](μ - σ , π -C≡CSiMe₃)₂}Cu]PF₆ (85a) was subjected to cyclic voltammetric studies (Figure 8).

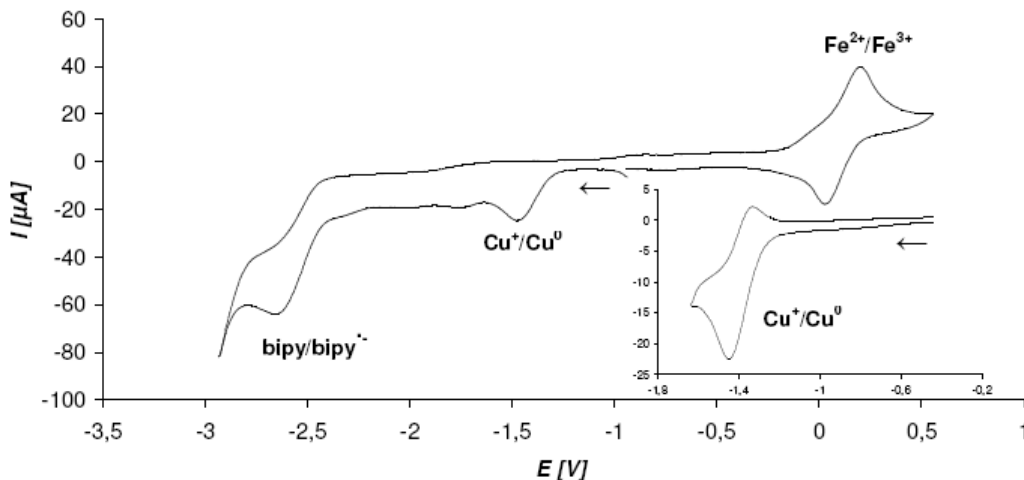


Figure 8. Cyclic voltammogram of 85a in tetrahydrofuran at 25 °C, [n Bu₄N]PF₆ supporting electrolyte (0.1 M), scan rate = 100 mV s⁻¹. All potentials are referenced to the FcH/FcH⁺ redox couple (FcH = (η^5 -C₅H₅)₂Fe) with E_0 = 0.00 V (ΔE_p = 150 mV) [14a, 48].

The relevant electrode potentials of 85a are for the iron(II) ion E_0 = 0.12 V (ΔE_p = 150 mV), the reduction of the copper ion at $E_{p,red}$ = -1.45 V and the reduction process bipy/bipy⁻ at $E_{p,red}$ = -2.67 V (Figure 8). The reduction of Cu(I) to Cu(0) is typical in Ti-Cu organometallic π-tweezer chemistry implying that in such complexes the reduction occurs initially at the Cu(I) ion resulting in fragmentation of the respective complexes (vide supra) [14a, 48]. However, when the cyclic voltammogram of 85a is measured only between -0.4 and -1.6 V (Figure 8, inset) the cathodic reduction of Cu(I) is followed by reoxidation of Cu(0) (E_0 = -1.39 V, ΔE_p = 120 mV) obviously without any change of the chemical identity of the molecule involved. In contrast, this is not the case for isostructural 85b, where instead of copper(I) a silver(I) ion is present. Next to the redox couples Fe²⁺/Fe³⁺ (E_0 = 0.13 V, ΔE_p = 145 mV) and bipy/bipy⁻ ($E_{p,red}$ = -2.66 V), respectively, an irreversible reduction peak for Ag(I)/Ag(0) is found at $E_{p,red}$ = -1.26 V, *i. e.*, no reoxidation peak is observed. In the second run the only observable potentials are those ones typical for free FcC≡C-bipy and [Ti](C≡CSiMe₃)₂ indicating that 85b fragmented into the starting materials.

Table 2. Electrochemical Data of 82 - 85. ^{a)}

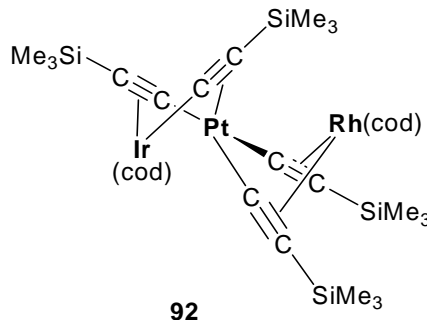
Compd.	Fe ²⁺ /Fe ³⁺	bipy/bipy ^{-b)}	bipy ⁻ /bipy ^{2-b)}	M' ⁺ /M' ^{c)}			
	E_0/V (ΔE_p mV)	$E_0(E_{p,red})/V$ (ΔE_p mV)	E_0/V (ΔE_p mV)	$E_{p,ox}$ V	$E_{p,red}/V$	E_0/V (ΔE_p mV)	
82	0.17 (130)	-1.59 (120)	-2.24 (130)	-	-	-	
83	0.16 (120)	-1.60 (130)	-2.23 (120)	-	-1.82	-	
84	0.10 (194)	-2.36 (200)	-2.76 (430)	-	-	-	
85a	0.12 (150)	-2.67	-	-1.33	-1.45	-1.39 (120)	
85b	0.13 (145)	-2.66	-	-	-1.26	-	

^{a)} In tetrahydrofuran. ^{b)} For electrode potentials of free bipy see ref. [73]. ^{c)} M' = Cu, Ag.

Related trimetallic compounds to 83 and 85 can be obtained, when the gold(I) and ruthenium(II) acetylides $\text{Ph}_3\text{PAu-C}\equiv\text{C-bipy}$ (86) and $(\eta^5\text{-C}_5\text{H}_5)(\text{PPh}_3)_2\text{RuC}\equiv\text{C-bipy}$ (87) are reacted with the organometallic π -tweezer $\{[\text{Ti}](\mu-\sigma,\pi-\text{C}\equiv\text{CSiMe}_3)_2\}\text{M}'\text{X}$ ($\text{M}'\text{X} = \text{Cu}(\text{N}\equiv\text{CMe})\text{PF}_6$, AgOCIO_3). After appropriate work-up, complexes $[\text{L}_n\text{MC}\equiv\text{C-bipy}\{[\text{Ti}](\mu-\sigma,\pi-\text{C}\equiv\text{CSiMe}_3)_2\}\text{M}'\text{JX}]$ (88a, $\text{L}_n\text{M} = (\text{Ph}_3\text{P})\text{Au}$, $\text{M}' = \text{Cu}$, $\text{X} = \text{PF}_6$; 88b, $\text{L}_n\text{M} = (\text{Ph}_3\text{P})\text{Au}$, $\text{M}' = \text{Ag}$, $\text{X} = \text{ClO}_4$; 89a, $\text{L}_n\text{M} = (\eta^5\text{-C}_5\text{H}_5)(\text{PPh}_3)_2\text{Ru}$, $\text{M}' = \text{Cu}$, $\text{X} = \text{PF}_6$; 89b, $\text{L}_n\text{M} = (\eta^5\text{-C}_5\text{H}_5)(\text{PPh}_3)_2\text{Ru}$, $\text{M}' = \text{Ag}$, $\text{X} = \text{ClO}_4$) can be isolated as red solids in excellent yield [48, 64]. They are fairly stable molecules, both in the solid state and in solution. The chemical and physical properties of the latter compounds correspond to those of other gold(I) [74] and ruthenium(II) [75] acetylides.

Another heterotrimetallic complex with a gold(I) acetylide unit is $\text{Ph}_3\text{PAu-C}\equiv\text{C-NCN-Pt-C}\equiv\text{C-Fc}$ (91), which can be obtained by combining $\text{Ph}_3\text{PAu-C}\equiv\text{C-NCN-PtCl}$ (90) with $\text{FcC}\equiv\text{CSnMe}_3$ [74k]. Complex 91 represents a rigid-rod shaped molecular wire molecule in which the transition metals Au, Pt, and Fe are spanned by acetylidyne, cyclopentadienyl and phenylene units.

A heterotrimetallic molecule featuring iridium, platinum and rhodium metals is 92, which is accessible by treatment of $(\text{NBu}_4)[\{\text{Ir-Pt}\}(\text{C}\equiv\text{CSiMe}_3)_2]$ with $[\text{Rh}(\text{cod})(\text{acetone})_x]^+$ ($\text{cod} = \text{cyclooctadiene}$) [76]. The molecular solid state structure of 92 proves the presence of the zwitterion $[(\text{cod})\text{Ir}(\mu-1\kappa\text{C}^\alpha:\eta^2-\text{C}\equiv\text{CSiMe}_3)(\mu-2\kappa\text{C}^\alpha:\eta^2-\text{C}\equiv\text{CSiMe}_3)\text{Pt}^-(\mu-2\kappa\text{C}^\alpha:\eta^2-\text{C}\equiv\text{CSiMe}_3)_2\text{Rh}^+(\text{cod})]$, resulting from the dinuclear anionic fragment $[(\text{cod})\text{Ir}(\mu-1\kappa\text{C}^\alpha:\eta^2-\text{C}\equiv\text{CSiMe}_3)(\mu-2\kappa\text{C}^\alpha:\eta^2-\text{C}\equiv\text{CSiMe}_3)\text{Pt}(\text{C}\equiv\text{CSiMe}_3)_2]^-$ which acts as a chelating dimetallocobidantate ligand towards the cationic $[\text{Rh}(\text{cod})]^+$ building block.



One more heterotrimetallic complex is represented by $(\text{dppf})(\eta^5\text{-C}_5\text{H}_5)\text{Ru-C}\equiv\text{C-C}_5\text{H}_4\text{-N}\rightarrow\text{W}(\text{CO})_4\text{PPh}_3$ (93) in which a linear carbon-rich dimetalla Ru-C≡C-C₅H₄N-W segment is present [77]. Replacement of the 4-ethynyl-pyridine by a 1-ethynyl-4-diphenylphosphino benzene entity gives access to a further series of complexes, *i. e.* $(\text{dppf})(\eta^5\text{-C}_5\text{H}_5)\text{Ru-C}\equiv\text{C-C}_6\text{H}_4\text{PPh}_2\text{-ML}_n$ (94, $\text{ML}_n = \text{AuCl}$; 95, $\text{ML}_n = (\eta^5\text{-C}_5\text{Me}_5)\text{RhCl}_2$; 96, $(\text{cod})\text{RhCl}$) [64]. Other trimetallic complexes featuring the dppf group as a basic building block are $(\text{dppf})\text{Pt}(\text{C}\equiv\text{CPPh}_2\text{ML}_n)_2$ (97a, $\text{ML}_n = \text{AuCl}$; 97b, $\text{ML}_n = (\eta^6\text{-C}_6\text{H}_4-1^i\text{Pr-4-Me})\text{RuCl}_2$) and $(\text{dppf})\text{Pt}[(\text{C}\equiv\text{CPPh}_2)_2\text{ML}_n]$ (98a, $\text{ML}_n = \text{PdCl}_2$; 98b, $\text{ML}_n = \text{PtCl}_2$; 98c, $\text{ML}_n = \text{Mo}(\text{CO})_4$) (Figure 9) which are accessible in consecutive reaction sequences as described in ref. [40]. Complex 98a was used as a catalyst in the Heck reaction of coupling iodobenzene with *tert*-butylacrylate to give *E-tert.-butyl cinnamate* [40].

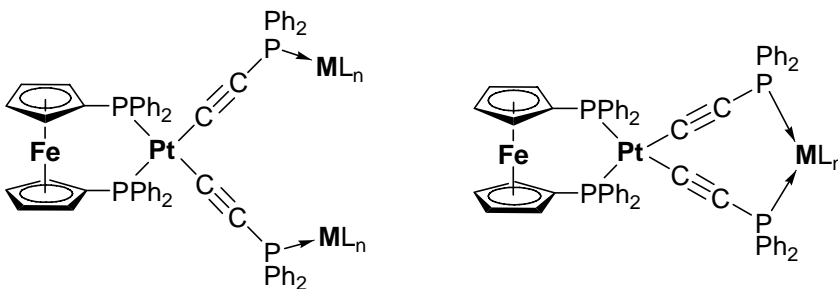


Figure 9. Complexes 97 (left) and 98 (right) [40].

The molecular solid state structures of 98a – 98c were established by single X-ray structure analyses showing that constraint $\text{Pt}(\text{C}\equiv\text{CP})_2\text{M}'$ rings ($\text{M}' = \text{Mo}, \text{Pd}, \text{Pt}$) are present. This corresponds with the observation made that 98a is a very efficient catalyst in Heck reactions showing very high activities [40].

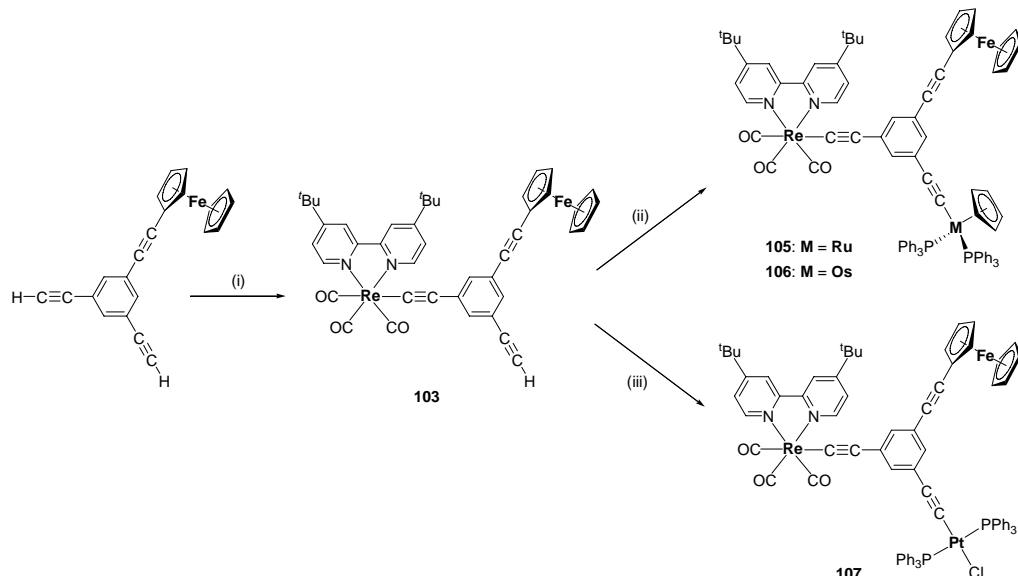
Examples of other heterotrimetallic complexes are $[(\eta^5\text{-C}_5\text{H}_4\text{terpyML}_n)\text{Fe}(\eta^5\text{-C}_5\text{H}_4\text{PPh}_2)]_2\text{M}'\text{Cl}_2$ ($\text{M}' = \text{Pd}$: 99, $\text{ML}_n = \text{Mo}(\text{CO})_4$; $\text{M}' = \text{Pt}$: 100, $\text{ML}_n = \text{Mo}(\text{CO})_4$) [61].

Another possibility to synthesize heterotrinuclear transition metal assemblies is the use of (poly)phenyleneethynes as connecting units to span different metal ions [78]. Recently, 1,3,5-triethynylbenzene was introduced as core in organometallic chemistry to prepare symmetrical and unsymmetrical bridged transition metal complexes. Due to its geometry and active coordination sites this molecule allows to extend the core into three directions by using, *e. g.* dehydrohalogenation and C-C coupling reactions. In general, there has been symmetric homo-substitution around the benzene core based on iron, iridium, chromium, gold and platinum containing metal building blocks (*i. e.*, $\text{C}_6\text{H}_3\text{-}1,3,5\text{-}(\text{Fe}(\eta^5\text{-C}_5\text{Me}_5)(\text{dppe}))_3$ (101)) [5i, 7b 79], while only less is known about unsymmetrical substituted complexes of 1,3,5-triethynylbenzene featuring, for example, *trans*- $[\text{Ru}(\text{dppm})_2\text{Cl}]$, *trans*- $[\text{Os}(\text{dppm})_2\text{Cl}]$, $[\text{Ru}(\eta^5\text{-C}_5\text{H}_5)(\text{PPh}_3)_2]$ ($\text{dppm} = \text{bis}(\text{diphenylphosphino)methane}$), and ferrocenyl end-grafted moieties [80]. These organometallic species are key molecules for the synthesis of metallo-dendrimers, megamers, and nanostructured materials [81], and play an important role in homogeneous catalysis and in many electron-transfer processes [81]. However, only two examples are known in which three different transition metal fragments are unsymmetrical arranged around the periphery of a 1,3,5-triethynylbenzene core [8c, 82].

A suitable starting material for the preparation of additional heterotrinuclear σ -alkynyl complexes is the 1,3,5-ethynylbenzene core 1-(Fc-C≡C)-3,5-(HC≡C)₂C₆H₃ (102) because alkynyl ferrocenes are known to be very robust to further reactions [8c]. Lithiation of 102 with LiN(SiMe₃)₂ followed by treatment with (bipy')(CO)₃ReCl (bipy' = 4,4'-di-*tert*-butyl-2,2'-bipyridine) afforded heterobimetallic 1-(FcC≡C)-3-[(bipy')(CO)₃ReC≡C)]-5-(HC≡C)-C₆H₃ (103). Complex 103 possesses with the free alkynyl entity a further reactive site and therefore should have a great potential to introduce a third transition metal building block and hence, forms oligomeric structures based on a 1,3,5-trisubstituted benzene core. Thus, the reaction behavior of the disubstituted iron-rhenium assembly 103 towards diverse transition metal complexes was studied.

The preferred synthetic method for the preparation of heterotrimetallic species was accomplished by the addition of the organometallic metal chloride $(\eta^5\text{-C}_5\text{H}_5)(\text{Ph}_3\text{P})_2\text{RuCl}$ to

103 in presence of the ammonium salt $[H_4N]PF_6$ and the base KO^tBu (Scheme 8). The analog osmium(II) complex could be prepared by the reaction of 103 with $(\eta^5-C_5H_5)(Ph_3P)_2OsBr$ in refluxing methanol in presence of $[H_4N]PF_6$ followed by deprotonation of the vinylidene intermediate $[1-(FcC\equiv C)-3-[(bipy')(CO)_3ReC\equiv C]-5-[(\eta^5-C_5H_5)(Ph_3P)_2Ru=C=CH]C_6H_3]^+$ (104) by addition of sodium metal. After appropriate work-up, $1-(FcC\equiv C)-3-[(bipy')(CO)_3ReC\equiv C]-5-[(\eta^5-C_5H_5)(Ph_3P)_2MC\equiv C]C_6H_3$ (105, M = Ru; 106, M = Os) could be isolated as orange powders in good yield [64]. A possibility to introduce a platinum building block exists in the reaction of 103 with $(PPh_3)_2PtCl_2$ in refluxing chloroform in presence of diethylamine (Scheme 8) [64]. To avoid the formation of the corresponding platinum bis(acetylide) complex the use of an excess of $(PPh_3)_2PtCl_2$ is required. $1-(FcC\equiv C)-3-[(bipy')(CO)_3ReC\equiv C]-5-[Cl(Ph_3P)_2PtC\equiv C]C_6H_3$ (107) could be isolated as a yellow solid.



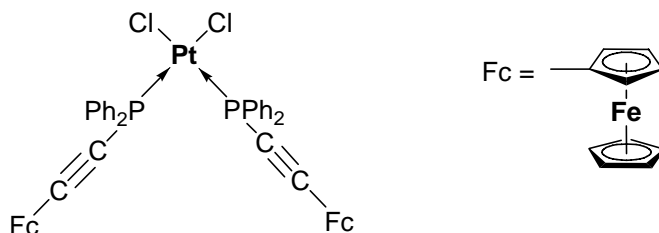
Scheme 8. Reaction chemistry of 103; synthesis of heterotrimetallic 105 – 107 ((i) 1. $LiN(Si-Me_3)_2$, toluene, $25\text{ }^\circ C$, 2 h; 2. $(bipy')_2(CO)_3ReCl$, toluene, reflux, 5 h. (ii) M = Ru: $(PPh_3)_2(\eta^5-C_5H_5)RuCl$, $[H_4N]PF_6$, KO^tBu , $CH_2Cl_2/MeOH$, 5 h; M = Os: 1. $(PPh_3)_2(\eta^5-C_5H_5)OsCl$, $[H_4N]PF_6$, MeOH, reflux, 3 h; 2. Na, MeOH, $25\text{ }^\circ C$, 1 h. (iii) *cis*- $(PPh_3)_2PtCl_2$, $CHCl_3/HNEt_2$, reflux, 3 h) [64].

The influence of connecting alkynyl-aromatic moieties has been considered through electrochemical measurements and is discussed in detail elsewhere [64].

A further series of trinuclear heterometallic complexes could be synthesized based on the 1,3,5-tri(ethynyl)benzene core as evidenced by $[1,3-\{Cl(PEt_3)_2PdC\equiv C\}_2-5-\{(Me_2bpy)(CO)_3-ReC\equiv C\}C_6H_3]$ (108) and $[1-\{Fc-C\equiv C\}-3-\{(CO)_3Cr(\eta^6-C_6H_5C\equiv C)\}-5-\{Ph_3PAuC\equiv C\}C_6H_3]$ (109) [83, 64]. For similar compounds see ref. [64].

Heterotrimetallic complexes based on the diphenylphosphino ferrocene building block are $FcPPh_2Au-C\equiv CRc$ (110), $FcPPh_2Au-C\equiv C[(\eta^6-C_6H_5)Cr(CO)_3]$ (111), and $FcPPh_2Au-C\equiv C-bipy[Mo(CO)_4]$ (112) ($Rc = (\eta^5-C_5H_4)(\eta^5-C_5H_5)Ru$) [48, 64, 84]. Redox-active multinuclear ferrocenyl ethynyl phosphanes and their palladium and platinum complexes $Ph_{3-n}P(C\equiv CFc)_n$ (113, n = 1; 114, n = 2; 115, n = 3) and $[Ph_{3-n}P(C\equiv CFc)_n]M'X_2$ ($M' = Pd$, X = Cl: 116a, n = 1; 116b, n = 2; 116c, n = 3; $M' = Pt$, X = I: 117, n = 1; $M' = Pt$, X = Cl: 118a, n = 1; 118b, n =

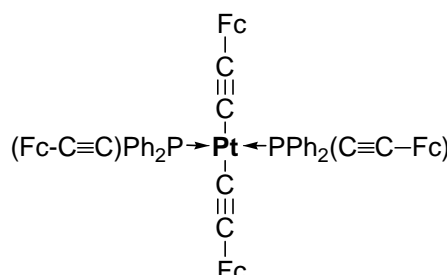
2; 118c, n = 3) were independently described by Baumgartner [85] and our group [84]. These ferrocenyl ethynyl phosphanes show an increasing number of ferrocenyl ethynyl units including the corresponding M'X₂ complexes.



118a

Solid state structures of this series of complexes were determined by X-ray structure analysis. The PdI₂-based complex shows a favourable *trans*-configuration with almost linear alkynyl ligands. The thermal behavior of some of the newly synthesized compounds indicated their utility as potential precursors for magnetic ceramic nanomaterials [85]. Although they can successfully be used as catalysts in, for example, the Heck, Suzuki and Buchwald-Hartwig reaction [84, 86]. Electrochemical investigations of the ferrocenyl ethynyl phosphane ligands and the appropriate palladium and platinum complexes, respectively, revealed that the structural motif of the ligands Ph_{3-n}P(C≡CFc)_n does not support multistep redox processes within these materials. All assemblies showed single, reversible redox processes whose potential is influenced by the substitution pattern of Ph_{3-n}P(C≡CFc)_n and the respective complex geometries [84, 85].

Reaction of 118a with two equivalents of HC≡CFc in diisopropyl amine in presence of catalytic amounts of [CuI], or treatment of 118c with LiC≡CFc in a 1:2 molar ratio produced the nonmetallic square-planar structured platinum(II) complex [(FcC≡C)Ph₂P]₂Pt(C≡CFc)₂ (119) in excellent yield [84]. In 119 a total of four ferrocene ethynyl groups are present.



119

(HETERO)TETRAMETALLIC TRANSITION METAL COMPLEXES

Organometallic π -tweezer complexes of structural type B (Scheme 1) can also successfully be used in the preparation of tetrametallic $Ti_2M_a'M_b'$ species ($M_a' = M_b'$; $M_a' \neq M_b'$; $M_a', M_b' = Cu, Ag$) [14, 87]. In this respect, halides, pseudohalides, dicarboxylates and, for example, nitrogen-based molecules have been utilized to connect tweezer-chelated copper(I) and silver(I) ions. For a detailed discussion on this topic see ref. [14b, e, 87]. The respective complexes may display metal-metal interactions, as the inorganic or organic connecting units permit rapid intramolecular electron transfer. The electrochemistry of selected complexes was studied by cyclic voltammetry. Semi-empirical calculations were additionally carried out. [14h] The results indicate a strong intramolecular interaction between the group-11 metals held in place by the organometallic bis(alkynyl) π -tweezers.

Other tetrametallic $MM'M_2''$ compounds are $\{[M](\mu-\sigma,\pi-C\equiv CFc)_2\}M'X$ ($[M] = (\eta^5-C_5H_4SiMe_3)_2Ti$: 120a, $M'X = Pd(PPh_3)$; 120b, $M'X = Ni(CO)$; 120c, $M'X = CuBr$; 120d, $M'X = CuCl$; 120e, $M'X = CuOTf$; 120f, $M'X = CuCl_2$; 120g, $M'X = ZnCl_2$; 120h, $M'X = ZnBr_2$; 120i, $M'X = AgCl$; 120j, $M'X = AgBF_4$; $[M] = (bipy)Pt$: 121a, $M'X = CuBr$; 121b, $M'X = CuOTf$; 121c, $M'X = CuBF_4$; 121d, $M'X = AgNO_3$; 121e, $M'X = AgClO_4$; 121f, $M'X = AgO_2CCF_3$; $[M] = [(Ph_2PCH_2PPh_2)_2Ru$: 122, $M'X = CuI$) [14, 61]. They are impressive examples of mixed early-late transition metal complexes in which reducible and oxidizable groups are present in close proximity to each other. Their electrochemical behavior is discussed in detail in refs. [14] and [61].

Further heterotetrametallic compounds are 125a and 125b (Figure 10) which are accessible in a two-step synthesis procedure including the Sonogashira cross-coupling reaction of 1,1'-bis(ethynyl) biferrocene (123) with I-1-NCN-4-Br and the oxidative addition of (1,1'-Br-4-NCN-C≡C)bfc (bfc = biferrocene) (124) to $[Pd_2(dbu)_3]$ and $[Pt(tol)_2(SEt_2)]_2$, respectively, [88].

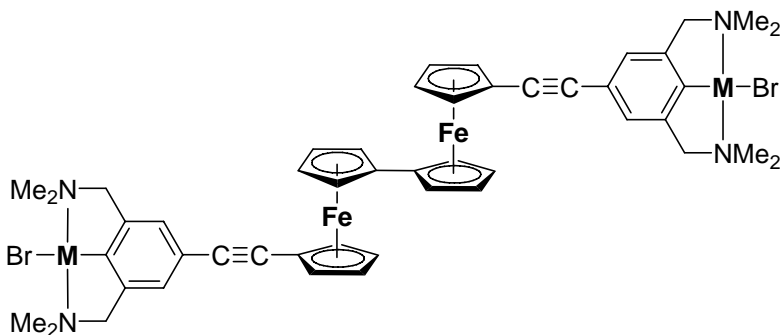


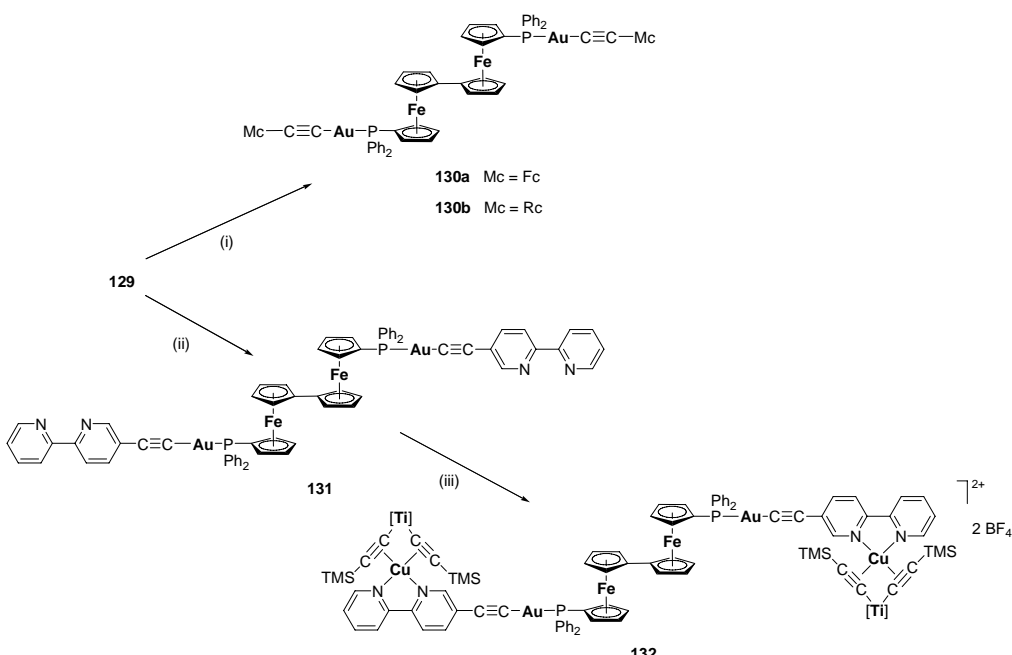
Figure 10. Biferrocene-based molecules 125a ($M = Pd$) and 125b ($M = Pt$) [88].

Cyclic voltammetric measurements of 125a and 125b show that the ferrocene moieties can be oxidized independently. The difference of the potentials of the Fe(II)/Fe(III) redox couples is 300 mV and is not affected by the NCN transition metal pincer [88].

Similar results are obtained for the biferrocene-based complexes $bfc(PPh_2ML_n)_2$ (127a, $ML_n = Cr(CO)_5$; 127b, $ML_n = Mo(CO)_5$; 127c, $ML_n = W(CO)_5$; 128, $ML_n = (C_6H_4-1-iPr-4-Me)RuCl_2$; 129, $ML_n = AuCl$), a series of complexes which can be prepared by the reaction of

bfc(PPh_2)₂ (126) with two equivalents of the ML_n sources $\text{M}(\text{CO})_5(\text{thf})$ ($\text{M} = \text{Cr, Mo, W}$), $[(\text{C}_6\text{H}_4-1^{\prime}\text{-Pr-4-Me})\text{RuCl}_2]_2$, or (tht) AuCl [89].

Tetrametallic Fe_2Au_2 129 affords with $\text{HC}\equiv\text{CMc}$ ($\text{Mc} = \text{Fc, Rc}$) in presence of $[\text{CuI}]$ and diethylamine in tetrahydrofuran at room temperature bfc($\text{PPh}_2\text{Au-C}\equiv\text{C-Mc}$)₂ (130a, $\text{Mc} = \text{Fc}$; 130b, $\text{Mc} = \text{Rc}$) (Scheme 9, route (i)) [90]. Under identical reaction conditions 129 reacted with a 20 % excess of 5-ethynyl-2,2'-bipyridine to give bfc($\text{PPh}_2\text{Au-C}\equiv\text{C-bipy}$)₂ (131) (Scheme 9, route (ii)) which contains with the bipy ligand a further N-ligating unit and hence, was reacted with stoichiometric amounts of the heterobimetallic early-late tweezer molecule $\{[\text{Ti}](\mu-\sigma,\pi-\text{C}\equiv\text{CSiMe}_3)_2\}\text{Cu}(\text{N}\equiv\text{CMe})\text{PF}_6$ (Scheme 9, route (iii)). On replacement of the weakly-bonded acetonitrile in the latter molecule by bipy octametallic 132 is formed which can be isolated after appropriate work-up in acceptable yield [90]. In 132 the bfc unit links the two heterotrimetallic Au-C≡C-bipy $\{[\text{Ti}](\mu-\sigma,\pi-\text{C}\equiv\text{CSiMe}_3)_2\}\text{Cu}^+$ building blocks and hence, represents a further example of a so far only barely discussed class of heterotetrametallic MM'M''M''' complexes. A detailed investigation of possible photophysical properties and electronic interactions between the appropriate metal atoms of 132 is in progress in our laboratory.



Scheme 9. Synthesis of heteromultimetallic 130, 131 and 132. (i) 1. (tht) AuCl ; 2. $\text{HC}\equiv\text{CMc}$, $[\text{CuI}]/\text{NEt}_3$. (ii) 1. (tht) AuCl ; 2. $\text{HC}\equiv\text{Cbipy}$, $[\text{CuI}]/\text{NEt}_3$. (iii) $\{[\text{Ti}]\text{C}\equiv\text{CSiMe}_3\}_2\text{Cu}(\text{N}\equiv\text{CMe})\text{PF}_6$ [90].

The development of polynuclear ruthenium(II) terpyridine molecular wire molecules based on the biferrrocene building block bfc were recently reported by Dong *et al.* [91]. The multinuclear supramolecules assembled from 1',1'''-bis(terpyridyl) biferrrocene redox-active sub-units attached to Ru(II) ions were prepared by, for example, the reaction of bfc-terpy (133) and bfc(terpy)₂ (134), respectively, with LRuCl_3 ($\text{L} = \text{terpy, fc-terpy}$), $\text{LRuCl}_2(\text{dmso})$ ($\text{L} = \text{bfc-terpy}$, dmso = dimethylsulfoxide) or $\text{RuCl}_2(\text{dmso})$ in the appropriate ratios as outlined in Figure 11 [91]. Complexes $\text{Ru}(\text{bfc-terpy})(\text{dmso})\text{Cl}_2$ (135), $[\text{Ru}(\text{terpy})(\text{bfc-terpy})](\text{PF}_6)_2$

(136), $[\text{Ru}(\text{bifc-terpy})_2](\text{PF}_6)_4$ (137), $[\text{bifc(terpy)}_2(\text{Ru(terpy)})_2](\text{PF}_6)_4$ (138), $[\text{bifc-terpy}_2(\text{Ru(terpy-Fc)})_2](\text{PF}_6)_4$ (139), $[\text{bifc(terpy)}_2(\text{Ru(terpy-bifc)})_2](\text{PF}_6)_4$ (140), $[(\text{Ru(terpy)})_2(\text{bifc(terpy)})_2](\text{PF}_6)_6$ (141), and $[(\text{Ru(terpy-Fc)})_2(\text{bifc(terpy)})_2](\text{PF}_6)_6$ (142) are thereby formed in good yield. The cyclic voltammograms of the ruthenium(II) coordinated bifc-terpy and fc-terpy species are dominated by the $\text{Ru}^{2+}/\text{Ru}^{3+}$ ($E_{1/2} \approx 1.35$ V), $\text{Fe}^{2+}/\text{Fe}^{3+}$ ($E_{1/2} \approx 0.4 - 0.9$ V), and the terpy (terpy⁻/terpy²⁻) redox couples ($E_{1/2} \approx -1.2 - -1.4$ V). The appreciable variations detected in the $\text{Fe}^{2+}/\text{Fe}^{3+}$ oxidation potentials indicated that this is an interaction between the respective spacer and the Ru²⁺ metal ions [91].

On the coordination of the 1,1''-bis(terpyridyl) biferrocene 133 to a ruthenium(II) ion there is a red-shifted and more intense ${}^1[(d(\pi)_{\text{Fe}})^6] \rightarrow {}^1[(d(\pi)_{\text{Fe}})^5(\pi^*_{\text{terpy}}{}^{\text{Ru}}_1)]$ transition found in the visible region ($[\text{Ru(terpy)}_2]^{2+}$, $[\text{Ru(terpy)(bifc-terpy)}]^{2+}$: ca. 510 nm; polynuclear ruthenium(II) 1,1''-bis(terpyridyl) biferrocenes: ca. 570 nm) [91]. This shift indicates that there is a qualitative electronic coupling within the appropriate assemblies. The coordination of Ru(II) ions lowers the energy of the π^*_{terpy} orbitals giving a more red-shifted transition.

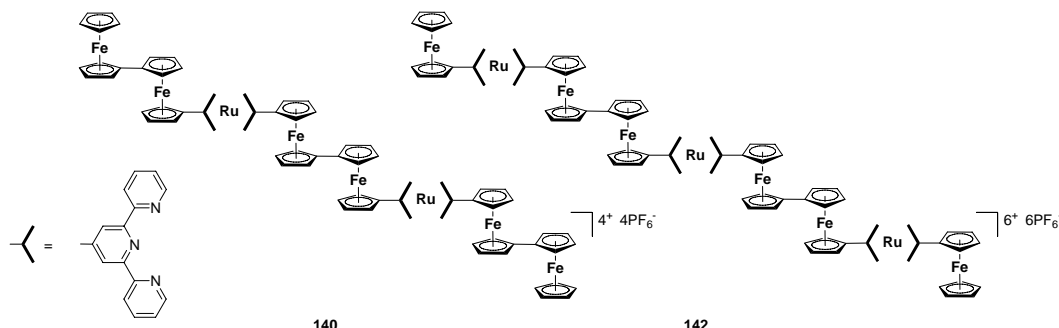


Figure 11. Complexes 140 (left) and 142 (right) [91].

Further examples of heterotetrametallic MM'M''M''' complexes with four different metals, based on organometallic π -tweezer units, can be obtained by joining heterobimetallic titanium-copper or titanium-silver tweezers with Fe-Pt or Fe-Au containing molecules (Figure 12). Thus, $\text{HC}\equiv\text{C}-\{\text{Pt}\}-\text{C}\equiv\text{C}-\text{Fc}$ (143) ($\{\text{Pt}\} = \text{Pt}(\text{C}_6\text{H}_2(\text{CH}_2\text{NMe}_2-2,6)_2)$) gives with $\{\text{[Ti]}(\mu-\sigma,\pi-\text{C}\equiv\text{C}'\text{Bu})_2\}\text{CuCH}_3$ on loss of CH_4 complex 144 [51], while $\text{FcPPPh}_2\text{Au-C}\equiv\text{C-bipy}$ affords with $\{\text{[Ti]}(\mu-\sigma,\pi-\text{C}\equiv\text{CSiMe}_3)_2\}\text{M}'\text{X}$ ($\text{M}'\text{X} = \text{Cu}(\text{N}\equiv\text{CMe})\text{PF}_6$, AgClO_4) tetrametallic 145 [92].

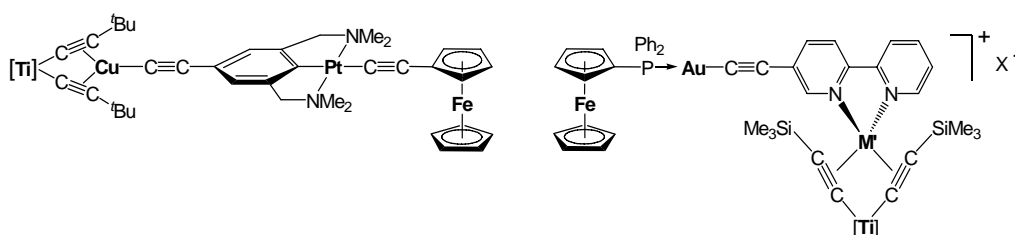
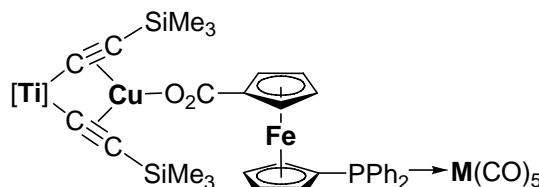


Figure 12. Complexes 144 (left) and 145 (right; 145a: $\text{M}' = \text{Cu}$, $\text{X} = \text{PF}_6^-$; 145b: $\text{M}' = \text{Ag}$, $\text{X} = \text{ClO}_4^-$) [51, 92].

Complexes 144 and 145 represent the first examples of heterotetrametallic transition metal complexes in which early and late metals are connected by π -conjugated organic bridging units. A striking feature of 144 is that all metals possess different coordination spheres: titanium shows a pseudo-tetrahedral environment, copper possesses a planar surrounding, platinum is square-planar coordinated and iron is part of a sandwich structure [51].

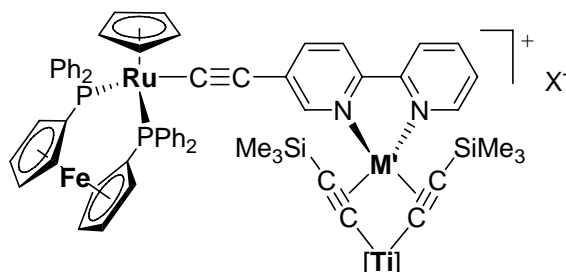
Based on the organometallic π -tweezer moiety $\{[\text{Ti}](\mu-\sigma,\pi\text{-C}\equiv\text{CSiMe}_3)_2\}\text{Cu}^+$ another heterotetrametallic species could be isolated from the reaction of $\{[\text{Ti}](\mu-\sigma,\pi\text{-C}\equiv\text{CSiMe}_3)_2\}\text{-CuMe}$ with $(\eta^5\text{-C}_5\text{H}_4\text{CO}_2\text{H})\text{Fe}(\eta^5\text{-C}_5\text{H}_4\text{PPh}_2)\text{Mo}(\text{CO})_5$ (146) [93]. The latter molecule is accessible by treatment of $\text{HO}_2\text{C-fc-PPh}_2$ (147) ($\text{fc} = \text{Fe}(\eta^5\text{-C}_5\text{H}_4)_2$) with $\text{M}(\text{CO})_5(\text{thf})$ [93]. The respective Ti-Cu-Fe-M complexes 148a - 148c (148a, $\text{M} = \text{Cr}$; 148b, $\text{M} = \text{Mo}$; 148c, $\text{M} = \text{W}$) are, however, very unstable molecules both in the solid state and in solution and hence, can only be handled at low temperature without significant decomposition [93].



148

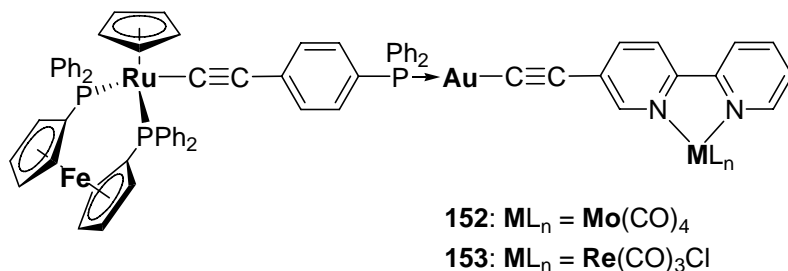
Isostructural systems to 148 can be obtained for the higher homologue of copper by combining $[\text{Ti}](\text{C}\equiv\text{CSiMe}_3)_2$ with equimolar amounts of the silver(I) salt $[\text{AgO}_2\text{C-fc-PPh}_2]$ to give $\{[\text{Ti}](\mu-\sigma,\pi\text{-C}\equiv\text{CSiMe}_3)_2\}\text{AgO}_2\text{C-fc-PPh}_2$ (149) [93]. Addition of $\text{M}(\text{CO})_5(\text{thf})$ to 149 produced the Ti-Ag-Fe-M complexes $\{[\text{Ti}](\mu-\sigma,\pi\text{-C}\equiv\text{CSiMe}_3)_2\}\text{AgO}_2\text{C-fc-PPh}_2\text{M}(\text{CO})_5$ (150a, $\text{M} = \text{Cr}$; 150b, $\text{M} = \text{Mo}$; 150c, $\text{M} = \text{W}$), which are, when compared with 148a - 148c, even more reactive. They readily decompose in solution and on exposure to sun light on formation of metallic silver, the free π -tweezer $[\text{Ti}](\text{C}\equiv\text{CSiMe}_3)_2$ and other unidentified materials.

When the FcPPh_2Au entity in 145 (Figure 12) is replaced by the $(\eta^2\text{-dppf})(\eta^5\text{-C}_5\text{H}_5)\text{Ru}$ building block related tetranuclear complexes of type $[(\eta^2\text{-dppf})(\eta^5\text{-C}_5\text{H}_5)\text{Ru}-\text{C}\equiv\text{C-bipy}\{[\text{Ti}](\mu-\sigma,\pi\text{-C}\equiv\text{CSiMe}_3)_2\}\text{M}']\text{X}$ (151a: $\text{M}' = \text{Cu}$, $\text{X} = \text{PF}_6^-$; 151b: $\text{M}' = \text{Ag}$, $\text{X} = \text{ClO}_4^-$) are accessible [64].



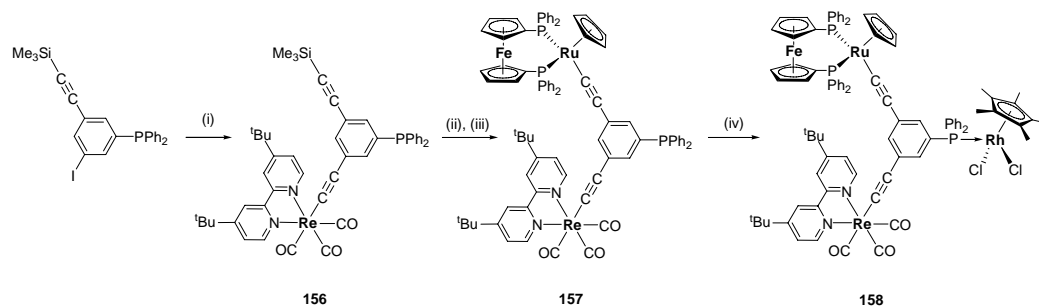
151

Extending the distance between the remote Fe-Ru and Ti-Cu fragments in 151 by an $\text{C}\equiv\text{C}-1-\text{C}_6\text{H}_4-4-\text{PPh}_2-\text{Au}$ moiety opens the possibility to create stable heteropentametallic transition metal complexes (see below). When the organometallic π -tweezer entity (vide supra) is substituted by mononuclear transition metal building blocks, such as $\text{Mo}(\text{CO})_4$ and $\text{Re}(\text{CO})_3\text{Cl}$, then tetrametallic $[(\eta^2\text{-dppf})(\eta^5\text{-C}_5\text{H}_5)\text{Ru}(\text{C}\equiv\text{C})-1-(\text{C}_6\text{H}_4)-4-\text{PPh}_2-\text{Au}-\text{C}\equiv\text{C}-\text{bipy}(\text{ML}_n)]$ (152, $\text{ML}_n = \text{Mo}(\text{CO})_4$; 153, $\text{ML}_n = \text{Re}(\text{CO})_3\text{Cl}$) is formed in which four different metal atoms are bridged by organic carbon-rich connecting units [64].



Compounds of the latter type are formed by treatment of $[(\eta^2\text{-dppf})(\eta^5\text{-C}_5\text{H}_5)\text{Ru}(\text{C}\equiv\text{C})-1-(\text{C}_6\text{H}_4)-4-\text{PPh}_2-\text{AuCl}]$ (154) with $\text{HC}\equiv\text{C}-\text{bipy}(\text{Re}(\text{CO})_3\text{Cl})$ (synthesis of 152) or combining $(\eta^2\text{-dppf})(\eta^5\text{-C}_5\text{H}_5)\text{Ru}(\text{C}\equiv\text{C})-1-(\text{C}_6\text{H}_4)-4-\text{PPh}_2-\text{Au}-\text{C}\equiv\text{C}-\text{bipy}$ (155) with $(\text{nbd})\text{Mo}(\text{CO})_4$ (synthesis of 153) [64].

An elegant approach to a novel Fe-Ru-Re-Rh tetrametallic complex, based on the 1,3-diethynyl-5-diphenylphosphino benzene core, is given by using a consecutive reaction methodology as presented in Scheme 10 including, dehydrohalogenation and carbon-carbon coupling reactions [64].



Scheme 10. Synthesis of heterotetrametallic 158 *via* the formation of 156 and 157, ((i) (bipy')($\text{CO})_3\text{ReC}\equiv\text{CH}$, $[(\text{PPh}_3)_2\text{PdCl}_2]$, $[\text{CuI}]$, HN^+Pr_2 , reflux, 5 h; (ii) $[^7\text{Bu}_4\text{N}]F$, thf , 25°C , 1 h; (iii) (dppf)($\eta^5\text{-C}_5\text{H}_5$) RuCl , $[\text{H}_4\text{N}]PF_6$, KO^+Bu , $\text{CH}_2\text{Cl}_2/\text{MeOH}$, 25°C , 3 h; (iv) $[(\eta^5\text{-C}_5\text{Me}_5)\text{RhCl}_2]$, CH_2Cl_2 , 25°C , 1 h) [64].

Exemplary, the molecular solid state structure of 158 was solved by X-ray structure analysis, thus confirming the structural assignment made from spectroscopic data [64]. An ORTEP drawing of this species is depicted in Figure 13.

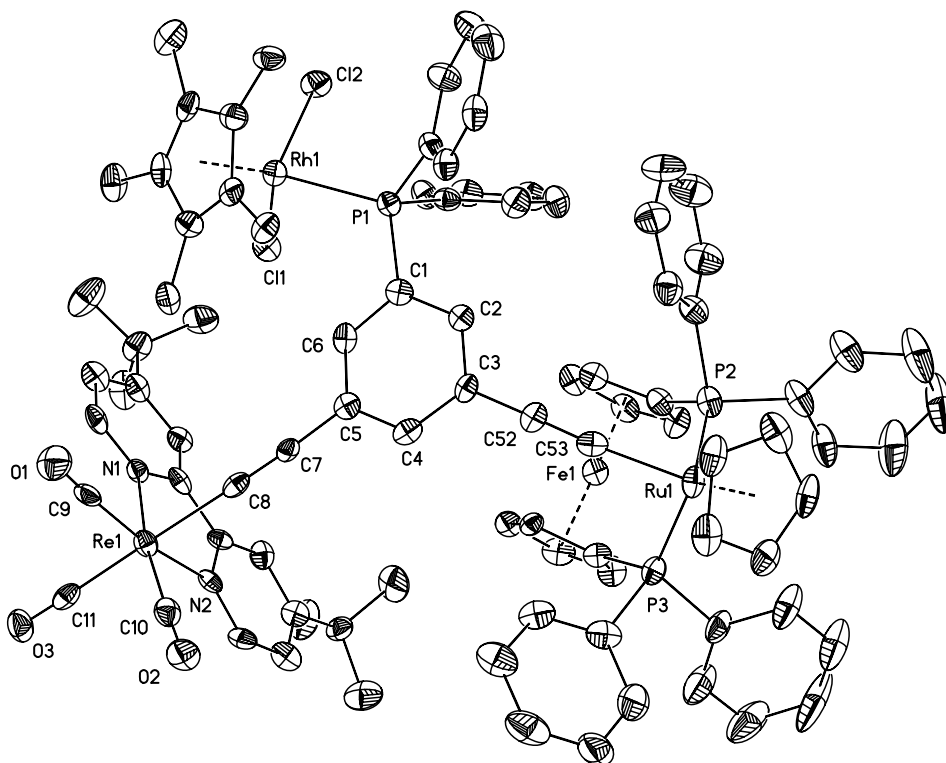
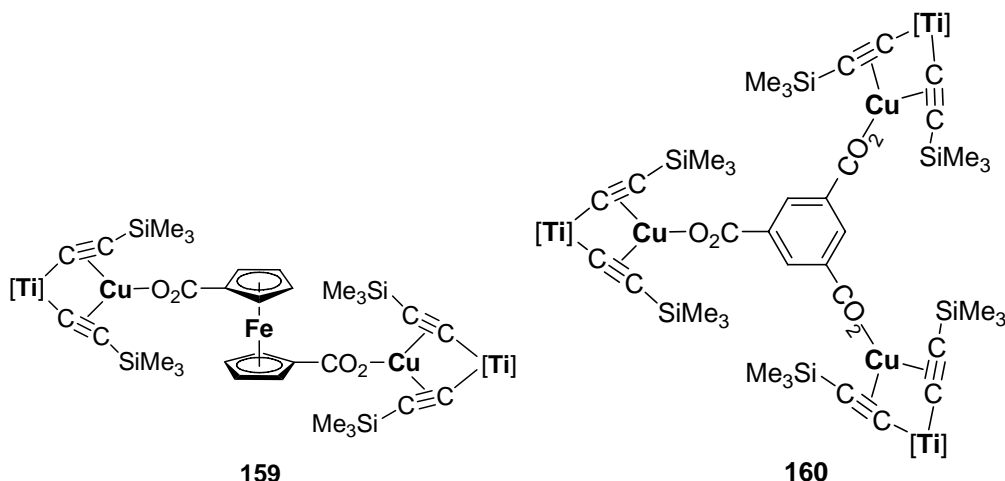


Figure 13. ORTEP drawing of 158. Thermal ellipsoids are shown at the 50% probability level. For selected bond lengths (\AA) and angles ($^\circ$) see ref. [64].

(HETERO)PENTA- TO (HETERO)UNDECAMETALLIC TRANSITION METAL COMPLEXES

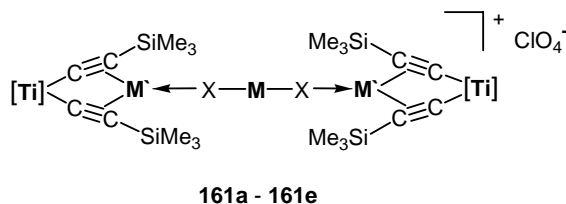
Further examples of the modular “Tinkertoy” approach includes the synthesis of (hetero)penta- to nona-metallic complexes. An important family of “Tinkertoys” are halide-, pseudohalide-, cyanoacetylide-, heterocyclic- and/or di- and tricarboxylic acid-functionalized transition metal building blocks.

There are mainly three methods which can successfully be applied for the preparation of the title compounds. The first synthesis protocol includes the reaction of $\{[\text{Ti}](\mu-\sigma,\pi\text{-C}\equiv\text{C-R})_2\}\text{CuMe}$ with diverse organic and organometallic di- and tricarboxylic acids, owing to the instability of the alkyl-copper system, and is based on the preparation of 159 and 160 [14m, 94].

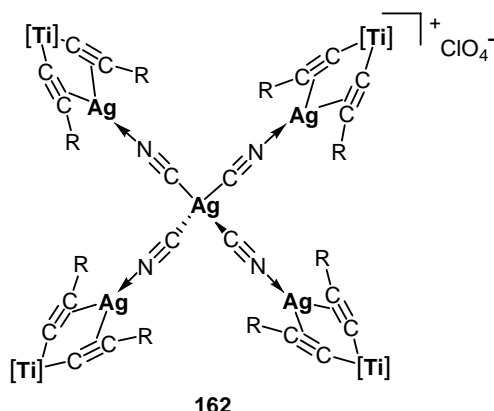


In the latter molecules organometallic π -tweezer units are connected by a 1,1'-ferrocenyl-dicarboxylate (159) or a 1,3,5-benzenetricarboxylic entity (160). However, electrochemical studies showed that the connecting carboxylates act as an impedance rather than a transmitter [14m, 94].

The 2nd and hence, more straightforward synthetic route to (hetero)multimetalloc π -tweezer-based complexes is the reaction of $\{[Ti](\mu-\sigma,\pi\text{-}C\equiv CSiMe_3)_2\}M'X$ ($M' = Cu, Ag$; $X = ClO_4, OTf$) with the metal salts $[MX_2]^-$ ($M = Cu, Ag, Au$; $X = CN, OCN$) (synthesis of 161a - 161e) or $[Ag(C\equiv N)_4]^{3-}$ (synthesis of 162) in the ratios of 2:1 and 4:1, respectively [14h, gg, 52, 56, 87, 95].



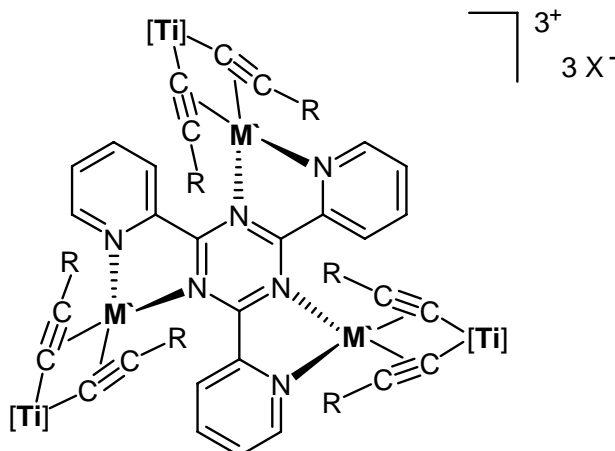
161a - 161e



162

Complexes 161a – 161e (161a, M = M' = Cu, X = C≡N; 161b, M = M' = Ag, X = C≡N; 161c, M = M' = Ag, X = NCO; 161d, M = Ag, M' = Cu, X = C≡N; 161e, M = Au, M' = Cu, X = C≡N) are linear structured and contain the features typical for 1-dimensional molecular wire molecules. Complex 162 is one of the outstanding examples of a cross-shaped molecule in which four titanium-silver tweezer parts are linked by a $[\text{Ag}(\text{C}\equiv\text{N})_4]^{3-}$ core. In 162 each cyanide is datively-bound to a silver(I) center of an individual π -tweezer fragment. While the inner silver atom possesses a tetrahedral environment, the outer silver(I) ions are planar coordinated and hence, possess coordination number 3 [95].

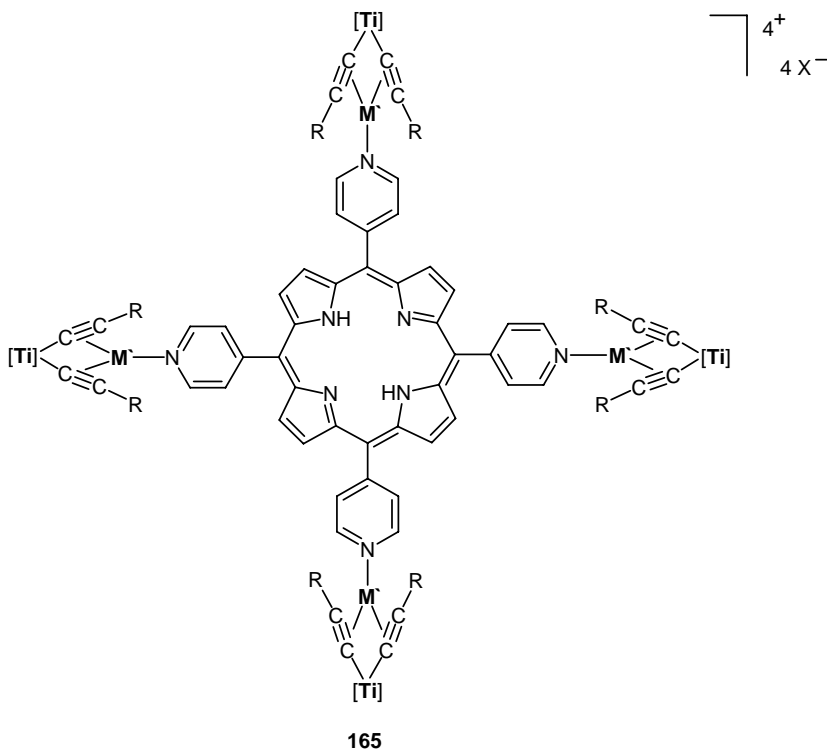
Multiple π -tweezers can also be linked together by bipyridyl, 2,4,6-tri(2-pyridyl)-1,3,5-triazine (tpt) or pyridyl-functionalized porphyrin connecting units [96, 97]. With tpt, complexes 163a – 163d (M' = Cu, X = PF₆: 163a, R = Ph; 163b, R = SiMe₃; M' = Ag, X = ClO₄: 163c, R = Ph; 163d, R = SiMe₃) are formed, when $\{[\text{Ti}](\mu-\sigma,\pi\text{-C}\equiv\text{CR})_2\}\text{M}'\text{X}$ is reacted with tpt in the stoichiometry of 3:1.



163a - 163d

In a similar manner, heptametallic FeAu₂Cu₂Ti₂ and FeAu₂Ag₂Ti₂ molecules Fe(η^5 -C₅H₄PPh₂AuC≡Cbipy-M'{(μ - σ , π -C≡CSiMe₃)₂[Ti]})₂ (164a, M' = Cu; 164b, M' = Ag) are accessible by treatment of Fe(η^5 -C₅H₄PPh₂AuC≡Cbipy)₂ with two equivalents of $\{[\text{Ti}](\mu-\sigma,\pi\text{-C}\equiv\text{CSiMe}_3)_2\}\text{M}'\text{X}$ (M'X = Cu(N≡CMe)PF₆, AgClO₄) [64].

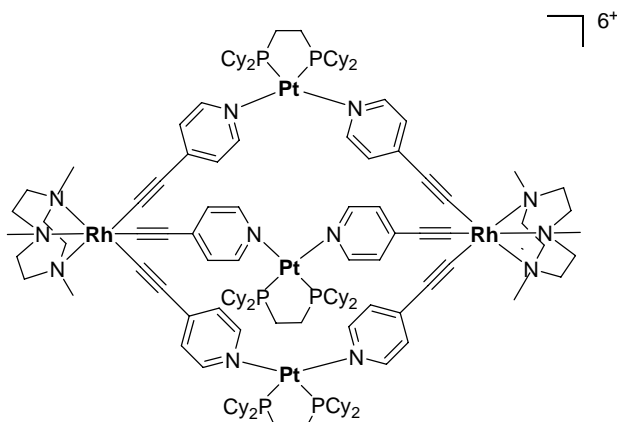
Pyridine-functionalized porphyrins allow the linkage of four organometallic π -tweezers as shown in 165a (M' = Cu) and 165b (M' = Ag). However, these molecules show a tendency to decompose in solution with formation of metallic copper or silver along with [Ti](C≡C-SiMe₃)₂ and the free porphyrin [97].



The reaction chemistry of 165a and 165b towards diverse transition and main-group element salts is in progress in our laboratories.

Ferrocene-based multimetallic species of type $M_xM'_y$ are $[Ph((\eta^5-C_5H_5)Fe(\eta^5-C_5H_4)_2P)AuC\equiv CAu[P((\eta^5-C_5H_5)Fe(\eta^5-C_5H_4))_2Ph]$ (166) [98], $(FcC\equiv C-C\equiv CFc)_2Os_2(CO)_6$ (167) [32c] and $(FcC\equiv C)_2Os_3(CO)_9$ (168) [32c].

As an instance, the pentametallic complex 171, a bipyramidal supramolecular cage based on rhodium and platinum atoms must be mentioned [99]. This compound is accessible by the consecutive reaction of 4-ethynyl-pyridine with $'BuLi$ followed by its addition to $(Me_3tacn)RhCl_3$ ($Me_3tacn = N,N',N''$ -trimethyl-1,4,7-triazacyclononane) giving the facial octahedral complex $(Me_3tacn)Rh(C\equiv Cpy)$ (169), condensation of which with the square-planar species *cis*-(dcpe) $Pt(NO_3)_2$ (170) (dcpe = 1,2-bis(dicyclohexylphosphino)ethane) results in a self-assembled trigonal-bipyramidal cage with Rh(III) and Pt(II) ions occupying the vertices. Multinuclear NMR analyses and single X-ray structure determination of 171 are consistent with the proposed structure.

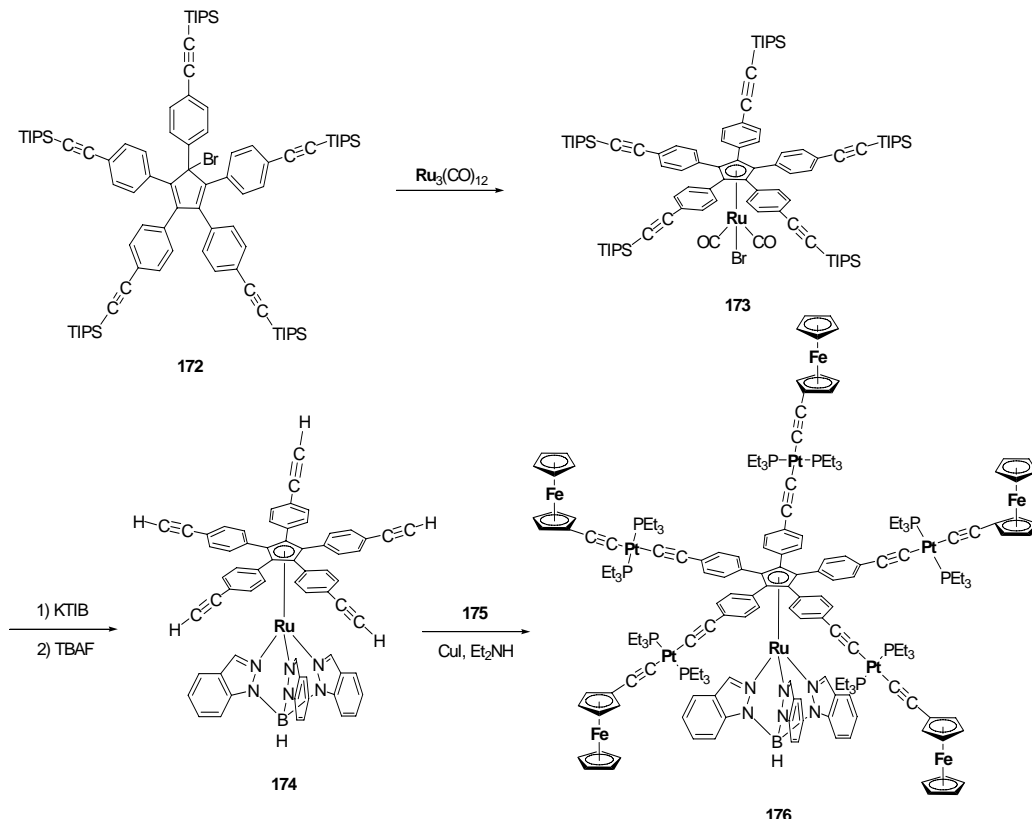


171

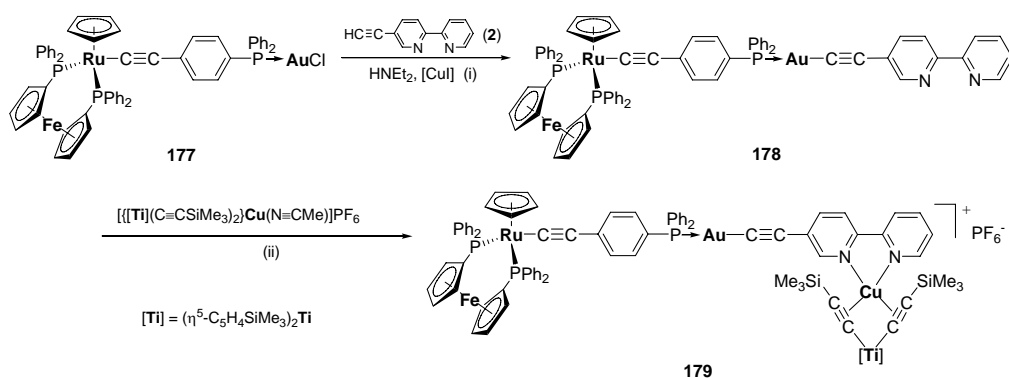
A star-shaped ruthenium complex (176) with five ferrocenyl end-grafted arms bridged by the *trans*- platinum fragments $\text{Pt}(\text{PEt}_3)_2$ represents an example of a undecanuclear $\text{Fe}_5\text{Pt}_5\text{Ru}$ assembly containing three different metals [100]. This complex can be synthesized by starting from the novel heteropolytopic penta(4-ethynyl)cyclopentadiene $\text{C}_5(\text{C}_6\text{H}_4\text{-4-C}\equiv\text{C-TIPS})_5(\text{Br})$ (TIPS = tri(*iso*-propyl)silyl) (172) (Scheme 11). Ruthenium was subsequently conducted to 172 affording 173 (Scheme 11). Compound 173 reacts with potassium tris(indazolyl)borate (= KTIB) and than with tetra-butylammonium fluoride (= TBAF) to yield 174, bearing five free $\text{HC}\equiv\text{C}$ terminal groups. These end-grafted units are available for coordination and hence, 174 was reacted with the ethynyl-ferrocenyl platinum fragment $\text{Fc-C}\equiv\text{C-Pt}(\text{PEt}_3)_2\text{Cl}$ (175) in presence of $[\text{CuI}]$ in Et_2NH as solvent (Scheme 11). In a quintuple coupling of 175 with 174, complex 176 was isolated. Oxidation of the five centers in 176 occurs simultaneously at a potential of 0.31 V followed by the oxidation of the Ru(II) ion at 0.60 V. However, the platinum atoms were not oxidized within the potential window of -1.8 to +1.5 V used. Finally, after performing a partial oxidation of the Fc units, no intervalence transition between $\text{Fe}^{2+}/\text{Fe}^{3+}$ was observed, thus confirming the absence of electronic communication between the electro-active ferrocenes [100].

Even the synthesis of heteropenta- and heterohexametallic complexes with the metals rhenium, iron, ruthenium, gold, copper and titanium is possible. Complex $[(\eta^2\text{-dppf})(\eta^5\text{-C}_5\text{H}_5)\text{RuC}\equiv\text{C-1-C}_6\text{H}_4\text{-4-PPh}_2\text{-Au-C}\equiv\text{C-bipy}\{\text{[Ti]}(\mu\text{-}\sigma,\pi\text{-C}\equiv\text{CSiMe}_3)_2\}\text{Cu}]\text{PF}_6$ (179) is accessible in a consecutive reaction sequence by using $(\eta^2\text{-dppf})(\eta^5\text{-C}_5\text{H}_5)\text{RuC}\equiv\text{C-1-C}_6\text{H}_4\text{-4-PPh}_2\text{-AuCl}$ (177) as key starting material [64, 101]. The newly synthesized compounds and the overall synthetic strategy employed are shown in Scheme 12. Compound 177 reacts with 5-ethynyl-2,2'-bipyridine, whereby this compound is added in a 20 % excess, in presence of $[\text{CuI}]$ and diethylamine to give $(\eta^2\text{-dppf})(\eta^5\text{-C}_5\text{H}_5)\text{RuC}\equiv\text{C-1-C}_6\text{H}_4\text{-4-PPh}_2\text{-Au-C}\equiv\text{C-bipy}$ (178) (Scheme 12, route (i)). This molecule contains with the 2,2'-bipyridine ligand a N-ligating unit and hence, was reacted with stoichiometric amounts of the heterobimetallic early-late tweezer molecule $\{\{\text{[Ti]}(\mu\text{-}\sigma,\pi\text{-C}\equiv\text{CSiMe}_3)_2\}\text{Cu}(\text{N}\equiv\text{CMe})\}\text{PF}_6$ (Scheme 12, route (ii)). On replacement of the copper-bonded acetonitrile in the organometallic π -tweezer part by bipyridine, complex 179 is formed which could be isolated after appropriate work-up in 92 % yield. Complex 179 is surprisingly a very stable species in which five different transition

metals are brought in close proximity to each other by connecting $C_5H_4PPh_2$, $C\equiv C$, C_6H_4 , and bipyridine units.



Scheme 11. Consecutive synthesis of 176 from 172 [100].



Scheme 12. Synthesis of trimetallic 178 and pentametallic 179 (route (i): tetrahydrofuran, 25 °C, 3 h; (ii): tetrahydrofuran, 25 °C, 2 h) [64, 101].

The formation of heteropentanuclear 179 was evidenced from spectroscopic studies and ESI-TOF mass spectrometric investigations. The ESI-TOF spectrum shows a prominent ion peak at m/z 1963.4 (100 %) corresponding to $[179\text{-}PF_6]^+$. Moreover, comparison of the

measured isotope pattern of 179 with the calculated one confirms the elemental composition and charge state (Figure 13).

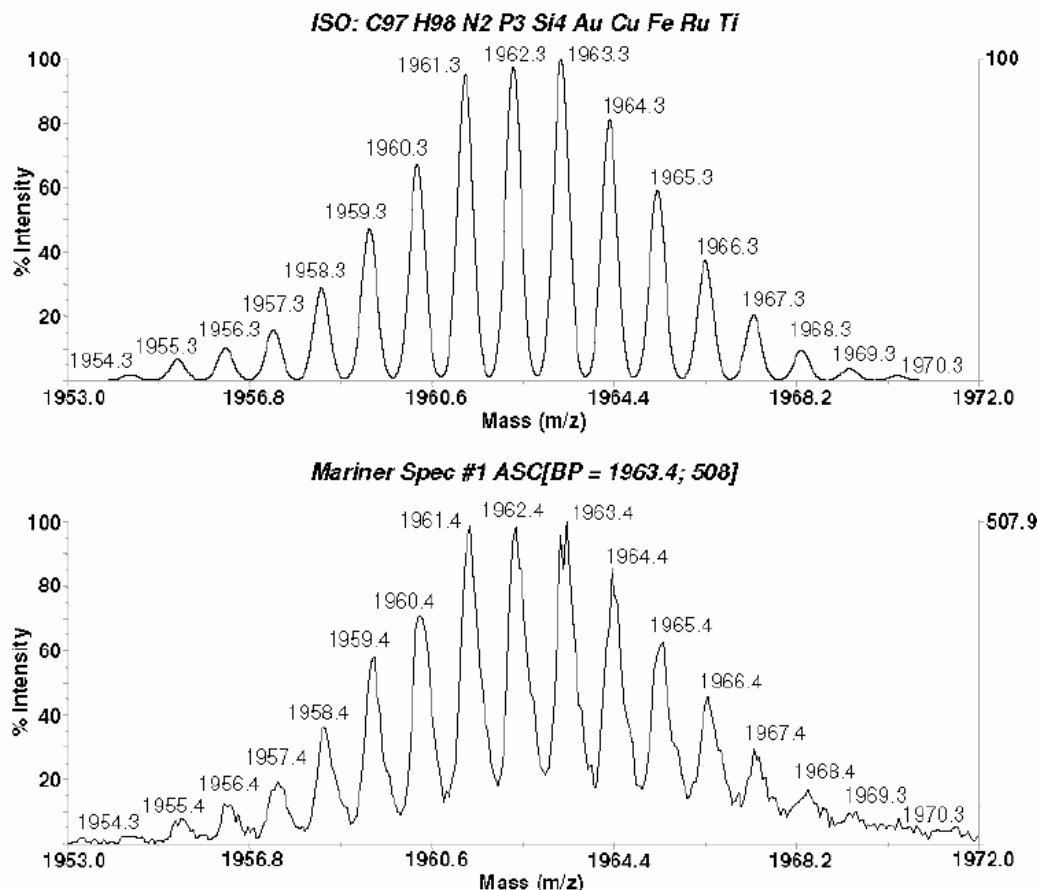
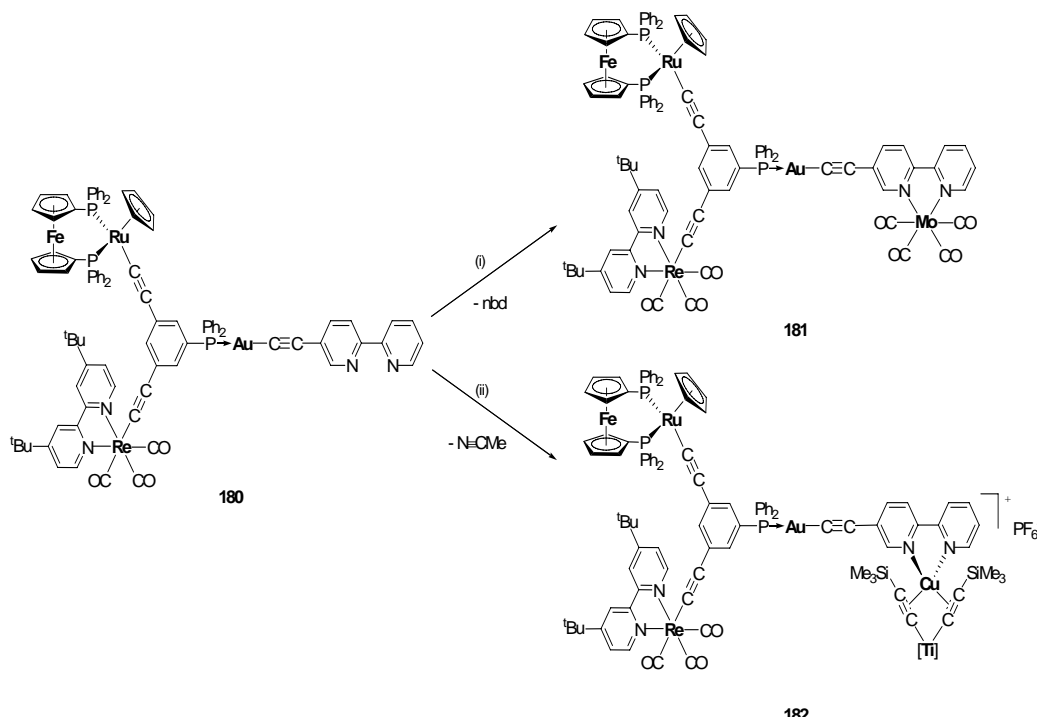


Figure 13. Comparison of the measured (bottom) and calculated (top) isotope pattern of the ion peak $[179\text{-PF}_6]^+$ in the ESI-MS spectrum of 179 [64, 101].

The bipyridine building block in $[(\eta^2\text{-dppf})(\eta^5\text{-C}_5\text{H}_5)\text{RuC}\equiv\text{C}]\text{-1-[}(4,4'\text{-}^1\text{Bu}_2\text{-}2,2'\text{-bipy})(\text{CO})_3\text{ReC}\equiv\text{C}]\text{-5-[PPh}_2\text{AuC}\equiv\text{C}\text{bipy}]\text{C}_6\text{H}_3$ (180) as bidentate binding site allows the preparation of Fe-Ru-Re-Au-Mo- and even Fe-Ru-Re-Au-Cu-Ti-based assemblies as outlined in Scheme 13. Addition of (nbd) $\text{Mo}(\text{CO})_4$ yields heteropentanuclear 181 upon replacement of nbd by bipy. Heterohexanuclear 182 is formed in a straightforward manner, when 180 is treated with $\{[\text{Ti}](\mu\text{-}\sigma,\pi\text{-C}\equiv\text{CSiMe}_3)_2\}\text{Cu}(\text{N}\equiv\text{CMe})\text{PF}_6$ [64]. Within this reaction the coordination number at copper is changed from three (planar) to four (tetrahedral).



Scheme 13. Synthesis of heteropentametallic 181 and heterohexanuclear 182 [(i) (nbd)Mo(CO)₄, dichloromethane, tetrahydrofuran, 25 °C, 8 h; (ii) {[Ti](C≡CSiMe₃)₂Cu(N≡CMe)]PF₆

The synthesis protocol developed to prepare heteromultinuclear 181 and 182 is directed to the use of modular shaped organometallic building blocks (vide supra) [64]. This allowed for the first time the synthesis of such unique complexes in which acetylenic and aromatic groups are connecting the different metal atoms.

The reports on the synthesis of transition metal complexes in which five different metals such as Fe, Ru, Au, Cu and Ti (complex 179), Fe, Ru, Re, Au and Mo (complex 181) or even six different metal atoms (Fe, Ru, Re, Au, Cu, Ti; complex 182) are spanned by carbon-rich bridging units demonstrate that such large heteronuclear assemblies can be synthesized in a straightforward manner by using the modular “Tinkertoy” approach. This procedure allows a fair control over the structure and composition of such molecules. A detailed investigation of possible photophysical properties and electronic interactions between the appropriate metal atoms of 179, 181 and 182 is in progress in our laboratory.

The identities of all described complexes within this article have been confirmed by elemental analysis, IR, ¹H, ¹³C{¹H} and ³¹P{¹H} NMR spectroscopy. From selected samples the ESI-TOF mass spectra were measured and the solid state structures determined by single X-ray structure analysis. In this respect, IR and NMR (¹H, ³¹P{¹H}) spectroscopy allows to monitor the progress of the reactions and verifies the structure and composition of the final assemblies.

CONCLUSION

This chapter addresses the chemistry of mono- and bis(alkynyl) transition metal complexes, diaminoaryl NCN and NN'N pincer molecules ($\text{NCN} = [\text{C}_6\text{H}_2(\text{CH}_2\text{NMe}_2-2,6)_2]$; $\text{NN}'\text{N} = [\text{C}_5\text{H}_3\text{N}(\text{CH}_2\text{NMe}_2-2,6)_2]$), modified ferrocenes and biferrocenes towards diverse metal complex fragments and serves to understand the manifold and sometimes unexpected reaction behavior of such systems. Interesting unique (hetero)bi- to (hetero)undecametallic compounds with often uncommon structural motifs are formed in which the respective transition metal building blocks are connected via π -conjugated carbon-rich organic and/or inorganic bridging units. The reactions based on the modular “Tinkertoys” approach depend on the steric and electronic properties of the metal atoms and ligands involved. Despite the large quantity of experimental work carried out in this field of chemistry, the exact factors which control the formation and/or interconversion of the structures in the (hetero)multimetallic complexes is still an open question and will continue to stimulate further work in this field of chemistry. A challenge is the preparation of even larger transition metal complexes featuring more than six different early-late metals and new functionalities. This chemistry opens the possibility for creating new materials with innovative electronic, catalytic, optical, and/or magnetic properties.

ACKNOWLEDGEMENT

The very creative and fruitful contributions of Drs. S. Back, W. Frosch, T. Stein, K. Köhler, M. Al-Anber, and Dipl.-Chem. S. Köcher, M. Lohan, J. Kühnert, A. del Villar, and D. Friedrich and specially R. Packheiser are gratefully acknowledged. The financial support from the Deutsche Forschungsgemeinschaft, the Fonds der Chemischen Industrie, and the VW-Foundation have been essentiell throughout.

REFERENCES

- [1] For example: (a) Balzani, V.; Juris A.; Venturi, M.; Campagna, S., and Serroni, S. (1996). Luminescent and Redox-Active Polynuclear Transition Metal Complexes. *Chem. Rev.*, *96*, 759-833. (b) Balzani, V.; Campagna, S.; Denti, G.; Juris A.; Serroni, S., and Venturi, M. (1998). Designing Dedrimers Based on Transition-Metal Complexes. Light-Harvesting Properties and Predetermined Redox Patterns. *Acc. Chem. Res.*, *31*, 26-34. (c) Long, N. J. (1995). Organometallic Compounds for Nonlinear Optics - The Search for En-light-Enment! *Angew. Chem., Int. Ed.*, *34*, 21–38. (d) Wong, K. M. C.; Lam, S. C. F.; Ko, C. C.; Zhu, N.; Yam, V. W. W.; Roué S.; Lapinte, C.; Fathallah, S.; Costuas, K.; Kahalal, S., and Halet, J. F. (2003). Electroswitchable Photoluminescence Activity: Synthesis, Spectroscopy, Electrochemistry, Photophysics, and X-ray Crystal and Electronic Structures of $[\text{Re}(\text{bpy})(\text{CO})_3(\text{C}\equiv\text{C-C}_6\text{H}_4-\text{C}\equiv\text{C})\text{Fe}(\text{C}_5\text{Me}_5)(\text{dppe})][\text{PF}_6]_n$ ($n = 0, 1$). *Inorg. Chem.*, *42*, 7086–7097. (e) Powell C. E., and Humphrey M. G. (2004). Nonlinear Optical Properties of Transition Metal Acetylides and their Derivatives. *Coord. Chem. Rev.*,

248, 725-756. (f) Cifuentes, M. P.; Humphrey, M. G; Morall J. P.; Samoc, M.; Paul, F.; Roisnel, T., and Lapinte C. (2005). Third-Order Nonlinear Optical Properties of Some Electron-Rich Iron Mono- and Trinuclear Alkynyl Complexes. *Organometallics*, 24, 4280-4288. (g) Low P. J. (2005). Metal Complexes in Molecular Electronics: Progress and Possibilities. *Dalton Trans.*, 17, 2821-2824. (h) Long, N. J.; Angela, A. J.; de Biani, F. F., and Zanello, P. (1998). Synthetic and Electrochemical Studies of Some Metal Complexes of 1,3,5-Triethynylbenzene *J. Chem. Soc., Dalton Trans.*, 2017-2022. (i) Koellner, C.; Pugin, B., and Togni, A. (1998). Dendrimers Containing Chiral Ferrocenyl Diphosphine Ligands for Asymmetric Catalysis. *J. Am. Chem. Soc.*, 120, 10274-10275. (j) Devadoss, C.; Bharathi, P., and Moore, J. S. (1996). Energy Transfer in Dendritic Macromolecules: Molecular Size Effects and the Role of an Energy Gradient. *J. Am. Chem. Soc.*, 118, 40, 9635-9644. (k) Hu, Q. S.; Pugh, V.; Sabat, M., and Pu, L. (1999). Structurally Rigid and Optically Active Dendrimers *J. Org. Chem.*, 64, 20, 7528-7536. (l) Paul, F., and Lapinte, C. (1998). Organometallic Molecular Wires and other Nanoscale-sized Devices: An Approach Using the Organoiron (dppe)Cp*Fe Building Block. *Coord. Chem. Rev.*, 178-180, 431-509. (m) Brunschwig, B. S.; Creutz, C., and Sutin, N. (2002). Optical Transitions of Symmetrical Mixed-Valence Systems in the Class II-III Transition Regime *Chem. Soc. Rev.*, 31, 168-184. (n) Nelson S. F. (2001). In V. Balzani (Ed.) *Electron Transfer in Chemistry* (Vol. 1, Chapter 10). Weinheim, Germany; Wiley-VCH. (o) Kaim, W.; Klein, A., and Glöckle, M. (2002). Exploration of Mixed-Valence Chemistry: Inventing New Analogues of the Creutz-Taube Ion. *Acc. Chem. Res.*, 33, 755-763. (p) Ceccon, A.; Santi, S.; Orian, L., and Bisello, A. (2004). Electronic Communication in Heterobinuclear Organometallic Complexes Through Unsaturated Hydrocarbon Bridges. *Coord. Chem. Rev.*, 248, 683-724. (q) Ward, M. D. (1995). Metal-Metal Interactions in Binuclear Complexes Exhibiting Mixed Valency; Molecular Wires and Switches. *Chem. Soc. Rev.*, 121-134. (r) Astruc D. (1997). From Organotransition-Metal Chemistry toward Molecular Electronics: Electronic Communication between Ligand-Bridged Metals. *Acc. Chem. Res.*, 30, 383-391. (s) Sarkar, B.; Kaim, W.; Fiedler, J., and Duboc, C. (2004). Molecule-Bridged Mixed-Valent Intermediates Involving the Ru^I Oxidation State. *J. Am. Chem. Soc.*; 126, 14706-14707. (t) Connelly, N. G., and Geiger, W. E. (1996). Chemical Redox Agents for Organometallic Chemistry. *Chem. Rev.*, 96, 877-910.

- [2] (a) Michl, J., and Magnera F. (2002). Two-dimensional Supramolecular Chemistry with Molecular Tinkertoys. *Proc. Natl. Acad. Sci. U.S.A.*, 99, 4788-4792. (b) Levin, M.; Kaszynski, P., and Michl, J. (2000). Bicyclo[1.1.1]pentanes, [n]Staffanes, [1.1.1]Propellanes, and Tricyclo[2.1.0.0^{2,5}]pentanes. *Chem. Rev.*, 100, 169-234. (c) Kaszynski, P., and Michl, J. (1998). [n]Staffanes: A Molecular-Size "Tinkertoy" Construction Set for Nanotechnology. Preparation of End-Functionalized Telomers and a Polymer of [1.1.1]Propellane. *J. Am. Chem. Soc.*, 120, 5225-5226.
- [3] (a) Stoddart, J. F. (1992). Constructing a Molecular LEGO Set. *Chem. Soc. Rev.*, 21, 215-225. (b) Raymo, F. M., and Stoddart, J. F. (1999). Interlocked Macromolecules. *Chem. Rev.*, 99, 1643-1663; (c) Kessler, V. G. (2003). Molecular Structure Design and Synthetic Approaches to the Heterometallic Alkoxide Complexes (Soft Chemistry Approach to Inorganic Materials by the Eyes of a Crystallographer) *Chem. Commun.*, 1213.

- [4] (a) Long, N. J., and Williams, C. K. (2003). Metal Alkynyl Complexes: Synthesis and Materials. *Angew. Chem., Int. Ed.*, 42, 2586-2617. (b) Yam V. W. W. (2004). Luminescent Metal Alkynyls – From Simple Molecules to Molecular Rods and Materials. *J. Organomet. Chem.*, 689, 1393. (c) Bruce, M. I.; Low, P. J.; Frantisek, F.; Humphrey, P. A.; De Montigny, F.; Jevric, M.; Lapinte, C.; Perkins, G. J.; Roberts, R. L.; Skelton, B. W., and White, A. H. (2005). Syntheses, Structures, some Reactions, and Electrochemical Oxidation of Ferrocenylethynyl Complexes of Iron, Ruthenium, and Osmium. *Organometallics*, 24, 5241-5255. (d) Low, P. J.; Roberts, R. L.; Cordiner, R. L., and Hartl F. J. (2005). Electrochemical Studies of Bi- and Polymetallic Complexes Featuring Acetylide Based Bridging Ligands. *Solid State Electrochem.*, 9, 717-731. (e) Szafert, S., and Gladysz, J. A. (2003). Carbon in One Dimension: Structural Analysis of the Higher Conjugated Polyynes. *Chem. Rev.*, 103, 4175-4205. (f) Bruce, M. I.; Low, P. J.; Costuas, K.; Halet, J. F.; Best, S. P., and Heath G. A. (2000). Oxidation Chemistry of Metal-Bonded C₄ Chains: A Combined Chemical, Spectroelectrochemical, and Computational Study: *J. Am. Chem. Soc.*, 122, 1949-1962. (g) Narvor, N. L.; Toupet, L., and Lapinte, C. (1995). Elemental Carbon Chain Bridging Two Iron Centers: Syntheses and Spectroscopic Properties of [Cp*(dppe)Fe-C₄-FeCp*(dppe)]_n⁺·n[PF₆]⁻. X-ray Crystal Structure of the Mixed Valence Complex (n = 1). *J. Am. Chem. Soc.*, 117, 7129-7138; (h) Baumgartner, T., and Reau, R. (2006). Organophosphorus π-Conjugated Materials. *Chem. Rev.*, 106, 4681-4727. (i) Yam, V. W. W.; Lo, K. K. W., and Wong K. M. C. (1999). Luminescent Polynuclear Metal Acetylides. *J. Organomet. Chem.*, 578, 3-30.
- [5] (a) Chawdhury, N.; Long, N. J.; Mahon, M. F.; Ooi, L.; Raithby, P. R.; Rooke, S.; White, A. J. P.; Williams, D. J., and Younus, M. (2004). Synthesis, Characterisation and Optical Spectroscopy of Platinum(II) Di-ynes and Poly-ynes Incorporating Condensed Aromatic Spacers in the Backbone. *J. Organomet. Chem.*, 689, 840-847. (b) de Montigny, F.; Argouarch, G.; Costuas, K.; Halet, J. F.; Roisnel, T.; Toupet, L., and Lapinte, C. (2005). Electron Transfer and Electron Exchange Between [Cp*(dppe)Fe]ⁿ⁺ (n = 0, 1) Building Blocks Mediated by the 9,10-Bis(ethynyl)anthracene Bridge *Organometallics*, 24, 4558-4572. (c) Callejas-Gaspar, B.; Laubender, M., and Werner, H. (2003). Synthesis and Reactivity of Dinuclear Rhodium Complexes with Rh=C=CHR and Rh=C=C=CRR' Units as Building Blocks. *J. Organomet. Chem.*, 684, 144-152. (d) Klein, A.; Lavastre, O., and Fiedler, J. (2006). Role of the Bridging Arylethynyl Ligand in Bi- and Trinuclear Ruthenium and Iron Complexes *Organometallics*, 25, 635-643. (e) Hurst, S. K.; Cifuentes, M. P.; McDonagh, A. M.; Humphrey, M. G.; Samoc, M.; Luther-Davies, B.; Asselberghs, I., and Persoons, A. (2002). Organometallic Complexes for Nonlinear Optics. Part 25. Quadratic and Cubic Hyperpolarizabilities of some Dipolar and Quadrupolar Gold and Ruthenium Complexes. *J. Organomet. Chem.*, 642, 259-262. (f) Hurst, S. K., and Ren, T. (2002). Synthesis, Characterization and Electrochemistry of Diruthenium Complexes Linked by Aryl Acetylide Bridges. *J. Organomet. Chem.*, 660, 1-5. (g) Fraysse, S.; Coudret, S., and Launay, J. P. (2003). Molecular Wires Built from Binuclear Cyclometalated Complexes. *J. Am. Chem. Soc.*, 125, 5880-5888. (h) Back, S.; Lutz, M.; Spek, A. L.; Lang, H., and van Koten, G. (2001). Preparation and Electrochemical Behaviour of Dinuclear Platinum Complexes Containing NCN Ligands (NCN=[C₆H₃(Me₂NCH₂)₂-2,6]⁻). The Crystal Structure of [C₆H₃(Me₂NCH₂)₂-1,3-(C≡C)-5]₂. *J. Organomet.*

- Chem.*, 620, 227-234. (i) Weyland, T.; Ledoux, I.; Brasselet, S.; Zyss, J., and Lapinte, C. (2000). Nonlinear Optical Properties of Redox-Active Mono-, Bi-, and Trimetallic σ -Acetylides Complexes Connected Through a Phenyl Ring in the $Cp^*(dppe)Fe$ Series. An Example of Electro-Switchable NLO Response *Organometallics*, 19, 5235-5237. (j) Colbert, M. C. B.; Lewis, J.; Long, N. J.; Raithby, P. R.; Younus, M.; White, A. J. P.; Williams, D. J.; Payne, N. N.; Yellowlees, L.; Beljonne, D.; Chawdhury, N., and Friend, R. H. (1998). Synthesis and Characterization of Dinuclear Metal σ -Acetylides and Mononuclear Metal σ -Allenylidenes. *Organometallics*, 17, 3034-3043. (k) Bruce, M. I.; Hall, B. C.; Kelly, B. D.; Low, P. J.; Skelton, B. W., and White, A. H. J. (1999). An Efficient Synthesis of Polyyynyl and Polyynediyi Complexes of Ruthenium(II). *J. Chem. Soc., Dalton Trans.*, 19, 3719-3728. (l) Lavastre, O.; Even, M.; Dixneuf, P. H.; Pacreau, A., and Vairon, J. (1996). Novel Ruthenium- or Iron-Containing Tetraynes as Precursors of Mixed-Metal Oligomers. *Organometallics*, 15, 1530-1531.
- [6] (a) Lam, S. C. F.; Yam, V. W. W.; Wong, K. M. C.; Cheng, E. C. C., and Zhu, N. (2005). Synthesis and Characterization of Luminescent Rhenium(I)-Platinum(II) Polypyridine Bichromophoric Alkynyl-Bridged Molecular Rods *Organometallics*, 24, 4298-4305. (b) Younus, M.; Long, N. J.; Raithby, P. R., and Lewis, J. (1998). Synthetic, Spectroscopic and Electrochemical Characterisation of Mixed-Metal Acetylide Complexes. *J. Organomet. Chem.*, 570, 55-62. (c) Lavastre, O.; Plass, J.; Bachmann, P.; Guesmi, S.; Moinet, C., and Dixneuf, P. H. (1997). Ruthenium or Ferrocenyl Homobimetallic and RuPdRu and FePdFe Heterotrimetallic Complexes Connected by Unsaturated, Carbon-Rich $-C\equiv CC_6H_4C\equiv C-$ Bridges. *Organometallics*, 16, 184-189.
- [7] (a) Fink, H.; Long, N. J.; Martin, A. J.; Opronolla, G.; White, A. J. P.; Williams, D. J., and Zanello, P. (1997). Ethynylferrocene Compounds of 1,3,5-Tribromobenzene. *Organometallics*, 16, 2646-2650. (b) Weyland, T.; Costuas, K.; Mari, A.; Halet, J. F., and Lapinte, C. (1998). $[(Cp^*)(dppe)Fe(III)]^+$ Units Bridged Through 1,3-Diethynylbenzene and 1,3,5-Triethynylbenzene Spacers: Ferromagnetic Metal-Metal Exchange Interaction. *Organometallics*, 17, 5569-5579. (c) Tykwinski, R. R., and Stang, P. J. (1994). Preparation of Rigid-Rod, Di- and Trimetallic, σ -Acetylide Complexes of Iridium(III) and Rhodium(III) via Alkynyl(phenyl)iodonium Chemistry *Organometallics*, 13, 3203-3208. (d) Müller, T. J. J., and Lindner, H. J. (1996). Palladium-Copper-Catalyzed Coupling of Tricarbonylchromium-Complexed Phenylacetylene with Iodoarenes. A Facile Access to Alkynyl-Bridged $Cr(CO)_3$ -Complexed Benzenes. *Chem. Ber.*, 129, 607-613. (e) Irwin, M. J.; Manojlovic-Muir, L.; Muir, K. W.; Puddephatt, R. J., and Yufit, D. S. (1997). Trigold Triacetylides: Polymerization Through Gold-Gold Bonding or Bridging Ligands. *Chem. Commun.*, 219-220. (f) Leininger, S.; Stang, P. J., and Huang S. (1998). Synthesis and Characterization of Organoplatinum Dendrimers with 1,3,5-Triethynylbenzene Building Blocks. *Organometallics*, 17, 3981-3987.
- [8] (a) Vicente, J.; Chicote, M. T., and Alvarez-Falcon, M. M. (2005). Platinum(II) and Mixed Platinum(II)/Gold(I) σ -Alkynyl Complexes. The First Anionic σ -Alkynyl Metal Polymers. *Organometallics*, 24, 2764-2772. (b) Chong, S. H. F.; Lam, S. C. F.; Yam, V. W. W.; Zhu, N.; Cheung, K. K.; Fathallah, S.; Costuas, K., and Halet, J. F. (2004). Luminescent Heterometallic Branched Alkynyl Complexes of Rhenium(I)-

- Palladium(II): Potential Building Blocks for Heterometallic Metallo-dendrimers. *Organometallics*, 23, 4924-4933. (c) Long, N. J.; Martin, A. J.; White, A. J. P.; Williams, D. J.; Fontani, M.; Laschi, F., and Zanello, P. (2000). Synthesis and Characterisation of Unsymmetrical Metal (RuII, OsII) and Ferrocenyl Complexes of 1,3,5-Triethynylbenzene. *J. Chem. Soc., Dalton Trans.*, 3387-3392. (d) Long, N. J.; Martin, A. J.; De Biani, F. F., and Zanello, P. (1998). Synthetic and Electrochemical Studies of some Metal Complexes of 1,3,5-Triethynylbenzene. *J. Chem. Soc., Dalton Trans.*, 2017-2022.
- [9] Lucas, N. T.; Cifuentes, M. P.; Nguyen, L. T., and Humphrey, M. G. (2001). Ruthenium Cluster Chemistry with Ph₂PC₆H₄-4-C≡CH. *J. Cluster Science*, 12, 201-221.
- [10] (a) Barbieri, A.; Ventura, B.; Flamigni, L.; Barigelli, F.; Fuhrmann, G.; Baeuerle, P.; Goeb, S., and Ziessel, R. (2005). Binuclear Wirelike Dimers Based on Ruthenium(II)-Bipyridine Units Linked by Ethynylene-Oligothiophene-Ethynylene Bridges. *Inorg. Chem.*, 44, 8033-8043. (b) Newkome, G. R.; Patri, A. K.; Holder, E., and Schubert, U. S. (2004). Synthesis of 2,2'-Bipyridines: Versatile Building Blocks for Sexy Architectures and Functional Nanomaterials. *Eur. J. Org. Chem.*, 2, 235-254. (c) Hissler, M.; Harriman, A.; Khatyr, A., and Ziessel, R. (1999). Intramolecular Triplet Energy Transfer in Pyrene-Metal Polypyridine Dyads: A Strategy for Extending the Triplet Lifetime of the Metal Complex. *Chem. Eur. J.*, 5, 3366-3381. (d) Constable, E. C. (1989). Homoleptic Complexes of 2,2'-Bipyridine. *Advan. Inorg. Chem.*, 1989, 34, 1-63. (e) McWhinnie, W. R., and Miller, J. D. (1969). Chemistry of Complexes Containing 2,2'-Bipyridyl, 1,10-Phenanthroline, or 2,2',6',2"-Terpyridyl as Ligands. *Advan. Inorg. Chem., Radiochem.*, 12, 135-215.
- [11] (a) Le Stang, S.; Paul, F., and Lapinte, C. (2000). Molecular Wires: Synthesis and Properties of the New Mixed-Valence Complex [Cp*(dppe)Fe-C≡C-X-C≡C-Fe(dppe)Cp*][PF₆] (X = 2,5 -C₄H₂S) and Comparison of its Properties with those of the Related All-Carbon-Bridged Complex (X = -C₄-). *Organometallics*, 19, 1035-1043.
- [12] (a) Wong, W. Y.; Lu, G. L.; Ng, K. F.; Choi, K. H., and Lin, Z. (2001). Synthesis, Structures and Properties of Platinum(II) Complexes of Oligothiophene-Functionalized Ferrocenylacetylene. *J. Chem. Soc., Dalton Trans.*, 22, 3250-3260. (b) Viola, E.; Lo Sterzo, C., and Trezzi, F. (1996). Formation of a Molybdenum-Iron Heterobimetallic Bis(acetylide) Derivative of 2,5-Diethynylthiophene via Palladium-Catalyzed Metal-Carbon Coupling. *Organometallics*, 15, 4352-4354.
- [13] Lang, H.; Packheiser, R., and Walfort, B. (2006). Organometallic π-Tweezers, NCN Pincers, and Ferrocenes as Molecular "Tinkertoys" in the Synthesis of Multiheterometallic Transition-Metal Complexes. *Organometallics*, 25, 1836-1851.
- [14] (a) Packheiser, R.; Walfort, B., and Lang, H. (2006). Heterobi- and Heterotrimetallic Transition Metal Complexes with Carbon-Rich Bridging Units. *Organometallics*, 25, 4579-4587. (b) Al-Anber, M.; Stein, T., and Lang, H. (2005). Organometallic π-Tweezers Incorporating Pyrazine- and Pyridine-Based Bridging Units. *Inorg. Chim. Acta*, 358, 50-56. (c) Bruce, M. I.; Zaitseva, N. N.; Skelton, B. W.; Somers, N., and White, A. H. (2003). Crystal and Molecular Structures of Some Alkynyl-Group 9/Group 11 Complexes [M₂m₄(C₂R)₈(PPh₃)₂] (M = Rh, Ir; m = Cu, Ag; R = Ph, Fc (Ir/Cu only)). *Aust. J. Chem.*, 56, 509-516. (d) Lang, H.; Stein, T.; Back, S., and Rheinwald, G. (2004). Titanocene-Based Group-11 Metal Ions; Solid-State Structure of

$[(\eta^5\text{-C}_5\text{H}_4\text{SiMe}_3)_2\text{Ti}(\text{C}\equiv\text{CPh})_2]_2\text{AgNO}_3$. *J. Organomet. Chem.*, 689, 2690-2696. (e) Al-Anber, M.; Walfort, B.; Stein, T., and Lang, H. (2004). $\{[\text{Ti}](\text{C}\equiv\text{CSiMe}_3)_2\}\text{Ag}(\text{OClO}_3)$ π -Tweezer Units Bridged by Pyrazine. *Inorg. Chim. Acta*, 357, 1675-1681. (f) Lang, H.; Meichel, E.; Stein, Th.; Weber, C.; Kralik, J.; Rheinwald, G., and Pritzkow, H. (2002). Stabilisierung niedervalenter Ni(CO)-Bausteine durch $[\text{Ti}](\text{C}\equiv\text{CR})_2$; Reaktionsverhalten von $\{[\text{Ti}](\text{C}\equiv\text{CR})_2\}\text{Ni}(\text{CO})$ gegenüber Triphenylphosphoran und Phosphiten. *J. Organomet. Chem.*, 664, 150-160. (g) Stein, T., and Lang, H. (2002). Monomere Kupfer(I)-Alkyle mit β -Wasserstoffatomen und Kupfer(I)-Aryle mit kondensierten Aromaten; die Festkörperstruktur von $[(\eta^5\text{-C}_5\text{H}_4\text{SiMe}_3)_2\text{Ti}(\text{C}\equiv\text{CSiMe}_3)_2]\text{Cu}^n\text{C}_4\text{H}_9$. *J. Organomet. Chem.*, 664, 142-149. (h) Stein, T.; Lang, H., and Holze, R. (2002). Intramolecular Intermetallic Interactions in Bi- and Tetrametallic Organometallic Complexes as Demonstrated with Cyclic Voltammetry, *J. Electro. Chem.*, 520, 163-167. (i) Back, S.; Stein, T.; Frosch, W.; Wu, I.-Y.; Kralik, J.; Büchner, M.; Huttner, G.; Rheinwald, G., and Lang, H. (2001). Heterometallic Early-Late π -Tweezer Complexes: Their Synthesis, Electrochemical Behaviour and the Solid-State Structures of $(\eta^5\text{-C}_5\text{H}_4\text{SiMe}_3)_2\text{Ti}(\text{C}\equiv\text{CPh})_2$ and $[(\eta^5\text{-C}_5\text{H}_4\text{SiMe}_3)_2\text{Ti}(\text{C}\equiv\text{CPh})_2]\text{Pd}(\text{PPh}_3)$. *Inorg. Chim. Acta*, 325, 94-102. (j) Frosch, W.; Back, S.; Müller, H.; Köhler, K.; Driess, A.; Schiemenz, B.; Huttner, G., and Lang, H. (2001). Donor-funktionalisierte Alkinyle von Titan(IV), Kupfer(I) und Silber(I); Festkörperstrukturen von $[\text{Ti}](\text{C}\equiv\text{CCH}_2\text{NMe}_2)_2$ und $\{[\text{Ti}](\text{C}\equiv\text{C}'\text{Bu})_2\}\text{CuC}\equiv\text{CC}\equiv\text{CC}_2\text{H}_5$. *J. Organomet. Chem.*, 619, 99-109. (k) Lang, H.; Mansilla, N., and Rheinwald, G. (2001). First Example of Zinc(II) Monomeric Species Stabilized by η^2 -Bonded Alkynes. *Organometallics*, 20, 1592-1596. (m) Frosch, W.; Back, S.; Rheinwald, G.; Köhler, K.; Zsolnai, L.; Huttner, G., and Lang, H. (2000). Mono-, Di-, and Tricarboxylic Acids: Central Building Blocks for the Formation of Multinuclear Transition Metal Complexes. *Organometallics*, 19, 5769-5779. (n) Lang, H.; George, D., and Rheinwald, G. (2000). Bis(alkynyl) Transition Metal Complexes, $\text{R}^1\text{C}\equiv\text{C}-[\text{M}]-\text{C}\equiv\text{CR}^2$, as Organometallic Chelating Ligands; Formation of $\mu,\eta^{1(2)}$ -Alkynyl-Bridged Binuclear and Oligonuclear Complexes. *Coord. Chem. Rev.*, 206-207, 101-197, and references cited therein. (o) Frosch, W.; Back, S.; Rheinwald, G.; Köhler, K.; Pritzkow, H., and Lang, H. (2000). $(\eta^2\text{-Alkyne})_2\text{CuMe}$ as a Synthetic Tool in the Preparation of Numerous Inorganic and Organic Copper(I) Species. *Organometallics*, 19, 4016-4024. (p) Rupp, R.; Huttner, G.; Lang, H.; Heinze, K.; Büchner, M., and Robert, E. (2000). Synthesis and π -Tweezer Properties of Tripod Cobalt-Bisalkynyl Compounds $[\text{CH}_3\text{C}(\text{CH}_2\text{PPh}_2)_3\text{Co}(\text{C}\equiv\text{CR})_2]$ - Application to the Oxidative Coupling of Alkynyl Groups. *Eur. J. Inorg. Chem.*, 9, 1953-1959. (q) Frosch, W.; del Vilar, A., and Lang, H. (2000). Heterobimetallische Komplexe von Titan(IV)-Quecksilber(II) und Platin(II)-Quecksilber(II). *J. Organomet. Chem.*, 602, 91-96. (r) Frosch, W.; Back, S.; Köhler, K., and Lang, H. (2000). Zur Umsetzung von Bis(alkynyl)-Titanocenen mit Übergangsmetall-Verbindungen von Cu(II), Pd(II), Pt(II), Fe(III) und Au(III). *J. Organomet. Chem.*, 601, 226-232. (s) Back, S.; Rheinwald, G., and Lang, H. (2000). Synthesis, Electrochemistry and Electronic Spectra of Tetranuclear Bis(η^2 -alkynyl) Transition-Metal Complexes. The Molecular Structure of $[(\eta^5\text{-C}_5\text{H}_4\text{SiMe}_3)_2\text{Ti}(\text{C}\equiv\text{CFc})_2]\text{CuBr}$. *J. Organomet. Chem.*, 601, 93-99. (t) Lang, H.; Weinmann, S.; Wu, I. Y.; Stein, T.; Jacobi, A., and Huttner, G. (1999). $(\eta^5\text{-C}_5\text{H}_4\text{SiMe}_3)_2\text{Ti}(\text{C}\equiv\text{C-SiMe}_2-\text{C}\equiv\text{CSiMe}_3)_2$: a Unique Entry to Monomeric and Oligomeric Alkyne-Copper(I) and Alkyne-Silver(I) Halides. *J. Organomet. Chem.*,

- 575, 133-140. (u) Lang, H., and Rheinwald, G. (1999). Kupfer, Silber, Gold; fixiert in metallorganischen π -Pinzetten. *J. Prakt. Chem.*, 341, 1-19. (v) Back, S.; Pritzkow, H., and Lang, H. (1998). C₂-Bridged Titanocene-Ferrocenyl Complexes: Synthesis, Reaction Chemistry, and Electrochemical Behavior. *Organometallics*, 17, 41-44. (w) Hayashi, Y.; Osawa, M.; Kobayashi, K.; Sato, T.; Sato, M., and Wakatsuki, Y. (1998). The Reaction of Titanocene Bis(ferrocenylacetylide) and Bis(ruthenocenylacetylide) with Silver Cation: Formation of Bis(Ti-Tweezers) Silver Complexes. *J. Organomet. Chem.*, 569, 169-175. (x) Back, S.; Rheinwald, G.; Zsolnai, L.; Huttner, G., and Lang, H. (1998). Synthesis, Reaction Chemistry and Electrochemical Behaviour of (η^5 -C₅H₄SiMe₃)₂Hf(C≡CFc)₂. *J. Organomet. Chem.*, 563, 73-79. (y) Koehler, K.; Silverio, S.; Hyla-Kryspin, I.; Gleiter, R.; Zsolnai, L.; Driess, A.; Huttner, G., and Lang, H. (1997). Trigonal-Planar-Coordinated Organogold(I) Complexes Stabilized by Organometallic 1,4-Diyne: Reaction Behavior, Structure, and Bonding. *Organometallics*, 16, 4970-4979. (z) Lang, H., and Weinmann, M. (1996). Bis(alkynyl) Titanocenes as Organometallic Chelating Ligands for the Stabilization of Monomeric Organo Copper(I) Compounds. *Synlett*, 1, 1-10. (aa) Hayashi, Y.; Osawa, M.; Kobayashi, K., and Wakatsuki, Y. (1996). Reductive Elimination by Remote Electron Transfer Activation in C₄-Bridged Titanocene-Ferrocenyl Complexes. *Chem. Commun.*, 1617-1618. (bb) Janssen, M. D.; Herres, M.; Zsolnai L.; Grove, D. M.; Spek, A. L., and Lang, H. (1995). A Stable Bimetallic Copper(I) Titanium Acetylide. *Organometallics*, 14, 1098-1100. (cc) Janssen, M. D.; Smeets, W. J. J.; Spek, A. L.; Grove, D.M.; Lang, H., and van Koten, G. (1995). Intramolecular Addition of Monomeric Arylcopper Entities Across an Alkyne Grouping in a Complex of Type [(η^5 -C₅H₄SiMe₃)₂Ti(C≡CSiMe₃)₂]CuR; X-ray Structure of [(η^5 -C₅H₄SiMe₃)₂Ti(C≡CSiMe₃)₂C=C(SiMe₃)(C₆H₃(CH₂NMe₂)₂-2,6)Cu]. *J. Organomet. Chem.*, 505, 123-126. (dd) Janssen, M. D.; Herres, M.; Spek, A. L.; Grove, D. M.; Lang, H., and van Koten, G. (1995). Monomeric Bis(η^2 -Alkyne) Complexes of (η^1 -Mesityl)Copper(I) and (η^1 -mesityl)Silver(I) Obtained from a Bis(Alkynyl)Titanocene; X-ray Structure of [(η^5 -C₅H₄SiMe₃)₂Ti(C≡CSiMe₃)₂]Cu(η^1 -Mes) (Mes = C₆H₂Me₃-2,4,6). *J. Chem. Soc., Chem. Commun.*, 925-926. (ee) Janssen, M. D.; Herres, M.; Zsolnai, L.; Spek, A. L.; Grove, D. M.; Lang, H., and van Koten, G. (1996). Monomeric Bis(η^2 -Alkyne)Copper(I) and -Silver(I) Halides, Pseudohalides, and Arenethiolates. *Inorg. Chem.*, 35, 2476-2483. (ff) Back, S.; Rheinwald, G., and Lang, H. (1999). Synthesis and Electrochemistry of a Bis- η^2 -Coordinated Tetrametallic Transition-Metal Complex. Crystal Structure of [(η^5 -C₅H₄SiMe₃)₂Ti(C≡CFc)₂]Pd(PPh₃). *Organometallics*, 18, 4119-4122. (gg) Lang, H., and Leschke, M. (2002). From Heterobimetallic Transition Metal Complexes to Linear Coordination Polymers Based on *cis*- and *trans*-L₂Pt(C≡CPh)₂. *Heteroat. Chem.*, 13, 521-533.
- [15] (a) Gosiewska, S.; Martinez, S. H.; Lutz, M.; Spek, A. L.; van Koten, G., and Klein Gebbink, R. J. M. (2006). Diastereopure Cationic NCN-Pincer Palladium Complexes with Square Planar η^4 -N,C,N,O Coordination. *Eur. J. Inorg. Chem.*, 22, 4600-4607. (b) Köcher, S.; Lutz, M.; Spek, A. L.; Prasad, R.; van Klink, G. P.M.; van Koten, G., and Lang, H. (2006). Heterobimetallic Fe-Pd and Fe-Pt NCN Pincer Complexes (NCN = [C₆H₂(CH₂NMe₂)₂-2,6]⁻). *Inorg. Chim. Acta*, 359, 4454-4462. (c) Szabo, K. J. (2006). Palladium-Pincer-Complex-Catalyzed Transformations Involving Organometallic Species. *Synlett*, 6, 811-824. (d) Slagt, M. Q.; van Zwieten, D. A.P.;

- Moerkerk, A. J. C. M.; Klein Gebbink, R. J. M., and van Koten, G. (2004). NCN-Pincer Palladium Complexes with Multiple Anchoring Points for Functional Groups. *Coord. Chem. Rev.*, **248**, 2275-2282. (e) van der Boom, M., and Milstein, D. (2003). Cyclometalated Phosphine-Based Pincer Complexes: Mechanistic Insight in Catalysis, Coordination, and Bond Activation. *Chem. Rev.*, **103**, 1759-1792. (f) Singleton, J. T. (2003). The Uses of Pincer Complexes in Organic Synthesis. *Tetrahedron*, **59**, 1837-1857. (g) Martin, A., and van Koten, G. (2001). Platinum Group Organometallics Based on „Pincer“ Complexes: Sensors, Switches, and Catalysts. *Angew. Chem. Int. Ed.*, **40**, 3750-3781. (h) Gossage, R.; van de Kuil, L. A., and van Koten, G. (1998). Diaminoarylnickel(II) "Pincer" Complexes: Mechanistic Considerations in the Kharasch Addition Reaction, Controlled Polymerization, and Dendrimeric Transition Metal Catalysts. *Acc. Chem. Res.*, **31**, 423-431. (i) Rietveld, M. H. P.; Grove, D. M., and van Koten, G. (1997). Recent Advances in the Organometallic Chemistry of Aryldiamine Anions that Can Function as N,C,N'- and C,N,N'- Chelating Terdentate "Pincer" Ligands: an Overview. *New J. Chem.*, **21**, 751-771.
- [16] (a) Sutcliffe, O. B., and Bryce, M. R. (2003). Planar Chiral 2-Ferrocenyloxazolines and 1,1'-Bis(oxazolinyl)ferrocenes: Syntheses and Applications in Asymmetric Catalysis. *Tetrahedron: Asymmetry*, **14**, 2297-2325. (b) Dai, L.-X.; Tu, T.; You, S.-L.; Deng, W.-P., and Hou, X.-L. (2003). Asymmetric Catalysis with Chiral Ferrocene Ligands. *Acc. Chem. Res.*, **36**, 659-667. (c) Herberhold, M. (2002). 1,1'-Ferrocenedi(amido) Chelate Ligands in Titanium and Zirconium Complexes. *Angew. Chem. Int. Ed.*, **41**, 956-958. (d) Colacot, T. J. (2001). Ferrocenyl Phosphine Complexes of the Platinum Metals in Non-Chiral Catalysis. *Platinum Metals Rev.*, **45**, 22-30. (e) Bandoli, G., and Dolmella, A. (2000). Ligating Ability of 1,1'-Bis(diphenylphosphino)ferrocene: a Structural Survey (1994-1998). *Coord. Chem. Rev.*, **209**, 161-196. (f) Vogler, A., and Kunkely, H. Photochemistry (2000). Induced by Metal-to-Ligand Charge Transfer Excitation. *Coord. Chem. Rev.*, **208**, 321-329. (g) Thomas, J. M.; Maschmeyer, T.; Johnson, B. F. G. (1999). Shephard, D. S. Constrained Chiral Catalysts. *J. Mol. Catalysis A: Chemical*, **141**, 139-144. (h) Beyer, L.; Richter, R., and Seidelmann, O. (1999). Ferrocensubstituierte 1,3-bidentate Liganden und ihre heteronuklearen Übergangsmetallchelate. *J. Prakt. Chem.*, **341**, 704-726. (i) Fong, A. S.-W., and Hor, A. T. S. (1998). Clusters and Aggregates of 1,1'-Bis(diphenylphosphino)ferrocene (dppf). *J. Cluster Sci.*, **9**, 351-392.
- [17] (a) Haussler, M.; Sun, Q.; Xu, K.; Lam, J. W. Y.; Dong, H., and Tang, B. Z. (2005). Hyperbranched Poly(ferrocenylene)s Containing Groups 14 and 15 Elements: Syntheses, Optical and Thermal Properties, and Pyrolytic Transformations into Nanostructured Magnetoceramics. *J. Inorg. Organomet. Poly. Mat.*, **15**, 67-81. (b) Fery-Forgues, S., and Delavaux-Nicot, B. (2000). Ferrocene and Ferrocenyl Derivatives in Luminescent Systems. *J. Photochem. Photobio.*, **132**, 137-159. (c) Yuan, Z.; Collings, J.; Taylor, N. J.; Marder, T. B.; Jardin, C., and Halet, J.-F. (2000). Linear and Nonlinear Optical Properties of Three-Coordinate Organoboron Compounds. *J. Solid State Chem.*, **154**, 5-12. (d) Delville, M.-H. (1999). Organometallic Electron Reservoir Sandwich Iron Complexes as Potential Agents for Redox and Electron Transfer Chain Catalysis. *Inorg. Chim. Acta*, **291**, 1-19. (e) Bethell, D.; Schiffrian, D. J., and Brust, M. (1996). Method of Synthesizing Materials Having Controlled Electronic, Magnetic, and/or Optical Properties. PCT Int. Appl., 56 pp. PIXXD2 WO 9607487 A1 19960314

- Can 125:24123 AN 1996:365688. (f) Sokolov, V. I. (1995). Optically Active Organometallic Compounds (a Personal Account from the Inside). *J. Organomet. Chem.*, 500, 299-306. (g) Astruc, D.; Desbois, M. -H.; Lacoste M., Moulines, F.; Hamon, J. -R., and Varret, F. (1990). Iron Sandwiches as Molecular Reservoir Materials: Design, Electronic Properties and Prospects. *Polyhedron*, 2727-2732.
- [18] Special issue, "50th Anniversary of the Discovery of Ferrocene". (2001). *J. Organomet. Chem.*, 637-639 (Adams, R. D., Ed.), and references cited therein.
- [19] For example: (a) Rüffer, T.; Ohashi, M.; Shima, A.; Mizomoto, H.; Kaneda, Y., and Mashima, K. (2004). Unique Oxidative Metal-Metal Bond Formation of Linearly Aligned Tetranuclear Rh-Mo-Mo-Rh Clusters. *J. Am. Chem. Soc.*, 126, 12244-12245 and references cited therein. (b) Sterenberg, B. T.; Scoles, L., and Carty, A. J. (2002). Synthesis, Structure, Bonding and Reactivity in Clusters of the Lower Phosphorus Oxides. *Coord. Chem. Rev.*, 231, 183-197. (c) Adams R. D., and Qu, B. (2001). Mixed Metal Cluster Complexes Containing the Bis-Ferrocenylbutadiyne Ligand: Their Structures and Electrochemical Responses. *J. Organomet. Chem.*, 620, 303-307. (d) Bruce, M. I.; Low, P. J.; Ke, M.; Kelly, B. D.; Skelton, B. W.; Smith, M. E.; White, A. H., and Witton, N. B. (2001). Some Chemistry of Diynyl-Tungsten Complexes. *Aust. J. Chem.*, 54, 453-460. (e) Bruce, M. I., and Humphrey, M. G. (2000). Organo-Transition Metal Cluster Compounds. *Organomet. Chem.*, 28, 275-366. (f) Blenkiron, P.; Enright, G. D., and Carty, A. J. (1997). Polycarbon Ligand Chemistry. Novel Behaviour of $\mu\text{-}\eta^1,\eta^2\text{-Butadiynyls}$ towards Metal Fragment Additions. *Chem. Commun.*, 5, 483-484. (g) Doherty, S.; Corrigan, J. F.; Carty, A. J., and Sappa, E. (1995). Homometallic and Heterometallic Transition Metal Allenyl Complexes: Synthesis, Structure, and Reactivity. *Adv. Organomet. Chem.*, 37, 39-130. (h) Bantel, H.; Powell, A. K., and Vahrenkamp, H. (1990). Alkyne-Bridged Tetranuclear Clusters by Expansion of Trinuclear Clusters. *Chem. Ber.*, 123, 677-684. (i) Huttner, G., and Knoll, K. (1987). RP-Bridged Carbonyl Metal Clusters: Synthesis, Properties and Reactions. *Angew. Chem.*, 99, 765-783.
- [20] (a) Taher, D., Walfort, B., and Lang, H. (2004). A New Approach to Novel Homobimetallic Palladium Complexes. *Inorg. Chem. Commun.*, 7, 1006-1009. (b) Taher, D.; Walfort, B.; van Koten, G., and Lang, H. (2006). Thiol End-Capped One-Dimensional Platinum and Palladium Complexes. *Inorg. Chem. Commun.*, 9, 955-958. (c) Lang, H.; Taher, D.; Walfort, B., and Pritzkow, H. (2006). Linear Homobimetallic Palladium Complexes. *J. Organomet. Chem.*, 691, 3834-3845. (d) Jung, D. R., and Czanderna, A. W. (1994). Chemical and Physical Interactions at Metal/Self-Assembled Organic Monolayer Interfaces. *Crit. Rev. Solid State Mater. Sci.*, 19, 1-54. (e) Herdt, G. C.; Jung, D. R., and Czanderna, A. W. (1995). Weak Interactions between Deposited Metal Overlays and Organic Functional Groups of Self-Assembled Monolayers. *Prog. Surf. Sci.*, 50, 103-129. (f) Tarlov, M. J. (1992). Silver Metalization of Octadecanethiol Monolayers Self -Assembled on Gold. *Langmuir*, 8, 80-89. (g) Ohgi, T.; Sheng, H. Y.; Dong, Z. C., and Nejoh, H. (1999). Observation of Au Deposited Self-Assembled Monolayers of Octanethiol by Scanning Tunneling Microscopy. *Surf. Sci.*, 442, 277-282. (h) Ohgi, T.; Fujita, D.; Dong, Z. C., and Nejoh, H. (2001). Scanning Tunneling Microscopy and X-Ray Photoelectron Spectroscopy of Silver Deposited Octanethiol Self-Assembled Monolayers. *Surf. Sci.*, 493, 453-459. (i) Fisher, G. L.; Hooper, A. E.; Opila, R. L.; Allara, D. L., and Winograd, N. (2000). The

Interaction of Vapor-Deposited al Atoms with CO₂H Groups at the Surface of a Self-Assembled Alkanethiolate Monolayer on Gold. *J. Phys. Chem. B*, **104**, 3267-3273. (j) Konstadinidis, K.; Zhang, P.; Opila, R. L., and Allara, D. L. (1995). An In-Situ X-Ray Photoelectron Study of the Interaction between Vapor-Deposited Ti Atoms and Functional Groups at the Surfaces of Self-Assembled Monolayers. *Surf. Sci.*, **338**, 300-312. (k) Hooper, A. E.; Fisher, G. L.; Konstadinidis, K.; Jung, D.; Nguyen, H.; Opila, R. L.; Collins, R. W.; Winograd, N., and Allara, D. L. (1999). Chemical Effects of Methyl and Methyl Ester Groups on the Nucleation and Growth of Vapor-Deposited Aluminum Films. *J. Am. Chem. Soc.*, **121**, 8052-8064. (l) Fisher, G. L.; Walker, A. V.; Hooper, A. E.; Tighe, T. B.; Bahnck, K. B.; Skriba, H. T.; Reinard, M. D.; Haynie, B. C.; Opila, R. L.; Winograd, N., and Allara, D. L. (2002). Bond Insertion, Complexation, and Penetration Pathways of Vapor-Deposited Aluminum Atoms with HO- and CH₃O-Terminated Organic Monolayers. *J. Am. Chem. Soc.*, **124**, 5528-5541. (m) Carlo, S. R.; Wagner, A. J., and Fairbrother, D. H. (2000). Iron Metalization of Fluorinated Organic Films: A Combined X-ray Photoelectron Spectroscopy and Atomic Force Microscopy Study. *J. Phys. Chem. B*, **104**, 6633-6641. (n) Nuzzo, R. G., and Allara, D. L. (1983). Adsorption of Bifunctional Organic Disulfides on Gold Surfaces. *J. Am. Chem. Soc.*, **105**, 4481-4483. (o) Lehn, J. M. (1995). *Supramolecular Chemistry-Concepts and Perspectives*. Weinheim, Germany: VCH. (p) Mayor, M.; von Hänsch, C.; Weber, H. B.; Reichert, J., and Beckmann, D. (2002). A *trans*-Platinum(II) Complex as a Single-Molecule Insulator. *Angew. Chem., Int. Ed.*, **41**, 1183-1186. (q) Mayor, M., and Weber, H. B. (2004). Statistical Analysis of Single-Molecule Junctions. *Angew. Chem.*, **43**, 2942-2884. (r) van Ryswyk, H.; Moore, E. E.; Joshi, N. S.; Zeni, R. J.; Eberspacher, A. T., and Collman, J. P. (2004). Surface-Confined Metalloporphyrin Oligomers. *Angew. Chem.*, **43**, 5827-5830.

- [21] (a) Creutz, C., and Taube, H. (1969). A Direct Approach to Measuring the Franck-Condon Barrier to Electron Transfer between Metal Ions. *J. Am. Chem. Soc.*, **91**, 3988-3989. (b) C. Creutz, C. (1983). Mixed Valence Complexes of d⁵-d⁶ Metal Centers. *Prog. Inorg. Chem.*, **30**, 1-73. (c) Creutz, C.; Newton, M. D., and Sutin, N. (1994). Metal-Ligand and Metal-Metal Coupling Elements. *J. Photochem. Photobiol. A: Chem.*, **82**, 47-59.
- [22] For further literature see: (a) Ward, M. D. (1995). Metal-Metal Interactions in Binuclear Complexes Exhibiting Mixed Valency; Molecular Wires and Switches. *Chem. Soc. Rev.*, **24**, 121-134. (b) Barlow, S., and O' Hare, D. (1997). Metal-Metal Interactions in Linked Metallocenes. *Chem. Rev.*, **97**, 637-669. (c) Whittall, I. R., McDonagh, A. M., Humphrey and M. G.; Samoc, M. (1998). Organometallic Complexes in Nonlinear Optics II: Third-Order Nonlinearities and Optical Limiting Studies. *Adv. Organomet. Chem.*, **43**, 349-405. (d) Astruc, D. (1997). From Organotransition-Metal Chemistry Toward Molecular Electronics: Electronic Communication Between Ligand-Bridged Metals. *Acc. Chem. Res.*, **30**, 383-391. (e) Skibar, W., Kopacka, H., Wurst, K., Salzmann, C., Ongania, K. H., de Biani, F. F., Zanello, P., and Bildstein, B. (2004). α,ω -Diferrocenyl Cumulene Molecular Wires. Synthesis, Spectroscopy, Structure, and Electrochemistry. *Organometallics*, **23**, 1024-1041. (f) Chung, M. C.; Gu, X.; Etzenhouser, R. A.; Spuches, A. M.; Rye, P. T.; Seetharaman, S. K.; Rose, D. J., Zubieta, J., and Sponsler, M. B. (2003). Intermetal Coupling in $[(\eta^5\text{-C}_5\text{R}_5)\text{Fe}(\text{dppe})]_2(\mu\text{-CH=CHCH=CH})$ and in Their Dicationic and Monocationic Mixed-Valence Forms.

Organometallics, 22, 3485-3494. (g) Zheng, Q.; Hampel, F., and Gladysz, J. A. (2004). Longitudinally Extended Molecular Wires Based upon PtC≡CC≡CC≡CC≡C Repeat Units: Iterative Syntheses of Functionalized Linear PtC₈Pt, PtC₈PtC₈Pt, and PtC₈PtC₈PtC₈Pt Assemblies. *Organometallics*, 23, 5896-5899. (h) Chanda, N.; Sarkar, B.; Fiedler, J.; Kaim, W., and Lahiri, C. K. (2003). Synthesis and Mixed Valence Aspects of $\{(\text{LClRu})_2(\mu\text{-tppz})\}^{n+}$ incorporating 2,2'-Dipyridylamine (L) as Ancillary and 2,3,5,6-Tetrakis(2-pyridyl)pyrazine (tppz) as Bridging Ligand. *Dalton Trans.*, 18, 3550-3555. (i) Venkatesan, K.; Blacque, O., and Berke, H. (2006). Metallacumulenes as Potential Electron Reservoir Devices. *Organometallics*, 25, 5190-5200. (j) Akita, M.; Sakurai, A.; Chung, M.-C., and Moro-oka, Y. (2003). Cluster Compounds Containing a Linear Carbon Chain Derived From Polyyneadiyl and Polyynyl Complexes, Fp^{*}-(C≡C)_n-X [X = Fp*, H; Fp^{*}=Fe(η^5 -C₅Me₅)(CO)₂]. *J. Organomet. Chem.*, 670, 2-10 and references cited therein. (k) Nguyen, P.; Gomez-Elipe, P., and Manners, I. (1999). Organometallic Polymers with Transition Metals in the Main Chain. *Chem. Rev.*, 99, 1515-1548. (l) Paul, F., and Lapinte C. (1998). Organometallic Molecular Wires and other Nanoscale-Sized Devices. An Approach Using the Organoiron (dppe)Cp^{*}Fe Building Block. *Coord. Chem. Rev.*, 178-180, 431-509. (m) Sauvage, J. P.; Collin, J. P.; Chambron, J. C.; Guillerez, S.; Coudret, C.; Balzani, V.; Barigelletti, F.; De Cola, L., and Flamigni, L. (1994). Ruthenium(II) and Osmium(II) Bis(terpyridine) Complexes in Covalently-Linked Multicomponent Systems: Synthesis, Electrochemical Behavior, Absorption Spectra, and Photochemical and Photophysical Properties. *Chem. Rev.*, 94, 993-1019. (n) Low, P. J., and Bruce, M. I. (2001). Transition Metal Chemistry of 1,3-Diynes, Polyynes, and Related Compounds. *Adv. Organomet. Chem.*, 48, 71-286. (o) Rigaut, S.; Massue, J.; Touchard, D.; Fillaut, J. L.; Golhen, S., and Dixneuf, P. H. (2002). Unprecedented Coupling of Allenylidene and Diynyl Metal Complexes: A Bimetallic Ruthenium System with a C₇ Conjugated Bridge. *Angew. Chem., Int. Ed.*, 41(23), 4513-4517. (p) Schwab, P. F. H.; Levin, M. D., and Michl, J. (1999). Molecular Rods. 1. Simple Axial Rods. *Chem. Rev.*, 99, 1863-1933. (q) Weyland, T.; Costuas, K.; Toupet, L.; Halet, J. F., and Lapinte, C. (2000). Organometallic Mixed-Valence Systems. Two-Center and Three-Center Compounds with *meta* Connections around a Central Phenylene Ring. *Organometallics*, 19, 4228-4239. (r) Ceccon, A.; Santi, S.; Orian, L., and Bisello, A. (2004). Electronic Communication in Heterobinuclear Organometallic Complexes through Unsaturated Hydrocarbon Bridges. *Coord. Chem. Rev.*, 248, 683-724. (s) Mantovani, N.; Brugnati, M.; Gonsalvi, L.; Grigiotti, E.; Laschi, F.; Marvelli, L.; Peruzzini, M.; Reginato, G.; Rossi, R., and Zanello, P. (2005). Synthesis, Characterization, and Electrochemical Behavior of Mono- and Bimetallic Ruthenium and Rhodium Allenylidenes Bearing Multiconjugated Organic Spacers. *Organometallics*, 24, 405-418. (t) Le Narvor, N., and Lapinte, C. (1993). First C₄ Bridged Mixed-Valence Iron(II)-Iron(III) Complex Delocalized on the Infrared TimeScale. *J. Chem. Soc., Chem. Commun.*, 4, 357-359. (u) Dewhurst, R. D.; Hill, A. F., and Willis, A. C. (2005). Stoichiometric and Catalytic Demercuration of Bis(tricarbido)mercurials: The First Dimetallaotatetraynes. *Organometallics*, 24, 3043-3046. (v) Roue, S.; Lapinte, C., and Bataille, T. (2005). Organometallic Mixed-Valence Systems. Electronic Coupling through an Alkyndiyl Bridge Incorporating Methylene Groups. *Organometallics*, 23, 2558-2567. (w) Coat, F.; Paul, F.; Lapinte, C.; Toupet, L.; Costuas, K., and Halet, J. F. (2003). Chemistry of the 1,3,5,7-Octatetracynediyl

Carbon Rod End-Capped by Two Electron-Rich ($\eta^5\text{-C}_5\text{Me}_5$)($\eta^2\text{-dppe}$)Fe Groups. *J. Organomet. Chem.*, 683, 368-378. (x) Roue, S.; Le Stang, S.; Toupet, L., and Lapinte, C. (2003). Magnetic Communication Between two [$(\eta^5\text{-C}_5\text{Me}_5)(\eta^2\text{-dppe})\text{Fe(III)}$] Units Mediated by the 2,5-Bis(ethynyl)thiophene Spacer. *C. R. Chim.*, 6, 353-366. (y) Jiao, H.; Costuas, K.; Gladysz, J. A.; Halet, J. F.; Guillemot, M.; Toupet, L.; Paul, F., and Lapinte, C. (2003). Bonding and Electronic Structure in Consanguineous and Conjugal Iron and Rhenium sp Carbon Chain Complexes $[\text{MC}_4\text{M}']^{n+}$: Computational Analyses of the Effect of the Metal. *J. Am. Chem. Soc.*, 125, 9511-9522. (z) Bruce, M. I.; Ellis, B. G.; Skelton, B. W., and White, A. H. (2005). Further Reactions of some Bis(vinylidene)diruthenium Complexes. *J. Organomet. Chem.*, 690, 792-801. (aa) Bruce, M. I.; Buntine, M. A.; Costuas, K.; Ellis, B. G.; Halet, J. F.; Low, P. J.; Skelton, B. W., and White, A. H. (2004). Some Ruthenium Complexes Containing Cyanocarbon Ligands: Syntheses, Structures and Extent of Electronic Communication in Binuclear Systems. *J. Organomet. Chem.*, 689, 3308-3326. (bb) Liu, S. H.; Xia, H.; Wan, K. L.; Yeung, R. C. Y.; Hu, Q. Y., and Jia, G. (2003). Synthesis of $[\text{TpRu}(\text{CO})(\text{PPh}_3)]_2(\mu\text{-CH=CH-CH=CH-C}_6\text{H}_4\text{-CH=CH-CH=CH})$ from Wittig Reactions. *J. Organomet. Chem.*, 683, 331-336. (cc) Cifuentes, M. P., and Humphrey, M. G. (2004). Alkynyl Compounds and Nonlinear Optics. *J. Organomet. Chem.*, 689, 3968-3981. (dd) Novikova, L. N.; Peterleitner, M. G.; Sevumyan, K. A.; Semeikin, O. V.; Valyaev, D. A.; Ustyuk, N. A.; Khrustalev, V. N.; Kuleshova, L. N., and Antipin, M. Y. (2001). Oxidative Dehydrodimerization of Manganese Phenylvinylidene Complex ($\eta^5\text{-C}_5\text{H}_5$)(CO)₂Mn=C=C(H)Ph. X-ray Structure of Phenyl(trityl)vinylidene Complex ($\eta^5\text{-C}_5\text{H}_5$)(CO)₂Mn=C=C(CPh₃)Ph. *J. Organomet. Chem.*, 631, 47-53. (ee) Vicente, J.; Chicote, M. T.; Alvarez-Falcon, M. M., and Bautista, D. (2004). The First Metal Complexes Derived from 3,5-Diethynylpyridine. X-ray Crystal Structure of $[(\text{AuPTo}_3)_2\{\mu\text{-(C}\equiv\text{C)}_2\text{Py}\}]$ (Py = Pyridine-3,5-diyl; To = *p*-Tolyl). *Organometallics*, 23, 5707-5712. (ff) Weyland, T.; Ledoux, I.; Brasselet, S.; Zyss, J., and Lapinte, C. (2000). Nonlinear Optical Properties of Redox-Active Mono-, Bi-, and Trimetallic σ -Acetylides Complexes Connected through a Phenyl Ring in the Cp*(dppe)Fe Series. An Example of Electro-Switchable NLO Response. *Organometallics*, 19, 5235-5237. (gg) Yam, V. W. W.; Tao, C. H.; Zhang, L.; Wong, K. M. C., and Cheung, K. K. (2001). Synthesis, Structural Characterization, and Luminescence Properties of Branched Palladium(II) and Platinum(II) Acetylides Complexes. *Organometallics*, 20, 453-459. (hh) Russo, M. V.; LoSterzo, C.; Franceschini, P.; Biagini, G., and Furlani, A. (2001). Synthesis of Highly Ethynylated Mono and Dinuclear Pt(II) Tethers Bearing the 4,4'-Bis(ethynyl)biphenyl (debp) Unit as Central Core. *J. Organomet. Chem.*, 619, 49-61. (ii) Hoshino, Y. (2001). Molecular Design for Long-Range Electronic Communication between Metals Polyyne and Ethynylated Aromatic Systems as Molecular Wires in Binuclear Ruthenium β -Diketone Complexes. *Platinum Met. Rev.*, 45, (1), 2-11. (jj) Meyer, W. E.; Amoroso, A. J.; Horn, C. R.; Jaeger, M., and Gladysz, J. A. (2001). Synthesis and Oxidation of Dirhenium C₄, C₆, and C₈ Complexes of the Formula ($\eta^5\text{-C}_5\text{Me}_5$)Re(NO)(PR₃)(C≡C)_n(R₃P)(ON)Re($\eta^5\text{-C}_5\text{Me}_5$) (R = 4-C₆H₄R', c-C₆H₁₁): In Search of Dications and Radical Cations with Enhanced Stabilities. *Organometallics*, 20, 1115-1127. (kk) Doppiu, A.; Minghetti, G.; Cinelli, M. A.; Stoccero, S.; Zucca, A., and Manassero, M. (2001). Unprecedented Behavior of 2,2':6',2' -Terpyridine:

Dinuclear Platinum(II) Derivatives with a New N,C⁺C,N Bridging Ligand. *Organometallics*, 20, 1148-1152. (ll) Matsuzaka, H.; Okimura, H.; Sato, Y.; Ishii, T.; Yamashita, M.; Kondo, M.; Kitagawa, S., and Shiro, M.; Yamasaki, M. (2001). Synthesis, Structure and Reactivities of the Dinuclear $\mu\text{-}\eta^1\text{:}\eta^6$ -Arylethynyl Ruthenium Complexes $[\text{Cp}(\text{PR}_3)_2\text{Ru}(\mu\text{-}\eta^1\text{:}\eta^6\text{-C}\equiv\text{CC}_6\text{H}_4\text{Me}-p)\text{RuCp}^*]\text{-Cl}$ ($\text{R} = \text{Ph, Me; Cp} = \eta^5\text{-C}_5\text{H}_5$, $\text{Cp}^* = \eta^5\text{-C}_5\text{Me}_5$). The Molecular Structure of $[\text{Cp}(\text{PPh}_3)_2\text{Ru}(\mu\text{-}\eta^1\text{:}\eta^6\text{-C}\equiv\text{CC}_6\text{H}_4\text{Me}-p)\text{RuCp}^*]\text{-PF}_6$. *J. Organomet. Chem.*, 625, 133-139. (mm) Ara, I.; Berenguer, J. R.; Eguizabal, E.; Fornies, J.; Gomez, J.; Lalinde, E., and Saez-Rocher, J. M. (2000). Synthesis, Photophysical Properties, and Theoretical Studies of Hydride-Alkynyl Platinum(II) Complexes. Molecular Structures of $[\text{trans-PtH(C}\equiv\text{CC}_5\text{H}_4\text{N-2)(PPh}_3)_2]$ and $[\text{Pt}(\eta^2\text{-HC}\equiv\text{CCPh}_2\text{OH})(\text{PPh}_3)_2]$. *Organometallics*, 19, 4385-4397. (nn) Hartmann, H.; Scheiring, T.; Fiedler, J., and Kaim, W. (2000). Structures and Spectroelectrochemistry (UV-vis, IR, EPR) of Complexes $[(\text{OC})_3\text{ClRe}]_n(\text{abpy})$, $n = 1, 2$; $\text{abpy} = 2,2'\text{-Azobispyridine}$. *J. Organomet. Chem.*, 604, 267-272. (oo) Hartbaum, C.; Mauz, E.; Roth, G.; Weissenbach, K., and Fischer, H. (1999). Bimetallic Complexes with Conjugated C_4 , C_6 , C_{10} , and C_{14} Bridges: Synthetic Routes to Alkynediyl-Bridged Bis(carbene) Complexes. *Organometallics*, 18, 2619-2627. (pp) Peters, T. B.; Bohling, J. C.; Arif, A. M., and Gladysz, J. A. (1999). C_8 and C_{12} sp Carbon Chains That Span Two Platinum Atoms: The First Structurally Characterized 1,3,5,7,9,11-Hexayne. *Organometallics*, 18, 3261-3263. (qq) Xia, H. P.; Ng, W. S.; Ye, J. S.; Li, X. Y.; Wong, W. T.; Lin, Z.; Yang, C., and Jia, G. (1999). Synthesis and Electrochemical Properties of C_5H -Bridged Bimetallic Iron, Ruthenium, and Osmium Complexes. *Organometallics*, 18, 4552-4557. (rr) Kheradmandan, S.; Heinze, K.; Schmalle, H. W., and Berke, H. (1999). Electronic Communication in C_4 -Bridged Binuclear Complexes with Paramagnetic Bisphosphane Manganese End Groups. *Angew. Chem. Int. Ed.*, 38, 2270-2273. (ss) Sato, M.; Iwai, A., and Watanabe, M. (1999). Synthesis and Redox Behavior of Ruthenium(II) 2,3,4,5-Tetramethylruthenocenylacetylide and Related Complexes. Formation of $\mu\text{-}\eta^6\text{:}\eta^1\text{-}[(\text{Cyclopentadienyldiene})\text{ethylidene}]\text{diruthenium}$ Complexes Containing a Strong Metal-Metal Interaction. *Organometallics*, 18, 3208-3219. (tt) Sakurai, A.; Akita, M., and Moro-oka, Y. (1999). Synthesis and Characterization of the Dodecahexaynediiron Complex, $\text{Fp}^*\text{-}(\text{C}\equiv\text{C})_6\text{-Fp}^*$ [$\text{Fp}^* = \text{Fe}(\eta^5\text{-C}_5\text{Me}_5)(\text{CO})_2$], the Longest Structurally Characterized Polyy nediy Complex. *Organometallics*, 18, 3241-3244. (uu) Glöckle, M., and Kaim, W. (1999). An Exceedingly Stable Diiron(II,III) Complex Ion $[(\text{tz})\{\text{Fe}(\text{CN})_5\}_2]^{5-}$ with Comproportionation Constants between 10^8 (in H_2O) and 10^{19} (in CH_3CN). *Angew. Chem. Int. Ed.*, 38, 3072-3074. (vv) Coat, F.; Guillemot, M.; Paul, F., and Lapinte, C. (1999). First Synthesis and Spectroscopic Characterization of Isolated Butatrienyldiene Complexes of Transition Metals. *J. Organomet. Chem.*, 578, 76-84. (ww) Akita, M.; Chung, M. C.; Sakurai, A.; Sugimoto, S.; Terada, M.; Tanaka, M., and Moro-oka, Y. (1997). Synthesis and Structure Determination of the Linear Conjugated Polyy nyl and Polyy nediy Iron Complexes $\text{Fp}^*\text{-}(\text{C}\equiv\text{C})_n\text{-X}$ ($\text{X} = \text{H}$ ($n = 1, 2$); $\text{X} = \text{Fp}^*$ ($n = 1, 2, 4$); $\text{Fp}^* = (\eta^5\text{-C}_5\text{Me}_5)\text{Fe}(\text{CO})_2$). *Organometallics*, 16, 4882-4888. (xx) Steenwinkel, P.; Grove, D. M.; Veldman, N.; Spek, A. L., and van Koten, G. (1998). Ionic 4,4'-Biphenylene-Bridged Bis-ruthenium Complexes $[\text{Ru}_2(4,4'\text{-}\{\text{C}_6\text{H}_2(\text{CH}_2\text{NMe}_2)_2\text{-2,6}\}_2)\text{(terpy)}_2]^{n+}$ ($n = 2$ and 4) and their Reversible Redox Interconversion: A Molecular Switch. *Organometallics*, 17, 5647-5655.

- [23] (a) Marcus, R. A., and Sutin, N. (1985). Electron Transfers in Chemistry and Biology. *Biochim. Biophys. Acta*, **811**, 233-322. (b) Hush, N. S. (1985). Distance Dependence of Electron Transfer Rates. *Coord. Chem. Rev.*, **64**, 135-157. (c) Coe, B. J. (1999). Molecular Materials Possessing Switchable Quadratic Nonlinear Optical Properties. *Chem. Eur. J.*, **5**, 2464-2471. (d) Bruce, M. I.; de Montigny, F.; Jevric, M.; Lapinte, C.; Skelton, B. W.; Smith, M. E., and White, A. H. (2004). Molecular Materials Possessing Switchable Quadratic Nonlinear Optical Properties. *J. Organomet. Chem.*, **689**, 2860-2871. (e) Weng, W.; Ramsden, J. A.; Arif, A. M., and Gladysz, J. A. (1993). A New Form of Coordinated Carbon: An Unsupported C₃ Chain Spanning Two Different Transition Metals. *J. Am. Chem. Soc.*, **115**, 3824-3825. (f) Bullock, R. M.; Femke, F. R., and Szalda, D. J. (1990). Complexes Containing a C₂ Bridge between an Electron-Rich Metal and an Electron-Deficient Metal. An Agostic Interaction in a RuCH₂CH₂Zr Moiety. *J. Am. Chem. Soc.*, **112**, 3244-3245. (g) Bürger, H., and Klüss, (1973). C. Titan-Stickstoff-Verbindungen XVII. σ-(Ferrocenyl)-Titan-Dialkylamide. *J. Organomet. Chem.*, **56**, 269-277. (h) Razuvayev, G. A.; Domrachev, G. A.; Sharutin, V. V., and Suvorova, O. N. (1977). Ferrocenyl Derivatives of Dicyclopentadienyl-Titanium, -Zirconium and -Hafnium. *J. Organomet. Chem.*, **141**, 313-317. (i) Zakharov, L. N.; Struchkov, V. T., Sharutin, V. V., and Suvorova, O. N. (1979). Crystal Structure of Diferrocenyltitanocene, C₃₀H₂₈Fe₂Ti. *Cryst. Struct. Commun.*, **8**, 439-444. (j) Dias, A. R.; Salema, M. S., and Simoes, J. A. M. (1982). Enthalpies of Formation of Bis(η⁵-cyclopentadienyl)diphenyltitanium and Bis(η⁵-cyclopentadienyl) Diferrocenyltitanium. *Organometallics*, **1**, 971-973. (k) Wedler, M.; Roesky, H. W., and Edelmann, F. T. (1988). Ferrocenyl Complexes of the Early Transition Metals - Synthesis and Structure. *Z. Naturforsch.*, **B43**, 1461-1467. (l) Lemke, F. R.; Szalda, D. J.; Bullock, R. M. (1991). Ruthenium/Zirconium Complexes Containing C₂ Bridges with Bond Orders of 3, 2, and 1. Synthesis and Structures of Cp(PMe₃)₂RuCH_nCH_nZrClCp₂ (*n* = 0, 1, 2). *J. Am. Chem. Soc.*, **113**, 8466-8477. (m) Gu, X., and Sponsler, M. B. (1998). Synthesis of Fe-C≡C-M Complexes through Condensation of Fe-C≡C-H with M-H or M-NMe₂. *Organometallics*, **17**, 5920-5923. (n) Mitani, M.; Hayakawa, M.; Yamada, T., and Mukaiyama, T. (1996). Novel Zirconium-Iron Multinuclear Complex Catalysts for Olefin Polymerizations. *Bull. Chem. Soc. Jpn.*, **69**, 2967-2976. (o) Qian, C.; Guo, J.; Sun, J.; Chen, J.; Zheng, P. (1997). Heterobimetallic Complexes with Phenylcyclopentadienyl Ligand: Syntheses and Structures of Tricarbonylchromium-η⁶,η⁵-Phenylcyclopentadienyl-Transition Metal Complexes. *Inorg. Chem.*, **36**, 1286-1295. (p) Weng, W.; Bartik, T., and Gladysz, J. A. (1994). On the Way to Coupling of Single Metals to One-Dimensional Carbon Wires: Charge Transfer between Terminal Rhenium and Manganese Centers in C₅-Cumulene. *Angew. Chem., Int. Ed. Engl.*, **33**, 2199-2202. (q) Stepnicka, P.; Podlaka, J.; Horacek, M.; Hanus, V., and Mach, K. (1999). A Directly Ring-to-Ring Linked Ferrocene-Pseudotitanocene Complex. *J. Organomet. Chem.*, **580**, 210-213. (r) Wong, W. Y.; Ho, K. Y.; Ho, S. L., and Lin, Z. (2003). Carbon-Rich Organometallic Materials Derived from 4-Ethynylphenyl-ferrocene. *J. Organomet. Chem.*, **683**, 341-353. (s) Yam, V. W. W.; Wong, K. M. C.; Chong, S. H. F.; Lau, V. C. Y.; Lam, S. C. F.; Zhang, L., and Cheung, K. K. (2003). Synthesis, Electrochemistry and Structural Characterization of Luminescent Rhenium(I) Monoynyl Complexes and their Homo- and Hetero-Metallic Binuclear Complexes. *J. Organomet. Chem.*, **670**, 205-220. (t) Launay, J. P. (2001). Long-

Distance Intervalence Electron Transfer. *Chem. Soc. Rev.*, 30, 386-397. (u) Brunschwig, B. S., and Sutin, N. (1999). Energy Surfaces, Reorganization Energies, and Coupling Elements in Electron Transfer. *Coord. Chem. Rev.*, 187, 233-254. (v) Wong, K. M. C.; Lam, S. C. F.; Ko, C. C.; Zhu, N.; Yam, V. W. W.; Roue, S.; Lapinte, C.; Fathallah, S.; Costuas, K.; Kahlal, S., and Halet, J. F. (2003). Electroswitchable Photoluminescence Activity: Synthesis, Spectroscopy, Electrochemistry, Photophysics, and X-ray Crystal and Electronic Structures of [Re(bpy)(CO)₃(C≡C-C₆H₄-C≡C)-Fe(C₅Me₅)(dppe)][PF₆]_n ($n = 0, 1$). *Inorg. Chem.*, 42, 7086-7097. (w) Paul, F.; Meyer, W. E.; Toupet, L.; Jiao, H.; Gladysz, J. A., and Lapinte, C. (2000). A "Conjugal" Consanguineous Family of Butadiynediyl-Derived Complexes: Synthesis and Electronic Ground States of Neutral, Radical Cationic, and Dicationic Iron/Rhenium C₄ Species. *J. Am. Chem. Soc.*, 122, 9405-9414. (x) Wheatley, N., and Kalck, P. (1999). Structure and Reactivity of Early-Late Heterobimetallic Complexes. *Chem. Rev.*, 99, 3379-3419. (y) Guo, J. H., and Qian, C. T. (1996). Synthesis and Reactivity of Heterobimetallic Complexes. *Youji Huaxue*, 16, 301-309. (z) Kuwabara, J.; Takeuchi, D., and Osakada, K. (2004). Preparation and Properties of Cp₂Zr(μ -N=CAr₂)₂PdCl(Me), New Zr/Pd Heterobimetallic Complexes with Bridging Alkylideneamido Ligands. *Organometallics*, 23, 5092-5095. (aa) Berenguer, J. R.; Bernechea, M.; Fornie's, J.; Garcia, A., and Lalinde, E. (2004). (*p*-Cymene)-Ruthenium(II)(diphenylphosphino)alkyne Complexes: Preparation of (μ -Cl)(μ -PPh₂C≡CR)-Bridged Ru/Pt Heterobimetallic Complexes. *Organometallics*, 23, 4288-4300. (bb) Gauthier, S.; Quebatte, L.; Scopelliti, R., and Severin, K. (2004). Syntheses and Structures of Homo- and Heterobimetallic, Chloro-Bridged Complexes Containing the RuCl₃(AsPh₃)_n Fragment ($n = 1, 2$). *Inorg. Chem. Commun.*, 7, 708-712. (cc) Thurston, J. H.; Tang, C. G. Z.; Trahan, D. W., and Whitmire, K. H. (2004). Toward Rational Control of Metal Stoichiometry in Heterobimetallic Coordination Complexes: Synthesis and Characterization of Pb(Hsal)₂(Cu(salen*))₂, [Pb(NO₃)(Cu(salen*))₂]-NO₃, Pb(OAc)₂(Cu(salen*)), and [Pb(OAc)(Ni(salen*))₂](OAc). *Inorg. Chem.*, 43, 2708-2713. (dd) Yang, Y.; Abboud, K. A., and McElwee-White, L. (2003). Heterobimetallic Complexes with dppm-Bridged Ru/Pd, Ru/Pt, Ru/Au and Ru/Cu Centers. *Dalton Trans.*, 22, 4288-4296. (ee) Berenguer, J. R.; Fornie's, J.; Lalinde, E., and Martinez, F. (1996). Reactions of (σ -Alkynyl)platinum Complexes with [Pd(η ³-C₃H₅)Cl]₂. Synthesis of Bis(η ²-alkyne)(η ³-allyl)palladium(II) Complexes. Crystal and Molecular Structure of [*cis*-(PPh₃)₂Pt(μ - η ¹: η ²-C≡C^tBu)₂Pd(η ³-C₃H₅)](ClO₄). *Organometallics*, 15, 4537-4546. (ff) Dennett, J. N. L.; Knox, S. A. R.; Anderson, K. M.; Charmant, J. P. H., and Orpen, A. G. (2005). The Synthesis of [FeRu(CO)₂(μ -CO)₂(η -C₅H₅)(η -C₅Me₅)] and Convenient Entries to its Organometallic Chemistry. *Dalton Trans.*, 1, 63-73. (gg) Friedrich, H. B.; Howie, R. A.; Laing, M., and Onani, M. O. (2004). Transition Metal-Substituted Paraffins: Synthesis and Properties of some μ -Saturated Heterobimetallic Complexes Containing Mo and W or Fe and the Crystal Structures of [(η ⁵-C₅H₅)(CO)₃W(CH₂)₃Mo(CO)₂(PPh₃)(η ⁵-C₅H₅)] and [(η ⁵-C₅H₅)(CO)₂(PPh₃)Mo(CH₂)₃Fe(CO)₂(η ⁵-C₅H₅)]. *J. Organomet. Chem.*, 689, 181-193. (hh) Li, Q. S.; Xu, F. B.; Cui, D. J.; Yu, K.; Zeng, X. S.; Leng, X. B.; Song, H. B., and Zhang, Z. Z. (2003). Heterobimetallic Pt(II)-M(I) (M = Cu, Ag) Eight-Membered Macrocyclic Complexes with Large-Bite P,N-Ligand Bridges. *Dalton Trans.*, 8, 1551-1557. (ii) Fornie's-Camer, J.; Claver, C.; Masdeu-Bulto, A. M., and Cardin, C. J.

(2002). New Half-Sandwich Heterobimetallic CpMPt (M = Rh, Ir) Dithiolato Bridged Complexes. X-Ray Structure of $[(\text{PPh}_3)_2\text{Pt}(\mu\text{-S}(\text{CH}_2)_2\text{S})\text{RhCl}(\eta^5\text{-C}_5\text{H}_5)]\text{BF}_4$. *J. Organomet. Chem.*, 662, 188-191. (jj) Meichel, E.; Stein, T.; Kralik, J.; Rheinwald, G., and Lang, H. (2002). Synthese von $[(\eta^5\text{-C}_5\text{H}_5)_2\text{Ti}(\text{Cl})(\text{C}\equiv\text{CSiMe}_3)]\text{Ni}(\text{CO})$ und dessen Reaktionsverhalten gegenüber Phosphiten: die Festkörperstruktur von $(\text{CO})_2\text{Ni}[\text{P}(\text{OC}_6\text{H}_4\text{CH}_3-2)_3]_2$. *J. Organomet. Chem.*, 649, 191-198. (kk) Le Gendre, P.; Picquet, M.; Richard, P., and Moise, C. (2002). Ti-Ru Bimetallic Complexes: Catalysts for Ring-Closing Metathesis. *J. Organomet. Chem.*, 643-644, 231-236. (ll) Burgos, F.; Chavez, I.; Manriquez, J. M.; Valderrama, M.; Lago, E.; Molins, E.; Delpech, F.; Castel, A., and Rivière, P. (2001). A New Heterobimetallic Ru, Rh Complex with a Dianionic Pentalene as Bridging Ligand. Synthesis, Crystal Structure, and Catalytic Activity of $[\text{Cp}^*\text{Ru}(\mu\text{-}\eta^5,\eta^3\text{-C}_8\text{H}_6)\text{Rh}(\eta^4\text{-COD})]$. *Organometallics*, 20, 1287-1291. (mm) Bruce, M. I.; De Montigny, F.; Jevric, M.; Lapinte, C.; Skelton, B. W.; Smith, M. E., and White, A. H. (2004). Synthesis, Structures and some Reactions of $\text{Ru}(\text{C}\equiv\text{CC}\equiv\text{CFc})(\text{PP})\text{Cp}$ (PP = dppm, dppe) and Related Compounds. *J. Organomet. Chem.*, 689, 2860-2871. (nn) Bruce, M. I., and Low, P. J. (2004). Transition Metal Complexes Containing All-Carbon Ligands. *Adv. Organomet. Chem.*, 50, 179-444. (oo) Antonova, A. B.; Bruce, M. I.; Ellis, B. G.; Gaudio, M.; Humphrey, P. A.; Jevric, M.; Melino, G.; Nicholson, B. K.; Perkins, G. J.; Skelton, B. W.; Stapleton, B.; White, A. H., and Zaitseva, N. N. (2004). A Novel Methodology for the Synthesis of Complexes Containing Long Carbon Chains Linking Metal Centres: Molecular Structures of $\{\text{Ru}(\text{dppe})\text{Cp}^*\}_2(\mu\text{-C}_{14})$ and $\{\text{Co}_3(\mu\text{-dppm})(\text{CO})_7\}_2(\mu_3\text{:}\mu_3\text{-C}_{16})$. *Chem. Commun.*, 8, 960-961. (pp) Bruce, M. I.; Skelton, B. W.; White, A. H., and Zaitseva, N. N. (2003). Preparation and Molecular Structures of some Complexes Containing C_5 Chains. *J. Organomet. Chem.*, 683, 398-405. (qq) Low, P. J., and Bruce, M. I. (2001). Transition Metal Chemistry of 1,3-Diynes, Poly-ynes, and Related Compounds. *Adv. Organomet. Chem.*, 48, 71-286. (rr) Bruce, M. I.; Ellis, B. G.; Gaudio, M.; Lapinte, C.; Melino, G.; Paul, F.; Skelton, B. W.; Smith, M. E.; Toupet, L., and White, A. H. (2004). Preparation, Structures and some Reactions of Novel Diynyl Complexes of Iron and Ruthenium. *Dalton Trans.*, 10, 1601-1609. (ss) Bruce, M. I.; Hall, B. C.; Low, P. J.; Smith, M. E.; Skelton, B. W., and White, A. H. (2000). Heterometallic Complexes Containing C_4 Chains. X-Ray Structures of $\{\text{Cp}(\text{OC})_3\text{W}\}\text{C}\equiv\text{C-C}\equiv\text{C}\{\text{Ir}(\text{CO})(\text{PPh}_3)_2\text{-}(\text{O}_2)\}$ and *cis*- $\text{Pt}\{\text{C}\equiv\text{CC}\equiv\text{C}[\text{W}(\text{CO})_3\text{Cp}]\}_2(\text{PEt}_3)_2$. *Inorg. Chim. Acta*, 300-302, 633-644. (tt) Cheung, K. L.; Yip, S. K., and Yam, V. W. W. (2004). Synthesis, Characterization, Electrochemistry and Luminescence Studies of Heterometallic Gold(I)-Rhenium(I) Alkynyl Complexes. *J. Organomet. Chem.*, 689, 4451-4462. (uu) Enders, M.; Kohl, G., and Pritzkow, H. (2002). Novel Heterobimetallic Compounds with Metal-Metal Bonds: The Use of Quinolyl-Substituted Metallocenes as Tridentate Ligands. *Organometallics*, 21, 1111-1117. (vv) Dewhurst, R. D.; Hill, A. F., and Smith, M. K. (2004). Heterobimetallic C_3 Complexes through Silylpropargylidyne Desilylation. *Angew. Chem. Int. Ed.*, 43, 476-478. (ww) Pizzotti, M.; Ugo, R.; Roberto, D.; Bruni, S.; Fantucci, P., and Rovizzi, C. (2002). Organometallic Counterparts of Push-Pull Aromatic Chromophores for Nonlinear Optics: Push-Pull Heteronuclear Bimetallic Complexes with Pyrazine and *trans*-1,2-Bis(4-pyridyl)ethylene as Linkers. *Organometallics*, 21, 5830-5840. (xx) Zhang, L. Y.; Chen, J. L.; Shi, L. X., and Chen, Z. N. (2002). Utilizing Diruthenium Components for the Design of Cyanide-Linked Tri- and Tetranuclear Organometallic

Complexes with Multistep One-Electron Redox Processes. *Organometallics*, 21, 5919-5925. (yy) Adams, C. J., and Raithby, P. R. (1999). Novel Mixed-Metal-Alkynyl Complexes Stabilised by Di-Imine Ligands: Synthesis, Characterisation and Electrochemistry of [(*t*Bu₂bipy)Pt(C≡CR)₂M(SCN)] (R = C₆H₄Me, SiMe₃; M = Cu, Ag). *J. Organomet. Chem.*, 578, 178-185. (zz) Thomas, K. R. J.; Lin, J. T.; Lin, H. M.; Chang, C. P., and Chuen, C. H. (2001). Ruthenium and Rhodium Complexes of Fluorene-Based Bipyridine Ligands: Synthesis, Spectra, and Electrochemistry. *Organometallics*, 20, 557-563. (aaa) Prim, D.; Auffrant, A.; Plyta, Z. F.; Tranchier, J. P.; Rose-Munch, F., and Rose, E. (2001). Bimetallic π -Conjugated Complexes Modulated by a Carbonyl Spacer: Synthesis of Arenetricarbonylchromium–Ferrocene Derivatives. *J. Organomet. Chem.*, 624, 124-130. (bbb) Richardson, G. N., and Vahrenkamp, H. (2000). Cyanide Bridged Trinuclear Complexes with Fe-CN-MCl₂-NC-Fe Backbones (M = Ni, Cu, Zn). *J. Organomet. Chem.*, 593-594, 44-48. (ccc) Low, P. J.; Rousseau, R.; Lam, P.; Udachin, K. A.; Enright, G. D.; Tse, J. S.; Wayner, D. D. M., and Carty, A. J. (1999). Polycarbon Ligand Chemistry: Electronic Interactions between a Mononuclear Ruthenium Fragment and a Cobalt-Carbon Cluster Core. *Organometallics*, 18, 3885-3897. (ddd) Bruce, M. I.; Hall, B. C.; Low, P. J.; Skelton, B. W., and White, A. H. (1999). Some Ruthenium Complexes Derived from 1,4-Diethynylbenzene: Molecular Structure of Ru{ η^3 -C[=C(CN)₂]C(C₆H₄C≡CH-4)=C(CN)₂}(PPh₃)Cp. *J. Organomet. Chem.*, 592, 74-83. (eee) Briel, O.; Fehn, A., and Beck, W. (1999). Hydrocarbon Bridged Metal Complexes XLV. Dinuclear Polyene-Bridged Fischer Carbene Complexes and a Star-Shaped Benzene-Bridged Tris(ferrocenyldecapentaenyl) Compound. *J. Organomet. Chem.*, 578, 247-251. (fff) Colbert, M. C. B.; Lewis, J.; Long, N. J.; Raithby, P. R.; White, A. J. P., and Williams, D. J. (1997). Synthetic, Structural, Electrochemical and Electronic Characterisation of Heterobimetallic Bis(acetylide) Ferrocene Complexes. *J. Chem. Soc., Dalton Trans.*, 99-104. (ggg) Lin, J. T.; Wu, J. J.; Li, C. S.; Wen, Y. S., and Lin, K. J. (1996). Conjugated Pyridines with an End-Capping Ferrocene. *Organometallics*, 15, 5028-5034. (hhh) Le Stang, S. L.; Lenz, D.; Paul, F., and Lapinte, C. (1999). New Pyridyl-Functionalized Organoiron Alkynyl Complexes. Easy Access to Polymetallic Architectures Featuring an Electroactive Site by Simple Coordination Reactions. *J. Organomet. Chem.*, 572, 189-192. (iii) Stepnicka, P.; Gyepes, R., and Cisarova, I. (1999). Synthesis and Structure of Titanocene Complexes with η^2 -Coordinated Internal Ferrocenylacetylenes. *Organometallics*, 18, 627-633.

- [24] (a) Laus, G.; Strasser, C. E.; Holzer, M.; Wurst, K.; Pürstinger, G.; Ongania, K.-H.; Rauch, M.; Bonn, G., and Schottenberger, H. (2005). The (*E*)-2-Ferrocenyl-ethenylcobaltocenium Cation. A Missing Link in Heteronuclear Bimetallocene-Based Donor-Acceptor Conjugate Chemistry Exhibiting Irregular Solvatochromism. *Organometallics*, 24, 6085-6093 (b) Obendorf, D.; Reichart, E; Rieker, C., and Schottenberger, H. (1994) Voltammetric Study of some Metallocene-Substituted (η^4 -1,3-Cyclopentadiene-5-exo-yl) Cobalt Complexes; ([CpCo(η^4 -C₅H₅R)], R = -C≡C-(η^5 -C₅H₄)FeCp; -(η^5 -C₅H₄)FeCp; -(η^5 C₅H₄)NiCp). *Electrochimica Acta*, 39, 2367-2375. (c) Wildschek, M.; Rieker, C.; Jaitner, P; Schottenberger, H., and Schwarzhans, K. E. (1990). Ethynylcobaltocenium Compounds as Precursors for Bridged, Heteronuclear Oligometallocenes: Preparation and Reactions of Ethynyl-,

- trimethylsilyl ethynyl- and Ferrocenylethynylcobaltocenium Salts. *J. Organomet. Chem.*, 396, 355-361.
- [25] Bartik, T.; Weng, W.; Ramsden, J. A.; Szafert, S.; Falloon, S. B.; Arif, A. M., and Gladysz, J. A. (1998). New Forms of Coordinated Carbon: Wirelike Cumulenic C₃ and C₅ sp Carbon Chains that Span Two Different Transition Metals and Mediate Charge Transfer. *J. Am. Chem. Soc.*, 120, 11071-11081.
- [26] (a) Venkatesan, K.; Fox, T.; Schmalle, H. W., and Berke, H. (2005). Synthesis and Characterization of Redox-Active C₄-Bridged Rigid-Rod Complexes with Acetylide-Substituted Manganese End Groups. *Organometallics*, 24, 2834-2847. (b) Venkatesan, K.; Blacque, O.; Fox, T.; Alfonso, M.; Schmalle, H. W., and Berke, H. (2004). Synthetic Access to Half-Sandwich Manganese C₄ Cumulenic Complexes. *Organometallics*, 23, 4646-4671. (c) Fernández, F. J.; Venkatesan, K.; Blacque, O.; Alfonso, M.; Schmalle, H. W., and Berke, H. (2003). Generation and Coupling of [Mn(dmpe)₂(C≡CR)(C≡C)][·] Radicals Producing Redox-Active C₄-Bridged Rigid-Rod Complexes. *Chem. Eur. J.*, 9, 6192-6206. (d) Venkatesan, K.; Fox, T.; Schmalle, H. W., and Berke, H. (2005). New Access to Homodinuclear Half-Sandwich Vinylidene-manganese Complexes. *Eur. J. Inorg. Chem.*, 901-909. (e) Venkatesan, K.; Blacque, O.; Fox, T.; Alfonso, M.; Schmalle, H. W.; Kheradmandan, S., and Berke, H. (2005). μ -Carbon-Carbon Bonds of Dinuclear Manganese Half-Sandwich Complexes as Electron Reservoirs. *Organometallics*, 24, 920-932.
- [27] Kheradmandan, S.; Venkatesan, K.; Blacque, O.; Schmalle, H. W., and Berke, H. (2004). Facile Access to Redox-Active C₂-Bridged Complexes with Half-Sandwich Manganese End Groups. *Chem. Eur. J.*, 10, 4872-4885.
- [28] (a) Herrmann, C.; Neugebauer, J.; Gladysz, J. A., and Reiher, M. (2005). Theoretical Study on the Spin-State Energy Splittings and Local Spin in Cationic [Re]-C_n-[Re] Complexes. *Inorg. Chem.*, 44, 6174-6182. (b) Neugebauer, J., and Reiher, M. Mode (2004). Tracking of Preselected Vibrations of One-Dimensional Molecular Wires. *J. Phys. Chem. A*, 108, 2053-2061. (c) Horn, C. R., and Gladysz, J. A. (2003). Syntheses of Dimetallamacrocycles by Intramolecular Oxidative Couplings of Dinuclear Bis(1,3-butadiynyl) Complexes: A New Approach to Steric Shielding in (sp-Carbon chain)dirhenium Complexes [(η^5 -C₅Me₅)Re(NO)(PR₃)(C≡CC≡CC≡C)(R₃P)(ON)-Re(η^5 -C₅Me₅)]. *Eur. J. Inorg. Chem.*, 2211-2218.
- [29] (a) Smith, M. E.; Cordiner, R. L.; Albesa-Jové, D.; Yufit, D. S.; Hartl, F.; Howard, J. A. K., and Low, P. J. (2006). The Synthesis, Structure, and Electrochemical Properties of Fe(C≡CC≡N)(dppe)Cp and Related Compounds. *Can. J. Chem.*, 84, 154-163. (b) Low, P. L.; Roberts, R. L.; Cordiner, R. L., and Hartl, F. (2005). Electrochemical Studies of Bi- and Polymetallic Complexes Featuring Acetylido Based Bridging Ligands. *J. Solid State Electrochem.*, 9, 717-731 (c) Cordiner, R. L. Corcoran, D.; Yufit, D. S.; Goeta, A. E.; Howard, J. A. K., and Low, P. J. (2003). Cyanoacetylenes and Cyanoacetylides: Versatile Ligands in Organometallic Chemistry. *Dalton Trans.*, 3541-3549.
- [30] LeVanda, C.; Cowan, D. O.; Leitch, C., and Bechgaard, K. (1974). Mixed-Valence Diferrocenylacetylene Cation. *J. Am. Chem. Soc.*, 96, 6788-6789.
- [31] (a) Y. Masuda, Y., and Shimizu, C. (2006). Solvent Effect on Intramolecular Electron Transfer Rates of Mixed-Valence Biferrocene Monocation Derivatives. *J. Phys. Chem.*, 110, 7019-7027. (b) Jiao, J.; Long, G. J.; Rebbouh, L.; Grandjean, F.; Beatty, A. M., and Fehlner, T. P. (2005). Properties of a Mixed-Valence (Fe^{II})₂(Fe^{III})₂ Square Cell for

Utilization in the Quantum Cellular Automata Paradigm for Molecular Electronics. *J. Am. Chem. Soc.*, **127**, 17819-17831. (c) Kramer, J. A., and Hendrickson, D. N. (1980). Electron Transfer in Mixed-Valent Diferrocenylacetylene and [2.2]-Ferrocenophane-1,13-diyne. *Inorg. Chem.*, **19**, 3330-3337. (d) Brady, M.; Weng, W.; Zhou, Y.; Seyler, J. W.; Amoroso; A. J.; Arif, A. M. Böhme, M.; Frenking, G., and Gladysz, J. A. (1997). Consanguineous Families of Coordinated Carbon: A ReC₄Re Assembly That is Isolable in Three Oxidation States, Including Crystallographically Characterized ReC≡CC≡CRe and ⁺Re=C=C=C=Re⁺ Adducts and a Radical Cation in which Charge is Delocalized between Rhenium Termini. *J. Am. Chem. Soc.*, **119**, 775-788.

- [32] (a) Mochida, T., and Yamazaki, S. (2002). Mono- and Diferrocenyl Complexes with Electron-Accepting Moieties Formed by the Reaction of Ferrocenylalkynes with Tetracyanoethylene. *J. Chem. Soc., Dalton Trans.*, 3559-3564. (b) Levanda, C. Bechgaard, K., and Cowan D. O. (1976). Mixed Valence Cations. Chemistry of n-Bridged Analogues of Biferrocene and Biferrocenylene. *J. Org. Chem.*, **41**, 2700-2704. (c) Adams, R. D.; Qu, B.; Smith, M. D., and Albright, T. A. (2002). Syntheses, Structures, Bonding, and Redox Behavior of 1,4-Bis(ferrocenyl)butadiyne Coordinated Osmium Clusters. *Organometallics*, **21**, 2970-2978. (d) McAdam, C. J.; Brunton, J. J.; Robinson, B. H., and Simpson, J. (1999). Ferrocenylethynylnaphthalenes and Acenaphthylenes; Communication Between Ferrocenyl and Cluster Redox Centres. *J. Chem. Soc. Dalton Trans.*, 2487-2496. (e) Jutzi, P., and Kleinebekel, B. (1997). Octamethylferrocenylethynyl Units as Peripheral Groups in Rigid, π -Conjugated Molecular Architectures. *J. Organomet. Chem.*, **545-546**, 573. (f) Levanda, C.; Cowan, D. O.; Leitch, C., and Bechgaard, K. (1974). Mixed-Valence Diferrocenylacetylene Cation. *J. Am. Chem. Soc.*, **96**, 6788-6789. (g) McManis, G. E.; Gochev, A.; Nielson, R. M., and Weaver, M. J. (1989). Solvent Effects on Intervalence Electron-Transfer Energies for Biferrocene Cations: Comparisons with Molecular Models of Solvent Reorganization. *J. Phys. Chem.*, **93**, 7733-7739. (h) Delgado-Pena, F.; Talham, D. R., and Cowan, D. O. (1983). Near-IR Spectroscopic Studies of Mixed-Valence Di-, Tri-, and Tetraferrocene Derivatives. *J. Organomet. Chem.*, **253**, C43-C46. (i) Powers, M. J. Meyer, T. J. (1978). Intervalence Transfer in Mixed-Valence Biferrocene Ions. *J Am. Chem. Soc.*, **100**, 4393-4398.
- [33] Schimanke, H., and Gleiter, R. (1998). Synthesis and Electrochemical Properties of Butadiyne-Bridged Cyclopentadienylcobalt-Cyclobutadiene Complexes. *Organometallics*, **17**, 275-277.
- [34] (a) Hore, L.-A.; John McAdam, C.; Kerr, J. L.; Duffy, N. W.; Robinson, B. H., and Simpson, J. (2000). Communication between Co₂(CO)₄dppm Units via Polyferrocenylalkyne Linkages. *Organometallics*, **19**, 5039-5048. (b) Richardson, D. E., and Taube, H. (1981). Determination of E20-E10 in Multistep Charge Transfer by Stationary-Electrode Pulse and Cyclic Voltammetry: Application to Binuclear Ruthenium Ammines. *Inorg. Chem.*, **20**, 1278-1285. (c) Cotton, F. A.; Donohue, J. P., and Murillo, C. A. (2003). Polyunsaturated Dicarboxylate Tethers Connecting Dimolybdenum Redox and Chromophoric Centers: Syntheses, Structures, and Electrochemistry. *J. Am. Chem. Soc.*, **125**, 5436-5450. (d) Berry, J. F.; Cotton, F. A., and Murillo, C. A. (2004). A Trinuclear EMAC-Type Molecular Wire with Redox-Active Ferrocenylacetylide "Alligator Clips" Attached. *Organometallics*, **23**, 2503-2506. (e) Sheng, T.; Appelt, R.; Comte, V., and Vahrenkamp, H. (2003). Chain-Like

- Tetra-, Penta- and Heptanuclear Cyanide-Bridged Complexes by Attachment of Organometallic Cyanides to M₂, M₃ and M₅ Units. *Eur. J. Inorg. Chem.*, 3731-3737.
- [35] Köcher, S. (2000). Mehrkernige Übergangsmetallkomplexe: Synthese, Reaktionsverhalten und elektronische Eigenschaften. Diploma Thesis, TU Chemnitz.
- [36] Hayashi, Y.; Osawa, M., and Wakatsuki, Y. (1997). Reductive Coupling Reaction Induced by Remote-Site Oxidation in Titanocene Bis(metallocenylacetylides), where Metallocenyl = Ferrocenyl or Ruthenocenyl: a Novel Route to C_n (n = 4, 6, and 8) Wire with the Metallocenyl Groups at Both Terminals. *J. Organomet. Chem.*, 542, 241-246.
- [37] Wetzold, N. (2003). Synthese Lewis-Basen-stabilisierter Bis(alkinyl)-Platin-Komplexe und deren Reaktionsverhalten. Diploma Thesis, TU Chemnitz.
- [38] (a) Osella, D.; Milone, L.; Nervi, C., and Ravera, M. (1995). Electronic Interactions in Organometallic Dimers. An Electrochemical Approach. *J. Organomet. Chem.*, 488, 1-7. (b) Osella, D.; Gobetto, R.; Nervi, C.; Ravera, M.; D'Amato, R., and Russo, M. V. (1998). Synthesis and Characterisation of Bis(ferrocenylethynyl) Complexes of Platinum (II) a Re-Investigation of their Electrochemical Behaviour. *Inorg. Chem. Commun.*, 1, 239-245. (c) Russo, M. V., and Furlani, A. (1994). Synthesis of some Bis(triphenylphosphine)(ethynylferrocenyl) Platinum(II) Complexes; Molecular Structure of [PtH(C≡C-C₅H₄FeC₅H₅)(PPh₃)₂]. *J. Organomet. Chem.*, 469, 245-252.
- [39] (a) Müller, T. J. J., and Lindner, H. J. (1996). Palladium-Copper-Catalyzed Coupling of Tricarbonylchromium-Complexed Phenylacetylene with Iodoarenes. A Facile Access to Alkynyl-Bridged Cr(CO)₃-Complexed Benzenes. *Chem. Ber.*, 129, 607-613. (b) Müller, T. J. J.; Ansorge, M., and Lindner, H. J. (1996). Synthesis and Substituent Interactions of Tricarbonylchromium-Complexed (Arylalkynyl)benzenes. Novel Organometallic Push-Pull Chromophores. *Chem. Ber.*, 129, 1433-1440. (c) Müller, T. J. J. (1999). Redox Active Alkenyl-Bridged Bi- and Trinuclear Arene-Cr(CO)₃-Complexes by Horner-Emmons-Wadsworth Olefinations. *J. Organomet. Chem.*, 578, 95. (d) Müller, T. J. J.; Netz, A.; Ansorge, M.; Schmälzlin, E.; Bräuchle, C., and Meerholz, K. (1999). Syntheses and NLO Properties of Chromium Carbonyl Arene Complexes with Conjugated Side Chains: The Amphoteric Nature of Chromium Carbonyl Complexation in Push-Pull Chromophores. *Organometallics*, 18, 5066.
- [40] Friedrich, D. (2006). Alkinyl-Übergangsmetallkomplexe: Synthese und Reaktionverhalten. Diploma Thesis, TU Chemnitz.
- [41] Sato, M., and Emiko, M. (1995). Unprecedented Promoting Effect of a Ferrocenyl Group for the Oxidatively Induced Reductive Elimination in cis-Aryl(ferrocenyl acetylidy)platinum(II) Complexes. *Organometallics*, 14, 3157-3159.
- [42] Kirchbauer, F. G.; Pellny, P.-M.; Sun, H.; Burlakov, V. V.; Arndt, P.; Baumann, W.; Spannenberg, A., and Rosenthal, U. (2001). Synthesis and Reactions with Carbon Dioxide of Mono(σ -alkynyl) Titanocene(III) Complexes Cp*₂Ti(C≡CR) (R = Me, t-Bu) and the Corresponding "Ate" Complexes [Cp*₂Ti(C≡CR)₂Li(THF)_n] (R = SiMe₃, t-Bu, Ph). *Organometallics*, 20, 5289-5296.
- [43] Erker, G.; Frömberg, W.; Benn, R.; Mynott, R.; Angermund, K., and Krüger, C. (1989). π -Conjugation and Dynamic Behavior in Doubly Acetylidy-Bridged Binuclear Group 4 Bent Metallocene Complexes. *Organometallics*, 8, 911-920.
- [44] Back, S.; Gossage, R. A.; Rheinwald, G.; Lang, H., and van Koten, G. (1999). Titanium σ -Acetylides as Building Blocks for Heterobimetallic Transition Metal Complexes:

Synthesis and Redox Behaviour of π -Conjugated Organometallic Systems. *J. Organomet. Chem.*, 582, 126.

- [45] Lang, H., and Stein, T. (2001). Bis(alkynyl)-Titanium and -Platinum Complexes in the Synthesis of Oligo- and Polynuclear Early-Late and/or Late-Late Transition Metal Species: An Overview. *Abhath Al-Yarmouk: Basic Sci. Eng.*, 10, 155; *Chem. Abstr.* (2001), 142, 38297.
- [46] Lemket, F. R., and Bullock, R. M. (1992). Insertion and Beta-Hydride Elimination Reactions of Ruthenium/Zirconium Complexes Containing C₂ Bridges with Bond Orders of 1, 2, and 3. *Organometallics*, 11, 4261-4267.
- [47] Back, S.; Gossage, R. A.; Lutz, M.; del Rio, I.; Spek, A. L.; Lang, H., and van Koten, G. (2000). Bis-*ortho*-chelated Diaminoaryl Platinum Compounds with -Acetylene Substituents. Investigations into Their Stability and Subsequent Construction of Multimetallic Systems. The Crystal Structure of $[(\mu^2-[(\eta^2\text{-NCN})\text{Pt}(\eta^1\text{-CO})\text{C}\equiv\text{C-SiMe}_3])\text{Co}_2(\text{CO})_6]$ (NCN = 2,6-Bis[(dimethylamino)methyl]phenyl). *Organometallics*, 19, 3296-3304.
- [48] Packheiser, R. (2003). Multimetallische Übergangsmetallkomplexe mit π -konjugierten organischen Bausteinen. Diploma Thesis, TU Chemnitz.
- [49] Köcher, S. (2007). Ph.D. Thesis, TU Chemnitz.
- [50] Köcher, S.; Walfort, B.; Lutz, M.; Spek, L. A.; Prasad, R.; van Koten, G., and Lang, H. Submitted for publication in *J. Organomet. Chem.*
- [51] Frosch, W.; Back, S.; del Río, I.; van Koten, G., and Lang, H. (1999). An Easy Entry to Novel Early–Late Oligonuclear Transition Metal Complexes Containing π -Conjugated Systems. *Inorg. Chem. Commun.*, 2, 584-586.
- [52] Back, S., and Lang, H. (2000). Heterometallic Assemblies with Bridging Cyano Ligands. *Organometallics*, 19, 749-751.
- [53] (a) Wilson, A. J. C. (1995). In *International Tables of Crystallography*; Kluwer Academic: London, Vol. C. (b) Lang, H. Köhler, K., and Schiemenz B. (1995). Lewis-basen Addukte monomerer bis(η^2 -alkin) Ag^IX-Verbindungen (X = BF₄ oder OSO₂CF₃). *J. Organomet. Chem.*, 495, 135-140.
- [54] Ara, I.; Berenguer, J. R.; Forniés, J.; Lalinde, E., and Moreno, M. T. (1996). Synthesis and Characterization of Cationic Heteronuclear Complexes of Platinum(II) and Silver(I) Bridged by Alkynyl Ligands. *J. Organomet. Chem.*, 510, 63-70.
- [55] del Villar, A.; Rheinwald, G., and Lang, H. Unpublished results.
- [56] Lang, H., and del Villar, A. (2003). Heterobimetallic Platinum–Copper and Platinum–Silver Transition Metal Complexes Based on *cis*-[Pt](C≡CPh)₂: An Overview. *J. Organomet. Chem.*, 670, 45-55.
- [57] Lang, H.; del Villar, A.; Walfort, B., and Rheinwald, G. (2007) in press *J. Organomet. Chem.*.
- [58] Wong, W.-Y.; Lu, G.-L., and Choi, K.-H. (2002). Synthesis, Characterization and Structural Studies of New Heterometallic Alkynyl Complexes of Platinum and Group 11 Metals with Chelating Bis(diphenylphosphino)ferrocene Ligand. *J. Organomet. Chem.*, 659, 107-116.
- [59] del Villar, A.; Rheinwald, G.; Walfort, B., and Lang, H. Unpublished.
- [60] (a) Bassetti, M. Floris, B., and Illuminati G. (1985). Reaction of Ethynylferrocene with Mercuric Acetate. *Organometallics*, 4, 617-623. (b) Cook, D. J.; Hill, A. F., and Wilson, D. J. (1998). Convenient Synthesis of Alkynyl Aryl Seleno- and Telluro-

- Ethers. *J. Chem. Soc. Dalton Trans.*, 7, 1171-1173. (c) Dewhurst, R. D.; Hill, A. F., and Smith, M. K. (2006). Hazards Associated with Bis(alkynyl)mercurials. *Organometallics*, 25, 2388-2389.
- [61] Wetzold, N. (2007). Bis(alkynyl)-Komplexe und Ferrocene als modulare Bausteine für den Aufbau mehrkerniger Übergangsmetallkomplexe. PhD Thesis, TU Chemnitz.
- [62] Köcher, S., and Lang, H. (2001). 4-Ethynyl-benzonitrile-ferrocenes Bridged by a Pd(PPh₃)₂ Unit; the Solid-State Structure of (η^5 -C₅H₅)Fe(η^5 -C₅H₄C≡CC₆H₄C≡N-1,4). *J. Organomet. Chem.*, 637-639, 198-203.
- [63] Köcher, S.; Walfort, B.; van Klink, G. P. M.; van Koten, G., and Lang, H. (2006). Trimetallic FePd₂ and FePt₂ 4-Ferrocenyl-NCN Pincer Complexes. *J. Organomet. Chem.*, 691, 3955-3961.
- [64] Packheiser, R. (2007). PhD Thesis, TU Chemnitz.
- [65] (a) Ohs, A. C.; Rheingold, A. L.; Shaw, M. J., and Nataro, C. (2004). Electrochemistry of Group VI Metal Carbonyl Compounds Containing 1,1'-Bis(diphenylphosphino)-ferrocene. *Organometallics*, 23, 4655-4660. (b) Koo, L. K.; Phang, L. T.; Hor, T. S. A., and Lee, H. K. (1991). High-Performance Liquid Chromatographic Separation of Metal Carbonyl Complexes Substituted with Bridging and Chelating 1,1'-Bis(diphenylphosphino)ferrocene. *J. Liquid Chromatography*, 14, 2079-2087. (c) Chan, H. S. O.; Hor, T. S. A.; Phang, L. T., and Tan, K. L. (1991). XVI. X-ray Photoelectron Spectroscopic Differentiation of Chemically Distinct Phosphorus Environments in Unidentate Complexes of 1,1'-Bis(diphenylphosphino)ferrocene. *J. Organomet. Chem.*, 407, 353-357. (d) Hor, T. S. A.; Phang, L.-T.; Liu, L.-K., and Wen, Y. S. (1991). Substituted Metal Carbonyls XV. Crystal and Molecular Structures of Two Isomorphous Singly Diphosphine-Bridged Complexes (OC)₅M(μ-dppf)M(CO)₅·CH₂Cl₂ (M = Cr, Mo; dppf = (Ph₂PC₅H₄)₂Fe). *J. Organomet. Chem.*, 397, 29-39. (e) Hor, T. S. A., and Phang, L.-T. (1989). Substituted Metal Carbonyls XI. 1,1'-Bis(diphenylphosphino)ferrocene — a Bridging, Chelating and Unidentate Ligand in the Synthesis of M₂(CO)₁₀(μ-P-P), M(CO)₄(η²-P-P) and M(CO)₅(η¹-P-P) (where M = Cr, Mo, W and P-P = Fe(C₅H₄PPh₂)₂). *J. Organomet. Chem.*, 373, 319-324. (f) Estevan, F.; Lahuerta, P.; Latorre, J.; Sanchez, A., and Sieiro, C. (1987). Electrochemical Study of Dinuclear Ruthenium(II)-Arene Compounds: Electrogeneration of Ru(II)-Ru(I) Species. *Polyhedron*, 6, 473-478. (g) Houlton, A.; Roberts, R. M. G., and Silver, J. (1991). Studies on Gold(I) Complexes of 1,1'-Bis(diphenylphosphino)ferrocene. *J. Organomet. Chem.*, 418, 269-275. (h) Mai, J.-F., and Yamamoto, Y. (1998). Preparations and Structures of (η^6 -Arene)ruthenium(II) Complexes Bearing 1,1'-Bis(diphenylphosphinomethyl)ferrocene or 1,1'-Bis(diphenylphosphino)ferrocene. *J. Organomet. Chem.*, 560, 223-232. (i) Delgado, E.; Hernandez, E.; Mansilla, N.; Moreno, M. T., and Sabat, M. (1999). Co-ordinative Ability of the New Compounds [Ti(η^5 -C₅H₄R)₂(C≡CBu^t)₂] (R = PPh₂, Ph₂P=O or Ph₂P=S) as Precursors in the Synthesis of Heterodi- and Heterotri-Nuclear Species. Crystal Structure of [ClCu(μ- η^5 : σ P-C₅H₄PPh₂)₂Ti(μ-η²-C≡CBu^t)₂CuCl]. *J. Chem. Soc., Dalton Trans.*, 4, 533-538. (j) Ara, I.; Berenguer, J. R.; Fornie's, J., and Lalinde, E. (1997). Synthesis, Characterisation and NMR Study of Paramagnetic Heteropolynuclear Anionic Pt-Co Species. Crystal Structures of [NBu₄]₂[cis-Pt(C₆F₅)₂(C≡CSiMe₃)₂CoCl₃]₂·0.5(CH₃)₂CO and NBu₄]₂[Pt(C≡CBu^t)₄]₂·1.5(CH₃)₂CO. *Inorg. Chim. Acta*, 264, 199-210.

- [66] Charmant, J. P. H.; Gomez, J.; Orpen, A. G.; Falvello, L. R.; Fornie's, J.; Rueda, A.; Gomez, J.; Lalinde, E., and Moreno, M. T. (1999). Synthesis, Structural Characterisation and Luminescence Studies of the First Alkynyl Stabilised Platinum–Cadmium Complexes. *Chem. Commun.*, 20, 2045-2046.
- [67] Zhang, D.; McConville, D. B.; Tessier, C. A., and Youngs, W. J. (1997). Synthesis and Crystallographic Characterization of the Planar Tetraethynylplatinum Complex $(\text{NBu}_4)_2[\text{Pt}(\text{OBET})_2]$ and its Double-Tweezer Mercury Dichloride Complex $(\text{NBu}_4)_2[\text{Pt}(\text{OBET})_2](\text{HgCl}_2)_2$. *Organometallics*, 16, 824-825.
- [68] Zhu, Y.; Olivier Clot, O.; Wolf, M. O., and Yap, G. P. A. (1998). Effect of Ancillary Ligands on Ru(II) on Electronic Delocalization in Ruthenium(II) Bisferrocenylacetylide Complexes. *J. Am. Chem. Soc.*, 120, 1812-1821.
- [69] (a) Lebreton, C.; Touchard, D.; Pichon, L. L.; Daridor, A.; Toupet, L., and Dixneuf, P. H. (1998). Mono- and Bis-Alkynyl Ruthenium(II) Complexes Containing the Ferrocenyl Moiety; Crystal Structure of *trans*- $[\text{Ru}(\text{C}\equiv\text{CC}_5\text{H}_4\text{FeC}_5\text{H}_5)_2(\text{Ph}_2\text{PCH}_2\text{CH}_2\text{PPh}_2)_2]$ and Electrochemical Studies. *Inorg. Chim. Acta*, 272, 188-196. (b) Jones, N. D., and Wolf, M. O. (1997). Synthesis of a Ferrocenyl-Capped Ruthenium(II) Bis-(acetylide) Complex: A Model for Organometallic Molecular Wires. *Organometallics*, 16, 1352-1354.
- [70] (a) Vives, G.; Carella, A.; Sistach, S.; Launay, J.-P., and Rapenne, G. (2006). Synthesis of Triester-Functionalized Molecular Motors Incorporating Bis-Acetylide *trans*-Platinum Insulating Fragments. *New J. Chem.*, 30, 1429-1438. (b) D'Amato, R.; Furlani, A.; Colapietro, M.; G. Portalone, G.; Casalboni, M.; Falconieri, M., and Russo, M. V. (2001). Synthesis, Characterisation and Optical Properties of Symmetrical and Unsymmetrical Pt(II) and Pd(II) Bis-Acetylates. Crystal Structure of *trans*- $[\text{Pt}(\text{PPh}_3)_2(\text{C}\equiv\text{C}-\text{C}_6\text{H}_5)(\text{C}\equiv\text{C}-\text{C}_6\text{H}_4\text{NO}_2)]$. *J. Organomet. Chem.*, 627, 13-22. (c) Osella, D.; Gambino, O.; Nervi, C.; Ravera, M.; Russo, M. V., and Infante, G. (1994). Electron Transfer in *trans*- $[\text{Pt}(\text{PPh}_3)_2(\text{C}\equiv\text{CFc})_2]$ and Related Compounds. *Inorg. Chim. Acta*, 225, 35-40.
- [71] Jakob, A., and Lang, H. Unpublished.
- [72] (a) Ferrocene/ferrocenium redox couple: Gritzner, G., and Kuta, J. (1984). Recommendations on Reporting Electrode Potentials in Nonaqueous Solvents. *Pure Appl. Chem.*, 56, 461. (b) Strehlow, H.; Knoche, W.; Schneider, H. (1973). A Conversion of Given Electrode Potentials to the Standard Normal Hydrogen Electrode is Possible. *Ber. Bunsen-Ges. Phys. Chem.*, 77, 760-717.
- [73] (a) Al-Anber, M.; Vatsadze, S.; Holze, R.; Thiel, W. R., and Lang, H. (2005). π -Conjugated *N*-heterocyclic Compounds: Correlation of Computational and ElectroChemical Data. *J. Chem. Soc., Dalton Trans.*, 3632. (b) Vatsadze, S.; Al-Anber, M.; Thiel, W. R.; Lang, H., and Holze, R. (2005). Electrochemical Studies and Semiempirical Calculations on *p*-Conjugated Dienones and Heterocyclic Nitrogen Containing Donor Ligand Molecules. *J. Solid State Electrochem.*, 9, 764.
- [74] For example: (a) Puddephatt, R. J. (1987). In *Comprehensive Coordination Chemistry*; G. Wilkinson, R. D. Gillard, J. A. McCleverty (Eds.); (Vol. 5, p 861) Oxford, U.K.: Pergamon. (b) Grohmann, A.; Schmidbaur, H. (1995). In *Comprehensive Organometallic Chemistry II*; E. W. Abel, F. G. A. Stone, G. Wilkinson, (Eds.); (Vol. 3, p 1). Oxford, U.K.: Pergamon. (c) Jia, G.; Puddephatt, R. J.; Scott, J. D., and Vittal, J. J. (1993). Organometallic Polymers with Gold(I) Centers Bridged by Diphosphines and

Diacetylides. *Organometallics*, 12, 3565-3574. (d) Mingos, D. M. P.; Yau, J.; Menzer, S., and Williams, D. J. (1995). A Gold(I) [2]-Catene. *Angew. Chem., Int. Ed. Engl.*, 34, 1894-1895. (e) Puddephatt, R. J. (1998). Precious Metal Polymers: Platinum or Gold Atoms in the Backbone. *Chem. Commun.*, 1055-1062. (f) Irwin, M. J.; Jia, G.; Payne, N. C., and Puddephatt, R. J. (1996). Rigid-Rod Polymers and Model Compounds with Gold(I) Centers Bridged by Diisocyanides and Diacetylides. *Organometallics*, 15, 51-57. (g) Irwin, M. J.; Vittal, J. J., and Puddephatt, R. J. (1997). Luminescent Gold(I) Acetylides: From Model Compounds to Polymers. *Organometallics*, 16, 3541-3547. (h) Yam, V. W. W.; Choi, S. W. K., and Cheung, K. K. (1996). Synthesis and Design of Novel Tetranuclear and Dinuclear Gold(I) Phosphine Acetylide Complexes. First X-ray Crystal Structures of a Tetranuclear ($[Au_4(tppb)(C\equiv CPh)_4]$) and a Related Dinuclear ($[Au_2(dppb)(C\equiv CPh)_2]$) Complex. *Organometallics*, 15, 1734-1739. (i) Irwin, M. J.; Manojlovic-Muir, L.; Muir, K. W.; Puddephatt, R. J., and Yufit, D. S. (1997). Trigold Triacetylides: Polymerization through Gold...Gold Bonding or Bridging ligands. *Chem. Commun.*, 219-220. (j) Lang, H.; Köcher, S.; Back, S.; Rheinwald, G., and van Koten, G. (2001). Synthesis and Coordination Chemistry of Gold(I) Acetylides. The Solid-State Structure of $\{[\eta^2-(Ph_3P)AuC\equiv CFc]Cu(\mu-Cl)\}_2$. *Organometallics*, 20, 1968-1972. (k) Back, S.; Gossage, R. A.; Lang, H., and van Koten, G. (2000). Mixed Metal Acetylides: The Pt(II) Aryl Acetylide "[PtC₆H₂(CH₂NMe₂)₂-2,6-(C≡C)-4]" as a Connective Fragment. *Eur. J. Inorg. Chem.*, 1457-1464. (l) Yam, V. W. W. (2002). Molecular Design of Transition Metal Alkynyl Complexes as Building Blocks for Luminescent Metal-Based Materials: Structural and Photophysical Aspects. *Acc. Chem. Res.*, 35, 555-563. (m) Whittall, I. R.; Humphrey, M. G.; Houbrechts, S.; Persoons, A., and Hockless, D. C. R. (1996). Organometallic Complexes for Nonlinear Optics. 8. Syntheses and Molecular Quadratic Hyperpolarizabilities of Systematically Varied (Triphenylphosphine)gold σ -Arylacetylides: X-ray Crystal Structures of Au(C≡CR)-(PPh₃) (R = 4-C₆H₄NO₂, 4,4'-C₆H₄C₆H₄NO₂). *Organometallics*, 15, 5738-5745. (n) Naulty, R. H.; Cifuentes, M. P.; Humphrey, M. G.; Houbrechts, S.; Boutton, C.; Persoons, A.; Heath, G. A.; Hockless, D. C. R.; Luther-Davies, B., and Samoc, M. (1997). Syntheses and Quadratic Hyperpolarizabilities of some (Pyridylalkynyl)metal Complexes: Crystal Structures of [Ni{2-(C≡C)C₅H₃NNO₂-5}](PPh₃)(η^5 -C₅H₅)], [Au{2-(C≡C)C₅H₃NNO₂-5}(PPh₃)] and [Au{2-(C≡C)C₅H₄N}(PPh₃)] . *J. Chem. Soc., Dalton Trans.*, 4167-4174. (o) Whittall, I. R.; Humphrey, M. G.; Samoc, M.; Luther-Davies, B., and Hockless, D. C. R. (1997). Organometallic Complexes for Non-Linear Optics XII Syntheses and Second-Order Susceptibilities of (Neomenthyldiphenylphosphine) Gold σ -Arylacetylides: X-ray Crystal Structures of Au(C≡CPh) (nmdpp) and Au((E)-4,4'-C≡CC₆H₄CH=CHC₆H₄NO₂)(nmdpp). *J. Organomet. Chem.*, 544, 189-196. (p) Whittall, I. R.; Humphrey, M. G.; Samoc, M., and Luther-Davies, B. (1997). Molecular Cubic Hyperpolarizabilities of Systematically Varied (Triphenylphosphane)-Gold- σ -Arylalkynyl Complexes. *Angew. Chem., Int. Ed. Engl.*, 36, 370-371. (q) Yamamoto, Y.; Shiotsuka, M., and Onaka, S. (2004). Luminescent Rhenium(I)-Gold(I) Hetero Organometallics Linked by Ethynylphenanthrolines. *J. Organomet. Chem.*, 689, 2905-2911. (r) Ferrer, M.; Rodriguez, L.; Rossell, O.; Lima, J. C.; Gomez-Sal, P., and Martin, A. (2004). Unexpected Alkyne Transfer between Gold and Rhenium Atoms and its Application to the Synthesis of Alkynyl Rhenium(I) Compounds. *Organometallics*, 23,

- 5096-5099. (s) Lu, X. X.; Li, C. K.; Cheng, E. C. C.; Zhu, N., and Yam, V. W. W. (2004). Syntheses, Structural Characterization, and Host-Guest Chemistry of Ethynylcrown Ether Containing Polynuclear Gold(I) Complexes. *Inorg. Chem.*, **43**, 2225-2227.
- [75] (a) Bruce, M. I.; Cole, M. L.; Gaudio, M.; Skelton, B. W., and White, A. H. (2006). Some Complexes Containing Carbon Chains End-Capped by $M(CO)_2Tp'$ [$M = Mo, W$; $Tp' = HB(pz)_3, HB(dmpz)_3$] Groups. *J. Organomet. Chem.*, **691**, 4601-4614. (b) Fillaut, J. L.; Dua, N. N.; Geneste, F.; Toupet, L., and Sinbandhit, S. (2006). Nitrile Ligands for Controlled Synthesis of Alkynyl-Ruthenium based homo and Hetero Bimetallic Systems. *J. Organomet. Chem.*, **691**, 5010-5018. (c) Onitsuka, K.; Ohara, N.; Takei, F., and Takahashi, S. (2006). Synthesis and Redox Properties of Trinuclear Ruthenium-Acetylide Complexes with Tri(ethynylphenyl)amine Bridge. *Dalton Trans.*, **3693**-3698. (d) Sato, M.; Kubota, Y.; Kawata, Y.; Fujihara, T.; Unoura, K., and Oyama, A. (2006). Synthesis and Some Properties of Binuclear Ruthenocenes Bridged by Oligoynes: Formation of Bis(cyclopentadienylidene)cumulene Diruthenium Complexes in the Two-Electron Oxidation. *Chem. Eup. J.*, **12**, 2282-2292. (e) Paul, F.; Ellis, B. G.; Bruce, M. I.; Toupet, L.; Roisnel, T.; Costuas, K.; Halet, J. F., and Lapinte, C. (2006). Bonding and Substituent Effects in Electron-Rich Mononuclear Ruthenium σ -Arylacetylides of the Formula $[(\eta^2-dppe)(\eta^5-C_5Me_5)Ru(C\equiv C)-1,4-(C_6H_4)X][PF_6]_n$ ($n = 0, 1$; $X = NO_2, CN, F, H, OMe, NH_2$). *Organometallics*, **25**, 649-665. (f) Kuo, C.-K.; Chang, J.-C.; Yeh, C.-Y.; Lee, G.-H.; Wang, C. C., and Peng, S. M. (2005). Synthesis, Structures, Magnetism and Electrochemical Properties of Triruthenium-Acetylide Complexes. *Dalton Trans.*, **3696**-3701. (g) Xu, G.-L.; Crutchley, R. J.; DeRosa, M. C.; Pan, Q.-J.; Zhang, H.-X.; Wang, X., and Ren, T. (2005). Strong Electronic Couplings between Ferrocenyl Centers Mediated by Bis-Ethynyl/Butadiynyl Diruthenium Bridges. *J. Am. Chem. Soc.*, **127**, 13354-13363. (h) Hu, Q. Y.; Lu, W. X.; Tang, H. D.; Sung, H. H. Y.; Wen, T. B.; Williams, I. D.; Wong, G. K. L.; Lin, Z., and Jia, G. (2005). Synthesis and Photophysical Properties of Trimetallic Acetylide Complexes with a 1,3,5-Triazine Core. *Organometallics*, **24**, 3966-3973. (i) Wilton-Ely, J. D. E. T.; Honarkhah, S. J.; Wang, M.; Tocher D. A., and Slawin, A. M. Z. (2005). σ -Organyl Complexes of Ruthenium and Osmium Supported by a Mixed-Donor Ligand. *Dalton Trans.*, **1930**-1939.
- [76] Ara, I.; Berenguer, J. R.; Eguizabal, E.; Fornies, J., and Lalinde, E. (2001). Formation of an Unsymmetrical Pt-Ir Tetraalkynyl Complex and Investigation into Subsequent Construction of Multimetallic Systems. *Organometallics*, **20**, 2686-2696.
- [77] Wu, I. Y.; Lin, J. T.; Luo, J.; Sun, S. S.; Li, C. S.; Lin, K. J.; Tsai, C.; Hsu, C. C., and Lin, J. L. (1997). Syntheses and Reactivity of Ruthenium σ -Pyridylacetylides. *Organometallics*, **16**, 2038-2048.
- [78] (a) Vicente, J.; Chicote, M.-T.; Alvarez-Falcón, M. M., and Jones, P. G. (2005). Platinum(II) and Mixed Platinum(II)/Gold(I) σ -Alkynyl Complexes. The First Anionic σ -Alkynyl Metal Polymers. *Organometallics*, **24**, 2764-2772. (b) Chin, C. S.; Kim, M.; Won, G.; Jung, H., and Lee, H. (2003). Diasterecontrolled Synthesis of *cis*-Olefins by Selective C-C Bond Formation Between Alkyl and Alkynyl Groups Coordinated to „ $Ir(CH=CHPPPh_3)(CO)(PPh_3)_2$ “. *Dalton Trans.*, **2325**-2328. (c) Albinati, A.; Leoni, P.; Marchetti, L., and Rizzato, S. (2003). Assembling Metal Clusters with Covalent

- Linkers: Synthesis and Structure of a Quasi-Planar Pt₁₈ Dendrimer Containing Five Clusters Connected by σ-Alkynyl Spacers. *Angew. Chem. Int. Ed.*, **42**, 5990-5993. (d) Chin, C. S.; Kim, M.; Lee, H.; Noh, S., and Ok, K. M. (2002). Regio- and Stereoselective C-C Bond Formation between Alkynes: Synthesis of Linear Dienynes from Alkynes. *Organometallics*, **21**, 4785-4793. (e) Bruce, M. I.; Davy, J.; Hall, B. C.; van Galen, Y.; Skelton, B. W., and White, A. H. (2002). Some Platinum(II) Complexes Derived from Aromatic Alkynes. *Appl. Organomet. Chem.*, **16**, 559-568.
- [79] Weyland, T.; Lapinte, C.; Frapper, G.; Calhorda, M. J.; Halet, J.-F., and Toupet, L. (1997). Bi- and Trimetallic σ-Acetylides Complexes Connected Through a Phenyl Ring in the Fe(Cp*)(dppe) Series. *Organometallics*, **16**, 2024-2031.
- [80] (a) Cifuentes, M. P.; Powell, C. E.; Morrall, J. P.; McDonagh, A. M.; Lucas, N. T.; Humphrey, M. G.; Samoc, M.; Houbrechts, S.; Asselberghs, I.; Clays, K.; Persoons, A., and Isoshima, T. (2006). Electrochemical, Spectroelectrochemical, and Molecular Quadratic and Cubic Nonlinear Optical Properties of Alkynylruthenium Dendrimers. *J. Am. Chem. Soc.*; **128**, 10819-10832. (b) McDonagh, A. M.; Powell, C. E.; Morrall, J. P.; Cifuentes, M. P., and Humphrey, M. G. (2003). Convergent Synthesis of Alkynylbis(bidentate phosphine)ruthenium Dendrimers. *Organometallics*, **22**, 1402-1413. (c) Long, N. J.; Martin, A. J.; White, A. J. P.; Williams, D. J.; Fontani, M.; Laschi, F., and Zanello, P. (2000). Synthesis and Characterisation of Unsymmetrical Metal (Ru^{II}, Os^{II}) and Ferrocenyl Complexes of 1,3,5-Triethynylbenzene. *J. Chem. Soc., Dalton Trans.*, 3387-3392.
- [81] (a) Hearshaw, M. A., and Moss, J. R. (1999). Organometallic and Related Metal-Containing Dendrimers. *Chem. Commun.* 1-8. (b) Stoddart, F. J., and Welton, T. (1999). Metal-Containing Dendritic Polymers. *Polyhedron*, **18**, 3575-3591. (c) Cuadrado, I.; Mora'n, M.; Casado, C. M.; Alonso, B., and Losada, J. (1999). Organometallic Dendrimers with Transition Metals. *Coord. Chem. Rev.*, **193-5**, 395-445. (d) Astruc, D.; Blais, J.-C.; Cloutet, E.; Djakovitch, L.; Rigaut, S.; Ruiz, J.; Sartor, V., and Vale'rio, C. (2000). The First Organometallic Dendrimers: Design and Redox Functions. In F. Vögtle, (Ed.), *Topics in Current Chemistry* (Vol. 210, p 229-259). Berlin, Germany: Springer. (e) Juris, A.; Venturi, M.; Ceroni, P.; Balzani, V.; Campagna, S., and Serroni, S. (2001). Dendrimers Based on Electroactive Metal Complexes. A Review of Recent Advances. *Collect. Czech. Chem. Commun.*, **66**, 1-32. (f) van Manen, H.-J.; van Veggel, F. C. J. M.; Reinhoudt, D. N. (2001). Non-Covalent Synthesis of Metallocendrimers. In F. Vögtle and C. A. Schalley, (Eds.) *Topics in Current Chemistry*; (Vol. 217, p 121-161). Berlin, Germany: Springer. (g) Kreiter, R.; Kleij, A. W.; Klein Gebbink, R. J. M.; van Koten, G. (2001). Dendritic Catalysts. In F. Vögtle, and C. A. Schalley, (Eds.) *Topics in Current Chemistry* (Vol. 217, p 163-199). Berlin, Germany: Springer. (h) Astruc, D. (2003). Organometallic Chemistry at the Nanoscale. Dendrimers for Redox Processes and Catalysis. *Pure Appl. Chem.*, **75**, 461481. (i) Sengupta, S. (2003). A Ferrocene Dendrimer Based on a Cyclotriphosphazene core. *Tetrahedron Lett.*, **44**, 7281-7284. (j) Poniatowska, E., and Salamon'czyk, G. M. (2003). Phosphite Dendrimers and their Organometallic Derivatives. *Tetrahedron Lett.*, **44**, 4315-4317. (k) Angurell, I.; Muller, G.; Rocamora, M.; Rossell, O., and Seco, M. (2003). Synthesis and Catalytic Properties of Neutral and Cationic Rhodium- and Iridium-Containing Carbosilane Dendrimers. *Dalton Trans.*,

- 1194-1200. (l) Angurell, I.; Muller, G.; Rocamora, M.; Rossell, O., and Seco, M. (2004). Single and Double Metallic Layer-Containing Ruthenium Dendrimers. Synthesis and Catalytic Properties. *Dalton Trans.*, 2450-2457. (n) Astruc, D. (2004). Organoiron Activation Combined with Electron- and Proton Transfer: Implications in Biology, Organic Synthesis, Catalysis and Nanosciences. *J. Organomet. Chem.*, 689, 4332-4344. (o) Busetto, L.; Cassani, M. C.; van Leeuwen, P. W. N. M.; Mazzoni, R. (2004). Synthesis of New Poly(propylenimine) Dendrimers DAB-dendr-[NH(O)COCH₂CH₂OC(O)C₅H₄Rh(NBD)]_n {n = 4, 8, 16, 32, 64} Functionalized with Alkoxy carbonylcyclopentadienyl Complexes of Rhodium(I). *Dalton Trans.*, 2767-2770. (p) Onitsuka, K.; Fujimoto, M.; Kitajima, H.; Ohshiro, N.; Takei, F., and Takahashi, S. (2004). Convergent Synthesis of Platinum-Acetylide Dendrimers. *Chem. Eur. J.*, 10, 6433-6446. (q) Caminade, A.-M., and Majoral, J.-P. (2005). Phosphorus Dendrimers Possessing Metallic Groups in their Internal Structure (Core or Branches): Syntheses and Properties. *Coord. Chem. Rev.*, 249, 1917-1926. (r) Turrin, C.-O.; Donnadieu, B.; Caminade, A.-M., and Majoral, J.-P. (2005). Organometallic Derivatives at the Core of Phosphorus-Containing Dendrimers. *Z. Anorg. Allg. Chem.*, 631, 2881-2887. (s) Angurell, I.; Rossell, O.; Seco, M., and Ruiz, E. (2005). Dendrimers Containing Two Metallic Layers. Chloride Migration from Peripheral Gold, Palladium, or Rhodium Metals to Internal Ruthenium Atoms. *Organometallics*, 24, 6365-6373. (t) Ornelas, C.; Vertlib, V.; Rodrigues, J., and Rissanen, K. (2006). Ruthenium Metalloc dendrimers Based on Nitrile-Functionalized Poly(alkylidene imine)s. *Eur. J. Inorg. Chem.*, 1, 47-50.
- [82] Mongin, O.; Papamicaël, C.; Hoyler, H., and Gossauer, A. (1998). Modular Synthesis of Benzene-Centered Porphyrin Trimers and a Dendritic Porphyrin Hexamer. *J. Org. Chem.*, 63, 5568-5580.
- [83] Chong, S. H-F.; Lam, S. C.-F.; Yam, V. W.-W.; Zhu, N., and Cheung, K.-K. (2004). Luminescent Heterometallic Branched Alkynyl Complexes of Rhenium(I)-Palladium(II): Potential Building Blocks for Heterometallic Metalloc dendrimers. *Organometallics*, 23, 4924-4933.
- [84] Jakob, A. (2007). PhD Thesis, TU Chemnitz.
- [85] Baumgartner, T.; Fiege, M.; Pontzen, F., and Arteaga-Müller, R. (2006). Redox-Active, Multinuclear (Ferrocenylethynyl)phosphanes and Their Palladium and Platinum Complexes. *Organometallics*, 25, 5657-5664.
- [86] Milde, B. (2007). Diploma Thesis, TU Chemnitz.
- [87] Stein, T. (2001). Bi- und oligonukleare Komplexe basierend auf Metallorganischen π -Pinzetten. PhD Thesis, TU Chemnitz.
- [88] Köcher, S.; van Klink, G. P. M.; van Koten, G., and Lang, H. (2006). Biferrocene NCN Pincer Metal-d⁸ Complexes: Synthesis, Reaction Chemistry and Cyclovoltammetric Studies. *J. Organomet. Chem.*, 691, 3319-3324.
- [89] (a) Horikoshi, R.; Mochida, T.; Torigoe, R., and Yamamoto, Y. (2002). Preparation and Electrochemical Properties of Polynuclear Organometallic Complexes Derived from Ferrocene-Containing Bidentate Ligands. *Eur. J. Inorg. Chem.*, 3197-3203. (b) Lohan, M. (2005). Biferrocene in der metallorganischen Synthese. Diploma Thesis, TU Chemnitz.
- [90] Lohan, M. PhD Thesis, TU Chemnitz.

- [91] Dong, T.-Y.; Lin, M.; Chiang, M. Y.-N., and Wu, J.-Y. (2004). Development of Polynuclear Molecular Wires Containing Ruthenium(II) Terpyridine Complexes. *Organometallics*, *23*, 3921-3930.
- [92] Packheiser, R.; Walfort, B., and Lang, H. (2007). Synthesis and Characterization of a Heterometallic Fe-Au-Ti-Cu Transition Metall Complex. *Jord. J. Chem.*, in press.
- [93] Kühnert, J. (2008). PhD Thesis, TU Chemnitz.
- [94] Frosch, W.; Back, S., and Lang, H. (1999). 1,1'-Ferrocenyldicarboxylic Acid as Starting Material for the Formation of Trimetallic Ti(IV)-Fe(II)-Cu(I) and Pentametallic Ti₂(IV)-Fe(II)-Cu₂(I) Complexes. *Organometallics*, *18*, 5725-5728.
- [95] Stein, T., and Lang, H. (2001). A Cross-Shaped Ag₅Ti₄ Molecule Based on a [Ag(C≡N)₄]³⁻ Core. *Chem. Commun.*, 1502-1503.
- [96] Al-Anber, M. (2003). Organic and/or Inorganic π -Conjugated Units in the Synthesis of Multinuclear Transition Metal Complexes. PhD Thesis, TU Chemnitz.
- [97] Al-Anber, M.; Taher, D.; Walfort, B., and Lang, H. (2007). Novel Heterotetrametallic Fe-Au-Ti-Cu Transition Metal Complexes. *Jordan J. Chem.*, *1*, 121-127.
- [98] (a) Müller, T. E.; Green, J. C.; Mingos, D. M. P.; McPartlin, C. M.; Whittingham, C.; Williams, D. J., and Woodroffe, T. M. (1998). Complexes of Gold(I) and Platinum(II) with Polyaromatic Phosphine Ligands. *J. Organomet. Chem.*, *551*, 313-330. (b) Müller, T. E.; Choi, S. W.-K.; Mingos, D. M. P.; Murphy, D.; Williams, D. J., and Yam, V. W.-W. (1994). Synthesis, Structural Characterization and Photophysical Properties of Ethyne-Gold(I) Complexes. *J. Organomet. Chem.*, *484*, 209-224.
- [99] Garrison, J. C.; Panzner, M. J.; Custer, P. D.; Reddy, D. V.; Rinaldi, P. L.; Tessier, C. A., and Youngs, W. J. (2006). Synthesis and Characterization of a Trigonal Bipyramidal Supramolecular Cage Based upon Rhodium and Platinum Metal Centers. *Chem. Commun.*, 4644-4646.
- [100] Vives, G.; Carella, A.; Launay, J.-P., and Rapenne, G. (2006). A Star-Shaped Ruthenium Complex with Five Ferrocenyl-Terminated Arms Bridged by *trans*-Platinum Fragments. *Chem. Commun.*, 2283-2285.
- [101] Packheiser, R., and Lang, H. (2007). A First Mixed Heteropentametallic Transition Metall Complex: Synthesis and Charcterisation. *Inorg. Chem. Commun.*, *10*, 580-582.

Chapter 5

RECENT ADVANCES IN ORGANOMETALLIC MATERIALS DERIVED FROM FERROCENYLACETYLIDE

Wai-Yeung Wong*

Department of Chemistry, Hong Kong Baptist University,
Waterloo Road, Kowloon Tong, Hong Kong, P.R. China.

ABSTRACT

There is a flurry of interest in the research community in the development of carbon-rich bi- or multi-metallic assemblies containing π -conjugated chains. It has been demonstrated that molecular wires comprising mixed-valence bimetallic fragments or remote redox-active organometallic building blocks linked by all-carbon chains could be used in molecular electronics, optoelectronic devices and chemical sensing appliances. In recent years, we have been engaged in the chemistry and material properties of oligoacetylenic ferrocenyl complexes and their organometallic derivatives by virtue of their potential in various areas of materials science. The synthesis, characterization, crystal structures, optical spectroscopy and electrochemistry of a series of homometallic and heterometallic alkynyl complexes end-capped with ferrocenyl entities which contain conjugated organic bridges will be presented. The electronic and redox properties will be examined as a function of the chain length and nature of the spacer group and the data are compared with the results obtained from theoretical computational studies.

Keywords: Alkynyl complexes; Butadiyne; Carbon-rich compounds; Ferrocene; Fluorene; Oligothiophene; Organometallics.

* Correspondence concerning this article should be addressed to Wai-Yeung Wong, Department of Chemistry, Hong Kong Baptist University, Waterloo Road, Kowloon Tong, Hong Kong, P.R. China. E-mail: rwywong@hkbu.edu.hk

ABBREVIATIONS

The following abbreviations are used throughout the text.

Ct	the center of a cyclopentadienyl ligand
CV	cyclic voltammetry
DFT	density functional theory
DBU	1,8-diazabicyclo[5.4.0]undec-7-ene
DP	degree of polymerization
EFISH	electric-field-induced second harmonic generation
FABMS	fast-atom bombardment mass spectrometry
Fc	ferrocenyl group ($\eta^5\text{-C}_5\text{H}_5$) $(\eta^5\text{-C}_5\text{H}_4)$ Fe
Fc/Fc ⁺	ferrocene/ferrocenium couple
FET	field-effect transistor
HOMO	highest occupied molecular orbitals
ICT	intramolecular charge-transfer
IR	infrared spectroscopy
ISC	intersystem crossing
LED	light-emitting diodes
LUMO	lowest unoccupied molecular orbitals
MLCT	metal to ligand charge-transfer
NLO	non-linear optics
NMR	nuclear magnetic resonance
OAc	acetate
PL	photoluminescence
T _{decomp} (onset)	onset decomposition temperature
TLC	thin-layer chromatography
UV/Vis	ultraviolet-visible

1. INTRODUCTION

There is a considerable research interest in the advance of carbon-rich organometallic systems containing rigid, π -conjugated chains due to their widespread applications in the syntheses of unsaturated organic species [1], organometallic polymers [2], and π -conjugated bi- or multimetallic systems [3]. These organometallic assemblies are important design goals for the investigation of electron-transfer processes [4], the generation of liquid crystalline materials [5], the construction of molecular devices [6], and the production of conjugated dendrimers [7]. In particular, the polyynyl systems $[\text{L}_n\text{M}-(\text{C}\equiv\text{C})_m-\text{R}]$ and $[\text{L}_n\text{M}-(\text{C}\equiv\text{C})_m-\text{M}'\text{L}_n]$ ($m = 1, 2, \dots$; $\text{M} = \text{M}'$, $\text{M} \neq \text{M}'$) are attractive candidates in the preparation of molecular wires and in the assembly of nanoscale electronic devices, in light of the possible charge delocalization along the entire conjugated backbone [8]. Molecular wires consisting of mixed-valence bimetallic fragments or remote redox-active organometallic building blocks assembled with all-carbon chains were shown to find applications in molecular electronics, optoelectronic devices and chemical sensing appliances [6b,9]. Since

the first report of the mixed-valence ion of diferrocenylacetylene in 1974 [10], the interest in these metal-capped linear polycarbon chains as models for materially useful compounds has tremendously increased and research efforts have been enthusiastically devoted to the molecular design of ferrocene-derived homo- and heterometallic molecular scaffolds spaced by various aromatic and heteroaromatic units including oligoene, oligoyne, thiophene, furan, phenylene, phenylacetyne, thienyl ethynyl and furanyl vinyl units [11]. As illustrated in Figure 1, two common models are employed to evaluate the capability of electrocommunication between two metal group termini “M₁” made possible by a conjugated organic spacer “M₁–spacer–M₁” (type A), and the influence of an organometallic fragment “M₂” in a conjugated organic chain “M₁–spacer–M₂–spacer–M₁” (type B) [11a,12]. In several cases, the redox active sites are strongly coupled electronically through the polyynyl fragments [12]. Among these, Adams and co-workers have studied extensively the coordination chemistry of various ferrocenyl-capped oligoynes toward metal cluster complexes and the electrocommunication between ferrocenyl groups in these compounds [13]. The introduction of a metallocene unit into rigid-rod one-dimensional oligomers and polymers may confer a range of interesting redox, optical, electrical as well as catalytic properties that differ significantly from those of conventional organic polymers. Previous work also demonstrated that a metal bis(acetylide) unit allows a significant ground-state interaction between terminal redox-active groups in some multimetallic molecular assemblages [12h,12i].

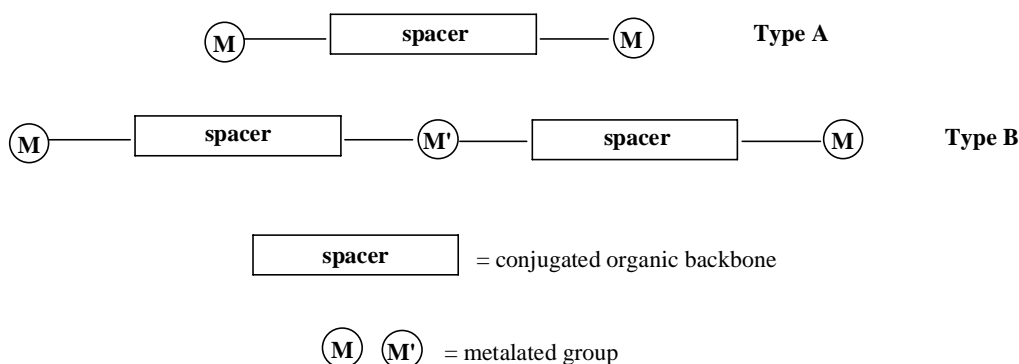


Figure 1. Three common types of metal-containing conjugated molecules.

Research on metal alkynyls covering a large body of transition metals across the Periodic Table is growing rapidly over the past decade and continues to attract enormous research attention. These organometallic complexes hold a fascination for synthetic chemists, structural chemists and materials scientists alike [14]. The linear geometry of the alkynyl unit and its unsaturated character have rendered these organometallic alkynyls versatile building blocks for the construction of molecular wires and organometallic oligomeric and polymeric materials. They can possess unique properties, such as luminescence, liquid crystallinity, optical non-linearity and electrical conductivity. Within this research regime, the use of ferrocenyl electrophores and their derivatives provides fascinating perspectives for the design and realization of such molecular wires, due to its stability in both the neutral and oxidized forms. Much efforts have been focused on the synthesis of ferrocene-derived materials with extensive π -conjugation [15]. Although the 1,4-diethynylbenzene $-\text{C}\equiv\text{CC}_6\text{H}_4\text{C}\equiv\text{C}-$ unit has been extensively used as the π -spacer in organic and homo- and heterometallic oligomers and

polymers [16], recent work has been paid on related materials based on oligothiophenes and fluorenes because of their remarkable electronic and optoelectronic properties [17,18]. With these concepts in mind, our research group is actively involved in developing new synthetic routes to a new series of alkyne-functionalized α -coupled thiophene oligomers as well as fluorene derivatives along the main chain which can then give a direct access to various metallated materials with these π -conjugated systems. The introduction of transition metal centers, with their large variety of ligand environments and oxidation states, can lead to interesting physical properties on the organic systems. In this chapter, we will concentrate on some recent advances in the synthesis and chemistry of a wide range of metallated complexes of ferrocenylacetylene functionalized with oligothienyl and various 9-substituted fluorene derivatives.

2. HOMOMETALLIC AND HETEROMETALLIC MATERIALS DERIVED FROM FERROCENYLACETYLIDE

2.1. Oligothienyl Spacers

The preparation and optoelectronic studies of metal-based conjugated organic materials and polymers have been the subject of diverse research interest in the past few decades because of their possible applications in various domains of the materials industry [19]. The driving force for this work lies in the possibility of coupling the chemical, optical and electronic properties of metal complexes to those of the organic backbone, thus accessing novel materials with new functional properties. Among the majority of organic backbones used, conjugated thiophene derivatives have been widely explored by virtue of their chemical stability and synthetic accessibility (Figure 2) [20]. It has been well-documented that α -coupled oligothiophenes play a vital role in the rapidly expanding field of electronic and optoelectronic devices such as field-effect transistors (FETs) [21], solar cells [22], and light-emitting diodes (LEDs) [23], and as the fluorescent biomarkers in biological research [24]. Polythiophene and its derivatives work very well in some of the above applications and remain one of the most studied conjugated polymer systems. Furthermore, highly organized molecular assemblies based on the thiophene oligomers are also systems of much interest [25]. Although the $-\text{C}\equiv\text{CC}_6\text{H}_4\text{C}\equiv\text{C}-$ unit has been extensively used as the π -spacer in organic and homo- and heterometallic oligomers and polymers [26], an increasing attention is currently being paid on materials based on oligothiophenes and polythiophenes in the scientific community because of their intriguing electronic and optoelectronic characteristics. The ease of modification and knowledge in the structure-property relationship of polythiophenes continue to make the synthesis of oligo- and polythiophenes a critical subject in the advance of new functional molecules [20-25]. Remarkably, π -conjugation of organometallic moieties into the oligothiophene chain should provide interesting models that possess unique properties which are not easily accessible in the classical organic counterparts. Insertion of these metal groups may promote or inhibit electron delocalization in such conjugated systems. Experimental evidences revealed that metal acetylide polymers containing oligothienyl bridges may be good candidates for electrically conducting materials. Following our recent reports of the synthesis and optical properties of dimeric and polymeric

platinum acetylides with oligothienyl bridges [26], we would like to expand the system to the alkynylferrocenyl complexes in the quest for some new ferrocene-containing materials. Here, we also present the chemistry of a series of platinum(II) complexes of oligothiophene-functionalized ferrocenylacetylene [27]. We believe that π -conjugation of organometallic moieties into the oligothiophene chain should provide interesting models that possess unique properties which are not observed in the organic counterparts.

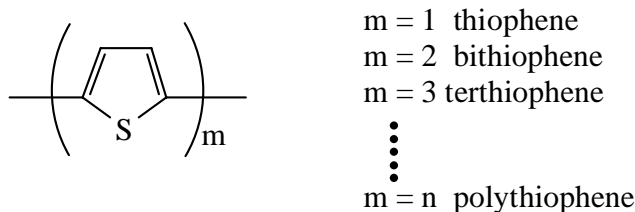
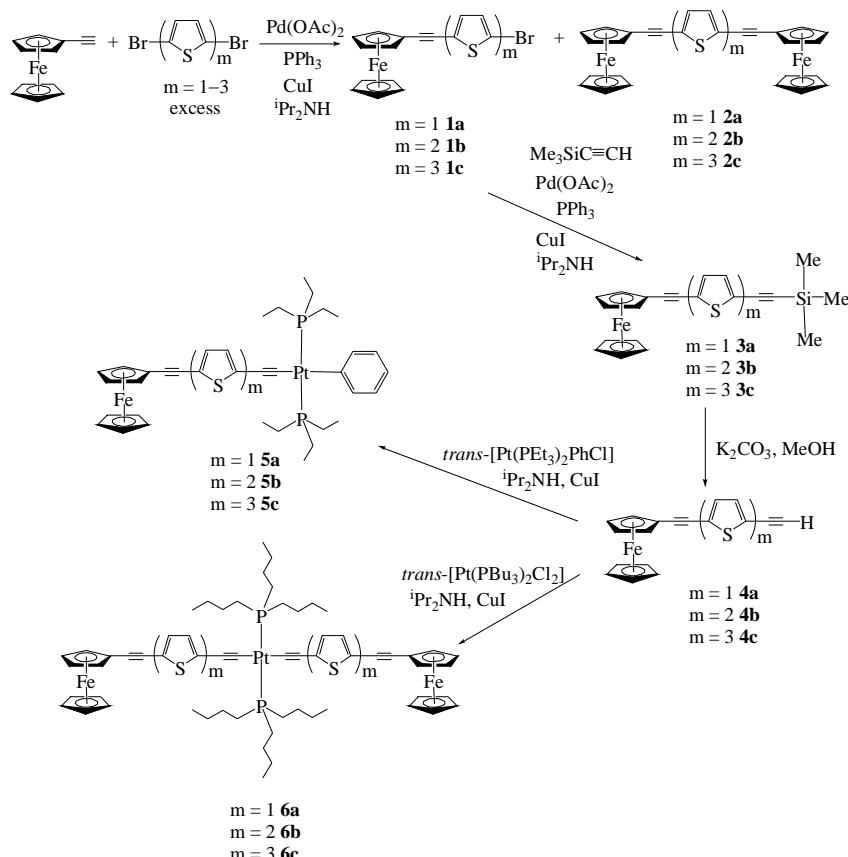


Figure 2. Chemical structures of oligothiophene.

Scheme 1 summarizes the reaction steps for the new ferrocenyl compounds functionalized with oligothienyl spacers, where m denotes the number of thiophene rings. The bromo-substituted ferrocenyl derivatives **1a–1c** can be prepared in good yields by the Sonogashira coupling reactions of ethynylferrocene with an excess of the corresponding dibromo-oligothiophenes [28]. Complexes **2a–2c** were also formed as the minor products in these preparations. Analogous cross-coupling reactions of **1a–1c** with trimethylsilylacetylene readily gave **3a–3c**. Removal of the Me_3Si groups in **3a–3c** was achieved by treatment with K_2CO_3 in MeOH to form **4a–4c** which can then be used as key synthons to the heterobimetallic and trimetallic systems. The dehydrohalogenating-type coupling reactions between **4a–4c** and *trans*- $[\text{Pt}(\text{PEt}_3)_2\text{PhCl}]$ or *trans*- $[\text{Pt}(\text{PBu}_3)_2\text{Cl}_2]$ under the $\text{CuI}/\text{iPr}_2\text{NH}$ condition provided **5a–5c** and **6a–6c**, respectively, as air-stable red crystalline solids in good to high yields. The feed mole ratios are 1:1 and 2:1 for the ferrocenyl precursors and platinum(II) chloride complexes, respectively.

The solid-state geometry of selected molecules were confirmed by X-ray crystallography. For the crystal structure of **2b** portrayed in Figure 3, two halves of the molecules are related by the center of symmetry with an iron–iron through-space distance of *ca.* 17 Å. The structure of **4b** (Figure 4) shows a *trans* geometry with respect to the two thiophene rings with the internal and terminal $\text{C}\equiv\text{C}$ bond lengths of 1.197(3) and 1.169(4) Å, respectively. For **5b**, the bithienyl ligand connects to a ferrocenyl unit at one end and a $[\text{Pt}(\text{PEt}_3)_2\text{Ph}]$ unit at the other extreme (Figure 5). The two PEt_3 ligands adopt a *trans* disposition at the Pt center. All the four five-membered rings within the molecule are nearly coplanar (dihedral angles 0.1–11.4°) and the phenyl ring is inclined by *ca.* 52° to the S(2) thiophene mean plane. For **6b**, the crystal structure shows a diferroacenyl end-capped molecule in which the two acetylidy linkages are bonded to the central square-planar Pt center in a *trans* orientation (Figure 6). On steric grounds, the bithienyl systems exhibit a *trans* conformation for the sulfur atoms and do not deviate significantly from planarity (mean deviation of *ca.* 0.019–0.035 Å). A slight lengthening of the alkynyl bond lengths (mean distance = 1.22(2) Å) suggests π -conjugation along the main chain. The rigidity of the complex is confirmed with four $\text{C}\equiv\text{C}$ bonds and four

thienyl rings connecting the metallated groups to result in an iron–iron through-space separation of *ca.* 32 Å.



Scheme 1. Synthesis of platinum(II) complexes of oligothiophene-based ferrocenylacetylene.

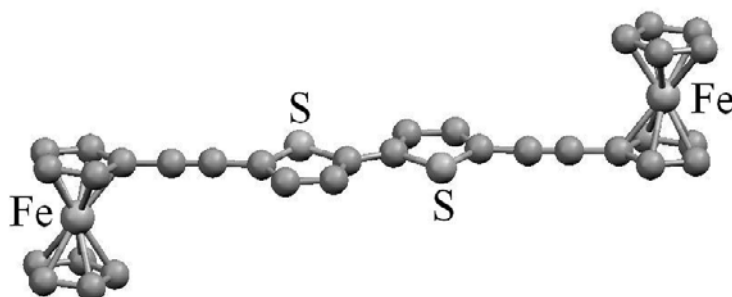
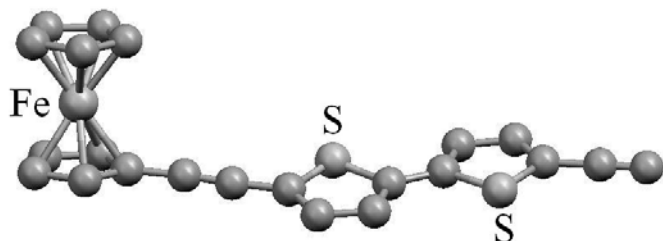
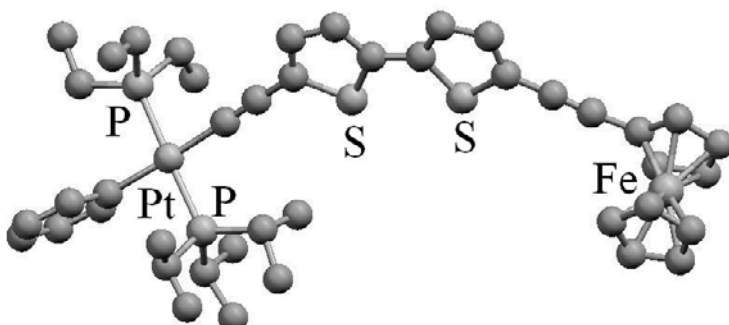
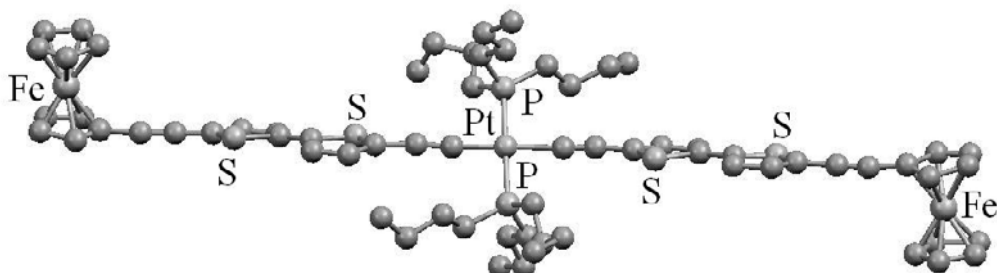


Figure 3. Molecular structure of **2b**.

Figure 4. Molecular structure of **4b**.Figure 5. Molecular structure of **5b**.Figure 6. Molecular structure of **6b**.

In general, the absorption spectra of **1–4** show intense, relatively high-energy bands in the near UV and visible region, which come from the $\pi-\pi^*$ transition of the oligothienyl fragments (table 1). This assignment is in good agreement with the notion that an increase in the extent of π -conjugation with additional thiényl units from one to three results in bathochromic shift of the $\pi-\pi^*$ transition and a notable increase in the molecular extinction coefficients. Increasing the value of *m* in the main chain stabilizes the LUMO of oligothiophene linkage. The electronic spectra of **5a–5c** and **6a–6c** are also dominated by the structureless $\pi-\pi^*$ transition bands of the organic bridges. The platinum(II) moiety tends to lower the transition energies and increase the absorption intensity, indicating an enhancement in the degree of π -delocalization through the metalated conjugated system. Also, increasing conjugation through more thiényl units leads to a decreased transition energy for **5a–5c** as

well as **6a–6c**. Thus, a red-shift of *ca.* 61 nm is observed from **5a** to **5c**, whereas the shift is 57 nm from **6a** to **6c**. We note that the absorption wavelength maximum (λ_{\max}) decreases according to the sequence **6** > **5** > **2** > **3** > **4** > **1**. However, the extent of bathochromic shifts induced by the end substitution of organometallic groups decreases significantly with an increase in the value of *m*. This substituent effect diminishes progressively as more thiophene units are added and there would be little advantage in increasing the number of thiophene units above 5 or 6. Figure 7 shows the plot of $\Delta\lambda$ against *m* where $\Delta\lambda$ corresponds to the red-shift in wavelength between the organometallic end-substituted complexes **2**, **5** and **6** and the free alkynes **4** from which the chain length dependence of the optical properties can be seen clearly. It is obvious that the shift is the largest for **6a–6c** at the same value of *m*.

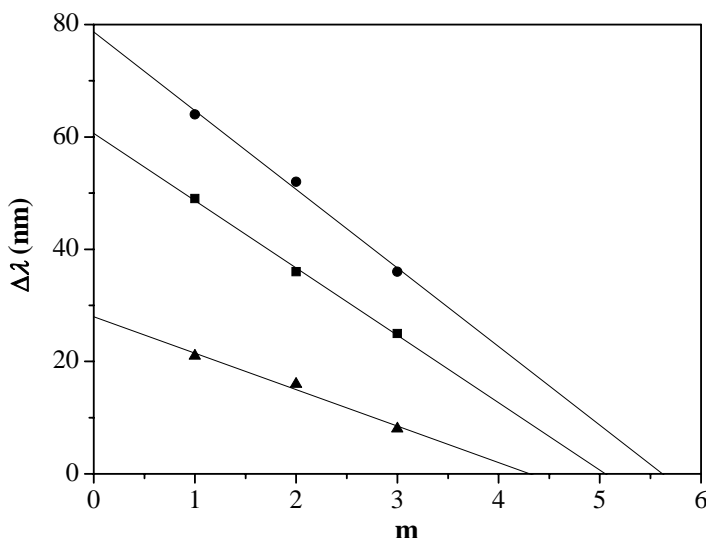


Figure 7. Bathochromic shifts of the absorption maximum induced by the end ferrocenyl substitution (▲), end -Pt(PEt₃)₂Ph substitution (■) and end -Pt(PBu₃)₂- substitution (●), relative to the number of thiophene rings, *m*, of the chain.

In each case, the cyclic voltammogram is characterized by a single quasi-reversible oxidation wave caused by the associated ferrocenyl electrophore (table 1). An anodic shift of the ferrocene/ferrocenium ion (Fc/Fc⁺) couple with respect to the ferrocene standard is consistent with the unsaturation of the ethynyl bridge which renders the removal of electron more difficult than the neat ferrocene. A small negative shift of the ferrocenyl redox potential occurs upon progressive addition of the thiophene rings because of the increased electron density in the ferrocene vicinity induced by the electron-rich thiophene groups. When the conjugation length is increased, oxidation is favored by the delocalization of charge along the chain which makes the ferrocenyl oxidation easier. Likewise, the slight but notable cathodic shift of the Fe(III)/Fe(II) couple for **5** and **6** can be attributed to the electron delocalization into the Pt segment through a $d\pi \rightarrow p\pi$ interaction. Experimentally, the first oxidation wave for each of **6a–6c** corresponds to a single-step two-electron oxidation involving the concomitant oxidation of the two terminal ferrocenyl groups. Analogous to **2b**, these two ferrocenyl end

groups only exhibit sparse electronic communication in **6a–6c**. Similar non-interacting diferrocenyl molecules are quite common in the literature [29].

Table 1. Electronic Absorption and Redox Data for Ferrocenyl Compounds 1–6

Compound	λ_{max} / nm ($\varepsilon / 10^3 \text{ M}^{-1} \text{ cm}^{-1}$) ^a	Optical gap / eV ^b	$E_{\text{ox}} / \text{V} (\Delta E_p)^{\text{c}}$
1a	311 (5.0), 445 sh (0.3)	3.12	0.15 (119)
1b	355 (14.4), 460 sh (1.2)	3.03	0.12 (119)
1c	394 (43.3)	2.74	0.11 (119), 0.82 ^d
2a	340 (26.7), 445 sh (3.4)	2.91	e
2b	385 (32.4)	2.72	e
2c	412 (44.7)	2.46	e
3a	327 (17.1), 442 sh (1.0)	3.04	0.16 (160)
3b	374 (30.1)	2.90	0.11 (139)
3c	405 (39.3)	2.63	0.10 (80), 0.80 ^d
4a	319 (7.1), 429 sh (0.6)	2.99	0.16 (139)
4b	369 (29.0)	2.92	0.11 (99)
4c	404 (40.7)	2.64	0.08 (119), 0.72 ^d
5a	368 (24.3), 421 (1.4)	2.93	0.12 (99), 0.67 ^d
5b	405 (32.9)	2.75	0.10 (119), 0.53 ^d
5c	429 (35.9)	2.49	0.06 (119), 0.38 ^d , 0.70 ^d
6a	383 (71.3)	2.90	0.07 (99), 0.65 ^d
6b	421 (89.4)	2.57	0.04 (116), 0.51 ^d
6c	440 (101.5)	2.44	0.02 (120), 0.35 ^d , 0.61 ^d

^a In CH_2Cl_2 . ^b Estimated from the absorption edge. ^c All the potential values are with reference to the external ferrocene standard. $E_{\text{ox}} = (E_{\text{pc}} + E_{\text{pa}})/2$ for reversible oxidation, and peak potential is reported for irreversible oxidation (in volts). ΔE_p in mV. Scan rate = 100 mV s⁻¹. ^d Irreversible wave. ^e Ref. 15b.

Another redox event was also observed at higher positive potentials in several compounds due to oxidation of the thiienyl fragments but such wave was absent for **1a**, **1b**, **3a**, **3b**, **4a** and **4b** with one or two thiophene units. However, complexes **1c**, **3c** and **4c** with an increased oligothienyl chain length were found to undergo an irreversible thiienyl oxidation peaking at 0.82, 0.80 and 0.72 V, respectively, which agrees with the common phenomenon that formation of the heteroaromatic cation radicals is more favored in the presence of electron-donating terminal groups [30] and increased conjugation chain [31]. It is well-documented that electrooxidation of oligothiophenes is often an irreversible process because the electrogenerated radical cations readily undergo rapid coupling reactions to yield higher oligomers or polymers. The stability of these radical cations increases when the oligomeric chain becomes longer [31]. Insertion of Pt(II) units in **5** and **6** also may facilitate the oxidation of the thiienyl chromophore. For **5a–5c** or **6a–6c**, each of them displays an irreversible thiienyl oxidation wave within 0.38–0.67 V for **5** and 0.35–0.65 V for **6**, and a second irreversible oxidation of the thiophene moiety also appears at 0.70 and 0.61 V for **5c** and **6c**, respectively (Figure 8). The waves become more reversible at higher scan rates (> 100 mV s⁻¹). Lowering of the redox potential of the thiophene units on increasing the chain length can be observed for **5a–5c** as well as **6a–6c**, which is a manifestation of a more π -delocalized system in the terthienyl counterparts. As noted for some thiénylenevinylene oligomers, it is likely that the

first thietyl oxidation step is generally followed by chemical reactions or the formation of a polymeric material [32].

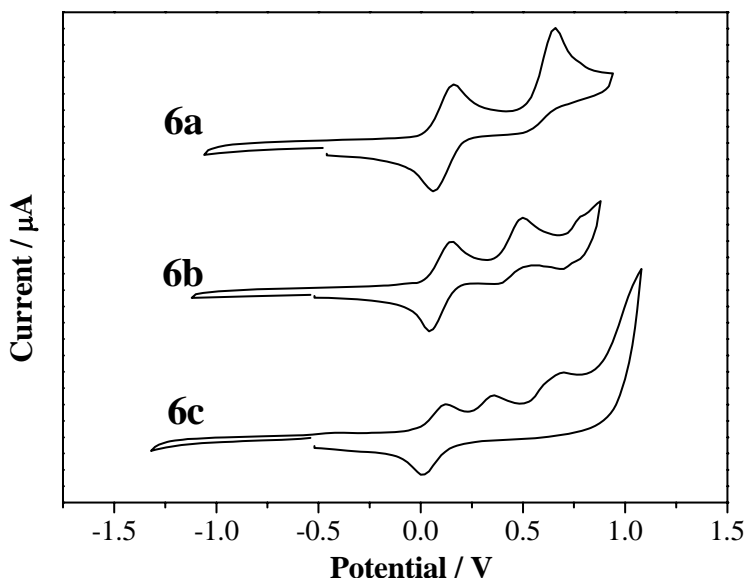


Figure 8. Cyclic voltammograms of **6a**–**6c** measured in CH_2Cl_2 at the scan rate of 100 mV s^{-1} .

To study the electronic structures of these newly synthesized ferrocenyl complexes, we have carried out molecular orbital calculations at the B3LYP level of density functional theory (DFT) for **1b**, **2b**, **4b**, **5b** and **6b** based on their experimental geometries obtained from the X-ray crystallographic data [33]. For theoretical simplicity, PH_3 was used to replace the phosphines bonded to the Pt(II) centre in the calculations. Examining the characteristics of the highest occupied (HOMO) and lowest unoccupied (LUMO) molecular orbitals for these complexes, we found that they are commonly related to π and π^* of the bithiophene structural unit(s). A correlation diagram, depicted in Figure 9, clearly shows the frontier molecular orbitals for 5,5'-diethynyl[2,2']bithiophene and **4b** [34], showing their common features. The HOMO and LUMO orbitals correspond to π and π^* of the bithiophene aromatic unit. The HOMO–LUMO gap for **4b** is smaller as compared to the parent bithiophene without the terminal ferrocenyl moiety. This is in line with the effect of metal coordination which enhances the delocalization along the conjugated structural backbone. The second and third HOMOs arise mainly from the Fe center, corresponding to the d_{xy} and $d_{x^2-y^2}$ orbitals of Fe, where the Cp–Fe–Cp axis is defined as the z-axis of the Cartesian system (Figure 9).

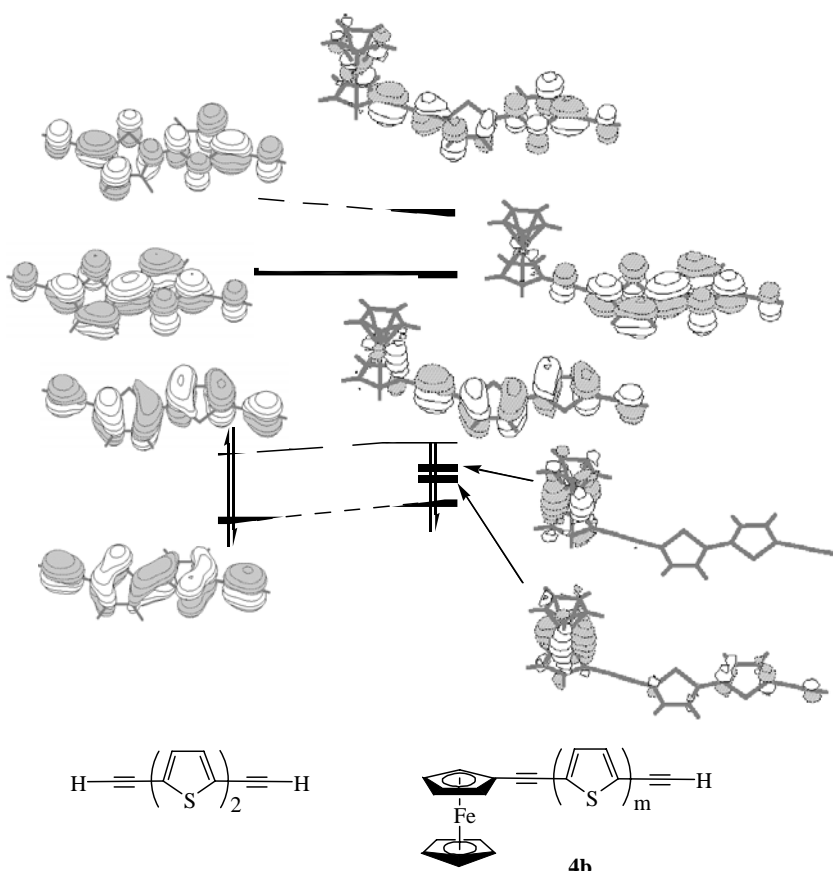


Figure 9. The frontier molecular orbitals for **4b** and 5,5'-diethynyl[2,2']bithiophene.

Molecular orbital calculations at the B3LYP level of DFT were carried out for **1b**, **2b**, **5b** and **6b** in order to study their electronic structures. As illustrated in Figure 10, the HOMO–LUMO transition is related to the $\pi-\pi^*$ excitation within the bithiophene structural unit(s) for each of them. There are two Fe's *d* orbitals immediately below the HOMO which may cause the high-energy Fe(*d*)-to-ligand(π^*) charge-transfer transition. For **5b** and **6b**, the energy levels are more complicated because of the presence of Pt–L(σ^*) components and the Pt's empty *p* orbital in the LUMO region. So, it is likely to observe ligand(π)-to-Pt charge transfer band in the UV/Vis spectra at higher energies. The increase of π -delocalization by extending the conjugation system or the use of metal coordination results in a smaller HOMO–LUMO gap. The calculated relative HOMO–LUMO gaps are consistent with the experimental energy gap order **4b** > **5b** > **2b** > **6b** and complex **6b** absorbs at the longest wavelength among the homologous bithiophene series.

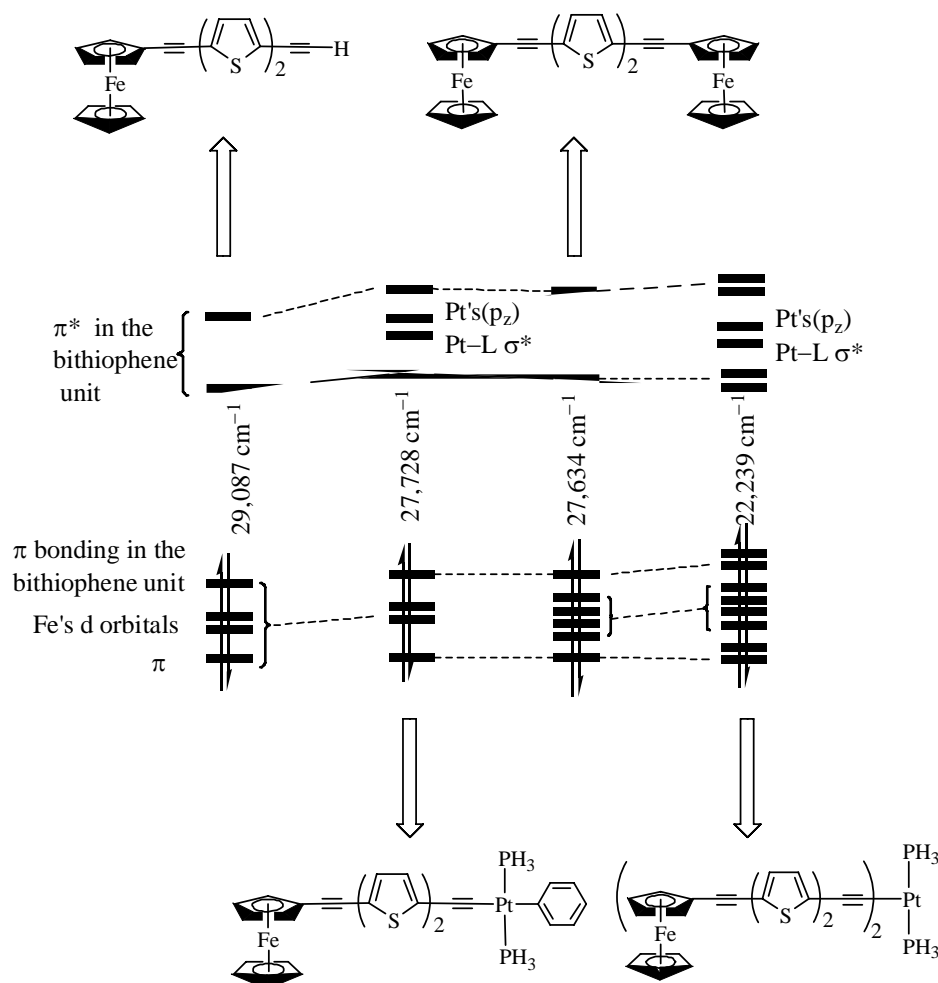


Figure 10. Bonding characteristics of the frontier molecular orbitals for the bithienyl-bridged ferrocenyl complexes.

2.2. Fluorenyl Spacers

Fluorenyl chromophores and other related derivatives such as carbazoles have attracted attention recently as structural variants of new molecular and polymeric materials for various optoelectronic applications [35]. The ease of modification and a good understanding of the structure-property relationship of polyfluorene homopolymers and copolymers can render fluorene-functionalized compounds very attractive candidates in the development of new functional materials. It was demonstrated that substituted poly(2,7-fluorene) derivatives (Figure 11) are attractive as active components of organic light-emitting diodes (LEDs) due to their thermal and chemical stability and their high emission quantum yields [36]. The fluorene moiety provides a rigidly planar biphenyl unit and substituent derivatization at the C-9 position of the monomeric fluorenes allows a control of the polymer properties such as

solubility, emission wavelengths as well as processibility and mediating potential interchain interactions in thin films [37]. Moreover, substituted fluorenes are widely used as electron acceptors in charge transfer complexes and electron transport materials [38]. More recently, a number of elegant synthetic means have been employed to generate fluorene-containing materials with enhanced device performance [35]. However, to our knowledge, related work on ferrocene-based functional materials of fluorenes is still rare. In this context, we have directed our research to the molecular design, synthesis and materials properties of new alkynylferrocene complexes of fluorene derivatives.

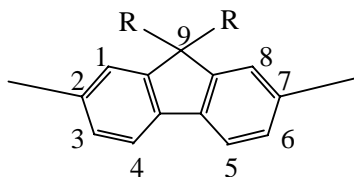
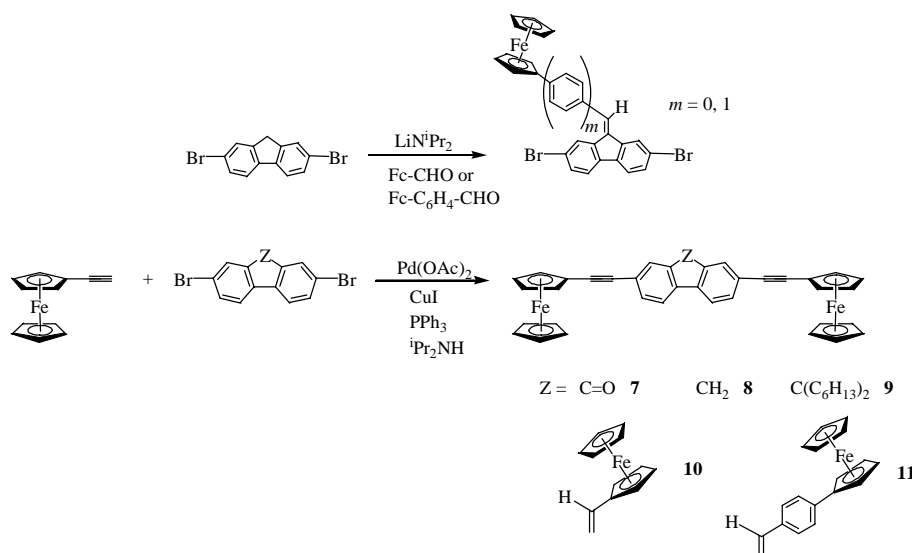


Figure 11. Chemical structure of 2,7-fluorenyl chromophore.

New bis(ferrocenylethyynyl) complexes with fluorenyl-based spacers $[(\eta^5\text{-C}_5\text{H}_5)\text{Fe}(\eta^5\text{-C}_5\text{H}_4)\text{C}\equiv\text{CRC}\equiv\text{C}(\eta^5\text{-C}_5\text{H}_4)\text{Fe}(\eta^5\text{-C}_5\text{H}_5)]$ (R = fluoren-9-one-2,7-diyl **7**, fluorene-2,7-diyl **8**, 9,9-dihexylfluorene-2,7-diyl **9**, 9-ferrocenylmethylenefluorene-2,7-diyl **10**, 9-ferrocenylphenylmethylenefluorene-2,7-diyl **11**) were prepared by the Sonogashira coupling reactions of ethynylferrocene with the corresponding dibromofluorene derivatives in a 2:1 molar ratio (Scheme 2) [39]. The product yields of **7–10** are very high (> 80%) and formation of the homocoupling compound, 1,4-diferrocenylbutadiyne, can be minimized under strictly anaerobic conditions. Compounds **7–11** are soluble in common organic solvents and characterized by satisfactory microanalysis, IR and NMR spectroscopies and fast-atom bombardment mass spectrometry (FABMS). Each of the X-ray crystal structures of **7** and **8** consists of two alkynylferrocene end groups appended to the central fluorenone unit at the 2,7 positions. The fluorenenediyl ring system is planar with a mean deviation from the plane of 0.016 Å. The cyclopentadienyl rings of both ferrocenyl groups are essentially planar and the tilt angles are 2.3 and 2.1° for the two C_5 rings in the two ferrocenyl units. The mean $\text{Fe-C(cyclopentadienyl)}$ bond length is 2.034(4) Å and the cyclopentadienyl rings produce an average distance of 1.647 Å from their centroids. One of the substituted C_5H_4 rings is nearly coplanar with the fluorenyl plane (dihedral angle 2.9°) while the other C_5H_4 ring is rotated by 76.0° relative to the plane of the attached fluorenone about the alkynyl bond. The crystal structure analysis of **8** shows the molecule to adopt a conformation in which the two ferrocenyl units are positioned on the opposite side over the plane of the central fluorene spacer. In both ferrocenyl moieties, the C_5 rings are essentially parallel, inclined by 1.9 and 2.7° for the iron centers. An eclipsed nature of the C_5 rings in the structure of **8** is observed with deviation angles of ca. 4.5 and 4.0°. The fluorenenediyl unit does not deviate significantly from planarity (mean deviation 0.015 Å) and makes small dihedral angles of 6.0 and 4.9° with the substituted C_5H_4 rings.



Scheme 2. Synthetic routes to bis(alkynylferrocene) complexes with fluorene spacers.

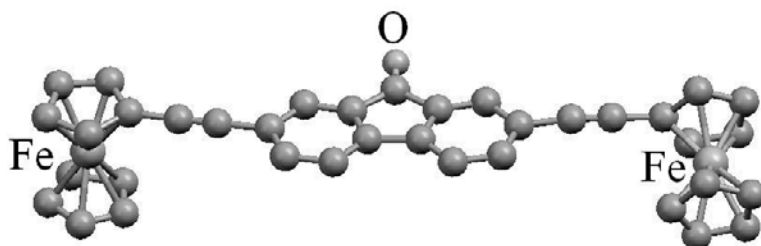


Figure 12. Molecular structure of 7.

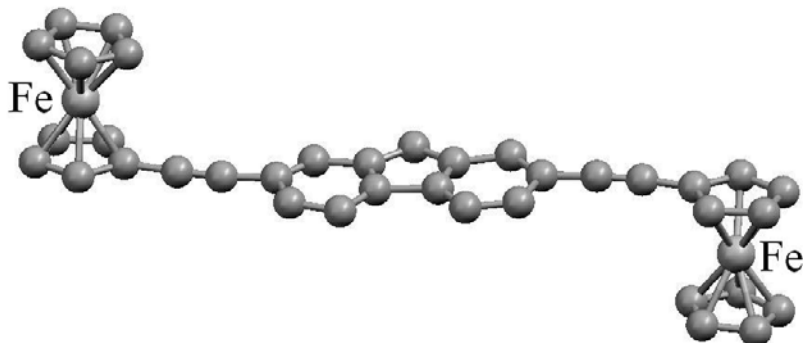


Figure 13. Molecular structure of 8.

Figure 14 shows the contour plots of the frontier molecular orbitals for the bis(ferrocenylethynyl) species 7. The HOMOs are very close to each other in orbital energies

and essentially consist of the four Fe d_{δ} metal orbitals together with small contributions from the highest π bonding orbitals from the fluorenone unit. There are four such d_{δ} orbitals since we have two Fe centers in the complex and each Fe metal center is expected to have two. The δ -type is defined by viewing the orbitals along the Ct-Fe-Ct axes (Ct: the center of each cyclopentadienyl ligand). When the the Ct-Fe-Ct axis is defined as the z axis, the two d_{δ} orbitals correspond to the d_{xy} and $d_{x^2-y^2}$ orbitals. Each iron center in the complex is formally considered as Fe(II). The two d_{z^2} orbitals (from the two Fe centers) are located in the lower energy region. The LUMOs correspond to the π^* orbitals of the organic aromatic entity. The calculated HOMO-LUMO gap for **7** is 3.20 eV.

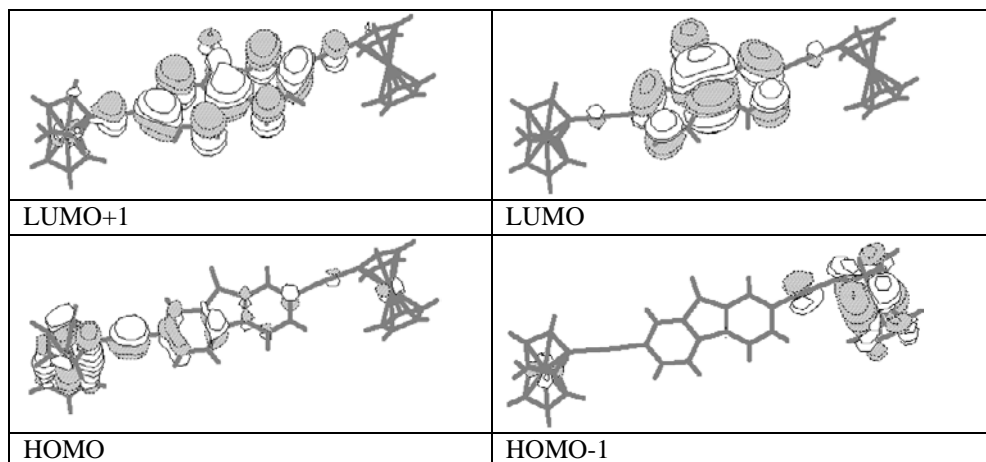


Figure 14. Spatial plots of the frontier molecular orbitals for **7**.

For **7–11**, the two ferrocenyl end groups only weakly communicate through the fluorenyl ring system as revealed by CV studies. Both diferrocenyl or triferrocenyl compounds were shown to undergo a single-step two- (or three-) electron oxidation involving the concomitant oxidation of the two (or three) ferrocenyl subunits at the experimental scan rate of 100 mV s^{-1} (table 2). The half-wave potential of the terminal ferrocenyl units shows a gradual increase in the order **9** \approx **10** $<$ **11** $<$ **8** $<$ **7** upon changing the 9-substituent of the fluorenyl ring from the electron-donating hexyl or ferrocenyl group in **9** and **10** to an electron-withdrawing oxo group in **7**. The potential is shifted to a more positive potential by ca. 120 mV from **10** to **7** and the low value for the oxidation potential in **10** shows that such a triferrocenyl species is more electron-rich. Loss of electron density from the ferrocenyl donor unit to the net electron-accepting fluorenone moiety through the alkynyl linking unit makes the oxidation wave appear at a more positive potential in **7**. For **7**, an additional irreversible wave was also observed at -0.95 V , which was attributable to the reduction of the fluorenone moiety.

Table 2. Photophysical and Redox Data for Fluorene-Derived Ferrocenylacetylides Complexes in CH₂Cl₂

Complex	$\lambda_{\text{max}} / \text{nm} (\varepsilon / 10^{-4} \text{ dm}^3 \text{ mol}^{-1} \text{ cm}^{-1})^{\text{a}}$	$E_{1/2} / \text{V} (\Delta E_p)^{\text{b}}$
7	288 (8.7), 349 (4.7), 493 (0.8)	0.14 (159), -0.95 ^c
8	342 (5.5), 429sh (0.3)	0.08 (120)
9	344 (4.0)	0.02 (122)
10	275 (4.6), 348 (6.1), 478sh (0.7)	0.03 (219)
11	267 (0.9), 275 (1.1), 339 (0.06), 364 (0.5)	0.05 (196)
12	279 (5.3), 338 (1.8), 472 (0.3)	0.17 (199), -0.74 ^c
13	284 (7.3), 344 (2.3), 474 (0.1)	0.17 (159), -0.73 ^c
14	272 sh (1.9), 298 (2.4), 307 (2.4), 368 (2.5), 496 (0.3)	0.71 ^c , 0.12 (99)
15	297 (7.1), 372 (8.2), 494 (1.1)	0.88 ^c , 0.11 (139)
16	297 (6.7), 349 (3.4), 476 (0.3)	0.13 (139)
17	289 (7.8), 343 (3.1), 474 (0.4)	0.14 (120)
18	279 (1.6), 306 (1.6), 349 (1.4), 457 (0.2)	0.07 (92), -1.56 ^c
19	257 (0.6), 304 (0.4), 348 (0.4), 451 (0.3), 490 (0.2)	0.06 (86), -1.58 ^c
20	258 (0.5), 336 (0.7), 449 (0.1)	0.04 (180)
21	240 (3.5), 283 (6.7), 309 (6.2), 354 (5.5), 454 (0.8)	0.10 (96), -1.59 ^c
22	263sh (3.8), 304 (5.3), 330 (3.7), 338 (3.2), 370 (4.6), 488 (0.5)	0.79 ^c , 0.07 (107)
23	262 (4.9), 305 (7.5), 378 (10.9), 485 (1.5)	0.82 ^c , 0.06 (158)
24	268 (3.0), 320 (1.7), 405 (1.3), 560 (0.2)	0.97 ^c , 0.08 (100)
25	302 (3.0), 421 (1.9), 598 (0.4)	0.95 ^c , 0.07 (107), -0.11 ^c
26	270 (5.0), 284 (4.0), 387sh (1.6), 404 (1.7), 592 (0.4)	0.27 (119), -1.13 ^c
27	320 (5.4), 461sh (0.3), 623 (0.1)	0.14 (99),
30	304 (1.5), 354 (1.1), 365 (1.1), 486br (0.2)	0.25 (130)
31	385 (1.8), 410 (1.7)	0.16 (148)
32	274 (1.6), 365 (1.3)	0.15 (180)
33	267 (0.6), 275 (0.9), 365 (0.7)	0.17 (198)

^a In CH₂Cl₂.

^b Scan rate = 100 mV s⁻¹, half-wave potential values $E_{1/2} = (E_{\text{pa}} + E_{\text{pc}})/2$ for reversible ferrocenyl oxidation, $\Delta E_p = E_{\text{pa}} - E_{\text{pc}}$ (in mV) for reversible waves are given in parentheses, where E_{pa} and E_{pc} are the anodic and cathodic peak potentials, respectively.

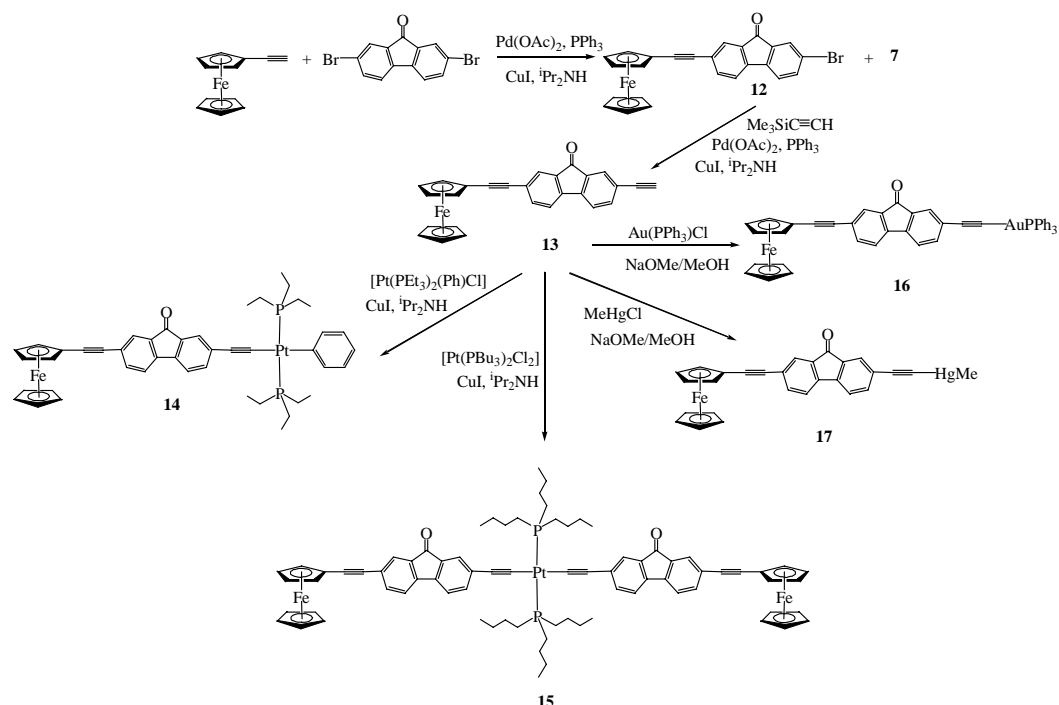
^c Irreversible wave.

sh = shoulder, br = broad.

New ferrocenyl heterometallic systems featuring such fluorene units were also investigated. In a multistep fashion, fluorenone-containing ferrocenylacetylene complex **13** (a perspective drawing of the molecule is shown in Figure 15), obtained from the bromo analogue **12**, was prepared which can provide a direct access to novel mixed-metal complexes **14–17** via the CuI-catalyzed dehydrohalogenative reactions with appropriate metal chloride compounds (Scheme 3) [40]. Complexes **14–17** dissolve very well in common organic solvents and their formulas were successfully confirmed by the intense molecular ion peak in each of the FAB mass spectra. The solid-state structures of **15–17** were determined by X-ray crystallography (Figures 16–18). For **15**, there is a centrosymmetry at the platinum center and the crystal structure shows a diferrocenyl end-capped species in which two deprotonated

forms of **13** are bound to a Pt(PBu₃)₂ unit in a *trans* geometry to furnish a rigid-rod, nanosized molecule with an iron–iron through-space separation of about 34 Å. The corresponding mean Fe–Pt distance is ca. 17 Å. The platinum center is square-planar with four ligand groups in the coordination sphere. The alkynyl bond lengths span the narrow range of 1.169(3)–1.189(3) Å, which are comparable to those in the bithienyl-linked analogue in section 2.1 [27]. The nearly linear bond angles around the alkyne units conform to the rigid and straight-chain nature of the molecule. The structures of the heterometallic complexes **16** and **17** have the isoelectronic fragments Au(PPh₃) and MeHg attached to the terminal alkyne unit of **13**, respectively. The geometry about the Au(I) and Hg(II) centers is essentially linear and the mean P–Au–C angle of 178.1(3)° and Au–C–C angle of 177.7(8)° in **16** as well as the C–Hg–C angle of 179.0(4)° and Hg–C–C angle of 178.5(9)° in **17** are typical of sp hybridization in the metal atom and acetylenic carbon.

Introduction of the platinum(II) segment in **14** and **15** can red-shift the lowest energy bands and increase the absorption intensity, suggesting an enhancement in the extent of π -delocalization through the platinum conjugated system that is fully consistent with the IR data. A red-shift of ~ 20 nm is observed from **13** to **14** and **15**. However, apart from an increase in the molar extinction coefficients, there is no significant difference in the lowest energy peak from **13** to **14** and **15**. Thus, delocalization of π electrons continues through the metal center to a different extent and the conjugation is greater for the Pt(II) complexes than the Au(I) and Hg(II) species. As far as the electrochemical behavior of these complexes is concerned, the cyclic voltammogram is dominated by one quasi-reversible ferrocenyl oxidation wave (table 2). An anodic shift of the Fc/Fc⁺ couple relative to the ferrocene standard is caused by the unsaturation of the ethynyl groups which makes the removal of electrons more difficult. When the conjugation length is increased upon capping the end group with an organometallic entity from **13** to **14–17**, oxidation is facilitated by the delocalization of charge along the main chain through a d π → p π interaction which leads to a lowering of the oxidation potentials. The most significant cathodic shift of ca. 0.06 V is noted in the most extended heterotrimetallic complex **15**, however, the two ferrocenyl end groups do not exhibit an observable electronic communication through the fluorenyl ring system in such case. Complex **15** only undergoes a single-step two-electron oxidation involving the concomitant oxidation of the two ferrocenyl subunits at a scan rate of 100 mV s^{−1}. In the literature, non-interacting diferrocenyl systems are known for *trans*-[FcC≡CPt(PR₃)₂C≡CFc] [29a,29b], **6a–c** [27] and *trans*-[Pd(PBu₃)₂(C≡CC₆H₄C≡CFc)₂] [29c], where Fc = (η^5 -C₅H₅)(η^5 -C₅H₄)Fe. The E_{1/2} value is slightly more anodic in **17** than in **16** because of the higher formal oxidation state of Hg(II) than that of Au(I), which would hinder the back-donation to π^* orbitals. Another irreversible redox event due to the Pt²⁺ → Pt³⁺ oxidation was also detected at higher positive potentials in **14** and **15**.



Scheme 3. Synthesis of heterometallic systems of fluorenone-based ferrocenylacetylene.

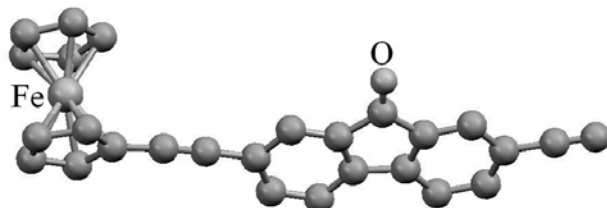


Figure 15. Molecular structure of **13**.

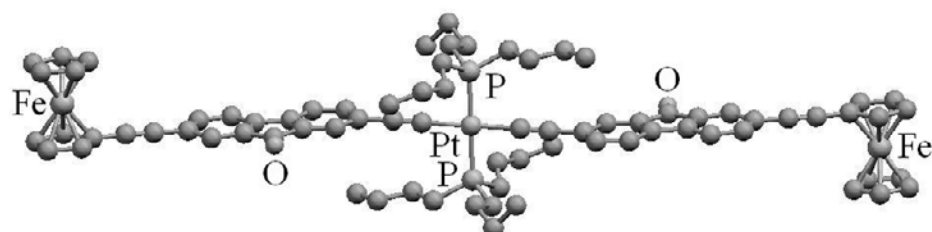
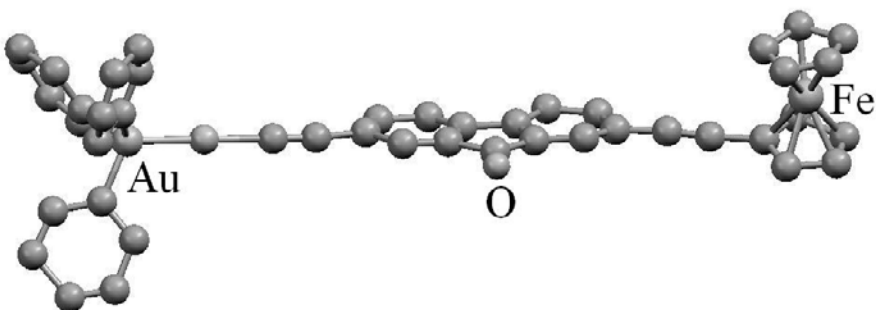
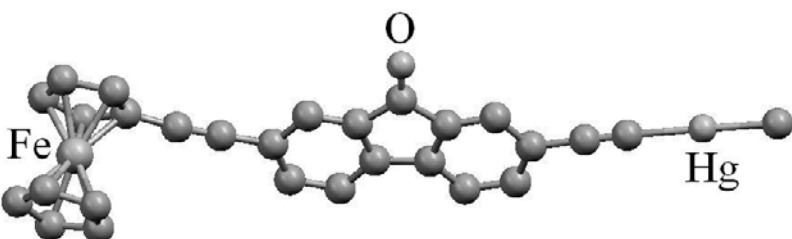
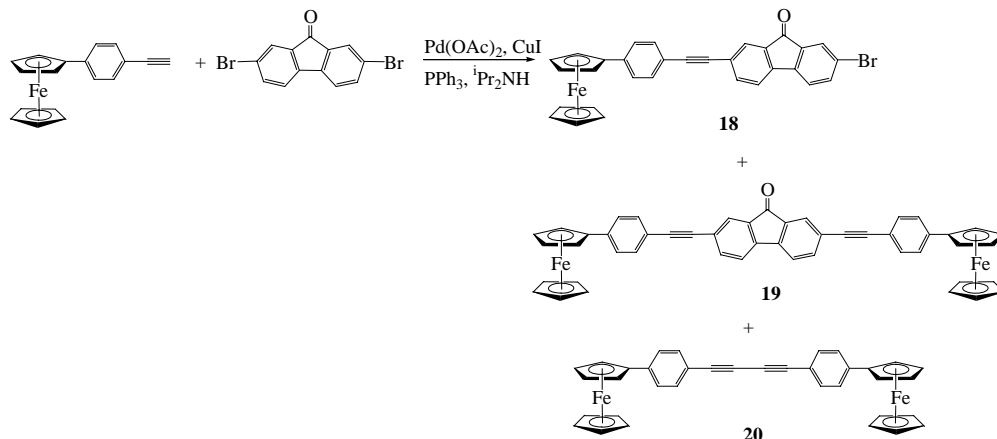


Figure 16. Molecular structure of **15**.

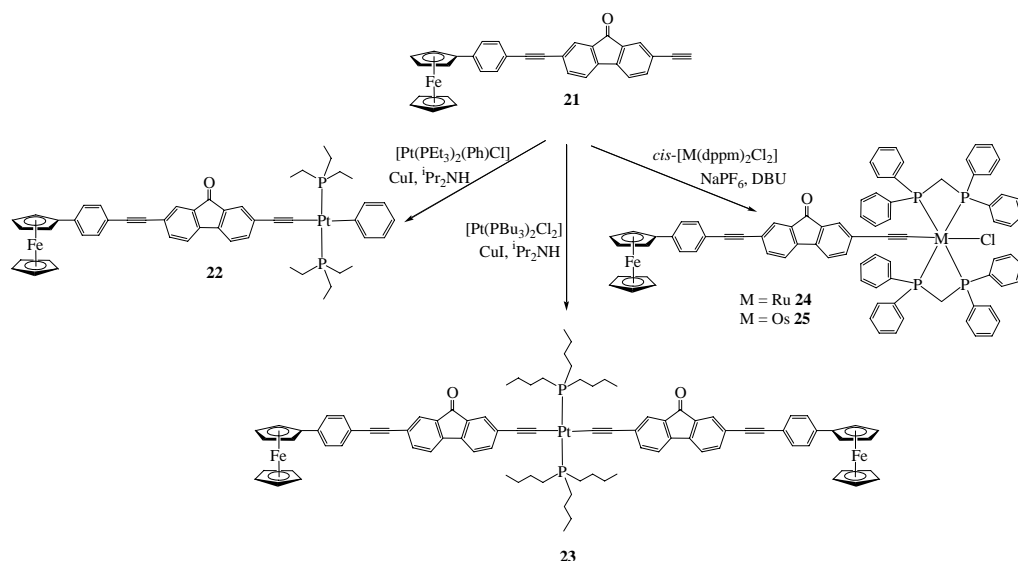
Figure 17. Molecular structure of **16**.Figure 18. Molecular structure of **17**.

In the quest for new alkynylferrocene-oriented materials, we also developed new molecular architectures based on the more extended congener, 4-ethynylphenylferrocene, and such a study should form an interesting protocol to the chemistry of systems of the longer homologue. The Sonogashira coupling reaction of 4-ethynylphenylferrocene with an excess of 2,7-dibromofluoren-9-one gave 2-bromo-7-(4-ferrocenylphenylethylnyl)fluoren-9-one **18** and 2,7-bis(4-ferrocenylphenylethylnyl)fluoren-9-one **19** as the major products, accompanied by the formation of 1,4-bis(4-ferrocenylphenyl)butadiyne **20** obtained via simultaneous oxidative coupling of 4-ethynylphenylferrocene in the presence of a trace amount of atmospheric O₂ (Scheme 4). We have been able to minimize the yield of the homocoupling product **20** (< 5%) under almost anaerobic conditions. 2-Ethynyl-7-(4-ferrocenylphenylethylnyl)fluoren-9-one **21** was prepared via three steps from 4-ethynylphenylferrocene and can be used for the build-up of new multimetallic systems. After the transformation of **18** to 2-trimethylsilylethylnyl-7-(4-ferrocenylphenylethylnyl)fluoren-9-one followed by desilylation with K₂CO₃ in MeOH, compound **21** was obtained. Scheme 5 outlines the synthetic routes to the bi- and trimetallic complexes **22–25** [41]. The classical dehydrohalogenation reactions between **21** and *trans*-[Pt(PEt₃)₂(Ph)Cl] or *trans*-[Pt(PBu₃)₂Cl₂] gave new platinum(II) alkynyl complexes **22** and **23**. New σ-acetylide complexes of Group 8 metals **24** and **25** were made by reacting *cis*-[M(dppm)₂Cl₂] (M = Ru, Os) with NaPF₆ to give first the vinylidene intermediates which can be deprotonated by 1,8-diazabicyclo[5.4.0]undec-7-ene (DBU) to furnish the desired compounds. The redox properties of **21–23** are very similar to those derived from ethynylferrocene. The structural properties of **23** and **25** were studied (Figures 22 and 23). For **23**, the X-ray structure shows a diferrocyll end-capped species in which two deprotonated forms of **21** are σ-bonded to the

central Pt(PBu₃)₂ unit in a *trans* configuration to afford a one-dimensional molecular rod of defined length and the through-space separation between the two Fe centers is estimated to be ~ 42 Å in the solid state. Hence, extension of the dimensions of these metal-capped molecules from the molecular scale to nanoscale is feasible based on this synthetic strategy.



Scheme 4. Synthesis of compounds **18–20**.



Scheme 5. Synthesis of heterometallic ferrocenyl alkynyl complexes of platinum, ruthenium and osmium containing fluorenone spacers.

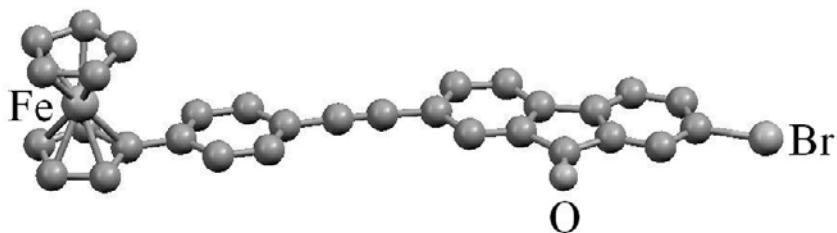


Figure 19. Molecular structure of **18**.

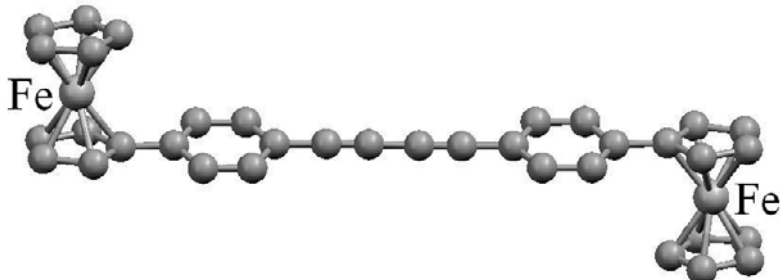


Figure 20. Molecular structure of **20**.

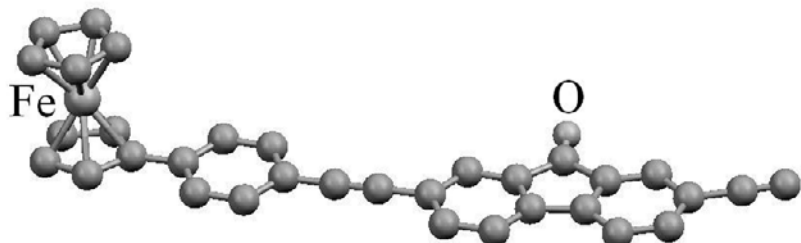


Figure 21. Molecular structure of **21**.

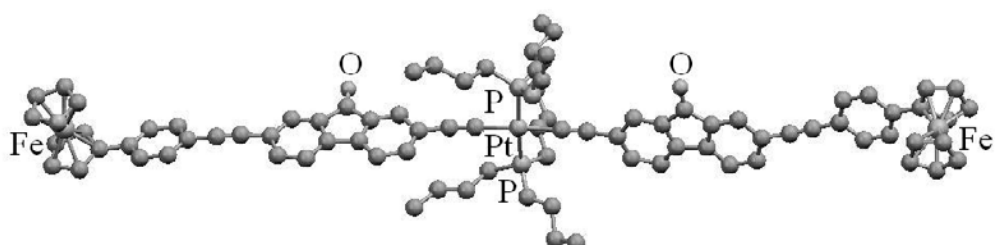


Figure 22. Molecular structure of **23**.

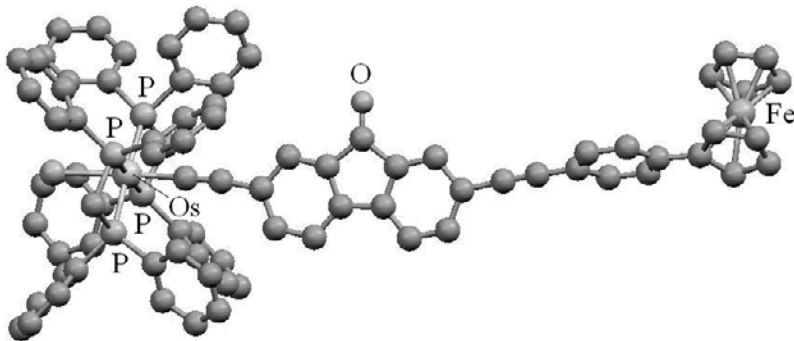


Figure 23. Molecular structure of **25**.

Molecular orbital calculations at the B3LYP level of DFT for complexes **21**, **23** and **25** based on their experimental geometries obtained from the X-ray data have been carried out. We found that the three HOMOs for **21** correspond to those derived from the mixing of the highest occupied orbitals of the conjugated organic structural unit and the two Fe(d_δ) orbitals. The δ -type is defined by viewing the orbitals along the Ct-Fe-Ct axes. When the Ct-Fe-Ct axis is defined as the z axis, the two d_δ orbitals correspond to the d_{xy} and $d_{x^2-y^2}$ orbitals. The LUMOs for **21** correspond to the π^* orbital in the structural unit having a carbonyl group. Carbonyl groups normally have lower π^* orbitals because of the electronegative oxygen atom. An orbital correlation diagram shown in Figure 24 is used to illustrate the change in the orbital patterns in **23** and **25** upon incorporation of different metal groups to **21**. The frontier orbitals of **23** consist of the orbital combinations of the two ferrocenyl-containing alkynyl ligands. The two HOMOs are contributed from the highest occupied π orbitals of the two ligands whereas the two LUMOs arise from the lowest unoccupied π^* orbitals of the organic portion in the two ligands. The two HOMOs of **25** are derived from the mixing of the Os metal d orbitals (i.e., d_{xz} and d_{yz} when the Os-Cl bond direction is defined as the z axis) and π orbitals of the Os-bonded C≡C unit. The LUMOs correspond to the lowest π^* orbitals of the carbonyl-containing conjugate structural moiety. Because of the π -donating properties of chloride ligand, there are π^* -antibonding characters between Os and Cl in the two HOMOs. In this way, the absorption band corresponding to the HOMO-LUMO transition probably has the MLCT character and the calculated HOMO-LUMO gap (2.69 eV) for **25** is considerably smaller than that for **21** (3.03 eV). The three HOMOs in **21** correspond to the 3rd to 5th HOMOs in **25**. Likewise, the smaller HOMO-LUMO gap for **23** (3.01 eV) as compared to **21** is in line with their observed UV/Vis data which indicates the possibility of π -conjugation through Pt.

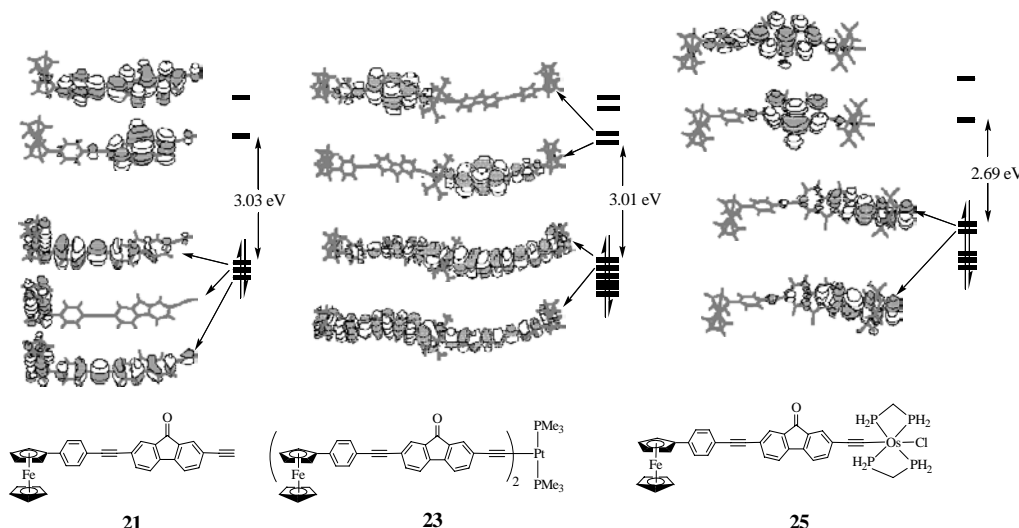


Figure 24. Contour plots of the HOMOs and the LUMOs for **21**, **23** and **25**. Here, the PBu_3 ligands in **23** were modeled by PMe_3 groups and the phenyl rings in **25** were modeled by H atoms.

As a further step, the coupling reaction of 2,7-dibromo-9-(dicyanomethylene)fluorene with ethynylferrocene was also studied. Although the palladium-catalyzed Sonogashira coupling of aryl halides with terminal acetylenes has been shown to be a versatile method for introducing an ethynyl group into organic molecules [28c], no direct coupling product was obtained in this case. Instead an unsymmetrical mono-cyano substituted fluorene compound **26** was generated in which one of the cyano groups is replaced by the incoming ferrocenylacetylide moiety [42]. This reaction also works in a general way for other organic terminal acetylenes. The synthesis of the symmetrical coupling product **27** thus requires the utilization of the corresponding fluoren-9-one derivative in the first step such that coupling reaction must take place first before the condensation reaction with malononitrile (Scheme 6). The crystal structure of **26** depicted in Figure 26 represents the first structurally characterized example of a fluorene derivative possessing an σ -acytlyide group at its 9-methylene position. The electronic spectra of **26** and **27** essentially show the structureless $\pi \rightarrow \pi^*$ transition bands of the corresponding fluorene π skeleton as well as the metal to ligand charge-transfer (MLCT) transitions at the low-energy regime, which were also supported by DFT calculations. From Figure 27, we found that the LUMO possesses the π^* anti-bonding orbitals in the conjugated unit, whereas the HOMO essentially contains mainly the Fe d_5 metal orbitals. The calculated HOMO–LUMO gap for **26** is 3.07 eV. The difference in the orbital characters in the HOMO explains why complex **26** has a smaller optical gap than that in the corresponding tolyl derivative because the metal orbitals generally have higher orbital energies than the π bonding orbitals of an aromatic C_6H_4 group in view of their ionization potentials. We note a bathochromic shift of ca. 130 nm in λ_{\max} in going from **7** (red in color) to **27** (green-blue in color) (see table 2). Comparing the data for **7** and **27**, the presence of the two π^* -accepting cyano groups lowers the optical gap value significantly by ~ 0.60 eV since these groups can stabilize the LUMO to a greater extent relative to that of the carbonyl group in **7**. We clearly notice a solvatochromic phenomenon for the lowest energy MLCT band in **26** (a red shift of 30 nm from hexane to CH_2Cl_2), consistent with a dipolar excited state due to

intramolecular charge-transfer (ICT) transition from the electron-donating ferrocenyl group to the electron-withdrawing cyano group through the conjugated framework. (compare the data of **26** in ethanol (nm): 267, 365, 400, 583 versus those in hexane: 257, 266, 274, 383, 400, 562). It is due to such MLCT band in **26** which gives rise to the deep blue colour of its solution in CH_2Cl_2 . In contrast, the higher-energy absorptions of **26** are relatively insensitive to the variation of solvent polarities. Analogous electron donor- π -acceptor chromophores **28** and **29** have also been reported by Perepichka and co-workers which can be obtained from the reaction between formylated ferrocenylacetylene and substituted fluorenes [43]. Compounds **28** and **29** also show ICT bands from the donor onto the acceptor moiety at 1.88 and 2.01 eV, respectively, and moderate second-order non-linear optical (NLO) properties as determined by the electric-field-induced second harmonic generation (EFISH) technique at $\lambda = 1.54 \mu\text{m}$ are observed for **29** [$\mu\beta(0) \approx 170 \pm 30 \times 10^{-48} \text{ esu}$].

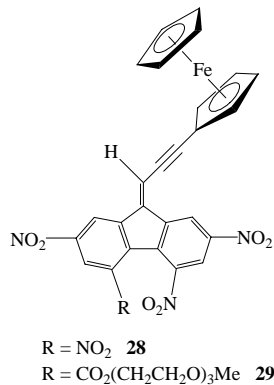


Figure 25. Chemical structures of **28** and **29**.

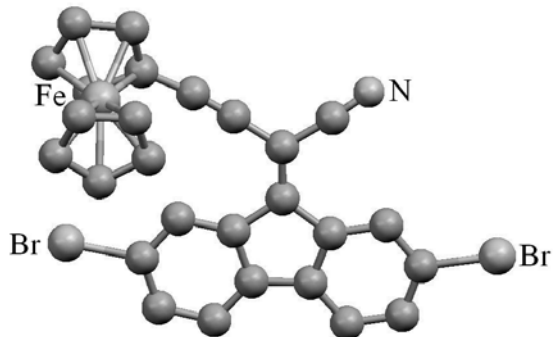
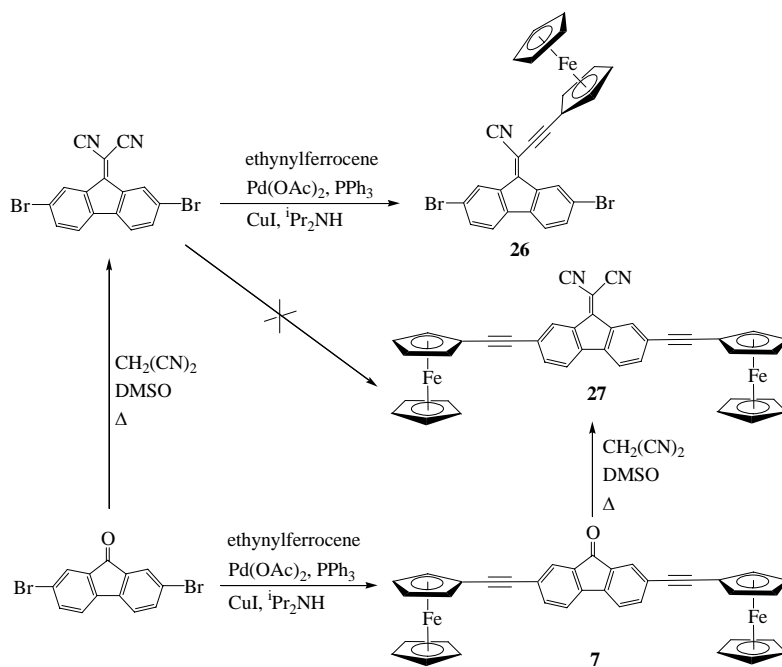


Figure 26. Molecular structure of **26**.



Scheme 6. Synthetic routes to 9-(dicyanomethylene)fluorene derivatives functionalized with substituted acetylenes.

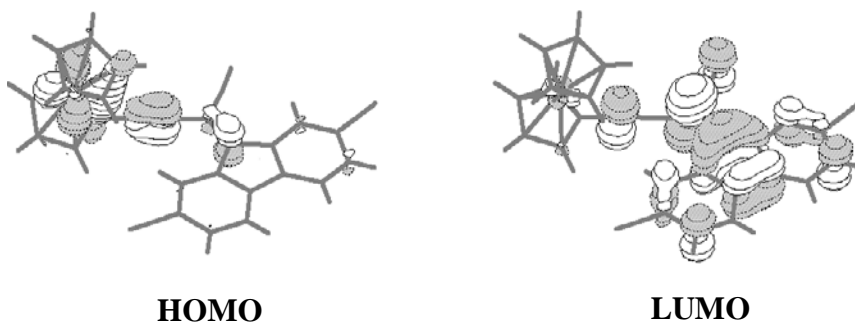
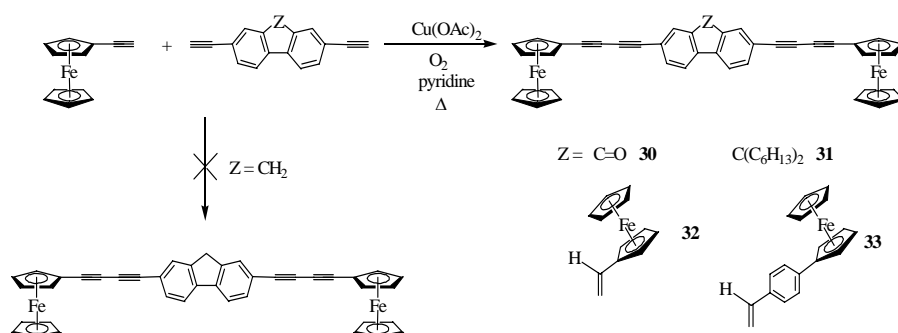


Figure 27. Spatial plots of the HOMO and LUMO for **26**.

While the above work in this area only highlighted on the use of monoalkynyl unit, it seemed an attractive goal to us to develop new molecular architectures based on the more extended 1,3-butadiynyl C₄ chain, and such a study will act as a spur to synthetic chemists working on the design of carbon-rich organometallics. In view of the fact that alkynyl ligands can offer structural rigidity and have great potentials to allow electronic communication between redox-active terminal end groups through delocalized bonds, we focused on the synthesis, characterization, redox and structural properties of a new series of carbon-rich ferrocenyl-capped bis(butadiynyl) complexes containing various fluorene-based spacers [44]. The spectroscopy and electrochemistry of these compounds were discussed as a function of the length of alkynyl bridges and the electronic effect of the fluorenyl substituents.

A new series of ferrocenyl end-capped bis(butadiynyl) fluorene complexes $[(\eta^5\text{-C}_5\text{H}_5)\text{Fe}(\eta^5\text{-C}_5\text{H}_4)\text{C}\equiv\text{CC}\equiv\text{CRC}\equiv\text{CC}\equiv\text{C}(\eta^5\text{-C}_5\text{H}_4)\text{Fe}(\eta^5\text{-C}_5\text{H}_5)]$ (R = fluoren-9-one-2,7-diyl **30**, 9,9-dihexylfluorene-2,7-diyl **31**, 9-ferrocenylmethylenefluorene-2,7-diyl **32**, 9-ferrocenylphenylmethylenefluorene-2,7-diyl **33**) have been synthesized in moderate yields by the oxidative coupling reactions of ethynylferrocene with half equivalents of the appropriate diethynylfluorene derivatives (Scheme 7). All the new complexes have been characterized by FTIR, NMR and UV/Vis spectroscopies and FABMS. The molecular structures of **30** and **33** have been determined by X-ray crystallographic techniques. The electronic absorption and redox properties of these carbon-rich molecules were investigated and the data were compared with those for the corresponding 2,7-bis(ferrocenylethynyl)fluorene counterparts **7** and **9–11**.



Scheme 7. Synthesis of carbon-rich ferrocenyl end-capped bis(butadiynyl) fluorene derivatives.

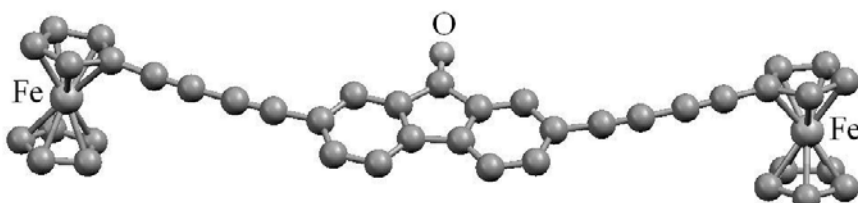


Figure 28. Molecular structure of **30**.

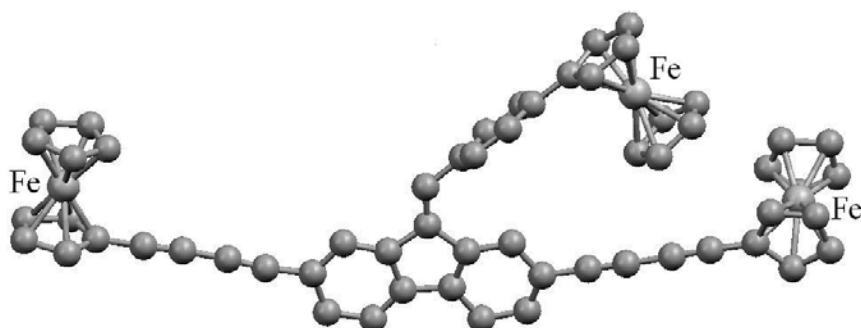


Figure 29. Molecular structure of **33**.

Based on the classical Hay- or Eglington-type synthetic procedures [45], the oxidative coupling reaction of 4-ethynylferrocene with half an equivalent of a series of 2,7-diethynylfluorene derivatives under a Cu(OAc)₂/O₂/pyridine system under reflux gave **30–33** as the major products, accompanied by the inevitable formation of 1,4-bis(ferrocenyl)butadiyne as a side product under such aerobic experimental conditions (Scheme 7). However, attempts to make a similar complex with the unsubstituted fluorene ring using 2,7-diethynylfluorene have met with little success and only compound **30** can be isolated probably due to the simultaneous oxidation of fluorene to fluoren-9-one under such air atmosphere. All the butadiynyl-containing compounds **30–33** show two weak to moderate $\nu(C\equiv C)$ absorptions in their IR spectra at around 2144 and 2213 cm⁻¹, which is different from the monoynе counterparts **7** and **9–11** where only one $\nu(C\equiv C)$ peak at about 2207 cm⁻¹ is observed in each case. From the single-crystal X-ray analyses, perspective views of the molecular structure of **30** and **33** are displayed in Figures 28 and 29. This represents the first structurally characterized example of such bis(ferrocenylbutadiynyl)arylene species in the literature. The structure of **30** consists of two ferrocenyl-1,3-butadiyne end groups appended to the central fluorenone unit at the 2,7-positions. An iron–iron through-space separation of ca. 21.9 Å was estimated in **30** which was found to be longer than that of 17.5 Å in **7** by 4.4 Å [39]. The two 1,3-butadiyne linear chains are essentially linear with C–C–C bond angles lying within 175.9(3)–177.2(3)°. The C–C triple bonds spanning the narrow range of 1.182(3)–1.195(3) Å are of the order of those observed in 1,4-diferrocenyl-1,3-butadiyne (1.198(4) Å) [46], 1,4-bis(4-ferrocenylphenyl)butadiyne (1.184(8) Å) [41] and 1,12-bis(ferrocenyl)-1,3,5,7,9,11-dodecahexayne (1.196(9)–1.224(10) Å) [13d].

It is clear that an increase in the number of ethynyl units from monoynе (for **7** and **9–11**) to diynе species (for **30–33**) leads to a bathochromic shift in the absorption maxima, consistent with the more extended π -conjugation for **30–33**. CV measurements in CH₂Cl₂ show that each of **30–33** is characterized by one quasi-reversible oxidation wave due to the ferrocenyl electrophore that is present (table 2). The half-wave potential of the terminal ferrocenyl moieties is anodically shifted when the number of ethynyl units increases and when the 9-substituent of the central fluorene ring changes from an electron-donating group to an electron-deficient group. A positive shift of the Fc/Fc⁺ couple relative to the ferrocene standard is caused by the unsaturation of the alkynе units which makes the removal of electrons more difficult than pure ferrocene. While no significant electronic interaction between terminal ferrocenyl moieties was detected in each case, we observe that those diferrocenyl complexes **30** and **31** (or triferoocenyl complexes **32** and **33**) only undergo a single-step two- (or three-) electron oxidation due to the concomitant oxidation of the two (or three) ferrocenyl subunits. It is worthwhile to note that the half-wave potential of the terminal ferrocenyl units follows the order **30** > **31** ≈ **32** ≈ **33** when the substituent at the 9-position of the central fluorene spacer varies from an electron-accepting fluoren-9-one to an electron-donating hexyl or ferrocenyl group. This is in line with the loss of electron density from the ferrocenyl group to the net electron-withdrawing fluorenone via the butadiynyl bridges. When the conjugation is extended from **7** and **9–11** to **30–33** upon incorporating an additional C≡C unit on each side of the fluorene group, the increased unsaturation of the conjugated backbone tends to increase the ferrocene-based oxidation potentials in the latter series.

3. CONCLUSIONS AND OUTLOOK

In this account, it is clear that a wide variety of ferrocenylacetylides complexes functionalized with the fluorene unit have been investigated. The properties of these compounds were completely elucidated by spectroscopic, electrochemical and X-ray structural techniques. The experimental results were also correlated with the theoretical calculations. These metalated systems have shown interesting optical, structural and redox characteristics. In many cases, variation of the 9-substituents on the fluorenyl ring can influence the optical and photophysical properties of these redox-active materials.

On another aspect, we have developed rational synthetic avenues to a new class of well-defined bis(ferrocenylethynyl) complexes and their heterometallic analogues with bridging units such as oligothiophenes and 2,7-functionalized fluorene derivatives. Various terminal ferrocenylacetylene synthons can serve as synthetic precursors to afford interesting multimetallic assemblages. Among these, we have been able to increase the dimensions of these rigid-rod-like complexes from the molecular scale to the nanoscale. Such studies may provide us a good platform to investigate novel multimetallic systems of nanosized dimensions which is of interest for the advance of nanoscale molecular wires and related nanomaterials. Remarkably, the X-ray crystal structures of several of these molecules in the solid-state were determined in which iron–iron through-space separations of ca. 32–42 Å can be obtained. We have also successfully extended the chemistry of bis(ethynylferrocene) complexes with different aromatic spacers to their bis(butadiynyl) congeners through the oxidative coupling reactions between two acetylenic precursors. The spectroscopic, structural and electrochemical properties of these carbon-rich compounds were examined in terms of the electronic nature of the 9-substituents of fluorene and the length of the C_n-bridges. Undoubtedly, there is still much scope to explore in the quest for a new series of rigid-rod multimetallic assemblies of nanosized dimensions displaying notable electronic communication along the conjugated chain.

4. ACKNOWLEDGMENT

This work was supported by CERG Grants from the Research Grants Council of the Hong Kong SAR, P.R. China (Project Nos. HKBU 2022/03P) and the Hong Kong Baptist University. Dr. Z. Lin at the Hong Kong University of Science and Technology is also gratefully acknowledged for his contribution on molecular orbital calculations. The author is also indebted to all the postgraduate students and postdoctoral associates whose names appear in the references of this chapter.

5. REFERENCES

- [1] (a) Bunz, U. H. F. *Angew. Chem., Int. Ed. Engl.* 1994, 33, 1073-1076; (b) Diederich, F. *Modern Acetylene Chemistry*, Stang, P. J.; Diederich, F. (Eds.), VCH Publishers, Weinheim, Germany, 1995, p.443; (c) Bunz, U. H. F.; Rubin, Y.; Tobe, Y. *Chem. Soc. Rev.* 1999, 28, 107-119.

- [2] (a) Manners, I. *Angew. Chem., Int. Ed. Engl.* 1996, **35**, 1602-1604; (b) Kingsborough, R. P.; Swager, T. M. *Prog. Inorg. Chem.* 1999, **48**, 123-231.
- [3] (a) Le Narvor, N.; Toupet, L.; Lapinte, C. *J. Am. Chem. Soc.* 1995, **117**, 7129-7135; (b) Weng, W.; Bartik, T.; Gladysz, J. A. *Angew. Chem., Int. Ed. Engl.* 1994, **33**, 2199-2202; (c) Colbert, M. C. B.; Lewis, J.; Long, N. J.; Raithby, P. R.; Younus, M.; White, A. J. P.; Williams, D. J.; Payne, N. N.; Yellowlees, L.; Beljonne, D.; Chawdhury, N.; Friend, R. H. *Organometallics* 1998, **17**, 3034-3043; (d) Bunz, U. H. F.; Wiegelmann-Kreiter, J. E. C. *Chem. Ber.* 1996, **129**, 785-797 and references therein; (e) Bruce, M. I.; Halet, J.-F.; Kahal, S.; Low, P. J.; Skelton, B. W.; White, A. H. *J. Organomet. Chem.* 1999, **578**, 155-168.
- [4] Grosshenny, V.; Harriman, A.; Ziessel, R. *Angew. Chem., Int. Ed. Engl.* 1995, **34**, 1100-1102.
- [5] (a) Altmann, M.; Bunz, U. H. F. *Angew. Chem., Int. Ed. Engl.* 1995, **34**, 569-571; (b) Oriol, L.; Serrano, J. L. *Adv. Mater.* 1995, **7**, 348-369.
- [6] (a) Lehn, J.-M. *Supramolecular Chemistry: Concepts and Perspectives*; VCH Publishers, Weinheim, Germany, 1995; (b) Ward, M. D. *Chem. Soc. Rev.* 1995, 121-134; (c) Tour, J. M. *Chem. Rev.* 1996, **96**, 537-554.
- [7] (a) Campagna, S.; Denti, G.; Serroni, S.; Juris, A.; Venturi, M.; Riceunto, V.; Balzani, V. *Chem. Eur. J.* 1995, **1**, 211-221; (b) Faust, R.; Diederich, F.; Gramlich, V.; Seiler, P. *Chem. Eur. J.* 1995, **1**, 111-117; (c) Amoroso, A. J.; Cargill-Thompson, A. M. W.; Maher, J. P.; McCleverty, J. A.; Ward, M. D. *Inorg. Chem.* 1995, **34**, 4828-4835; (d) Achar, S. Puddephatt, R. J. *Angew. Chem., Int. Ed. Engl.* 1994, **33**, 847-848.
- [8] (a) Ward, M. D. *Chem. Ind.* 1996, 568-573; (b) Bunz, U. H. F. *Angew. Chem., Int. Ed. Engl.* 1996, **35**, 969-971; (c) Lang, H. *Angew. Chem., Int. Ed. Engl.* 1994, **33**, 547-550; (d) Beck, W.; Niemer, B.; Wieser, M. *Angew. Chem., Int. Ed. Engl.* 1993, **32**, 923-950 and references therein; (e) Markwell, R. D.; Butler, I. S.; Kakkar, A. K.; Khan, M. S.; Al-Zakwani, Z. H.; Lewis, J. *Organometallics*. 1996, **15**, 2331-2337.
- [9] McCleverty, J. A.; Ward, M. D. *Acc. Chem. Res.* 1998, **31**, 842-851.
- [10] Le Vanda, C.; Cowan, D. O. *J. Am. Chem. Soc.* 1974, **96**, 6728-6729.
- [11] (a) Lavastre, O.; Plass, J.; Bachmann, P.; Salaheddine, A.; Moinet, C.; Dixneuf, P. H. *Organometallics*, 1997, **16**, 184-189; (b) Brady, M.; Weng, W.; Zhou, Y.; Seyler, J. W.; Amoroso, A. J.; Arif, A. M.; Böhme, M.; Frenking, G.; Gladysz, J. A. *J. Am. Chem. Soc.* 1997, **119**, 775-788; (c) Schimanke, H.; Gleiter, R. *Organometallics*. 1998, **17**, 275-277.
- [12] (a) Yuan, Z.; Stringer, G.; Jobe, I. R.; Kreller, D.; Scott, K.; Koch, L.; Taylor, N. J.; Marder, T. B. *J. Organomet. Chem.* 1993, **452**, 115-120; (b) Thomas, J. A.; Jones, C. J.; McCleverty, J. A.; Hutchings, M. G. *Polyhedron* 1996, **15**, 1409-1414; (c) Justin Thomas, K. R.; Lin, J.-T.; Lin, K.-J. *Organometallics*, 1999, **18**, 5285-5291; (d) Hradsky, A.; Bildstein, B.; Schuler, N.; Schottenberger, H.; Jaitner, P.; Ongania, K.-H.; Wurst, K.; Launay, J.-P. *Organometallics* 1997, **16**, 392-402; (e) Stang, S. L.; Paul, F.; Lapinte, C. *Organometallics* 2000, **19**, 1035-1043; (f) Brady, M.; Weng, W.; Gladysz, J. A. *J. Chem. Soc., Chem. Commun.* 1994, 2655-2656; (g) Justin Thomas, K. R.; Lin, J. T.; Wen, Y. S. *J. Organomet. Chem.* 1999, **575**, 301-309; (h) Jones, N. D.; Wolf, M. O.; Giaquinta, D. M. *Organometallics* 1997, **16**, 1352-1354; (i) Colbert, M. C. B.; Lewis, J.; Long, N. J.; Raithby, P. R.; White, A. J. P.; Williams, D. J. *J. Chem. Soc., Dalton*

- Trans.* 1997, 99-104; (j) Grosshenny, V.; Harriman, A.; Hissler, M.; Ziessel, R. *J. Chem. Soc., Faraday Trans.* 1996, 92, 2223-2238.
- [13] (a) Adams, R. D.; Qu, B. *Organometallics* 2000, 19, 2411-2413; (b) Adams, R. D.; Kwon, O. S.; Qu, B.; Smith, M. D. *Organometallics* 2001, 20, 5225-5232; (c) Adams, R. D.; Qu, B.; Smith, M. D.; Albright, T. A. *Organometallics* 2002, 21, 2970-2978; (d) Adams, R. D.; Qu, B.; Smith, M. D. *Organometallics* 2002, 21, 3867-3872; (e) Adams, R. D.; Qu, B.; Smith, M. D. *Organometallics* 2002, 21, 4847-4852.
- [14] (a) Wong, W.-Y.; Ho, C.-L. *Coord. Chem. Rev.* 2006, 250, 2627-2690; (b) Wong, W.-Y. *J. Inorg. Organomet. Polym. Mater.* 2005, 15, 197-219; (c) Long, N. J.; Williams, C. K. *Angew. Chem. Int. Ed.* 2003, 42, 2586-2617.
- [15] (a) Long, N. J. *Metallocenes: An Introduction to Sandwich Complexes*, Blackwell Science, Oxford, UK, 1998; (b) Justin Thomas, K. R.; Lin, J. T.; Wen, Y. S. *Organometallics*, 2000, 19, 1008-1012; (c) Colbert, M. C. B.; Edwards, A. J.; Lewis, J.; Long, N. J.; Page, N. A.; Parker, D. G.; Raithby, P. R. *J. Chem. Soc., Dalton Trans.* 1994, 2589-2590; (d) Colbert, M. C. B.; Hodgson, D.; Lewis, J.; Raithby, P. R.; Long, N. J. *Polyhedron* 1995, 14, 2759-2766; (e) Lee, S.-M.; Marcaccio, M.; McCleverty, J. A.; Ward, M. D. *Chem. Mater.* 1998, 10, 3272-3274.
- [16] (a) Sonogashira, K.; Ohga, K.; Takahashi, S.; Hagihara, N. *J. Organomet. Chem.* 1980, 188, 237-243; (b) Takahashi, S.; Sonogashira, K.; Morimoto, H.; Murata, E.; Kataoka, S.; Hagihara, N. *J. Polym. Sci., Polym. Chem. Ed.* 1982, 20, 565-573; (c) Lavastre, O.; Even, M.; Dixneuf, P. H.; Pacreau, A.; Vairon, J. P. *Organometallics*. 1996, 15, 1530-1531.
- [17] (a) McCullough, R. D. *Adv. Mater.* 1998, 10, 93-116 and references therein; (b) Skotheim, T. A. (Ed.), *Handbook of Conducting Polymers*, Marcel Dekker, New York, 1986; (c) Roncali, J. *Chem. Rev.*, 1997, 97, 173-205; (d) Kraft, A.; Grimsdale, A. C.; Holmes, A. B. *Angew. Chem., Int. Ed.* 1998, 37, 402-428; (e) Wong, W.-Y. *Comments Inorg. Chem.* 2005, 26, 39-74.
- [18] (a) Wong, W.-Y. *Coord. Chem. Rev.* 2005, 249, 971-997. (b) Nehr, D. *Macromol. Rapid Commun.* 2001, 22, 1365-1385.
- [19] (a) Nuguyen, P.; Gomez-Elipe, P.; Manners, I. *Chem. Rev.* 1999, 99, 1515-1548; (b) Manners, I. *Synthetic Metal-Containing Polymers*, Wiley-VCH, 2005; (c) Wong, W.-Y.; Ho, C.-L. *Rigid-rod Polymetallaynes in Frontiers in Transition Metal-Containing Polymers*, Abd-El-Aziz, A. S.; Manners, I. (Eds.), Wiley-Interscience, 2007, Chap. 6.
- [20] (a) Perepichka, I. F.; Perepichka, D. F.; Meng, H.; Wudi, F. *Adv. Mater.* 2005, 17, 2281-2305; (b) Fichou, D. (Ed.), *Handbook of Oligo- and Polythiophenes*, Wiley-VCH, New York, 1999.
- [21] (a) Garnier, F. *Acc. Chem. Res.* 1999, 32, 209-215; (b) Dodabalapur, A.; Torsi, L.; Katz, H. E. *Science* 1995, 268, 270-271; (c) Hajlaoui, R.; Fichou, D.; Horowitz, G.; Nessakh, B.; Constant, M.; Garnier, F. *Adv. Mater.* 1997, 9, 557-561.
- [22] (a) Kim, J. Y.; Kim, S. H.; Lee, H.-H.; Lee, K.; Ma, W.; Gong, X.; Heeger, A. J. *Adv. Mater.* 2006, 18, 572-576; (b) Reyes-Reyes, M.; Kim, K.; Carroll, D. J. *Appl. Phys. Lett.* 2005, 87, 083506-1-083506-3; (c) Kim, Y.; Cook, S.; Tuladhar, S. M.; Choulis, S. A.; Nelson, J.; Durrant, J. R.; Bradley, D. D. C.; Giles, M.; McCulloch, I.; Ha, C. S.; Ree, M. *Nature Mater.* 2006, 5, 197-203; (d) Li, G.; Shrotriya, V.; Huang, J.; Yao, Y.; Moriarty, T.; Emery, K.; Yang, Y. *Nature Mater.* 2005, 4, 864-868; (e) Li, G.; Shrotriya, V.; Yao, Y.; Yang, Y. *J. Appl. Phys.* 2005, 98, 043704-1-043704-5; (f) Kim,

- Y.; Choulis, S. A.; Nelson, J.; Bradley, D. D. C.; Cook, S.; Durrant, J. R. *Appl. Phys. Lett.* 2006, **86**, 063502-1-063502-3; (g) Chirvase, D.; Parisi, J.; Hummelen, J. C.; Dyakonov, V. *Nanotechnology* 2004, **15**, 1317-1323; (h) De Bettignies, R.; Leroy, J.; Firon, M.; Sentein, C. *Synth. Met.* 2006, **156**, 510-513; (i) Mihailetschi, V. D.; Xie, H.; de Boer, B.; Popescu, L. M.; Hummelen, J. C.; Blom, P. W. M.; Koster, L. J. A. *Appl. Phys. Lett.* 2006, **89**, 012107-1-012107-3.
- [23] (a) Chisholm, M. H.; Epstein, A. J.; Gallucci, J. C.; Feil, F.; Pirkle, W. *Angew. Chem. Int. Ed.* 2005, **44**, 6537-6540; (b) Ma, C.-Q.; Mena-Osteritz, E.; Debaerdemaeker, T.; Wienk, M. M.; Janssen, R. A. J.; Bäuerke, P. *Angew. Chem. Int. Ed.* 2007, **46**, 1679-1683; (c) Barta, P.; Birgersson, J.; Guo, S.; Arwin, H.; Salaneck, W. R.; Zagorska, M. *Adv. Mater.* 1997, **9**, 135; (d) Birgerson, J.; Kaeriyama, K.; Barta, P.; Broms, P.; Fahlman, M.; Granlund, T.; Salaneck, W. R. *Adv. Mater.* 1996, **8**, 982-985; (e) Harrison, M. G.; Friend, R. H. *Electronic Materials: The Oligomer Approach*, Mullen, K.; Wegner, G. (Eds.), Wiley-VCH, 1998, Chap. 10.
- [24] Barbarella, G. *Chem. Eur. J.* 2002, **8**, 5073-5077; (b) Li, C.; Numata, M.; Takeuchi, M.; Shinkai, S. *Angew. Chem. Int. Ed.* 2005, **44**, 6371-6374.
- [25] Stott, T. L.; Wolf, M. O. *Coord. Chem. Rev.* 2002, **226**, 81-101.
- [26] (a) Lewis, J.; Long, N. J.; Raithby, P. R.; Shields, G. P.; Wong, W.-Y.; Younus, M. *J. Chem. Soc., Dalton Trans.* 1997, 4283-4288; (b) Chawdhury, N.; Köhler, A.; Friend, R. H.; Wong, W.-Y.; Lewis, J.; Younus, M.; Raithby, P. R.; Corcoran, T. C.; Al-Mandhary, M. R. A.; Khan, M. S. *J. Chem. Phys.* 1999, **110**, 4963-4970; (c) Chawdhury, N.; Köhler, A.; Friend, R. H.; Younus, M.; Long, N. J.; Raithby, P. R.; Lewis, J. *Macromolecules* 1998, **31**, 722-727.
- [27] Wong, W.-Y.; Lu, G.-L.; Ng, K.-F.; Choi, K.-H.; Lin, Z. *J. Chem. Soc., Dalton Trans.* 2001, 3250-3260.
- [28] (a) Sonogashira, K.; Tohda, Y.; Hagihara, N. *Tetrahedron Lett.* 1975, 4467-4470; (b) Khan, M. S.; Kakkar, A. K.; Long, N. J.; Lewis, J.; Raithby, P. R.; Nguyen, P.; Marder, T. B.; Wittmann, F.; Friend, R. H. *J. Mater. Chem.* 1994, **4**, 1227-1232; (c) Takahashi, S.; Kuroyama, Y.; Sonogashira, K.; Hagihara, N. *Synthesis* 1980, 627-630.
- [29] (a) Osella, D.; Milone, L.; Nervi, C.; Ravera, M. *J. Organomet. Chem.* 1995, **488**, 1-3; (b) Osella D.; Gobetto, R.; Nervi, C.; Ravera, M.; D'Amato, R.; Russo, M. V. *Inorg. Chem. Commun.* 1998, **1**, 239-245.
- [30] Bäuerle, P. *Adv. Mater.* 1992, **4**, 102-105.
- [31] Garcia, P.; Pernaut, J. M.; Hapiot, P.; Wintgens, V.; Valat, P.; Garnier, F.; Delabougline, D. *J. Phys. Chem.* 1993, **97**, 513-516.
- [32] Jestin, I.; Frère, P.; Mercier, N.; Levillain, E.; Stievenard, D.; Roncali, J. *J. Am. Chem. Soc.* 1998, **120**, 8150-8158.
- [33] (a) Becke, A. D. *J. Chem. Phys.* 1993, **98**, 5648-5652; (b) Miehlich, B.; Savin, A.; Stoll, H.; Preuss, H. *Chem. Phys. Lett.* 1989, **157**, 200-206; (c) Lee, C.; Yang, W.; Parr, G. *Phys. Rev. B* 1988, **37**, 785-789.
- [34] Schaftenaar, G. Molden v3.5, CAOS/CAMM Center Nijmegen, Toernooiveld, Nijmegen (Netherlands), 1999.
- [35] (a) Lewis, J.; Raithby, P. R.; Wong, W.-Y. *J. Organomet. Chem.* 1998, **556**, 219-228; (b) Wong, W.-Y.; Lu, G.-L.; Choi, K.-H.; Shi, J.-X. *Macromolecules* 2002, **25**, 3506-3513; (c) Zhou, G.-J.; Wong, W.-Y.; Cui, D.; Ye, C. *Chem. Mater.* 2005, **17**, 5209-5217; (d) Wong, W.-Y.; Choi, K.-H.; Lu, G.-L.; Shi, J.-X. *Macromol. Rapid Commun.*

- 2001, 22, 461-465; (e) Wong, W.-Y.; Liu, L.; Poon, S.-Y.; Choi, K.-H.; Cheah, K.-W.; Shi, J.-X. *Macromolecules* 2004, 37, 4496-4504. (f) Wong, W.-Y.; Poon, S.-Y.; Lee, A. W.-M.; Shi, J.-X.; Cheah, K.-W. *Chem. Commun.* 2004, 2420-2421; (g) Wong, W.-Y.; Poon, S.-Y.; Shi, J.-X.; Cheah, K.-W. *J. Polym. Sci.: Part A: Polym. Chem.* 2006, 44, 4804-4824; (h) Liu, L.; Wong, W.-Y.; Poon, S.-Y.; Shi, J.-X.; Cheah, K.-W.; Lin, Z. *Chem. Mater.* 2006, 18, 1369-1378; (i) Ho, C.-L.; Wong, W.-Y. *J. Organomet. Chem.* 2006, 691, 395-402. (j) Zhou, G.-J.; Wong, W.-Y.; Lin, Z.; Ye, C. *Angew. Chem. Int. Ed.* 2006, 45, 6189-6193.
- [36] (a) Tsuie, B.; Reddinger, J. L.; Sotzing, G. A.; Soloducho, J.; Katritzky, A. R.; Reynolds, J. R. *J. Mater. Chem.* 1999, 9, 2189-2200; (b) Wong, K.-T.; Chien, Y.-Y.; Chen, R.-T.; Wang, C.-F.; Lin, Y.-T.; Chiang, H.-H.; Hsieh, P.-Y.; Wu, C.-C.; Chou, C.-H.; Su, Y. O. *J. Am. Chem. Soc.* 2002, 124, 11576-11577; (c) Yu, W.-L.; Pei, J.; Huang, W.; Heeger, A. J. *Adv. Mater.* 2000, 12, 828-831; (d) Setayesh, S.; Grimsdale, A. C.; Weil, T.; Enkelmann, V.; Müllen, K.; Meghdadi, F.; List, E. J. W.; Leising, G. J. *Am. Chem. Soc.* 2001, 123, 946-953; (e) Marsitzky, D.; Vestberg, R.; Blainey, P.; Tang, B. T.; Hawker, C. J.; Carter, K. R. *J. Am. Chem. Soc.* 2001, 123, 6965-6972.
- [37] (a) Janietz, S.; Bradley, D. D. C.; Grell, M.; Glebeler, C.; Inbasekaran, M.; Woo, E. P. *Appl. Phys. Lett.* 1998, 73, 2453-2455; (b) Yu, W.-L.; Pei, Y.; Cao, Y.; Huang, W.; Heeger, A. J. *Chem. Commun.* 1999, 1837-1838; (c) Pschirer, N. G.; Bunz, U. H. F. *Macromolecules* 2000, 33, 3961-3963; (d) Scherf, U.; List, E. J. *Adv. Mater.* 2002, 14, 477-487.
- [38] (a) Mysyk, D. D.; Perepichka, I. F.; Perepichka, D. F.; Bryce, M. R.; Popov, A. F.; Goldenberg, L. M.; Moore, A. J. *J. Org. Chem.* 1999, 64, 6937-6950; (b) Perepichka, I. F.; Popov, A. F.; Orekhova, T. V.; Bryce, M. R.; Andrievskii, A. M.; Batsanov, A. S.; Howard, J. A. K.; Sokolov, N. I. *J. Org. Chem.* 2000, 65, 3053-3063.
- [39] Wong, W.-Y.; Lu, G.-L.; Ng, K.-F.; Wong, C.-K.; Choi, K.-H. *J. Organomet. Chem.* 2001, 637-639, 159-166.
- [40] Wong, W.-Y.; Ho, K.-Y.; Choi, K.-H. *J. Organomet. Chem.* 2003, 670, 17-26.
- [41] Wong, W.-Y.; Ho, K.-Y.; Ho, S.-L.; Lin, Z. *J. Organomet. Chem.* 2003, 683, 341-353.
- [42] Wong, W.-Y.; Lu, G.-L.; Choi, K.-H.; Lin, Z. *Eur. J. Org. Chem.* 2003, 365-373.
- [43] Moore, A. J.; Chesney, A.; Bryce, M. R.; Batsanov, A. S.; Kelly, J. E.; Howard, J. A. K.; Perepichka, I. F.; Perepichka, D. F.; Meshulam, G.; Berkovic, G.; Kotler, Z.; Mazor, R.; Khodorkovsky, V. *Eur. J. Org. Chem.* 2001, 2671-2687.
- [44] Wong, W.-Y.; Lu, G.-L.; Choi, K.-H.; Guo, Y.-H. *J. Organomet. Chem.* 2005, 690, 177-186.
- [45] (a) Hay, A. S. *J. Org. Chem.* 1962, 27, 3320-3321; (b) Peters, T. B.; Bohling, J. C.; Arif, A. M.; Gladysz, J. A. *Organometallics* 1999, 18, 3261-3263; (c) Mohr, W.; Stahl, J.; Hampel, F.; Gladysz, J. A. *Inorg. Chem.* 2001, 40, 3263-3264.
- [46] Rodriguez, J.-G.; Oñate, A.; Martin-Villamil, R. M.; Fonseca, I. *J. Organomet. Chem.* 1996, 513, 71-76.

Chapter 6

THE BIO-ORGANOMETALLIC CHEMISTRY OF [2FE2S] MODELS RELATED TO IRON HYDROGENASE ACTIVE SITE

Xiaojun Peng* and Jun Hou

State Key Laboratory of Fine Chemicals, Dalian University of Technology,
116012 Dalian, P. R. China

ABSTRACT

Hydrogenases are enzymes that catalyze the reversible uptake/evolution hydrogen. The X-ray single crystal structure determinations have shown that the active site of iron hydrogenase features the organometallic community of [2Fe2S] compounds. Small molecular synthetic models, which structurally mimic the [2Fe2S] centre, serve as important probes of structure and chemistry at the active site of Fe-only hydrogenase. The azadithiolate-bridged diiron compounds that have been developed as structural model systems for Fe-only hydrogenase are reviewed in this article. The functionalized diiron complexes which show some ability to generate hydrogen are surveyed, with emphasis on the synthesis and the electrocatalytic properties. The electrocatalytic properties of all complexes investigated by cyclic voltammetry in the presence and absence of acid are described. In addition, the application of electrochemical and IR spectroelectrochemical (SEC) techniques to the elucidation of the details of the electrocatalytic proton reduction is described. The functional mechanistic proposals are discussed from these work.

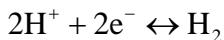
Keywords: Bioinorganic; Bioorganometallic chemistry; Electrochemistry; Hydrogen evolution; IR spectroelectrochemistry; Iron hydrogenase; Synthetic models.

* Xiaojun Peng: E-mail: pengxj@dlut.edu.cn

1. INTRODUCTION

Hydrogen is being considered as a clean and highly efficient energy carrier in the future. [1] However, hydrogen evolution from the reduction of protons and electrons is now efficiently catalyzed by the expensive platinum-containing catalysts.[2] For this reason, a search for the less expensive and more efficient catalysts to replace platinum-based materials become a challenge for the hydrogen energy applications.[3, 4]

To date, no molecular system but hydrogenases can achieve this goal. Many microorganisms, such as methanogenic, acetogenic, nitrogen-fixing, photosynthetic, or sulfate-reducing bacteria, can metabolize hydrogen, which is controlled by hydrogenases.[5, 6] Not surprisingly, hydrogenases catalyze the reversible uptake/evolution hydrogen according to the following reaction:



Hydrogenases can be classified into three groups on the basis of the metal content of their respective active sites, NiFe hydrogenases,[7, 8] NiFeSe hydrogenases, [7] and Fe-only hydrogenases.[9, 10] The NiFe hydrogenases and NiFeSe hydrogenases contain at least a Ni and an Fe atom, which tend to be more involved in hydrogen oxidation. The Fe-only hydrogenases contain two Fe atoms, with responsibility of hydrogen production. Fe-only hydrogenases are 50–100 times more active than [NiFe] hydrogenases. The maximum turnover frequencies for Fe-only hydrogenase are in the range 6000–60,000 molecules $\text{H}_2 \text{ s}^{-1}$ per site. [11, 12] In recent years, Fe-only hydrogenases are of particular interest because of their high rates of hydrogen production. This article focuses on the Fe-only hydrogenase and their model systems.

The structural definition of the Fe-only hydrogenase has initiated significant interest in developing model systems for the active site. Remarkably, earlier work by bioinorganic and organometallic chemists had already generated many diiron organometallic compounds that significantly resembles the Fe-hydrogenase active site. [13–16] According to the crystallographic results on the proteins, several groups prepared the biomimetic models by modifying the parent dinuclear $\text{Fe}_2\text{S}_2(\text{CO})_6$ structure [17] using the 1,3–propane dithiolate ligand [18, 19] or azadithiolate ligands [20–22] as the source of the bridging S ligands. The relatively simple structures which have been easily prepared and their close resemblance to the active site suggests that this dinuclear arrangement are readily assembled and might constitute easily accessible. Therefore, this diiron organometallic chemistry not only provides structural and spectroscopic analogues, and, eventually, reactivity models, but might offers the prospects of understanding the properties of the active site and the catalytic reaction that takes place in the Fe hydrogenase.

One of the main directions of study, among many others, of the bioinorganic chemist is to prepare diiron azadithiolate complexes which have been considered as relevant to the diiron subsite chemistry. So, in this article, we will present a short non-exhaustive overview of diiron azadithiolate model complexes related to the Fe-only hydrogenase active site. Several diiron complexes reported by our laboratory will be discussed, including the electrocatalytic properties.

Although few detailed electrochemical studies have been reported until now, several diiron azadithiolate complexes have been used as catalysts for the electrochemical reduction of protons to H₂, including protonation and reduction behavior. The electrochemistry data cited in this article all have been converted to values relative to the Fc⁺/Fc.

2. ACTIVE SITE STRUCTURE OF FE-ONLY HYDROGENASE

The Fe-only enzymes have been identified only in certain anaerobic bacteria and some anaerobic eukaryotes [5, 6]. X-ray crystallographic structures [23, 24] and spectroscopies [25–28] of Fe-only hydrogenases, from *Clostridium pasteurianum* and *D. desulfuricans*, respectively, reveal that the active site, wherein the catalytic chemistry takes place, possesses a common core, which consists of an “organometallic” [2Fe2S] sub-site linked to a [4Fe4S] cluster by a bridging cysteinyl sulfur. [23, 24] The core is deeply buried the protein of Fe-only hydrogenases. This common core also harbors three [4Fe4S] clusters. [25] The Fe-only hydrogenase from *C. pasteurianum* contains two additional domains, each with one iron-sulfur cluster, which gives the molecule a mushroom aspect.[23] The moiety including the dinuclear center, the thiolate bridging ligand, and the proximal [4Fe4S] cluster is known as the “H-cluster”. [6] The [4Fe4S] unit is probably responsible for electron transfer while the 2Fe2S subsite is utilized as a catalytic center for hydrogen formation and activation.[12]

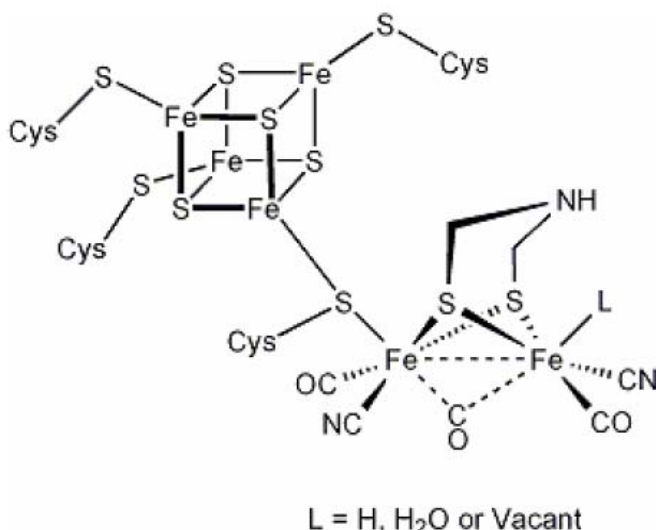


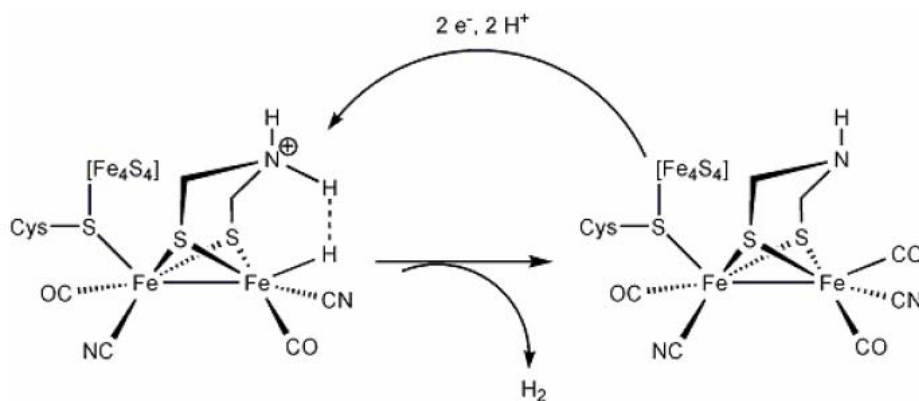
Figure 1. Schematic structure for the H-cluster of the Fe-only hydrogenase active site.

At the Fe–Fe dinuclear center, the two iron atoms are bridged by the sulfur atoms of a 1, 3-propanedithiolate ligand having a structure –SCH₂CH₂CH₂S– (PDT),[23] while the spectroscopic studies show the ligand favors di(thiomethyl)amine ligand having a structure –SCH₂NCH₂S– (ADT).[26–28] The biologically unusual ligands CO and CN[−] are found in the diiron unit. The diiron subunit adopts a bi-octahedral butterfly geometry. The Fe–Fe distance is *ca.* 2.60 Å. In the oxidized form, one CO bridges the two Fe atoms at the catalytic site

whereas in the reduced form this same CO is terminally bound to the Fe atom distal to the [4Fe4S] cluster. The Fe atom distal to the [4Fe4S] cluster is coordinated by water molecule (or vacancy) in the partially reduced or reduced form of the Fe-only hydrogenase. In the CO inhibited form of the Fe-only hydrogenase, this site is thought to be occupied by CO for hydride/dihydrogen binding.

The electronic structure of the two Fe in the sub-site of the Fe-only hydrogenase is intriguing. By using the Mössbauer [29], FTIR [26, 28, 30] and EPR [31, 32] spectroscopy for DdH and CpI, several redox states in the diiron unit have been observed. The three most likely states are a reduced state (H_{red}), an oxidized state (H_{ox}), and a CO-inhibited state (H_{ox-CO}). In the reduced state (H_{red}), the proximal iron atom is diamagnetic, and probably contains a low-spin Fe^{II} . The diiron center in both H_{ox} and H_{ox-CO} states is paramagnetic ($S = 1/2$). The main question is whether the formal oxidation state in diiron unit is Fe^{III} or is unprecedented Fe^I state. Mössbauer studies show that the distal iron is in a conventional Fe^{III} state, but not Fe^I . [29] However, FTIR ^{13}CO labelling studies of the Fe hydrogenase by De Lacey and co-workers strongly support an Fe^I oxidation state for the distal iron centre in $\{H_{ox-CO}\}$. DFT calculations suggest that H_{ox} is a mixed state Fe^I-Fe^{II} . [33, 34]

Whether the bridging dithiolate in the diiron unit is 1,3-propanedithiolate or a di(thiomethyl)amine ligand is still a considerable question. Early crystallographic studies indicate that the diiron centers in the Fe-only hydrogenase are bridged by 1,3-propanedithiolate. However, Studies on spectroscopy and theory of Fe-only hydrogenases favoured di(thiomethyl)amine ligand. The natural selection of the azadithiolate cofactor is probably the reason that azadithiolates could be easily biosynthesized. On the other hand, the amine in the cofactor could participate in the proton transfer required in the process of hydrogen evolution, as shown in Scheme 1. [35] The amine functionality in the azadithiolate could complement the catalytic function of the diiron unit by interacting with flanking ligands.



Scheme 1. The possible role of di(thiomethyl)amine unit in catalytic H_2 evolution.

3. STRUCTURAL MODELS RELATED TO THE ACTIVE SITE OF FE-ONLY HYDROGENASE

3.1. Azadithiolate Diiron Complexes

Since the discoveries of hydrogenases in bacteria in 1931 [36] and in archaea in 1981,[5] their importance in all areas of natural sciences and their potential for technological application in fuel cells [37–39] have attracted significant interest in understanding the structure and function of the Fe-only hydrogenase active site. In the context, some catalysts for proton reduction have been developed, which are attractive base metal alternatives to platinum-based materials typical for H₂ production.[3]

Rauchfuss and co-workers have prepared diiron azadithiolates $\{(\mu\text{-SCH}_2)_2\text{NR}\}\text{Fe}_2(\text{CO})_6$ by the reaction of $[(\mu\text{-SLi})_2\text{Fe}_2(\text{CO})_6]$ and $(\text{ClCH}_2)_2\text{NR}$.[20] Bis(chloromethyl)amines proligands can be prepared by the reaction of primary amines, formaldehyde, and SOCl₂. This methodology have provided us to attach diverse substituents to the amine, and in this way they have generated thioether- and alkene-functionalized derivatives, as shown in Figure 2.

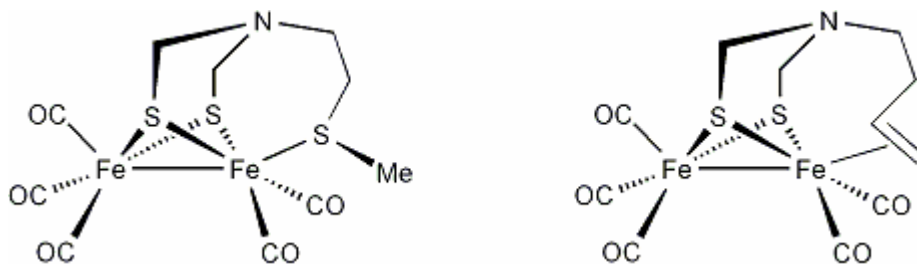
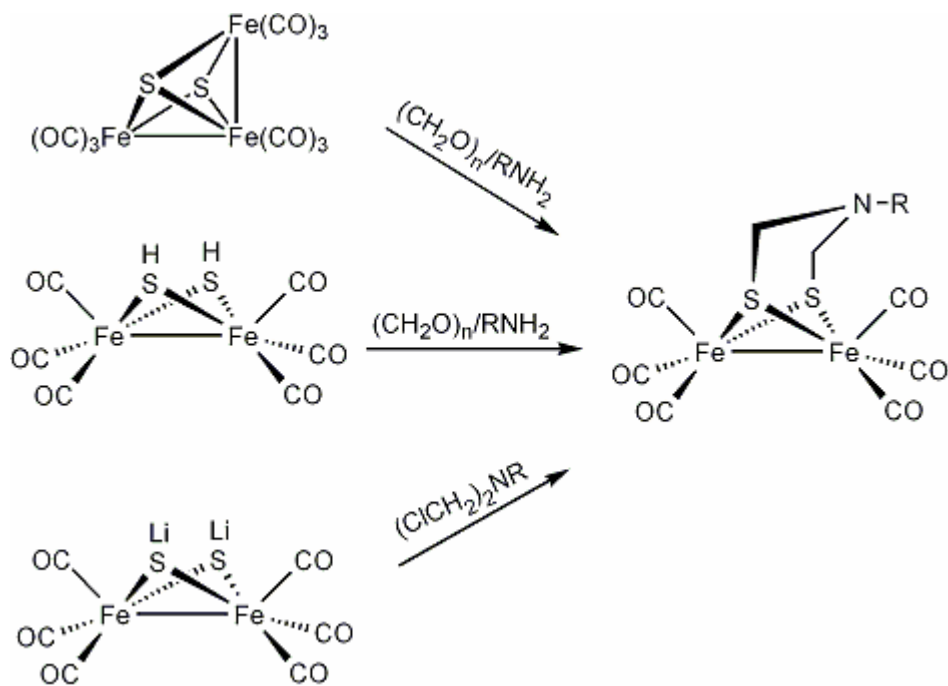


Figure 2.

Crystallographic studies have revealed that $(\text{Et}_4\text{N})_2\{(\mu\text{-SCH}_2)_2\text{NMe}\}\{\text{Fe}_2(\text{CN})_2(\text{CO})_4\}$ (1) has two conformers cocrystallize.[21] In the major conformer, the *N*-methyl group sterically clashes with the underlying CN ligand, manifested by a flattening of the amine. In the minor conformer, the *N*-methyl group is sterically unencumbered and the amine is pyramidal. The implication of these results is that the encumbered conformer must be stabilized electronically; otherwise only the sterically unencumbered isomer would be observed.

At the same time, they also have reported that $[(\mu\text{-SH})_2\text{Fe}_2(\text{CO})_6]$ efficiently condenses with formaldehyde in the presence of primary amines to give the corresponding azadithiolates (Scheme 2).[22] Alkyl and arylamines also participate in this reaction to give $\{(\mu\text{-SCH}_2)_2\text{NR}\}\text{Fe}_2(\text{CO})_6$ (R= *t*-Bu, Bn, and Ph). The cluster $[\text{Fe}_3\text{S}_2(\text{CO})_9]$ also reacts with aqueous formaldehyde and amines or ammonia to give $\{(\mu\text{-SCH}_2)_2\text{NR}\}\text{Fe}_2(\text{CO})_6$. To synthesize $\{(\mu\text{-SCH}_2)_2\text{NH}\}\text{Fe}_2(\text{CO})_6$ (3), which contains the proposed secondary amine, they used (NH₄)₂CO₃ as a source of ammonia.



Scheme 2. Syntheses of the diiron azadithiolate complexes.

The mechanism of these reactions is that $[(\mu\text{-SH})_2\text{Fe}_2(\text{CO})_6]$ initially reacts with aqueous formaldehyde in the absence of amines to afford $[(\mu\text{-SCH}_2\text{OH})_2\text{Fe}_2(\text{CO})_6]$, which reacts at room temperature with amines to give the corresponding azadithiolates. Since amines and formaldehyde condense to give imines, $[(\mu\text{-SH})_2\text{Fe}_2(\text{CO})_6]$ condenses efficiently with $1,3,5\text{-}(\text{CH}_2)_3(\text{NR})_3$ to afford $\{(\mu\text{-SCH}_2)_2\text{NR}\}\text{Fe}_2(\text{CO})_6$ ($\text{R}=\text{Me, Ph}$). The NH derivative is also obtained via the reaction of $[(\mu\text{-SH})_2\text{Fe}_2(\text{CO})_6]$ and hexamethylenetetramine, $(\text{CH}_2)_6\text{N}_4$.

The structure of $(\text{Et}_4\text{N})_2[\{(\mu\text{-SCH}_2)_2\text{NH}\}\{\text{Fe}_2(\text{CN})_2(\text{CO})_4\}]$ (4) established that the N-H is axial, the orientation favored by the anomeric effect, and the amine is pyramidal. The amine in 3 can be protonated by HOTf. Such an acidic ammonium center should be capable of protonating even weakly basic iron hydrides to give coordinated H_2 .

3.2. Protonated Azadithiolate Diiron Complexes

Sun and co-workers have found that $\{(\mu\text{-SCH}_2)_2\text{N}(\text{CH}_2\text{C}_6\text{H}_4\text{-2-Br})\}\text{Fe}_2(\text{CO})_6$ (5) can be N-protonated $\{(\mu\text{-SCH}_2)_2\text{NH}(\text{CH}_2\text{C}_6\text{H}_4\text{-2-Br})\}\text{Fe}_2(\text{CO})_6^+\text{ClO}_4^-$ (6). [40] Protonation of 5 in CHCl_3 with an excess of aqueous HClO_4 solution have afforded the N-protonated species 6 in good yield, which is successfully isolated and crystallographically identified for the first time. The IR spectrum of the N-protonated species 6 indicates that the wavenumbers of three CO bands shift *ca.* 17 cm^{-1} to higher frequencies. As 5 equiv. of HClO_4 is added to the CD_3CN solution of 5, ^1H NMR displays that the singlet of the CH_2 group of the benzyl moiety at δ 4.01 shifts down field by 0.53 ppm, and the singlet of the CH_2S groups at δ 3.73 splits into two broad signals at δ 3.37 and 4.19. A triplet with $^1J_{\text{NH}} = 53$ Hz appears at δ 5.92 is attributed

to the proton of the NH group. All observations in the ^1H NMR spectra are consistent with the protonation of the bridging-N atom.

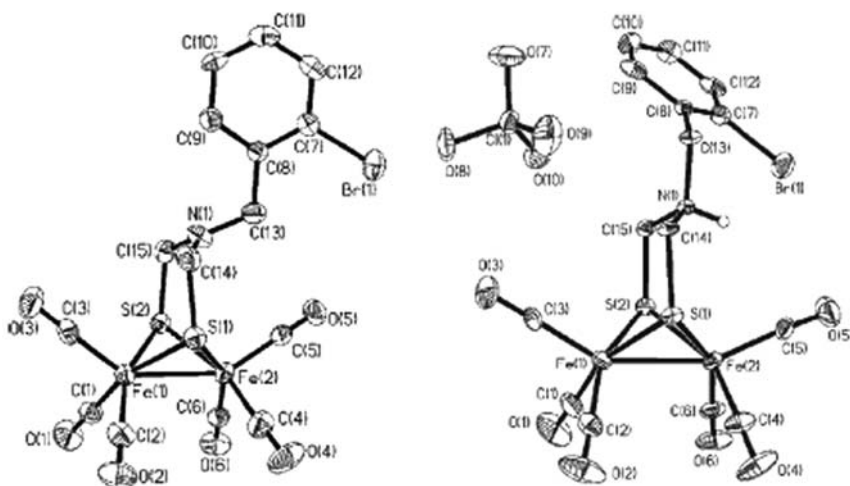


Figure 3. ORTEP (ellipsoids at 30 % probability level) view of diiron complexes 5 and 6: (a) 5; (b) 6.

The molecular structures of 5 and its protonated form 6 were determined by X-ray analyses of single crystals, shown in Figure 3. The central 2Fe2S structures are both in the butterfly framework and each Fe atom is coordinated in the familiar pseudo-pyramidal geometry as in previously reported 2Fe2S models. The results of this work give experimental support to the argument that the bridging-N atom of the Fe-only hydrogenase active site may perform a function as the proton capturer and carrier in the enzymatic H₂-production process.

They have also reported that PMe₃-disubstituted diiron azadithiolate complex, $\{(\mu-\text{SCH}_2)_2\text{N}(\text{C}_6\text{H}_4-p\text{-NO}_2)\}\{\text{Fe}_2(\text{CO})_4(\text{PMe}_3)_2\}$ (7) can be protonated at Fe-Fe bond to afford a μ -hydride species $\{(\mu\text{-H})(\mu-\text{SCH}_2)_2\text{N}(\text{C}_6\text{H}_4-p\text{-NO}_2)\}\{\text{Fe}_2(\text{CO})_4(\text{PMe}_3)_2\}$ (8). [41] The μ -hydride species 8 was prepared by the addition of HOTf to the solution of PMe₃-disubstituted diiron azadithiolate complex 7 in CH₃CN. The protonation process of 7 was recorded by the in situ IR and $^{31}\text{P}\{1\text{H}\}$ NMR spectra of 7. With an increase of 4 mol HOTf, the $\nu(\text{CO})$ bands of 7 completely disappeared and four blue-shifted bands at 2111, 2071, 2035 and 1995 cm⁻¹ were observed, as compared with that of the non-protonated complex 7. At the same time two new signals at $\delta = 22.52$ and 21.09 appeared in the $^{31}\text{P}\{1\text{H}\}$ NMR spectrum, shifting high field by 4.67 and 28.28 ppm, respectively. The Single crystal X-ray diffraction analyses of 7 and its μ -hydride diiron complex species 8 indicates that the PMe₃-disubstituted complex 7 exists in the crystalline state as two configurational isomers, transoid basal-basal (*ba-ba*) and apical-basal (*ap-ba*), while the μ -hydride species 8 possesses the sole transoid *ba-ba* geometry, as shown in Figure 4. The Fe-Fe distance (2.5879(8) Å) of 8 shows a slight increase as compared to the corresponding *ba-ba* isomer (2.5671(10) Å) of 7.

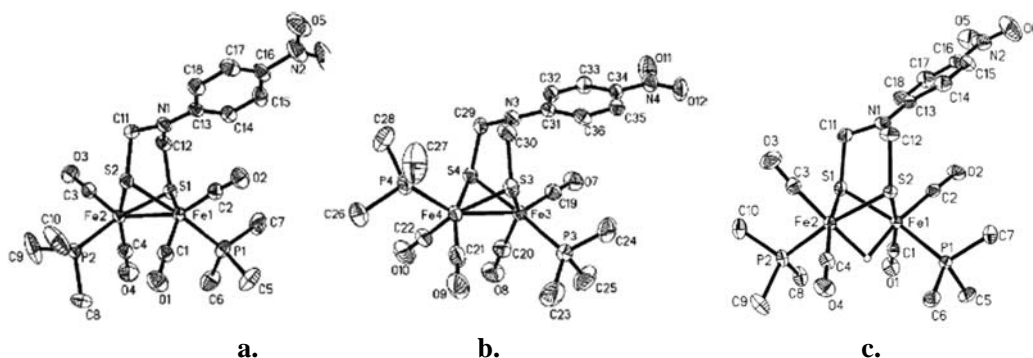


Figure 4. ORTEP (ellipsoids at 30 % probability level) view of diiron complexes 7 and 8: (a) 7 (*ba-ba*); (b) 7 (*ap-ba*); (c) 8.

Similarly, Ott and co-workers have synthesized PMe₃-disubstituted diiron azadithiolate complex, [{(μ-SCH₂)₂N(CH₂Ph)}{Fe₂(CO)₄(PMe₃)₂}] (9) (Figure 5), which can be protonated on either the Fe-Fe bond or the ADT nitrogen as well as on both sites simultaneously. [42] All four protonation states are well-defined and have been characterized by IR and NMR spectroscopy. As one equivalent of triflic acid was added to a solution of 9 in CH₃CN, the nitrogen heteroatom in ADT bridge was initially protonated. The IR spectra show a shift of $\nu_{(CO)} = 16$ cm⁻¹ to higher energy. Upon addition of excess triflic acid, the ³¹P NMR spectra feature two phosphorus signals at $\delta = 25.3, 21.3$ ppm, with an additional average shift of $\nu_{(CO)} = 80$ cm⁻¹, which can be assigned to the doubly protonated species, [{(μ-H)(SCH₂)₂N(CH₂Ph)}{Fe₂(CO)₄(PMe₃)₂}] (10) (Figure 5).

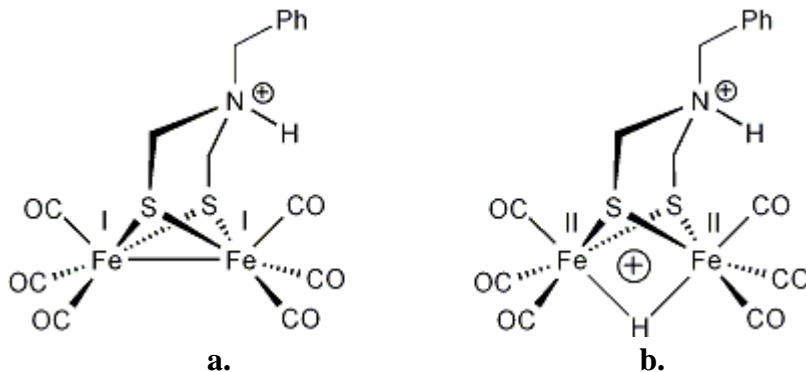
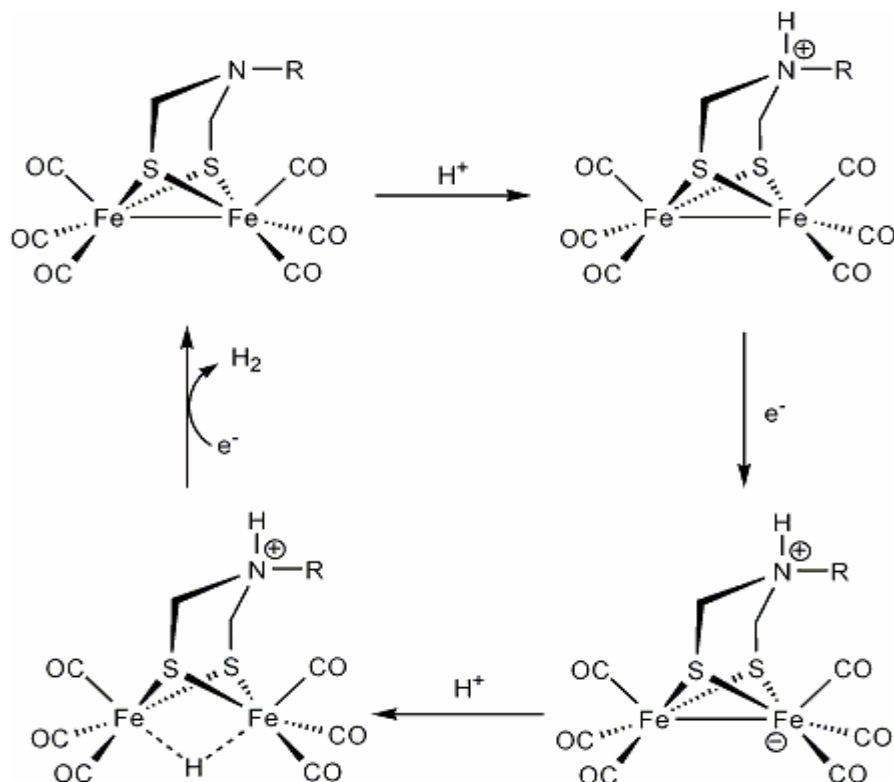


Figure 5.

4. FUNCTIONAL MODELS FOR HYDROGEN EVOLUTION FROM THE ACTIVE SITE OF FE-ONLY HYDROGENASE

4.1. Azadithiolate Diiron Hexacarbonyl Complex

As early as 1998, the first biomimetic study for H₂ evolution has been reported by Rauchfuss and co-workers. [43] Since then, a variety of PDT-bridged (PDT=1, 3-propanedithiol) diiron complexes as functionalized models have been synthesized to catalyze the proton to H₂ in the presence of acid, such as H₂SO₄, HOTS and acetic acid, etc. [44–47] In the search for synthetic competitive catalysts that function with Fe-only hydrogenase-like capability, the azadithiolate diiron complexes attracted particular interest because of their possible role in a low-energy route to H₂ evolution. Sun and co-workers have reported the first azadithiolate diiron complex, [{(μ-SCH₂)₂N(4-BrC₆H₄CH₂)}Fe₂(CO)₆] (11), can catalyze proton reduction to H₂ in the presence of HClO₄, which the potential was only -1.48 V. [48] The proposed catalytic mechanism is shown in Scheme 3. In the presence of acid, the N site in ADT bridge is initially protonated, followed by an electrochemical reduction event. The electron-rich Fe-Fe bond is then available for protonation, which leads to a hydride. The double protonated species undergoes a second reduction to release molecular hydrogen. In this system, the introduction of the ADT nitrogen atom leads to shift the potential for H₂ production to a more positive value and thus makes the proton reduction significantly easier.

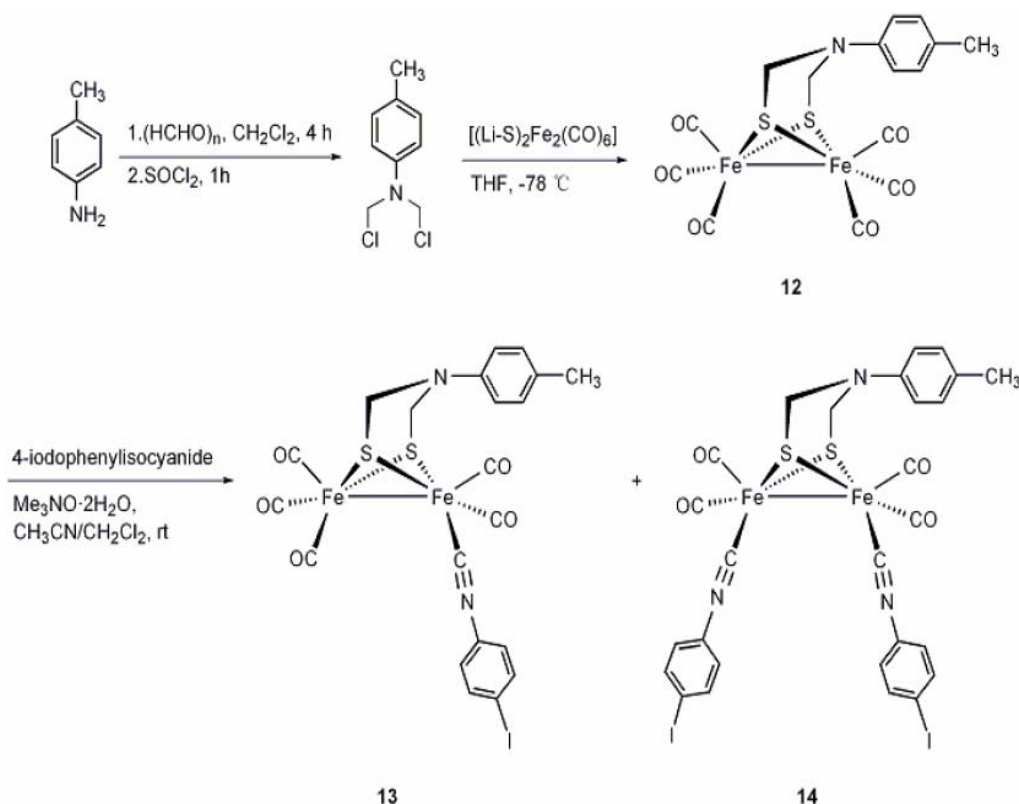


Scheme 3. The possible mechanism for H₂ evolution catalyzed by 11, R=benzyl.

4.2. Isocyanide Disubstituted Azadithiolate Diiron Complex

In spite of the biological importance of the bridgehead N atom in the active site of Fe-only hydrogenase, the synthesis of functionalized diiron azadithiolate may be an alternative in the search for synthetic catalysts with [Fe]hydrogenase-like capability. Although ADT-bridged diiron complexes have been extensively studied, to the best of our knowledge, the structural and functional azadithiolate model complexes have been much less investigated. To further develop the biomimetic chemistry of Fe-only hydrogenase, we have presented the synthesis, structures and properties of a new series of diiron ADT-type model complexes, in which some substituents are attached to the N atom and Fe atoms in the diiron ADT framework $\{(\mu\text{-SCH}_2)_2\text{N}\}\text{Fe}_2(\text{CO})_n$ ($n = 4, 5$). [49]

The lithium salt of hexacarbonyldisulfidodiiron, freshly derived from $[(\mu\text{-S})_2\text{Fe}_2(\text{CO})_6]$, was treated with *N,N*-bis(chloromethyl)-4-methylaniline to give diiron complex $\{(\mu\text{-SCH}_2)_2\text{N}(4\text{-CH}_3\text{Ph})\}\text{Fe}_2(\text{CO})_6$ (12) in moderate yield. Treatment of 12 with two equivalents of *p*-iodophenylisocyanide in CH_2Cl_2 or CH_3CN solution afforded monosubstituted diiron complex $\{(\mu\text{-SCH}_2)_2\text{N}(4\text{-CH}_3\text{Ph})\}\{\text{Fe}_2(\text{CO})_5(4\text{-IPhNC})\}$ (13) as a main product (Scheme 4). However, reaction of complex 12 with *p*-iodophenylisocyanide in mixed solvent system $\text{CH}_3\text{CN}/\text{CH}_2\text{Cl}_2$ (2:1, v/v) solution in the presence of the decarbonylating agent $\text{Me}_3\text{NO}\cdot 2\text{H}_2\text{O}$ at room temperature gave the disubstituted isocyanide derivative $\{(\mu\text{-SCH}_2)_2\text{N}(4\text{-CH}_3\text{Ph})\}\{\text{Fe}_2(\text{CO})_4(4\text{-IPhNC})_2\}$ (14) in reasonable yield (Scheme 4).



Scheme 4. The synthesis of diiron azadithiolate complexes of 12, 13 and 14.

The IR spectrum of complex 12 in CH_2Cl_2 shows three major bands in the CO region at 2071, 2030, and 2000 cm^{-1} . Compared with the bands of 12, the CO stretching frequencies of 14 are shifted to lower wavenumbers by about 50 cm^{-1} on average, consistent with the better electron-donating ability of *p*-iodophenylisocyanide with respect to the CO ligand. This indicates that the introduction of aromatic isocyanide ligands to the diiron center increases the electron density of the Fe-Fe bond.

The solid-state structures of 12 and 14 were determined by X-ray diffraction, as shown in Figure 6 and Figure 7, respectively. It is noteworthy that the C(6)–Fe(2)–Fe(1) angle in 12 is about 7° larger than the C(2)–Fe(1)–Fe(2) angle (Figure 6), thus indicating an interaction between the arene group and Fe(2)(CO)₃ unit. Like the “parent” 12, the central 2Fe2S unit of 14 (Figure 7) adopts a face-shared bi-octahedral structure. The Fe–Fe bond length of 2.5121(11) Å is somewhat longer than that observed in 12, indicating that the metal–metal distance in diiron(I) compounds is slightly affected by the nature of terminal ligands with a better electron-donating ability. The p–π conjugation between the 4-methylphenyl ring and the bridging N p orbital is somewhat weakened, therefore the bridging N atom is not in the plane defined by the atoms C(12), C(10), and C(19). It is interesting to note that the two phenylisocyanide ligands in the basal positions on each iron unit are nearly parallel to each other. The crystal packing view along the *b* axis showed π–π stacking interactions of the *p*-iodophenylisocyanide ligands within the column (Figure 8). Complex 14 is unusual compared to related diiron isocyanide complexes where the two isocyanide ligands are in apical positions in the solid state and are not parallel to each other.

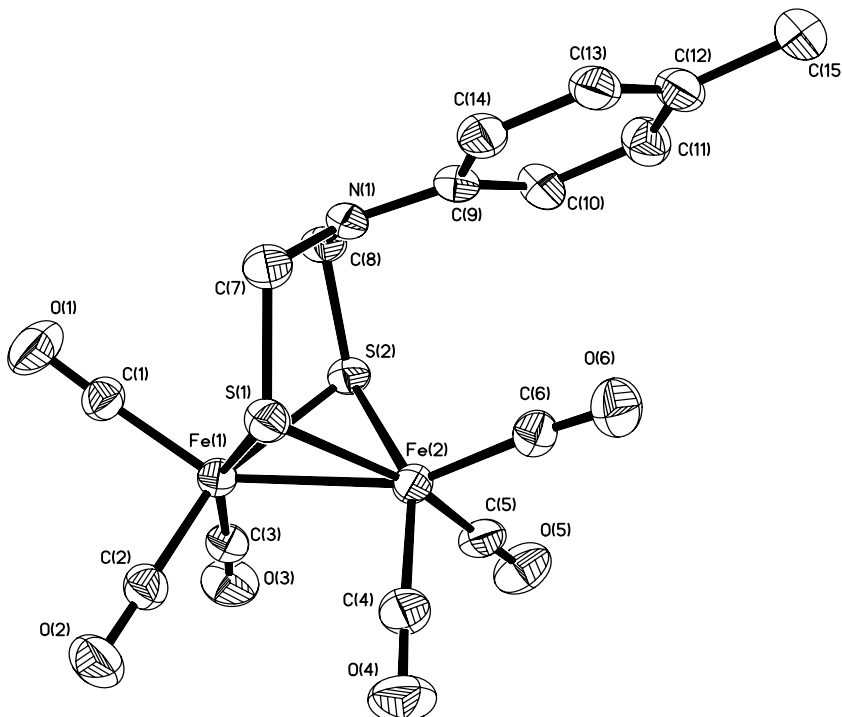


Figure 6. ORTEP (ellipsoids at 30 % probability level) view of diiron complex 12.

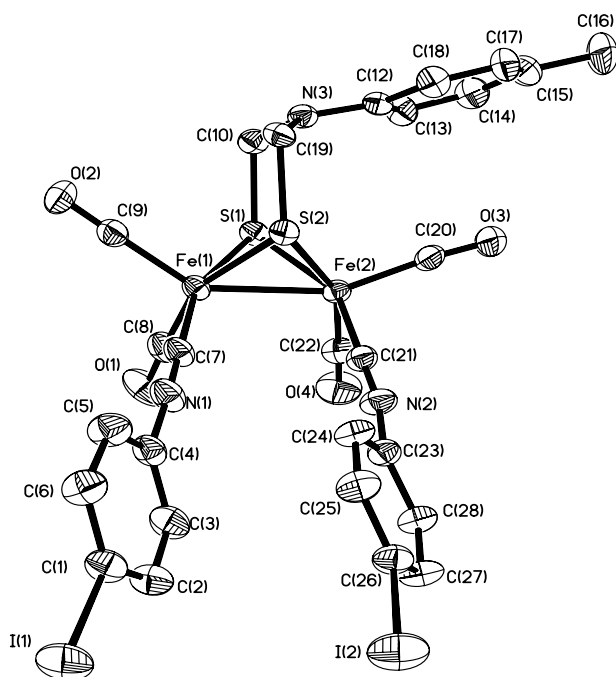


Figure 7. ORTEP (ellipsoids at 30 % probability level) view of diiron complex 14.

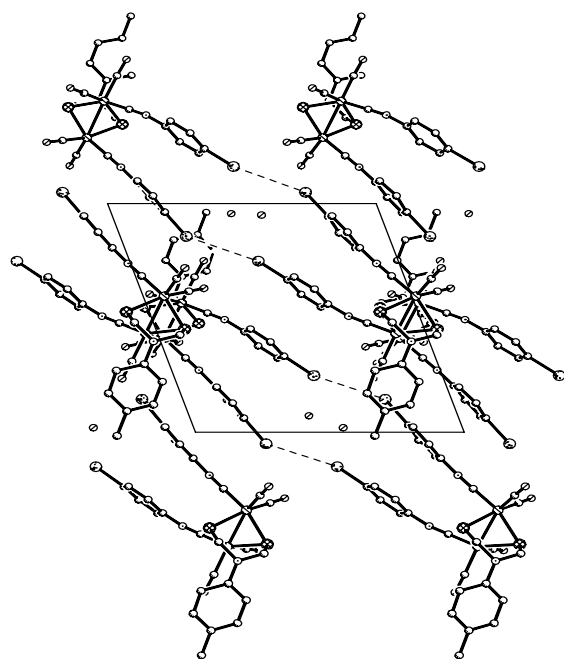


Figure 8. The crystal packing view of diiron complexe 14 along with b axis.

The electrochemical properties were investigated by cyclic voltammetry in CH_3CN solution. Complexes 12 and 14 display a quasi-reversible reduction peak and an irreversible oxidation wave, respectively. The reduction peaks at -1.55 V for 12 and -1.70 V for 14 can be assigned to the one-electron reduction process of $\text{Fe}^{\text{I}}\text{Fe}^{\text{I}}$ to $\text{Fe}^{\text{I}}\text{Fe}^{\text{0}}$. In comparison to that of the parent complex 12, the reduction potential of 14 shifts by about 0.15 V to a more negative value. The shift of potential indicate that the introduction of *p*-iodophenylisocyanide ligands in 14 makes the reduction of the iron core more difficult and the oxidation easier, which is consistent with the better donor capacity of *p*-iodophenylisocyanide relative to CO.

Upon addition of 1 mM of HOTs, a new reduction peak was observed at around -1.48 and -1.43 V for 12 and 14, respectively. As can be seen in Figure 9, the current height of the reduction peak around -1.48 and -1.43 V displayed a significant increases with an increase of acid concentration, respectively, which showed an electrocatalytic response. The current intensity of these reduction peaks gradually increased and the potentials were shifted to relatively more negative values with increasing acid concentration. These features are typical of a catalytic proton reduction process. We conclude that the reduction peaks around -1.48 V for 12 and -1.43 V for 14 display electrocatalytic responses to proton reduction.

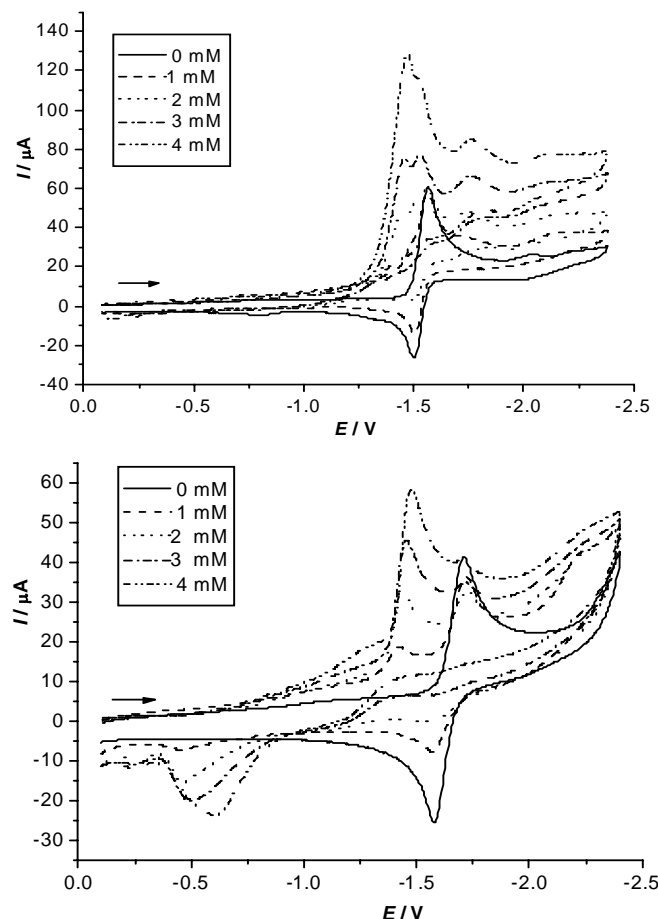


Figure 9. Cyclic voltammograms of 12 (top) and 14 (below) (1 mM) with $0\text{--}4\text{ mM}$ HOTs in 0.1 M $n\text{-Bu}_4\text{NPF}_6/\text{CH}_3\text{CN}$ solution at a potential scan rate of 100 mVs^{-1} .

Complexes 12 and 14 also has considerably more positive potentials of proton reduction. A reasonable interpretation for this is that the utilization of the basicity of the ADT heteronitrogen atom [48] and the introduction of isocyanide ligands shift the potential to a more positive value and therefore makes the reduction of protons remarkably easier.

The iodo functionality in 14 could be used for further elaboration by incorporating a redox species. This offers a possibility of linking a ruthenium photosensitizer to the azadithiolatodiiron system 14 in an attempt to produce H₂ by action of light.[50] Further experimental efforts in these directions are underway.

4.3. Spectroelectrochemistry of Phosphine Monosubstituted Diiron Complex

Although there are many reports on proton reduction to H₂ catalyzed by diiron models related to the Fe-only hydrogenase active site, the catalytic mechanism was still ambiguous so far. In biological system of Fe-only hydrogenase, the bridging or terminal CO group is usually suggested to be a crucial role during the catalytic H₂ evolution cycle. We have been wondering if the active transition of the asymmetric diiron model complexes during electrocatalysis has such CO bridged conformation. We have thus prepared tris(N-pyrrolidinyl)phosphine monosubstituted diiron compound 15, $[(\mu\text{-pdt})\text{Fe}_2(\text{CO})_5\text{P}(\text{NC}_4\text{H}_8)_3]$, and investigated the electrochemical and spectroelectrochemical properties of complex 15. [51] The formation of a bridging CO group during one-electron reduction of 15 has been identified using IR spectroelectrochemical techniques. Cyclic voltammograms results show that this model system is electrocatalytically active in terms of proton reduction.

The complex 15 was readily prepared in a good yield by reaction of $[(\mu\text{-pdt})\text{Fe}_2(\text{CO})_6]$ and $\text{P}(\text{NC}_4\text{H}_8)_3$ in refluxing toluene. The geometry of 15 is nearly identical with that of those tertiary phosphosphine-monosubstituted derivatives (Figure 10). The $\text{P}(\text{NC}_4\text{H}_8)_3$ ligand of 15 is in basal position and roughly *cis* to the Fe-Fe bond, which may minimize the $\text{P}(\text{NC}_4\text{H}_8)_3$ ligand steric interactions with the six-membered ring of propanedithiolate. The Fe-Fe distance of 2.5527(9) \AA is enlarged by ca. 0.01–0.04 \AA than those found in phosphine momosubstituted complexes, and nearly identical with those in disubstituted complexes. The geometries of nitrogen heteroatoms in $\text{P}(\text{NC}_4\text{H}_8)_3$ ligand are notable. The $\text{P}(\text{NC}_4\text{H}_8)_3$ ligand shares two nearly planar nitrogen atoms (N1 and N2) and a pyramidal nitrogen (N3). The sum of C–N–C angles around N1 and N2 are 355° and 357°, respectively, while the sum of C–N–C angle around N3 is 351°.

The IR spectrum shows three major bands in CO region at 2034, 1973, 1912 cm^{-1} which shifts to lower frequencies by an average value ca. 55 cm^{-1} as compared with the parent complex $[(\mu\text{-pdt})\text{Fe}_2(\text{CO})_6]$. As compared with those of other highly electron rich phosphine, the value of ν_{CO} for 15 is significantly shifted to lower frequencies. The better electron-donating ability of $\text{P}(\text{NC}_4\text{H}_8)_3$ ligand can be attributed to the donation towards phosphorus atom from lone pair electron of two planar nitrogens [52, 53].

Complex 15 displays an electrochemically irreversible reduction at -1.98 V. We have described the proton electroreduction catalyzed by 15 in the presence of weak proton acid (HOAc) by cyclic voltammogram. The results show that the first reduction event at -1.98 V is significantly sensitive to the acid concentration. That is, the first reduction event at -1.98 V is electrocatalytically active in terms of proton reduction. Bulk electrolysis shows that the total

charge passed through the cell approached 12 F per mol of 15 per hour, which is equivalent to 6 turnover.

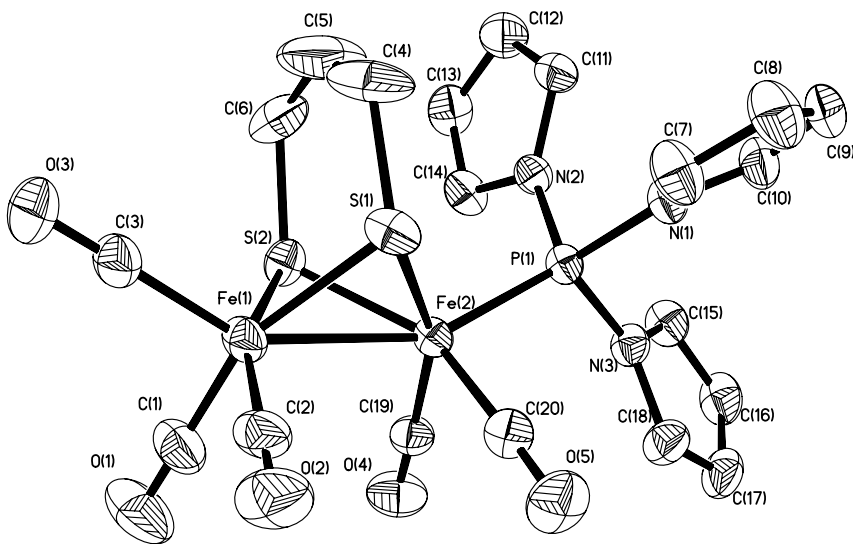


Figure 10. ORTEP (ellipsoids at 30 % probability level) view of diiron complex 15.

The IR changes of 15 at a reduction applied potential at -1.98 V was investigated by IR spectroelectrochemical technique in CO and N_2 -saturated THF solution. The IR spectral changes in CO region during the electrochemical reduction of 15 in a thin-layer IR cell were shown in Figure 11. Upon reduction of 10 mM 15 in THF solution under CO, the three major $\nu_{(CO)}$ IR bands at 2034, 1974 and 1953 cm^{-1} of the starting material display a loss of intensity, with the growth of bands at lower frequencies with 2014, 1938, 1921, 1908 and 1888 cm^{-1} (Figure 11b and c). These bands at lower wavenumbers can be attributed to the terminal CO ligands coordinated to two Fe atoms of the diiron unit. As compared with the IR bands of terminal CO ligands of 15 (Figure 11a), a shift of the $\nu_{(CO)}$ bands of one-electron reduced species 15B on average ca. 30 cm^{-1} to lower energy. The IR bands of terminal CO ligands of 15B show a significant similarity to those of the one-electron reduced species $[(\mu-pdt)Fe_2(CO)_6]^-$ [54], generated by the reduction of complex $[(\mu-pdt)Fe_2(CO)_6]$. Interestingly, we found a peak at 1778 cm^{-1} (Figure 11b and c) attributed to a bridging CO ligand during the reduction of 15.

The final spectrum obtained following the reduction of 15 is nearly attributed to 15B with no contribution of 15 (Figure 11c), indicating 15 completely converts into 15B, as shown in Figure 12.

The IR spectra obtained in N_2 -saturated solution (Figure 11d and e) are similar to those recorded in CO-saturated solution (Figure 11b and c), but the conversion rate of 15 to 15B as given at 2014 cm^{-1} in N_2 -saturated solution is faster than that recorded in CO-saturated solution. We conclude either additional CO impedes the formation of one-electron reduced species or CO reacts with the transient intermediate to inhibit the efficient conversion into 15B.

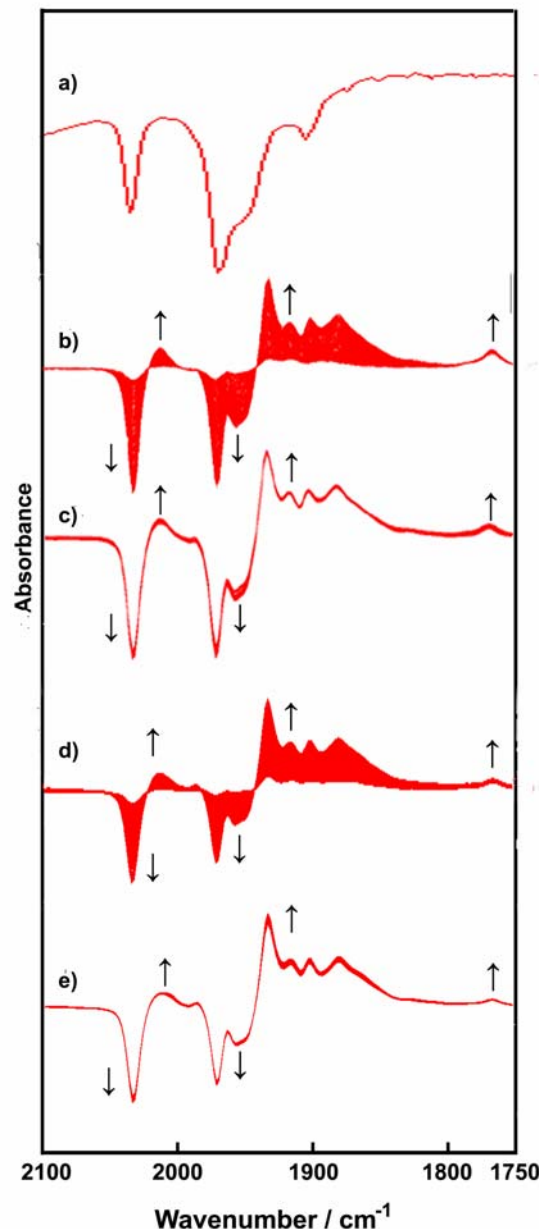


Figure 11. IR spectra in the CO region recorded during the reduction of 10 mM 15 in THF (0.1M *n*-Bu₄NPF₆) in the SEC cell at -1.98 V. (a) In CO-saturated solution prior to the application of the potential; (b, c) in CO-saturated solution; (d, e) in N₂-saturated solution.

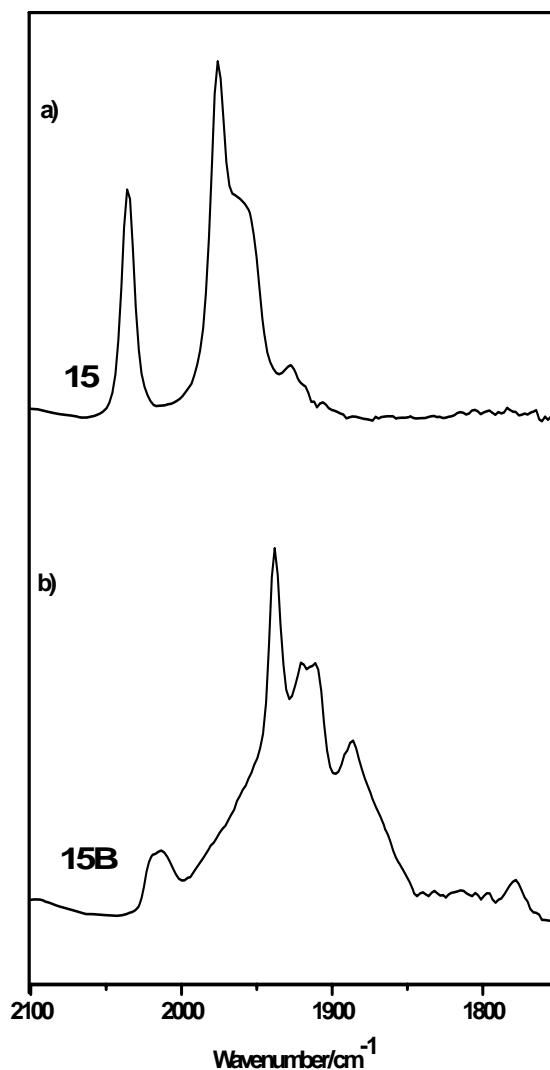
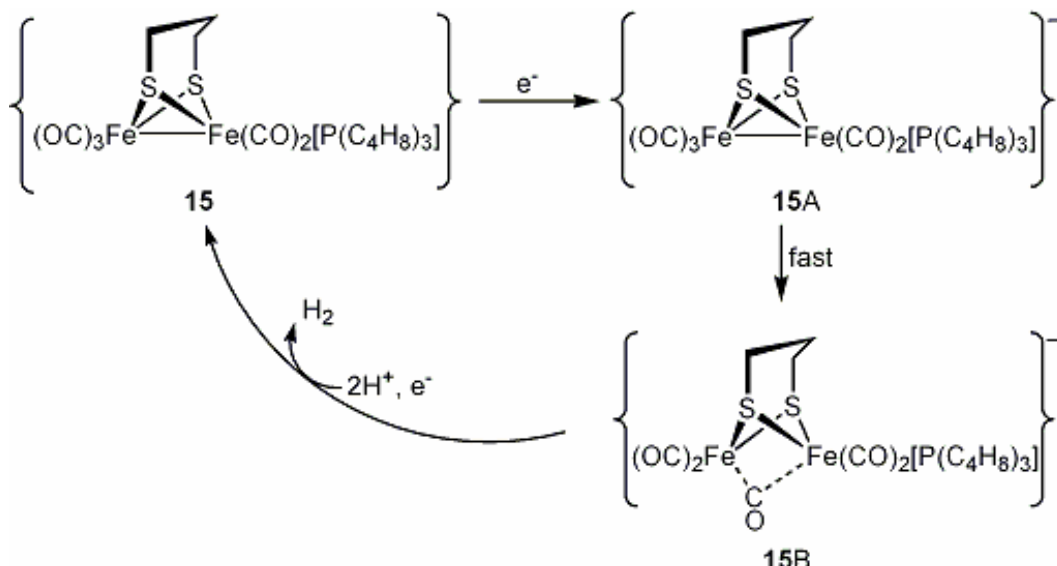


Figure 12. IR spectra in CO region of 15 (a) and the electrochemically reduced product 15B (b).

In view of the similarity in IR spectra of the terminal and bridging CO ligands, we conclude that the structure of 15B has a bridging CO group. A reasonable interpretation for the formation of a bridging CO group is that an asymmetrical charge distribution and the structural asymmetry at the two iron centers due to the coordination of an electron-donating P(NC₄H₈)₃ ligand make the rotation of Fe(CO)₃ unit when diiron center is reduced. A more electron-rich Fe(CO)₂P(NC₄H₈)₃ unit favors the transformation of CO ligand in Fe(CO)₃ unit from terminal to bridging binding. Excessive electron density could be transferred to Fe(CO)₃ unit through a bridging CO bond, which stabilizes of one-electron reduced species Fe⁰Fe¹. In addition, the strong electron-donating ability of P(NC₄H₈)₃ ligand facilitates the stability of the conformation of a CO bridging group. Our results confirm the formation of a bridging CO group during electrocatalytic H₂-production by an asymmetrically substituted diiron complex having a good electron-donating ligand.

For these results described above for cyclic voltammograms and SEC experiments, an ECCE mechanism for the electrocatalytic proton reduction of 15 could be proposed (Scheme 5). Complex 15 initially undergoes an electrochemical reduction to generate a one-electron reduced intermediate 15A. The transition 15A rapidly converts into a CO-bridged species 15B. After double protonation of 15B and a second electroreduction event, hydrogen is evolved, and the starting material is reclaimed to fulfill the catalytic cycle. This work also shows the formation of a CO bridge is a reasonable activation step in the enzymatic H₂-evolution process.

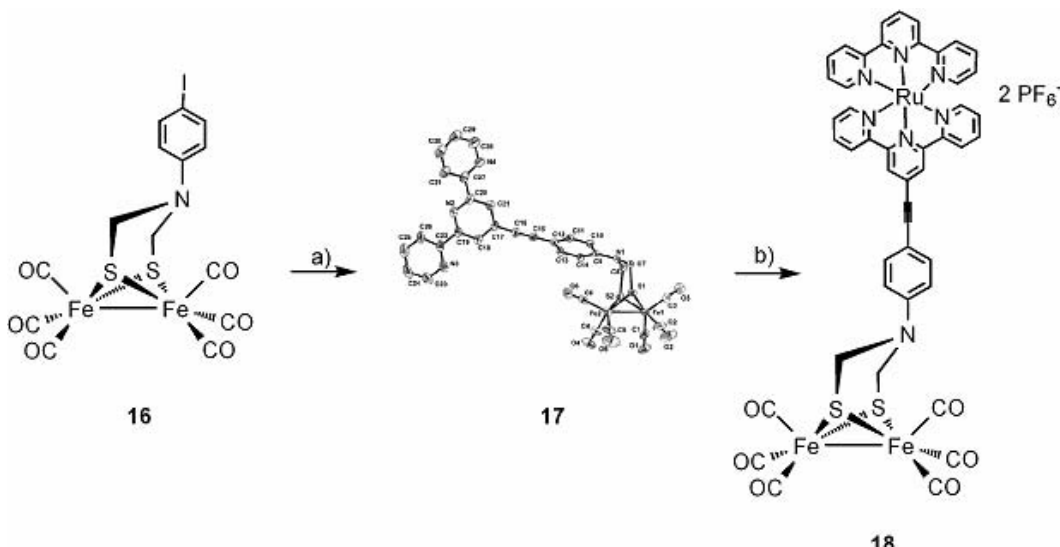


Scheme 5. A possible electrocatalytic mechanism for 15.

5. SUPRAMOLECULAR MODELS RELATED TO THE ACTIVE SITE OF FE-ONLY HYDROGENASE AIMING FOR LIGHT-DRIVEN HYDROGEN PRODUCTION

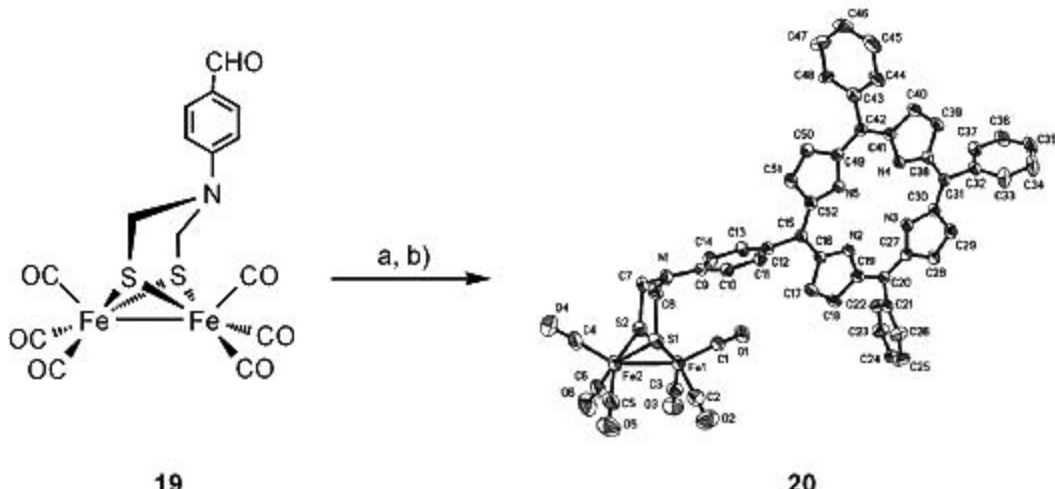
In context of interest in photochemical fuel production, Sun and co-workers became intrigued by the possibility to covalently link a biomimetic model of the iron hydrogenase active site to a ruthenium photosensitizer in an attempt to afford hydrogen production by light. [50] The projected process can be seen in the reference. The iodo-functionalized diiron complex 16 could be converted to the corresponding dyad by reacting the former complex with 4'-ethynyl-2,2':6', 2''-terpyridine [55] under Sonogashira cross-coupling conditions [56] to afford the diiron complex 17 with an appended terpyridine metal binding site (Scheme 5). In the solid state, the iron carbonyl portion of 17 is stable towards ligand substitution by the polypyridine as unambiguously demonstrated by single crystal X-ray diffraction. Ligand 17 coordinates readily to the (terpy)Ru fragment, afforded the desired trinuclear complex 18. The excited state energies of complexes 18 was 1.89 eV calculated from the emission spectra, the driving force was calculated to be uphill with $\Delta G^0 = 0.59$ eV. The excited state decay lifetime was 6.5 ns for 18. The quenching rate constant k_q can be estimated as $k_q = 1.1 \times 10^8 \text{ s}^{-1}$, which

the quenching is not induced by electron transfer but rather by dipole-dipole energy transfer. The excited state lifetime of this mode is generally shorter and the excited state energy is lower. Furthermore, the potential proton reduction site is composed of a diiron hexacarbonyl portion in both dyads, but differs in the nature of the central atom in the dithiolate bridge. Thus, this limits its further applications.



Scheme 6. Synthesis of 18. (a) 4'-ethynyl-2', 2:6', 2''-terpyridine, $[\text{PdCl}_2(\text{PPh}_3)_2]$, CuI , Et_3N , toluene, 40°C ; (b) $[\text{RuCl}_2(\text{terpy})]\cdot\text{DMSO}$, MeOH , reflux.

More recently, Song and co-workers reported a new type of light-driven model compounds, in which a photosensitizing tetraphenylporphyrin group (TPP) was covalently linked to the N atom of the diiron parent complex $\{(\mu\text{-SCH}_2)_2\text{N}\}\text{Fe}_2(\text{CO})_6$. [57] The target model 20 was synthesized by treatment of 19 with pyrrole and benzaldehyde followed by the oxidant *p*-chloranil. The IR spectrum of 20 shows three absorption bands at 1558, 1472 and 1350 cm^{-1} , assigned to the skeletal vibrations of the pyrrole rings in the porphyrin unit, [58] and strong absorption bands at 2073, 2033, and 1996 cm^{-1} due to the terminal CO groups in the diiron unit. There is one Soret band at 419 nm in the near-UV region and four Q bands at 516, 552, 592, and 647 nm in the visible region. [59] The fluorescence emission spectrum of 20 displayed the two fluorescence emission bands at 655 and 719 nm. Further, their intensities are strongly quenched relative to those of the TPP bands. They conclude that the remarkably decreased intensities of the two fluorescence bands of 20 are most likely due to strong intramolecular electron transfer from the photoexcited state of the porphyrin macrocycle of TPP to the covalently bonded diiron unit.



Scheme 7. Synthesis of 20. (a) PhCHO, pyrrole, $\text{CF}_3\text{CO}_2\text{H}$, CH_2Cl_2 ; (b) p-chloranil, reflux, 1 h.

6. CONCLUSION

The [2Fe2S] organometallic Chemistry related to the Fe-only hydrogenase is developing very rapidly and providing some prospects to understand the enzymatic mechanism. In the context, we are beginning to understand the structure-reactivity relationships of [2Fe2S] complexes. The nitrogen heteroatom in ADT bridge might play a key role in the catalytic H_2 evolution cycle. Research on diiron azadithiolate complexes has proven to be fruitful with respect to novel structural and functional models, and catalytic proton reduction to H_2 .

This review provides an overview of the [2Fe2S] organometallic coordination chemistry appropriate to understand the significant discovery of the diiron azadithiolate complexes related to the Fe-only hydrogenase active site. Compared with those PDT-bridged diiron complexes, introduction of nitrogen atom in ADT bridge could give access to shift the potentials of H_2 evolution to more positive values. It is worth noting that, so far, very few detailed electrochemical studies of diiron azadithiolate models have been developed. Furthermore, the synthetic diiron azadithiolate complexes have only been shown to display electrocatalysis of proton reduction and this at relatively negative potentials. Thus, a search for synthetic competitive catalysts that function with iron hydrogenase-like capability is an important goal for the hydrogen energy applications. The introduction of photosensitizer in [2Fe2S] unit offer us a possibility to achieve H_2 evolution driven by light.

ACKNOWLEDGEMENTS

We are grateful to the Ministry of Education of China and National Natural Science Foundation of China (Projects 20128005, 20376010, and 20472012).

REFERENCES

- [1] Service, R. F. *The hydrogen backlash*. *Science*. 2004, *305*, 958–961.
- [2] Koelle, U. Transition metal catalyzed proton reduction. *New. J. Chem.* 1992, *16*, 157–169.
- [3] Cammack, R. Bioinorganic chemistry: Hydrogenase sophistication. *Nature*. 1999, *397*, 214–215.
- [4] Darensbourg, M. Y. Synthetic chemistry: Making a natural fuel cell. *Nature*. 2005, *433*, 589–591.
- [5] Adams, M. W. W.; Mortenson, L. E.; Chen, J. S. Hydrogenase. *Biochim. Biophys. Acta*. 1981, *594*, 105–176.
- [6] Adams, M. W. W. The structure and mechanism of iron-hydrogenase. *Biochim. Biophys. Acta*. 1990, *1020*, 115–145.
- [7] Albracht, S. P. J. Nickel hydrogenases: In search of the active site. *Biochim. Biophys. Acta* 1994, *1188*, 167–204.
- [8] Albracht, S. P. J.; Graf E. G.; Thauer, R. K. The EPR properties of nickel in hydrogenase from *Methanobacterium thermoautotrophicum*. *FEBS Lett.* 1982, *140*, 311–313.
- [9] Adams, M. W.; Stiefel, E. I. Organometallic iron: the key to biological hydrogen metabolism. *Curr. Opin. Chem. Biol.* 2000, *4*, 214–220.
- [10] Adams, M. W.; Mortenson, L. E. The physical and catalytic properties of hydrogenase II of Clostridium pasteurianum: A comparison with hydrogenase I. *J. Biol. Chem.* 1984, *259*, 7045–7055.
- [11] Peters, J. W. Structure and mechanism of Fe-only hydrogenase. *Curr. Opin. Struct. Biol.* 1999, *6*, 670–676.
- [12] Frey, M. Hydrogenases: Hydrogen-activating enzymes. *Chem. Bio. Chem.* 2002, *3*, 153–160.
- [13] Darensbourg, M. Y.; Lyon, E. J.; Zhao, X.; Georgakaki, I. P. Bioinorganic chemistry special feature: The organometallic active site of [Fe]hydrogenase: Models and entatic states. *Proc. Natl. Acad. Sci. U. S. A.* 2003, *100*, 3683–3688.
- [14] Evans, D. J.; Pickett, C. J. Chemistry and the hydrogenases. *Chem. Soc. Rev.* 2003, *32*, 268–275.
- [15] Rauchfuss, T. B. Research on Soluble Metal Sulfides: From polysulfido complexes to functional models for the hydrogenases. *Inorg. Chem.* 2004, *43*, 14–26.
- [16] Sun, L. C.; Åkermark, B.; Ott, S. Iron hydrogenase active site mimics in supramolecular systems aiming for light-driven hydrogen production. *Coord. Chem. Rev.* 2005, *249*, 1653–1663.
- [17] Seyferth, D., Henderson, R. S., Song, L. C. The dithiobis(tricarbonyliron) dianion: improved preparation and new chemistry. *J. Organomet. Chem.* 1980, *192*, C1–C5.
- [18] Lyon, E. J.; Georgakaki, I. P.; Reibenspies, J. H.; Darensbourg, M. Y. Carbon monoxide and cyanide ligands in a classical organometallic complex model for Fe-only hydrogenase. *Angew. Chem. Int. Ed. Engl.* 1999, *38*, 3178–3180.
- [19] Schmidt, M.; Contakes, S. M.; Rauchfuss, T. B. First generation analogues of the binuclear site in the Fe-only hydrogenases: $\text{Fe}_2(\mu-\text{SR})_2(\text{CO})_4(\text{CN})_2^{2-}$. *J. Am. Chem. Soc.* 1999, *121*, 9736–9737.

- [20] Lawrence, J. D.; Li, H.; Rauchfuss, T. B. Beyond Fe-only hydrogenases: N-functionalized 2-aza-1,3-dithiolates $\text{Fe}_2[(\text{SCH}_2)_2\text{NR}](\text{CO})_\chi$ ($\chi = 5, 6$). *Chem. Commun.* 2001, *16*, 1482–1483.
- [21] Lawrence, J. D.; Li, H.; Rauchfuss, T. B.; Bénard, M.; Rohmer, M.-M. Diiron azadithiolates as models for the iron-only hydrogenase active site: synthesis, structure, and stereoelectronics. *Angew. Chem. Int. Ed. Engl.* 2001, *40*, 1768–1771.
- [22] Li, H.; Rauchfuss, T. B. Iron carbonyl sulfides, formaldehyde, and amines condense to give the proposed azadithiolate cofactor of the fe-only hydrogenases. *J. Am. Chem. Soc.* 2002, *124*, 726–727.
- [23] Peters, J. W.; Lanzilotta, W. N.; Lemon, B. J.; Seefeldt, L. C. X-ray crystal structure of the Fe-only hydrogenase (CpI) from *Clostridium pasteurianum* to 1.8 Angstrom Resolution. *Science*. 1998, *282*, 1853–1858.
- [24] Nicolet, Y.; Piras, C.; Legrand, P.; Hatchikian, C. E.; Fontecilla-Camps, J. C. Desulfovibrio desulfuricans iron hydrogenase: the structure shows unusual coordination to an active site Fe binuclear center. *Structure*. 1999, *7*, 13–23.
- [25] Spek, T. M.; Arendsen, A. F.; Happe, R. P.; Yun, S. Y.; Bagley, K. A.; Stukens, D. J.; Hagen, W. R.; Albracht, S. P. J. Similarities in the architecture of the active sites of Ni-hydrogenases and Fe-hydrogenases detected by means of infrared spectroscopy. *Eur. J. Biochem.* 1996, *237*, 629–634.
- [26] Nicolet, Y.; De Lacey, A.; Vernède, X.; Fernandez, V. M.; Hatchikian, E. C.; Fontecilla-Camps, J. C. Crystallographic and ftir spectroscopic evidence of changes in fe coordination upon reduction of the active site of the Fe-only hydrogenase from *Desulfovibrio desulfuricans*. *J. Am. Chem. Soc.* 2001, *123*, 1596–1601.
- [27] Fan, H. J.; Hall, M. B. A capable bridging ligand for Fe-only hydrogenase: density functional calculations of a low-energy route for heterolytic cleavage and formation of dihydrogen. *J. Am. Chem. Soc.* 2001, *123*, 3828–3829.
- [28] De Lacey, A. L.; Stadler, C.; Cavazza, C.; Hatchikian, E.C.; Fernandez, V. M. FTIR characterization of the active site of the Fe-hydrogenase from *Desulfovibrio desulfuricans*. *J. Am. Chem. Soc.* 2000, *122*, 11232–11233.
- [29] Popescu, C. V.; Münck, E. Electronic structure of the H cluster in [Fe]-Hydrogenases. *J. Am. Chem. Soc.* 1999, *121*, 7877–7884.
- [30] Chem, Z.; Lemon, B. J.; Huang, S.; Swartz, D. J.; Peters, J. W.; Bagley, K. A. Infrared studies of the co-inhibited form of the Fe-only hydrogenase from *Clostridium pasteurianum* I: examination of its light sensitivity at cryogenic temperatures. *Biochemistry*. 2002, *41*, 2036–2043.
- [31] Adams, M. W. W. The mechanisms of H_2 activation and co binding by hydrogenase I and hydrogenase II of *Clostridium pasteurianum*. *J. Biol. Chem.* 1987, *262*, 15054–15061.
- [32] Bennett, B.; Lemon, B. J.; Peters, J. W. Reversible carbon monoxide binding and inhibition at the active site of the Fe-Only hydrogenase. *Biochemistry*. 2000, *39*, 7455–7460.
- [33] Liu, Z. P.; Hu, P. A density functional theory study on the active center of fe-only hydrogenase: characterization and electronic structure of the redox states. *J. Am. Chem. Soc.*, 2002, *124*, 5175–5182.
- [34] Liu, Z. P.; Hu, P. J. Mechanism of H_2 metabolism on Fe-only hydrogenases. *Chem. Phys.* 2002, *117*, 8177–8180.

- [35] Nicolet, Y.; Lemon, B. J.; Fontecilla-Camps, J. C.; Peters, J. W. A novel FeS cluster in Fe-only hydrogenases. *Trends Biochem. Sci.* 2000, **25**, 138–143.
- [36] Stephenson, M.; Stickland, L. H. Hydrogenase: a bacterial enzyme activating molecular hydrogen: The properties of the enzyme. *Biochem. J.* 1931, **25**, 205–214.
- [37] “A survey of energy” in *The Economist*. 2001, February 10th, p. 20.
- [38] Cammack, R.; Frey, M.; Robson, R. Hydrogen as a fuel: Learning from nature, Taylor & Francis, London, 2001, p. 267.
- [39] Hoffmann, P. *Tomorrow’s Energy: Hydrogen, fuel cells, and prospects for a cleaner planet*. MIT Press, Cambridge, MA. 2001.
- [40] Wang, F. J.; Wang, M.; Liu, X. Y.; Jin, K.; Dong, W. B.; Li, G. H.; Åkermark, B.; Sun, L. C. Spectroscopic and crystallographic evidence for the N-protonated Fe^IFe^I azadithiolate complex related to the active site of Fe-only hydrogenases. *Chem. Commun.* 2005, 3221–3223.
- [41] Dong, W. B.; Wang, M.; Liu, X. Y.; Jin, K.; Li, G. H.; Wang, F. J.; Sun, L. C. An insight into the protonation property of a diiron azadithiolate complex pertinent to the active site of Fe-only hydrogenases. *Chem. Commun.* 2006, 305–307.
- [42] Schwartz, L.; Eilers, G.; Eriksson, L.; Gogoll, A.; Lomoth, R.; Ott, S. Iron hydrogenase active site mimic holding a proton and a hydride. *Chem. Commun.* 2006, 520–522.
- [43] Gloaguen, F.; Lawrence, J. D.; Rauchfuss, T. B. Biomimetic hydrogen evolution catalyzed by an iron carbonyl thiolate. *J. Am. Chem. Soc.* 2001, **123**, 9476–9477.
- [44] Gloaguen, F.; Lawrence, J. D.; Rauchfuss, T. B.; Bénard, M.; Rohmer, M.-M.. Bimetallic carbonyl thiolates as functional models for fe-only hydrogenases. *Inorg. Chem.* 2002, **41**, 6573–6582.
- [45] Izutsu, K. *Acid-base dissociation constants in dipolar aprotic solvents*, Blackwell Scientific Publications, Oxford, 1990.
- [46] Chong, D.; Georgakaki, I. P.; Mejia-Rodriguez, R.; Sanabria-Chinchilla, J.; Soriaga, M. P.; Daresbourg, M. Y. Electrocatalysis of hydrogen production by active site analogues of the iron hydrogenase enzyme: structure/function relationships. *J. Chem. Soc. Dalton Trans.* 2003, 4158–4163.
- [47] Mejia-Rodriguez, R.; Chong, D.; Reibenspies, J. H., Soriaga, M. P.; Daresbourg, M. Y. The hydrophilic phosphatriazaadamantane ligand in the development of h₂ production electrocatalysts: Iron hydrogenase model complexes. *J. Am. Chem. Soc.* 2004, **126**, 12004–12014.
- [48] Ott, S.; Kritikos, M.; Åkermark, B.; Sun, L. C.; Lomoth, R. A biomimetic pathway for hydrogen evolution from a model of the iron hydrogenase active site. *Angew. Chem. Int. Ed.* 2004, **43**, 1006–1009.
- [49] Hou, J.; Peng, X.J.; Liu, J. F.; Gao, Y. L.; Zhao, X.; Gao, S.; Han, K.L. A binuclear isocyanide azadithiolatoiron complex relevant to the active site of Fe-only hydrogenases: Synthesis, structure and electrochemical properties. *Eur. J. Inorg. Chem.* 2006, 4679–4686.
- [50] Ott, S.; Kritikos, M.; Åkermark, B.; Sun, L. C. Synthesis and structure of a biomimetic model of the iron hydrogenase active site covalently linked to a ruthenium photosensitizer. *Angew. Chem. Int. Ed.* 2003, **42**, 3285–3288.
- [51] Hou, J.; Peng, X. J.; Zhou, Z. Y.; Sun, S. G.; Zhao, X.; Gao, S. Tris(N-pyrrolidinyl)phosphine substituted diiron dithiolate related to iron-only hydrogenase

- active site: Synthesis, characterization and electrochemical properties. *J. Organomet. Chem.* 2006, **691**, 4633–4640.
- [52] Moloy, K.G.; Petersen, J. L. N-Pyrrolyl Phosphines: An unexploited class of phosphine ligands with exceptional π -acceptor character. *J. Am. Chem. Soc.* 1995, **117**, 7696–7710.
- [53] Clarke, M.L.; Holliday, G. L.; Slawin, A. M. Z.; Woollins, J. D. Highly electron rich alkyl- and dialkyl-N-pyrrolidinyl phosphines: an evaluation of their electronic and structural properties. *J. Chem. Soc. Dalton Trans.* 2002, 1093–1103.
- [54] Borg, S.J.; Behrsing, T.; Best, S.P.; Razavet, M.; Liu, X.; Pickett, C. J. Electron transfer at a dithiolate-bridged diiron assembly: Electrocatalytic hydrogen evolution. *J. Am. Chem. Soc.* 2004, **126**, 16988–16999.
- [55] Grosshenny, V.; Romero, F. M.; Ziessel, R. Construction of preorganized polytopic ligands via palladium-promoted cross-coupling reactions. *J. Org. Chem.* 1997, **62**, 1491–1500.
- [56] Sonogashira, K.; Tohda, Y.; Hagiwara, N. A convenient of acetylenes:catalytic substitutions of acetylenic hydrogen with bromoalkens, iodoarenes, and bromopyridines. *Tetrahedron Lett.* 1975, **16**, 4467–4470.
- [57] Song, L.C. Tang, M.Y.; Su, F. H; Hu, Q. M. A biomimetic model for the active site of iron-only hydrogenases covalently bonded to a porphyrin photosensitizer. *Angew. Chem. Int. Ed.* 2006, **45**, 1130–1133.
- [58] Bookser, B. C.; Bruice, T. C. Syntheses of quadruply two- and three-atom, aza-bridged, cofacial bis(5,10,15,20-tetraphenylporphyrins). *J. Am. Chem. Soc.* 1991, **113**, 4208–4218.
- [59] Shaw, J. L.; Garrison, S. A.; AlemPn, E. A.; Ziegler, C. J.; Modarelli, D. A. Synthesis and Spectroscopy of a Series of Substituted N-Confused Tetraphenylporphyrins. *J. Org. Chem.* 2004, **69**, 7423–7427.

Chapter 7

RECENT ADVANCES IN ORGANOTIN(IV) COMPLEXES CONTAINING Sn-S BONDS

Abbas Tarassoli and Tahereh Sedaghat

Department of Chemistry, College of Sciences,
Shahid Chamran University, Ahvaz, Iran

ABSTRACT

In view of widespread industrial and biomedical applications of organotin(IV) compounds containing Sn-S bond, the synthesis, spectroscopic characterization and X-ray strucrural studies of some novel organotin complexes with 2-amino-1-cyclopentene-1-carbodithioic acid (ACDA) and its N-alkyl derivatives (RACDA) are investigated and reviewed. The presence of competing reactive center in these aminodithiocarboxylato ligands and the remarkable diversity in structure of organotin dithiolates lead to the interest in the study of such sulfur-nitrogen containing ligands. X-ray crystallographic studies of these organotin complexes show the bonding take place through the dithioate moiety and reveal a variety of coordination geometry around the Sn atom. These studies also show that an intramolecular hydrogen bond is formed between NH proton of amine group and one of sulfur atoms from dithiolate moiety. In ACDA complexes the neighboring molecules are oriented in such a way that an intermolecular hydrogen bond is also formed between another NH proton and one sulfur atom of the neighboring molecule, so that this sulfur atom is involved in one intra- and one inter-molecular hydrogen bonding. In this chapter the reaction of ACDA and RACDA (R= Et, Bu and Bz) with di- and tri-organotin chlorides will be discussed and the characterization of complexes will be investigated in solution and in solid state by spectroscopic methods and X-ray crystallography.

INTRODUCTION

Tin has played a considerable role upon increasing of activity in organometallic chemistry and this was stimulated by the discovery of a variety of applications. Tin chemistry acknowledges a wealth of academic and industrial applications, which are extremely

widespread and well documented. The history of organotin chemistry began in about 1849, when Frankland reported the preparation of diethyltindiiodide [1]. Organotin compounds are characterized by the presence of at least one bond between tin and carbon. As a member of group 14 in the periodic table, tin is indisputably a main group element, yet has also transition metal characteristics. Accordingly, it forms strong covalent bonds with carbon and heteroelements, as well as weaker coordination bonds [2]. Consequently, organotin chemistry is very rich in applications in many areas.

Among organometallic compounds of tin, the most well known ones are derivatives of tin(IV). The organotin(IV) compounds contain tetravalent Sn center and are classified as mono-, di-, tri- and tetraorganotin(IV)s, depending on the number of alkyl (R) or aryl (Ar) moieties. The anion is usually chloride, fluoride, oxide, hydroxide, carboxylate, thiolate, etc. Over the last few decades, research into the chemistry of organometallic compounds of tin in the +4 oxidation state has represented one of the most prolific areas of chemical investigations [3]. This is because of several reasons; these compounds have been studied by more techniques and have found more industrial, agricultural and medicinal applications than any other organometallic compounds. Many organotin complexes are biologically active and may interact with biological systems in many different ways as for instance bactericides, fungicides, acaricides and industrial biocides. Investigations have established the powerful biocidal properties of the trialkyltin and triaryltin compounds. Triphenyltin compounds were known to have fungicidal activity combined with very low phytotoxicity. Some organotins have also been developed as agrochemicals [4-7]. Organotin compounds are employed in a number of fields in the plastic industry, as stabilizer for PVC and as catalysts for certain silicon oligomers and in the manufactures of polyurethane foam and polyesters. Plastic has to protect against the degradative effects of heat and light and certain organotin compounds are amongst the most effective stabilizers known for the plastic. There are three major types of tin stabilizers and are distinguished by their respective alkyl groups: methyl, butyl and octyl [7].

Organotin compounds are being increasingly important in area of antitumour activity and cancer chemotherapy [8-10]. Several organotin complexes are effective antineoplastic (mainly antileukaemic) and antiviral agents. Diorganotin dihalide and diseudohalide octahedral complexes with bidentate N-donor ligands, containing *trans* organic groups and *cis* halogens, which bear a close structural resemblance to the platinum anti-tumor drug *cis*-Pt(NH₃)₂Cl₂, are active *in vivo* towards the P388 lymphocytic leukemia tumor in mice. Dibutyltin dichloride and dioctyltin dichloride exert a selective cytotoxic action on T-lymphocytes and may therefore hold potential as anti-T-cell tumor agents [11, 12]. The precise mechanism of the activity of these complexes requires an understanding of their structure and isomerism. In attempts to correlate the anti-tumor activity with structure, it has been generally assumed that the organic ligand would facilitate the transport of the complex across cell membranes, while the anti-tumor activity would be exerted by the dissociated diorganotin(IV) moieties [13]. In order to make the best use of the antiproliferative activity of tin, in recent years many organotin compounds have been synthesized and tested for their antitumor activity and have been found to be as effective as or even better than traditional heavy anticancer drugs [14].

In addition to their biological activity, organotin compounds have been used as reagents or catalysts in organic reactions [15]. Among organometallic reagents, organotins occupy a special place in organic synthesis; the nature of tin-hydrogen, tin-oxygen and tin-carbon bonds, strong enough to provide stable reagents but labile enough to allow high reactivity in

mild conditions, provide valuable and versatile use in organic chemistry. Organostannanes are known to be valuable reagents in organic synthesis due to the variety of carbon-carbon bond forming reactions they undergo. Several organotin compounds have been shown to be extremely versatile catalysts for transesterification reactions [16-19]. Although in recent years there are general environmental concerns about the toxicity and disposal of organostannanes [20], these compounds are much easier to use and to dispose safely than their mercury, thallium, and lead counterparts. It is inappropriate to generalize that all tin compounds, as having equivalent toxicological and ecotoxicological profiles.

In addition to the aforesaid applications, organotin compounds are also of interest in view of the considerable structural diversity that they possess. Many studies on the structural chemistry of organotin systems, as determined by X-ray crystallography, have shown that remarkable diversity in structure may sometimes be observed even when only small changes in chemistry exist. This aspect has been attracting the attention of a number of researchers and a multitude of structural types have been discovered.

SYNTHESIS OF ORGANOTIN COMPOUNDS

The alkyl (or aryl) groups are usually introduced onto tin by complete alkylation of tin tetrachloride with an organometallic reagent. Then the various alkyltin chlorides, R_nSnCl_{4-n} ($n=3, 2, \text{ or } 1$), are prepared by the Kocheshkov disproportion reaction in which the tetraalkyltin and tin tetrachloride in the appropriate proportions are heated together at about 200°C [3, 21, 22]. Organotin mixed dihalides were prepared by redistribution method or by halogen exchange [23, 24]. Reaction of alkyltin chlorides with the appropriate nucleophiles gives the alkyltin alkoxides, amines, thioalkoxides, carboxylates, thiolates, etc. [25]. Major structural issues in organotin chemistry are induced by the high coordination ability of tin, more specifically its ability to be involved in both weak or strong intra- and intermolecular coordinations. Since tin has *d* orbitals and it can expand its valence shell beyond eight electrons, the presence of electronegative groups on the tin renders the metal susceptible to coordination by Lewis bases and complexes with a higher coordination number are formed [26, 27]. Organotin compounds are now known to contain tin in coordination numbers three through to seven, in varying isomeric forms and lattice arrays. The organotin halides, R_nSnX_{4-n} ($n=3, 2, \text{ or } 1$), provide the starting materials from which most other organotin compounds are prepared [28-30]. The Lewis acid strengths of the organotin halides decrease as n increases and when the halide is varied in the sequence Cl > Br > I. The reaction of organotin halides with nucleophiles may be a substitution reaction and $R_nSnX_{4-n-m}Y_m$ (Y is an anionic nucleophile) is formed, or may be an addition reaction and $R_nSnX_{4-n}L_m$ (L is a neutral nucleophile) is formed [31-34]. Therefore organotin chemistry has always intrigued chemists due to their synthetic challenges and unique structural features ranging from monomeric to cluster networks with rich variety of structures, reactions and applications.

SPECTROSCOPIC METHODS FOR STUDY OF ORGANOTIN(IV) COMPOUNDS

Compounds of tin are studied by more techniques than those of any other element. Beside the other conventional methods, some of the more specialized techniques are also well-suited to solve structural problems in organotin chemistry. The fact that tin has more stable isotopes than any other element gives it very characteristic mass spectra and these isotopes give rise to the characteristic pattern of peaks. Amongst the isotopes of tin, the ^{115}Sn , ^{117}Sn and ^{119}Sn nuclei have spin 1/2, therefore zero quadrupole moment, and are in principle suitable for NMR studies. With respect to both higher abundance and greater sensitivity to NMR detection, most measurements have been made with ^{119}Sn . This nucleus has a natural abundance of 8.7 %, negative magnetogyric ratio and consequently negative nuclear Overhauser enhancement. ^{119}Sn nucleus is less sensitive than proton but about 25.5 times more sensitive than ^{13}C [35]. The ^{119}Sn chemical shifts, quoted against tetramethyltin as zero, are influenced by the variation in the coordination number and bond angles at tin, by any $\delta\pi$ -bonding effect and by the presence of electronegative substituents [36-39]. A very important property of ^{119}Sn chemical shift is that $\delta(^{119}\text{Sn})$ is strongly dependent on the coordination number of tin atom and an increase in coordination number produces a large upfield shift. $\delta(^{119}\text{Sn})$ moves upfield by 60-150 ppm with a change of coordination number of tin from 4 to 5, by 130-200 ppm from 5 to 6, and approximately 150-300 ppm from 6 to 7 [40, 41]. Therefore ^{119}Sn NMR is an excellent technique for studying of organotin complexes in solution. Satellites due to coupling by the ^{117}Sn and ^{119}Sn isotopes can be observed in the ^1H NMR spectra and the value of $J(\text{Sn}-\text{CH})$ for ^{119}Sn being always greater than for ^{117}Sn . The coupling constant shows an increase in magnitude with increasing coordination number of the tin atom. Nuclear spin coupling also increases with increasing *s*-character of bonds [35, 42]. Nowadays tin NMR methodologies are applied to the advanced structure determination of tin compounds in solution. Two structural issues specific to tin chemistry in the solution state have been considered: (i) obtaining evidence for the existence of coordination, sometimes very weak ones, from a Lewis donor, present as a functionality on an organic substituent of the organotin compound under examination, to the tin atom itself; while trivial in X-ray crystal structures, it is not at all in solution; (ii) confirming or even unraveling the covalent structure pattern of complex organotin compounds, either micro-clusters or bioorganotin derivatives, including not only the full atom assignment to the multinuclear NMR resonances but also, when meaningful, spatial arrangements and conformational features in the complex tin derivatives.

Solid-state tin NMR has also experienced a welcome breakthrough in tin chemistry since the early 1990s [43, 44]. Recently high-resolution solid-state NMR spectroscopy investigations can provide an invaluable 'bridge' between the structural data obtained on a single crystal and the NMR spectroscopic data obtained in solution. With the help of this bridge it is possible to make clear statements about the structure of the compound in solid state and in solution, and thus to develop better models for understanding the mechanisms involved in reactions carried out in the liquid state. This holds especially for tin compounds which are amorphous in the solid state, and therefore, not amenable to X-ray diffraction [45, 46]. However, solid-state tin NMR is a technique which has so far been used by relatively few research groups working in the organotin field. This may well be due to the fact that it still

appears too many to be a very difficult technique which can be successfully practiced only by ‘experts’.

The radioactive isotope ^{119m}Sn is appropriate for Mössbauer spectroscopy. The Mössbauer effect is now generally termed the recoil-free emission and resonant absorption of nuclear γ -rays. Information extracted from ^{119}Sn Mössbauer spectroscopy of tin compounds essentially concerns (1) the valence state in inorganic derivatives, (2) structure and bonding in the metal environment (mainly in organotins) and (3) the dynamics of tin nuclei, the latter possibly correlated to the nature of the substrate (mono- or polymeric) [47]. Measurements are effected on solids, gels and frozen solutions. A Mössbauer spectrum furnishes the parameters isomer shifts (IS or δ) and quadrupole splitting (QS or Δ). The isomer shift gives a measure of the s -electron density at the tin nucleus. A decrease in the s -electron density at the nucleus corresponds with a more positive isomer shift [48, 49]. Isomer shift values also depend on the electronegativity of ligands, on the coordination number, and on the stereochemistry. The value of δ is seen to fall with increasing electronegativity of ligand [50]. The quadrupole splitting QS arises because the excited state with $I\ 3/2$ has quadrupolar charge separation and this can interact with a local electric field gradient due to the ligands about the tin. Deviations of the electronic environment of the nucleus from cubic, octahedral, or tetrahedral symmetry result in a splitting of the Mössbauer signal. Quadrupole splitting supplies additional structural information. For example, a tetrahedral compound R_4Sn , with zero field gradient at the tin, will show only a singlet signal, but a compound R_3SnX with only axial symmetry, will show the signal split into a doublet. The ^{119m}Sn -Mössbauer spectroscopy is used less now that the more discriminating technique of high resolution solid state NMR spectroscopy has been developed, and X-ray diffraction is more generally available for investigating crystalline samples. However, this technique stands the test in cases where crystalline material for the application of diffraction is not available.

Despite the contribution of ^{119}Sn NMR and Mössbauer spectroscopies, no new structural form of tin can be firmly established without crystallographic confirmation.

ORGANOTIN COMPOUNDS WITH Sn-S BONDS

Up to now considerable efforts have been made to synthesize and characterize organotin compounds of ligands having heterodonor atoms (O, N, S) and many studies have been focused on structure–activity correlations [51-55]. It seems that the sulfur coordinated complexes are very stable as compared with those coordinated by oxygen or nitrogen.

Organotin compounds with Sn-S bonds can be prepared by substitution at tin by sulfur nucleophile. There are many parallels between the chemistry of compounds containing Sn-S bonds and those containing Sn-O bonds. An important difference between them is that whereas Sn-O bonded compounds often self-associate to give oligomers or polymers with 5-coordinate tin, the sulfur compounds show fewer tendencies to associate. The Sn-S bonds also less easily cleaved in substitution (e. g. hydrolysis) and addition reactions [54,56].

Interest in the coordination chemistry of metal-sulfur complexes arises from their potential relevance to active sites in metalloenzymes and also from their ability to adopt various nuclearities and significant structural complexity [57-59]. In addition, interaction of toxic main group metals with biological systems frequently involves bonding to enzymes

sulfhydryl groups and main group metal complexes are of some interest in the design of detoxification reagents [60]. This interest has led researchers to study organotin compounds that in a biological medium react with thiol groups in relevant molecules, yielding products characterized by Sn-S bonds [61, 62]. On the other hand some organotin thiolates and sulfides have found industrial application, especially as stabilizers of polyvinylchlorides [7]. Much of the work on organotin compounds of sulfur has been directed towards this end, and it has been mostly published only in the patent literature. Increasing industrial use of organotin(IV) compounds containing an Sn-S bond and recognition of the importance of this bond for the biological properties of organotin compounds have together spurred on the study of thiolates of tin.

ORGANOTIN(IV) THIOLATES AND DITHIOLATES

Simple organotin alkyl thiolates have been known for a number of years but a proposal that the biocidal activity of diorganotin compounds arises from binding to enzymatic dithiolates, such as reduced lipoic acid, has renewed interest in this area of chemistry, and several new thiolates have been reported. The organotin thiolates (mercaptides) are usually prepared by substitution by a sulfur nucleophile at a tin center. Suitable pairs of reactants are: (a) thiol and tin oxides, alkoxides, or amide, (b) thiol and tin halide in the presence of a base or (c) metal thiolate and tin halide [63-65]. The tin thiolates are usually stable towards air and water, and, in general, the reactivity in both substitution and addition process follows the sequence $\text{Sn-NR}_2 > \text{Sn-OR} > \text{Sn-SR}$. They are normally monomeric in solution and dithia-stannolanes show a few tendency to undergo self-association as compared with dioxa- and oxathia-stannolanes. The degree of self association is reduced as sulfur is introduced in place of oxygen, and when bridging does occur in the oxathiastannolanes, it involves the oxygen rather than sulfur [66]. The Sn-SR bond is cleaved by protic acids (e. g. carboxylic acids) and by Lewis acids such as BCl_3 , HgCl_2 , and PCl_3 , and bromine or iodine react quantitatively with $\text{R}_3\text{SnSR}'$ to give R_3SnX and $\text{R}'\text{SSR}'$ [56]. Their reactions with HCl and with tin halides are keys to their operation as stabilizers for PVC [7].

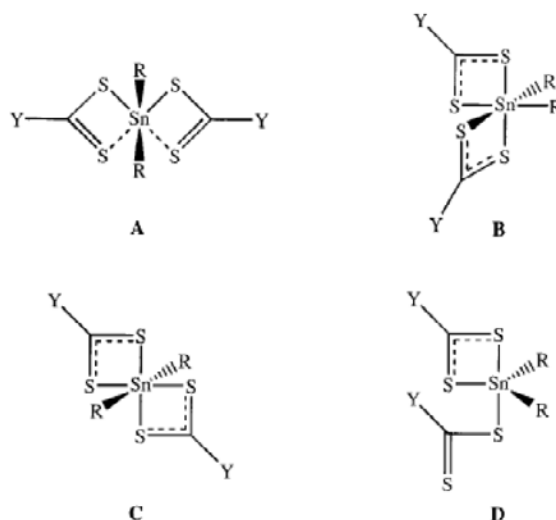
Organotin halides also react with 1,1-dithiolates and each halide can be simply replaced by dithiolate anions [e. g., 1,1-dithiolate = S_2CNR_2 (dithiocarbamate = R_2dtc^-), S_2COR (Xanthate = RXan^-), $\text{S}_2\text{P(OR)}_2$ (dithiophosphate = R_2dtp^-), etc.]. Effective coordination numbers between four and six can be contemplated for such series of complexes in the solid state, depending on whether the dithiolate ligands behave as monodentate or bidentate donors toward the tin atom. In solution the tin complexes may undergo dynamic processes such as intermolecular ligand exchange and intramolecular monodentate-bidentate dithiolate ligand exchange as well as molecular fluxionality. Furthermore, steric and electronic effects of organoyl R group substituent at tin may also influence the stereochemistry of the hypervalent tin(IV) complex in solution [67].

The solid-state structures of a number of triorganoyl- and diorganoyltin(IV) dithiolate complexes have been described in literatures. These structures are generally characterized by asymmetric coordination of the dithiolate to the tin atom (with a S-S distance spanning the range 2.5-3.2 Å) so that the coordination number of the tin atom may appear ambiguous, depending on the significance given to S-S distances which are longer than normal covalent

bonds but shorter than the sum of the respective van der Waals radii. Accordingly, even within the fairly simple series derived from R_3SnCl , the structure of the resultant tin complex in the solid state may be either five-coordinate as in $Me_3Sn(Me_2dtc)$ or four-coordinate as in $Ph_3Sn(Et_2dtp)$ [68]. In the diorganoyl series $Ph_2SnCl(^iPr(xan))$ the tin atom is effectively five coordinate whereas in $Ph_2Sn(Et_2dtc)_2$, $Ph_2Sn(Et_2dtp)_2$, $Me_2Sn(Et_2dtc)_2$, $Me_2Sn(Me_2dtp)_2$, and $Me_2Sn(Et(xan))_2$ the tin atoms appear to be six coordinate in the solid state [69-71]. These complexes exhibit a rich diversity of geometries even if small changes in the structure of the groups around the central tin atom are made. Examples of this feature are the related compounds bis(diisopropyl-dithiophosphate)diphenyltin(IV), $[(^iPrO)_2PS_2]_2SnPh_2$, and bis(diethyldithiophosphate)diphenyltin(IV), $[(EtO)_2PS_2]_2SnPh_2$. The former has an octahedral geometry around the tin atom (Ph–Sn–Ph angle is 180°) with the phosphorodithioate ligand coordinated symmetrically, whereas the latter has a skewed trapezoidal bipyramidal geometry with the dithiolate ligand coordinated in an asymmetric fashion. In this compound the angle Ph–Sn–Ph is 135° [72]. The difference between both compounds is the methyl group at the alkoxy moiety of the dithiophosphate ligand. Crystal packing effects may not entirely account for the different geometries around tin between these two structures.

For six-coordinated diorganotin bis(1,1-dithiolates) four structural motifs are found, as shown in Scheme 1 [73]. The majority of structures adopt motif A, which features a skew-trapezoidal bipyramidal geometry. The trapezoidal plane is defined by four sulfur atoms derived from two asymmetrically coordinating 1,1-dithiolate ligands and the tin-bound organo substituents are orientated over the weakly bound sulfur atoms so that the C–Sn–C angles lie in the range $121.8(5)$ - $150.2(4)^\circ$. In motif B, the organo substituents occupy mutually cis positions so that the coordination geometry is best described as distorted octahedral. A distorted octahedral geometry is also found in motif C, where the organo substituents occupy mutually trans positions. Finally, a reduced coordination number is found in motif D, where the tin atom exists in a distorted trigonal bipyramidal geometry owing to the presence of a monodentate dithiocarbamate ligand. The reasons for the adoption of the different structural motifs have yet to be ascertained. These may relate to electronic, steric, or crystal packing effects or some combination of these. Clearly, systematic investigations are required in order to determine the relative importance of these factors [73].

Recent investigations have shown that such a combined crystallographic/theoretical protocol proves very useful in examining the relative importance of electronic, steric, and crystal packing effects on molecular structure in organotin systems and indeed in other systems containing heavy elements [74-77]. One of the key result of such studies has been the demonstration that the often ignored crystal packing effects, i.e., intermolecular forces, do indeed exert a significant influence on coordination geometry as well as on the derived interatomic parameters. For example, calculations have repeatedly shown that non-symmetric structures converge to symmetric structures in the absence of solid-state effects. In the same way, calculations on polymorphs invariably demonstrate that differences in conformation and/or bond distances can be related to crystal packing effects [73].



Scheme 1.

There is a paucity of data describing the stereochemistry of such hypervalent tin(IV) complexes in solution. Tin-119 NMR spectroscopy is a particularly sensitive probe for determination of the coordination environment of the tin atom in many of its complexes. In general tin-119 chemical shifts move to lower frequency with increasing coordination number. There is an approximate linear relationship between the $\delta(^{119}\text{Sn})$ values and the coordination numbers of organotin(IV) dithiocarbamate complexes. Although the shift ranges are somewhat dependent on the nature of the substituents at the tin atom, the following ranges have been proposed for some tin(IV) dithiocarbamato complexes: -150 to -250 ppm for five-coordinate compounds, -300 to -500 ppm for six-coordinate compounds, and -700 to -800 ppm for seven-coordinate compounds [40, 41, 78, 79]. Furthermore, NMR spectroscopy is well-suited for studying dynamic processes such as inter- and intramolecular ligand exchange as well as stereochemical non-rigidity arising from fluxionality [67].

As part of an ongoing study of dithiolate complexes of main group elements and of the coordination chemistry of tin(IV) compound, we now report the results of synthesis and structural investigation of several organotin complexes with a series of aminodithiocarboxylate ligands in solution and solid state.

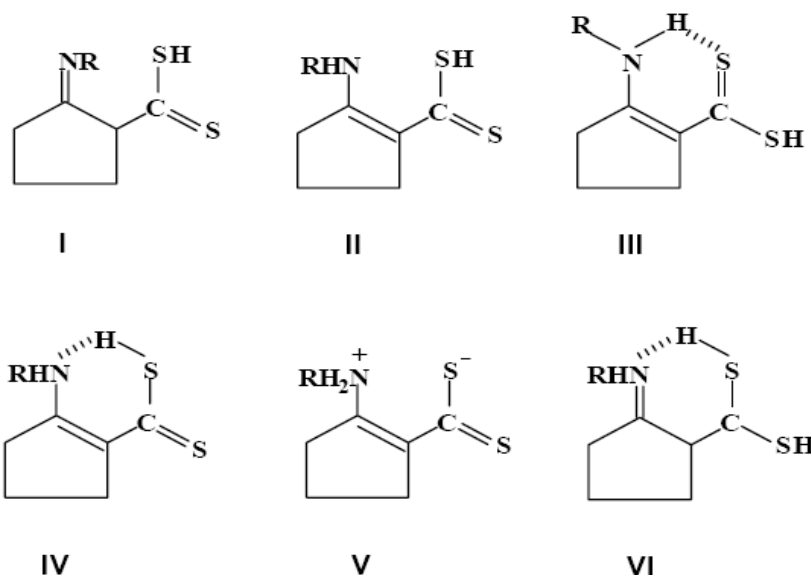
ORGANOTIN(IV) COMPLEXES WITH 2-AMINO-1-CYCLOPENTENE-1-CARBODITHIOATE AND ITS N-ALKYL DERIVATIVES

In view of the interesting role played by aminocarboxylic acid complexes in body systems and also because of the current interest in metal-sulfur compounds in biological molecules, delineation of the nature of metal ion binding and stereochemistry in aminodithiocarboxylic acid complexes warrant investigations. Among these, 2-amino-1-cyclopentene-1-carbodithioic acid (ACDA) and its N-alkyl derivatives (RACDA) are good chelatig agents. These ligands contain the backbone $-\text{NH}-\text{C}=\text{C}-\text{C}(\text{S})\text{S}^-$ which has some

similarity with derivatives of dithiocarbazate, $-N-N-C(S)S^-$, and dithiocarbamate, $-N-C(S)S^-$, ligands.

2-Amino-1-cyclopentene-1-carbodithioc acid (ACDA) is prepared as the ammonium salt through the reaction of cyclopentanone, carbon disulfide and ammonia [80-82]. Then N-alkyl derivatives of 2-amino-1-cyclopentene-1-carbodithioc acid are obtained from transamination reaction between aminodithiocarboxylic acid and corresponding amine [83-85].

2-amino-1-cyclopentene-1-carbodithioic acid and its N-alkyl derivatives may be assumed to exist in the six tautomeric forms (Scheme 2). On the basis of low temperature 1H NMR spectrum, Singh *et al.* suggested existence of tautomeric form **III** exclusively for ACDA and its derivatives [86].



Scheme 2.

The molecular structure of the benzyl derivative of ACDA (BzACDA), which is prepared from the reaction of benzylamine with ACDA, is shown in Figure 1 [85]. On the basis of crystallographic data, there are intramolecular hydrogen bonds between $N(1)H \cdots S(2)$ and intermolecular bonds between $S(1)H$ and $S(2)$. This crystal structure confirms, among the above possible tautomeric forms, **III** exists exclusively.

ACDA and its derivatives are interesting sulfur-nitrogen containing ligands with suitable competing reactive centers. The ligands may act in monodentate fashion, fully or partially bidentate and even bridging, so that the coordination number of metal may appear ambiguous. In bidentate coordination mode, bonding takes place either from the amino nitrogen and the deprotonated thiol sulfur or from the 1,1-dithiolate moiety. In the studies performed on complexes of ACDA and its derivatives with transition metals, for a large number of complexes the N and S sites are involved in bond formation (Scheme 3a) but with Co(II), Ni(II) and some other metal ions disulfur chelation (Scheme 3b) occurs [87-91].

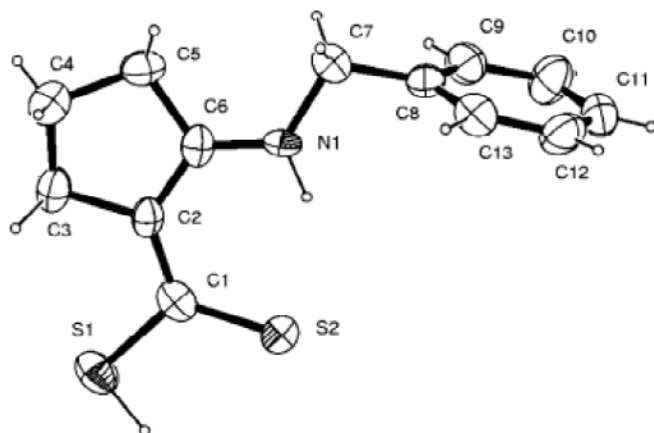
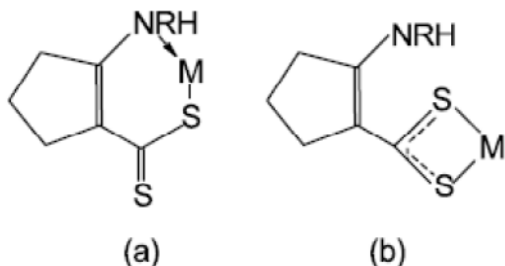


Figure 1. Crystal structure of BzACDA.



Scheme 3.

Until 2001, only a few attempts have been made to synthesize organotin complexes of these ligands and no crystallographic structure have been reported for them [92-94]. As we have seen earlier, the family of organotin compounds covers a spectrum of products used in a wide variety of biological applications. One of the interesting works in the field of bioorganotin chemistry is the introducing ligands which are bioactive themselves [52, 53]. Of particular interest among these, are certain complexes of potentially chelating dithioanionic ligands. In view of antifungal activity of ACDA and its derivatives and because they can mimic sulfur protein compounds, it is worthwhile to synthesize organotin(IV) complexes of them and investigate the structural features and nature of bonding with tin. Therefore, interest in ACDA and its derivatives complexes of organotin species arises in part because of their probable biological and industrial uses as well as because of their variable structures. Presence of hydrogen bonding in ACDA and its derivatives also adds to the interest in the study of organotin complexes of these ligands, because hydrogen bonding is an interesting feature of the structure of organotin(IV) complexes [95-98].

SYNTHESIS OF ORGANOTIN(IV) COMPLEXES WITH ACDA AND RACDA

Di- and tri-organotin(IV) chlorides, R_2SnCl_2 ($R = Ph, Bu, Bz$) and R_3SnCl ($R = Ph, Bz$), react with ACDA or its ammonium salt (AACD) to give complexes 1-7 [99, 100]. Complex 8 was obtained by Flores *et al.* from reaction of Et_2SnCl_2 with sodium salt of ACDA [101]. Complexes 9-20 are synthesized by reaction of di- and tri-organotin(IV) chlorides, R_2SnCl_2 ($R = Ph, Bu, Bz$) and R_3SnCl ($R = Ph, Bz$), with RACDA ($R = Et, Bu, Bz$) in neutral medium or in presence of triethylamine [85, 102]. In all of reactions chloride ion is replaced by dithiolate ligand and according to starting materials and reaction conditions, mono- or di-substituted complexes are formed. Stoichiometry of products may be confirmed by elemental analysis and mass spectroscopy. Also in the 1H NMR spectra of complexes, the ratio of the integrals of the signals from protons of the ligand to those of from protons of the organic groups on the tin provides a reliable measure of metal to ligand ratio in the complexes.

Because of low bond dissociation energy for organotins, molecular ion peak for most of complexes was not observed in mass spectrum [103, 104]. Since the most abundance isotope of tin is ^{120}Sn , highest intensity peak in isotope patterns of all spectra is corresponding to the fragment containing this isotope. Figure 2 shows the result of isotope pattern calculation for 10. The highest intensity peak is related to $^{120}SnPh_2(BuACDA)$ fragment.

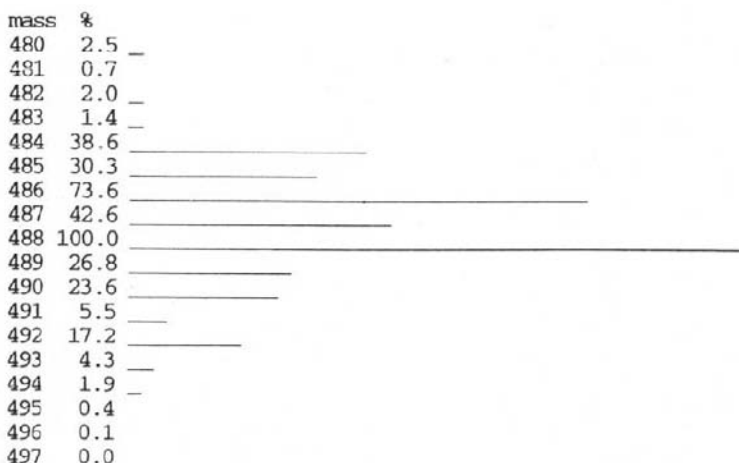
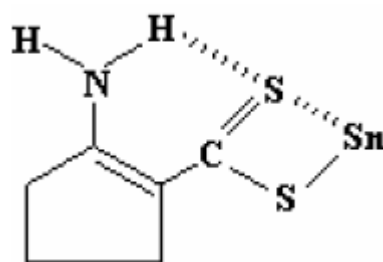


Figure 2. the result of isotope pattern calculation for 10.

Because it is not uncommon that the coordination characteristics of the tin atom and hence the structure of an organotin compound differ in solution and solid states, the potential duality in solid and solution state organotin structures requires therefore parallel structural investigations.

STRUCTURE OF ORGANOTIN (IV) COMPLEXES OF ACDA AND RACDA IN SOLUTION

A comparison of the ^1H NMR spectrum of complexes with that of the ligands shows the disappearance of the signal for the –SH proton indicating formation of dithiolate complexes. In the ^1H NMR spectrum of ACDA, two signals assigned to the –NH₂ protons are appeared at δ 6.1 and δ 11.2 ppm, showing the nonequivalence of the protons of the amino group. This is attributed to the involvement of one of the NH₂ protons in hydrogen bonding through the sulfur atom of the –C=S group in structure III of scheme 2 [86]. In the spectra of the ACDA complexes (1-8) one of the two signals (6.1 ppm) appears almost in the same region while the second signal shifts upfield, particularly in 1 and 2. This shift may be ascribed to coordination of dithiolate moiety and weakening of the hydrogen bond (N-H···S=C) on complexation. However, the existence of two signals for the –NH₂ protons, instead of one signal in complexes, indicates remaining of hydrogen bonding between one of the NH₂ protons and the sulfur atom (–C=S) of the dithiocarboxylate group even after complexation (structure VII).



VII

Similarly, in the organotin complexes of RACDA, NH signal of the free ligand (~12 ppm) shift to upfield, particularly in 9-12. It is indicating of (S, S⁻) type of bonding and weakening of hydrogen bonding in the complex. Table 1 compares chemical shift of NH proton involving in hydrogen bond (NH···S=C) for the ligands and the complexes. It is suggested that the stronger metal-sulfur bond (–C=S–Sn) results the weaker hydrogen bonding (NH···S=C-). The central tin atom in R₂SnCl(S–S) complexes should display enhanced acceptor strength owing to the presence of the more electronegative Cl atom in comparison to the other complexes. Such an enhancement in acidity of the tin center should spread over both the coordination sites of the NCS₂ skeleton, strengthening the bonding interaction of the ligand (–C=S–Sn) and weakening the hydrogen bonding (NH···S=C). Therefore in the chloroorganotin complexes (1, 2, 9-12) chemical shift values for the proton of the amine group are at much lower frequencies than those observed for other complexes (see table 1).

Table 1. $\delta(^1\text{H})$ for NH involving in hydrogen bonding (-NH---S=C) in CDCl_3

Compound	$\delta(^1\text{H})$	Ref.	Compound	$\delta(^1\text{H})$	Ref.
ACDA	11.2	86	$\text{Ph}_2\text{SnCl}(\text{EtACDA})$ (9)	9.5	102
$\text{Ph}_2\text{SnCl}(\text{ACDA})$ (1)	8.8	99	$\text{Ph}_2\text{SnCl}(\text{BuACDA})$ (10)	9.6	102
$\text{Bz}_2\text{SnCl}(\text{ACDA})$ (2)	8.7	100	$\text{Bz}_2\text{SnCl}(\text{EtACDA})$ (11)	9.56	85
$\text{Ph}_2\text{Sn}(\text{ACDA})_2$ (3) ^a	8.9	99	$\text{Bz}_2\text{SnCl}(\text{BzACDA})$ (12)	9.9	85
$\text{Bu}_2\text{Sn}(\text{ACDA})_2$ (4)	10.0	99	$\text{Bu}_2\text{Sn}(\text{EtACDA})_2$ (13)	11.1	102
$\text{Bz}_2\text{Sn}(\text{ACDA})_2$ (5)	9.7	100	$\text{Bu}_2\text{Sn}(\text{BuACDA})_2$ (14)	11.1	102
$\text{Ph}_3\text{Sn}(\text{ACDA})$ (6)	10.0	99	$\text{Bz}_2\text{Sn}(\text{EtACDA})_2$ (15)	10.9	85
$\text{Bz}_3\text{Sn}(\text{ACDA})$ (7)	10.3	100	$\text{Bz}_2\text{Sn}(\text{BzACDA})_2$ (16)	11.2	85
$\text{Et}_2\text{Sn}(\text{ACDA})_2$ (8)	10.7	101	$\text{Ph}_3\text{Sn}(\text{EtACDA})$ (17)	11.0	102
EtACDA	12.1	102	$\text{Ph}_3\text{Sn}(\text{BuACDA})$ (18)	11.1	102
BuACDA	12.6	102	$\text{Bz}_3\text{Sn}(\text{EtACDA})$ (19)	11.5	85
BzACDA	12.1	85	$\text{Bz}_3\text{Sn}(\text{BzACDA})$ (20)	11.9	85

^a Solvent: DMSO.

The ^1H NMR of 14 in toluene-d₈ has also been examined as a function of temperature (between 100 and -50°C) to evaluate behavior of the -NH proton within complex (Figure 3). In high temperature, NMR spectra show only one singlet for -NH proton. Decreasing the temperature caused this singlet to split and a triplet appeared. This splitting is due to coupling with nitrogen (I=1) in which rate of spin change would be slow with lowering of temperature and coupling with proton could be observed. Note that upon varying the temperature the position of -NH signal show no significant shift. So variation of temperature has no effect on the behavior of the hydrogen bonding in the complex.

The $^{119}\text{Sn}\{\text{H}\}$ NMR data for all complexes and original organotin chlorides are given in table 2. The $^{119}\text{Sn}\{\text{H}\}$ chemical shifts for all complexes are at much higher field than those of the original chloroorganotin(IV) compounds, because the electronegative group has been removed and the coordination number has increased. On the basis of the chemical shift ranges proposed for some of the tin(IV) dithiocarbamato complexes [67], it appears reasonable to assume that for 9, 19 and 20 coordination number of tin is four and in other complexes the effective coordination number in solution is five. However, these NMR data themselves do not indicate whether in solution the dithioate ligands are symmetrically or asymmetrically coordinated to tin. In most dithioates one of the Sn-S bonds is weaker than the other, so that there are two sets of intramolecular distances [105-107]. In ^1H NMR spectra of complexes $\text{R}_2\text{Sn}(\text{ACDA})_2$ and $\text{R}_2\text{Sn}(\text{RACDA})_2$ only one signal was observed for NH proton involving in hydrogen bonding, NH---S=C, indicating that the two ACDA (or RACDA) groups are chemically equivalent. Each dithioate ligand effectively behaves as a bidentate sulfur donor ligand coordinated asymmetrically to the metal center. The distribution of charge on tin leads to shifts in the ^{119}Sn NMR spectra consistent with a coordination number of five. Fluxional behavior of chelates, S=C—S—Sn(S₂C)↔(CS₂)Sn—S—C=S in solution may also be responsible for the two equivalent NH features in the ^1H NMR spectrum and thus the effective coordination number of five in ^{119}Sn NMR.

In the ^{119}Sn NMR spectrum of 9 after standing in CDCl_3 , another signal at -157.6 ppm is appeared. Apparently at room temperature, the dithioate ligand can undergo slow monodentate–bidentate equilibrium in solution [67, 108]; appearance of an additional signal in higher frequency is consistent with an effective decrease in coordination number at the tin

atom which would arise from this intramolecular monodentate-bidentate exchange that is slow on the NMR timescale.

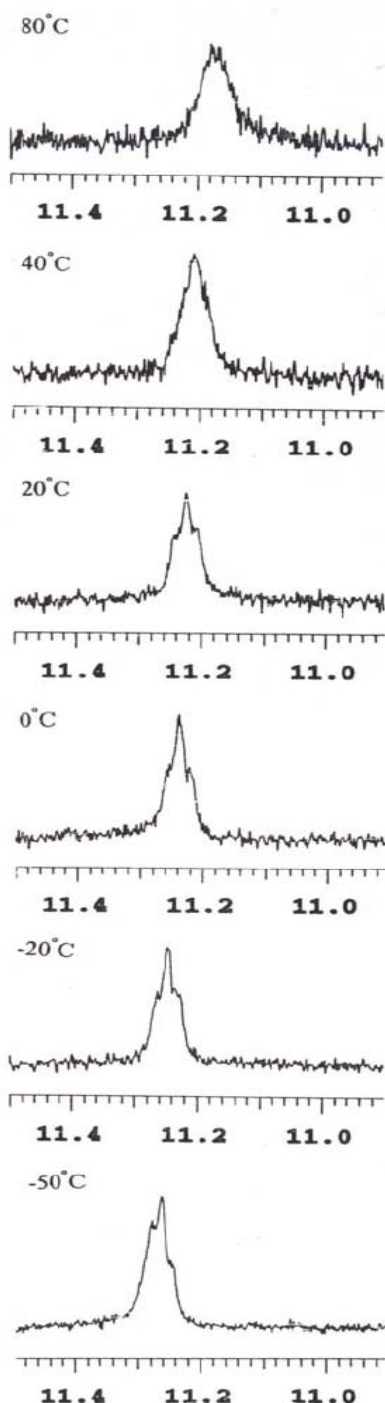


Figure 3. ^1H NMR spectra of 14 as a function of temperature.

Table 2. $\delta(^{119}\text{Sn})$ for organotin chlorides and complexes 1-20 (in CDCl_3)

Compound	$\delta(^{119}\text{Sn})$	Ref.	Compound	$\delta(^{119}\text{Sn})$	Ref.
Ph_2SnCl_2	-27	67	$\text{Et}_2\text{Sn}(\text{ACDA})_2$ (8)	-191.6	101
Bz_2SnCl_2	-35	85	$\text{Ph}_2\text{SnCl}(\text{EtACDA})$ (9)	-252.3	102
Bu_2SnCl_2	122	123	$\text{Ph}_2\text{SnCl}(\text{BuACDA})$ (10)	-183.5	102
Et_2SnCl_2	125	36	$\text{Bz}_2\text{SnCl}(\text{EtACDA})$ (11)	-168.0	85
Ph_3SnCl	-43	35	$\text{Bz}_2\text{SnCl}(\text{BzACDA})$ (12)	-166	85
Bz_3SnCl	-52	85	$\text{Bu}_2\text{Sn}(\text{EtACDA})_2$ (13)	-185.4	102
$\text{Ph}_2\text{SnCl}(\text{ACDA})$ (1)	-258.0	99	$\text{Bu}_2\text{Sn}(\text{BuACDA})_2$ (14)	-183.7	102
$\text{Bz}_2\text{SnCl}(\text{ACDA})$ (2)	- ^a	-	$\text{Bz}_2\text{Sn}(\text{EtACDA})_2$ (15)	-222	85
$\text{Ph}_2\text{Sn}(\text{ACDA})_2$ (3)	- ^a	-	$\text{Bz}_2\text{Sn}(\text{BzACDA})_2$ (16)	-221	85
$\text{Bu}_2\text{Sn}(\text{ACDA})_2$ (4)	-200.2	99	$\text{Ph}_3\text{Sn}(\text{EtACDA})$ (17)	-155.1	102
$\text{Bz}_2\text{Sn}(\text{ACDA})_2$ (5)	- ^a	-	$\text{Ph}_3\text{Sn}(\text{BuACDA})$ (18)	-153.2	102
$\text{Ph}_3\text{Sn}(\text{ACDA})$ (6)	-155.0	99	$\text{Bz}_3\text{Sn}(\text{EtACDA})$ (19)	-38.0	85
$\text{Bz}_3\text{Sn}(\text{ACDA})$ (7)	-36.2	100	$\text{Bz}_3\text{Sn}(\text{BzACDA})$ (20)	-36	85

^a Because of low solubility in common solvents, no data could be obtained.

STRUCTURE OF ORGANOTIN COMPLEXES OF ACDA IN SOLID STATE

Structure of [Ph₂SnCl(ACDA)] (1) [99]: Although a number of penta-coordinated diorganotin complexes of the type R₂ClSnS₂C have been reported, examples of structural studies are limited [69, 109-111]. Figure 4 shows the molecular structure of [Ph₂SnCl(ACDA)] and atomic numbering scheme used. Figure 5 shows the molecular packing diagram in unit cell. It can be seen that the configuration about the tin atom is penta-coordinated distorted trigonal bipyramidal with atoms S(1), C(7) and C(8) occupying equatorial positions. The sum of ligand–Sn–ligand angle in the trigonal girdle of the compound is 359.5°. So the tin atom shows no significant deviation from the equatorial plane. The Cl atom occupies one of apical positions of the trigonal bipyramidal. Due to being part of a chelate the angle S(1)–Sn–S(2) is not 90° but only 70.65°, so the S(2) cannot occupy exactly the corresponding *trans* axial position of Cl and the angle Cl–Sn–S(2) being 157.10°. The Sn–S(2) bond is markedly elongated (2.649 Å) compared to the Sn–S(1) bond (2.439 Å). This makes the dithioate coordination unsymmetrical. In this anisobidentate ligand, also the C–S bond length are unequal and both of them lie between the average value for the double C=S bond in thioureas (1.681 Å) and the single C–S bond in the C–S–Me fragment (1.789 Å) [112], suggesting that the both carbon-sulfur bonds have some double bond character in the deprotonated ACDA. In the complex, the shorter tin-sulfur bond is associated with a longer carbon–sulfur bond and vice versa, this is consonance with the bonding asymmetry of ligands.

As shown in Figure 4, the orientation of the ACDA enables it to form an intramolecular hydrogen bond between N–H(2)---S(2). Also neighboring molecules are held together by intermolecular Cl---H(1)–N hydrogen bonds. These hydrogen bonds can lend the crystal stability and compactness and the result is the chain arrangement from the intermolecular bonds (Figure 5).

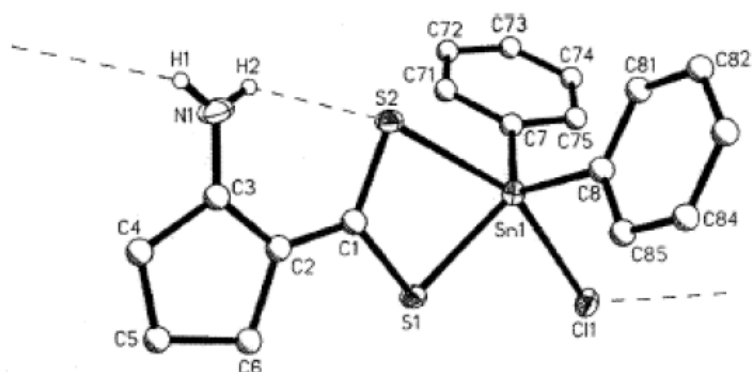


Figure 4. Molecular structure of $[Ph_2SnCl(ACDA)]$ (1).

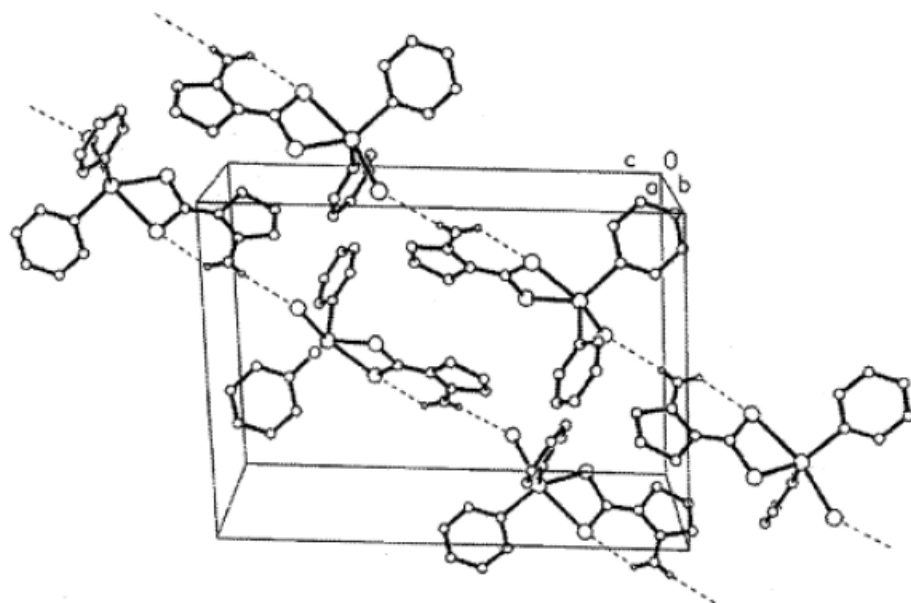


Figure 5. Molecular packing diagram in unit cell of $[Ph_2SnCl(ACDA)]$ (1).

Crystal structure of $Bz_2SnCl(ACDA)$ (2) [100]: The unit cell contains two independent molecules that show only minor differences. Atomic numbering scheme and a view of one of the two molecules are represented in Figure 6. The geometry around the Sn atom is pentacoordinated distorted trigonal bipyramidal with two benzylic carbon atoms and S(1) in the equatorial plane. As in all similar molecules, the chloride ion occupies an axial position [67, 99, 102, 103, 110, 111] while the other apical position is occupied by S(2) atom. The sum of the ligand–Sn–ligand angles in the trigonal girdle of the compound is 357.17° instead of the ideal 360° . The Sn–S(2) bond is markedly elongated compared to the Sn–S(1) bond. This makes the dithioate coordination unsymmetrical.

Because of being part of a chelate, the atom S(2) cannot occupy exactly the corresponding *trans* axial position, the angle Cl–Sn–S(2) being 158.92° and also the angle S(1)–Sn–S(2) is not 90° but only 69.15° . There are an intramolecular hydrogen bond between

one of the two proton atoms of NH₂ and S(2) and an intermolecular hydrogen bond between the other NH₂ proton and Cl of neighboring molecule.

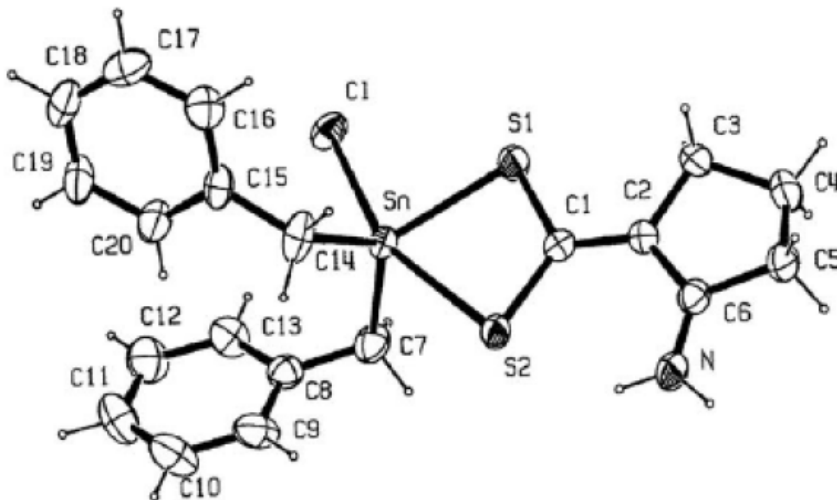


Figure 6. Crystal structure of Bz₂SnCl(ACDA) (2).

Structure of [Bu₂Sn(ACDA)₂] (4) [99]: The crystal consists of relatively isolated molecules that differ in conformation of butyl group. Figure 7 shows a view of one of molecules. The Sn atom shows extremely irregular octahedral coordination. The four S atoms lie in the equatorial plane. The C(1) and C(5) atoms of the butyl groups define C-Sn-C angles 134.2° is intermediate between *cis* and *trans*. The ACDA ligand is anisobidentately chelated to Sn, with one longer and one shorter Sn-S bond. From X-ray studies the dithioate ligands act as anisobidentate in most of the diorganotin(IV) dithioate complexes [113, 114]. As indicated in Figure 5 by dashed lines, there are intramolecular hydrogen bonds between N(1)H(2)--S(2) and N(2)H(4)--S(4) similar to previously described molecules.

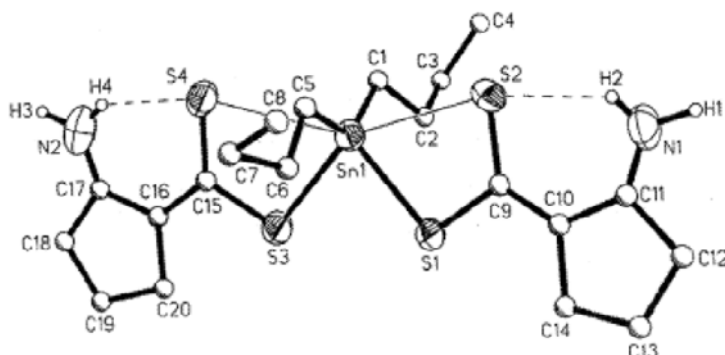


Figure 7. Molecular structure of [Bu₂Sn(ACDA)₂] (4).

Crystal structure of Bz₂Sn(ACDA)₂ (5) [100]: A view of the molecule including numbering scheme is shown in Figure 8. The crystals of 5 contain a molecule of THF from which it was recrystallized. The dithioate ligands are coordinated asymmetrically with short

Sn–S(1) [2.5082 Å] and Sn–S(3) [2.5006 Å] and long Sn–S [3.1001 Å] and Sn–S(4) [2.9530 Å] distances. The long Sn–S distances are significantly less than the sum of the van der Waals radii (4.0 Å), and the coordination number of tin is assigned as six. The overall geometry at tin is, however, highly distorted from *trans* octahedral: the C–Sn–C angle is only 130.64° which is intermediate between *cis* and *trans*, the tin and four S atoms of the ligands are nearly coplanar but distorted from square-planar geometry, so that Sn–S(2) is about 0.05 Å longer than Sn–S(4) and also while *cis* S(1)-Sn–S(3) angle is only 82.89°, the *cis* S(2)-Sn–S(4) is 149.81°. In both anisobidentate ligands each shorter tin-sulfur bond is associated with a longer carbon–sulfur bond and vice versa; this is in consonance with the bonding asymmetry of the ligands. The bond angles subtended at the tin atom by the methylene carbons and S(1) and S(3) atoms range from 104.50° to 113.85° demonstrating that the tin–carbon bonds are bent toward the longer tin–sulfur bonds. This is obviously a consequence of repulsion between the bonding electron pairs around the central tin atom. Electronic and steric arguments have also been invoked to account for the distortion of similar structures from regular octahedral geometry.

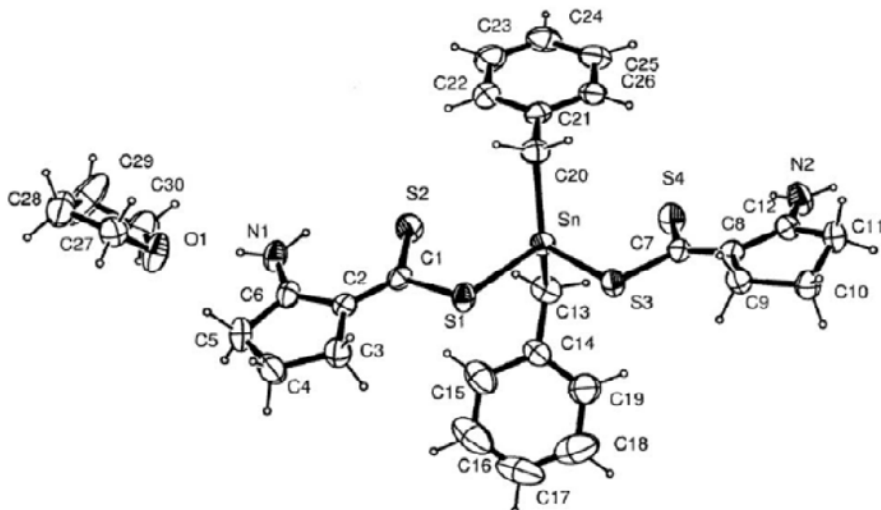


Figure 8. Crystal structure of $\text{Bz}_2\text{Sn}(\text{ACDA})_2 \cdot \text{THF}(5)$.

Structure of $[\text{Ph}_3\text{Sn}(\text{ACDA})]$ (6) [99]: A stereoview of the molecule and atomic numbering is shown in Figure 9. The crystal consists of two molecules which both have the same ligand shell but two different positions for the tin center. The crystal structure shows the tin atom is coordinated to the two sulfur atoms of the ACDA ligand and to the one carbon atom of each of the three phenyl groups. One of the Sn–S bonds (2.462 Å) lies in the range recently reported for triphenyltin thiolates (2.405–2.481 Å) [115, 116], close to the sum of the covalent radii of tin and sulfur (2.42 Å) [117], while the other Sn–S bond is considered as a weak coordinative bond corresponding to an anisobidentate ligand (thin lines in Figure 7). This might suggest description of the tin environment as a trigonal bipyramidal with S(2) and C(13) in the apical positions and S(1), C(7) and C(19) in the equatorial positions, this bipyramid is distorted: The sum of the equatorial angles is 350.2° instead of the ideal 360° and the tin atom lies out of the equatorial plane. As indicated by dashed lines in Figure 9, an

intramolecular hydrogen bond is formed between one of the NH_2 protons and the sulfur atom which is involved in the weaker Sn–S bond ($\text{N}(1)\text{H}(1)\cdots\text{S}(2)$ and $\text{N}(2)\text{H}(3)\cdots\text{S}(4)$ in Figure 9). Also as shown in this Figure the neighboring molecules are oriented in the way that an intermolecular hydrogen bond is formed between another NH_2 proton and one sulfur atom of the neighboring molecule ($\text{N}(1)\text{H}(2)\cdots\text{S}(4)$ in Figure 9), so that this sulfur atom is involved in one intra- and one inter-molecular hydrogen bond. The structure is held in two-dimensional space by these intermolecular hydrogen bonding forces.

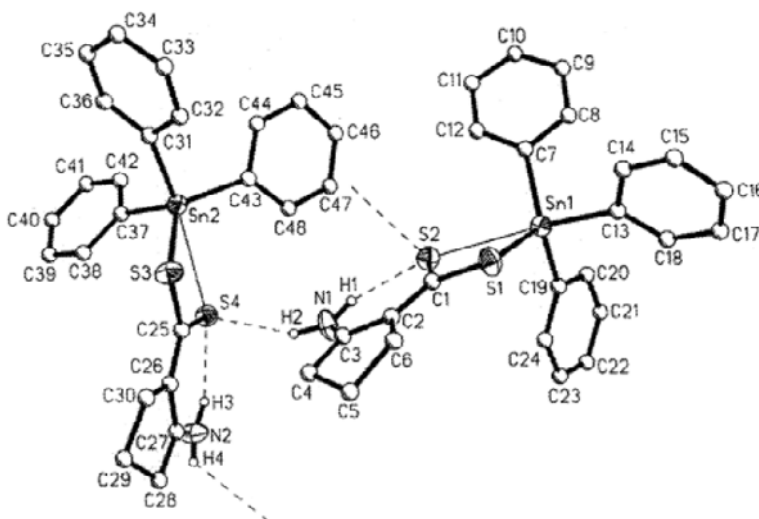


Figure 9. Molecular structure of $[\text{Ph}_3\text{Sn}(\text{ACDA})]$ (6).

Structure of $\text{Et}_2\text{Sn}(\text{ACDA})_2$ (8): The X-ray structure of 8 has been reported by Flores *et al.* [101] In this complex geometry obtained around tin is a skew trapezoidal bipyramidal with both organic residues in mutual trans-positions. The coordination occurs through both sulfur atoms in an asymmetric fashion and there is hydrogen bond between the NH and one of the sulfur atoms of the carbodithioate moiety. Therefore the coordination mode of ligand in 8 is similar to our complexes, so the steric hinderance on tin has little effect over the coordination pattern.

STRUCTURE OF ORGANOTIN COMPLEXES OF RACDA IN SOLID STATE

Structure of $[\text{Ph}_2\text{SnCl}(\text{BuACDA})]$ (10) [102]: The crystal consists of two independent molecules in the unit cell with their corresponding bond distances and angles being slightly different. Figure 10(a) shows the crystal structure of one of the molecules with the atom-numbering scheme and Figure 10(b) shows the structure around the tin. The geometry around the Sn atom is described as a distorted trigonal bipyramidal. The three atoms S(2), C(21) and C(31) lie on the equatorial plane of the bipyramid. The sum of the equatorial angles formed at the Sn atom is 358.5° instead of the ideal 360° , owing to the slight displacement of Sn out of

the plane. The Cl and S(1) atoms occupy apical positions. Owing to the constraint of the chelate, the average angle between these axial groups is 156.84° . As in the other known organotin dithiolates, an anisobidentate coordination is observed for this complex. The Average of the shorter Sn–S bond lengths is 2.453\AA which is very close to the sum of the covalent radii of tin and sulfur (2.42 \AA), and the average of the longer Sn–S distances is 2.730 \AA , which is significantly less than the sum of van der Waals radii (4.0 \AA) [114]. The longer C–S bond is associated with the shorter Sn–S bond, and likewise, the shorter C–S' bond is associated with the longer Sn–S' bond.

The average distances between S(1) and the H atom of the amine group [S(1)–H(1), 2.324\AA] are similar to the value reported for NH---S hydrogen bonds ($\sim 2.4\text{ \AA}$) [118]. This suggests an intramolecular hydrogen bond between sulfur and proton of the amine group.

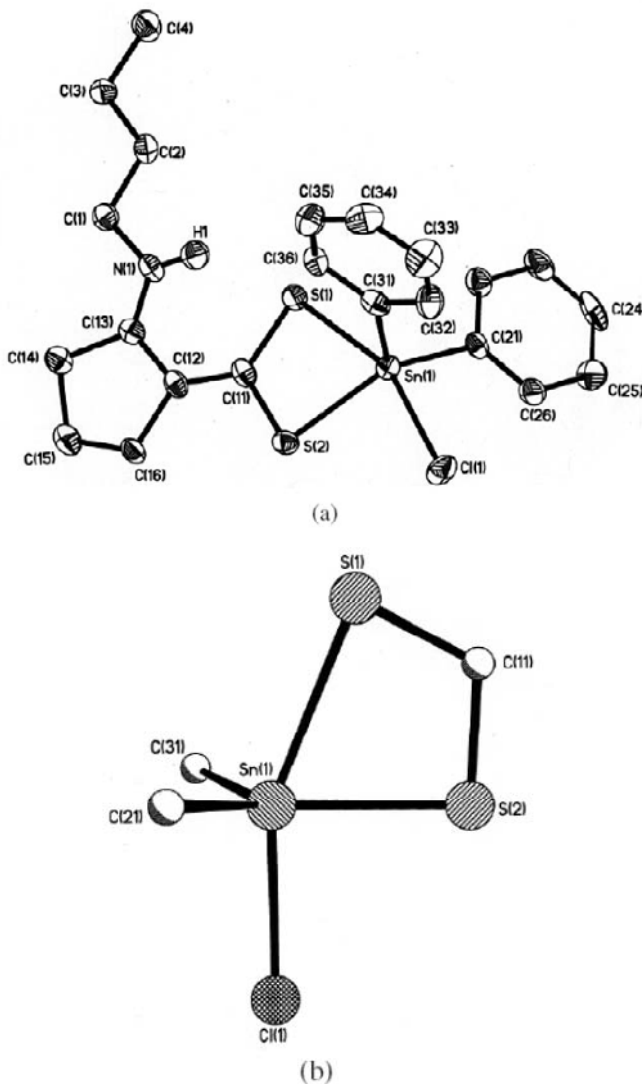
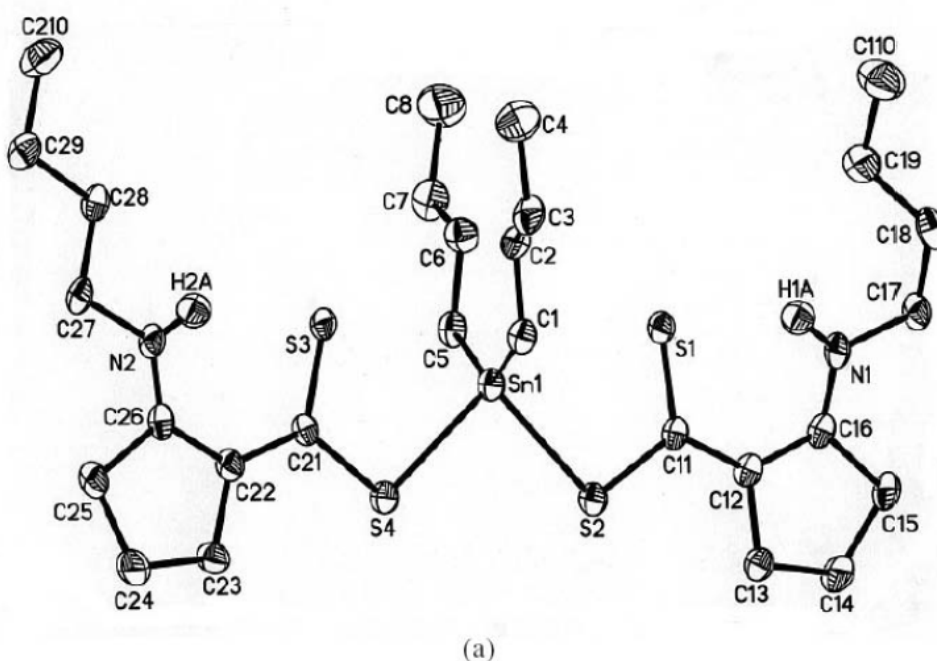
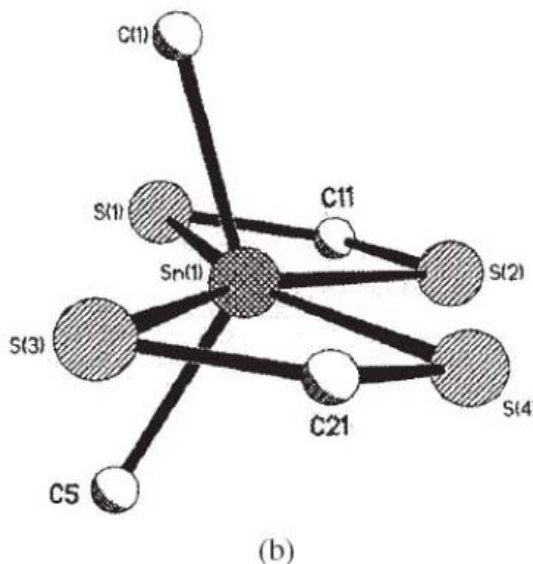


Figure 10. (a) Crystal structure for $[\text{Ph}_2\text{SnCl}(\text{BuACDA})]$ (10); (b) Crystal structure for 10 around tin atom.

Structure of $[Bu_2Sn(BuACDA)_2]$ (14) [102]: Figure 11(a) shows the crystal structure of 14 with the atom numbering scheme. Figure 11(b) shows the crystal structure only around the tin atom. The molecular structure shows an unsymmetrical environment for the tin atom. One sulfur atom of each ligand is covalently bonded with an average distance of 2.5137 Å, only 0.09 Å longer than the sum of the covalent radii (2.42 Å), while the other is located at an average distance of 2.9831 Å. This may be considered as a weak coordinate bond corresponding to an anisobidentate ligand. The long Sn–S distances are significantly less than the sum of the van der Waals radii (4.0 Å), and the coordination number of tin is unambiguously assigned as six. The overall geometry at tin is, however, highly distorted from *trans* octahedral. The C–Sn–C angle is only 134.45, intermediate between *cis* and *trans*. The tin and four sulfur atoms of BuACDA are nearly coplanar but are highly distorted from square-planar geometry, *cis* S–Sn–S angles range from 64.79° to 152.04°. The deviations from regular octahedral geometry may be a result of the difference in the steric effect and the electronegativity of ligand groups attached to the Sn atom [119, 120]. The distances between S and the H atom of the NHR group are 2.3203 Å and 2.2494 Å for S(1)–H(1A) and S(3)–H(2A), respectively. This again suggests an intramolecular hydrogen bond between sulfur and the proton of the amine ($-\text{C}=\text{S}1\cdots\text{HN}-$).



Figures 11. (a) Crystal structure of $[Bu_2Sn(BuACDA)_2]$ (14)



Figures 11. (b) Crystal structure of 14 around tin atom.

Structure of $Bz_2Sn(BzACDA)_2$ (16) [85]: The molecular structure and the numbering scheme are shown in Figure 12. The tin atom has a highly distorted octahedral environment in which the four S atoms lie in the equatorial plane. The atoms C(27) and C(34) of the benzyl groups define a C-Sn-C angle of 129.22° which is intermediate between those for *cis*- and *trans*-substitution. The deviation from the regular octahedral geometry may result from steric effects and differences in the electronegativities of the ligands attached to the tin atom [113]. The S-Sn-S bond angles range from 79° in the chelate ring to 154° for the angle between the ligands. The BzACDA ligands are anisobidentately chelated to Sn, with one longer and one shorter Sn-S bond [105, 114]. The Sn-S-C-S' bonding system in 16 is easy to discern [67]. The longer C-S bond is associated with the shorter Sn-S bond, and the shorter C-S' bond is associated with the longer Sn-S' bond. The long Sn-S distances are significantly shorter than the sum of the van der Waals radii (4.0 \AA) and the coordination number of Sn is effectively six [114]. The bond distances and bond angles within the five member rings and benzyl groups are unexceptional. Intramolecular hydrogen bonds between S and the adjacent amine groups are observed. The distances between S and H atoms are 2.33 and 2.38 \AA for S(2)-H(1) and S(4)-H(2), respectively.

Structure of $Bz_3Sn(EtACDA)$ (19) [85]: In the unit cell of this compound, there are two crystallographically independent molecules that show only minor differences. Crystal structure for one of the molecules is shown in Figure 13. The molecules contain essentially the four-coordinate tin, but with distortion from the normal tetrahedral environment. However, the long Sn···S(2) interactions (3.1001 \AA) can be regarded as weak coordinate bonds corresponding to an anisobidentate ligand [115]. The tin atom is also coordinated to the other sulfur atom and to the one carbon atom of each of the three benzyl groups. The Sn-S bond length lies toward the middle of the range reported for triphenyl thiolates ($2.405\text{--}2.481 \text{ \AA}$) close to the sum of the covalent radii of tin and sulfur (2.42 \AA) [115, 116]. Around the tin, the angles C(14)-Sn-C(7), C(14)-Sn-S(1) and C(7)-Sn-S(1) are wider and C(14)-Sn-C(21),

C(7)-Sn-C(21) and especially C(21)-Sn-S(1) are narrower than the ideal tetrahedral angle. This might suggest the description of the tin environment as *cis*-trigonal bipyramidal with S(2) and C(21) in the apical positions and S(1), C(7) and C(14) in the equatorial positions, but this bipyramid is extremely distorted: the sum of the equatorial angles is only 344° and the axial Sn-C bond lengths are very similar to the equatorial ones. Thus, the environment of tin is best described as distorted tetrahedral [116, 121].

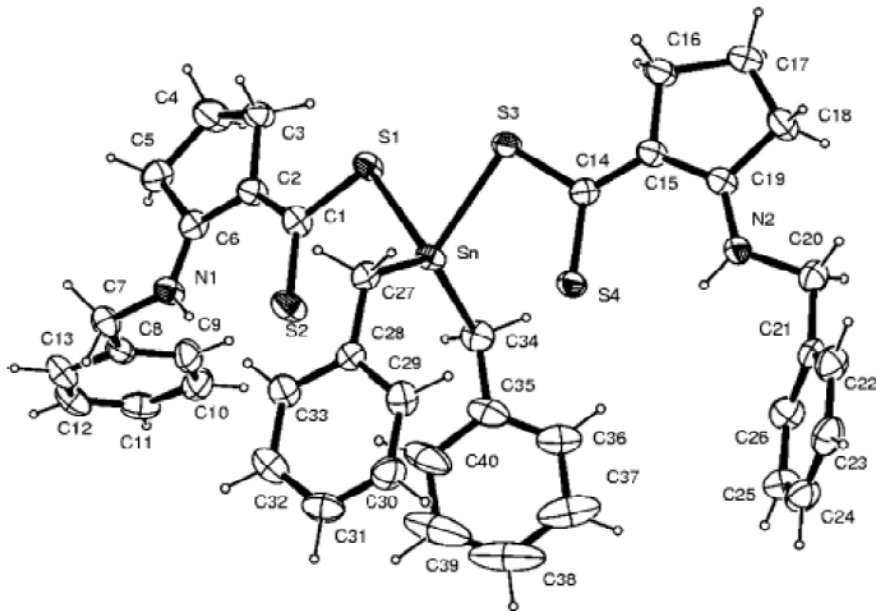


Figure 12. Crystal structure of Bz₂Sn(BzACDA)₂ (16).

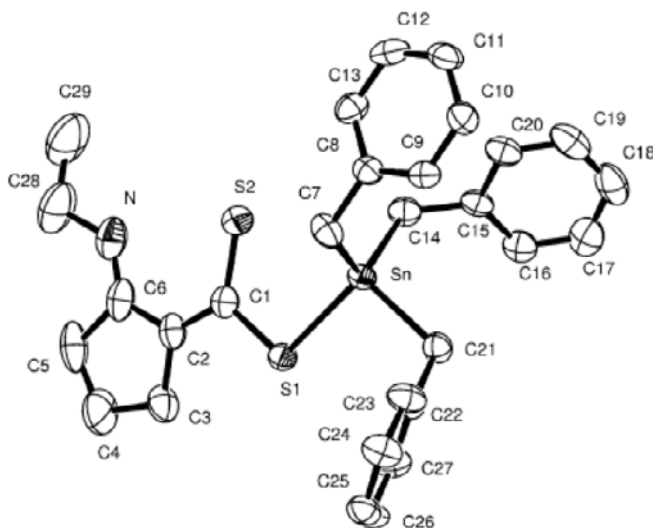


Figure 13. Crystal structure of Bz₃Sn(EtACDA) (19).

CONCLUSION

X-ray crystallographic studies of all the complexes investigated here clearly show that in solid state the Sn atom is bound asymmetrically to the dithiolate group of aminodithiocarboxylate ligands and the amine group has no participation in coordination to tin. This is in consistent with HSAB principle and with the higher stabilization of sulfur-coordinated organotin complexes in comparison with those coordinated by hard donors (nitrogen or oxygen). According to the NMR spectra data, the structure of the complexes in the solution must be similar to that of in the solid state. However the NMR data themselves do not indicate whether in solution the dithioate ligands are symmetrically or asymmetrically coordinated to tin. A combined crystallographic and theoretical study of selected organotin systems has shown [74] that in the absence of crystal packing effects, the solid state geometries uniformly converged to more symmetric structures and hence it is possible to conclude that the crystal packing influence the molecular geometry about the tin. The intramolecular hydrogen bond between NH and one of the sulfur atoms of carbodithioate moiety present in the free ligand remain in the complex both in the solid state and in the solution. In the ACDA complexes the packing is also stabilized by an intermolecular hydrogen bonding and orientation of ligand is determined by this hydrogen bond. The reasons for the adoption of diverse motifs in the solid state for many organotin systems are electronic and steric factors of the organotin entities and/or ligands. It seems that for the organotin complexes of ACDA and RACDA, the steric hindrance of alkyl on the amine group and on the tin has a little or even negligible effect and the electronic factor is more effective over the coordination pattern. The information about these complexes could lead us towards the design of sulfur-nitrogen ligands with the suitable competing reactive centers for the tin.

REFERENCES

- [1] Davies, A.G. *Organotin Chemistry*; WILEY-VCH: Weinheim, 2003; chapter 1.
- [2] Harrison, P.G. In *Chemistry of Tin*; P.J. Smith; 2nd ed.; Blackie: London, 1998; chapter 2, p. 10.
- [3] Molloy, K.C. In *Chemistry of Tin*; P.J. Smith; 2nd ed.; Blackie: London, 1998; chapter 5, p. 138.
- [4] Molloy, K. C.; Quill, K.; Nowell, I. W. *J. Organomet. Chem.* 1985, 289, 271-279
- [5] Kovala-Demertz, D.; Tauridou, P.; Russo U.; Gielen M. *Inorg. Chim. Acta*. 1995, 239, 177-183
- [6] Pellerito, C.; Nagy, L.; Pellerito, L.; Szorcsik A. *J. Organomet. Chem.* 2006, 691, 1733-1747
- [7] Evans, C.J. In *Chemistry of Tin*; P.J. Smith; 2nd ed.; Blackie: London, 1998; chapter 12, p. 442.
- [8] McManus, J.; Cunningham, D.; Hynes, M. *J. J. Organomet. Chem.* 1994, 468, 87-92.
- [9] Carcelli, M.; Pelizzi, C.; Pelizzi, G.; Mazza, P.; Zani, F.; *J. Organomet. Chem.* 1995, 488, 55-61.
- [10] Tabassum, S.; Pettinari, C. *J. Organomet. Chem.* 2006, 691, 1761-1766.
- [11] Ruarola, F.; Camalli, M.; Caruso, F. *Inorg. Chim. Acta*. 1987, 126, 1-6.

- [12] Saxena, A. K.; Huber, F. *Coord. Chem. Rev.* 1989, 95, 109-123.
- [13] Huber, F.; Roge, G.; Carl, L.; Atassi, G.; Spreafico, F.; Filippes Chi, S.; Barbieri, R.; Silvestri, A.; Rivarola, E.; Di Bianaca, F.; Alnozo, G. *J. Chem. Soc. Dalton Trans.*, 1985, 523.
- [14] Arakawa Y., In *Chemistry of Tin*; P.J. Smith; 2nd ed.; Blackie: London, 1998; chapter 10, p. 388.
- [15] Jousseau, B.; Pereyre, M. In *Chemistry of Tin*; P.J. Smith; 2nd ed.; Blackie: London, 1998; chapter 9, p. 290.
- [16] Komiya, S. *Synthesis of Organometallic Compounds*, Willy, 1997, chapter 17
- [17] Neumann, W. P. *J. Organomet. Chem.* 1992, 437, 23-39.
- [18] Hernán, A. G.; Horton, P.N.; Hursthouse, M. B. ; Kilburn, J. D. *J. Organomet. Chem.* 2006, 691, 1466-1475.
- [19] Prieto, O.; Woodward, S. *J. Organomet. Chem.* 2006, 691, 1515-1519.
- [20] Smith, P.J. *Chemistry of Tin*, 2nd ed, Blackie: London, 1998, chapter 11, p. 429.
- [21] Wardell, J.L. In *Chemistry of Tin*; Smith, P.J.; 2nd ed.; Blackie: London, 1998; chapter 4, p. 95.
- [22] Davies, A.G. *Organotin Chemistry*; WILEY-VCH: Weinheim, 2003; chapter 11, p. 166.
- [23] Armitage, D. A.; Tarassoli, A. *Inorg. Nucl. Chem. Letters*, 1973, 9, 1225-1227
- [24] Armitage, D. A.; Tarassoli, A. *Inorg. Chem.* 1975, 14, 1210-1211
- [25] Davies, A.G.; Smith, P.J. In *Comprehensive Organometallic Chemistry*; Wilkinson, G.; Stone, F.G.A.; Abel, E.W.; Pergamon: Oxford, 1982. p. 159.
- [26] Robert, K.I.; Sanders, D.R.; Henry, G.; *Chem. Rev.*, 1960, 60, 459-539
- [27] Massey, A.G. *Main Group Chemistry*, Ellis Horwood: London, 1990.
- [28] Tarassoli, A. Ph. D Thesis (under supervision of Armitage, D. A.), London University, England (1975)
- [29] Sedaghat, T. Ph. D Thesis (under supervision of Tarassoli A.) Shahid Chamran University, Iran (2000)
- [30] Asadi, A. Ph. D Thesis (under supervision of Tarassoli A.) Shahid Chamran University, Iran (2001)
- [31] Sedaghat, T.; Goodarzi, K. *Main Group Chemistry*. 2005, 4, 121–126.
- [32] Tarassoli, A.; Khodamoradpur, Z; *Phosphorus, Sulfur and Silicon*. 2005, 180, 527-532.
- [33] Tarassoli, A.; Sedaghat, T. *Inorg. Chem. Commun.* 2 (1999) 595–598.
- [34] Sedaghat, T.; Menati, S. *Inorg. Chem. Commun.* 7 (2004) 760–762.
- [35] Davies, A.G. *Organotin Chemistry*; WILEY-VCH: Weinheim, 2003; chapter 2.
- [36] Smith, P. J.; Smith, L. A. P. *Inorg. Chim. Acta Rev.* 1973, 7, 11-33.
- [37] Clark, H. C.; Jain, V. K ; Mehrotra, R. C.; Singh, B. P. ; Srivastava, G. ; Birchall, T. J. *Organomet. Chem.* 1985, 279, 385-394.
- [38] Dakternieks, D.; Rolls, C. L.; *Inorg. Chim. Acta*. 1989, 161, 105-111.
- [39] McManus, J.; Cunningham D.; Hynes, M. *J. J. Organomet. Chem.* 1994, 468, 87-92.
- [40] Otera, J. *J. Organomet. Chem.* 1981, 221, 57-61.
- [41] Otera, J.; Kusaba, A.; Hinoishi, T.; Kawasaki, Y. *J. Organomet. Chem.* 1982, 228, 223-228.
- [42] Colton, R. ; Dakternieks, D. *Inorg. Chim. Acta.*, 1988, 148, 31-36.
- [43] Martins, J.C.; Biesemans, M.; Willem, R. *Progress in Nuclear Magnetic Resonance Spectroscopy*. 2000, 36, 271–322.

- [44] Kuemmerlen, J.; Sebald, A. *J. Am. Chem. Soc.* 1993, 115, 1134-1142.
- [45] Lappert, M. F.; Misra, M.; Onyszchuk, M.; Rowe, R. S.; Power, P. P.; Slade, M. J. *J. Organomet. Chem.* 1987, 330, 31-46.
- [46] Mitchell, T.N. In *Chemistry of Tin*; P.J. Smith; 2nd ed.; Blackie: London, 1998; chapter 13, p. 480.
- [47] Barbieri R., Huber F., Pellerito L. Ruisi G. Silvestri A. In *Chemistry of Tin*; P.J. Smith; 2nd ed.; Blackie: London, 1998; chapter 14, p. 496.
- [48] R. Barbieri and A. Silvestri, *J. Chem. Soc. Dalton Trans.*, 1984, 1019-1026.
- [49] Camalli, M.; Caruso, D.; Mattogno G.; Rivarola, E. *Inorg. Chim. Acta.* 1990, 170, 225-231.
- [50] Tudela, D.; Maira, A. J.; Cunningham, D.; Timminus, B. *Inorg. Chim. Acta.*, 1995, 232, 195-197.
- [51] Gupta, S.P. *Chem. Rev.* 1994, 94, 1507-1551.
- [52] Nath, M.; Pokharia, S.; Ydav, R. *Coord. Chem. Rev.* 2001, 215, 99-149.
- [53] Pellerito, L.; Nagy, L. *Coord. Chem. Rev.*, 2002, 224, 111-150.
- [54] Chandrasekhar, V.; Nagendran, S.; Baskar, V. *Coord. Chem. Rev.* 2001, 235, 1-52.
- [55] Song, X.; Zapata A.; Eng, G. *J. Organomet. Chem.* 2006, 691, 1756-1760.
- [56] Davies, A.G. *Organotin Chemistry*; WILEY-VCH: Weinheim, 2003; chapter 17.
- [57] Raper, E.S. *Coord. Chem. Rev.* 1996, 153, 199-255.
- [58] Raper, E.S. *Coord. Chem. Rev.* 1997, 165, 475-567.
- [59] Dance, I.G. *Polyhedron* 1986, 5 , 1037-1104.
- [60] E. Block, G. Ofori-Okai, J. Zubietta, *J. Am. Chem. Soc.* 111 (1989) 2327-2329.
- [61] Buck-Koehntop, B. A.; Porcelli, F.; Lewin, J. L.; Cramer, C. J.; Veglia, G. *J. Organomet. Chem.* 2006, 691, 1748-1755.
- [62] Pérez-Lourido, P.; Romero, J.; García-Vázquez, J.A.; Sousa, A.; Zubietta, J.; Russo, U. *J. Organomet. Chem.* 2000, 595, 59-65.
- [63] Hager, C. D.; Huber, F.; Silvestri, A.; Barbieri, R. *Inorg. Chim. Acta.* 1981, 49, 31-36.
- [64] Cea-Olivares, R.; Gomez-Ortiz, L. A.; Garcia-Montalvo, V.; Gavino-Ramirez, R. L.; Hernandez-Ortega, S. *Inorg. Chem.* 2000, 39, 2284-2288.
- [65] Gómez-Ortiz, L. A.; Cea-Olivares, R.; García-Montalvo, V.; Hernández-Ortega, S. *J. Organomet. Chem..* 2002, 654, 51-55.
- [66] Bates, P. A.; Hursthouse, M. B.; Davies, A. G.; Slater, S. D.; *J. Organomet. Chem.* 1989, 363, 45-60.
- [67] Dakternieks, D.; Zhu, H. ; Masi, D.; Mealli, C. *Inorg. Chem.* 1992, 31, 3601-3606.
- [68] Molloy, K. C.; Hossain, M. B.; van der Helm, D.; Zuckerman, J. J.; Haiduc, I. *Inorg. Chem.* 1979, 18, 3507-3511.
- [69] Dakternieks, D.; Hoskins, B. F.; Jackson.P. A.; Tiekkink,E. R.T.; Winter, G. *Inorg. Chim. Acta.* 1985, 101, 203-206.
- [70] Molloy, K. C.; Hossain, M. B.; van der Helm, D.; Zuckerman, J. J.; Mullins, F. P. *Inorg. Chem.* 1981, 20, 2172-2177.
- [71] Dakternieks, D.; Hoskins, B. F.; Tiekkink, E. R. T.; Winter, G. *Inorg. Chim. Acta.* 1984, 85, 215-218.
- [72] Molloy, K. C.; Hossain, M. B.; van der Helm, D.; Zuckerman, J. J.; Haiduc, I. *Inorg. Chem.* 1980, 19, 2041-2045.
- [73] Mohamed-Ibrahim, M. I.; Chee, S. S. *Organometallics.* 2000, 19, 5410-5415.

- [74] Buntine, M. A.; Hall, V. J.; Kosovel, F. J.; Tiekink, E. R. T. *J. Phys. Chem. A* 1998, 102, 2472-2485.
- [75] Burda, J. V.; Sponer, J.; Hobza, P. *J. Phys. Chem.* 1996, 100, 7250-7255.
- [76] Jiang, S.; Dasgupta, S.; Blanco, M.; Frazier, R.; Yamaguchi, E. S.; Tang, Y.; Goddard, W. A. *J. Phys. Chem.* 1996, 100, 15760-15769.
- [77] Stewart, G. M.; Tiekink, E. R. T.; Buntine, M. A. *J. Phys. Chem. A* 1997, 101, 5368-5373.
- [78] Otera, J.; Hinoishi, T.; Okaware, R. *J. Organomet. Chem.* 1980, 202, C93-C94.
- [79] Holecek, J.; Nadvornik, M.; Handler, K.; Lycka,A. *J. Organomet. Chem.* 1983, 241, 177-184.
- [80] Nag, K.; Joardar, D. S. *Inorg. Chim. Acta.*, 1975, 14, 133-141.
- [81] Baid, D. M. *J. Chem. Edu.*, 1985, 621, 168-169.
- [82] Takeshima, T.; Yokoyama, M.; Imamoto, T.; Akano, M.; Asaba, H. *J. Org. Chem.* 1969, 34, 730-732.
- [83] Bordas, B.; Shohar, P.; Matolcsy, G.; Berencsi, P. *J. Org. Chem.* 1972, 37, 1727-1730.
- [84] Nag, K.; Joardar, D. S. *Can. J. Chem.* 1976, 54, 2827-2831.
- [85] Tarassoli, A.; Asadi, A.; Hitchcock, P. B. *J. Organomet. Chem.* 2002, 645, 105-111
- [86] Singh, S. K.; Singh, Y.; Rai, A. K.; Mehrotra, R. C. *Polyhedron.* 1989, 8, 633-639.
- [87] Bereman, R. D.; Dorfman, J. R. *Polyhedron.* 1983, 2, 1013-1017.
- [88] Martin, E. M.; Bereman, R. D. *Inorg. Chim. Acta.* 1991, 188, 221-231.
- [89] Burman, S.; Sathyanarayana, D. N. *J. Coord. Chem.* 1983, 13 , 51-55.
- [90] Martin, E. M.; Bereman, R.D. *Inorg. Chim. Acta.* 1991, 188, 233-242.
- [91] Kumar, S. B.; Chaudhury, M. J. *Chem. Soc. Dalton Trans.* 1992, 3439-3443.
- [92] Singh, B.; Gupta, V. D. *J. Ind. Chem. Soc.* 1982, 59, 793-795.
- [93] Singh, B.; Gupta, V. D. *Ind. J. Chem.* 1981, 20A, 526-528.
- [94] Sharma, R. K.; Singh, Y.; Rai, A. K. *Phosphorus, Sulfur and Silicon.* 2000, 166, 221-230.
- [95] Casas, J.S.; Castellano, E. E.; Barros, F. J. G.; Sanchez, A.; Gonzalez, A. S.; Sordo, J.; Schpector, J. Z. *J. Organomet. Chem.* 1996, 519, 209-216.
- [96] Demertizi, D. K.; Tauridou, P.; Russo, U.; Gielen, M. *Inorg. Chim. Acta.* 1995, 239, 177-183.
- [97] Valle, G.; Ettorre, R.; Peruzzo, V.; Plazzogna, G. *J. Organomet. Chem.* 1987, 326, 169-172.
- [98] Casellato, U.; Graziani, R.; Peruzzo, V.; Plazzogna, G. *J. Organomet. Chem.* 1995, 486, 105-107.
- [99] Tarassoli, A.; Sedaghat, T.; Neumüller, B.; Ghassemzadeh, M. *Inorg. Chim. Acta.* 2001, 318, 15-22.
- [100] Tarassoli, A.; Asadi, A.; Hitchcock, P. B. *J. Organomet. Chem.* 2006, 691, 1631-1636.
- [101] Barroso-Flores, J.; Cea-Olivares, R.; Toscano, R. A.; Cogordan, J.A. *J. Organomet. Chem.* 2004, 689, 2096-2102.
- [102] Tarassoli, A.; Sedaghat, T.; Helm, M.; Norman, A. D. *J. Coord. Chem.* 2003, 56, 1179-1189.
- [103] Kumar Das, V. G.; Keong, Y. C.; Smith, P. J.; *J. Organomet. Chem.* 1987, 327, 311-326.
- [104] Martinez, E. G.; Gonzalez, A. S.; Casas, J. S.; Sordo, J.; Casellato, U.; Graziani, R.; Russo, U. *J. Organomet. Chem.* 1993, 463, 91-96.

- [105] Thormas, P. L.; Manders, W. F.; Schlemper, E. O. *J. Am. Chem. Soc.* 1985, 107, 7451-7453.
- [106] Kim, K.; Ibers, J. A.; Jung, O. S.; Sohn, Y. S. *Acta Cryst.* 1987, C43, 2317-2319.
- [107] Harrison, P. G.; Mangia, A. *J. Organomet. Chem.* 1976, 120, 211-216.
- [108] Dakternieks, D.; Zhu, H.; Masi, D.; Mealli, C. *Inorg. Chim. Acta.* 1993, 211, 155-160.
- [109] Furue, K.; Kimura, T.; Yasuoka, N.; Kasai, N.; Masao, K. *Bull. Chem. Soc. Jpn.* 1970, 43, 1661-1667.
- [110] Wei, C.; Kumar Das, V. G.; Sinn, E. *Inorg. Chim. Acta.* 1985, 100, 245-249.
- [111] Othman, A. H.; Fun, H. K.; Yamin, B. M. *Acta Cryst.* 1997, C53, 1228-1230.
- [112] Allen, F. H.; Kennard, O.; Watson, D. G.; Brammer, L.; Orpen, A. G.; Taylor, R. *J. Chem. Soc. Perkin Trans. II.* 1987, S1-S19.
- [113] Vrabel, V.; Lokay, J.; Kello, E.; Rattay, V. *Acta Cryst.* 1992, C48, 627-629.
- [114] Vrabel, V.; Lokay, J.; Kello, E.; Garaj, J. *Acta Cryst.* 1992, C48, 633-635.
- [115] James, B. D.; Magee, R. J.; Patalinghug, W. C.; Skelton, B. W.; White, A. H. *J. Organomet. Chem.* 1994, 467, 51-55.
- [116] Casas, J. S.; Castinrriras, A.; Martinez, E. G.; S. Gonzalez, A.; Sanchez, A.; Sordo, J. *Polyhedron.* 1997, 16, 795-800.
- [117] Casas, J. S.; Castineiras, A.; Couse, M. D.; Playa, N.; Russo, U.; Sanchez, A.; Sordo, J.; Varela, J. M. *J. Chem. Soc. Dalton Trans.* 1998, 1513-1521.
- [118] Ueyama, N.; Nishikawa, N.; Yamada, Y.; Okamura, T.; Oka, S.; Sakurai, H.; Nakamura, A. *Inorg. Chem.* 1998, 37, 2415-2421.
- [119] Kimura, T., Yasuoka, N.; Kasai, N.; Kakudo, M. *Bull. Chem. Soc. Jpn.* 1972, 45, 1649-1654.
- [120] Kepert, D. L. *J. Organomet. Chem.* 1976, 107, 49-54.
- [121] Chandra, S.; James, B. D.; Magee, R. J.; Patalinghug, W. C.; Skelton, B. W.; White, A. H. *J. Organomet. Chem.* 1988, 346, 7-12.

Chapter 8

ORGANOMETALLIC COMPLEXES OF RHODIUM(I), IRIDIUM(I) AND RUTHENIUM(II) CONTAINING HEMILABILE FUNCTIONALIZED PHOSPHINE- CHALCOGEN DONOR LIGANDS : SYNTHESIS, REACTIVITIES AND APPLICATIONS

Dipak Kumar Dutta*

Material Science Division, Regional Research Laboratory (CSIR);
Jorhat 785 006, Assam, INDIA

ABSTRACT

Organometallic complexes of rhodium, iridium and ruthenium have gained much importance because of their novelty, reactivity and applications in diverse fields. Some important examples of applications of such metal complexes as commercial homogeneous catalysts are : *L-DOPA* synthesis(Rhodium(I)-chiral catalyst); Monsanto / B. P. Chemicals process for carbonylation of methanol to acetic acid (Rhodium(I) catalyst) and the process called '*Cativa*' (Iridium(I) catalyst with Ru-complex activator). Neutral and cationic rhodium(I), iridium(I) and ruthenium(II) complexes of functionalized phosphine-chalcogen donors P-X (X = O, S, Se) ligands are of much interest in recent time because of expected novel structures and stereo-chemical control in catalytic applications in various important organic synthesis. Different types of P-X ligands like $R_2P-(CH_2)_n-COOX'$, X' = H / alkyl, n = 1-3; $R_2P-(CH_2)_nXR$, R = alkyl/aryl; $Ph_2PC_6H_4COOMe$; mono-, di- and tri-chalcogen functionalized poly-phosphines such as $Ph_2P(CH_2)_nP(X)Ph_2$, (n = 1-4), $MeC(CH_2PPh_2)_2(CH_2P(X)Ph_2)$ and other ligands CO, COD (1,5-cyclooctadiene) etc. form interesting metal complexes. Rhodium(I) carbonyl complexes containing bidentate chelating ligand such as diphenylphosphinomethane oxide / sulphide / selenide have shown interesting structural features. The chelated complex of the type $[Rh(CO)Cl(2-Ph_2PC_6H_4COOMe)]$ has been synthesized and the X-ray structure indicates a long range intramolecular 'Secondary' Rh...O interactions (Rh – O distance 3.18 Å). The effect of chain length of the bifunctional i.e. 'Soft and Hard'

* Dipak Kumar Dutta: Fax : +91-376-2370011; Ph. +91-376-2370081; Email : dipakkrdutta@yahoo.com

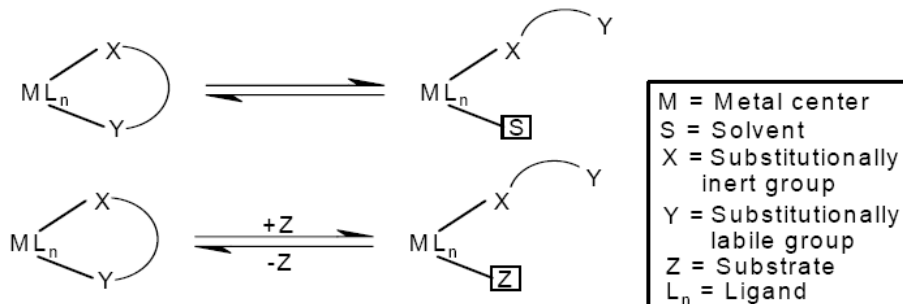
donors chelating ligands of tertiary phosphines with functional carboxylic acid or ester, or unequal softness of the chelating donors i.e. tertiary phosphines functionalised with sulfur or selenium donors having aliphatic and aromatic backbones on the '*Hemilability*' of the metal - O / S / Se bonds are discussed. In chelate metal complexes containing hemilabile ligands like P-X, the labile M-X bonds cleave and provide a vacant potential coordination site for reversible binding of substrates to metal centre by dynamic chelating ability i.e. by '*Opening and Closing*' mechanism. The steric effect, electronic effect and kinetics of oxidative addition (OA) reactions of the complexes with different electrophiles like CH₃I, C₂H₅I, C₆H₅CH₂Cl etc. are discussed. The activation of small molecules like CO, CH₃I, I₂, etc. by the metal complexes and evaluation as catalysts precursors for carbonylation of alcohol are also discussed. The catalytic activities of suitable metal complexes are reported for carbonylation, hydrogenation and hydroformylation of important substrates for potential industrial organic compounds. The metal complexes of types [Rh(CO)₂Cl(P~O)] and [Rh(CO)Cl(P~O)₂]; show high catalytic carbonylation reactions of methanol to acetic acid / ester with high Turn Over Number(TON) of about 1500. The metal complexes and the products were characterized mainly by Infrared, UV-Visible spectroscopy, NMR studies, X-ray crystallography and GCMS technique.

INTRODUCTION

Platinum metal complexes of unsymmetrical chelating ligands such as functionalized phosphines have aroused much interest in recent time because of their structural novelty, reactivity and catalytic applications [1-14] such as hydrogenation, carbonylation and hydroformylation reactions. Homogeneous catalysis by transition metal complexes has become a major synthetic tool in industrial processes [8]. The potential of such catalytic reactions are due to the fact that most of these reactions are low energy processes. One of such metal-complex systems is rhodium(I)-complexes which play a big role as industrial homogeneous catalysts. The catalytic reactions span a wide range of complexes such as from syntheses of fine chemicals like that of *L-DOPA* (a drug for curing Parkinson's diseases) by an asymmetric hydrogenation of prochiral substrates with rhodium(I)-complexes containing optically active ligands [15] to syntheses of bulk chemicals like carbonylation of methanol for producing acetic acid by *Monsanto's* process [16-18] where [Rh(CO)₂I₂]⁻ is the active catalytic species (presently owned by B.P. Chemicals, UK). Recently, a new industrial catalytic process called "*Cativa*" has been introduced [19,20] involving iridium complexes with ruthenium-complex activator for carbonylation of methanol where high efficacy was reported.

Tertiary phosphines functionalized with chalcogen donors like oxygen [9, 21-25], sulfur [26-30] and selenium [31,32] containing "Soft" phosphorus and "Hard" oxygen donors or "Soft" phosphorus and relatively less "Softer" sulfur and selenium donor ligands with distinctly different π -acceptor strength [9] form a variety of metal complexes due to their different bonding abilities. Oxygen being "Hard" donor is capable of stabilizing metal ions in higher oxydation state which can be ascribed as due to absence of d π -back bonding. On the other hand, "Soft" phosphorus donors stabilize metal ion in low oxidation state by d π -p π -back bonding. The metal-oxygen bond is weak and may dissociate reversibly to generate a vacant site for substrate binding and such ligands are called "Hemilabile". When P-S and P-Se donors ligands are chelated, the M-S/Se bonds are comparatively labile than the M-P bonds

and thus may permit facile generation of a "Vacant site" at the metal centre [9,33,34] and may show interesting dynamic stereo-chemistry. Such types of creation of vacant coordination site through a reversible "Opening and Closing" mechanism [34] is useful for coordination and activation of the small molecules for further reaction with other organic substrates (Scheme 1).

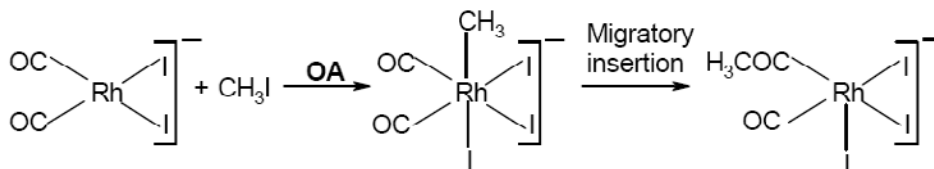


Scheme 1. Opening-closing mechanism of hemilabile ligands.

OXIDATIVE ADDITION REACTIONS

Oxidative addition (OA) reactions of transition metal complexes, particularly rhodium(I) and iridium(I) with small molecules, being the key step in many catalytic transformation reactions such as carbonylation, hydrogenation and hydroformylation have gained much attention [19,35-39]. Rhodium(I) complexes (low spin d^8 -ions) undergo two electrons OA reaction with small molecules like H_2 , X_2 , ICl , CH_3I , C_2H_5I etc. producing six coordinated rhodium(III) species (d^6 -ions). In many cases, the OA reactions may be reversible and this reversibility between rhodium(I) and rhodium(III) is responsible for many of the catalytic organic transformation [9,40]. It is well known that the Rh^I-Rh^{III} couple stabilized by phosphates play an important role in homogeneous catalysis [40]. Activation of substrates by transition metal complexes has become most important for both stoichiometric and catalytic reactions. The complexation of substrates by transition metal complexes represent an important step in the course of catalytic processes. OA reactions are of much importance because they involve scission of comparatively inert substrate bonds and thus enable further reactions. The tendency of a metal complex to undergo OA reactions increases with increase in basicity of the metal centre [1,3]. Thus, a low oxidation state in which the metal centre is electron rich is favoured and ligands that increase the electron density of the metal centre will enhance the reactivity. It is anticipated that a direct interaction of a σ -donor ligand would significantly increase the electron density at the metal atom and consequently lowers the activation barrier of an OA reaction. Rhodium complexes are generally found to activate hydrogen by dihydride formation, the metal must be in a low oxidation state that can readily increased by two units, site of unsaturation must be available and the basicity of the complex must be high enough to ensure that the metal centre is reactive towards hydrogen. Wilkinson's complex, $[RhCl(PPh_3)_3]$ is one of the famous example of the transition metal hydrogenation catalysts. One PPh_3 ligand in this complex can be replaced by CO group to form $[Rh(CO)Cl(PPh_3)_2]$ which, although closely related to $[RhCl(PPh_3)_3]$, does not form

rhodium(III) dihydride complex. Replacement of a PPh_3 by CO group (a stronger π -acceptor) lowers the basicity of the metal centre considerably to prevent it from undergoing OA reactions under moderate condition. It is worth to mention here that by changing the halide in the rhodium complexes, the activity and selectivity can be affected remarkably for e.g. $[\text{RhBr}(\text{PPh}_3)_3]$ and $[\text{RhI}(\text{PPh}_3)_3]$ show higher catalytic activity in hydrogenation of terminal alkene than $[\text{RhCl}(\text{PPh}_3)_3]$ [41]. The OA reactions of alkyl or aryl halides to various types of rhodium(I) carbonyl complexes had been widely studied and it followed a migratory insertion pathways where a methyl group is migrated to coordinated carbonyl group to form acyl complex. In these studies the formation of rhodium acyl species have been established from the observation of new characteristic carbonyl stretching band at around 1700 cm^{-1} [42-44]. For instance, OA reaction of $[\text{Rh}(\text{CO})_2\text{I}_2]^-$ with CH_3I gave a five-coordinated rhodium(III) acyl complex $[\text{Rh}(\text{COCH}_3)\text{COI}_3]^-$ which exhibits a terminal $\nu(\text{CO})$ band at 2061 cm^{-1} and an acyl $\nu(\text{CO})$ band at 1740 cm^{-1} . It was proposed that the reaction was proceeded via an unstable six-coordinated rhodium(III) intermediate $[\text{Rh}(\text{CO})_2\text{CH}_3\text{I}_3]^-$ (Scheme 2) which on alkyl group migration produced the acyl complex.



Scheme 2. OA reaction of $[\text{Rh}(\text{CO})_2\text{I}_2]^-$ with CH_3I .

The OA reaction of alkyl halide to the metal centre is the key rate determining step in the metal complex catalyzed carbonylation of alcohol [45,46]. The oxidative reactivity of the metal complexes depends on the nucleophilicity of the metal center, which in turn depends upon the steric and electronic characteristics of the ligand. Kinetic study of the OA reaction of CH_3I with the complexes $[\text{Rh}(\text{CO})_2\text{ClL}]$ (L = ligands) and the course of the reaction was monitored by IR spectroscopy.

Recently, Cole-Hamilton et. al. [47] have investigated the use of trialkyl-phosphines as strongly electron donating ligand in rhodium complexes such as $[\text{Rh}(\text{PEt}_3)_2(\text{CO})\text{X}]$ ($\text{X} = \text{Cl}, \text{Br}$ or I) exhibiting $\nu(\text{CO})$ at 1960 cm^{-1} indicating more electron rich than that of $[\text{Rh}(\text{CO})_2\text{I}_2]^-$ where $\nu(\text{CO})$ are at 1988 and 2059 cm^{-1} . The complex $[\text{Rh}(\text{PEt}_3)_2(\text{CO})\text{I}]$ undergoes OA with MeI to form $[\text{RhMeI}_2(\text{CO})(\text{PEt}_3)_2]$ exhibiting iodide and methyl trans to each other (X-ray structure: Figure 1). The complex $[\text{Rh}(\text{PEt}_3)_2(\text{CO})\text{I}]$ exhibits high catalytic activity in converting methanol to acetic acid under the experimental conditions $120 - 150^\circ\text{C}$ and 27 bar pressure.

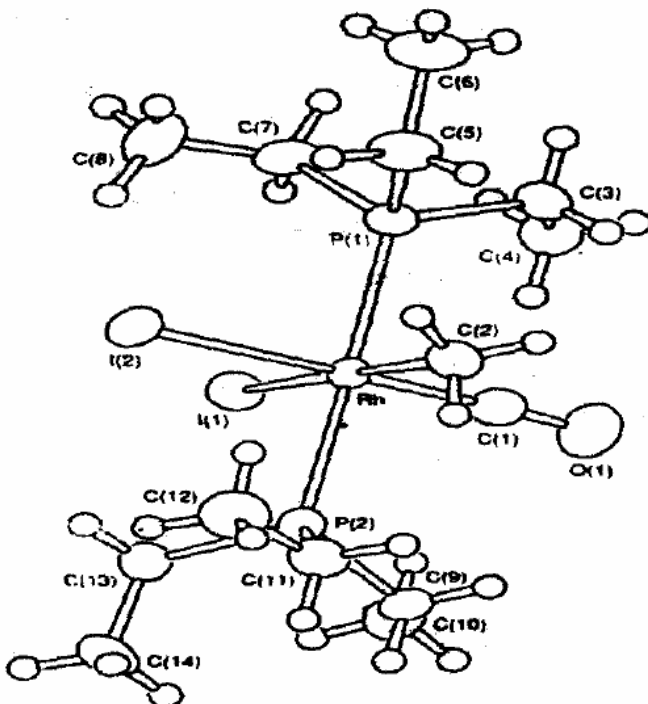
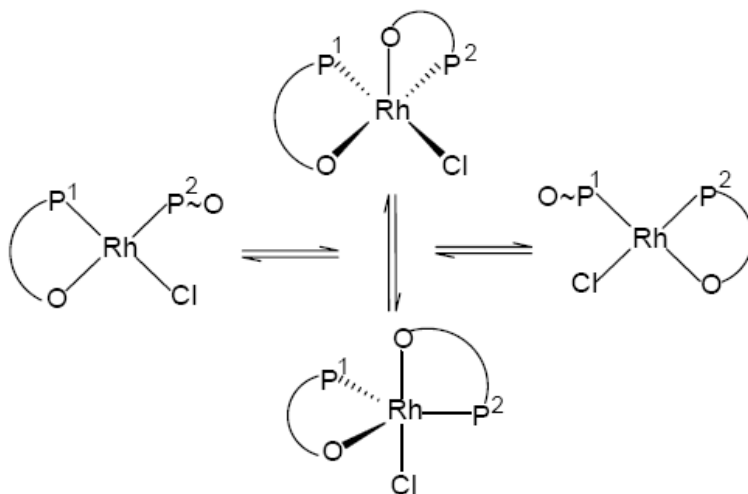


Figure 1. X-ray structure of $[\text{RhMeI}_2(\text{CO})(\text{PPh}_3)_2]$ [J. Rankin, A. D. Poole, A. C. Benyei and D. J. Cole - Hamilton, J. Chem. Soc., Chem. Commun., 1997, 1835] – Reproduced by permission of The Royal Society of Chemistry.

Few complexes containing mixed donor ligands which promote carbonylation under mild reaction condition have been reported [25,29,30a,48,49]. The complex, $[\text{RhCl}(\text{CO})_2(\text{Ph}_2\text{PCH}_2\text{CH}_2\text{P}(\text{O})\text{Ph}_2)]$ [25] acts as active catalytic species during carbonylation of methanol and shows a turnover frequencies approaching 400 h^{-1} at 80°C and 50 psig of CO. Rhodium(I) forms a complex of the type $[\text{Rh}(\text{CO})_2\text{Cl}(\text{Ph}_2\text{PCH}_2\text{P}(\text{S})\text{Ph}_2)]$ which shows [29,30a] about 8 times more catalytic activity in carbonylation of methanol than the famous industrial species $[\text{Rh}(\text{CO})_2\text{I}_2]$. This higher catalytic efficiency is attributed to more electron rich species than the $[\text{Rh}(\text{CO})_2\text{I}_2]$. Rhodium(I) forms complexes of the type $[\text{RhCl}(\text{CO})(\text{Ph}_2\text{PCH}_2\text{SPh})]$. When the P and S are coordinated to the metal, the M-S bond is expected to be more labile than the M-P, permitting facile generation of a vacant site at the metal centre. Rhodium(I) also forms compounds by the reaction of $[\text{Rh}(\text{CO})_2\text{Cl}]_2$ with 2-(diphenyl-phosphino)benzenethiol and 2-(diphenylphosphino)ethanethiol in presence of base. Similarly, rhodium(I) forms monomer complex by the reaction of $[\text{Rh}(\text{CO})_2\text{Cl}]_2$ with diphenyl(2-methylthiophenyl)phosphine in appropriate mol ratio. The rhodium(I) carbonyl complexes containing phosphino-thiolate and thioether ligands are almost four times active compared to the species $[\text{Rh}(\text{CO})_2\text{I}_2]$ in catalyzing the carbonylation of methanol [30a]. The Rh(I) complex $[\text{Rh}(\text{CO})\text{I}(\text{dppms})]$ where dppms = $\text{Ph}_2\text{PCH}_2\text{P}(\text{S})\text{Ph}_2$ has been reported [29] to show some dynamic steric effect on the rate of migratory CO insertion in catalytic carbonylation of methanol. The ligand in such complex is able to promote both OA and migratory insertion reaction.

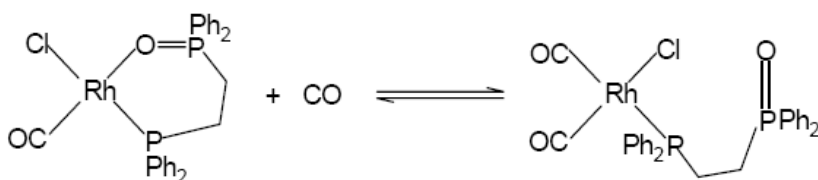
FLUXIONAL AND HEMILABILE BEHAVIOR

Neutral monochelate complex $[\text{RhCl}(\text{P}\sim\text{O})(\text{P}\cap\text{O})]$ ($\text{P}\sim\text{O} = \eta^1\text{-}(\text{P})$ coordinated $\text{Cy}_2\text{PCH}_2\text{CH}_2\text{OCH}_3$; $\text{P}\cap\text{O} = \eta^2\text{-}(\text{O},\text{P})$ chelated) was reported by Lindner et al. [9] and the complex exhibits fluxional behavior as demonstrated by variable temperature $^{31}\text{P}\{\text{H}\}$ NMR spectroscopy. The observed dynamic phenomena are reversible and proceed with an associative mechanism involving a five-coordinated species as shown below (Scheme 3) :



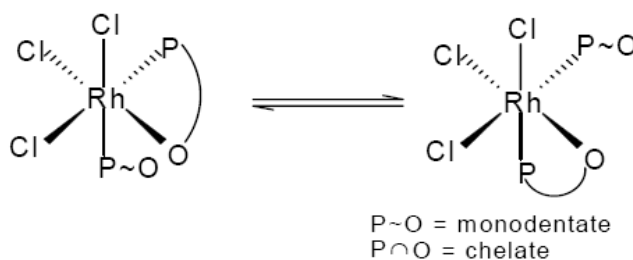
Scheme 3: Fluxional behaviour of $[\text{Rh}(\text{Cy}_2\text{PCH}_2\text{CH}_2\text{OMe})(\text{Cy}_2\text{PCH}_2\text{CH}_2\text{OMe})\text{Cl}]$

The dimeric complex $[\text{Rh}(\text{CO})_2\text{Cl}]_2$ reacts with $\text{Ph}_2\text{P}(\text{CH}_2)\text{P}(\text{O})\text{Ph}_2$ to form a monocarbonyl complex $[\text{Rh}(\text{CO})\text{Cl}(\text{P}\cap\text{O})]$ [25]. The formation of Rh-O chelate bond is indicated by the shifting of $\nu(\text{P}=\text{O})$ stretching band towards lower wave number. The five membered ring, according to Bayer's strain theory is more stable than six member one and therefore, the five member ring complex $[\text{Rh}(\text{CO})\text{Cl}(\text{Ph}_2\text{PCH}_2\text{P}(\text{O})\text{Ph}_2)]$ does not react with CO under low pressure, though at high pressure trace amount of *cis*- $[\text{Rh}(\text{CO})_2\text{Cl}(\text{Ph}_2\text{PCH}_2\text{P}(\text{O})\text{Ph}_2)]$ has been formed. On the other hand, the six member chelate ring in complex $[\text{Rh}(\text{CO})\text{Cl}(\text{Ph}_2\text{PCH}_2\text{CH}_2\text{P}(\text{O})\text{Ph}_2)]$ can be reversibly cleaved by CO even at low pressure (1-3 bar) to give *cis*- $[\text{Rh}(\text{CO})_2\text{Cl}(\text{Ph}_2\text{PCH}_2\text{CH}_2\text{P}(\text{O})\text{Ph}_2)]$ as shown in the Scheme 4.



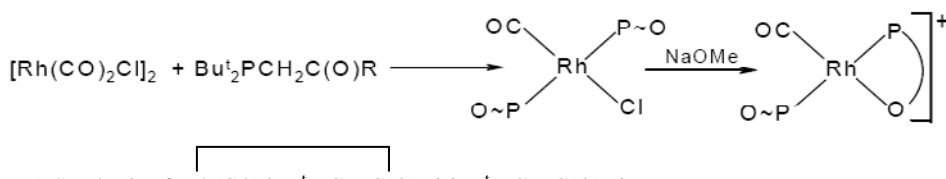
Scheme 4. Ring opening and closing mechanism [R. W. Wegman, A. G. Abatjoglou and A. M. Harrison, J. Chem. Soc., Chem. Commun. 1987, 1891] – Reproduced by permission of The Royal Society of Chemistry.

$\text{RhCl}_3 \cdot 3\text{H}_2\text{O}$ reacts with $\text{Ph}_2\text{PCH}_2\text{COOEt}$ at ambient condition to afford an orange compound *fac*- $[\text{RhCl}_3(\text{P}\sim\text{O})(\text{P}\sim\text{O})]$ [50] containing both the chelated and monodentate phosphines. Such complexes often show fluxional isomerism [9] (Scheme below) which is the most significant properties of hemilabile ligands. The ester moieties of the two vicinal ester-phosphine ligands in this compound act for a common coordination sites. And thus, the fluxionality may be regarded as an entirely reversible intramolecular mutual substitution reaction in which the donor atoms of the same kinds are involved. This is an excellent example of the “Opening and Closing” mechanism [9,40]. The fluxional behavior is monitored by low temperature $^{31}\text{P}\{\text{H}\}$ NMR spectroscopy.



Fluxional behaviour of $[\text{RhCl}_3(\text{P}\sim\text{O})(\text{P}\cap\text{O})]$

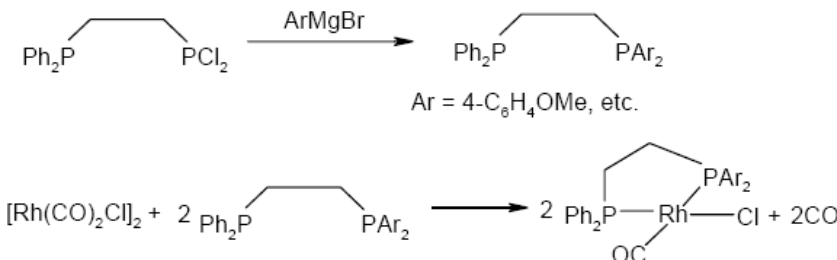
The keto-phosphine ligands, $\text{Bu}^t_2\text{PCH}_2\text{C(O)R}$ ($\text{R} = \text{Ph}, \text{Bu}^t$), react with $\text{RhCl}_3 \cdot 3\text{H}_2\text{O}$ to give a penta-coordinate Rh(III) complex $[\text{RhCl}_2(\text{P}\cap\text{O})(\text{P}\sim\text{O})]$ [51] in which the presence of both coordinated and uncoordinated $-\text{C=O}$ of keto-phosphine ligand has been indicated by two different types of ketonic $\nu(\text{CO})$ bands. The lower value of which is due to the chelated one. The keto-phosphine ligand $\text{Bu}^t_2\text{PCH}_2\text{C(O)R}$ also forms rhodium(I) complex of the type *trans*- $[\text{Rh}(\text{CO})\text{Cl}(\text{P}\sim\text{O})_2]$, [51] when ethanolic solution of $[\text{Rh}(\text{CO})_2\text{Cl}]_2$ was treated with two equivalent of the $\text{Bu}^t_2\text{PCH}_2\text{C(O)R}$ ligand. The complex *trans*- $[\text{Rh}(\text{CO})\text{Cl}(\text{P}\sim\text{O})_2]$ on subsequent reaction with NaOMe resulted corresponding chelate complex *trans*- $[\text{Rh}(\text{CO})(\text{P}\cap\text{O})(\text{P}\sim\text{O})]^+$ (Scheme 5). The ^{31}P NMR spectra of the complex *trans*- $[\text{Rh}(\text{CO})(\text{P}\cap\text{O})(\text{P}\sim\text{O})]^+$ displayed an ABX pattern for two different types of phosphorous and the *trans* disposition of the two phosphorous atoms had been reflected from large $J(\text{PP})$ values.



Scheme 5: Synthesis of $[\text{Rh}(\text{CO})\{\text{Bu}^t_2\text{PCH}_2\text{C(O)R}\}\{\text{Bu}^t_2\text{PCH}_2\text{C(O)R}\}]$.

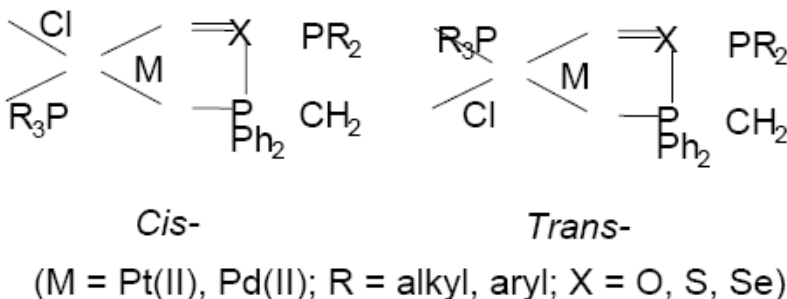
Recently, Pringle et. al. reported [52] that rhodium complexes of unsymmetrical ethylene diphosphine ligands are more efficient catalysts than the symmetrical ethylenediphosphine analogues for methanol carbonylation. The catalysts were prepared by addition of diphosphines to $[\text{Rh}(\text{CO})_2\text{Cl}]_2$ as shown below (Scheme 6). The catalysts show methanol

conversion to acetic acid greater than 98% and selectivity higher than 99%, however, the rate of reaction is lower than species $[\text{Rh}(\text{CO})_2\text{I}_2]^-$.

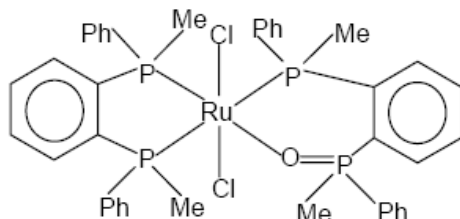


Scheme 6. Synthesis of ligands and rhodium complexes.

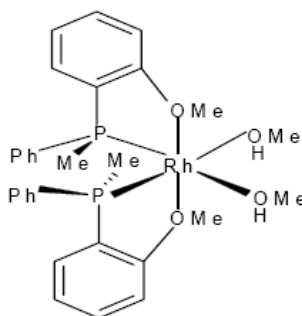
Platinum(II) and palladium(II) react with bisphosphine monochalcogenides $[\text{Ph}_2\text{PCH}_2\text{P}(\text{X})\text{R}_2]$, $\text{X} = \text{O}, \text{S}$ or Se , $\text{R} = \text{alkyl, aryl}$ to form complexes [53] of the type $[\text{MCIL}(\text{Ph}_2\text{PCH}_2\text{P}(\text{X})\text{R}_2)]$ (as shown below) where L = monodentate ligands like PR_3 . Such complexes show one strong (M-P) and another weak coordinated chelated (M-X) bonds and is likely to show interesting dynamic stereochemistry.



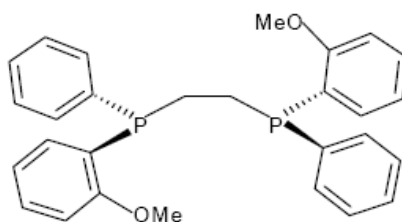
Interesting complex (shown below) is formed between diphos ligands and RuCl_3 in presence of formaldehyde [54], where the Ru-P bond trans to oxygen is considerably shorter (222 pm) than the other two Ru-P bonds and Ru-O is weak.



Brown et. al. [55] reported that $2\text{-MeOC}_6\text{H}_4\text{PPhMe}$ forms Rh(I) complexes where a weak bonding between the methoxy oxygen atom and the metal is suggested.

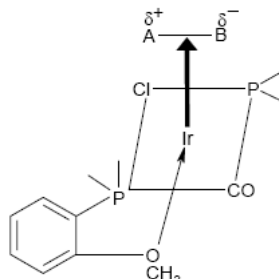


Knowles et. al. [56] and others [57] found that rhodium complexes containing ortho-methoxy substituted aryl phosphines are effective catalyst for asymmetric hydrogenation reactions. The stereoselectivity of such complexes has been attributed to the ability of the –OMe group to bind to the substrate.

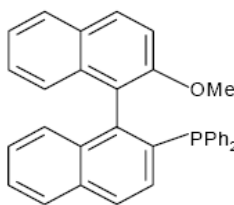


The invention of another type of ligand by Monsanto group was R,R-PPh(2-PhOCH₃)CH₂CH₂PPh(2-PhOCH₃) (DIPAM) and its use as rhodium complex in asym-mmetric hydrogenation for production of L-DOPA, has improved the yield (> 95 %).

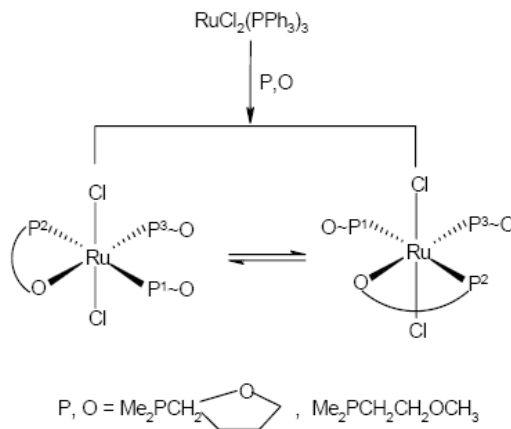
Miller and Shaw [58] have shown that in metal complex like, trans-[IrCl(CO){PMe₂(2-MeOC₆H₄)₂}], the ortho –OMe group forms directly Ir-O bond. The –OMe group by donating electron density to the metal enhances nucleophilicity and thus lowers the activation energy required for oxidation reaction. Such electron donation and activation is shown schematically as.



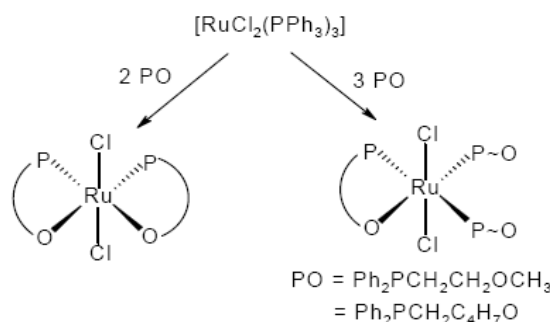
Another type of P-O ligands i.e. 2-(diphenylphosphino)-2-methoxy-1,1-binaphthyl (shown below) is reported to show good catalytic activity as palladium complex in asymmetric hydrosilylation reaction(59) in converting terminal olefin into optically active secondary alcohols (yield > 94 %)



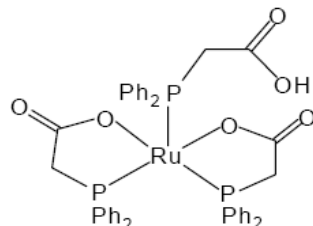
Ru(II) forms complex such as $[\text{RuCl}_2(\text{P}\cap\text{O})(\text{P}\sim\text{O})_2]$ by the reaction between $[\text{RuCl}_2(\text{PPh}_3)_3]$ and P,O ligands. The complex shows fluxional behaviour [60] as shown below –



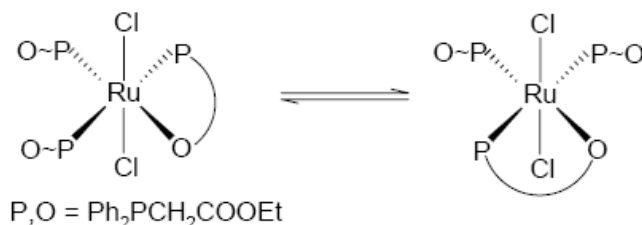
Ruthenium complexes are expected to give rise to a large number of isomeric compounds because of its coordination number i.e. six. A considerable amount of work has been done on the ruthenium metal complexes of hemilabile (P,O) ligands [61-64]. For example, $[\text{RuCl}_2(\text{PPh}_3)_3]$ reacts with two equivalent of ether-phosphine ligand such as $\text{Ph}_2\text{PCH}_2\text{CH}_2\text{OCH}_3$, $\text{Ph}_2\text{PCH}_2\text{C}_4\text{H}_7\text{O}$ in refluxing ethanol to afford a complex of the type *trans,cis*- $[\text{RuCl}_2(\text{P}\cap\text{O})_2]$ [60], while the use of three equivalent of these ligand gives *trans,cis,cis*- $[\text{RuCl}_2(\text{P}\cap\text{O})(\text{P}\sim\text{O})_2]$. The schematic representation of the reactions has been shown below.



Reaction of $[\text{RuCl}_2(\text{PPh}_3)_3]$ with diphenylphosphinoacetic acid ($\text{Ph}_2\text{PCH}_2\text{COOH}$) in 1:3 molar ratio under refluxing condition produced the complex $[\text{Ru}(\text{P}\cap\text{O})_2(\text{POH})]$ ($\text{P}\cap\text{O} = \eta^2\text{-}(\text{P},\text{O})$ chelated $\text{Ph}_2\text{PCH}_2\text{COO}^-$; $\text{POH} = \eta^1\text{-}(\text{P})$ coordinated $\text{Ph}_2\text{PCH}_2\text{COOH}$) [65]. On the basis of IR and $^{31}\text{P}\{\text{H}\}$ NMR spectroscopy the structure has been assigned as five coordinated square pyramidal geometry as shown below –

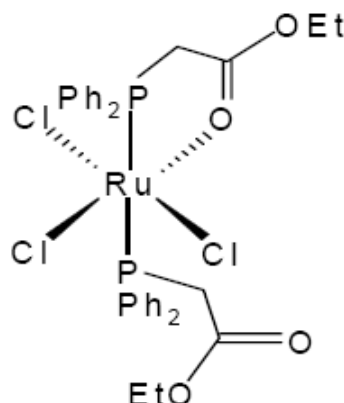


$\text{RuCl}_3 \cdot 3\text{H}_2\text{O}$ can also be used as starting material for synthesis of some metal complexes with hemilabile (P,O) ligand. Thus, $\text{RuCl}_3 \cdot 3\text{H}_2\text{O}$ reacts with $\text{Ph}_2\text{PCH}_2\text{COOEt}$ in 1:3 molar ratio to yield the complex *trans*- $[\text{RuCl}_2(\text{P}\cap\text{O})(\text{P}\sim\text{O})_2]$ [62]. The hemilabile nature of the P,O ligand in the complex is evidenced from a Scheme (shown below) and the stereo-dynamic behavior was observed by variable temperature $^{31}\text{P}\{\text{H}\}$ NMR spectroscopy.

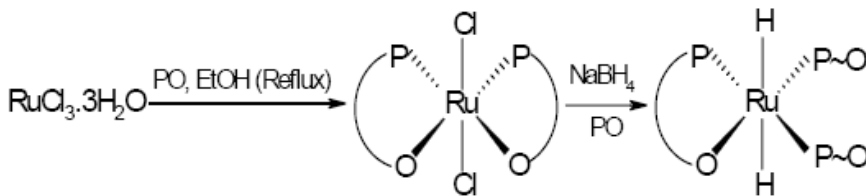


Stereodynamic behaviour of *trans*- $[\text{RuCl}_2(\text{P}\cap\text{O})(\text{P}\sim\text{O})_2]$

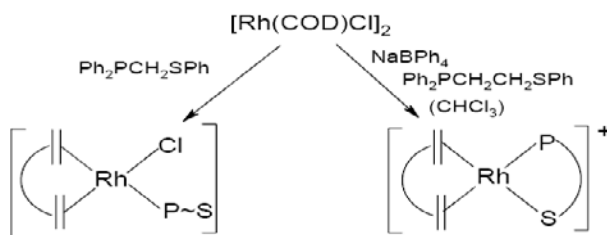
The phosphinoester ligand $\text{Ph}_2\text{PCH}_2\text{COOEt}$ also forms ruthenium(III) complex of the type *mer*- $[\text{RuCl}_3(\text{P}\cap\text{O})(\text{P}\sim\text{O})]$ [66] by reacting with ethanolic solution of $\text{RuCl}_3 \cdot 3\text{H}_2\text{O}$ in presence of HCl at room temperature. The structure of the complex is shown below –



$\text{RuCl}_3 \cdot 3\text{H}_2\text{O}$ also reacts with ether-phosphine ligand such as $\text{R}_2\text{PCH}_2\text{CH}_2\text{OMe}$, $\text{R}_2\text{PCH}_2\text{C}_4\text{H}_7\text{O}$ (PO) ($\text{R} = \text{Cy, Ph}$) to yield octahedral ruthenium(II) complexes of the type *trans*- $[\text{RuCl}_2(\text{P}\cap\text{O})_2]$. The bis-chelate complex *trans*- $[\text{RuCl}_2(\text{P}\cap\text{O})_2]$ reacts with NaBH_4 in presence of excess of PO ligand to form complexes *trans*- $[\text{RuH}_2(\text{P}\cap\text{O})(\text{P}\sim\text{O})_2]$ [9].



There are a few reports available on the rhodium metal complexes of various types of (P, S) donors ligands [29,30,67,68]. In most of the cases the dimeric complex $[\text{Rh}(\text{COD})\text{Cl}]_2$ or $[\text{Rh}(\text{CO})_2\text{Cl}]_2$ are used as starting rhodium complex. It has been observed that sometimes ligands of the same homologous series behave different way [68]. For example, the ligand $\text{Ph}_2\text{PCH}_2\text{SPh}$ reacts with $[\text{Rh}(\text{COD})\text{Cl}]_2$ in 2:1 molar ratio to afford a complex $[\text{Rh}(\text{COD})\text{Cl}(\text{P}\sim\text{S})]$ ($\text{P}\sim\text{S} = \eta^1$ -(P) coordinated PS) where as its homologue $\text{Ph}_2\text{PCH}_2\text{CH}_2\text{SPh}$ does not normally react with $[\text{Rh}(\text{COD})\text{Cl}]_2$. But when CHCl_3 solution of $[\text{Rh}(\text{COD})\text{Cl}]_2$ was treated with $\text{Ph}_2\text{PCH}_2\text{CH}_2\text{SPh}$ in presence of NaBPh_4 , a cationic bis-chelate complex, $[\text{Rh}(\text{COD})(\text{P}\cap\text{S})]^+$ ($\text{P}\cap\text{S} = \eta^2$ -(P, S) coordinated) are formed. Similar types of cationic bis-chelate complex have also been reported [67] for other ligands such as $\text{Ph}_2\text{PCH}_2\text{CH}_2\text{SR}$ ($\text{R} = \text{Me, Et}$).

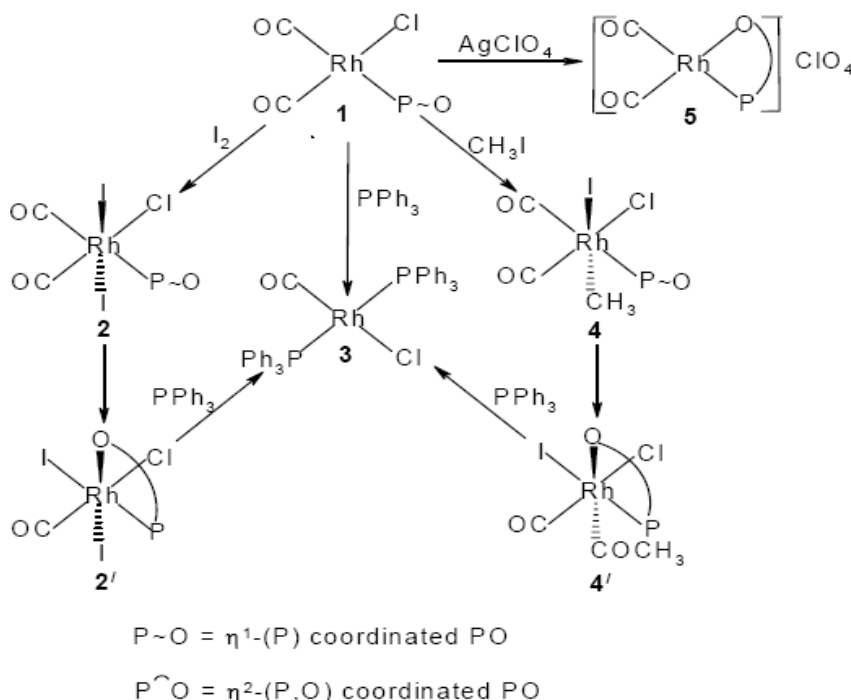


The coordination chemistry of ruthenium(II) with bidentate ligands containing phosphorous and sulfur donor atoms has got less attention. Recently few reports [69,70] on ruthenium metal complexes with (P, S) donors are found. Del Zotto et. al. [71] reported a few ruthenium(II) complexes with thioether-phosphine ligand of the type $\text{Ph}_2\text{P}(\text{CH}_2)_2\text{SR}$ ($\text{R} = \text{Me, Et, cyclo-C}_6\text{H}_{11}$).

Triphenylphosphinechalcogenides Ph_3PX ($\text{X} = \text{O, S, Se}$) are a class of σ - donor ligands and form a number of complexes with platinum metals and some of them are reported to act as catalysts for organic synthesis [46a, 72-74]. A neutral rhodium(I) complex $[\text{Rh}(\text{CO})\text{Cl}(\text{Cy}_3\text{PO})]$ ($\text{Cy} = \text{C}_6\text{H}_{11}$) was reported [75]. Ruthenium(II) also forms complex of the type $[\text{RuCl}_2(\text{DMSO})(\text{PPh}_3\text{O})]$ [76].

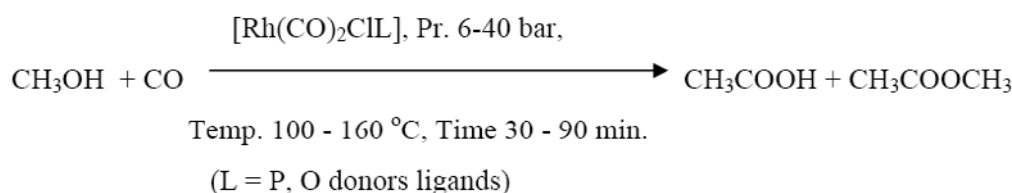
During the last few years, our group at Regional Research Laboratory(CSIR), India, is pursuing works relating to synthesis, reactivity and catalytic applications of Rh(I) and Ru(II) complexes containing ligands like tertiaryphosphine functionlized with chalcogen-

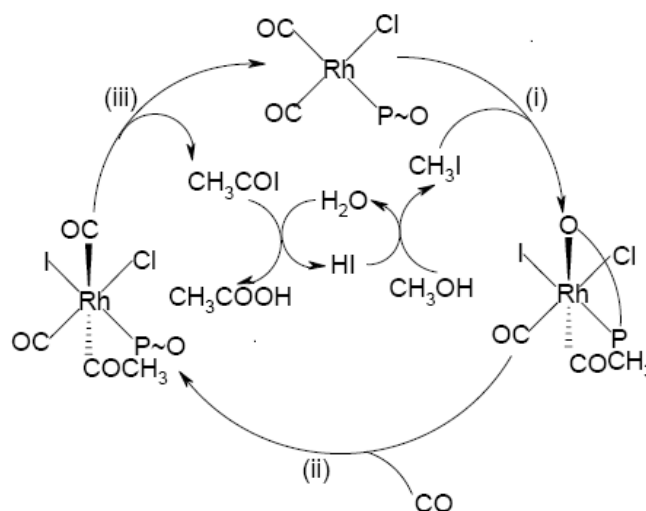
donors(O,S,Se) groups [14,46a,74,77-83]. Some of the metal complexes synthesized at our laboratory are highlighted in respect with their variety of reactivities (Scheme 7).



Scheme 7. Reactivity of complex $[\text{Rh}(\text{CO})_2\text{Cl}(\text{P}\sim\text{O})]$.

A brief description of the process / product of carbonylation reaction and proposed mechanism are given below [74,78] :





PO = Ph₂PCH₂COOEt, Ph₂PCH₂CH₂COOEt, Ph₂PCH(Me)COOMe

P~O = η^1 -(P) coordinated PO

P~O = η^2 -(P,O) chelated PO

(i) Oxidative addition of CH₃I followed by insertion of CO

(ii) Ring opening by CO

(iii) Reductive elimination of CH₃COI

Scheme 8. Catalytic cycle for carbonylation of methanol in presence of [Rh(CO)₂Cl(P~O)] as catalyst precursors.

COMPLEXES WITH P-O LIGANDS

Recently, we have reported [14] the complexes [Rh(CO)Cl(2-Ph₂PC₆H₄COOMe)]1 and *trans*-[Rh(CO)Cl(2-Ph₂PC₆H₄COOMe)]₂2 synthesized by the reaction of the dimer [Rh(CO)₂Cl]₂ with 2 and 4 molar equivalents of 2-(diphenylphosphino)methyl benzoate. The complexes 1 and 2 show terminal v(CO) bands at 1979 and 1949 cm⁻¹ respectively indicating high electron density at the metal center. The lower v(CO) at 1949 cm⁻¹ indicates lowest value so far reported of such complexes which suggest a high electron density at the central metal atom and expected to show higher catalytic activity for carbonylation of methanol to acetic acid. The molecular structure of the complex 2 has been determined by single crystal X-ray diffraction which shows a Rh - O 'Secondary' interaction established from X-ray structure (Figure 2). The rhodium atom lies in an approximately square planar environment formed by the two phosphorus donors, Rh, C (of CO) and Cl atoms. The ester carbonyl

oxygen atom of the two phosphine ligands points towards the rhodium centre above and below the vacant axial sites of the planar complex. The observed rhodium-oxygen distances (Rh....O(49) 3.18 Å; Rh....O(19) 3.08 Å) and the angle O(19)....Rh....O(49) 179° indicate a long range intramolecular secondary Rh...O interactions leading to a pseudo hexa-coordinated complex. In order to ascertain the influence of the position of the substituted COOCH₃ on the phenyl ring of the triphenylphosphine ligand, we have also prepared the complex *trans*-[RhCOCl(4-Ph₂PC₆H₄COOMe)₂] 3 which shows the terminal $\nu(\text{CO})$ band at 1977 cm⁻¹ and the ester $\nu(\text{COO})$ band at 1717 cm⁻¹ indicating non-formation of 'Secondary bond'.

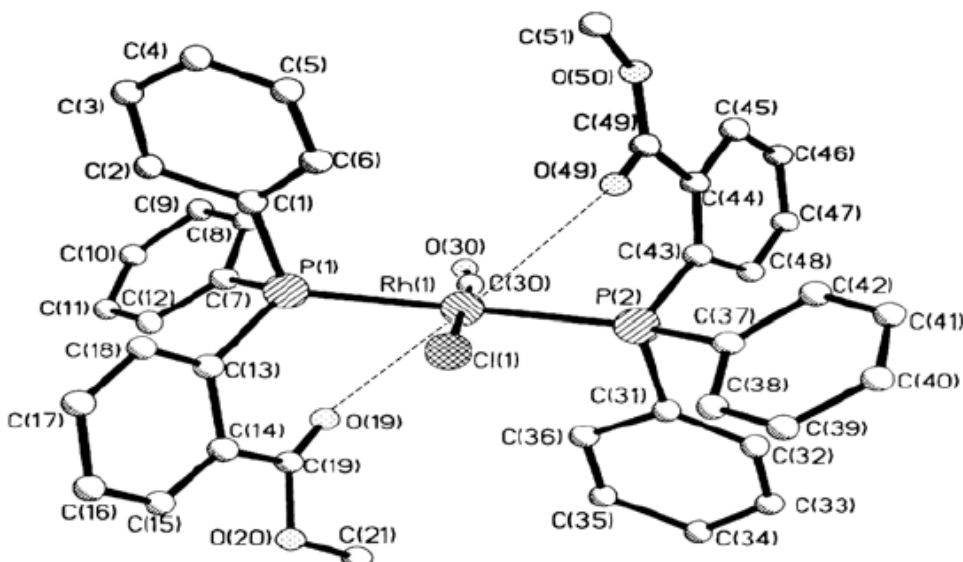
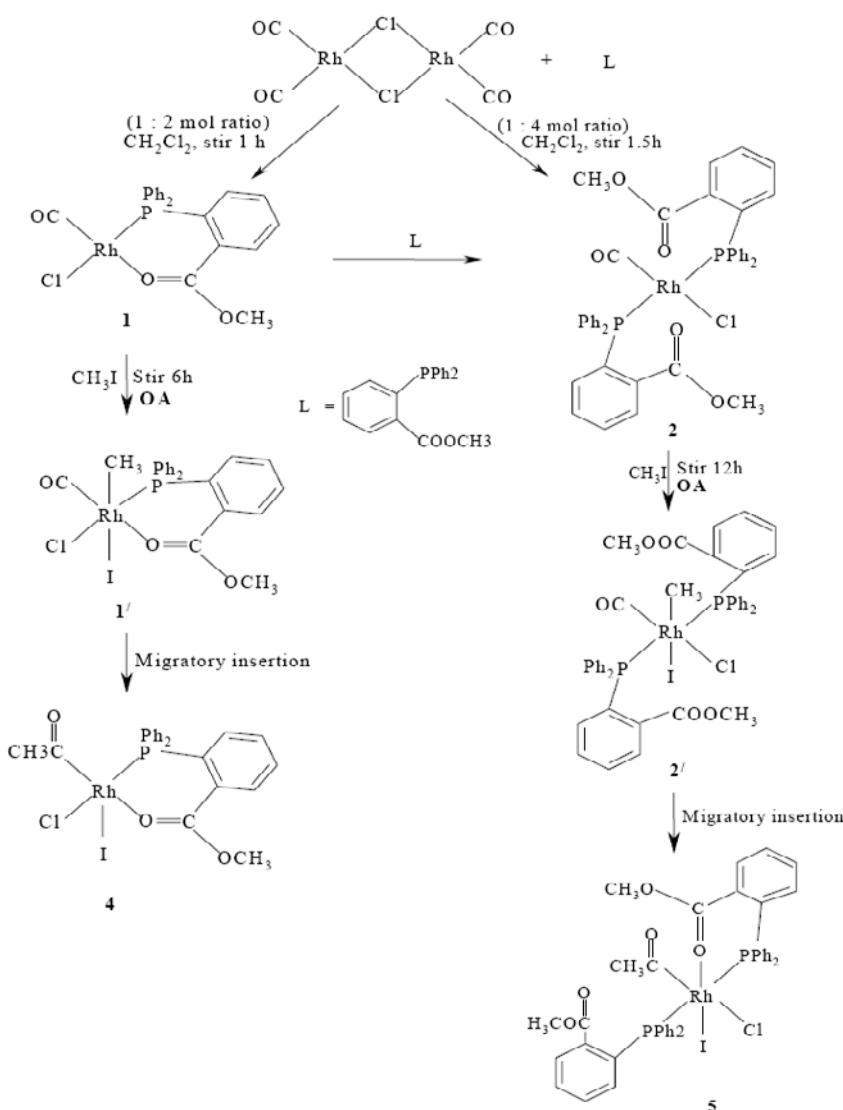


Figure 2. Crystal structure of the complex *trans*-[Rh(CO)Cl(2-Ph₂PC₆H₄COOCH₃)₂][D. K. Dutta, et. al. Dalton Transaction 2003, 2674]-Reproduced by permission of The Royal Society of Chemistry.

The OA reactions of the complexes 1 and 2 with excess CH₃I yield complexes

[Rh(COCH₃)ClI(2-Ph₂PC₆H₄COOMe)]4 and *trans*-[Rh(COCH₃)ClI(2-Ph₂PC₆H₄COOCH₃)(2-Ph₂PC₆H₄COOMe)]5 respectively through their corresponding unisolable alkyl-Rhodium(III) intermediates 1' and 2' (Scheme 9).



Scheme 9. Synthesis of complexes 1 and 2 and their OA reactions with MeI.

Catalytic Activity of Complexes 1 and 2 for Carbonylation of Methanol

The results of batch carbonylation of methanol to acetic acid and its ester in the presence of complexes 1, 2, *trans*-[Rh(CO)Cl(PPh₃)₂] and [Rh(CO)₂I₂] as catalyst precursors are shown in table 1. GC analyses of the products reveal that as the reaction time increases from 0.5 to 1.5 hours, the total conversion as well as Turn Over Number (TON) for the different catalyst precursors increases irrespective of the complexes. Maximum conversion of methanol with corresponding maximum TON were observed during the entire catalytic reaction period for the complex 1 compared to others and the highest conversion (95 %) and TON (1563) were observed for 1.5 hour reaction period (table 1). Under the same

experimental condition, the well-known catalyst precursor $[\text{Rh}(\text{CO})_2\text{I}_2]^-$ generated *in-situ* from $[\text{Rh}(\text{CO})_2\text{Cl}]_2$ shows 64 % conversion with a TON 1052 while that the complex 2 and *trans*- $[\text{Rh}(\text{CO})\text{Cl}(\text{PPh}_3)_2]$ exhibit 82 % and 76 % conversions respectively with corresponding TON 1349 and 1228. Data from table 1. in general, reveal an order of efficiency of the catalytic activity of the precursors as - complex 1 > complex 2 > *trans*- $[\text{Rh}(\text{CO})\text{Cl}(\text{PPh}_3)_2]$ > $[\text{Rh}(\text{CO})_2\text{I}_2]^-$. It therefore becomes obvious that the functionalized phosphine show higher catalytic activity than the unfunctionalized phosphine and this higher activity may be due to higher electron density on the central metal by the chelate formation through ester oxygen donors of the ligand. From the electronic point of view (indicated by the $\nu(\text{CO})$ value), 2 should show higher catalytic activity than 1, but in practice, the reverse situation was observed. Similar behavior has already been observed (*vide supra*) and was attributed to steric and electronic factors. Thus the steric factor due to two bulky $-\text{COOCH}_3$ group on the two phosphine ligands in 2 sterically restrict the path of MeI addition which is the rate determining step for carbonylation of methanol. On examining the catalytic reaction mixture by IR spectroscopy at different time intervals, and at the end of the catalytic reactions, multiple $\nu(\text{CO})$ bands were obtained that matched well with the $\nu(\text{CO})$ values of solution containing a mixture of the parent rhodium(I) carbonyl complexes 1 and 2 and rhodium(III) acyl complexes 4 and 5. Thus, it may be inferred that the ligands remained bound to the metal centre throughout the entire course of the catalytic reactions.

The importance of steric effects of *ortho* substituted bidentate phosphines in polyketone catalysts has been neatly demonstrated by Pringle and co-workers[52]. We believe this work demonstrates the potential for *ortho* substituents to provide electron density to the metal center via secondary coordination with effects which are as profound as those associated with major R group manipulation in phosphines.

Table 1. Results of carbonylation reaction of methanol

Catalyst Precursor	Time (hour)	Total Conversion ^a (%)	Methyl acetate ^b (%)	Ethanoic acid ^b (%)	TON ^c
$[\text{Rh}(\text{CO})_2\text{I}_2]^-$ ^d	0.5	30	26.0	4.0	493
	1.0	48	38.5	9.5	790
	1.5	64	52.0	12.0	1052
1	0.5	71	32.6	37.4	1168
	1.0	77	60.8	16.2	1267
	1.5	95	28.7	65.3	1563
2	0.5	36	30.6	5.4	609
	1.0	69	59.6	9.4	1135
	1.5	82	30.9	51.1	1349
$[\text{Rh}(\text{CO})\text{Cl}(\text{PPh}_3)_2]$	0.5	37	27.1	9.9	592
	1.0	57	34.0	23.0	938
	1.5	76	16.1	59.9	1228

^a Conversion = $\{[\text{CO consumed (mol)}]/[\text{CO charged (mol)}]\} \times 100$. CO consumption was determined from analysis of products by GC. ^bYields of methyl acetate and acetic acid were obtained from GC analyses. ^cTON = [Amount of product (mol)] / [Amount of catalyst (Rh mol)]. ^dFormed from added $[\text{Rh}(\text{CO})_2\text{Cl}]_2$ under the catalytic condition.

COMPLEXES WITH P-S LIGANDS

Hexa-coordinated chelate complex *cis*-[Ru(CO)₂I₂(P~S)](1a) {P~S= η^2 -(P,S)-coordinated} and penta-coordinated non-chelate complexes *cis*-[Ru(CO)₂I₂(P~S)](1b-d) {P~S= η^1 -(P)-coordinated} are produced [81] by the reaction of polymeric [Ru(CO)₂I₂]_n with equimolar quantity of the ligands Ph₂P(CH₂)_nP(S)Ph₂{n=1(a), 2(b), 3(c), 4(d)} in dichloromethane at room temperature (Scheme 10). The bidentate nature of the ligand a in the complex 1a leads to the formation of five membered chelate ring which confers extra stability to the complex. On the other hand, 1:2 (Ru:L) molar ratio reaction affords the hexa-coordinated non chelate complexes *cis*-[Ru(CO)₂I₂(P~S)₂](2a-d) irrespective of the ligands. All the complexes show two equally intense terminal ν (CO) bands in the range 2028-2103 cm⁻¹. The ν (PS) band of complex 1a occurs 23 cm⁻¹ lower region compared to the corresponding free ligand suggesting chelation via metal-sulfur bond formation. X-ray crystallography reveals (Figure 3) that the Ru(II) atom occupies the center of a slightly distorted octahedral geometry. The complexes have also been characterized by elemental analysis, ¹H, ¹³C and ³¹P NMR spectroscopy.

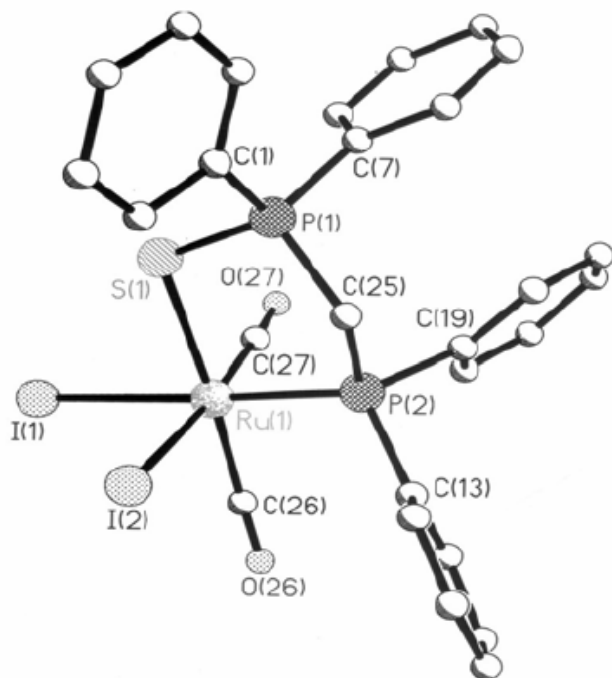
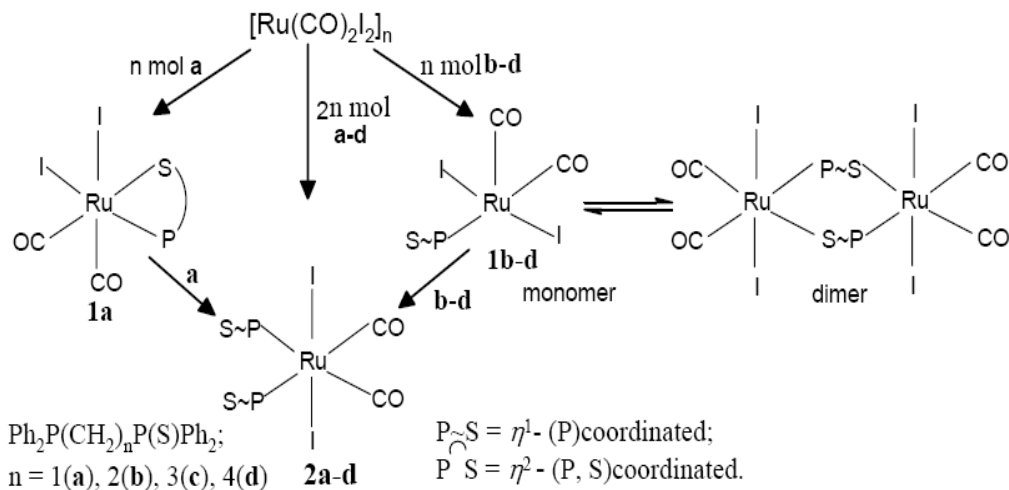


Figure 3. The structure of [Ru(CO)₂I₂(Ph₂PCH₂P(S)Ph₂)](1a). Hydrogen atoms are omitted for clarity.

In order to obtain unambiguous characterization of the complexes 1a-d and 2a-d, an X-ray diffraction study was undertaken. Fortunately, a good crystal suitable for X-ray analysis was developed for the complex 1a, [Ru(CO)₂I₂(P~S)]. Figure 3 shows the arrangements and numbering of atoms in the crystal. The crystal contains a metal occupying the centre of a slightly distorted octahedron with two *cis* carbonyl, two *cis* iodides and one *bis* phosphine

sulfide ligand bonding via P and S atom to the metal completing the coordination sphere. This atomic arrangement is sterically less hindered and energetically most favoured because the carbon monoxide is a very strongly double bonding ligand and prefers not to be in a *trans* position to another carbon monoxide. Moreover, the more *trans* influencing nature of the tertiary phosphine and CO, favour strong *trans* directing iodides in their *trans* position. This shortening of the Ru-P bond length is due to the strong π -acceptor property of the two carbonyl groups as a result of which a strong d π -p π bonding is formed between the Ru and the P atom. The Ru-CO and Ru-S bond lengths are not significantly different from those observed for similar complexes $[\text{Ru}(\text{CO})_2(\text{BzIPPh}_2)\text{Cl}_2]$ and $[\eta^6\text{-MeC}_6\text{H}_4\text{Pr}^i\text{Ru}\{\eta^3\text{-}(\text{SPPH}_2)_2\text{CMe-C,S,S'}\}]\text{PF}_6$. The observed deviation from usual bond angles (180° and 90°) of a regular octahedral geometry is probably due to steric requirement to get a most stable structure, where the uncoordinated phenyl rings are oriented away from the plane containing the all bonding groups and atoms to the metal. Although, we successfully grew crystals for $[\text{Ru}(\text{CO})_2\text{I}_2(\text{P}\cap\text{S})](1\text{a})$, no crystal was developed for the same type of complex $[\text{Ru}(\text{CO})_2\text{Cl}_2(\text{P}\cap\text{S})]$. The soft Ru metal will prefer to bind with the softest I atom rather than Cl. Moreover, in the absence of the other interaction between the halide and the metal, iodide would be expected to form the strongest bond due to the σ -interaction with the metal. Conversely, we can explain the decarbonylation reaction taking place in the complex $[\text{Ru}(\text{CO})_2\text{Cl}_2(\text{P}\sim\text{S})_2](\text{P}\sim\text{S} = \eta^1\text{-P coordinated Ph}_2\text{PCH}_2\text{P}(\text{S})\text{Ph}_2)$ to give a new chelate complex $[\text{Ru}(\text{CO})_2\text{Cl}(\text{P}\cap\text{S})_2]\text{Cl}$. The molecular structure of this new complex was established by a single crystal X-ray study but, no such decarbonylation was observed in our present complex $[\text{Ru}(\text{CO})_2\text{I}_2(\text{P}\sim\text{S})_2](2\text{a})$. We have reacted the complex 1a under vigorous reaction condition with various σ -donor ligands such as Ph_3P , Ph_3As , Ph_3Sb and Ph_3PX ; X = O, S, Se in order to investigate the lability of the Ru-S bond in the molecule. Interestingly, these ligands were not able to break the relatively labile metal-sulfur bond as expected.



Scheme 10. Synthesis of iodo-carbonyl ruthenium(II) complexes of P-S ligands.

Reaction of $[\text{Ru}(\text{CO})_2\text{Cl}_2]_n$ with ligands $\text{Ph}_2\text{P}(\text{CH}_2)_n\text{P}(\text{S})\text{Ph}_2$ [n = 1(a), 2(b), 3(c), 4(d)] in 1:1 molar ratio produces complex *cis*- $[\text{Ru}(\text{CO})_2\text{Cl}_2(\text{P}\cap\text{S})](1\text{a})$ ($\text{P}\cap\text{S} = \eta^2\text{-}(\text{P}, \text{S})$ coordinated)

and *cis*-[Ru(CO)₂Cl₂(P~S)](1b-d) (P~S = η^1 -(P) coordinated), while 1:2 molar ratio yields complex [79] of the type *cis*-[Ru(CO)₂Cl₂(P~S)₂](2a-d)(Scheme 11). The complex 2a undergoes partial decarbonylation reaction in CH₂Cl₂-hexane solution to give a new chelated complex [Ru(CO)Cl(P~S)₂]Cl(2a') (Scheme 12). Abstraction of halide with AgClO₄ from the nonchelated complexes 1b-d and 2a-d afford corresponding chelated complexes [Ru(CO)₂Cl(P~S)](ClO₄)(3b-d) and [Ru(CO)₂(P~S)₂](ClO₄)₂(4a-d). The molecular structure of the complex 2a' has been determined by single crystal X-ray diffraction (Figure 4). The ruthenium atom is at the centre of slightly distorted octahedral structure having the two phosphorus atoms of the two chelated P, S coordinated ligands at *trans* to each other, one CO group and Cl atom completing the coordination sphere. Other complexes have been characterized by elemental analysis, IR, ¹H and ³¹P-{H} NMR spectroscopy.

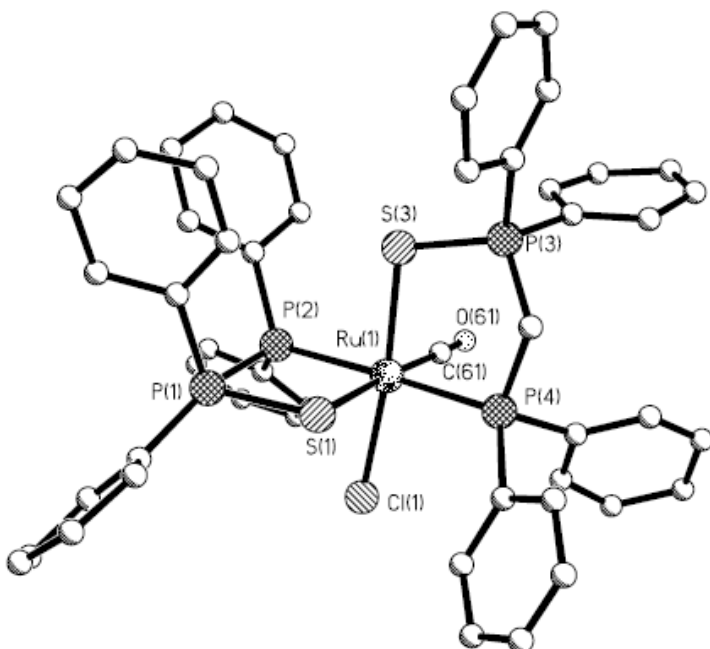
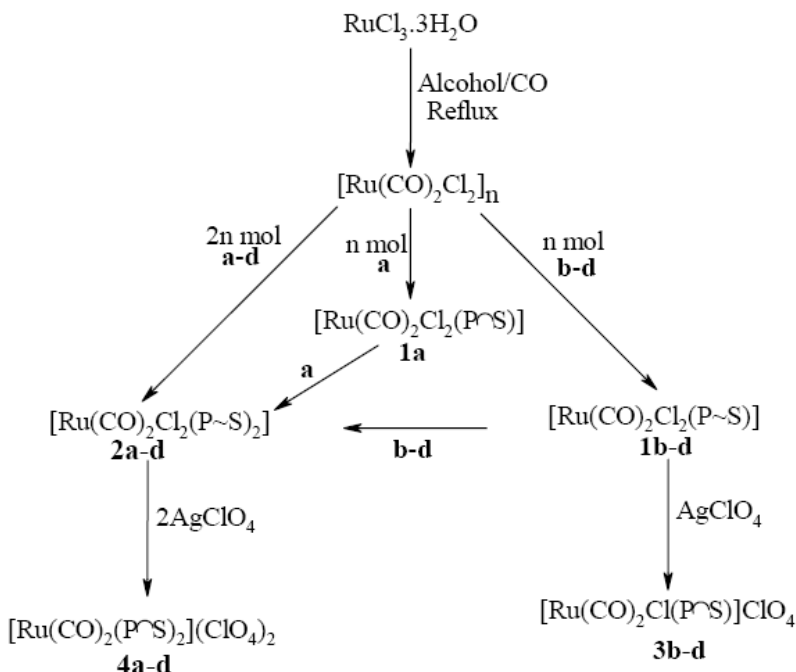


Figure 4. Crystal structure of [Ru(CO)Cl{Ph₂PCH₂P(S)Ph₂}₂]Cl(2a').



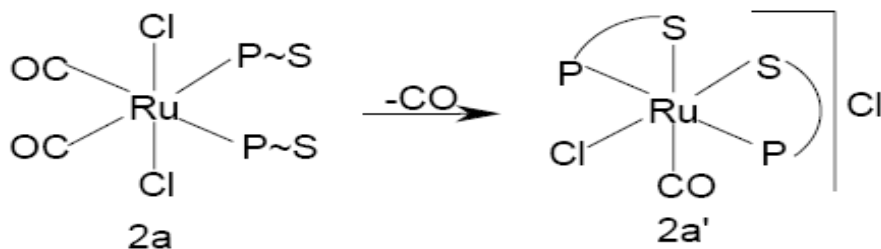
$\text{Ph}_2\text{P}(\text{CH}_2)_n\text{P}(\text{S})\text{Ph}_2$; $n = 1(\mathbf{a}), 2(\mathbf{b}), 3(\mathbf{c}), 4(\mathbf{d})$

$\text{P}\sim\text{S} = \eta^1 - (\text{P})\text{coordinated}$.

$\text{P}\sim\text{S} = \eta^2 - (\text{P}, \text{S})\text{coordinated}$.

Scheme 11. Synthesis of ruthenium (II) carbonyl complexes of P-S ligands.

It is interesting that the dicarbonyl complex $2\mathbf{a}$ on storing in CH_2Cl_2 -hexane solution for about 15 days undergoes a partial decarbonylation reaction resulting a monocarbonyl chelated complex $[\text{Ru}(\text{CO})\text{Cl}(\text{P}\sim\text{S})_2]\text{Cl}$ ($2\mathbf{a}'$) (Scheme 12) as indicated by a single terminal $\nu(\text{CO})$ band at 1969 cm^{-1} . Such decarbonylation reaction was also observed in rhodium α -(2-furyl)-N-phenylnitron complex. The two dangling P,S coordinated ligands undergo chelation which is corroborated by the shifting of free $\nu(\text{PS})$ band at 606 to 577 cm^{-1} . In order to obtain an unambiguous characterization of the complex $2\mathbf{a}'$, an X-ray diffraction study was undertaken. The arrangement of the atoms in the crystal are shown in the Figure 4. In the molecule, Ru(II) is situated at the centre of a slightly distorted octahedral coordination environment with two chelated P, S coordinated ligands, one CO group and one Cl atom. Due to the strong *trans* effect, both the phosphorus atoms are mutually *trans* to each other and hence the complex is apparently preferred. The Ru-Cl and Ru-P distances are within the range of values typical for Ru(II) complexes. The Ru-S(1) distance is slightly larger than Ru-S(3) and the weakening of the bond in the former results from the stronger *trans* influence of the CO group compared to Cl atom. The bond angles for S(3)-Ru-Cl, P(2)-Ru-P(4) and C(61)-Ru-S(1) are 174.06° , 175.54° and 175.90° respectively and are therefore slightly deviated from 180° . This deviation is probably due to steric effect of the bulky phenyl rings. In the five member chelate rings, the angles P(4)-Ru-S(3) and P(2)-Ru-S(1) are 90.96° and 90.68° respectively and the slight deviation from 90° is probably due to strain of five member ring.



Scheme 12.

COMPLEXES WITH P-SE LIGANDS

The chelate complexes of the types $[\text{Rh}(\text{CO})\text{Cl}(\text{Ph}_2\text{PCH}_2\text{P}(\text{Se})\text{Ph}_2)](1)$ and $[\text{Rh}(\text{CO})\text{Cl}(\text{Ph}_2\text{PN}(\text{CH}_3)\text{P}(\text{Se})\text{Ph}_2)](2)$ have been synthesized and characterized by IR and NMR spectroscopy[82]. The lower shift of the $\nu(\text{P-Se})$ bands and downfield shift of the ^{31}P - $\{^1\text{H}\}$ NMR signals for both P(III) and P(V) atoms in 1 and 2 compared to the corresponding free ligands indicate chelate formation through selenium donor. 1 and 2 show terminal $\nu(\text{CO})$ bands at 1977 and 1981 cm^{-1} respectively suggesting high electron density at the metal center. The molecular structure of 2 has been determined by single crystal X-ray diffraction (Figure 5). The rhodium atom is at the center of a square planar geometry having the phosphorus and selenium atoms of the chelating ligand at *cis*- position, one carbonyl group *trans*- to selenium and one chlorine atom *trans*- to phosphorus atom. 1 and 2 undergo oxidative addition (OA) reaction with CH_3I to produce acyl complexes $[\text{Rh}(\text{COCH}_3)\text{Cl}(\text{Ph}_2\text{PCH}_2\text{P}(\text{Se})\text{Ph}_2)](3)$ and $[\text{Rh}(\text{COCH}_3)\text{-Cl}(\text{Ph}_2\text{PN}(\text{CH}_3)\text{P}(\text{Se})\text{Ph}_2)](4)$ respectively. The kinetics of the OA reactions reveal that 1 undergoes faster reaction by about 4.5 times than 2. The catalytic activity of 1 and 2 in carbonylation of methanol was higher than that of the well known species $[\text{Rh}(\text{CO})_2\text{I}_2]$ and 2 shows higher catalytic activity compared to 1.

Kinetic studies for the OA reaction of CH_3I with 1 and 2 were carried out in order to understand the effect of ligand backbone. Figure 6a. shows a plot of absorbance against time for the disappearance of the terminal $\nu(\text{CO})$ band of 1 (1977 cm^{-1}) and formation of a new terminal $\nu(\text{CO})$ band at higher energy 2063 cm^{-1} which is a characteristic band for Rh(III) alkyl intermediate ($[\text{Rh}(\text{CO})(\text{CH}_3)\text{Cl}(\text{Ph}_2\text{PCH}_2\text{P}(\text{Se})\text{Ph}_2)]1'$) along with the formation of acyl $\nu(\text{CO})$ band at around 1700 cm^{-1} . The decay of the terminal $\nu(\text{CO})$ band of 1 indicates that the course of the reaction proceeds in an exponential manner while the initial formation and then decay of the terminal $\nu(\text{CO})$ band of 1' indicates that at a reaction time of about 5 min the concentration of the intermediate reaches a maximum after which it follows a similar kinetics to that of 1. Similar type of plot (Figure 6b) was also obtained for 2 in which the decay of the terminal $\nu(\text{CO})$ band at 1981 cm^{-1} accompanies with the growth and decay of another new terminal $\nu(\text{CO})$ band at around 2060 cm^{-1} which is due to formation of a hexacoordinated Rh(III)-alkyl intermediate ($[\text{Rh}(\text{CO})(\text{CH}_3)\text{Cl}(\text{Ph}_2\text{PN}(\text{CH}_3)\text{P}(\text{Se})\text{Ph}_2)]2'$). From Figure 6b, it is clear that the concentration of the intermediate increases up to a period of about 15 minutes

and then starts decreasing in a manner similar to that of the decaying curve of 2. The rate of decay of the terminal $\nu(\text{CO})$ band of 2 was slower than 1 and the course of the reaction proceeds exponentially. The growth of the acyl $\nu(\text{CO})$ bands at 1700 and 1717 cm^{-1} for 3 and 4 were also found to follow a similar type of kinetics as that of decay of terminal $\nu(\text{CO})$ bands for 1 and 2. Kinetics measurements were done by applying pseudo first order conditions i.e. at high concentration of CH_3I . A linear fit of pseudo-first-order was observed for the entire course of the OA reactions of CH_3I with 1 and 2 as is evidenced from the plot of $\ln(A_0/A_t)$ vs time, where A_0 and A_t are the absorbance at time $t = 0$ and t respectively. From the slope of the plot, the rate constants for both the reactions were calculated and found to be 24.67×10^{-4} and $5.47 \times 10^{-4} \text{ s}^{-1}$ for 1 and 2 respectively. The values of the rate constants clearly indicate that the OA reaction of 1 is almost 4.5 times faster than that of 2. This can be substantiated by higher electron density, i.e. higher nucleophilicity of 1 over 2.

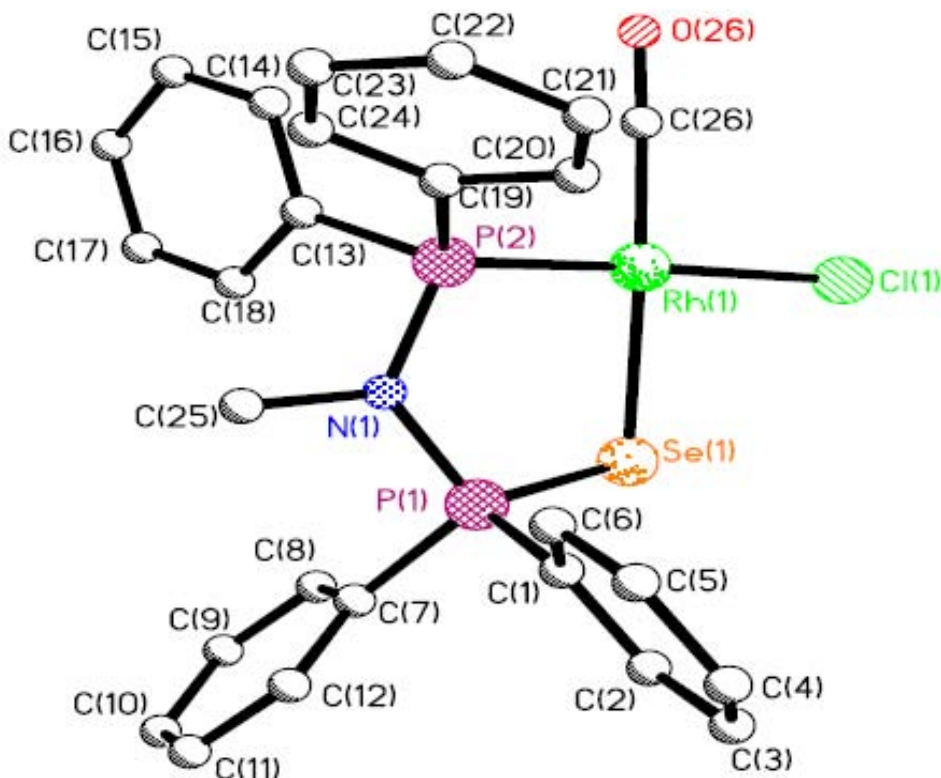


Figure 5. Molecular structure of 2 showing atomic labeling.

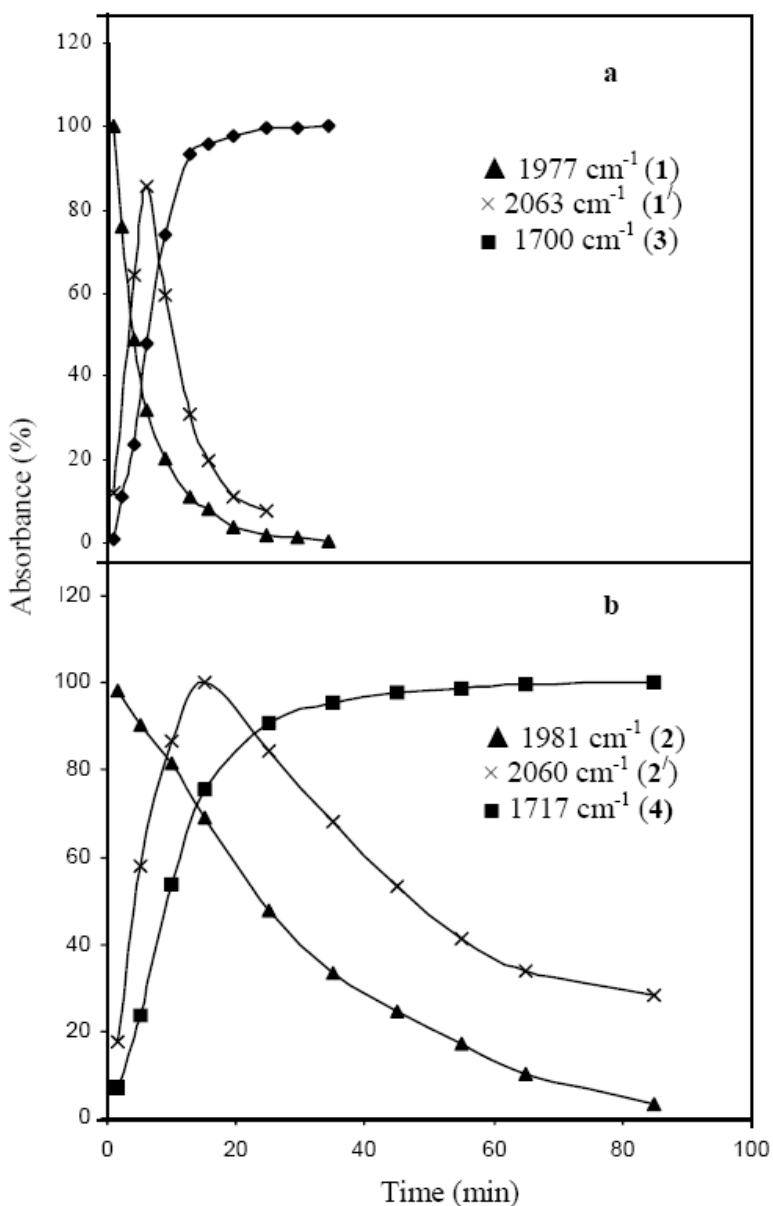


Figure 6. Absorbance of $\nu(\text{CO})$ against time for different carbonyl species: decay (\blacktriangle) of terminal $\nu(\text{CO})$ band (a) for the complexes 1 and (b) for 2; variation (\times) of terminal $\nu(\text{CO})$ band (a) for intermediate (1') and (b) for (2'); and the growth (\blacksquare) of the acyl $\nu(\text{CO})$ band (a) for the complex 3 and (b) for 4 during the course of OA reactions with CH_3I .

Catalytic Activity of 1 and 2 for Carbonylation of Methanol

The results of batch carbonylation of methanol to acetic acid and its ester in the presence of 1, 2, and $[\text{Rh}(\text{CO})_2\text{Cl}]_2$ as catalyst precursors are shown in table 2. GC analyses of the products reveal that 2 exhibits a maximum conversion of 42.4 % with the highest Turn Over

Number (TON) 901 compared to the other complexes. Under the same experimental condition, the well-known catalyst precursor $[\text{Rh}(\text{CO})_2\text{I}_2]^-$ generated *in-situ* from $[\text{Rh}(\text{CO})_2\text{Cl}]_2$ shows 34.08 % conversion with a TON 648 while 1 exhibits 38.8 % conversion with TON 870. Data from table 2, in general, reveal an order of efficiency of the catalytic activity of the precursors as $2 > 1 > [\text{Rh}(\text{CO})_2\text{I}_2]^-$. It is well known that OA step plays a key role in enhancing the catalytic efficacy of such reaction. As expected from higher OA reaction rate of 1 over 2, the former should act more efficiently over the latter in the carbonylation reaction. But in practice, the reverse situation was observed. To explain this, one must consider the fact that higher electron donating ligands makes the metal center more nucleophilic and may lead to the formation of stronger Rh-C (acyl) bond which may cause retardation of the rate of the reductive elimination reaction required for completion of the catalytic cycle. On examining the catalytic reaction mixture by IR spectroscopy at different time intervals and at the end of the catalytic reactions, the $\nu(\text{CO})$ bands compared well with the $\nu(\text{CO})$ values of a solution containing a mixture of the parent rhodium(I) carbonyl complexes and the rhodium(III)-acyl complexes. Thus, it may be inferred that the ligands remained bound to the metal centre during the entire course of the catalytic reactions. It is worth to mention that the catalysts showed almost the same efficacy for their recycled experiments (table 2), indicating adequate stability of the catalysts.

Table 2. Results of carbonylation of methanol

Catalyst precursor	Acetic acid (%)	Methyl acetate (%)	Total conversion (%)	TON ^b
$[\text{Rh}(\text{CO})_2\text{I}_2]\text{-1c}$	3.34	30.74	34.08	648
1	9.6	29.2	38.8	870
1 ^d	9.1	27.8	36.9	827
2	7.2	35.2	42.4	901
2 ^d	6.8	33.8	40.6	863

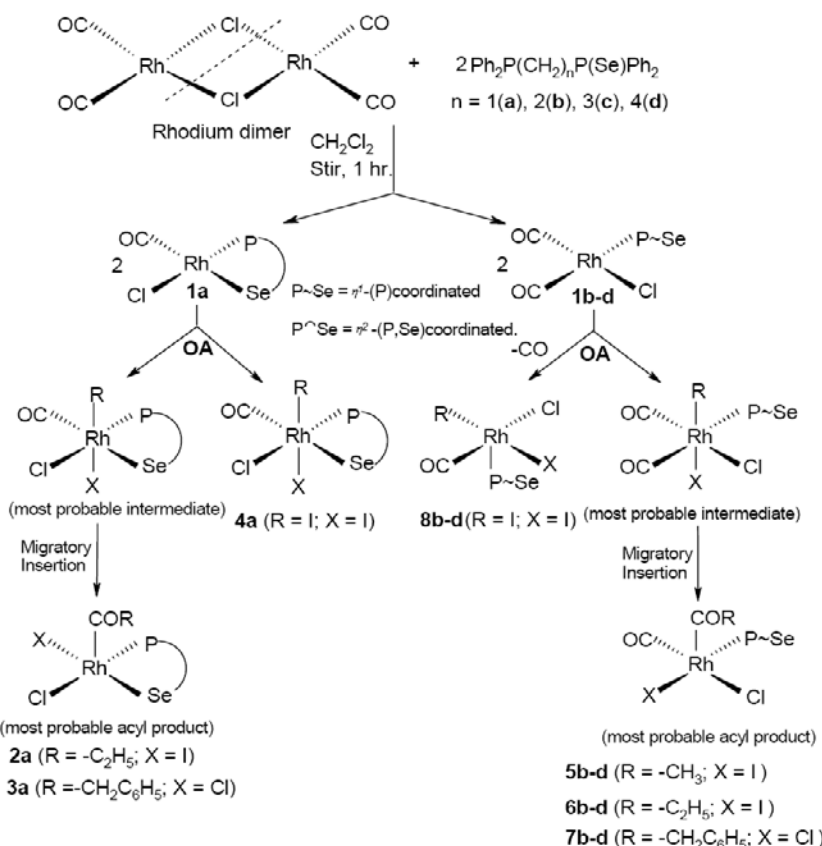
^a Yields of methyl acetate and acetic acid were obtained from GC analyses; ^b TON = [Amount of product (mol)] / [Amount of catalyst (Rh mol)]. ^c Formed from added $[\text{Rh}(\text{CO})_2\text{Cl}]_2$ under the catalytic condition. ^d Recycled.

The complex $[\text{Rh}(\text{CO})_2\text{Cl}]_2$ reacts with two equivalents of a series of unsymmetrical phosphine-phosphine monoselenide ligands, $\text{Ph}_2\text{P}(\text{CH}_2)_n\text{P}(\text{Se})\text{Ph}_2$ { $n = 1\text{(a)}, 2\text{(b)}, 3\text{(c)}, 4\text{(d)}$ } to form chelate complex $[\text{Rh}(\text{CO})\text{Cl}(\text{P}\cap\text{Se})](1\text{a})$ { $\text{P}\cap\text{Se} = \eta^2\text{-(P,Se)}$ coordinated} and non-chelate complexes $[\text{Rh}(\text{CO})_2\text{Cl}(\text{P}\sim\text{Se})](1\text{b-d})$ { $\text{P}\sim\text{Se} = \eta^1\text{-(P)}$ coordinated}[83]. The complexes 1 undergo oxidative addition reactions with different electrophiles such as CH_3I , $\text{C}_2\text{H}_5\text{I}$, $\text{C}_6\text{H}_5\text{CH}_2\text{Cl}$ and I_2 to produce Rh(III) complexes of the type $[\text{Rh}(\text{COR})\text{ClX}(\text{P}\cap\text{Se})]$ {where $\text{R} = -\text{C}_2\text{H}_5\text{(2a)}$, $\text{X} = \text{I}$; $\text{R} = -\text{CH}_2\text{C}_6\text{H}_5\text{ (3a)}$, $\text{X} = \text{Cl}$ }, $[\text{Rh}(\text{CO})\text{ClI}_2(\text{P}\cap\text{Se})](4\text{a})$, $[\text{Rh}(\text{CO})(\text{COCH}_3)\text{ClI}(\text{P}\sim\text{Se})](5\text{b-d})$, $[\text{Rh}(\text{CO})(\text{COC}_2\text{H}_5)\text{ClI}(\text{P}\sim\text{Se})](6\text{b-d})$, $[\text{Rh}(\text{CO})(\text{COCH}_2\text{C}_6\text{H}_5)\text{Cl}_2(\text{P}\sim\text{Se})](7\text{b-d})$ and $[\text{Rh}(\text{CO})\text{ClI}_2(\text{P}\sim\text{Se})](8\text{b-d})$ (Scheme 13). The kinetic study of the oxidative addition (OA) reactions of the complexes 1 with CH_3I and $\text{C}_2\text{H}_5\text{I}$ reveals a single stage kinetics. The rate of OA of the complexes varies with the length of the ligand backbone and follows the order $1\text{a} > 1\text{b} > 1\text{c} > 1\text{d}$. The CH_3I reacts with the different complexes at a rate 10-100 time faster than the $\text{C}_2\text{H}_5\text{I}$. The catalytic activity of complexes 1b-

d for carbonylation of methanol is evaluated and a higher turn over number (TON) is obtained compared with that of the well-known commercial species $[\text{Rh}(\text{CO})_2\text{I}_2]^-$.

Kinetics of OA Reactions of Rh(I) Complexes with CH_3I and $\text{C}_2\text{H}_5\text{I}$:

The dicarbonyl rhodium(I) complexes $[\text{Rh}(\text{CO})_2\text{Cl}(\text{P}\sim\text{Se})](1\text{b-d})$ are coordinately unsaturated and undergo rapid OA reactions with CH_3I . The reactivities of the complexes vary with the chain-length of the ligand backbones. To find out the rate of OA, *in situ* IR was taken during the course of the reaction (Figure 7). The reaction kinetics are monitored by following the simultaneous decay of the lower $\nu(\text{CO})$ absorption of the complexes 1b-d in the region $1984\text{-}1992\text{ cm}^{-1}$ and the formation of acyl $\nu(\text{CO})$ band of the corresponding acyl complexes 5b-d in the range $1702\text{-}1713\text{ cm}^{-1}$. During the course of the OA reactions of the complexes with CH_3I , a series of IR spectra are recorded at different time intervals and a typical set of spectral pattern for complex 1b is shown in the Figure 1. It is clear that out of the two terminal $\nu(\text{CO})$ bands, the intensity of the lower $\nu(\text{CO})$ band occurring at 1988 cm^{-1} decreases while the higher $\nu(\text{CO})$ band at 2067 cm^{-1} shifts to 2071 cm^{-1} .



Scheme 13. Synthesis of Rh(I) and Rh(III) carbonyl complexes containing P-Se donors ligands.

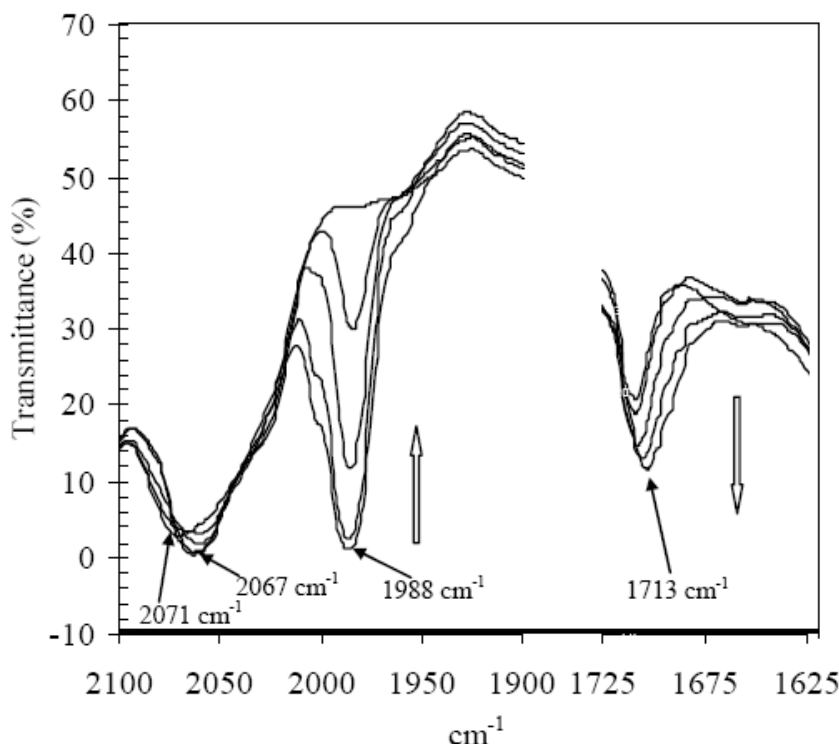


Figure 7. Series of IR spectra ($\nu(\text{CO})$ region) showing the OA reaction of 1b with CH_3I at room temperature. The arrows (↑) and (↓) indicate the decrease and increase in intensity of the terminal and acyl $\nu(\text{CO})$ bands respectively with the progress of the reaction.

The rate of OA reaction is evaluated by applying pseudo-first order condition, i.e. at high concentration (neat) of CH_3I . The formations of acyl complexes from the parent complexes 1b-d as a function of time are shown in Figure 8. The decaying curves of the parent complexes 1b-d indicate that the entire course of the OA reactions proceed in an exponential manner and are completed at around 30, 35 and 40 minutes respectively. Applying the pseudo-first order condition, the plot of $\ln(A_0/A_t)$ versus t (Figure 9), where A_0 and A_t are the concentrations of the complexes at time $t = 0$ and t respectively, shows a good linear fit for the entire course of the reaction. The slope of the plots gives the rate constants $k_{\text{obs}} = 2.34 \times 10^{-3}$, 2.30×10^{-3} and $1.67 \times 10^{-3} \text{ s}^{-1}$ for the complexes 1b-d respectively. Thus the reactivity of the complexes follows the order 1a > 1b > 1c > 1d and the trend may be due to steric hindrance of the ligands where it increases with increase of the chain-length of the backbone.

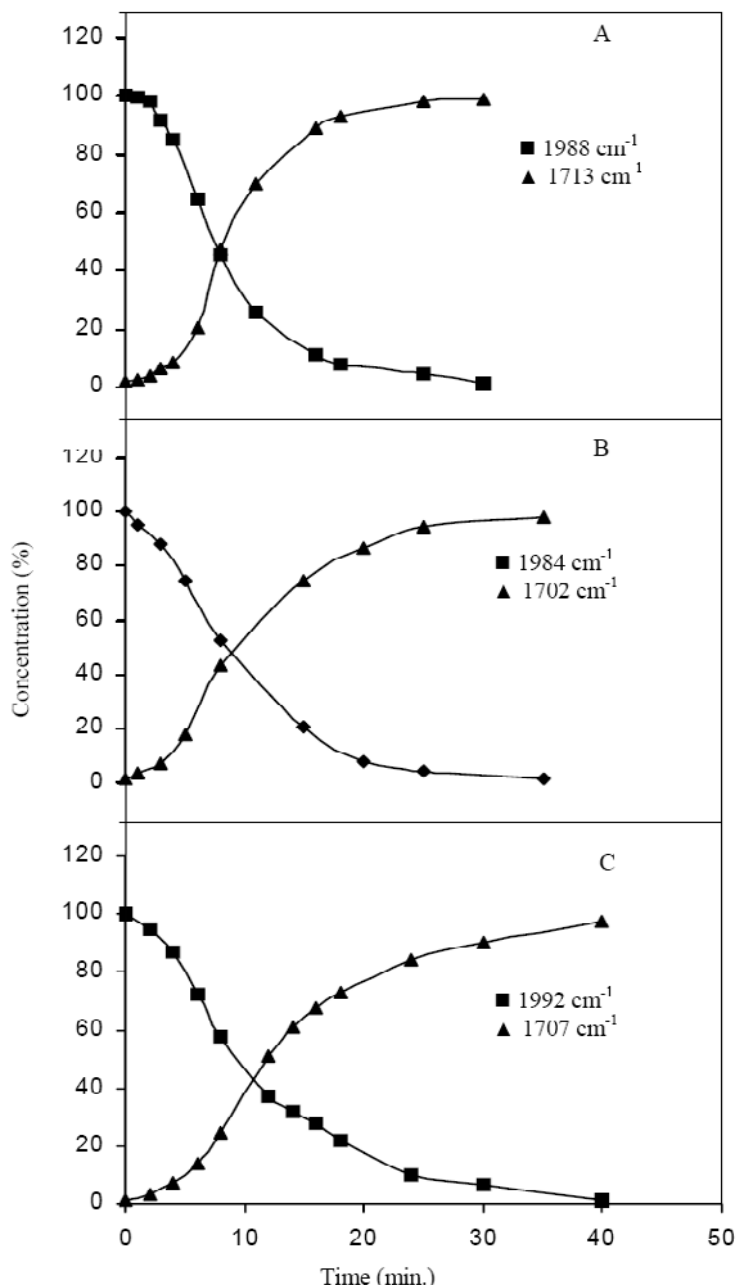


Figure 8. Simultaneous decay (■) of terminal $\nu(\text{CO})$ bands in complexes 1b (A), 1c(B) and 1d(C) and increase in intensity (▲) of acyl $\nu(\text{CO})$ bands of the corresponding acyl complexes 5b-d during the OA reaction with CH_3I against time.

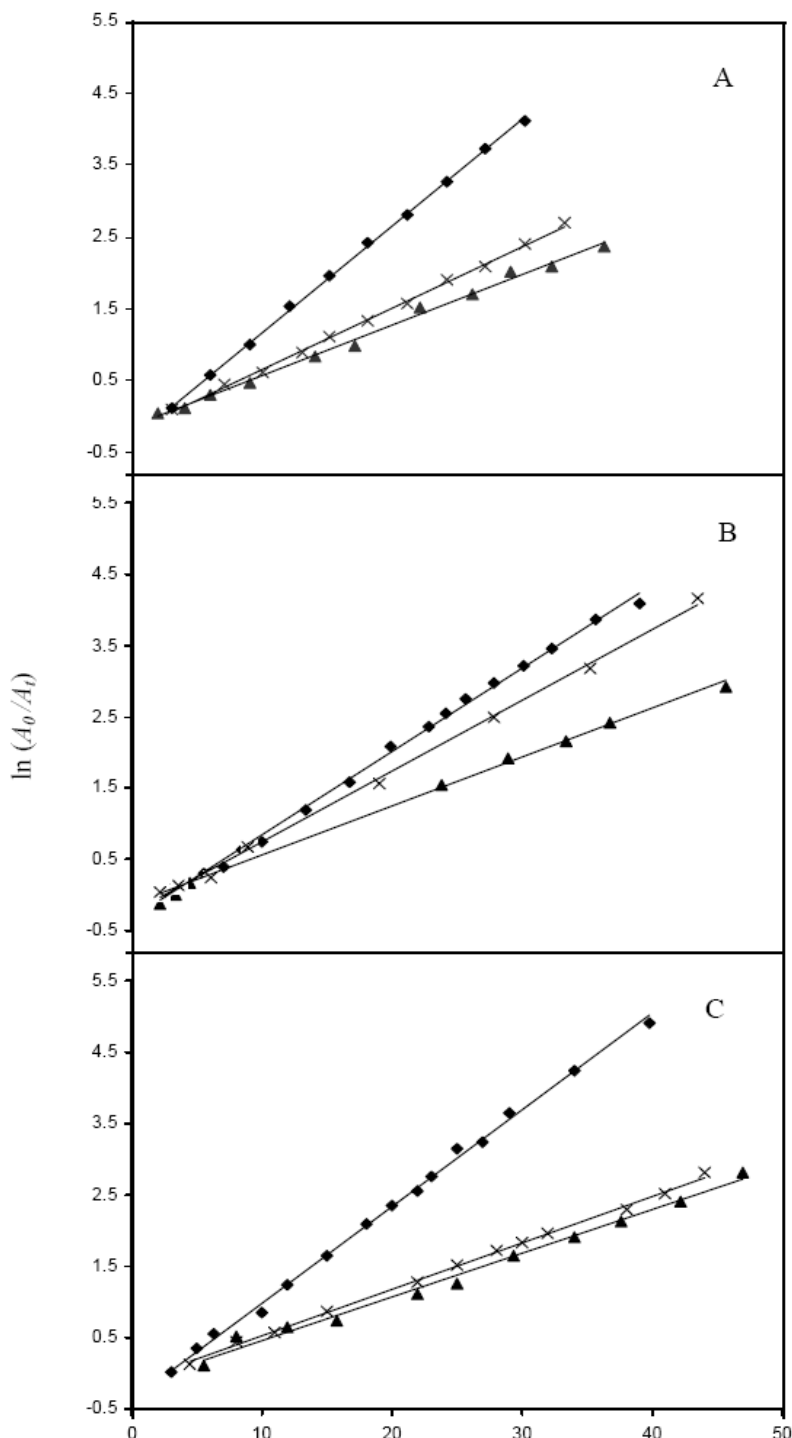
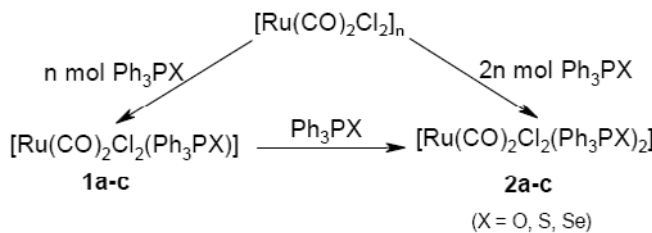


Figure 9. Plot of $\ln(A_0/A_t)$ against time (min.) : OA of each complexes 1b (A), 1c (B) and 1d (C) in (◆) 1, (x) 0.75 and (▲) 0.5 cm^3 of CH_3I .

In order to compare the reactivity (OA) of CH_3I , the OA reactions of $\text{C}_2\text{H}_5\text{I}$ with complexes 1a-d have also been carried out. Applying the same conditions as above, similar types of kinetics are observed from the decay of lower $\nu(\text{CO})$ bands of the complexes 1a-d and increase of intensity of the corresponding acyl complexes. It is found that OA reaction of the complexes with $\text{C}_2\text{H}_5\text{I}$ is slower than with CH_3I . The reaction follows the single-stage kinetics and k_{obs} values for the complexes 1a-d are found to be 2.07×10^{-4} , 1.4×10^{-4} , 9.33×10^{-5} and $8.50 \times 10^{-5} \text{ s}^{-1}$ which are about 10-100 times slower than the corresponding k_{obs} of the complexes with CH_3I . The trend of reactivity (OA) of $\text{C}_2\text{H}_5\text{I}$ with complexes 1a-d follows the order 1a > 1b > 1c > 1d which was also observed in case of CH_3I reactivities.

COMPLEXES WITH P-X LIGANDS (X = O, S, Se)

The reactions of polymeric complex $[\text{Ru}(\text{CO})_2\text{Cl}_2]_n$ with triphenylphosphinechalcogenides ligands Ph_3PX ; X = O(a), S(b), Se(c) in 1:1 molar ratio form five coordinated complexes of the types $[\text{Ru}(\text{CO})_2\text{Cl}_2(\text{Ph}_3\text{PX})](1\text{a-c})$ while 1:2 molar ratio produces six coordinated $[\text{Ru}(\text{CO})_2\text{Cl}_2(\text{Ph}_3\text{PX})_2](2\text{a-c})$ complexes[80]. The complexes 1a-c and 2a-c exhibit two equally intense $\nu(\text{CO})$ bands in the range $2059\text{-}1989 \text{ cm}^{-1}$ and $2050\text{-}1980 \text{ cm}^{-1}$ respectively indicating *cis*-disposition of the two terminal carbonyl groups(Scheme 14). The values of $\nu(\text{CO})$ frequencies irrespective of the complexes, in general, follow the order : $\text{Ph}_3\text{PO} > \text{Ph}_3\text{PS} > \text{Ph}_3\text{PSe}$ which may be ascribed in terms of "Soft-Hard" ($\text{Ru}(\text{II})\text{-O}$) and "Soft-Soft" ($\text{Ru}(\text{II})\text{-S/Se}$) interactions. The $\nu(\text{PX})$ bands of the complexes observed in the range $1173\text{-}538 \text{ cm}^{-1}$ are $19\text{-}41 \text{ cm}^{-1}$ lower than those of the corresponding free ligands substantiating the formation of Ru-X bonds. The molecular structure of the complex, $[\text{Ru}(\text{CO})_2\text{Cl}_2(\text{Ph}_3\text{PS})_2]$ was determined by single X-ray crystallography (Figure 10). The crystal is monoclinic, space group Cc; $a = 11.4990 \text{ \AA}$, $b = 17.3966 \text{ \AA}$, $c = 18.4788 \text{ \AA}$; $\alpha = 90^\circ$, $\beta = 98.160^\circ$, $\gamma = 90^\circ$. In the molecule, the Ru(II) atom occupies the center of a slightly distorted octahedral geometry which consists of two *trans*-S atoms of two Ph_3PS ligands, two *cis*-CO groups and two *cis*-chlorides. The complexes have also been characterized by elemental analysis, ^1H , ^{13}C and ^{31}P NMR spectroscopy.



Scheme 14. Synthesis of complexes (1a-c and 2a-c).

In order to confirm the structures and to determine the detailed geometry, we tried to develop crystals of the complexes. A good crystal suitable for X-ray structural determination was developed for the complex 2b. The conclusions derived from IR and different NMR data are well agreed with the structure. The arrangements and numbering of the atoms in the

crystal are shown in Figure 10. In the molecule, the ruthenium atom has a slightly distorted octahedral coordination with two Ph_3PS ligands occupying two *trans*-octahedral sites via two sulfur atoms, two *cis* CO groups and two *cis* chlorides. This atomic arrangement is sterically less hindered and is apparently preferred because both the bonded sulfur atoms of the ligands are *trans* to each other. The basal Ru-Cl(2) and Ru-C(38) bond lengths are 1.865 and 2.449 Å while their corresponding apical bonds Ru-Cl(1) and Ru-C(37) are little shorter (1.836 and 2.432 Å respectively)(Figure 10). This shortening of the apical bonds may be due to a steric effect. The bond angles for C(37)-Ru-Cl(1), C(38)-Ru-Cl(2) and S(2)-Ru-S(1) are 177.7°, 179° and 163.32° respectively and the deviation from 180° is probably due to steric effect of the bulky phenyl rings. The angles C(37)-Ru-C(38), C(37)-Ru-S(2), C(38)-Ru-S(2), C(37)-Ru-S(1), C(38)-Ru-S(1), C(38)-Ru-Cl(1), S(2)-Ru-Cl(1), S(1)-Ru-Cl(1), C(37)-Ru-Cl(2), S(2)-Ru-Cl(2), S(1)-Ru-Cl(2) and Cl(1)-Ru-Cl(2) exhibit different values in the range 80.17-100.5° with the deviation from 90°, may be due to inter and intra atomic repulsions amongst the bonding atoms and with the bulky phenyl rings.

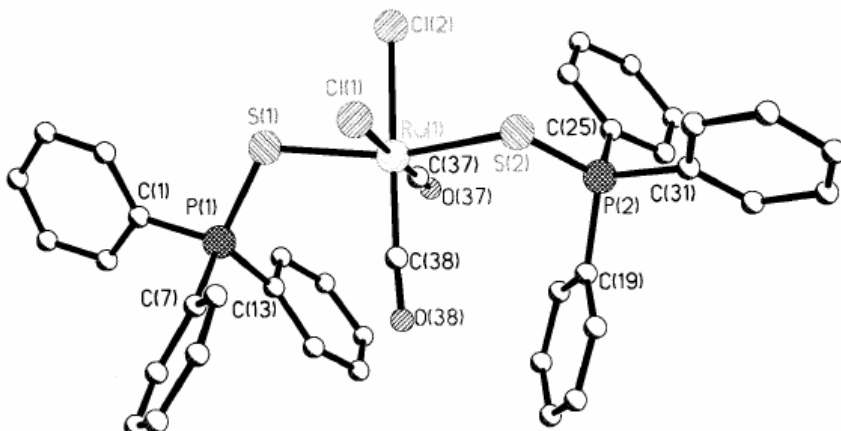
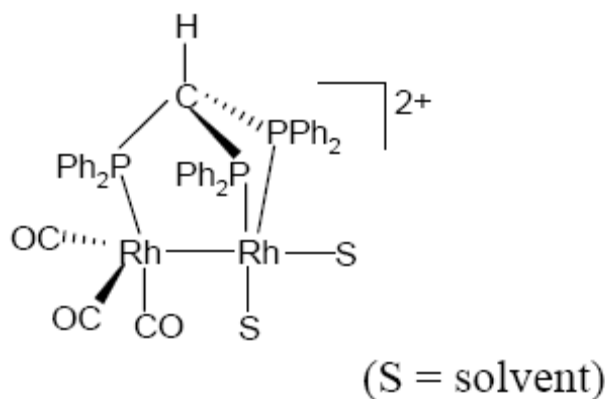


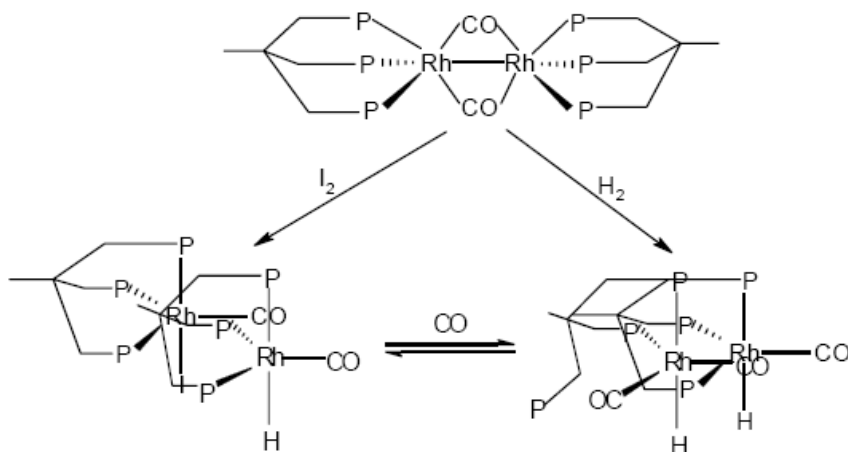
Figure 10. Crystal structure of $[\text{Ru}(\text{CO})_2\text{Cl}_2(\text{PPh}_3\text{S})_2](2\text{b})$.

Polyphosphines as ligands show several advantages like (i) excellent bonding ability to metal, (ii) create high electron density at the metal center (high nucleophilicity), (iii) formation of stable metal-complexes, (iv) stabilize different oxidation states of metals, (v) provide structural and bonding information due to the metal-phosphorous and phosphorous-phosphorous coupling constants. Metal complexes of such ligands are thermodynamically more stable than monophosphine analogues. A review [84] on stereochemical control of transition metal complexes by polyphosphines elaborates the different aspects of the complexes and their catalytic chemical reactions particularly hydrogenation and hydroformylation. Some of the important metal complexes containing polyphosphines are highlighted below :

Tripod, $\text{HC}(\text{PPh}_2)_3$ with least steric constraints forms small rhodium cluster having metal-metal bond [85,86] as shown below –

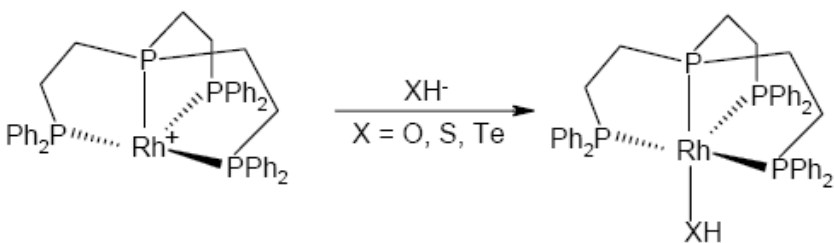


The d^8 metal complexes of $\text{MeC}(\text{CH}_2\text{PPh}_2)_3$ were much studied [87,88]. The *fac*-coordinating character of the ligand prompted the formation of metal-metal bonded complexes but the Rh-Rh bond can be cleaved by suitable reagents to monomeric complexes (shown below).



In metal-tripod complex based catalytic reactions like hydroformylation, at least one of the ligand($\text{MeC}(\text{CH}_2\text{PPh}_2)_3$)-metal bonds dissociate to create free coordination site for substrate binding [89] as shown below –

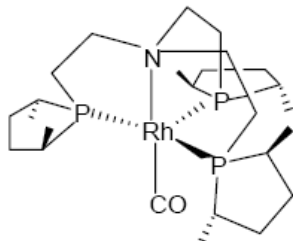
There are many reactions involving the ligand (tdpme)-metal complexes, which can be explained on the basis of an “arm-off” [84] process during the course of the reactions demonstrating the kinetic lability in contrast to the thermodynamic stability of the M-P bond in chelating phosphine complexes [87,90,91].



Polyphosphine ligands form complexes of the type (shown below) which undergo facile substitution at the vacant trigonal-bipyramidal site [92].

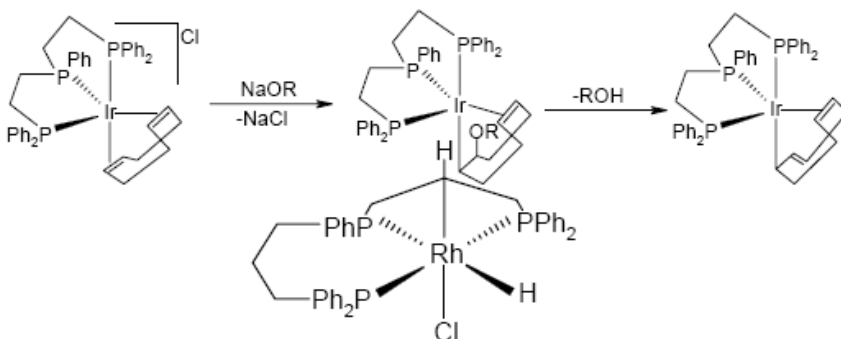
The polyphosphine ligands are used in chiral hydrogenation [93,94]. Most important of such chiral complex of rhodium is shown below –

All (S) complex



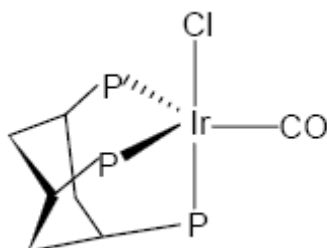
The tripodal ligand $\text{PhP}(\text{CH}_2\text{CH}_2\text{CH}_2\text{PPh}_2)_2$ forms a rhodium complex [95] (shown below) which does not require dissociation of a phosphorous donor during the catalytic hydrogenation of alkene involving coordination of the alkene, hydride transfer to produce a metal alkyl, oxidative addition of H_2 , a second hydride transfer, elimination of the alkane, and regeneration of the catalyst.

The tripodal ligand $\text{PhP}(\text{CH}_2\text{CH}_2\text{PPh}_2)_2$ forms iridium complexes (shown below) which interact with bases in different ways to form different products [96].

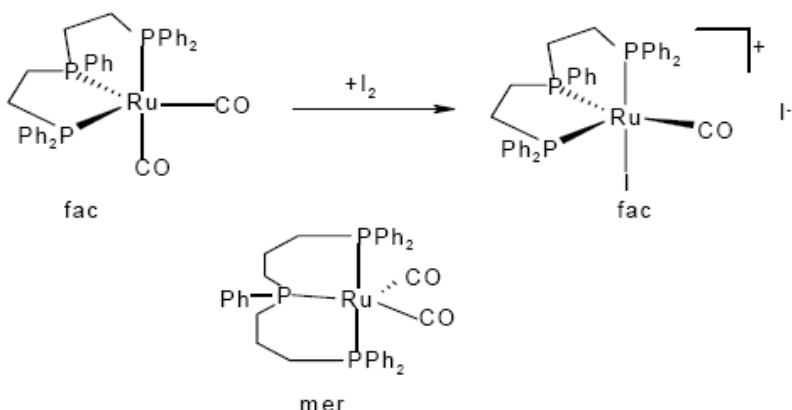


The cyclohexane frame was introduced as a backbone in tripodal phosphine ligands and iridium complex with such ligand forms (shown below). The complexation behaviour of these

kinds of ligands is not only a function of the bite angle but also depends on the flexibility of the cyclohexane ring and the specific cis, cis arrangement of the phosphine functional group[84].



The tripodal ligand PhP(CH₂CH₂CH₂PPh₂)₂ prefers *mer*-arrangement (shown below), while PhP(CH₂CH₂PPh₂)₂ forms *fac*-coordinated complex. This is because of smaller bite angle in the latter ligand [97,98].



Suzuki et. al. reported [99] the preparation of metal(III)-tripodal tridentate phosphine complexes of the type [MCl(acac)(tdmme)]PF₆ where M = Co and Rh; acac = pentane-2,4-dionate; tdmme = 1,1,1-tris(dimethylphosphinomethyl)ethane. The crystal structure and spectroscopic properties of the complexes were evaluated. Recently, the preparation, crystal structure and spectroscopic properties of novel series of complexes [M^{III}Cl_{3-n}P_{3-n}]ⁿ⁺ (M = Co, Rh; n = 0, 1, 2, 3) containing tripodal tridentate phosphine, 1,1,1-tris(dimethylphosphinomethyl)ethane have been reported [100]. Heins et. al. reported [101] the synthesis of metal complexes containing functionalized tripodal phosphine ligands. Mononuclear complexes of metals Rh, Ir and Pt containing tripod ligand (Ph₂P)₃CH are reported [102]. Heinze et. al. reported [103] cobalt-catalysed selective oxidation of the tertiary phosphane triphos with molecular oxygen. The novel ligand triphosO₂ can be obtained in quantitative yield using catalytic amounts of [CoCl₂{CH₃C(CH₂PPh₂)₃}].

Colton et.al. [104,105] reported synthesis and characterization of a number of functionalized (chalcogens) tri- and tetra-tertiary phosphines. Dean and Hughes reported [106] characterization of complexes of Cd(II) with some phosphine oxides, sulphides and

selenides. Grim et. al. reported [107,108] synthesis and characterization of a number of functionalized polyphosphines particularly with chalcogenide donors. Bianchini et.al. reported [109,110] some interesting rhodium(I) complexes of $\text{MeC(CH}_2\text{PPh}_2)_3$ and their reactivities in some transformations.

CONCLUSION

Rhodium(I), iridium(I) and ruthenium(II) complexes of tertiary phosphines functionalized with chalcogen donors P-X (X = O, S, Se) are of much interest in recent time because of expected novel structures and stereo-chemical control in catalytic applications in various important organic synthesis. Some important examples of applications of such metal complexes as commercial homogeneous catalysts are - *L-DOPA* synthesis(Rhodium(I)-chiral catalyst); Monsanto / B. P. Chemicals process for carbonylation of methanol to acetic acid (Rhodium(I) catalyst) and the process called ‘*Cativa*’ (Iridium(I) catalyst with Ru-complex activator). Rhodium(I) carbonyl complexes containing bidentate chelating ligand such as diphenylphosphinomethane oxide / sulphide / selenide have shown interesting structural features. The chelated complex of the type $[\text{Rh}(\text{CO})\text{Cl}(\text{2-Ph}_2\text{PC}_6\text{H}_4\text{COOMe})]$ show a long range intramolecular ‘*Secondary*’ Rh...O interactions (Rh – O distance 3.18 Å). The effect of chain length of the bifunctional i.e. ‘Soft and Hard’ donors chelating ligands of tertiary phosphines with functional carboxylic acid or ester, or unequal softness of the chelating donors i.e. tertiary phosphines functionalised with sulfur or selenium donors having aliphatic and aromatic backbones on the ‘*Hemilability*’ of the metal - O / S / Se bonds are demonstrated. In chelate metal complexes containing hemilabile ligands like P-X, the labile M-X bonds cleave and provide a vacant potential coordination site for reversible binding of substrates to metal centre by dynamic chelating ability i.e. by ‘*Opening and Closing*’ mechanism. The steric effect, electronic effect and kinetics of oxidative addition (**OA**) reactions of the complexes with different electrophiles like CH_3I , $\text{C}_2\text{H}_5\text{I}$, $\text{C}_6\text{H}_5\text{CH}_2\text{Cl}$ etc. show interesting features. The activation of small molecules like CO, CH_3I , I_2 , etc. by the metal complexes and their evaluation as catalysts precursors for carbonylation of alcohol are interesting. The metal complexes of types $[\text{Rh}(\text{CO})_2\text{Cl}(\text{P}\sim\text{O})]$ and $[\text{Rh}(\text{CO})\text{Cl}(\text{P}\sim\text{O})_2]$ show high catalytic carbonylation reactions of methanol to acetic acid / ester with high Turn Over Number(TON) of about 1500.

REFERENCES

- [1] R. H. Crabtree, *The organometallic chemistry of the transition metal*, 2nd Ed., John Wiley and Sons, New York, 1994.
- [2] B. R. James, *Homogeneous hydrogenation*, Wiley, New York, 1973.
- [3] F. A. Cotton and G. Wilkinson, Advanced Inorganic Chemistry, A comprehensive Text, 4 th Ed., Interscience, New York, 1980.
- [4] G. N. Schrauzer (Ed.), *Transition metals in homogeneous catalysis*, Marcell Dekker, New York, 1971.

- [5] A. Mullen; Carbonylations Catalyzed by metal carbonyls - Reppe reactions. In *new Synthesis with carbon monoxide*, J. Falbe (Ed), Springer -Verlag, Heidelberg, New York, 1980, 11, 286.
- [6] T. W. Dekleva and D. Forster, Mechanistic aspects of transition-metal catalysed alcohol carbonylations, in *Advances in catalysis*, Academic Press, Vol. 34, 1986, pp- 81.
- [7] H-U. Blaser, A. Indolese and A. Schynder, *Current Science*. 2000, 78, 11, 1336.
- [8] (a) P.W.N.M. van Leeuwen, *Homogeneous Catalysis*, Kluwer Academic Publishers, 2004; (b) B. Cornils, *J. Mol. Catal.*, A : *Chemical*, 1999, 143, 1; (c) C. M. Thomas and G. S-Fink, *Coordination Chem. Rev.*, 2003, 243, 125.
- [9] A. Bader and E. Lindner, *Coord. Chem. Rev.*, 1991, 108, 27.
- [10] R. A. M. Robertson, A. D. Poole, M. J. Payne and D. J. Cole-Hamilton, *J. Chem. Soc., Chem. Commun.*, 2001, 147.
- [11] T. B. Rouchfuss and D. M. Roundhill, *J. Am. Chem. Soc.*, 1974, 96, 3098.
- [12] P. Braunstein, D. Math, Y. Dusausoy, J. Fischer, A. Mitschler and L. Richard, *J. Am. Chem. Soc.*, 1981, 103, 5115.
- [13] W. S. Knowles, *Acc. Chem. Res.*, 1983, 16, 206.
- [14] D. K. Dutta, J. D. Woollins, A. M. Z. Slawin, D. Konwar, P. Das, M. Sharma, P. Bhattacharyya and S. M. Aucott, *Dalton Transaction*. 2003, 2674.
- [15] W.S. Knowels, *J. Chem. Edu.*, 1986, 63, 222.
- [16] F. E. Paulik and J. F. Roth, *Chem. Commun*, 1968, 1578.
- [17] D. Forster, *J. Am.Chem. Soc.*, 1976, 98, 846.
- [18] D. Forster, *Adv. Organomet. Chem.*, 1979, 17, 255.
- [19] G.J. Sunley and D.J. Watson, *Catal. Today*, 2000, 58, 293.
- [20] J. Jones, *Platinum Metals Rev.*, 2000, 44(3), 94.
- [21] E. Lindner, K. Gierling, R. Fawzi and M. Steimann, *Inorg. Chim. Acta..*, 1998, 13, 269.
- [22] Le. Gall, P. Laurent, E. Soulier, J. Y. Salaiin and H. D. Abbayes, *J. Organomet. Chem.*, 1998, 13, 567.
- [23] P. Braunstein, Y. Chauvin, J. Nahring, A. Decian and J. Fischer, *J. Chem. Soc., Dalton. Trans.*, 1995, 863.
- [24] P. Braunstein, Y. Chauvin, J. Fischer, H. Oliver, C. Strohmann and D. V. Toronto, *New. J. Chem.*, 2000, 24 (6), 437.
- [25] R. W. Wegman, A. G. Abatjoglou and A. M. Harrison, *J. Chem. Soc., Chem. Commun.* 1987, 1891.
- [26] G. K. Anderson and R. Kumar, *Inorg. Chim. Acta..*, 1985, L21, 97.
- [27] S. Kim, J. H. Reibenspies and M. Y. Darenbourg, *J. Am. Chem. Soc.*, 1996, 118, 4115.
- [28] M. Thomas and G. Suss-Fink, *Coord. Chem. Rev.*, 2003, 243, 125.
- [29] M. J. Baker , M. F. Giles, A. G. Orpen, M. J. Taylor and R. J. Watt, *J. Chem. Soc. Chem. Commun.*, 1995, 197.
- [30] (a) J. R. Dilworth, J. R. Miller, N. Wheatley, M. J. Baker and J. G. Sunley, *J. Chem. Soc. Chem. Commun.*, 1995, 1579; (b) L. Gonsalvi, H. Adams, G.J. Sunley, E. Ditzel and A. Hynes, *J. Am. Chem. Soc.*, 2000, 124, 13597.
- [31] T. C. Blagborough, R. Devis and P. Ivison, *J. Organometet. Chem.*, 1994, 467, 85.
- [32] C. Cauzzi, M. Graiff, G. P. Lanfranchi, and A. Tripicchio, *Inorg. Chim. Acta..*, 1998, 273, 320.
- [33] E. Lindner, Q. Wang, H. A. Mayer, R. Fawzi and M. Steimann, *Organometallics*, 1993, 12, 1865.

- [34] E. Lindner, Q. Wang, H. A. Mayer, A. Bader, H. Kuhbauch and P. Wegner, *Organometallics*, 1993, 12, 3291.
- [35] P. R. Ellis, J. M. Pearson, A. Haynes, H. Adams, N. A. Bailey and P. M. Maitlis, *Organometallics*, 1994, 13 (8), 3215.
- [36] T. R Griffin, D. B. Cook, A. Haynes, J. M. Pearson, D. Monti and G. E. Morris, *J. Am. Chem. Soc.*, 1996, 118, 3029.
- [37] E. Eduardo, M. Angles, A. Huet, A. C. Francisco, J. L. Farnando and L. A. Oro, *Inorg. Chem.*, 2000, 39 (21), 4868.
- [38] P. Paolo, B. Alessia, B. Carta, C. Mauro, C. Mireo, P. Corrado and C. Vivorio, *Organometallics*, 2000, 25, 19.
- [39] A. Doppiu, U. Englert, V. Peters and A. Salzer, *Inorg. Chim. Acta.*, 2004, 357, 1773.
- [40] P. Braunstein, Y. Chauvin, J. Nahring, A. Decian, J. Fischer, A. Tiripicchio and F. Uguzzoli, *Organometallics*, 1996, 15, 555.
- [41] D. N. Lawson, J.A. Osborn and G. Wilkinson, *J. Am. Chem. Soc.*, 1966, 1733.
- [42] G. Deganello, P. Uguagliati, B. Crociani and U. Belluco, *J. Chem. Soc. A.*, 1969, 2726.
- [43] F. Steel and T. A. Stephenson, *J. Chem. Soc., Dalton Trans.*, 1972, 2161.
- [44] F. Faraone, *J. Chem. Soc., Dalton Trans.*, 1975, 541.
- [45] A. Haynes, P.M. Maitlis, I. A. Stanbridge, S. Haak, J.M. Pearson, H. Adams and N.A. Bailey, *Inorg. Chim. Acta.* 2004, 357, 3027.
- [46] (a) P. Das, D. Konwar, P. Sengupta and D. K. Dutta, *Trans. Met. Chem.*, 2000, 25, 426; (b) A. Haynes, B. E. Mann, G. E. Morris and P. M. Maitlis, *J. Am. Chem. Soc.*, 1993, 115, 4093.
- [47] J. Rankin, A. D. Poole, A. C. Benyei and D. J. Cole - Hamilton, *J. Chem. Soc., Chem. Commun.*, 1997, 1835.
- [48] M. J. Howard, M. D. Jones, M. S. Roberts and S. A. Taylor, *Cat. Today.*, 1993, 18, 325.
- [49] M. J. Baker, J. R. Dilworth, J. G. Sunley and N. Wheatley, *US Patent.* 5, 1996, 488.
- [50] P. Braunstein, D. Matt, F. Mathey and D. Thavard, *J. Chem. Res. (S)*, 1978, 232.
- [51] D. Empsall, S. Johanson and B. L. Shaw, *J. Chem. Soc., Dalton Trans.*, 1980, 302.
- [52] C. A. Carraz, E. J. Ditzel, A. G. Orpen, D. D. Ellis, P. G. Pringle and G. J. Sunley *J. Chem. Soc., Chem. Commun.*, 2000, 1277.
- [53] D.E. Berry, J. Browning, K. R. Dixon and R. W. Hilts, *Can. J. Chem.*, 66, 1988, 1272.
- [54] S. R. Hall, B. W. Skelton and A. H. Hite, *Aust. J. Chem.*, 36, 1983, 267.
- [55] J. M. Brown, P. A. Chaloner and P. N. Nicholson, *J. Chem. Soc. Chem. Com.*, 1978, 646.
- [56] W. S. Knowels, M. J. Sabacky and B. D. Vineyard, *J. Chem. Soc. Chem. Com.*, 1972, 10.
- [57] J. M. Brown and B. A. Murrer, *Tet. Lett.*, 1980, 21, 581.
- [58] E. M. Miller and B. L. Shaw, *J. Chem. Soc., Dalton Trans.*, 1974, 480.
- [59] Y. Uozumi and T. Hayashi, *J. Am. Chem. Soc.*, 1991, 113, 9887.
- [60] E. Lindner and B. Karle, *Z. Natureforsch.*, 1990, 45, 1108.
- [61] J. C. Jeffrey and T. B. Rouchfuss, *Inorg. Chem.*, 1979, 18, 2658.
- [62] P. Braunstein, D. Matt and Y. Dusausoy, *Inorg. Chem.*, 1983, 22, 2043.
- [63] E. Lindner, M. Haustein, R. Fawzi, M. Steimann and P. Wegner, *Organometallics.*, 1994, 3, 5021.
- [64] E. Lindner, M. Geprags, K. Gierling, R. Fawzi and M. Steimann, *Inorg. Chem.*, 1995, 34, 6106.

- [65] M.M. Taqui Khan and Md. K. Nazeeruddin, *Inorg. Chim. Acta.*, 1988, 147, 33.
- [66] P. Braunstein, D. Matt, D. Nobel, S. E. Bouaoud, B. Carluer, D. Grandjean and P. Lemoine, *J. Chem. Soc., Dalton Trans.*, 1986, 415.
- [67] M. Bressan, F. Morandini and P. Rigo, *Inorg .Chim. Acta.*, 1983, L139, 77.
- [68] R. Sanger, *Can. J. Chem.*, 1983, 61, 2214.
- [69] G. K. Anderson and R. Kumar, *Inorg. Chem.*, 1984, 23, 4064.
- [70] D. Cauzzi, C. Graiff, M. Lanfranchi, G. Predieri and A. Tripicchio, *Inorg. Chim. Acta.*, 1998, 273, 320.
- [71] Del. Zotto, B. D. Ricca, E. Zangrando and P. Rigo, *Inorg. Chim. Acta.*, 1997, 261, 147.
- [72] T. S. Lobana, Coordination Chemistry of Phosphine Chalcogenides and their analytical and catalytic applications. In *the Chemistry of Organophosphorous Compounds*; F.R. Hartley, Ed.; Wiley: New York, 1992; Vol. 2; pp. 521.
- [73] T. S. Lobana, *Prog. Inorg. Chem.*, 1989, 37, 495.
- [74] P. Das, P. Chutia and D. K. Dutta, *Chem. Lett.*, 2002, 766.
- [75] G. Bandoli, D. A. Clementi, G. Deganello, G. Carturan, P. Uguagliati and U. Belluco, *J. Organomet. Chem.*, 1974, 71,125.
- [76] C. Paul, U. C. Sharma and R. K. Poddar, *Inorg. Chim. Acta.*, 1991, 179, 17.
- [77] P. Das, M. Baruah, N. Kumari, M. Sharma, D. Konwar and D.K. Dutta, *J. Mol. Cat. A (Chemical)*, 2002, 178, 283.
- [78] P. Das, M, Sharma, N. Kumari, D. Konwar and D. K. Dutta, *Appl. Organomet. Chem.*, 2002, 16, 302.
- [79] P. Chutia, M. Sharma, P. Das, N. Kumari, J. D. Woollins, A. M. Z. Slawin and D. K. Dutta , *Polyhedron*, 2003, 22, 2725.
- [80] P. Chutia, N. Kumari, M. Sharma, J. D. Woollins, A. M. Z. Slawin and D. K. Dutta, *Polyhedron*, 2004, 23, 1657.
- [81] D. K. Dutta, P. Chutia, J. D. Woollins and A. M. Z. Slawin, *Inorg. Chim. Acta.* 2006, 359, 877.
- [82] D. K. Dutta, J. D. Woollins, A. M. Z. Slawin, D. Konwar, M. Sharma, P. Bhattacharyya and S.. M. Aucott, *J. Organomet. Chem.* 2006, 69, 1229-1234.
- [83] P. Chutia, B. Jyoti Sarmah and D. K. Dutta, *Appl. Organomet. Chem.*, 2006, 20, 512.
- [84] H. A. Mayer and W. C. Kaska, *Chem. Rev.* 1994, 94, 1239.
- [85] H. E-Amouri, A.A. Bahsoun, J. Fischer and J.A. Osborn, *Angew. Chem. Int. Ed. Engl.*, 1987, 26, 1169.
- [86] G.F. Holland, D.E. Ellis, D.R. Tylor, H.B. Gray and W.C. Trogler, *J. Am. Chem. Soc.*, 1987, 109, 4276.
- [87] W.O. Siegel, S.J. Laporte, and J.D. Collman, *Inorg. Chem.*, 1971, 10, 2158.
- [88] M.M. Taqui Khan and A.E. Martell, *Inorg. Chem.*, 1974, 13,
- [89] T. Horvath and G. Kiss, *Organometallics*, 10, 1991, 3798.
- [90] J. Otto, L.M. Vananzi, C. A.Ghilardi, S. Midollini and A. Orlandini, *J. Organomet. Chem.*, 1985, 291, 89.
- [91] D. Rouscher, E.G. Thaler, J.C. Huffman and K.G. Caulton, *Organometallics*, 1991, 10, 2209.
- [92] C. Bianchini, E. Farnetti, M. Graziani, M. Pwruzzini and A. Polo, *Organometallics*, 1993, 12, 3753.
- [93] M.J. Burk and R.I. Harlow, *Angew. Chem. Int. Ed. Engl.*, 1990, 29, 1467.

- [94] T.R. Ward, L. M. Vananzi, F. Lianza, T. Gerfin, V. Gramlich and G. M. Ramos Tomba, *Helv. Chim. Acta.* 1991, 74, 983.
- [95] D. Dubois and D.W. Meek, *Inorg. Chim. Acta.*, 1976, 19, L.29.
- [96] A. M. Gull, P.E. Fanwick and C. P. Kubiak, *Organometallics*, 1993, 12, 2121.
- [97] J. B. Letts, T.J. Mazanec and D.W. Meek, *Organometallics*, 1983, 2, 695.
- [98] G. Jia and D.W. Meek, *Inorg. Chim. Acta.*, 1990, 178, 195.
- [99] T. Suzuki, T. Imamura, S. Kaizaki and K. Kashiwabara, *Polyhedron*, 2002, 21, 835.
- [100] T. Suzuki, T. Tsukuda, K. Kiki, S. Kaizaki, K. Isobe, H.D. Takagi and K. Kashiwabara, *Inorg. Chim. Acta.*, 2005, 358, 2501.
- [101] W. Heins, P. Stobel, H.A. Mayer, R. Fawzi and M. Steimann., *J. Organomet. Chem.* 1999, 587, 258.
- [102] K. J. Beckett and S. J. Loeb, *Can. J. Chem.*, 1988, 66, 1073.
- [103] K. Heinze, G. Huttner and L. Zsolnai, *Chem. Ber.*, 1997, 130, 1393.
- [104] R. Colton and T. Whyte, *Aust. J. Chem.*, 1991, 44, 525.
- [105] S. W. Car and R. Colton, *Aust. J. Chem.*, 1981, 34, 35.
- [106] P. A. W. Dean and M. K. Hughes, *Can. J. Chem.*, 1980, 58, 180.
- [107] S. O. Grim and E.D. Walton, *Phosphorus and Sulfur*, 1980, 9, 123.
- [108] S.O. Grim, S. A. Sangokoya and E. Delaubenfels, *Phosphorus and Sulfur*, 1988, 38, 79.
- [109] C. Bianchini, C. Mealli, A. Mali and M. Sabat, . *J. Am. Chem. Soc*, 1985, 107, 5317.
- [110] C. Bianchini, D. Masi, C. Mealli, A. Meli and M. Sabat. *Inorg. Chem.*, 1988, 27, 3716.

Chapter 9

ELECTRONIC PROPERTIES OF TRANSITION METAL CARBENE AND SILYLENE COMPLEXES - A QUANTUM CHEMICAL STUDY AT SELECTED MODEL COMPLEXES

Uwe Böhme*

Institut für Anorganische Chemie, TU Bergakademie Freiberg
Leipziger Str. 29, 09596 Freiberg, Germany

ABSTRACT

Common features and principal differences between carbene and silylene complexes of early and late transition metals are analyzed from a quantum chemical point of view. $\text{Cp}_2\text{Ti}=\text{EH}_2$ and $(\text{OC})_4\text{Fe}=\text{EH}_2$ with E= C, Si were chosen as representative examples for that purpose. The nature of the transition metal carbon and silicon bond was analyzed with CDA, NBO and the EHT-method. The distinctive properties of transition metal silylene complexes are caused by two main reasons: the silylene substituent acts mainly as σ -donor, and there is very weak π -bonding in silylene complexes.

Keywords: Silylene Complexes, Carbene Complexes, Iron, Titanium, Quantum Chemical Calculations.

INTRODUCTION

Transition metal carbene complexes were already discovered in the early years of organometallic chemistry [1]. Since then exciting reactions [2] with these complexes have been found and a number of useful applications were developed [3,4,5,6]. In contrast to that, transition metal silylene complexes have been explored only during the last decade

* Uwe Böhme: e-mail: uwe.boehme@chemie.tu-freiberg.de

[7,8,9,10,11,12,13,14,15,16]. The preparative potential of these compounds is mainly unexplored. Detailed quantum chemical investigations at transition metal carbenes and higher homologues have been published earlier [17].

This article is focused on common features and principal differences between carbene and silylene complexes of early and late transition metals from a quantum chemical point of view. The bonding properties of the metal carbon and metal silicon bond were investigated for that purpose at the model compounds 1 to 4 (Fig. 1). The molecules were optimized with DFT methods and the electronic properties were analyzed with CDA, NBO and the EHT-method.

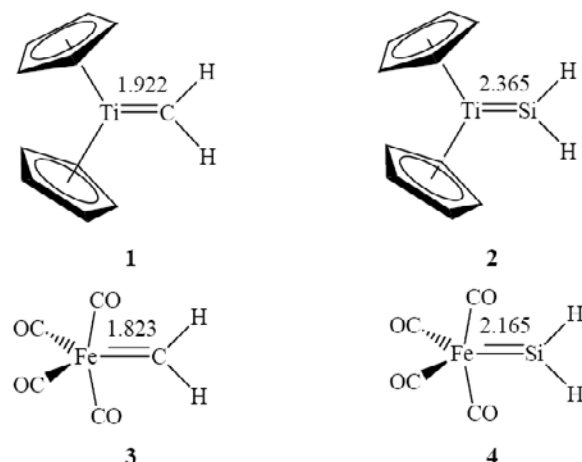


Figure 1. Selected examples for Schrock-carbene / -silylene (top) and Fischer-carbene / -silylene (bottom). M-E-bond lengths in Å.

CHARGE-DECOMPOSITION-ANALYSIS (CDA)

CDA is a method of population analysis on the basis of orbital interactions [18]. This method allows the analysis of donor-acceptor interactions. Synergetic interactions between donor and acceptor are analyzed quantitatively with this method according to the Dewar-Chatt-Duncanson-model [19, 20]. The σ -donor bond from the ligand to the metal and the π -back bond from the metal to the ligand are considered as the most important factors of the interaction. The CDA builds the wavefunction of the complex $L_nM \cdot D$ as linear combination of the molecule orbitals of the donor D and the complex fragment L_nM . Both fragments must have closed shell configuration. The contributions of the orbitals of both fragments to the wavefunction of the molecule are decomposed into four different interactions:

d - interaction of occupied MOs of D with unoccupied MOs of L_nM
(donor bond $D \rightarrow ML_n$)

b - interaction of unoccupied MOs of D with occupied MOs of L_nM
(back donation $D \leftarrow ML_n$)

r - interaction of occupied MOs of D with occupied MOs of L_nM

(repulsive polarization $D \leftrightarrow ML_n$)

Δ - interaction of unoccupied MOs of D with unoccupied MOs of L_nM
(rest term)

The last term should not contribute to the electronic structure of the complex and should have values equal or close to zero. A considerable deviation of Δ from zero hints to the fact, that the bond under investigation has the character of a normal covalent bond between two fragments with non-closed shell configuration and therefore this interaction cannot be considered as donor-acceptor interaction. The donor bond and the back donation are calculated separately for every molecule orbital. This allows to evaluate the contributions of the σ -bond from the ligand to the metal and the π -back donation from the metal to the ligand to the overall interaction. The CDA-method can be performed on the basis of orbitals from Hartree-Fock- or with Kohn-Sham-orbitals from DFT-calculations.

The results of the CDA are summarized in table 1. The compounds 1 to 4 were divided for that purpose into the fragments Cp_2Ti , $(OC)_4Fe$ and SiH_2 , CH_2 respectively and the interaction of the orbitals of the fragments were analyzed. The residual value Δ is too large for the Schrock-complexes 1 and 2. Therefore the bonds between the titanium atom and Si and C respectively in these two compounds cannot be regarded as donor-acceptor interactions between closed-shell fragments. These are interactions between open-shell fragments according to the bonding model of Taylor and Hall [21]. The residual value for the compounds 3 and 4 is nearly zero, this justifies to consider these complexes as donor-acceptor complexes. If someone compares the values for electron donation (d) and back bonding (b) it is obvious that the silylene fragment in 4 is a stronger donor than the carbene fragment in 3. The values for back bonding are nearly equal in both complexes.

The electron density at the bond critical point between the transition metal and C or Si respectively gives further information [22]. The carbene complexes 1 and 3 (0.951 and 1.032 $e\cdot\text{\AA}^{-3}$) have substantial more electron density at the bond critical point than the silylene complexes 2 and 4 (0.506 and 0.655 $e\cdot\text{\AA}^{-3}$, see table 1).

Table 1. CDA results and electron density at the bond critical points for the compounds 1-4

molecule	d	b	r	Δ	ED
$Cp_2Ti=CH_2$ (1)	0.426	0.003	-0.217	0.413	0.951
$Cp_2Ti=SiH_2$ (2)	0.131	0.036	-0.050	0.046	0.506
$(OC)_4Fe=CH_2$ (3)	0.477	0.378	-0.332	0.003	1.032
$(OC)_4Fe=SiH_2$ (4)	0.540	0.384	-0.373	0.008	0.655

(d – electron donation; b – back donation; r - repulsive polarization; Δ - residual value; ED – electron density at the bond critical point between transition metal and C or Si in $e\cdot\text{\AA}^{-3}$).

NATURAL BOND ORBITAL ANALYSIS (NBO)

An alternative description of the chemical bonding between a transition metal atom and its surrounding atoms is provided by the natural bond orbital analysis (NBO). This method developed by Weinhold et al. [23] uses the one-electron matrix as starting point to find the

best Lewis structure of the molecule. Bond polarizations, hybridizations of the atoms, partial charges and the electron configuration of the atoms can be concluded from this method. The NBO-method has been described previously in detail [23]. Through a series of mathematical operations the molecular orbital wavefunction is transformed to a NBO wavefunction consisting of highly occupied one-center (lone pair) and two-center (bond) orbitals, and formally unoccupied one-center Rydberg and two-center antibonding orbitals [24]. This set of orbitals corresponds to the localized “natural Lewis structure” and serves as a zeroth-order description of the system. Delocalization effects from this Lewis structure are taken into account by a charge transfer from the highly occupied bond orbitals into unoccupied orbitals. The energy lowering achieved by these donor-acceptor interactions can be described by a second-order perturbative treatment of the Fock-matrix in the NBO-basis.

The Wiberg-bond index (BO) [25] is calculated as sum of the quadratic non-diagonal elements of the density matrix between two atoms. This is done in the NAO-basis. The index has always positive values, therefore one cannot differentiate between bonding and antibonding character of the interaction between the two atoms.

Further conclusions about the bonding properties can be drawn from the NBO-analysis. The main results with respect to the MC- and the MSi-bonds of the four compounds under investigation are summarized in table 2. The titanium atoms in the complexes 1 and 2 have a substantial higher positive charge than the iron atoms in 3 and 4. This is caused by the more electropositive character of the titanium atom and the different ligand environment at the metal atoms. The carbene carbon atom is negatively charged in the compounds 1 (- 0.67) and 3 (- 0.53). In contrast to that the more electropositive silicon atom is positively charged in the 2 (+ 0.48) and 4 (+ 0.57). The Wiberg bond index is substantial larger than 1.00 for the metal carbon and the metal silicon bond in the Schrock-complexes (1.59 for 1 and 1.41 for 2). The Fischer complexes 3 and 4 have drastically reduced bond indices. That means the ME-bond in the Schrock-complexes have a substantial higher double bond character. The differences in the bond order become plausible if someone looks at the polarity of the ME-bond. The polarity might be derived from the percentage share of the atomic orbital of the metal to the bond orbital (% M in table 2). The ME-bonds in the Schrock-complexes are rather less polar. The titanium atom has a share of 31.5 (1) and 40.3 % (2) of the σ -bond and 53.8 and 59.7 % of the π -bond. In contrast to that the ME-bonds in the Fischer-complexes 3 and 4 are quite more polar. The share of the iron atom of the σ -bond is only 16.6 (3) and 37.8% (4) respectively. The π -orbitals are mainly localized at the iron atom (83.4 % in 3 and 79.3 % in 4). This corresponds to the classical description of bonding interactions in Fischer-complexes as coupling of singlet fragments according to Taylor and Hall [26].

Table 2. Results of the NBO-analysis for the compounds 1-4

molecule	q (Fe, Ti)	q (C, Si)	BO	Occ	%M
$Cp_2Ti=CH_2$ (1)	0.72	-0.67	1.59	σ 1.96	31.5
				π 1.90	53.8
$Cp_2Ti=SiH_2$ (2)	0.24	0.48	1.41	σ 1.92	40.3
				π 1.84	59.7
$(OC)_4Fe=CH_2$ (3)	-0.44	-0.53	0.93	σ 1.53	16.6
				π 1.84	83.4
$(OC)_4Fe=SiH_2$ (4)	-0.61	0.57	0.75	σ 1.62	37.8
				π 1.79	79.3

Table 2. (Continued).

	bond	AO of the metal atom (%)				AO of C or Si (%)		
		s	p	d	f	s	p	d
(1)	σ	16.8		83.1		42.9	57.1	
	π		0.70	99.3			100	
(2)	σ	22.0		77.9		46.4	53.4	0.2
	π			99.8			99.7	0.3
(3)	σ	14.9	34.8	49.8	0.5	37.7	62.3	
	π		0.3	99.7			100	
(4)		49.8	0.1	50.1		44.7	55.2	0.1
	π		0.1	99.9			99.7	0.3

(q – charge of the atom, BO –Wiberg bond index, Occ – occupancy of the bond, % M –share of the atomic orbital of the metal atom to the molecule orbital in %, AO – atomic orbitals which contribute to the bonds in %).

FRAGMENT ORBITAL ANALYSIS

A fragment orbital analysis with the EHT method [26,27,28,29,30] was performed additional to the bonding analyses. The interaction of the frontier orbitals of the fragments are shown in Figure 2 and 3. The MO's of the titanium complexes **1** and **2** were constructed from the fragments Cp_2Ti , CH_2 and SiH_2 respectively as shown in Figure 1. All these fragments and the resulting molecules have C_{2v} -symmetry, therefore the orbitals have a_1 - or b_2 -symmetry. The bent titanocene fragment has three frontier orbitals which are denoted as $1a_1$, b_2 and $2a_1$ [29]. The shape of these orbitals is sketched in Figure 1. The occupation of the fragment MO's is done according to the model of Taylor and Hall as interaction of triplet fragments, since the fragment orbital analysis with the EHT-method does not give any information about the electronic state of the system.

The fragments methylene and silylene have frontier orbitals of a_1 - and b_2 symmetry. These orbitals form σ - and π -bonds with the transition metal fragment according to their symmetry along the bonding axis. The fragment orbitals of carbene and silylene and the resulting molecule orbitals of $Cp_2Ti=CH_2$ (1) und $Cp_2Ti=CH_2$ (2) have the same order and similar shape. The fragment orbitals of SiH_2 have substantial higher energy compared to the orbitals of CH_2 . This leads to differences in the energy of the resulting molecule orbitals. The σ - and π -bonding orbitals of $Cp_2Ti=SiH_2$ (2) have higher energy than the corresponding orbitals of $Cp_2Ti=CH_2$ (1). Similar differences have been found between cationic ruthenium carbene- and silylene-complexes $[CpL_2Ru=EX_2]^+$ with $E = C, Si$ [31].

The empty nonbonding orbitals of 1 and 2 have very similar energy. The nonbonding orbital of 1 has mixed in the a_1 orbital of CH_2 . The nonbonding orbital of 2 is exclusively localised at the titanocene fragment.

Some qualitative conclusions can be drawn from the energetic differences of the MOs: Titanocenesilylene (2) is stronger nucleophile, easier to oxidize and kinetic less stable than titanocenecarbene (1). This statement should be valid also for the comparison of other Schrock-silylenes with their structural analogous carbenes.

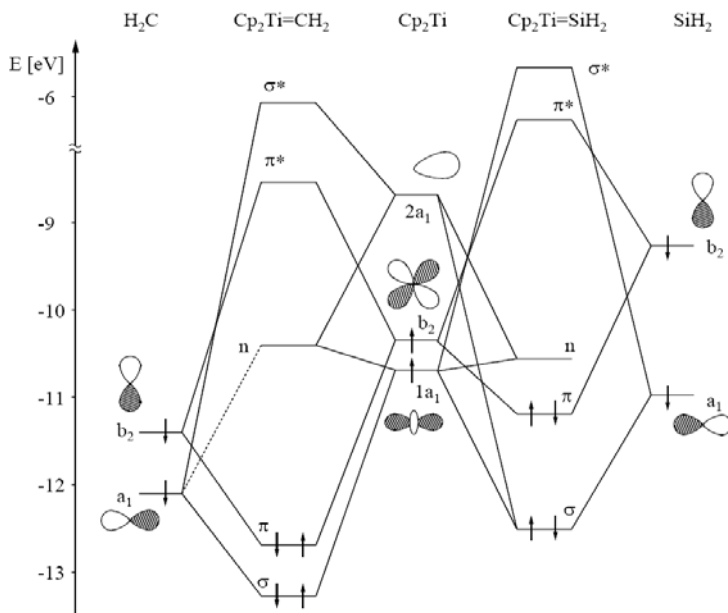


Figure 2. Fragment orbital analysis of 1 and 2.

The Fischer-complexes 3 and 4 have been divided into fragments in the same way (Figure 3). The fragment (OC)₄Fe has also C_{2v}-symmetry, therefore we find the same Mulliken-symbols for the fragment orbitals as before. The (OC)₄Fe-fragment has 16 valence electrons, leading to occupied 1a₁- and b₂-orbitals. The fragment orbitals were filled with electron pairs according to the bonding model of Taylor and Hall, which proposes an interaction of singulet fragments for these complexes. The combination of the (OC)₄Fe-fragment with CH₂ or SiH₂ leads to complexes with 18 valence electrons. Therefore the nonbonding MO is also occupied in 3 and 4.

The order of the molecule orbitals is the same, the shape of the orbitals is similar in 3 and 4. The higher energy of the frontier orbitals of the silylene fragment causes again some differences in the energetic position of the resulting MOs of 4 compared to the MOs of 3. The HOMO of (OC)₄Fe=SiH₂ (4) has higher energy compared with the HOMO of 3. Therefore 4 should be a stronger nucleophile than 3. The π-orbital of 4 should be localised mainly at the iron atom due to the big energy gap between the b₂-orbital of (OC)₄Fe and the b₂-orbital of SiH₂. Vice versa the π*-orbital should be localised mainly at the silicon atom. This is in fact the case as one can see in Figure 4 (right). The π-orbitals in (OC)₄Fe=CH₂ (3) are localised at the iron atom and at the carbon atom (Figure 4, left).

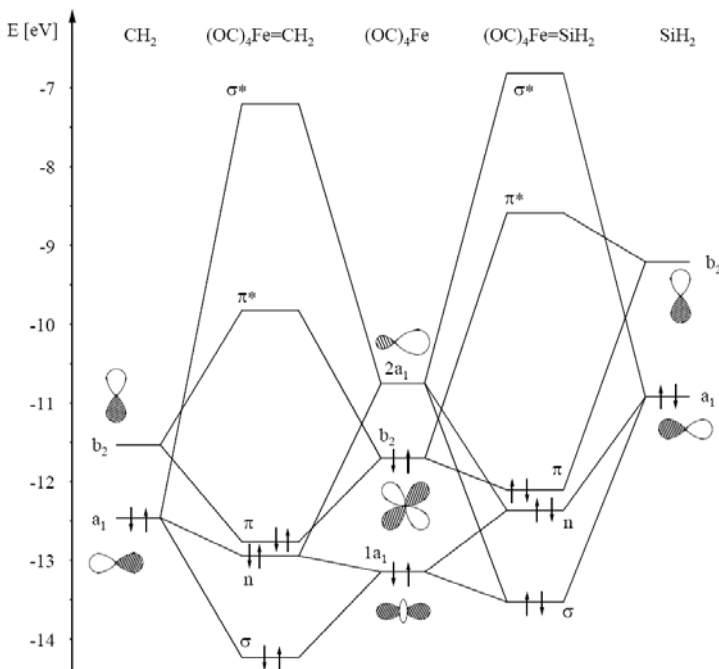


Figure 3. Fragment orbital analysis of 3 and 4.

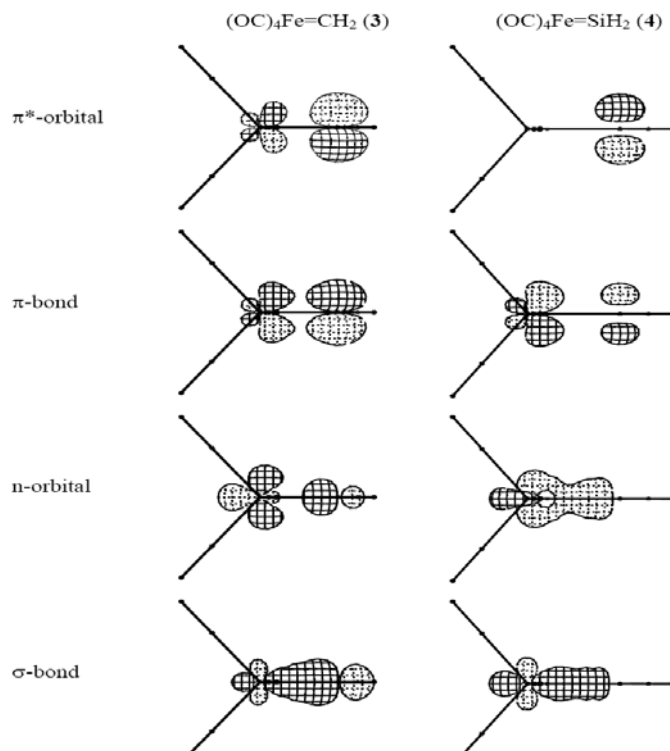


Figure 4. Selected molecular orbitals of 3 (left) and 4 (right).

CONCLUSION

With the differences in the electronic properties described above one can explain the different reactivity of these compounds. The high energy HOMO of $(OC)_4Fe=SiH_2$ (4) causes stronger nucleophilicity. An electrophilic attack should occur preferably at the iron atom, whereas a nucleophilic attack should occur preferably at the silicon atom due to the unequal distribution of the coefficients of the π -orbitals. The numerous donor adducts of transition metal silylenes [32,33,34] are excellent examples for a nucleophilic attack at the silicon atom.

Obviously the very weak π -bonding in transition metal silylenes is the key to understand the different bonding properties in transition metal carbenes and silylenes [17, 35]. The silylene substituent acts mainly as σ -donor and accepts the coordination of additional donor ligands due to the weak back bonding from the transition metal atom.

Quantum Chemical Calculations

The DFT calculations have been performed with the programme suite GAUSSIAN 03 [36]. The molecular geometries of **1** to **4** have been fully optimized. Becke's three parameter hybrid exchange functional in combination with the correlation functionals of Lee, Yang und Parr (B3LYP) was the used DFT method [37,38]. Geometry optimizations and frequency calculations have been performed with an effective core potential and a valence double zeta basis set for titanium and iron [39] and the basis set 6-31G* for all main group elements [40,41]. An additional polarization function of f-type has been used for the elements iron and titanium [42]. The optimized geometries were characterized as minima with 0 imaginary frequencies by calculating the Hessian matrices. Full geometric parameters of the optimized molecules can be obtained on request from the author.

The NBO-analysis [23] has been performed with the programme code implemented in GAUSSIAN 03 (NBO version 3). The bond critical points [22] were analysed using the AIMPAC programs which can be obtained from the official Atoms in Molecules Download Site at <http://www.chemistry.mcmaster.ca/aimpac/>. Extended Hückel calculations were performed with CACAO using the default atom parameters of the software package [30].

ACKNOWLEDGMENT

The author thanks the Bundesland Sachsen for financial support and the computing centre of the TU Bergakademie Freiberg for computing time and support during installation of programmes.

REFERENCES

- [1] E. O. Fischer, A. Maasböl, *Angew. Chem.* 1964, **76**, 645; *Angew. Chem. Int. Ed. Engl.* 1964, **3**, 580.
- [2] For a concise introduction see: Ch. Elschenbroich , A. Salzer, *Organometallics*, Second Edition, Wiley-VCH, Weinheim 2005, 210.
- [3] K. H. Dötz, *Angew. Chem.* 96 (1984) 573-594.
- [4] F. Z. Dörwald, *Metal Carbenes in Organic Synthesis*, Wiley-VCH, Weinheim 1999.
- [5] J. R. Stille, Transition Metal Carbene Complexes: Tebbe's Reagent and Related Nucleophilic Alkylidenes; in Comprehensive Organomet. Chem. (Eds.: E. W. Abel, F. G. A. Wilkinson, G. Stone), Pergamon, Oxford, 1995, Vol. 12, 577-599.
- [6] R. H. Grubbs, R. H. Pine, *Alkene Metathesis and Related Reactions*; in *Comprehensive Organic Synthesis*. (Ed.: B. M. Trost), Pergamon, New York, 1991, 5, 1115-1127.
- [7] C. Zybill, Topics in Current Chem. 1991, **160**, 1-45.
- [8] S. D. Grumbine, T. D. Tilley, F. P. Arnold, A. L. Rheingold, *J. Am. Chem. Soc.*, 1993, **115**, 7884-7885.
- [9] S. K. Grumbine, T. D. Tilley, F. P. Arnold, A. L. Rheingold, *J. Am. Chem. Soc.*, 1994, **116**, 5495-5496.
- [10] M. Denk, R. K. Hayashi, R. West, *J. Chem. Soc., Chem. Commun.* 1994, 33-34.
- [11] B. Gehrhus, P. B. Hitchcock, M. F. Lappert, H. Maciejewski, *Organometallics*. 1998, **17**, 5599-5601.
- [12] S. K. Grumbine, G. P. Mitchell, D. A. Straus, T. D. Tilley, A. L. Rheingold, *Organometallics*. 1998, **17**, 5607-5619.
- [13] T. A. Schmedake, M. Haaf, B. J. Paradise, D. Powell, R. West, *Organometallics*. 2000, **19**, 3263-3265.
- [14] T. A. Schmedake, M. Haaf, B. J. Paradise, A. J. Millevolte, D. R. Powell, R. West, *J. Organomet. Chem.* 2001, **636**, 17-25.
- [15] J. D. Feldman, J. C. Peters, T. D. Tilley, *Organometallics*. 2002, **21**, 4065-4075.
- [16] D. Amoroso, M. Haaf, G. P. Yap, R. West, D. E. Fogg, *Organometallics*. 2002, **21**, 534-540.
- [17] G. Frenking und N. Fröhlich, *Chem. Rev.* 2000, **100**, 717-774 and references cited therein.
- [18] S. Dapprich, G. Frenking, *J. Phys. Chem.* 1995, **99**, 9352-9362.
- [19] M. J. S. Dewar, *Bull. Soc. Chim. Fr.* 1951, **18**, C71-C79.
- [20] J. Chatt, L. A. Duncanson, *J. Chem. Soc.* 1953, 2939-2947.
- [21] T. E. Taylor, M. B. Hall, *J. Am. Chem. Soc.* 1984, **106**, 1576-1584.
- [22] R. F. W. Bader, *Atoms in Molecules. A Quantum Theory*, Oxford University Press, Oxford, 1990.
- [23] A. E. Reed, L. A. Curtiss, F. Weinhold, *Chem. Rev.* 1988, **88**, 899-926.
- [24] Explanation taken from: J. T. Nelson, W. J. Pietro, *Inorg. Chem.* 1989, **28**, 544-548.
- [25] K. Wiberg, *Tetrahedron*. 1968, **24**, 1083-1096.
- [26] R. Hoffmann, *J. Chem. Phys.* 1963, **39**, 1397-1412.
- [27] R. Hoffmann, W. N. Lipscomb, *J. Chem. Phys.* 1962, **36**, 2179-2189.
- [28] R. Hoffmann, W. N. Lipscomb, *J. Chem. Phys.* 1962, **37**, 2872-2883.
- [29] J. W. Lauher, R. Hoffmann, *J. Am. Chem. Soc.* 1976, **98**, 1729-1742.

- [30] C. Mealli, D. M. Proserpio, *J. Chem. Educ.* 1990, **67**, 399-402.
- [31] F. P. Arnold Jr., *Organomet.* 1999, **18**, 4800-4809.
- [32] C. Zybill, G. Müller, *Angew. Chem.* 1987, **99**, 683-684; *Angew. Chem., Int. Ed. Engl.* 1987, **26**, 669-670.
- [33] C. Zybill, G. Müller, *Organometallics.* 1988, **7**, 1368-1372.
- [34] D. A. Straus, T. D. Tilley, A. L. Rheingold, S. J. Geib, *J. Am. Chem. Soc.* 1987, **109**, 5872-5873.
- [35] T. R. Cundari, *Chem. Rev.* 2000, **100**, 807-818.
- [36] Gaussian 03, Revision C.02, M. J. Frisch, G. W. Trucks, H. B. Schlegel, G. E. Scuseria, M. A. Robb, J. R. Cheeseman, J. A. Montgomery, Jr., T. Vreven, K. N. Kudin, J. C. Burant, J. M. Millam, S. S. Iyengar, J. Tomasi, V. Barone, B. Mennucci, M. Cossi, G. Scalmani, N. Rega, G. A. Petersson, H. Nakatsuji, M. Hada, M. Ehara, K. Toyota, R. Fukuda, J. Hasegawa, M. Ishida, T. Nakajima, Y. Honda, O. Kitao, H. Nakai, M. Klene, X. Li, J. E. Knox, H. P. Hratchian, J. B. Cross, C. Adamo, J. Jaramillo, R. Gomperts, R. E. Stratmann, O. Yazyev, A. J. Austin, R. Cammi, C. Pomelli, J. W. Ochterski, P. Y. Ayala, K. Morokuma, G. A. Voth, P. Salvador, J. J. Dannenberg, V. G. Zakrzewski, S. Dapprich, A. D. Daniels, M. C. Strain, O. Farkas, D. K. Malick, A. D. Rabuck, K. Raghavachari, J. B. Foresman, J. V. Ortiz, Q. Cui, A. G. Baboul, S. Clifford, J. Cioslowski, B. B. Stefanov, G. Liu, A. Liashenko, P. Piskorz, I. Komaromi, R. L. Martin, D. J. Fox, T. Keith, M. A. Al-Laham, C. Y. Peng, A. Nanayakkara, M. Challacombe, P. M. W. Gill, B. Johnson, W. Chen, M. W. Wong, C. Gonzalez, and J. A. Pople, Gaussian, Inc., Wallingford CT, 2004.
- [37] A. D. Becke, *J. Chem. Phys.* 1993, **98**, 5648-5652.
- [38] C. Lee, W. Yang, R. G. Parr, *Physical Rev.* 1988, **B37**, 785-789.
- [39] P. J. Hay, W. R. Wadt, *J. Chem. Phys.* 1985, **82**, 270-283.
- [40] P.C. Hariharan, J.A. Pople, *Theoret. Chim. Acta.* 1973, **28**, 213-222.
- [41] M. M. Franci, W. J. Pietro, W. J. Hehre, J. S. Binkley, M. S. Gordon, D. J. DeFrees, J. A. Pople, *J. Chem. Phys.* 1982, **77**, 3654-3665.
- [42] A. W. Ehlers, M. Böhme, S. Dapprich, A. Gobbi, A. Höllwarth, V. Jonas, K. F. Köhler, R. Stegmann, A. Veldkamp, G. Frenking, *Chem. Phys. Lett.* 1993, **208**, 111-114.

INDEX

A

absorption spectra, 171
accelerator, 19, 20
access, 120, 168, 180, 216
accessibility, 168
acetic acid, x, 88, 114, 205, 249, 250, 252, 256, 262, 264, 265, 272, 273, 283
acetone, 64, 65, 109, 120
acetonitrile, 66, 125, 133
achievement, 62
acid, ix, x, 3, 4, 9, 18, 31, 34, 35, 41, 62, 63, 64, 88, 96, 197, 204, 205, 209, 210, 221, 223, 226, 228, 229, 250, 258, 283
acidity, 34, 41, 232
activation, x, 199, 214, 218, 250, 251, 257, 283
activation energy, 257
active site, ix, 167, 197, 198, 199, 201, 203, 206, 210, 214, 216, 217, 218, 219, 220, 225
additives, 88
adenocarcinoma, 20
adsorption, viii, 61, 64
agent, 7, 16, 27, 30, 32, 85, 88, 206
aggregation, 2
albumin, 26
alcohol(s), viii, x, 4, 18, 61, 62, 63, 91, 94, 250, 252, 257, 283, 284
aldehydes, 4, 35
aliphatic amines, 91
alkane, 281
alkenes, 35, 36
alkylation, 223
alkynyls, viii, 99, 100, 167
alternative(s), 4, 5, 6, 29, 30, 86, 95, 201, 206, 291
amines, viii, 4, 18, 24, 83, 88, 89, 90, 91, 201, 202, 218, 223
amino acid(s), 7, 9, 10, 24
ammonia, 201, 229
ammonium, 122, 202, 229, 231
anaerobic bacteria, 199

animal models, 11
animals, 12
anion, 2, 3, 4, 11, 17, 23, 24, 34, 35, 37, 38, 40, 41, 222
annihilation, 21
anthracene, 139
antibody, 16, 17, 24, 29
anti-cancer, 14, 32, 34
anticancer drug, 32, 222
antigen, 24
antitumor, vii, 1, 33, 222
Argentina, 20
arginine, 18
argument, 203
aromatic compounds, 2
arthritis, 20
aspartate, 18
assignment, 128, 171, 224
astatine, 27
asymmetric synthesis, 91
asymmetry, 213, 235, 238
atmospheric pressure, viii, 83, 84, 85, 86, 88, 89, 91, 92
atomic orbitals, 293
atoms, ix, 2, 4, 6, 16, 17, 23, 30, 62, 69, 71, 74, 101, 103, 104, 107, 108, 110, 113, 114, 115, 125, 128, 132, 133, 136, 137, 169, 187, 198, 199, 206, 207, 210, 211, 221, 225, 227, 235, 237, 238, 239, 241, 242, 244, 255, 260, 262, 266, 268, 269, 270, 278, 291, 292
attachment, vii, 1, 11, 16, 18, 21, 24, 27
attention, vii, 1, 7, 10, 13, 37, 40, 62, 101, 103, 105, 167, 168, 176, 223, 251, 260
autoimmune disease, 20
availability, 22

B

backlash, 217
bacteria, 198, 201

- bactericides, 222
 basicity, 210, 251
 batteries, 41
 behavior, viii, 39, 61, 62, 75, 78, 99, 106, 109, 111, 114, 121, 123, 124, 137, 181, 199, 233, 254, 255, 259, 265
 benzene, viii, 30, 34, 35, 41, 99, 100, 105, 120, 121, 122, 128
 binding, x, 10, 14, 17, 21, 24, 29, 30, 33, 63, 100, 118, 135, 200, 213, 214, 218, 226, 228, 250, 280, 283
 biological activity, 33, 222
 biological systems, 222, 225
 biomarkers, 168
 biomedical applications, ix, 221
 biomolecules, vii, 1, 9, 10, 21, 27, 29
 biotin, 17, 27, 28
 blood, 27
 bonding, ix, x, 2, 35, 107, 113, 179, 187, 221, 224, 225, 229, 230, 232, 233, 235, 238, 239, 242, 244, 250, 256, 267, 279, 289, 290, 291, 292, 293, 294, 296
 bonds, x, 2, 3, 4, 24, 36, 62, 63, 64, 69, 71, 85, 104, 106, 169, 189, 191, 222, 224, 225, 226, 227, 229, 233, 235, 238, 242, 250, 251, 256, 278, 279, 280, 283, 291, 292, 293
 boric acid, 3
 boron neutron capture therapy, 21
 brain, 12
 branching, 17
 breast cancer, 24
 bromine, 226
 building blocks, viii, ix, 7, 11, 99, 100, 106, 107, 108, 112, 114, 121, 125, 128, 129, 136, 137, 165, 166, 167
 burning, vii, 1, 5
 by-products, 63

C

- cadmium, 6
 calcium, 3
 Canada, 51
 cancer, vii, 1, 5, 6, 11, 14, 16, 18, 21, 27, 32, 34, 222
 cancer cells, 14, 16, 18, 21, 27, 32
 cancer treatment, vii, 1
 candidates, 7, 20, 41, 88, 166, 168, 176
 capillary, 94
 capital cost, 19
 carbohydrate(s), 7, 10, 17, 18
 carbon, vii, viii, ix, x, 4, 24, 35, 36, 64, 69, 70, 71, 76, 77, 83, 84, 85, 86, 88, 89, 91, 92, 94, 95, 99, 102, 103, 106, 107, 109, 120, 128, 136, 137, 165, 166, 181, 189, 190, 192, 218, 222, 229, 235, 236, 238, 242, 267, 284, 289, 290, 292, 294
 carbon atoms, 4, 35, 69, 71, 76, 104, 236
 carbon dioxide, 4
 carbon monoxide, viii, 83, 84, 85, 86, 88, 89, 91, 92, 95, 218, 267, 284
 carbonyl groups, 267, 278
 carboxylic acids, 17, 226
 carboxylic groups, 10
 carrier, 22, 198, 203
 catalysis, 84, 95, 121, 250, 251, 283, 284
 catalyst(s), vii, viii, x, 1, 34, 35, 36, 63, 66, 83, 84, 85, 86, 88, 89, 90, 91, 92, 93, 94, 120, 121, 123, 198, 199, 201, 205, 206, 216, 222, 249, 250, 251, 255, 257, 260, 262, 264, 265, 272, 273, 281, 283
 catalytic activity, 36, 252, 253, 257, 262, 265, 270, 273
 catalytic hydrogenation, 281
 catalytic properties, 101, 167, 217
 catalytic system, 89, 90
 cation, 35, 62, 64, 113, 173
 C-C, 103, 106, 108, 110, 115, 120, 121, 132, 137, 151, 156, 161, 228
 cell, vii, 1, 5, 7, 10, 14, 16, 17, 18, 22, 23, 24, 32, 33, 64, 85, 89, 94, 211, 212, 217, 222, 235, 236, 239, 242
 cell culture, 16
 cell growth, 14
 cell line(s), 32, 33
 cell membranes, 222
 cell surface, 10
 ceramic, 123
 cesium, 40
 chelates, 29, 233
 chemical properties, 4, 21
 chemical reactions, 174, 279
 chemical stability, 40, 41, 168, 176
 chemotherapy, 7, 20, 222
 China, 165, 192, 197, 216
 chiral catalyst, x, 249, 283
 chlorine, 70, 270
 chloroform, 4, 122
 cholesterol, 17, 18, 19, 31
 chromatography, 97, 166
 chromium, 105, 121
 circulation, 18
 cisplatin, 32, 33
 cisplatin resistance, 33
 cleavage, 24, 106, 218
 clinical trials, 6, 20
 cluster network, 223
 clusters, 6, 21, 29, 37, 38, 39, 102, 199, 224
 C-N, 97, 109, 120

- coatings, 40
cobalt, 4, 8, 9, 11, 38, 40, 104, 282
colon, 20
communication, 102, 105, 133, 173, 181, 189, 192
community, ix, 165, 197
competition, 29, 88
complement, 200
complexity, 225
components, 5, 18, 37, 41, 174, 176
composition, 10, 114, 135, 136
compounds, vii, viii, ix, 1, 2, 5, 6, 7, 10, 11, 13, 14, 16, 17, 18, 21, 24, 30, 31, 33, 35, 37, 38, 39, 62, 63, 72, 74, 80, 83, 85, 88, 99, 100, 101, 103, 106, 107, 108, 114, 115, 120, 122, 123, 124, 129, 133, 137, 165, 167, 169, 173, 176, 179, 180, 183, 184, 189, 191, 192, 197, 198, 207, 215, 221, 222, 223, 224, 225, 226, 227, 228, 230, 233, 253, 258, 290, 291, 292, 296
computed tomography, 21, 30
computing, 296
concentration, vii, 1, 5, 7, 16, 21, 209, 210, 271, 275
condensation, 11, 71, 132, 187
configuration, 123, 184, 235, 290, 291, 292
Congress, iv
conjugation, 16, 27, 29, 167, 168, 169, 171, 172, 173, 175, 181, 186, 191, 207
constraints, 279
construction, 2, 18, 38, 101, 166, 167
consumption, 2, 265
consumption rates, 2
contact time, 64
control, x, 100, 136, 137, 177, 249, 279, 283
conversion, 4, 35, 37, 211, 256, 264, 273
conversion rate, 211
copolymers, 176
copper, viii, 83, 85, 88, 89, 103, 106, 110, 111, 112, 116, 117, 119, 124, 126, 127, 129, 131, 133, 135
correlation(s), 174, 186, 225, 296
correlation function, 296
costs, 19
couples, 119, 124, 126
coupling, 17, 24, 25, 26, 29, 103, 104, 106, 108, 109, 114, 120, 121, 124, 126, 128, 133, 168, 169, 173, 177, 183, 187, 190, 191, 192, 214, 220, 224, 233, 279, 292
coupling constants, 279
covalent bond, vii, 62, 63, 222, 227, 291
covering, 167
CRR, 139
crystal structure, ix, 34, 66, 75, 165, 169, 177, 180, 187, 192, 197, 218, 224, 229, 238, 239, 241, 282
crystalline, 35, 39, 166, 169, 203, 225
crystalline solids, 169
crystallinity, 167
crystallographic studies, ix, 200, 221, 244
crystals, 38, 39, 237, 267, 278
culture, 16
curing, 250
currency, 2
cyanide, 4, 110, 131, 217
cycles, 41
cyclohexanol, 87
cyclopentadiene, 133
cytotoxic action, 222
cytotoxicity, 7, 21, 33
Czech Republic, 20

D

- decay, 21, 22, 23, 214, 271, 272, 274, 276, 278
decomposition, 34, 75, 127, 166
decomposition temperature, 166
definition, 198
degradation, 23, 26, 29
delivery, 5, 10, 14, 16, 17, 18, 20, 21
density, 166, 174, 218, 225, 251, 262, 291, 292
density functional theory, 166, 174, 218
derivatives, vii, viii, ix, 1, 3, 4, 9, 12, 14, 17, 18, 21, 24, 25, 26, 27, 28, 29, 30, 31, 33, 34, 37, 38, 40, 41, 62, 63, 67, 68, 69, 91, 96, 99, 115, 165, 167, 168, 169, 176, 177, 189, 190, 191, 192, 201, 210, 221, 222, 224, 225, 228, 229, 230
destruction, vii, 1, 11
detection, 21, 41, 109, 224
deviation, 169, 177, 235, 242, 267, 269, 279, 291
DFT, 166, 174, 186, 187, 200, 290, 291, 296
differentiation, 14, 17
diffraction, 207, 225
diffusion, 7, 23
digestion, 23
diluent, 40
dimer, 262
dimethylsulfoxide, 125
displacement, 239
disposition, 36, 169, 255, 278
dissociation, 29, 219, 231, 281
distilled water, 64
distribution, 23, 27, 63, 213, 233, 296
diversity, ix, 221, 223, 227
DMF, 91, 96
DNA, 7, 13, 14, 23, 32, 33
donors, x, 100, 226, 244, 249, 250, 260, 262, 265, 274, 283
dosage, 21
drugs, 6, 7, 10, 20, 93
drying, 64, 66

dyes, 14, 88

E

elaboration, 210
 electric field, 225
 electrical conductivity, 167
 electrocatalysis, 210, 216
 electrocatalytic, ix, 90, 197, 198, 209, 213, 214
 electrochemistry, viii, ix, 83, 84, 88, 95, 124, 165, 189, 199
 electrodes, vii, 1, 41, 84, 103
 electroluminescence, 100
 electrolysis, 85, 86, 89, 91, 96, 97, 210
 electrolyte, 84, 85, 89, 91, 107, 117, 119
 electron(s), vii, 2, 21, 22, 23, 24, 37, 38, 41, 84, 85, 88, 100, 101, 102, 103, 104, 105, 106, 108, 109, 111, 114, 118, 121, 124, 166, 168, 172, 173, 177, 179, 181, 188, 191, 198, 199, 205, 207, 209, 210, 211, 213, 214, 215, 220, 223, 225, 238, 251, 252, 253, 257, 262, 265, 270, 271, 273, 279, 291, 294
 electron density, 103, 172, 179, 191, 207, 213, 225, 251, 257, 262, 265, 270, 271, 279, 291
 electron diffraction, vii
 electron pairs, 238, 294
 electronic structure, 39, 174, 200, 218, 291
 electroreduction, 210, 214
 electrostatic interactions, 14
 emission, 21, 22, 23, 29, 64, 176, 214, 215, 225
 emitters, 20
 energy, 5, 19, 20, 21, 22, 23, 30, 38, 100, 104, 126, 171, 174, 179, 181, 187, 198, 204, 205, 211, 215, 216, 218, 219, 231, 250, 271, 292, 293, 294, 296
 energy density, 5
 energy transfer, 5, 23, 215
 England, 245
 environment, viii, 65, 71, 73, 74, 75, 76, 83, 84, 103, 127, 131, 225, 228, 238, 241, 242, 262, 269, 292
 enzymes, ix, 7, 16, 197, 199, 217, 225
 epidermal growth factor, 16, 17, 27
 equilibrium, 36, 233
 ESI, 135, 136
 ESR, 104
 ester, x, 38, 250, 255, 262, 263, 264, 272, 283
 estradiol, 30, 31
 estrogen, 30
 ethanol, 92, 188, 258
 ethyl acetate, 97
 ethylene, 152, 255
 Europe, 20
 European Union, 20
 evolution, ix, 197, 198, 200, 205, 210, 214, 216, 219, 220

excision, 20
 excitation, 174
 excretion, 23
 exocytosis, 23
 experimental condition, 191, 252, 265, 273
 exposure, 23, 117, 127
 extinction, 171, 181
 extraction, vii, 1, 40

F

family, 2, 23, 40, 105, 129, 230
 family members, 23
 fatigue, 62
 ferrocenyl, ix, 104, 105, 121, 122, 123, 133, 155, 156, 165, 166, 167, 169, 172, 174, 176, 177, 179, 180, 181, 184, 186, 188, 189, 190, 191
 ferromagnets, 38
 fillers, 40
 financial support, 137, 296
 Finland, 20
 first generation, 104
 fission, vii, 1
 flexibility, 282
 fluid, 38
 fluorescence, 64, 215
 fluorine, 34
 folate, 17
 folic acid, 17, 18
 formaldehyde, 4, 201, 202, 218, 256
 fragmentation, 116, 119
 free volume, 77
 FTIR, 190, 200, 218
 fuel, 2, 201, 214, 217, 219
 fullerene, 35, 37
 furan, 167

G

gamma rays, 22
 gases, 91
 gene, 20, 31
 gene therapy, 20
 generation, 7, 17, 20, 166, 188, 217, 251, 253
 geography, 20
 Germany, 99, 138, 146, 162, 192, 193, 289
 gifted, 2
 glass, 65, 94
 glioblastoma, 12, 20
 glioblastoma multiforme, 20
 glioma, 12, 14
 glucose, 17

- glycine, 18
glycol, 40
goals, 166
gold, 110, 120, 121, 133, 160
government, 2
grants, 42
graphite, viii, 83, 84, 85, 88, 89, 91
Grignard reagents, vii
groups, viii, 3, 4, 7, 10, 16, 17, 21, 24, 26, 27, 29, 37, 38, 39, 61, 62, 63, 69, 70, 71, 72, 73, 74, 75, 76, 77, 78, 100, 103, 104, 105, 108, 113, 115, 118, 123, 124, 133, 136, 167, 168, 169, 170, 172, 173, 177, 179, 181, 186, 187, 189, 191, 198, 202, 215, 222, 223, 224, 226, 227, 231, 233, 237, 238, 240, 241, 242, 260, 267, 278, 279
growth, 17, 18, 20, 30, 211, 271, 272
growth factor, 17, 18

H

- half-life, 21, 22, 23, 29
halogen(s), 22, 23, 24, 34, 85, 222, 223
H-bonding, 30
health, 23
health care, 23
health care professionals, 23
heat, 222
heating, 66
heating rate, 66
height, 209
heterogeneity, 17
hexane, 65, 66, 97, 188, 268, 269
higher quality, 22
histidine, 30
HIV, 88
homogeneous catalyst, x, 249, 250, 283
homopolymers, 176
Honda, 298
Hong Kong, 165, 192
hospitals, 19, 21
host, 41
hybrid, 296
hybridization, 181
hydrazine, 2
hydrides, vii, 1, 2, 3, 4, 5, 10, 18, 22, 30, 36, 37, 38, 39, 41, 42, 202
hydrocarbon fuels, 2
hydroformylation, x, 250, 251, 279, 280
hydrogen, ix, 2, 3, 4, 34, 41, 62, 63, 118, 197, 198, 199, 200, 205, 214, 216, 217, 219, 220, 221, 222, 229, 230, 232, 233, 235, 236, 237, 239, 240, 241, 242, 244, 251
hydrogen atoms, 3, 4, 118
hydrogen bonds, 62, 63, 229, 235, 237, 240, 242
hydrogen fluoride, 34
hydrogenation, x, 35, 36, 250, 251, 257, 279, 281, 283
hydrolysis, 71, 74, 96, 225
hydrophobic interactions, 30
hydrophobicity, 10
hydrosilylation, viii, 61, 63, 71, 72, 73, 74, 75, 76, 78, 257
hydroxide, 222
hydroxyl, 11
- I
- identity, 119
images, 22
imaging, 21, 22, 23, 29, 30
immobilization, 62, 63, 69
immunoreactivity, 16, 17, 24
immunotherapy, 20
implementation, 20
impurities, 65, 75, 77, 78
in situ, 3, 4, 203, 274
in transition, 296
in vitro, 14, 24, 27, 32, 33
in vivo, 6, 14, 16, 21, 23, 27, 29, 30, 222
India, 260
indices, 292
industrial application, 221, 226
industrial production, 5
industry, 38, 63, 168, 222
inflammation, 20
infrared spectroscopy, 166, 218
inhibition, 218
insertion, 4, 252, 253
insight, 219
instability, 110, 129
instruments, 21
insulation, 40
integrin, 18
intensity, 74, 75, 171, 181, 209, 211, 231, 274, 275, 276, 278
interaction(s), vii, x, 1, 22, 23, 36, 37, 38, 39, 84, 102, 106, 111, 115, 124, 125, 126, 136, 167, 172, 177, 181, 191, 207, 210, 225, 232, 242, 249, 251, 262, 263, 267, 278, 283, 290, 291, 292, 293, 294
internalization, 23
internalizing, 23, 26
interpretation, 210, 213
iodine, 3, 30, 226
ionization, 22, 187
ionization potentials, 187

ions, viii, 5, 21, 29, 35, 62, 64, 83, 89, 112, 117, 121, 124, 125, 126, 131, 132, 229, 250, 251
 IR, viii, ix, 61, 64, 65, 68, 69, 71, 72, 73, 75, 104, 113, 136, 149, 155, 166, 177, 181, 191, 197, 202, 203, 204, 207, 210, 211, 212, 213, 215, 252, 259, 265, 268, 270, 273, 274, 275, 278
 IR spectra, 68, 71, 73, 75, 191, 204, 211, 212, 213, 274, 275
 IR spectroscopy, 252, 265, 273
 Iran, 221, 245
 iridium, x, 35, 120, 121, 249, 250, 251, 281, 283
 iron, ix, 38, 104, 106, 108, 119, 121, 127, 133, 169, 177, 179, 181, 191, 192, 197, 199, 200, 202, 207, 209, 213, 214, 216, 217, 218, 219, 220, 292, 294, 296
 irradiation, 19, 20
 ISC, 166
 isolation, 35
 isomerization, 4
 isomers, 9, 203
 isotope, 5, 6, 22, 29, 135, 225, 231
 Italy, 83

J

Japan, 20, 61, 78
 joints, 20
 Jordan, 54, 55, 164

K

KBr, 64
 ketones, 35
 kidneys, 24
 killing, 5
 kinetics, x, 250, 270, 271, 273, 274, 278, 283
 KOH, 94

L

labeling, 21, 22, 23, 24, 25, 27, 29, 270
 lactose, 10
 lattice parameters, 64
 LDL, 17, 18
 leakage, 20, 23
 LED, 166
 leukemia, 222
 Lewis acids, 226
 lifetime, 214
 ligand(s), ix, x, 10, 14, 16, 18, 29, 32, 35, 36, 38, 86, 89, 99, 100, 101, 102, 103, 104, 105, 106, 109, 110, 111, 112, 113, 115, 116, 117, 118, 120, 123,

125, 133, 137, 160, 166, 168, 169, 174, 179, 181, 186, 187, 189, 198, 199, 200, 201, 207, 209, 210, 211, 213, 214, 217, 218, 219, 220, 221, 222, 225, 226, 227, 228, 229, 230, 231, 232, 233, 235, 236, 237, 238, 239, 241, 242, 244, 249, 250, 251, 252, 253, 255, 256, 257, 258, 259, 260, 263, 265, 266, 267, 269, 270, 271, 273, 274, 275, 278, 279, 280, 281, 282, 283, 290, 291, 292, 296

light-emitting diodes, 166, 168, 176

limitation, 34

linkage, 7, 17, 29, 131, 171

links, 125

lipoproteins, 18

liposomes, 16, 18

liquid crystal phase, 38

liquid crystals, vii, 1, 38, 39

liquids, 41

lithium, vii, 41, 206

liver, 20, 26

location, 23

low-density lipoprotein, 17

luciferase, 31

luminescence, 167

lying, 37, 191

lymphocytes, 222

M

mAb, 16, 17, 27
 macromolecules, 17
 magnesium, vii
 magnetic properties, 101, 137
 magnets, vii, 1
 malignant cells, vii, 1, 10, 21, 23
 malignant tumors, 16
 manipulation, 265
 manufacturing, 100
 market, 30
 MAS, viii, 61, 64, 69, 70, 71, 72, 73, 74, 75, 76, 78
 mass spectrometry, 166, 177
 materials science, ix, 165
 matrix, 38, 291, 292
 measurement, 64
 media, 30
 melanoma, 17
 melting, 38
 membranes, 23, 26, 40, 41
 Mendeleev, 47
 mercury, 41, 114, 223
 Mercury, 159
 metabolism, 16, 17, 217, 218
 metal salts, 130

- metals, vii, viii, 36, 38, 83, 100, 102, 103, 104, 107, 120, 124, 126, 127, 133, 136, 137, 183, 225, 260, 279, 282, 283
metastatic cancer, 23
methane, 35, 110, 121
methanol, x, 65, 85, 122, 249, 250, 252, 253, 255, 262, 264, 265, 270, 272, 273, 274, 283
mice, 24, 222
migration, 252
military, 2
Ministry of Education, 78, 216
mixing, 186
model system, ix, 197, 198, 210
models, ix, 12, 167, 168, 197, 198, 203, 205, 210, 216, 217, 218, 219, 224
modified polymers, 40
moisture, 34, 35, 71
mole, 169
molecular orbitals, 166, 174, 175, 176, 179, 295
molecular oxygen, 11, 282
molecular structure, 190, 191, 203, 227, 229, 235, 241, 242, 262, 267, 268, 270, 278
molecular weight, 7, 13, 16, 18, 25, 30, 65
molecules, viii, ix, x, 24, 30, 35, 38, 41, 62, 63, 69, 78, 99, 100, 101, 102, 103, 104, 105, 107, 109, 111, 114, 115, 120, 121, 124, 125, 126, 127, 130, 131, 136, 137, 167, 168, 169, 173, 184, 187, 190, 192, 198, 221, 226, 228, 235, 236, 237, 238, 239, 242, 250, 251, 283, 290, 293, 296
monoclonal antibody, 16, 24, 27
monohydrogen, 41
monomer, 253
MRI, 30
mutant, 16

N

- nanomaterials, 123, 192
nanostructured materials, 121
nanotube, 36
natural science(s), 201
natural selection, 200
NCS, 24, 25
Netherlands, 195
neutrons, vii, 1, 5, 19, 20
nickel, 38, 217
NIR, 104
nitrobenzene, 40
nitrogen, ix, 65, 66, 124, 198, 204, 205, 210, 216, 221, 225, 229, 233, 244
NMR, viii, x, 35, 61, 64, 65, 69, 70, 71, 72, 73, 74, 75, 76, 78, 80, 97, 132, 136, 158, 166, 177, 190,

- 202, 203, 204, 224, 225, 228, 229, 231, 232, 233, 234, 244, 250, 254, 255, 259, 266, 268, 270, 278
N-N, 228
non-linear optics, 166
novel materials, 168
novelty, x, 249, 250
nuclear magnetic resonance, viii, 61, 64, 96, 166
nuclei, 14, 224, 225
nucleic acid, 7
nucleophiles, 35, 223
nucleophilicity, 35, 252, 257, 271, 279, 296
nucleus, vii, 1, 22, 23, 224, 225

O

- observations, 72, 74, 202
octane, 94
olefins, 35, 36, 86
oligomeric structures, 112, 121
oligomers, 167, 168, 173, 222, 225
oligosaccharide, 10
opacity, 30
optical properties, 62, 168, 172
optimization, 21
optoelectronic devices, ix, 165, 166, 168
optoelectronic properties, 168
organ, vii, ix, 4, 38, 62, 78, 95, 100, 101, 102, 103, 105, 107, 108, 109, 110, 111, 113, 115, 116, 117, 119, 120, 121, 124, 126, 127, 128, 129, 130, 131, 133, 136, 165, 166, 167, 168, 172, 181, 197, 198, 199, 216, 217, 221, 222, 223, 283, 289
organic compounds, viii, x, 83, 84, 91, 93, 250
organic polymers, vii, 167
organic solvent(s), 40, 177, 180
organo-lithium compound, vii
organomagnesium, vii
organomagnesium compounds, vii
organometallic, vii, ix, 62, 100, 102, 103, 109, 111, 121, 165, 166, 167, 169, 172, 198, 222
organotin compounds, 222, 223, 224, 225, 226, 230
orientation, 169, 202, 235, 244
osmium, 122, 184
ovarian cancer, 32
oxidation, vii, viii, 3, 83, 84, 85, 95, 104, 105, 106, 116, 126, 133, 168, 172, 173, 174, 179, 180, 181, 191, 198, 200, 209, 222, 250, 251, 257, 279, 282
oxides, 282
oxygen, viii, 11, 62, 69, 76, 77, 83, 186, 222, 225, 226, 244, 250, 256, 263, 265

P

palladium, viii, 83, 84, 85, 86, 88, 89, 90, 91, 92, 94, 108, 109, 114, 122, 123, 151, 187, 220, 256, 257
 parameter, 64, 296
 parotid, 20
 particles, 23
 passive, 7
 pathways, 252
 peptides, 18, 21, 23, 24, 30
 Periodic Table, 167
 permit, 124, 251
 PET, 21, 22
 petroleum products, vii
 pH, 30
 pharmacokinetics, 21
 phenylalanine, 30
 phosphates, 251
 phospholipids, 17, 18
 phosphorous, 255, 260, 279, 281
 phosphorus, 204, 210, 250, 262, 268, 269, 270
 photoluminescence, 166
 photons, 21, 23
 physical properties, 103, 120, 168
 physical therapy, 20
 plants, 2
 plasma, 41, 64
 plasmid, 33
 platinum, 32, 33, 94, 104, 106, 108, 113, 116, 120, 121, 122, 123, 127, 132, 133, 151, 156, 169, 170, 171, 180, 181, 183, 184, 198, 201, 222, 260
 polarity, 292
 polarizability, 39
 polarization, 64, 291, 296
 polydimethylsiloxane, viii, 61, 63, 78
 polyesters, 222
 polymer(s), vii, ix, 1, 17, 36, 39, 40, 74, 88, 99, 115, 166, 168, 173, 177, 225
 polymer chains, 74
 polymer properties, 177
 polymer systems, 168
 polymeric chains, 34
 polymeric materials, 167, 176
 polymerization, 35, 36, 166
 polypeptides, 30
 polyurethane, 222
 polyurethane foam, 222
 poor, 111
 population, 20, 290
 porphyrins, 11, 12, 13, 18, 131
 positron(s), 21, 22, 24
 positron emission tomography, 21
 potassium, 3, 133

pressure, viii, 35, 65, 66, 83, 85, 86, 88, 89, 91, 94, 95, 252, 254
 probability, 118, 129, 203, 204, 207, 208, 211
 probe, 228
 prodrugs, 7
 production, vii, 1, 2, 166, 198, 201, 203, 205, 213, 214, 217, 219, 257
 program, 2, 40
 propane, 89, 198
 protease inhibitors, 88
 protein structure, 26
 proteins, 21, 23, 24, 26, 27, 29, 198
 proteolytic enzyme, 26
 protocol, 108, 109, 129, 136, 183, 227
 protons, 64, 198, 199, 210, 231, 232, 239
 pulse, 64
 PVC, 222, 226
 pyrimidine, 7
 pyrolysis, viii, 2, 3, 61, 66, 75, 78

Q

quantum yields, 176
 quantum-chemical calculations, 3

R

race, 9
 radiation, 7, 20, 21, 22, 40, 64
 radical polymerization, 35
 radio, 23
 radiotherapy, 19, 20
 range, vii, x, 1, 2, 4, 5, 23, 34, 70, 76, 109, 167, 168, 181, 191, 198, 226, 227, 238, 241, 242, 249, 250, 263, 266, 269, 274, 278, 279, 283
 reactants, 112, 226
 reaction center, 36
 reaction mechanism, 92, 114
 reaction rate, 273
 reaction time, 112, 264, 271
 reactive groups, 100
 reactivity, viii, x, 34, 70, 83, 84, 92, 198, 216, 222, 226, 249, 250, 251, 252, 260, 275, 278, 296
 reagents, viii, 3, 4, 35, 83, 84, 222, 226, 280
 receptor agonist, 30, 31
 receptors, 10, 17, 18, 21, 22, 30
 recognition, 7, 10, 226
 recovery, 40
 recycling, viii, 83, 84, 88, 89
 red shift, 188
 redistribution, 223
 redox groups, 115

- redox-active, ix, 103, 105, 125, 165, 166, 189, 192
reduction, ix, 84, 106, 116, 119, 179, 197, 198, 199, 201, 205, 209, 210, 211, 212, 214, 215, 216, 217, 218
reflection, 70, 72, 74, 75, 78
regeneration, 281
regulations, 19
rehabilitation, 20
relationship(s), 8, 31, 168, 176, 216, 219, 228
relevance, 225
replacement, vii, 125, 133, 135
replication, 7
residues, 10, 26, 30, 75, 239
resistance, 32, 40
resolution, 21, 22, 224, 225
retardation, 273
retention, 7, 16, 17, 23, 24
rhenium, 121, 133
rheumatoid arthritis, 20
rhodium, x, 36, 120, 132, 249, 250, 251, 252, 253, 255, 256, 257, 260, 262, 263, 265, 269, 270, 273, 274, 279, 281, 283
rigidity, 169, 189, 228
rings, 18, 30, 38, 121, 169, 172, 177, 187, 215, 242, 267, 269, 279
rodents, 16
room temperature, 35, 38, 41, 64, 84, 85, 110, 125, 202, 206, 233, 259, 266, 275
Royal Society, 57, 253, 254, 263
Russia, 1, 40
ruthenium, x, 108, 120, 125, 126, 133, 149, 158, 162, 184, 210, 214, 219, 249, 250, 258, 259, 260, 267, 268, 269, 279, 283, 293

S

- salt(s), 5, 34, 35, 38, 40, 41, 88, 111, 122, 127, 132, 206, 229, 231
sample, 64
scientific community, 168
search, 35, 198, 205, 206, 216, 217
second generation, 6
selectivity, 88, 89, 90, 91, 252, 256
selenium, vii, x, 250, 270, 283
semiconductors, vii, 1, 38
semimetals, vii
sensing, ix, 165, 166
sensitivity, 218, 224
sensors, 41
separation, 40, 104, 170, 181, 184, 191, 225
series, ix, 8, 14, 30, 31, 32, 36, 37, 38, 40, 108, 110, 115, 120, 122, 123, 124, 165, 168, 169, 175, 189, 190, 191, 192, 206, 226, 227, 228, 260, 273, 274, 282, 292
serum, 16, 29
serum albumin, 16
serum transferrin, 29
shape, 293, 294
shares, 210
signals, 69, 71, 72, 73, 75, 76, 104, 202, 203, 204, 231, 232, 270
silicon, x, 35, 63, 78, 222, 289, 290, 292, 294, 296
silver, 35, 103, 106, 110, 111, 113, 117, 119, 124, 126, 127, 131
silylenes, vii, 293, 296
similarity, 211, 213, 228
single crystals, 203
sites, 22, 100, 104, 110, 113, 115, 121, 204, 229, 232, 255, 263, 279
skeleton, 11, 105, 187, 232
sodium, 3, 4, 65, 122, 231
software, 296
solar cells, 168
sol-gel, 62
solid state, vii, x, 2, 111, 113, 117, 118, 120, 121, 127, 128, 136, 184, 207, 214, 221, 224, 225, 226, 227, 228, 231, 244
solid tumors, 22
solubility, 10, 30, 40, 41, 177, 235
solvent molecules, 84
solvents, 35, 41, 90, 114, 219, 235
Soviet Union, 40
species, vii, viii, 1, 5, 11, 18, 35, 36, 37, 84, 91, 95, 99, 100, 102, 103, 104, 105, 106, 107, 111, 113, 121, 124, 126, 127, 128, 132, 133, 166, 179, 180, 181, 184, 191, 202, 203, 204, 205, 210, 211, 213, 214, 230, 250, 251, 253, 254, 256, 270, 272, 274
specific surface, 72
specificity, 7, 14, 16, 21
spectroscopic methods, x, 221
spectroscopy, ix, 35, 37, 136, 165, 189, 200, 204, 224, 225, 228, 231, 254, 255, 259, 266, 268, 270, 278
spectrum, 19, 32, 64, 65, 69, 71, 72, 73, 75, 76, 135, 202, 203, 207, 210, 211, 215, 225, 229, 230, 231, 232, 233
speed, 2, 76
spin, 200, 224, 233, 251
squamous cell, 20, 24
squamous cell carcinoma, 20, 24
stability, 26, 27, 30, 34, 37, 100, 101, 167, 173, 213, 235, 266, 273
stabilization, 35, 100, 106, 244
stabilizers, 222, 226
standards, 85

- stoichiometry, 112, 131
 storage, 100
 strain, 254, 269
 strategies, 18
 strength, 24, 34, 232, 250
 stretching, 207, 252, 254
 strontium, 40
 students, 192
 substitution, 3, 18, 34, 35, 121, 123, 172, 214, 223, 225, 226, 242, 255, 281
 substitution reaction, 223, 255
 substrates, x, 11, 16, 93, 250, 251, 283
 sugar, 10
 sulfate, 41, 198
 sulfur, ix, x, 109, 169, 199, 221, 225, 226, 227, 228, 229, 230, 232, 233, 235, 238, 239, 240, 241, 242, 244, 250, 260, 266, 267, 279, 283
 sulfur dioxide, 109
 Sun, 58, 144, 150, 156, 161, 202, 205, 214, 217, 219
 supervision, 245
 surface modification, 63
 surprise, 112
 Sweden, 20
 symbols, 294
 symmetry, 38, 169, 225, 293, 294
 synthesis, vii, viii, ix, x, 1, 2, 3, 4, 6, 7, 9, 11, 16, 18, 29, 30, 36, 37, 38, 39, 71, 83, 84, 85, 88, 89, 90, 91, 93, 94, 95, 100, 101, 107, 108, 114, 115, 121, 122, 124, 128, 129, 130, 133, 134, 136, 165, 167, 168, 177, 187, 189, 197, 206, 218, 221, 222, 228, 249, 259, 260, 282, 283
 systems, ix, 5, 12, 23, 24, 29, 37, 84, 90, 92, 95, 99, 100, 101, 103, 104, 107, 114, 115, 127, 137, 166, 168, 169, 180, 181, 182, 183, 192, 217, 223, 227, 228, 244, 250

T

- tamoxifen, 30
 technological advancement, 2
 technology, 17
 temperature, 35, 64, 65, 75, 91, 112, 127, 229, 233, 234, 254, 255, 259
 testosterone, 31
 tetrahydrofuran, 65, 66, 113, 117, 119, 125, 134, 136
 thallium, 223
 theory, 200, 254
 therapy, vii, 1, 5, 6, 11, 13, 20, 21, 22, 23, 24, 27
 thermal stability, 34, 39
 thermodynamic stability, 280
 thermogravimetry, 64
 thin films, 177
 thyroid, 23, 24

- time, x, 1, 2, 4, 5, 6, 9, 14, 16, 18, 20, 21, 25, 27, 101, 136, 201, 202, 203, 249, 250, 265, 271, 272, 273, 274, 275, 276, 277, 283, 296
 tin, 222, 223, 224, 225, 226, 227, 228, 230, 231, 232, 233, 235, 238, 239, 240, 241, 242, 244
 tin oxide, 226
 tissue, vii, 1, 5, 20, 21, 22, 23
 titanium, 106, 110, 126, 127, 131, 133, 291, 292, 293, 296
 toluene, 2, 34, 65, 66, 122, 210, 233
 toxicity, 5, 7, 12, 14, 16, 30, 32, 223
 Toyota, 298
 trade, 40
 transesterification, 223
 transferrin, 18
 transformation(s), 84, 90, 183, 213, 251, 283
 transistor, 166
 transition(s), viii, x, 36, 63, 83, 84, 88, 99, 100, 101, 103, 105, 106, 107, 108, 109, 110, 111, 114, 115, 116, 120, 121, 124, 126, 127, 128, 129, 132, 133, 136, 137, 167, 171, 174, 186, 187, 210, 214, 222, 229, 250, 251, 279, 283, 284, 289, 290, 291, 293, 296
 transition metal, viii, x, 36, 63, 83, 84, 88, 99, 100, 101, 103, 105, 106, 107, 108, 109, 110, 111, 114, 115, 116, 120, 121, 124, 126, 127, 128, 129, 134, 136, 137, 167, 222, 229, 250, 251, 279, 283, 289, 290, 291, 293, 296
 transmission, 37, 38
 transport, 14, 21, 105, 177, 222
 trend, 275, 278
 trial, 12
 tricarboxylic acid, 129
 triflic acid, 204
 triphenylphosphine, 94, 156, 263
 trust, 42
 TSH, 17
 tuberculosis, 42
 tumor(s), vii, 1, 5, 7, 10, 11, 12, 14, 16, 17, 18, 19, 20, 21, 22, 23, 24, 27, 32, 33, 222
 tumor cells, vii, 1, 5, 7, 11, 14, 16, 17, 18
 tunneling, 38
 turnover, 198, 211, 253
 two-dimensional space, 239
 tyrosine, 9, 26, 30

U

- UK, 194, 250
 ultrasound, 30
 uniform, 74
 United States, 30
 urea, 88, 89, 90, 91

USSR, 2, 4, 43, 55
UV, x, 37, 149, 166, 171, 174, 186, 190, 215, 250
UV-Visible spectroscopy, x, 250

V

vacuum, 34
valence, ix, 2, 100, 102, 104, 109, 111, 165, 166,
223, 225, 294, 296
values, 32, 33, 37, 64, 66, 173, 180, 199, 209, 216,
225, 228, 232, 255, 265, 269, 271, 273, 278, 279,
291, 292
variable, 104, 230, 254, 259
variation, 104, 115, 188, 192, 224, 233, 272
vehicles, 20
vesicle, 17

W

waste treatment, 40
wave number, 254
wavelengths, 177
weak interaction, 62
wealth, 221
wires, ix, 165, 166, 167, 192

workers, 88, 167, 188, 200, 201, 202, 204, 205, 214,
215, 265

X

X-ray analysis, 266
X-ray crystallography, x, 169, 180, 221, 223, 250,
266, 278
X-ray diffraction, vii, viii, 35, 61, 64, 113, 203, 214,
224, 225, 262, 266, 268, 269, 270
X-ray diffraction (XRD), viii, 61, 64
XRD, viii, 61, 64, 66, 67, 70, 72, 73, 74, 75, 76, 78

Y

yield, 2, 3, 4, 9, 27, 29, 84, 85, 89, 90, 92, 93, 94,
114, 120, 122, 123, 125, 126, 133, 173, 183, 202,
206, 210, 257, 259, 263, 282

Z

zirconium, 62, 108